Préparation et étude de Membranes Asymétriques Polyalcoxyétherimides (PEI) pour la séparation de composés organiques de l'eau

Ayman Taha Elgendi

Nancy-Université INPL

Institut National Polytechnique de Lorraine- Ecole doctorale RP2E

Ecole Nationale Supérieure des Industries Chimiques

Laboratoire Réactions et Génie des Procédés

THESE

Présentée pour obtenir le titre de

DOCTEUR DE L'INPL

Spécialité :

GENIE DES PROCEDES ET DES PRODUITS

Présentée par

Ayman Taha ELGENDI

Préparation et Etude de Membranes Asymétriques Polyalcoxyétherimides (PEI) pour la Séparation de Composés Organiques de l'Eau

Soutenue publiquement le 11 Octobre 2010 devant le jury composé de :

Rapporteurs :	**RABILLER-BAUDRY Murielle**	**(Professeur, Université Rennes 1)**
	CABASSUD Corinne	**(Professeur, INSA)**
Examinateurs :	**DERATANI André**	**(Directeur de Recherche, CNRS)**
	LANGEVIN Dominique	**(Chargé de Recherche, CNRS)**
	ROIZARD Denis	**(Directeur de Recherche, CNRS)**
	FAVRE Eric	**(Professeur, INPL)**

LRGP Laboratoire Réactions et Génie des Procédés - UPR3349 CNRS – ENSIC

NANCY, France 2010

Nancy-Université INPL

Institut National Polytechnique de Lorraine- Ecole doctorale RP2E

Ecole Nationale Supérieure des Industries Chimiques

Laboratoire Réactions et Génie des Procédés

Thesis

Submitted as requirement to get the degree of

Doctor of the Institut National Polytechnique de Lorraine

speciality

CHEMICAL ENGINEERING

by

Ayman Taha ELGENDI

Preparation and Evaluation of Asymmetric Polyetherimide Membranes (PEI) for the Separation of Organic Compounds from Water

Graduation committee:

Rewiers :	**RABILLER-BAUDRY Murielle**	**(Professor, Université Rennes 1)**
	CABASSUD Corinne	**(Professor, INSA)**
Examiners :	**DERATANI André**	**(Research Director, CNRS)**
	LANGEVIN Dominique	**(Researcher, CNRS)**
	ROIZARD Denis	**(Research Director, CNRS)**
	FAVRE Eric	**(Professor, INPL)**

publicly defended: 11th October 2010

To my parents

To my loving my wife, sahar

To my daughters, Lamyaa, Kholoud and Jana

Acknowledgements

Thanks to Allah whom without thee, this work would not have been done. I owe a deep debt of gratitude to my advisors, Profs. ROIZARD Denis and FAVRE Eric, for their continuous guidance, great supervision, Valuable advices, time offered, support, and encouragement through this study.Their have also guided my personal development and maturation as an independent, confident, and strong researcher, something I never could have learned from a book.

I would like to extend my gratefully acknowledge for the financial support from the Egyptian ministry of higher education and from Laboratoire Réactions et Génie des Procédés/ CNRS. I appreciate my friends Jaques and Fleur for helping me to understand french culture and politics, advice for overcoming culture difference and achieving a successful career. I am fortunate to work in a wonderful group and I appreciate all of the kind help. I would like to thank constructive suggestions and valuable comments from committee members: RABILLER-BAUDRY Murielle, CABASSUD Corinne, DERATANI André and LANGEVIN Dominique. A special dept goes to my wife **Dr.Sahar Hassan** for continuous help during the study and writing this thesis, understanding, encouragement, and love, which inspired me to pursue my dream and finish my Ph.D study in France. Many thanks also to all the staff of Equipe Membranes, Séparations, Procédés and all the employment. To my friends and family, thank you for the time, care and support, they have offered as I have strived to complete this mammoth task.

Table of Contents

Table of contents

Acknowledgements **7**

List of Tables ***17***

List of Figures ***21***

1. Symbols ***29***

2. Abbreviations ***29***

General Introduction ***33***

General Introduction ***35***

References ***39***

Chapter (1) Bibliographic study ***45***

1.1 Introduction ***45***

1.2 Part 1: An outloook in membrane processes ***46***

1.2.1 Definition of membrane ***46***

1.2.2 Classification of membranes ***47***

1.2.3 The principal types of membranes based on morphology ***50***

1.2.4 Mixture types separated by membranes ***52***

1.2.5 Transfer parameters of membrane separation processes ***52***

1.2.6 The advantages and limitations of membrane separation processes ***52***

1.3 Membrane separation processes ***53***

1.3.1 Pervaporation (PV) ***54***

1.3.2 Pressure- driven membranes process ***64***

1.3.3 Problem of the extraction of low molecular weight organic compounds from water by membranes ***73***

1.3.4 Interest of nanofiltration **74**

1.3.5 Separation mechanism with NF membranes ***75***

1.3.6 Traditional methods to remove pollutants from water and wastewater ***78***

1.3.7 Rejection of organic compounds using nanofiltration (NF) membranes ***79***

1.3.8 Inorganic rejection using nanofiltration (NF) membranes ***81***

1.3.9 Rejection of aqueous organic/inorganic by asymmetric polyetherimide membranes **82**

1.4 Part 2: Membrane preparations ***84***

1.4.1 Interest of polyimide membranes ***84***

1.4.2 Preparation of membranes 86

1.4.3 Symmetrical membrane 87

1.4.4 Preparation of porous membrane 88

1.4.5 Asymmetric membrane preparation and phase inversion process 89

1.4.6 Thermodynamic description of phase inversion..... 91

Mechanism of microporous formation by thermal gelation of a binary system..... 91

1.4.7 Phase inversion process and ternary phase diagram 93

1.4.8 Demixing types in a ternary system..... 96

1.4.9 Mechanism of formation skin toplayer and porous sublayer..... 97

1.4.10 Study of some parameters which have an influence on membrane morphology 99

1.4.11 Preparing new asymmetric block copolyimide membranes: Asymmetric polyetherimide (PEI) copolyimide membranes..... 102

References Chapter 1..... 103

Chapter (2) 123

Materials and Methods..... 123

2.1 Materials and Methods 123

2.1.1 Materials..... 123

2.1.2 Part 1: Preparation of PEI and Kapton™ membranes..... 124

2.2 Part 2: Membrane characterizations..... 132

2.2.1 Phase diagram 132

2.2.2 Scanning electron microscopy (SEM)..... 134

2.2.3 Thermo-mechanical property..... 134

2.2.4 Thermo-gravimetric analysis (TGA)..... 134

2.2.5 FTIR characterizations..... 135

2.2.6 Swelling properties..... 135

2.3 Part 3: Separation properties..... 136

2.3.1 Pervaporation (PV) experiments..... 136

2.3.2 Nanofiltration (NF) system experiments..... 143

2.3.3 Characteristic flow rates of NF set-up 150

References Chapter 2 154

Chapter 3..... 161

Results and discussion of synthesis and characterization of membranes *161*

3.1 Membrane preparation *161*

3.2 Phase diagrams *161*

3.2.1 Phase diagram and the determination of the binodal demixing curve by alternating addition of nonsolvent and solvent to the polymer solution. *162*

3.2.2 Turbid points values (binodal demixing curve) and phase diagrams *164*

3.3 Studing of membrane morphology with scanning electron microscope (SEM) *166*

3.3.1 Preparation of PEI dense membrane *166*

3.3.2 Preparation of PEI asymmetric membranes by phase inversion process *167*

3.3.3 SEM for Hybrid silica-PEI membranes *193*

3.3.4 Kapton membranes preparation *194*

3.3.5 Asymmetric PEI membranes preparation with strong mechanical support *198*

3.4 Study of the stability of PEI dense membranes in organic solvents and in water ... *200*

3.5 Physical characterizations *207*

3.5.1 Infrared spectra (FT-IR) *207*

3.5.2 Mechanical property *210*

3.5.3 Thermogravimetric analysis (TGA) *211*

Conclusions and Recommendations for Future work *217*

References **219**

Chapter 4 ..... *227*

Pervaporation results and discussion *227*

4.1 Pervaporation performances with pure solvents (Water, Heptane, Toluene) and 50-50 wt% Toluene-Heptane mixtures (organic –organic mixture) *227*

4.1.1 Effect of feed concentration and operating temperature on the performances of PEI dense membrane. *229*

4.1.2 Effect of membrane and temperature on membrane performances *232*

4.2 Pure solvents and 0-100 wt. % aqueous solution of water- ethanol *237*

4.2.1 Effect of temperature and feed composition on membrane selectivity *240*

4.2.2 Effect of temperature and feed composition on membrane flux *246*

4.3 Effect of soft block on pervaporation performances of PEI membranes *250*

4.3.1 Effect of membrane type and operating temperature on selectivity *251*

4.3.2 Effect of operating temperature and membrane morphology on flux *253*

4.4 Dehydration of alcohols 254

4.5 Separation properties with the hybrid silica- PEI membranes 260

4.5.1 Effect of operating temperature on flux and selectivity 261

4.5.2 Effect of TMOS content on flux, swelling and selectivity 264

Conclusions and Recommendations for Future work 267

References 269

Chapter (5) 279

Nanofiltration (NF) results and discussion 279

5.1 Results with PEI-NF 279

5.1.1 Hydraulic flux of dense membranes 279

5.1.2 Hydraulic flux of asymmetric membranes 282

5.2 Separation of aqueous polluted solutions by NF-PEI membranes 287

5.2.1 Nanofiltration of aqueous inorganic feeds with asymmetric PEI membranes 287

5.2.2 Nanofiltration of aqueous organic solutions with asymmetric PEI membrane 292

Conclusions and Recommendations for Future work 321

References 322

General Conclusions and Perspectives 327

Appendix A: List of publications 329

Appendix B: Résumé Français 333

SOMMAIRE Résumé Français 337

Introduction Générale 343

1. PARTIE 1: Etude bibliographique ..... - 349 -

2. Partie 2: Matériels et Méthodes ..... - 365 -

2.1 Les matériaux et leurs propriétés ..... - 365 -

2.2 Préparation de membranes denses PEI et membranes asymétriques PEI…… - 366 -

2.2.1 Protocole de préparation membrane dense ..... - 366 -

2.2.2 Protocole de préparation des membranes asymétriques ..... - 367 -

2.3 Synthèse de membranes hybrides Organique/Inorganique ..... - 368 -

2.3.2 Protocole de préparation de membranes hybrides dense ..... - 369 -

2.3.3 Préparation de membranes hybrides asymétriques ..... - 370 -

2.4 Protocoles de préparation de membranes Kapton^{TM} (PI) denses et membranes Kapton^{TM} (PI) asymétriques ..... - 370 -

2.5 Caractérisation des membranes ..... - 370 -

2.6 Propriétés de séparation..... - 373 -

2.6.1 La pervaporation..... - 373 -

2.6.2 Mise en place du montage de nanofiltration (NF)..... - 380 -

3. Partie 3: Résultats et discussions ..... - 387 -

3.1 Caractérisation des membrane PEI.....- 387 -

3.2 Principaux résultats et discussions ..... - 403 -

3.2.1 Etude des propriétés de pervaporation ..... - 403 -

3.2.2 Résultats de Nanofiltration (NF) avec les membranes PEI ..... - 419 -

Conclusion générale.....435

List of Tables

Table 1.1: Manufacturers who obtained the grant of European patents by the European Patent Office between 1980 and 1999 for the areas of pervaporation field.

Table 2.1: Patents by the European and USA Patent Office between 1976 and 1999 for the areas of pervaporation field

Table 3.1: illustrates the characteristics of feed, permeate and concentrate for some applications of pressure-driven membrane system

Table 4.1: Inorganic rejection using a commercial nanofiltration (NF) membrane

Table 5.1: Physical properties of the salts ions tested

Table 6.1: Asymmetric PEI ultrafiltration membranes made from monomers for organic solution separation

Table 7.1: Comparison of nanofiltration performance of the asymmetric PEI membranes prepared from commercial pure polymers for organic liquid solution separation

Table 1.2: Characteristics of different raw materials

Table 2.2: The properties of the non-polar mixture (Toluene/n-Heptane).

Table 3.2: The properties of alcohols.

Table 4.2: Operating parameters for NF cell system

Table 5.2: Characteristics of organic

Table 1.3: Points of alternating addition of nonsolvent (cloud point) and solvent (clearing point) to the polymer solution at 10 °C

Table 2.3: The composition of turbid point at 10 °C

Table 3.3: Operating parameters tested on preparation of PEI membranes (membranes M_1:M_6).

Table 4.3: The operating parameters tested for preparation of PEI membranes (membranes M_7:M_{12}).

Table 5.3: The operating parameters tested for preparation of PEI membranes (test 4, test 5)

Table 6.3: Operating prameters for studying the effect of change of immersion bath temperature.

Table 7.3: The operating parameter tested for preparation of PEI membranes

Table 8.3: Operating parameter tested for preparation of PEI membranes

Table 9.3: Operating parameters tested for preparation of Kapton membranes

Table 10.3: Effect of soft block (Jeff600) content on the swelling degree.

Table 11.3: Stability of dense PEI (0.4 Jeff) with solvents at room temperature (20^{o}C).

Table12.3: Mechanical properties of PEI and Kapton™ (present work and literature data).

Table 13.3: TGA features of PEI membranes

Table 14.3: Effect of addition non solvent (water) to polymer solutions (membranes M_7:M_{12}).

Table 15.3: Effect of the polymer solution concentration

Table 16.3:Effect of change immersion bath temperature

Table 1.4: Pervaporation results of PEI dense and asymmetric membranes with feed 50 wt.% Toluene-Heptane.

Table 2.4: Effect of PEI membranes types on the separation factor (α) and on the permeate enrichment (Cp) with 50 wt% Toluene-Heptane feed(CP ±2-3%).

Table 3.4: Pervaporation results of PEI dense and asymmetric membranes with pure solvents and water.

Table 4.4: Effect of operating temperature on the total real flux of PEI dense and asymmetric membranes.

Table 5.4: Effect of temperature on the partial real flux of feed with asymmetric PEI membrane 25 wt % PAA ($m_{as,\ 60\ um}$).

Table 6.4: Effect of operating temperature on the normal flux for dense PEI membranes.

Table 7.4: Effect of temperature on the partial normal flux with dense PEI membrane ($m_{d1,60\mu m}$).

Table 8.4: Effect of temperature on the partial normal flux with dense PEI membrane ($m_{d2,30\mu m}$).

Table 9.4: separation factor of PEI membranes.

Table 10.4: Comparing between dense, asymmetric PEI (0.4 Jeff 600) and dense PI Kapton™ membranes prepared from commercial PAA (feed 50 wt% ethanol/water).

Table 11.4: Pervaporation performance of PEI membranes in aqueous alcohol systems.

Table 12.4: Activation energy for asymmetric PEI membrane.

Table 13.4: Pervaporation performance of polyimide membranes in aqueous alcohol systems.

Table 14.4: Effect of TMOS content and temperature on flux.

Table 15.4: Separation factor (**α)** and permeate enrichment (Cp).

Table 16.4 : Review table results of PEI membranes with pervaporation (PV)

Table 1.5: NF test results with dense membranes at 40 bar, active membrane area 41 cm^2.

Table 2.5: Nanofiltration results with PEI and kapton membranes (feed pure water).

Table 3.5: Physical properties of the salts ions

Table 4.5: Results of salt separation with asymmetric PEI membranes

Table 5.5: Effect of operating pressure and feed on membrane performances.

Table 6, a.5: Operating parameters for preparing asymmetric PEI membranes.

Table 6, b.5: Effect of Mw on average rejection of aqueous organic by PEI membranes (feed 500 ppm of organic/water, pressure 10 bar).

Table 7.5: Organic solutes size taken from literature

Table 8.5: Selected physico-chemical properties of the organic compounds tested

Table 9.5: Flux of aqueous organic compounds by asymmetric PEI membranes (feed 500 ppm of organic/water, pressure 10 bar for asymmetric PEI membrane and 20 bar for asymmetric Kapton™ membranes).

Table 10 .5: Membrane permeance of aqueous organics by PEI membranes (feed 500 ppm of organic/water, pressure 10 bar for asymmetric membranes and 20 bar for asymmetric kapton).

Table 11.5: Effect of salt solution on performance of PEI-NF membrane

Table 12,a.5: Nanofiltration results with PEI and Kapton membranes (feed pure water).

Table 12,b.5: Separation of H_2O/ EtOH mixtures by NF membrane performance.

Table 12,c.5: Comparison between nanofiltration and pervaporation

List of Figures

Figure 1.1: Schematic of size based membrane exclusion

Figure 2.1: Schematic diagrams of the principal types of membranes based on structure

Figure 3.1: Classification of membrane separation methods by size according to separated compounds

Figure 4.1: Schematic diagram of the basic membrane separation process.

Figure 5.1: Schematic diagram of the basic pervaporation process

Figure 6.1: Pervaporation patents by the European and USA Patent Office between 1976 and 1999.

Figure 7.1: Schematic of solution-diffusion model through non-porous polymeric materials.

Figure 8.1: Classification of organic–organic pervaporation separation

Figure 9.1: Definitions of pressure-driven membrane processes based on the smallest particle (molecule) retained.

Figure 10.1: Classified consumption of membrane in the world

Figure 11.1: Retention of spherical and linear molecules in NF membrane by a steric exclusion mechanism

Figure 12.1: Typical sigmoidal rejection curve (rejection as a function of molecular weight) obtained for rejection of uncharged solutes with a nanofiltration membrane

Figure 13.1: Structure of a polyimide a) linear b) heterocyclic aromatic

Figure 14.1: Structure of Ultem and Kapton.

Figure 15.1: General reaction for synthesis the polyimide

Figure 16.1: Structure of the polyetherimide (PEI).

Figure 17.1: Phase inversion process by immersion precipitation

Figure 18.1: Schematic diagram showing the formation of a microporous system by thermal gelation

Figure 19.1: Ternary-phase diagram of polymer(P)–solvent(S)–nonsolvent(NS) system

Figure 20.1: Schematic diagram showing the formation of a microporous system

Figure 21.1: Mechanism of formation of asymmetric membrane

Figure 22.1: Formation symmetric microporous membrane

Figure 1.2: Chemical structures of the raw materials

Figure 2.2: PAA and PEI synthesis with two steps mechanism

Figure 3.2: Process flow sheet for asymmetric PEI membranes preparation.

Figure 4.2: The hydrolysis (1) and condensation (2) reactions of the sol–gel process.

Figure 5.2: Schematic representation of the phase diagram and the determination of the binodal demixing curve.

Figure 6.2: Shape and dimensions of PEI and PI specimens used in mechanical testing.

Figure 7.2: Schematic diagram of the pervaporation experimental set-up

Figure 8.2: a) the pervaporation unit b) trap during pervaporation c) Condensation of the permeate through contact with liquid nitrogen

Figure 9.2: Calibration curve of toluene – heptane (gas chromatography-FID)

Figure 10.2: Calibration curve of water – ethanol (gas chromatography-TCD).

Figure 11.2: Calibration curve of water – butanol (gas chromatography-TCD)

Figure 12.2: The SEPACF II Membrane Element Cell

Figure 13.2: SEPA CF II Membrane element cell major components and flow sequence

Figure14.2: NF permeation system set-up

Figure 15.2: a; Membrane element cell, b; NF setup.

Figure 16.2: NF cell tests without membrane with pure water (characteristic of the cell hydrodynamics).

Figure 1.3: Schematic representation of the phase diagram and the determination of the binodal demixing curve

Figure 2.3: Ternary phase diagram and the determination of the binodal demixing curve of PAA-DMF-H_2O system build

Figure 3.3: SEM Photograph of PEI dense membranes

Figure 4.3: SEM Photograph surface of M_1 (30%-70%-0/1min/1hr/85µm)

Figure 5.3: SEM Photograph surface of M_2 (30%-70%-0/1min/2hr /50µm)

Figure 6.3: SEM Photograph surface of M_3 (30%-70%-0/1min/3hr/55µm)

Figure 7.3: SEM Photograph surface of M_4 (30%-70%-0/3min/1hr/70µm)

Figure 8.3: SEM photograph surface of M_5 (30%-70%-0/3min/2hr/45µm)

Figure 9.3: SEM photograph surface of M_6 (30%-70%-0/3min/3hr/50µm)

Figure 10.3: Cross section view of PEI membrane M_7 (28-67-5/1min/1hr/120 µm)

Figure 11.3: Cross section view of PEI membrane M_8 (25-60-15 /1min/1hr/ 150µm)

Figure 12.3: Cross section views of M_9 (24-56-20/1min/1hr/170µm)

Figure 13.3: Cross section view of M_{10} (23-53-24/1min/1hr/170µm)

Figure 14.3. SEM view of SEM view of M_{11} (PAA-DMF-water: 20-49-31/1min/1hr)

Figure 15.3: Schematic representation of the ternary phase diagram with membrane morphology

Figure 16.3: cross section views of PEI membranes with change polymer solution composition test 4

Figure 17.3: Cross section view of PEI membranes versus polymer solution composition test5

Figure 18.3: Cross section view of M_{19} (30%-70%-0 /1min/1hr/35µm).

Figure 19.3: Cross section view of M_{20} (25%-75%-0 /1min/1hr/20-40µm)

Figure 20.3: Cross section view of M_{21} (25%-75%-1% /1min/1hr/30µm)

Figure 21.3: SEM Photograph surface of M_{24}

Figure 22.3: Cross sections view of PEI membranes

Figure 23.3: cross section view for hybrid dense PEI membrane M_{dc1} (5%TMOS,95% PAA)

Figure 24.3: Cross section views for hybrid asymmetric PEI membrane.

Figure 25.3: cross section views for asymmetric PEI membrane M_{c4} (5%SiO2 12 nm, 95%PAA).

Figure 26.3: Surface view of PI membrane M_{kd1}.

Figure 27.3: Cross section view of Kapton M_{k1} (11PAA%-89NMP%0% /1min/1hr/70µm)

Figure 28.3: Cross section view for M_{k2} (11PAA%-89NMP%/60min/1hr/75µm)

Figure 29.3: SEM view of Kapton M_{k3} (15PAA%-85NMP%/5min/1hr/145µm)

Figure 30.3: SEM view of Kapton M_{k4} (15PAA%-85NMP%/10min/1hr/165µm)

Figure 31.3: SEM view of Kapton M_{k5} (15PAA%-85NMP%/15min/1hr/140µm)

Figure 32.3: Cross sections view of PEI membranes coated on support

Figure 33.3: Isothermal swelling equilibrium of PEI dense membrane at (20^0C).

Figure 34.3: Effect of temperature on swelling in PEI dense membranes.

Figure 35.3: Swelling degrees of PEI and Kapton™ dense membranes in different liquids at 20°C

Figure 36.3: Relation between solubility parameter of some solvents and swelling percent of PEI dense membranes.

Figure 37.3: Infra-red spectrum for dense and asymmetric PAA membrane 30% PAA in DMF.

Figure 38 a, b, c.3: Infra-red spectra for PAA, PEI and Kapton™ membranes.

Figure 39.3: Stress-strain curve of PEI with Jeff 600 (0.4).

Figure 40.3: TGA showing the membranes weight loss of PEI and Kapto

Figure 41.3: Differential curves of the TGA signals of PEI and Kapton™.

Figure 42.3: Evolution of the total weight loss with the polymer structures after degradation at 800°C.

Figure 43.3: Evolution of PEI decomposition temperatures rate of Jeff 600.

Figure 1.4: Toluene enrichment in PEI dense membrane (60µm).

Figure 2.4: Effect of feed wt. % on the partial normalized flux of PEI dense membrane (60µm)

Figure 3.4: SEM photograph surface of PEI membranes

Figure 4.4: Effect of membrane (type, thickness) and operating temperature on selectivity

Figure 5.4: Effect of membrane type on partial real flux (feed 50% T/H).

Figure 6.4: Effect of the feed concentration on separation performance of PEI membranes.

Figure 7.4 a, b, c: Enrichment comparison for the PEI dense membranes (30PAA& 25PAA) at temperature 30 - 60^0C, where (cp d); (30PAA)

Figure 8.4, a b c: Enrichement comparison of asymmetric (cp as) / dense membrane (cp d) (25PAA) at temperature 30 - 60 ^{0}C, CP±2-3%.

Figure 9.4: Effect of operating conditions (temperature, feed composition) and membrane type on separation factor.

Figure10.4: Effect of feed concentration on the partial real flux of asymmetric membrane (25 PAA& 60um).

Figure 11.4: Effect of feed content on partial normal flux with dense membrane 30 PAA

Figure 12.4: Effect of feed content on partial real flux with dense membrane 25 PAA.

Figure 13.4: Cross section view of PEI asymmetric membrane 25% PAA in DMF at immersion bath temperature 16°C.

Figure 14 a, b.4: PV results obtained with PI or PEI membranes either as dense or asymmetric membranes – Feed mixture: 50 wt% water/ethanol(at 40 and 60°C)

Figure 15.4: Asymmetric PEI membrane performance with aqueous alcohol systems

Figure 16.4: Plot of molar ln (j)/ verses 1 / T for the asymmatric membrane (25%PAA).

Figure17.4: Effect of TMOS on membrane performance.

Figure 18.4: Effect of operating temperature and membrane type on flux

Figure 19.4: Plot of molar ln (j)/ verses 1 / T for a hybrid dense membrane (20% TMOS).

Figure 20.4: Effect of TMOS% on swelling% of silca-PEI membranes.

Figure 1.5: Effect of operating pressure on performance of Kapton^{TM} and PEI dense Membranes, feed pure water at 30°C±2.

Figure 2.5: Cross section view of porous symmetric Kapton membrane.

Figure 3.5: Cross section view of homogenous PEI asymmetric membrane.

Figure 4.5: Cross sections view of composite PEI asymmetric membranes.

Figure 5.5: Effect of pressure and membrane type on membrane performance.

Figure 6.5: SEM of asymmetric PEI membranes.

Figure 7.5: Effect of operating pressure on membrane performances (flux, permeability) {$M1_{(25PAA+15w)}$, $M2_{(25PAA+20w)}$}.

Figure 8.5: Effect of operating pressure and feed on performances of $Mc_{(25PAA+s15PAA)}$

Figure 9.5: Effect of operating pressure and feed on performance of $M_{(20PAA+25w).}$

Figure 10.5: Effect of membrane type on organic molecule rejection (10bar, feed 500ppm).

Figure 11,a .5: Cross section view of Kapton M_{k1} (11PAA%-89NMP%/1min/1hr/50µm) at immersion bath temperature 11°C**.**

Figure 11, b,c,d.5: SEM view of Kapton^{TM} at immersion bath temperature 11°C**.**

Figure 12 .5: Effect of membrane type on organic molecule rejection for $M_{(25PAA+15W)}$ (10bar, feed 500ppm) and PEI (UItem 1000) (4:14 bar, feed 1000ppm).

Figure 13.5: Effect of organic solute molecular weight on rejection.

Figure 14.5: Solute rejection as a function of solute radius.

Figure 15.5: Correlation between solute hydrophobicity expressed as log $_{ow}$ and retention of PEI asymmetric membranes for 3 aliphatic alcohols, toluene and cyclohexane.

Figure 16.5: Effect of membrane type on membrane performances at 10 bar and feed 500ppm.

Figure 17.5: Effect of operating pressure on flux and on membrane permeance by asymmetric PEI membranes (aqueous organic feed 500 ppm).

Figure 18 .5: SEM for asymmetric PEI $M_{(25PAA)}$ membrane.

Figure 19 .5: SEM for asymmetric PEI $M_{(25PAA+15W)}$ membrane .

Figure 20.5: SEM for asymmetric PEI $M_{(20PAA+25W)}$ membrane.

Figure 21.5: SEM for asymmetric PEI $M_{(15PAA+25W)}$ membrane.

Figure 22 .5: SEM for Mc (dense 30PAA+ support Kapton 11PAA).

Figure 23.5: Effect of inorganic solution on organic rejection as a function of Mw for a series of organic compounds in the feed. The feed temperature was 20°C±2; the pressure was 10 bar.

Figure 24 .5: Effect of aqueous inorganic addition on flux. The feed temperature was 20°C at 10 bar.

Symbols and Abbreviations

Symbols and Abbreviations

1. **Symbols**

C_p	weight fraction in the permeate (%)
C_f	weight fraction in the feed (%)
Wd	initial dry sample weight recorded before immersion (g)
Ws	final sample weight noted after immersion (g)
Q	total mass of permeate (kg)
A	effective area of membrane (m^2)
T_t	PV experiment duration (h)
J	total flux (kg / $h.m^2$)
J_T	partial toluene real flux,
J_H	heptane partial real flux
α	selectivity or separation factor
ΔG	free energy of mixing
φx	volume fraction
μ	dipole moment
ρ	density
R	rejection

2. **Abbreviations**

BSA	bovine serum albumin
CA	Cellulose acetate
DMA	dimethylacetamide

DMAC	N, N-dimethyl acetamide
DSI	Desalination Systems, Inc.
EA	egg albumen
ESR	electron spin resonance
FA	formic acid
ICL	isophthaloyl chloride
MWCO	molecular weigh cut off
MABH	m-amino benzhydrazide
MD	Membrane distillation
MF	Microfiltration
NF	Nanofiltration
NMP	N-methyl-2-pyrrolidone
SEM	scanning electron microscopy
ODA	4, 4'Oxydianiline
Jeff	Jeffamine® ED-600
DMF	N, N-Dimethylformamide
TCL	terephthaloylchloride
TFC	thin-film composite membranes
TFM	thin-film composite membranes
TGA	Thermogravimetric analysis
RO	Reverse osmosis
SEIP	solvent exchange cum immersion precipitation

SEM	Scanning Electron Microscopy
PMDA	pyromellic dianhydride
PASA	poly (amidesulfonamide)
PEAH	polyetheramide hydrazide
PEG	polyethylene glycol
PAA	poly(amic acid)
PI	aromatic polyimides such as Kapton™
PEI	polyetherimide
PV	pervaporation
PPSS	poly (phenylene sulfide sulfone)
PSf	polysulfone
PSO	polysulfone
PTMSP	poly (1-trimethylsilyl-1-propyne)
PVA	polyvinyl alcohol
PVDF	polyvinylidenedifluoride
PA	propionic acid
PA-6	polyamide-6
PABH	p-amino benzhydrazide
PAH	polyamide-hydrazides
PAN	polyacrylonitrile
PP	polypropylene
PPO	polyphenyleneoxide
PTFE	Teflon (polytetrafluoro ethylene)

PVAC	poly(vinyl acetate)
PVC	poly(vinyl chloride)
PVDC	poly(vinylidene chloride)
ZrO2	zirconium oxide

General Introduction

General Introduction

I. The problem of organic pollutants in drinking water

This thesis intends to use membrane separation processes for purification of aqueous solutions containing molecules of organic pollutants based on the selectivity of the membrane, such as the preferential permeation of water (classical selectivity) or the solute (reverse selectivity). In the classical case, the goal is most often the purification of water downstream (production of drinking water by ultra-or nanofiltration) or the upstream concentration of organic species (application for molecules with high added values). In the case of a reverse selectivity, the organic molecules is passed, the energy balance is much more interesting because it is the minority species for the permeate.

However in the case of aqueous solutions containing organic molecules of small sizes or low molecular weights, the applicability of the nanofiltration technology remains poorly understood. The objectives of the thesis is to contribute to improve the knowledge in this area by testing the separation of aqueous mixtures containing molecules of various molecular weights and polarities. For example, industrial potential targets include ethanol, urea, 2-propanol ...

Nanofiltration (NF) is one of the promising technologies for the treatment of organic and inorganic pollutants in water. The rejection of organics by membrane depends on both the membrane properties like pore size, membrane material, membrane charge and solute characteristics such as molecule size, charge and polarity, as well as on the membrane-solute interactions. For neutral species, the rejection mechanism of organic compounds by nanofiltration is prevalently governed by the sieving mechanism based on the solute size and the membrane pore size. However, the physicochemical effects in organic rejection cannot be totally neglected, and they can contribute to the rejection of the specific pairs membrane-solute. The effect of solute molecule charge is obvious, the effect of solute molecule polarity and solute molecule hydrophobicity are likely. Although, NF technology has a rapidly growing field in the membrane industry. The question of whether NF technology presents an appropriate barrier for low molecular weight (LMW) organic solutes is still controversial [1,2,3].

In this work, we focus particularly on two membrane separation techniques, which are nanofiltration and pervaporation for liquid mixtures. These two processes will be used to test

dense and asymmetric membranes with one of the components of the mixtures to be treated. For both methods, as with any membrane process, the membrane is one of the most important characteristics which determines the usefulness and effectiveness of the entire process. For this reason, several targets of research have shifted in recent years towards developing new and more efficient materials that allow for a compromise between two fundamental properties of the separation, often antagonistic, namely the selectivity and permeability.

However, membrane processes are becoming economically competitive after the development of highly permeable polymer membranes. These membranes are less expensive than inorganic membranes and their implementation is much easier. Several types of polymers can be used such as polysulfones, polyamides and polyimides.

The aromatic polyimides (PI) are well known as a class of polymer materials, which have been widely studied for over 20 years in the field of membrane separation [4]. Aromatic polyimides are also known to exhibit a very good stability to a great number of solvents. As glassy polymers, they possess remarkable mechanical and chemical properties for organic materials, but generally their permeability coefficients are low because of their rigid carbon skeleton and of their low available free volume; consequently their applications in separation are mainly limited to gas separations or to filtration processes (MF, UF) [5,6].

To broaden the application area of polyimides in liquid separations, we decided to prepare and study the properties of a block ether aromatic copolyimide series where the ether soft block acts both as a selective and a permeable block. Furthermore, in our laboratory (Laboratoire Réactions et Génie des Procédés) we are interested with polyetherimides. Several researchs have been done with polyetherimide such as preparing dense membranes by M.Kréa and J. Grignard. So, in this thesis we used polyetherimide to prepare dense and asymmetric membranes to benefit from the experiences gained before with polyetherimide.

- **Design of polyetherimide (PEI) membranes**

This dissertation aims at preparing polymeric nanofiltration membranes in order to get water selective membranes suitable for the retention of relatively small organic molecules ($Mw<6000$ $g.mol^{-1}$) from polluted water mixtures. Hence two objectives must be reached: first, the selection of water selective materials well resistant in almost pure water, and secondly the preparation of high flux membranes needed for the recovery of water.

To satisfy the first objective, a copolyimide (PEI) including alkyloxy- rubbery blocks was used; indeed, propyloxy- and more particularly ethyloxy- ether blocks are known to have high affinity with water (water-selective blocks). On the other hand, the imide block was prepared from pyromellitic dianhydride (PMDA) and oxydianiline (ODA) to provide a water resistant polymer structure after the formation of the imide cycle. The physico-chemical properties of PEI membranes were determined by swelling experiments in several pure liquids.

To get high fluxes membranes, asymmetric polyetherimide membranes (PEI) structures were prepared by the phase inversion method and the influence of the experimental conditions on the membrane microstructure was characterized by scanning electron microscope (SEM). The characterization of the membranes was carried out by swelling, phase diagram, SEM, FT-IR, mechanical properties and thermal analysis. Thus, it is expected that the development of new types of asymmetric membranes copolyimide block can lead to high performance membranes. However, it was not possible to predict the exact influence of this second type of block (soft block) on the preparation of asymmetric membranes or to know if a molecular separation could be achieved in nanofiltation or pervaporation with such asymmetric membranes.

To control if the top layer of asymmetric membrane was either tight or porous, pervaporation and nanofiltration experiments of pure liquids and mixtures were routinely carried out and compared with results obtained from homogenous dense membranes.

As a matter of fact, the preparation of polymeric membranes usually involves the phase inversion (separation) process, in which a homogeneous casting solution induces phase separation into a polymer-rich phase and a polymer-poor phase by the exchange of solvent with nonsolvent in a immersion bath (i.e: as water bath). Phase separation would continue to form the membrane structure until the polymer rich phase is solidified. Solidification during phase inversion could be induced by gelation and/or crystallization of the casted polymer solution. The equilibrium ternary phase diagram system is still a good tool for controlling the morphology and interpreting the membrane structure. Significantly, knowledge of phase equilibria (cloud points, binodals, spinodals, and critical compositions) enables one to change the conditions for the preparation of membranes such as the compositions of the casting solution, the temperature and of the coagulation bath type to obtain an optimum membrane structure.

In this work, different types of membranes are used: KaptonTM membrane as a reference and original polyetherimide membranes. These types of membranes were prepared in the laboratory. The influence of different parameters on the performance efficiency of nanofiltration/ pervaporation were studied such as:

-Molecular parameters of solutes (molecular weight, shape, polarity),

- Effect of the type and morphology of membrane on separation

-Effect of applied pressure on rejection and flux.

Based on the existing literature, the main steps of this thesis are:

- The installation of a new experimental set-up of NF water system,
- The preparation of original membranes, including pervaporation and nanofiltration types;
- The characterization of membranes (surface properties, porosity, permeability to pure water, ..)
- The study of the separation of mixtures by pervaporation models (separation factor, ..);
- The study of the separation of mixtures by nanofiltration models (concentration factor, ..);
- The analysis of results. Particular attention will be paid to understand the mechanisms of permeation.

This thesis is divided into five chapters:

- **Chapter (1) Bibliographic study**: This first chapter discusses the bibliography of membrane technology, it provides a detailed reminder of the different methods of membrane separation characteristics of pervaporation and pressure driven membrane processes.
- **Chapter (2) Materials and methods**: This second chapter explains the different methods and experimental devices used both for synthesis of dense and asymmetric membranes and for characterization by pervaporation and nanofiltration.
- **Chapter (3) Results and discussion** of synthesis and characterization of membranes: this third chapter displays results of methods used for synthesis of dense and asymmetric PEI membranes and to characterize membranes.
- **Chapter (4) Pervaporation results and discussion**: This fourth chapter discusses pervaporation performances. The PEI dense and asymmetric membranes are evaluated by pervaporation using pure solvents, to check structure, to estimate dense layer of asymmetric membrane and to understand effect of operating temperature. Furthermore, the testing of

mixtures to check molecular separation and to reach optimum for structure of asymmetric membrane with flux and selectivity.

– **Chapter (5) Nanofiltration (NF) results and discussion**: This chapter presents information relevant to the characterization of asymmetric PEI membranes by nanofiltration. On one hand, characteristic flow rates of NF set-up system because it is a new experimental set-up of NF water system. On the other hand, PEI membranes sheets which have been prepared by wet phase inversion are applied to pure water as a feed at different operating pressures to evaluate their performances and flexibility of operation. Finally, rejection characteristics of aqueous solutions (organic and inorganic compounds) by asymmetric PEI membrane sheets are determined.

This thesis finishes with conclusions and recommendations in which further comments on the previous chapters will be given. Ways of continuation of the work described in this thesis will be discussed. A methodology for development of NF processes is presented, which allows the determination of the optimal process conditions, results in a more founded selection of membranes and a better understanding of the process. An outlook to future developments and needs is presented also.

References

1. H. Ozaki, H Li, Rejection of organic compounds by ultra-low pressure reverse osmosis membrane, Water Res. 36 (2002) 123-130.
2. I. Sibille, L. Mathieu, J. Paquin, D. Gatel, J. Block, Microbial characteristics of a distribution system fed with nanofiltered drinking water, Water Res. 31 (1997) 2318–2326.
3. K. Agbekodo, B. Legube, P. Cote, Organic in NF permeate, Am. Water Works Assoc. 88 (1996) 67–74.
4. S. Stern, R. Vaidyanathan, J. Pratt, Structure/permeability relationships of silicon-containing polyimides, J. Membr. Sci. 49 (1990) 1-14.
5. R. Baker, W. Koros, Polymeric gas separation membranes: London, CRC Press, 1994.
6. X. Shude, Y Robert, F. Xianshe, Synthetic 6FDA-ODA copolyimide membranes for gas separation and pervaporation: Functional groups and separation properties, Polymer 48(2007) 5355-5368.

Chapter (1)

Bibiographic study

Table of contents chapter 1

Chapter 1 Bibiographic study 45

1.1 Introduction 45

1.2 Part 1: An outloook in membrane processes 46

1.2.1 Definition of membrane 46

1.2.2 Classification of membranes 47

1.2.3 The principal types of membranes based on morphology 50

1.2.4 Mixture types separated by membranes 52

1.2.5 Transfer parameters of membrane separation processes 52

1.2.6 The advantages and limitations of membrane separation processes 52

1.3 Membrane separation processes 53

1.3.1 Pervaporation (PV) 54

1.3.2 Pressure- driven membranes process 64

1.3.3 Problem of the extraction of low molecular weight organic compounds from water by membranes 73

1.3.4 Interest of nanofiltration 74

1.3.5 Separation mechanism with NF membranes 75

1.3.6 Traditional methods to remove pollutants from water and wastewater 78

1.3.7 Rejection of organic compounds using nanofiltration (NF) membranes 79

1.3.8 Inorganic rejection using nanofiltration (NF) membranes 81

1.3.9 Rejection of aqueous organic/inorganic by asymmetric polyetherimide membranes 82

1.4 Part 2: Membrane preparations 84

1.4.1 Interest of polyimide membranes 84

1.4.2 Preparation of membranes 86

1.4.3 Symmetrical membrane 87

1.4.4 Preparation of porous membrane 88

1.4.5 Asymmetric membrane preparation and phase inversion process 89

1.4.6 Thermodynamic description of phase inversion 91

1.4.7 Mechanism of microporous formation by thermal gelation of a binary system 91

1.4.8 Phase inversion process and ternary phase diagram 93

1.4.9 Demixing types in a ternary system 96

1.4.10 Mechanism of formation skin toplayer and porous sublayer 97

1.4.11 Study of some parameters which have an influence on membrane morphology 99

1.4.12 Preparing new asymmetric block copolyimide membranes: Asymmetric polyetherimide (PEI) copolyimide membranes *102*

References Chapter 1 ..... *103*

Chapter (1) Bibliographic study

1.1 Introduction

This chapter is dedicated to a literature survey of separation of organics in water solution by membranes. Thus, an analysis study for practical and applied references connected with membrane technologies with background takes place. Also, the membrane background and the membrane materials are outlined.

Typically, several raw materials can be used for preparing membrane films which include either organic or inorganic materials such as polyimide, ceramic, natural or artificial polymers. Therefore, as a result of the variety of the raw materials which already exist in all the world, different membrane separation processes might be applied dependent on the nature of the membrane sheet and the requirements of treatment process. In addition, there are different engineering forms which have been established for membranes that include flat, tubular, spiral wound or hollow fiber [1,2]. Generally, the membrane preparation techniques are classified as a function of the raw materials used, the engineering forms and the characteristics of the required separation process. Over the past decades, the polymeric membranes have achieved commercial importance in a variety of separations applications in the chemical, food, pharmaceutical, and biotechnology industries. Today, the membrane industry is faced with the challenge of inventing new membrane materials.

In the field of the water treatment, reverse osmosis, nanofiltration, ultrafiltration and microfiltration membranes are increasingly used for a different applications in the field of waste water purfication. Sourirajan and Loeb [3] developed the early progress on the spiral wound cellulose acetate membrane and the invention of capillary technology, to the introduction of a low fouling composite (LFC) spiral RO membrane and the back washable capillary ultrafiltration membrane. Recently, the evolution of membrane development has improved performance to lower operating costs and membranes have become the preferred

This chapter contains two parts:

- Part 1: An outloook in membrane processes
- Part 2: Membrane preparation

1.2 Part 1: An outloook in membrane processes

In this section a general introduction on membrane science and technology is given. It begins with the definition of terms and provides a description of membranes structures and membrane separation process. The advantages as well as the limitations of membrane process are indicated. A short overview over the developments of membranes science and technology is given .

1.2.1 Definition of membrane

C. Mark [2] defined a membrane as follows: what is a membrane? possibly the broadest definition is: a region of discontinuity interposed between two phases. This statement implies that membranes can be gaseous, liquid, or solid, or combinations of these phases. The term "region" in the definition is used to eliminate ordinary interfaces. Thus, the interfaces of two immiscible liquids, of a gas and a liquid, or of a gas and a solid would not ordinarily be considered as membrane structures.

A. Zydney et al. [4**]** defined a (bio-) membrane as: a membrane is a flexible layer surrounding a cell, organelle (such as the nucleus), or other bodily structure. The movement of molecules across a membrane is strictly regulated in both directions. Therfore, a membrane is a layer of material which serves as a selective barrier between two phases and remains impermeable to specific particles, molecules, or substances when exposed to the action of a driving force. Some components are allowed to pass through the membrane into a permeate stream, whereas others are retained by it and accumulate in the retentate stream.

From Wikipedia [5**]:** membranes can be of various thicknesses, with homogeneous or heterogeneous structure. Membranes can also be classified according to their pore diameter (Fig.1.1). There are three different types of pore size classifications: microporous ($dp < 2nm$), mesoporous ($2nm < dp < 50nm$) and macroporous ($dp > 50nm$). Membranes can be neutral or charged, and particles transport can be active or passive. The latter can be facilitated by pressure, concentration, chemical or electrical gradients of the membrane process. Membranes can be generally classified into three groups: inorganic, polymeric or biological membranes. These three types of membranes differ significantly in their structure and functionality.

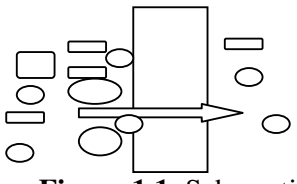

Figure 1.1: Schematic of size based membrane exclusion

1.2.2 Classification of membranes [1,2,6]

This part explores the various approaches to classifying membranes. Even a cursory examination of the variety of membranes that exist makes it evident that a single classification scheme is unlikely to permit a clear and concise presentation. However, a rather informative picture is obtained by using multiple schemes, which can readily be interrelated. Such arrangements are represented by the following:

A. Classification by nature of membrane.

B. Classification by structure of membrane.

C. Classification by application of membrane.

D. Classification by mechanism of membrane function.

A. Classification by nature of membrane

. *Natural membranes*

- Living membranes.
- Natural substances – modified or regenerated.

. *Synthetic membranes*

1. Inorganic : Metals, Ceramics and Glass.
2. Organic – Polymers: Films ,Tubing and Hollow fibers.

B. Classification by structure of membrane

b.1 Porous membranes

1. Microporous media.
   Compressed powders, Microporous glass (Corning), Microporous ceramics, Microporous silver membrane (Selas), Millipore filters, Porous polymer structures, Cellulose acetate and Nuclepore (General Electric).
2. Macropores: Filters for gases and liquids, some Millipore filters and Ultrafilters.

b.2 Nonporous membranes

1. Inorganic : Metal films and Glass.
2. Polymeric structures: Films,Tubes and Hollow fibers.

b.3 Morphological distinction

1. Crystalline: Inorganic (metals, ceramics) and organic.
2. Amorphous: Glass and polymers.

b.4 Liquid membranes

1. Monomolecular film: Fatty acid spreading on water.
2. Liquid drop surrounded by stable liquid film.

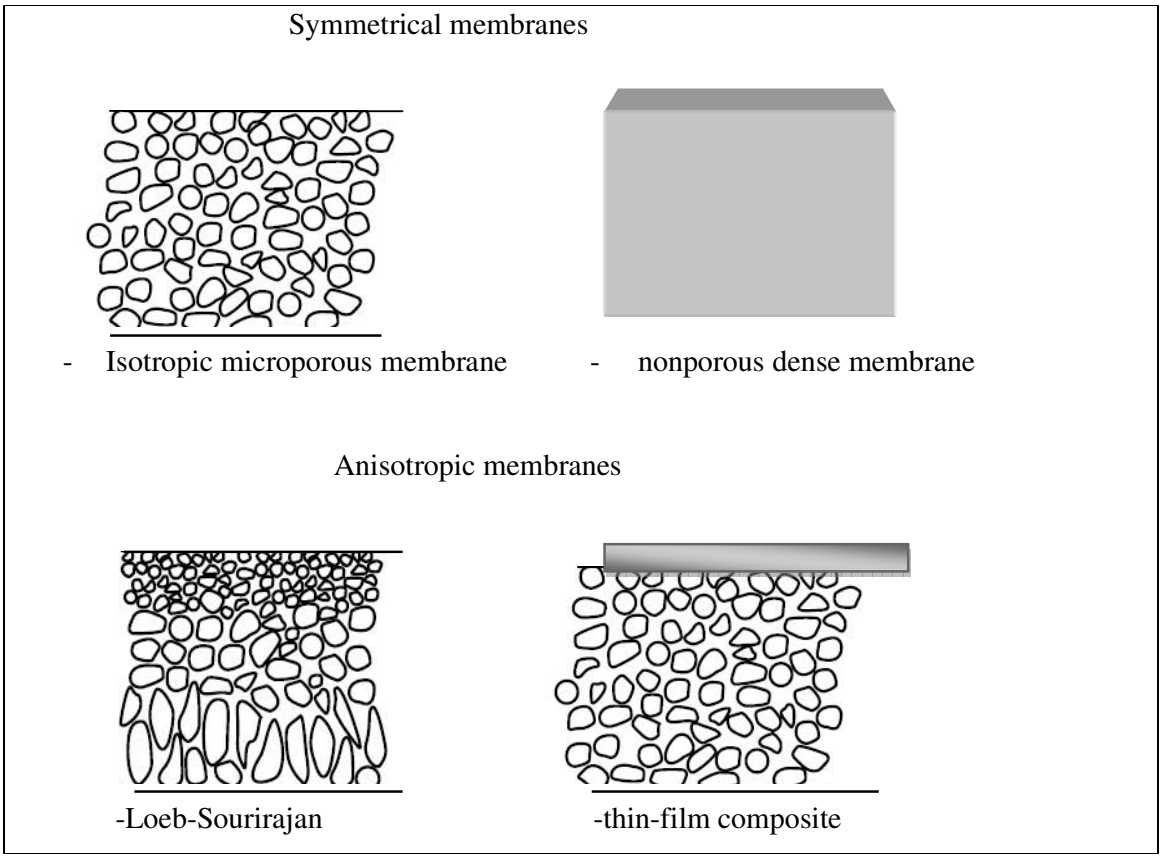

Figure 2.1: Schematic diagrams of the principal types of membranes based on structure [6**].**

C. Classification by application of membrane

Here, a membrane, gaseous, liquid, or solid, is interspersed between phases, as, for instance, gas-membrane-gas:

I. Gaseous-phase systems *:*

1. Molecular flow – size of pores and molecular velocity determine separation.
2. Molecular flow with surface flow (surface or diffusive flow results from adsorptive properties of microporous media).
3. Sweep gas diffusion – use of carrier gas.
4. Diffusive solubility flow of polymeric structures – solubility of diffusing gases or vapors is controlling parameter.
5. Diffusive flow in solvated polymers – occurs with liquids or vapors that swell or modify membrane properties.

II. Gas-liquid systems

1. Macropore structure :

   Removal of liquid entertainment in gas stream.

   Introduction of gas into liquid phase.
2. Microporous structure : Ultrafine filters.
3. Polymeric structures.

   Gas diffusion from or into liquid, that is, blood oxygenation (oxygenation and CO_2 removal).

III. Liquid-liquid systems

1. Gas transport from one phase to another liquid phase.

   Organ preservation devices, blood oxygenation.
2. Osmotic processes.

   Reverse osmosis and gel permeation.
3. Liquid membranes.

   Selective flow through liquid film.

D. Classification by mechanism of membrane action

I. Adsorptive membranes

1. Microporous membranes: Porous Vycor and Activated charcoal
2. Reactive membranes.

II. Diffusive membranes

1. Polymeric membranes: Diffusive solubility flow.
2. Metallic: Atomic-state diffusion.
3. Glass: Molecular state or affinity phenomena.

III. Ion-exchange membranes

1. Cation-exchange resins.
2. Anion-exchange resins.

IV. Osmotic membranes

1. Regular osmotic membranes.
2. Reverse osmotic membranes.
3. Electro-osmotic membranes.

V. Non selective membranes: case of fritted glass

1.2.3 The principal types of membranes based on morphology [1,2,6]

The principle types of membranes is divided in to three categories: Isotropic membranes, Anisotropic membranes (polymeric, ceramic, metal) and liquid membranes. These types will be outlined below.

1.2.3.1 Isotropic membranes

Isotropic membranes is divided in to three types: Microporous membranes, Nonporous and Electrically charged membranes.

1.2.3.1.1 Microporous membranes (ultrafiltration and microfiltration)

The microporous membrane filtration is similar to some extent to a traditional liquid filtration; but significant differences can arise with complexes molecules such as proteines. The membrane itself has a rigid, highly voided structure with unorganized distributed and interconnected pores. Moreover, these pores differ from those in a conventional filter by being smaller, on the order of 0.01 to 10 μm in diameter. Therefore, all particles larger than the largest pores will be completely rejected by the membrane. While, particles smaller than the largest pores, but larger than the smallest pores could be partially rejected, according to the pore size distribution of the membrane. However, particles much smaller than the smallest pores could pass through the membrane. Thus, separation of solutes by microporous membranes is mainly dependent on the molecular size and pore size distribution. In general, only molecules that differ considerably in size could be rejected effectively by microporous membranes, for example, in ultrafiltration and microfiltration.

1.2.3.1.2 Nonporous, dense membranes

Nonporous, dense membranes composed of a dense film through which material can pass on by diffusion under the driving force of a pressure, concentration, or electrical potential gradient. However, the separation efficiency of various solutes of a mixture is dependent on their transport rate through the membrane, which is determined by their solubility and diffusivity in the membrane material. In addition, nonporous, dense membranes could reject charged or uncharged solutes of similar size if their concentration in the membrane material differs significantly. Typically, pervaporation, most gas separation, and reverse osmosis membranes use nonporous membranes to do the separation process.

1.2.3.1.3 Electrically charged membranes

Electrically charged membranes are dense or microporous. A membrane with fixed positively charged ions is called an anion-exchange membrane. Similarly, a membrane containing fixed negatively charged ions is referred to as a cation-exchange membrane. Separation with charged membranes is achieved mainly by exclusion of ions of the same charge as the fixed ions of the membrane structure. The separation is affected by the charge and concentration of the ions in solution. For example, monovalent ions are excluded less effectively than divalent ions and, in solutions of high ionic strength, selectivity decreases. Electrically charged membranes are used for processing electrolyte solutions in electrodialysis.

1.2.3.2 Anisotropic membranes (asymmetric membrane)

The permeate flux through a membrane is inversely proportional to the membrane thickness. Really, high permeabilities are desirable in membrane separation processes for economic reasons; therefore, the membrane thickness should be as thin as possible. Conventional film fabrication technology limits manufacture of mechanically strong, defect-free films to about 20 μm thickness. Moreover, the development of a new membrane fabrication technique to produce asymmetric membrane was one of the major breakthroughs of membrane fabrication technology during the last years. Asymmetric membranes consist of an extremely thin surface layer supported on a much thicker surface layer, porous substructure. The surface layer and its substructure may be formed in a single operation or separately. In composite membranes, the layers are usually made from different polymers. The rejection properties and flow rates of the membrane are determined exclusively by the surface layer; the substructure functions as a mechanical support. The advantages of the higher fluxes provided by anisotropic membranes are so great that almost all commercial processes use such membranes.

1.2.3.3 Ceramic, metal and liquid membranes

Ceramic membranes are special class of microporous membranes, are being used in ultrafiltration and microfiltration applications for which solvent resistance and thermal stability are required.

*NB: The case of nanofitration membranes is not treated here but in the close section **1.3.4***

1.2.4 Mixture types separated by membranes

The mixtures which can be separated by membranes are:

- homogeneous type, mono-phasic (miscible liquid or gas- gas)
- bi phasic, heterogeneous (immiscible liquids, liquid-solid,liquid-gas).

Depending on their size, the separate components can be classified into:

- particles, micro-particles, molecules and macromolecules [7].

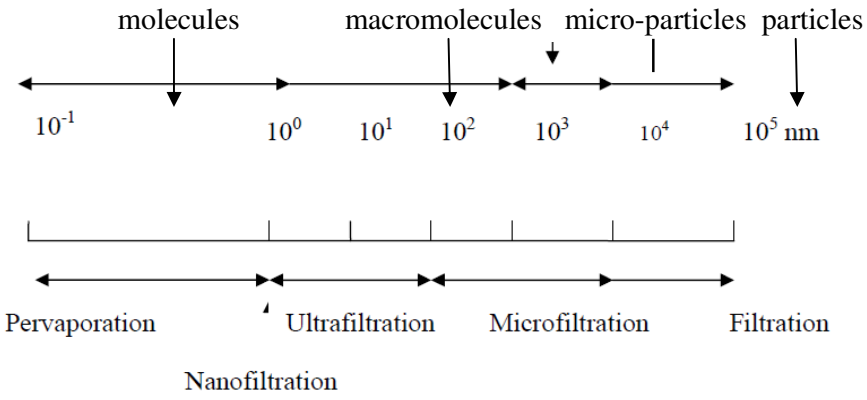

Figure 3.1: Classification of membrane separation methods by size according to separated compounds [8].

1.2.5 Transfer parameters of membrane separation processes

The transfer in membrane takes place under the effect of different driving forces:

- Pressure: microfiltration (MF), ultrafiltration (UF), nanofiltration (NF), reverse osmosis (RO).
- Gravity: particle filter (PF).
- Temperature: membrane distillation (MD), thermal osmosis (TO), thermodialysis (TD).
- Chemical potential (concentration gradient) [9]: dialysis (D), hemodialysis (HD),osmosis (O), pervaporation (PV), perstraction (PS), vapor permeation, gas permeation (GP) .
- Electric potential :electromembrane techniques: membrane electrolysis (EM), Electroosmosis (EO), conventional electrodialysis (ED), electrodialysis bipolar membrane (EDMB), electro-ultrafiltration (EUF) .

1.2.6 The advantages and limitations of membrane separation processes [1,2,10,11]

The membrane separation processes have in common, several advantages and some limitations compared to other separation processes (energy limited environmental, ...) that are outlined below.

1.2.6.1 The advantages

The membrane separation methods can work in favorable conditions following:

1. Clean process method, great respect for the environment and low discharge of pollutant(no addition of chemicals).

2. An energy requirement essentially limited to energy transport of the permeat

3- A moderate temperature favors the separation of temperature sensitive compounds, avoiding any change or degradation of products.

4- A high selectivity, can split azeotropes.

5 - A moderate operating costs: electricity as running, no consumable products.

6- Possibility of designing hybrid processes, combined with other methods separation (distillation, gas scrubbing, decantation).

7 - A compact and modular nature of plants and maintenance flexibility.

9- Separation is easier to automate.

10- More simple to operate, easy up and down scaling

11- reduced number of unit operations, recycle process water, and recover valuable products for other applications

12- Additional inherent advantages, such as selective separation, continuous and automatic operation

13- Easy scale-up and low space requirement.

1.2.6.2 Limitations

Besides the many advantages cited, the methods suffer from certain membrane limitations:

- The life of membranes can be limited to a few years (4 -10 years depending on the processes) and the membrane long-term reliability is not always proven.
- A cost of relatively high investment.
- Chemical resistance and thermal constraints of membranes, especially the polymeric membranes, the phenomenon of clogging pores (MF, UF, NF).
-Excessive pretreatment can be required to limit fouling

1.3 Membrane separation processes [12]

The membrane separation techniques have been used in several applications as biological, industrial, drinking water and wastewater treatment purposes. Moreover, The advantages of this separation system are their powerful separation capacity of small and large

molecules and compounds from mixtures, organic and inorganic solutions. In addition, they are characterized by their low power consumption and area required comparing to other separation techniques. Furthermore, membrane separation technologies have some advantages over other mass transfer processes, including high rejection, low energy consumption, low cost to performance ratio, and compact and modular designs. Thus, they are generally considered to be “clean technologies˝.

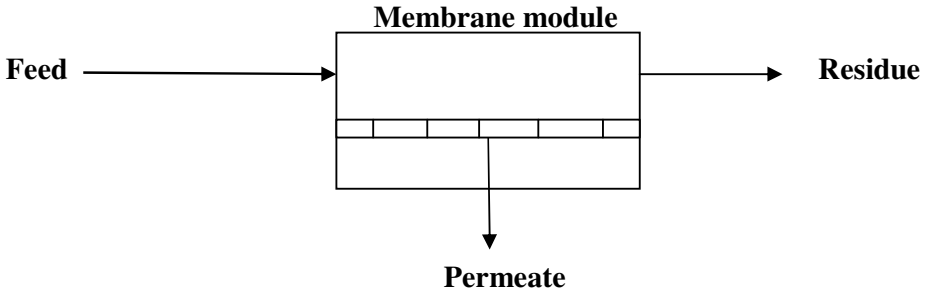

Figure 4.1: Schematic diagram of the basic membrane separation process.

Membrane separation processes are often used since these applications realize high removals of constituents such as charged solutes, uncharged solutes, and organic molecules. In the recent years, membrane separation techniques have grown from a simple laboratory tool to an industrial process with considerable technical and commercial impact. Really, membrane separation processes are more easier, more efficient and more economical than conventional separation techniques. The separation is usually performed at ambient temperature by using membrane process, this is allowing temperature-sensitive solutions to be produced without the constituents being damaged [2]. In fact, this is very important where temperature-sensitive products have to be processed (i.e: food like milk at 50°C, drug industry, biotechnology, lactoserum at 15°C). The main membrane separation processes are pervaporation and pressure driven membrane processes, as outlined below in detail.

1.3.1 Pervaporation (PV)

Pervaporation process is recognized to be an alternative technology for liquid separations when more classical technologies are either not efficient (too close boiling points, thermal sensitive compounds) or too expensive; for instance, breaking azeotropes can be an easy task by pervaporation [13] and also an energy-saving process [14]. Pervaporation can be used either for organic liquid separations [15,16,17,18] or for dehydration of organic liquids [19]. According to the separation type, the permeate or the retentate can be valorised; in

addition, an interesting feature of pervaporation is that it is a clean technology which does not emit pollutant [20].

Pervaporation is a liquid mixture separation process in which mixture or solvent contacts with the membrane at the feed side while the permeate side is kept dry, most of the time with low pressure [14,15]. The attraction of pervaporation is that the separation obtained is proportional to the rate of permeation of the components of the liquid mixture through the selective membrane. The separation process is carried out by solubility difference to the membrane and diffusivity difference of permeants in the membrane of pervaporation [21]. On the other hand, swelling of one component of the permeant to the membrane is a necessary factor to realize the separation performance, but enhancement of solubility causes membrane swelling [14,15]. Accordingly, suppressing swelling is important to prepare the membrane with high separation performance. Discriminating affinity existing between the feed mixture and the membrane results in the partition of mixtures components and separation achieves.

I. Process overview [6]

A typical pervaporation process is shown schematically in figure 5.1. A liquid mixture contacts one side of a membrane at the feed side while the permeate is removed as a vapor from the other side at low pressure. Therefore, transport through the membrane film is done by the difference in partial pressure between the feed solution and the permeate vapor. This partial-pressure difference can be obtained by several ways. On one hand, in the laboratory a vacuum pump is usually used to get a vacuum on the permeate side for the system. On the other hand, industrially, the permeate vacuum is most economically generated by cooling the permeate vapor, causing it to condensate. Moreover, the components of the feed solution permeate the membrane at rates determined by their feed solution vapor pressures, that is, their relative volatilities and their intrinsic permeabilities through the membrane. However, pervaporation is a rate-controlled process, and the permeation flux through a membrane is generally low. Therefore, pervaporation becomes economically more attractive when the preferentially permeable component is present in the feed at low concentrations.

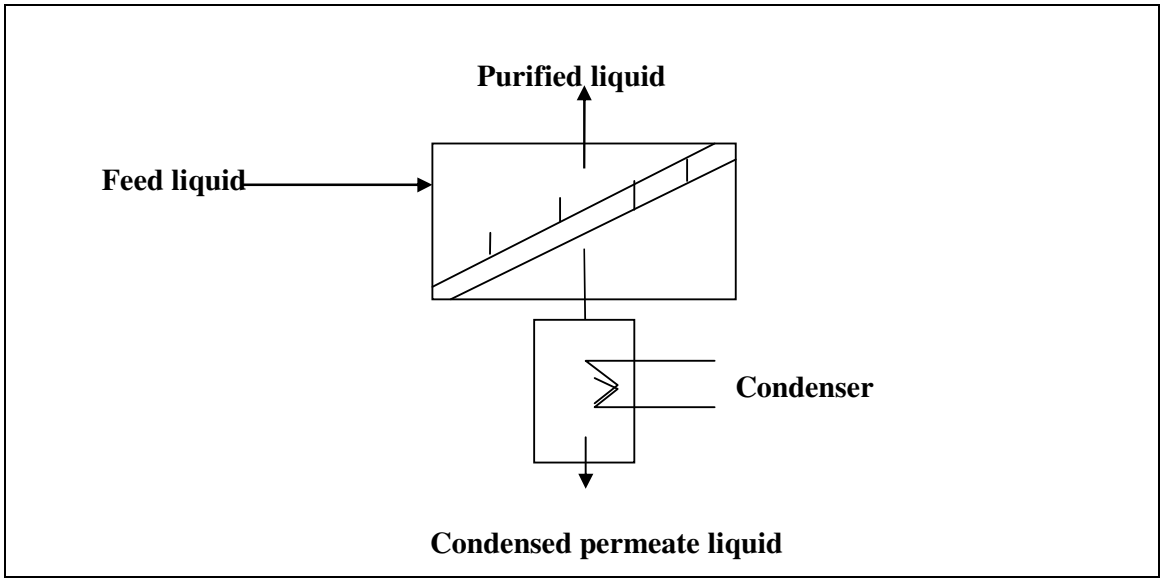

Figure 5.1: Schematic diagram of the basic pervaporation process [22]

II. Historical trends [6]

The pervaporation process essential dates back to the 19th century. Kober [23] was the first researcher who described the PV technique in 1917 when he was dialyzing and noticed liquid evaporated through a tightly closed collodion bag suspended in air. But the pervaporation process was first studied in a systematic fashion at the laboratory level by Binning, Lee and co-workers at American Oil in the early 1950s [24]. Because of the limitations of membrane preparation at that time, the pervaporation process was not commercialized in the laboratory or industrial until 1980s. However, advancements in membrane technology made it possible to prepare economically viable pervaporation systems. The interest in the process started in 1976. Jonquières et al. [25] provide a detailed list of patents represented in table 1.1. The number of registered European and USA/Canadian PV related patents peaked in the early 1990s, illustrated in Fig. 6.1 which tabulates the increase in the quantity of pervaporation literature over the last 40 years.

Table 1.1: Manufacturers having obtained the grant of European patents by the European Patent Office between 1980 and 1999 for the areas of pervaporation field.

Industrial Company	Number of European patents
GFT and associates (Germany)	13
GKSS (Germany)	10
Ube industries(Japan)	2
Akzo GmbH(Germany)	1
Atenburger Electronic GmbH(Germany)	1
Bend Research Inc. (USA)	1
Hoechst Celanese Corporation(Germany)	1
Krebs (Suisse)	1
Metallgesellschaft (Germany)	1
Naturin GmbH(Germany)	1
Novamont (Italy)	1
Starcosa GmbH(Germany)	1
Tenneco Canada Inc. (Canada)	1
TNO (The Netherlands)	1
X Flow(The Netherlands)	1
Total	37

Generally, pervaporation process has been commercialized for two applications. The most important is the separation of water from alcohol mixture solutions. GFT in Germany is the leader in this field at that time and they installed their first major plant in 1982 [26]. Currently, more than 100 plants have been installed by GFT for this application [27]. The other application in pervaporation is the separation of small amounts of organic solvents from contaminated waters, for which the technology has been developed by MTR in USA [28]. Both of the current commercial processes concentrate on the separation of organics from water. This separation is relatively easy, because organic solvents and water, due to their difference in polarity, exhibit distinct membrane permeation properties. The separation is also amenable to membrane pervaporation because the feed solutions are relatively non-aggressive and do not chemically degrade the membrane.

Table 2.1: Patents deposited at the European and USA Patent Office between 1976 and 1999 for the areas of pervaporation field [25,31].

Year	Number of patents in European and USA	Number of European patents	Number of USA patents
1976	2		2
1977	1		1
1984	1		1
1985	1		1
1986	3	1	2
1987	6	2	4
1988	16	2	14
1989	22	2	20
1990	49	3	46
1991	43	1	42
1992	38		38
1993	26	4	22
1994	19	5	14
1995	24	6	18
1996	20	4	16
1997	20	4	16
1998	12	2	10
1999	19	1	18

The first pilot-plant for an organic-organic application, the separation of methanol from methyltertiobutyl ether/isobutene mixtures, was reported by Air Products in 1989 [29]. Until now no commercial systems have yet been used for the separation of the industrially organic/organic mixtures. However, current technology now makes development of pervaporation for these applications to possibly take place and the process is being actively researched in a number of laboratories.

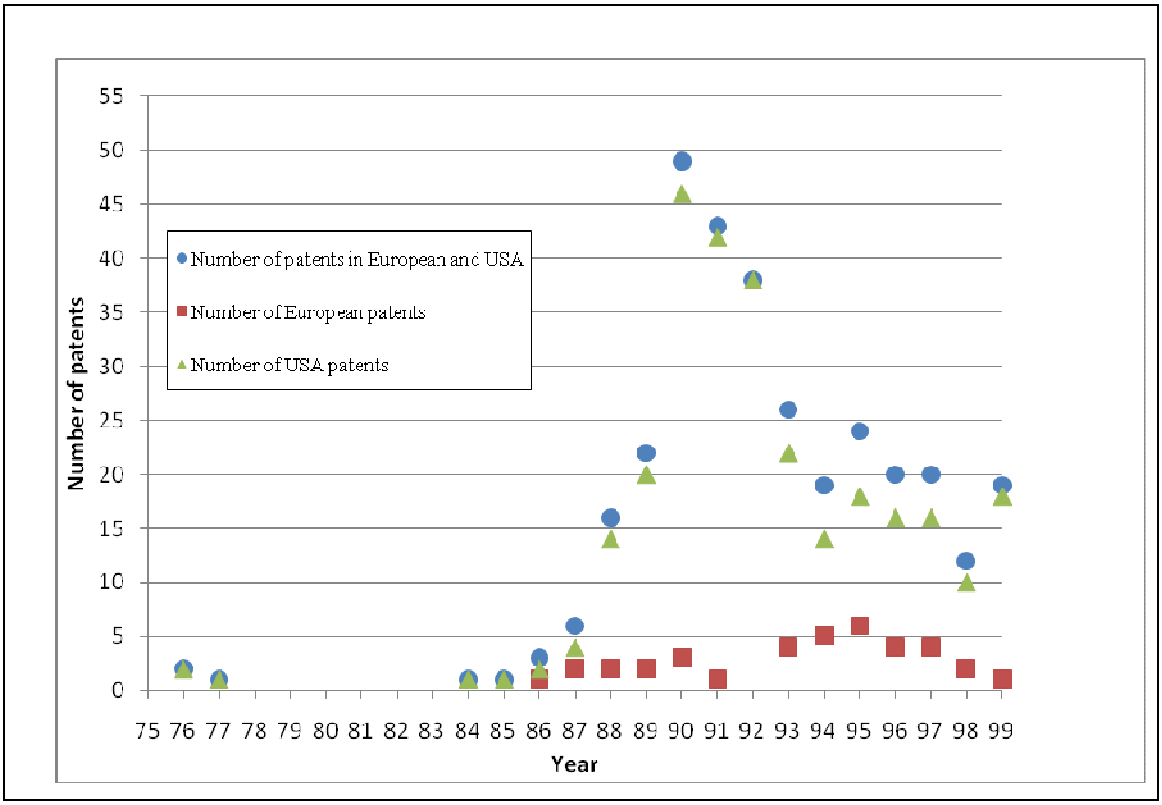

Figure 6.1: Pervaporation patents by the European and USA Patent Office between 1976 and 1999.

III. Advantages of pervaporation

The separation processes by PV have in common several advantages :

- Simpler processing
- One step separation
- Energy saving
- Cleaner end products
- Either stand alone or easy add on with

e.g. distillation in separation of azeotropic top product

- Less down-stream processing
- multi-purpose unit operation
- Enables new chemical reaction routes in esterifications

IV. Mechanism of separation with dense film in PV

The separation of the mixtures using PV can be divided into three fields [22,1]:

• Dehydration of aqueous–organic mixtures;

• Removal of trace volatile organic compounds (VOC) from aqueous solution;

• Separation of organic–organic solvent mixtures.

Separation mechanism with PV is carried out by permeation through non-porous (dense) polymeric films which is usually described by the solution diffusion model [22,30] that considers three successive steps for mass transfer (Fig. 7.1):

1- The dissolution (or sorption) of molecules at the membrane upstream side in contact with the vapor or liquid

2- The diffusion step driven by the chemical potential across the membrane

3- The desorption of the permeated species at the membrane downstream side, that is usually considered as a non-limiting step.

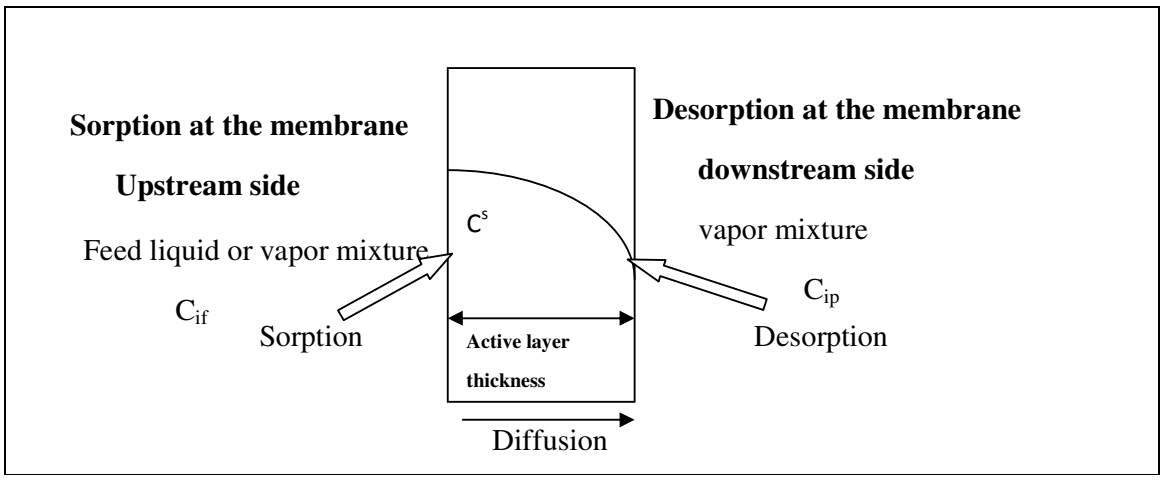

Figure 7.1: Schematic of solution-diffusion model through non-porous polymeric materials. C_i, C^S and C_{ip} are the compositions of the feed, sorbed and permeated mixture, respectively, conventionally expressed as the mass fractions of the preferentially permeated species [22].

Furthermore, the separation is based on the selective solution and diffusion, i.e., the physical–chemical interactions between the membrane material and the permeating molecules. Therefore, PV separation is usually governed by the chemical nature of the macromolecules in the membrane, the physical structure of the membrane, the physicochemical properties of the mixtures to be separated, and the permeant–permeant and permeant–membrane interactions [31].

V. Selection of the polymer materials for development of membranes in PV process

As the other membrane separation techniques, the suitable membrane polymer material and its membrane-forming technique should be firstly found out to study separation of organics mixtures systems with PV process [15].

Really, selection of the polymer membrane materials for separation with PV process is based mainly on three important features: good chemical resistance, sorption capacity and high mechanical strength of the polymer film in the mixture solution. Therefore, it should have good interaction preferably with one of the components of the mixture for separation.

Hence, the solubility parameter and membrane polarity [32,33] are the indices of interest in the development of new polymer membrane materials. In the sorption experiment, more component A (as toluene, water) was sorbed into the membrane than component B (heptane, ethanol) and as expected, exceptionally high selectivity was obtained with this membrane to separate component A from its mixture with component B. Thus, the solubility parameter may be used as a guide for the selection of the PV polymer membrane materials being suitable for separating organic mixtures [34].

Separation performances of membrane is also dependent on the membrane polarity. Hence, in separation of a particular molecule in feed mixture, the polarity of one of the molecules must be close to the polarity of the membrane. For example, Shimidzu and Yoshikawa [35] reported the separation of water–ethanol mixture using polystyrene membrane, the membrane polarity (31.7 kcal /mol) was close to the polarity of ethanol (30 kcal /mol) and as expected the membrane preferably permeated ethanol compared to water (63.1 kcal/ mol) because of the increasing distance between the membrane polarity and water polarity.

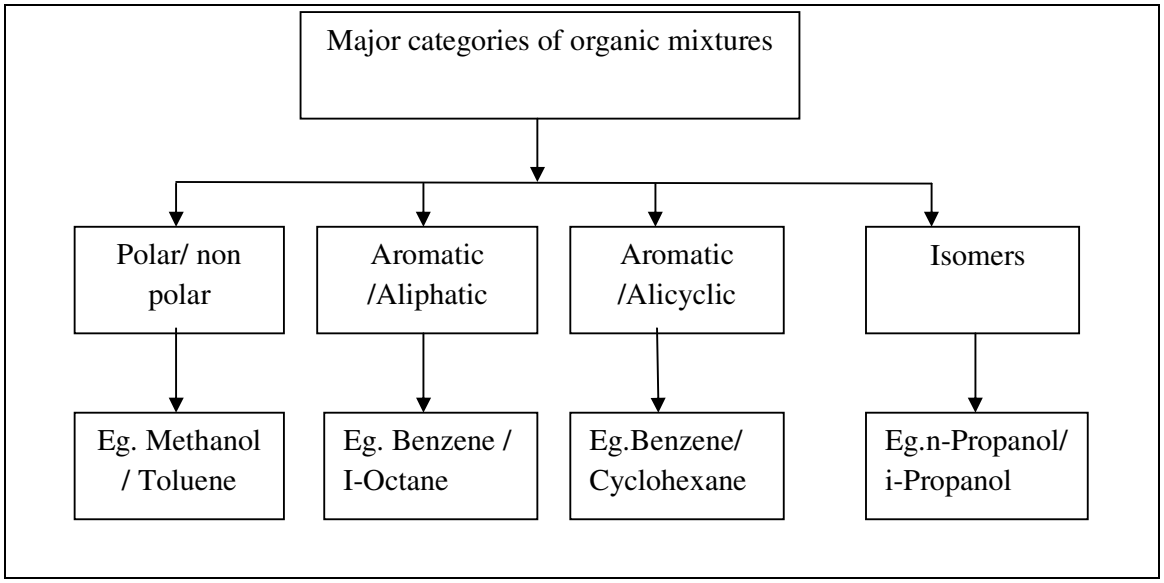

Figure 8.1: Classification of organic–organic pervaporation separation [15].

VI. The major parameters affecting membrane performance with PV

An example of a basic laboratory PV experimental set-up is shown in Fig (5.1). Therefore, there are several factors affecting the membrane performance, which have to be kept in mind by any investigator before attempting to work on pervaporation they are:

(i) **Membrane thickness** [36]

Generally, thin membranes are used in order to obtain a high permeation rate. It is usually perceived that in an ideal case where the membrane is homogeneous and free of defects, the permeation rate is inversely proportional to the membrane thickness while the membrane thickness has no impact on the membrane selectivity. This is why in [15,37**,**38] the reported permeation fluxes were normalized to a given membrane thickness by assuming a reciprocal relationship between permeation flux and the membrane.

(ii) **Feed composition and concentration** [39]

The membrane selectivity for pervaporation depends mainly on the equilibrium swelling which stands at the upstream face. Furthermore, the swelling depends on the composition of the mixture studied. A change in the feed mixture composition directly has influence on the sorption phenomena (swelling) at the liquid membrane interface, as proved by the solution-diffusion principle, and as the diffusion of the molecules in the membrane is dependent on the concentration of the components. Hence, the permeation characteristics is dependent on the concentration of feed as well.

(iii) **Feed and permeate pressure**

The downstream pressure has a great influence on the efficiency of pervaporation. It must be kept below the saturation vapor pressure of the permeate. In all cases, an increase in downstream pressure causes a reduction of permeation flux. the activity gradient of the components in the membrane is the main driving force in pervaporation. The permeate pressure is dependent on the activity of the components at the downstream side of the membrane and hence affects the pervaporation properties [40]**.**

(iv) **Temperature[41]:**

The influence of temperature occurs at the level of the sorption and diffusion. The permeate flux generally increases as the operating temperature of the feed increases and follows an Arrhenius-type law [42**,**43] ($J = J_0 \exp(-Ep/RT)$. The selectivity is always dependent on operating temperature; in most cases a small decrease in membrane selectivity is done with increasing operating temperature [44]**.** If the activation energies for the two components are equivalent, the selectivity is independent of operating temperature, but if the temperature has an influence on swelling, thus the selectivity will change. Otherwise, an increase in operating temperature causes an increase in the flux.

(v) **Concentration polarization (CP)**

The more concentrated boundary solution and the less concentrated bulk is termed as concentration polarization; this concentration gradient takes place when a binary liquid

mixture is permeating through a semi-permeable membrane, with different individual component permeation rates, an increase of the less permeable component in the boundary layer near the membrane surface occurs. Researchers [45,46] have dealt with problems related to concentration polarization in pervaporation of organic–water mixtures and have generally reported that CP gives order of magnitude, a very significant role.

VII. Characteristic equations of pervaporation [22,47,48]

The membrane permeation total flux has been investigated according to the following equation:-

$J=Q/A*T$ [1.2]

Where:

J: the total flux ($kg / m^2 h$)

Q: the total mass of permeate collected kg

A: effective area of membrane film m^2

T: time of permeate sample h

The total flux is most usually inversely proportional to the thickness of the dense permeable film [49]. Thus, to allow a comparison of the properties of films with close but not constant thicknesses, a normalized flux can be calculated for a reference thickness of the dense film (e.g: 10 μm). The normalized flux is calculated from the following equation:

J_n= (total membrane thickness*J)/10 [2.1]

Where;

J_n: the normal flux ($kg / m^2 h$)

• Another very common definition of selectivity permeation is given by the selectivity parameter (also known as the separation factor) α, which was initially defined by analogy with the relative volatility used in distillation. The separation factor (α) is defined by

$$\alpha= (Y_i*X_j)/(X_i*Y_j) \quad [3.1]$$

Where

Y_i: represent the weight fractions of the fastest compound in the permeate

Y_j : represent the weight fractions of the slowest compound in the permeate

and X_i , X_j represent the weight fractions of the component in the feed.

• Another feature of the selectivity, the enrichment factor β, is defined:

$$\beta = C_P/C_F = Y_i/X_i \quad [4.1]$$

where C_P (permeate enrichment, downstream mass) and C_F (feed concentration, upstream in weight) are the weight fractions of target compound in the permeate and in the feed, respectively.

1.3.2 Pressure- driven membranes process

Pressure-driven membrane process techniques have become an alternative to conventional water treatment methods, as well as in the treatment and concentration of waste water of both industrial and municipal origin [50]. The occurrence and prevalence of organic micropollutants such as pesticides, and other organic micropollutants are becoming a concern in drinking water, wastewater, and water reuse applications due to potential adverse health effects associated with these compounds. Thus, membrane processes are becoming increasingly widespread in water treatment and wastewater reclamation/reuse applications where a high product quality is desired [51,52,53].

1.3.2.1 Main types of pressure driven membrane separation processes [1,2,54]

There are four main types of pressure driven membrane separation processes, namely:-

- Microfiltration (MF)
- Ultrafiltration (UF)
- Nanofiltration (NF)
- Reverse osmosis (RO)

Literally all RO, NF and UF membranes are asymmetric. This differentiates easily most membranes from traditional filters, which are symmetric or, in other words, are identical on the both sides of the common filter. In addition, membrane has a tight top layer facing the pollutant solution to be treated. This layer, also called the skin layer, is thin typically <<0.1 micron. The membrane thickness is about 150 - 250 micron, the bulk of the membrane simply providing structural support for the skin layer. The asymmetric structure means that the pores are wider, which prevents the pores from being plugged. This provides good fouling resistance, since foulants have a tendency to either be totally rejected or to pass all the way through a membrane.

Pressure-driven membrane filtrations processes are classified by pressure into two categories:

- High-pressure membrane processes, such as reverse osmosis (RO) and nanofiltration (NF),

RO needing dense membranes (no detectable pore below the nanoscale range), NF membranes having a relatively small pore size compared to low-pressure membranes since small pore size membranes require higher driven force to drive fluid through the membrane compared to big pore size membranes. Further, these types of membranes normally require a relatively high pressure from 4 bar to 70 bar. In addition, these high-pressure processes primarily remove contaminants through chemical diffusion.

- And low-driven pressure membrane, such as microfiltration (MF) and ultrationfiltration (UF), normally require a low pressure from 0.4 to 7 bar. These membranes primarily remove contaminants through physical sieving. More details about these types are outlined below.

- **Microfiltration (MF)**

Microfiltration is characterized by a membrane pore size between 0.05 and 10 μm and operating pressures below 1 bar. MF is primarily used to separate particles and bacteria from other smaller solutes. Further, MF is a low-pressure technique that removes particles with a molecular weight above 50,000 or a particle size over 0.05 μm**.** In addition, MF is a process where ideally only suspended solids are rejected; in fact agglomeration of proteins (like in micelles), or caseine are also retained whereas seric proteins freely pass through .

- **Ultrafiltration (UF)**

Ultrafiltration refers to membranes having smaller pore size compared to microfiltration membranes. Ultrafiltration (UF) is characterized by a membrane pore size between 2 nm and 0.05 μm and operating pressures between 1 and 5 bar. UF is a low-pressure technique also where single proteins and suspended solids are rejected freely. Neutral organic species (sugars, peptides) and neutral salts usually show no rejection.

- **Nanofiltration (NF)**

Nanofiltration (NF) is characterized by a membrane pore size between 0.5 and 2 nm and operating pressures between 5 and 40 bar. NF is used to achieve a separation between sugars, other organic molecules and multivalent salts on one hand and monovalent salts and water on the other. True NF rejects only ions with more than one negative charge, such as sulfate or phosphate, while passing single charged ions. Non charged NF membrane also rejects uncharged and dissolved materials according to the size and shape of the molecule in

question; for positively charges ions, the rejection may vary with charge beard by the membrane and according to the membrane fouling.

Although Nanofiltration (NF) membrane appeared at the end of the 1970s under various names, it was only really recognized as a useful separation process in the 1980s, mainly aiming at combined softening and organics removal [55]. NF membranes have been on the market at 1984s, but have gained in popularity at 1990s . Since then, the application ranges of nanofiltration membranes have extended tremendously. Large plants were constructed, the best documented example being the Mery-sur-Oise plant in France (140,00 m3/day of permeate), which was started in the second half of the 1990s [56].

Today most membrane manufacturers also produce NF membranes. The membranes are made of many different materials, mostly from polymers such as aromatic polyamides, polyethersulfones, poly(acrylonitrile) and poly(phenylene oxide) as well as from different modifications of them. The better the flux, the more open and less retentive is the membrane.

Nanofiltration membranes consist of an active skin layer, determining the separation properties, and a support porous structure, giving mechanical strength. The skin layer may be integrally connected to the support structure, such as membranes prepared via phase inversion (immersion precipitation) process [57]. This type of membrane has distinct pores in the nanometer range at the active layer. The skin layer can also be an extra coating layer on a tailor-made support structure. A dense skin layer was assumed by the Torell–Meyer–Sievers Model (TMC) and the Hybrid Model. On the other hand, the Space-Charge Model and the Donnan–Steric Pore Model (DSPM) described a porous skin layer [58]. These models have been applied in the prediction of electrolyte rejection by NF membranes in aqueous solutions.

Recently, Bowen et al. [58] reported the observation of distinctive pores by atomic force microscopy (AFM) in the surface of commercial membranes prepared by phase inversion process. The research supported the hypothesis that a dense coating layer swells at working conditions, resulting in water passages and NF properties.

Nanofiltration (NF) process is widely applied in many industries for the separation and purification of drinking and waste water. The energy consumption of NF can be reduced by choosing the process operating conditions (temperature, pressure,….) carefully. Some of researchers [59-60] study how operating temperature influences on the transport of water and neutral solutes across Nanofiltration membranes and the mass transfer and pressure drop

directly and indirectly and thus the energy consumption. Employing Nanofiltration (NF) process directly on warm process streams ($T > 50$ °C) may be beneficial comparison to Nanofiltration at normal temperatures (T 25 °C). A high process temperature changes the separation performance due to temperature-dependent changes in the active layer of the membrane, as well as temperature effects that may be directly or indirectly related to the decrease in viscosity, such as reduced pressure drop, increased water flux and increased external mass transfer (lower concentration polarization).

M. Nilsson et al. [60] evaluated the influence of temperature on cost and energy consumption during Nanofiltration, and reported that the concentration polarization was found to be less at the higher operating temperature. However, this effect was small in comparison to the effect of temperature on fouling and the membrane performance. The influence of cleaning procedure on flux and retention was very dependent on the processing temperature due to time and temperature dependent changes in the membrane performance. Nanofiltration at 55 °C was found to be slightly better than Nanofiltration at 25 °C. The energy required for pumping was lower at 55 °C. However, the energy required for heating is high and processing at 55 °C is only advantageous if the feed is already warm, if there is excess heat in the factory, or if the heat can be recycled.

Pressure driven membrane processes are characterized by their low specific energy consumption. NF membranes are characterized by lower retention than RO membranes, but they operate at lower pressures and correspondingly lower energy requirements. Table 1 [61] compares the differences in operating pressure, power consumption, and effluent quality that can be obtained with the Dow Filmtec NF90-4040 membranes and with the low pressure RO Dow Filmtec BW30-4040 membranes.Table 2 shows that given identical feed water and plant design characteristics, RO membranes operate at a 45% higher pressure than NF membranes (9.04 bar vs. 5 bar). The difference in operating pressure translates into significantly lower specific energy costs for the NF membranes relative to the RO membranes

Membrane fouling is a major constraint on the implementation of membrane processes for use in water treatment, but for nanofiltration it might be even somewhat more complex because of the interactions leading to fouling take place at nanoscale, and are therefore difficult to understand [62]. Membrane fouling occurs through one or more of the following mechanisms: adsorption and accumulation of solute near the membrane surface (concentration polarization), gradual irreversible changes to the polarized layer and deposition

of particles on the membrane, so flux decline may be caused. Flux decline can be decomposed into a reversible and an irreversible component. The fraction of the initial water flux which cannot be recovered by a water washing is called irreversible fouling and is related to adsorption or precipitation and/or membrane pore clogging by organic and inorganic compounds [63]. Therefore, the identification of foulants and their fouling mechanisms is very important to reduce or avoid membrane fouling, to optimize pretreatment, and to decide upon optimal cleaning agents and cleaning procedures.

Table 3,a.1: Operating pressures, power consumption, and permeate quality with NF and RO membranes [61].

Membrane type	RO (Dow Filmtec BW30-4040)	NF(Dow Filmtec NF90-4040)
Operating pressure, bar	9.04	5
Power consumption on, kW	0.37	0.22
Specific energy costs, kWh m^{-3}	1.47	0.89
Permeate TDS, ppm	65	318

Foulants playing a role for nanofiltration membranes can be organic solutes, inorganic solutes, colloids, or biological solids [64]. Depending on the relative size of colloidal particles and membrane pores, colloidal fouling may occur either due to accumulation of particles on the membrane surface and build-up of a cake or by penetration within the membrane pores. The size, charge and concentration of the colloids also influence fouling in nanofiltration. An increase in colloid concentration leads to an increase in fouling. Inorganic fouling is related to scaling, i.e., precipitation of salts on the membrane surface. Nanofiltration membranes retain ions, causing an increase of the concentration at the membrane surface. Classical solutions to fouling are the optimization of pretreatment methods and cleaning of membranes.

Such studies [65] reported that hydrophilic surfaces are less foulant than hydrophobic surfaces. For example, based on free energy of adhesion calculations from contact angle measurements, cellulose acetate and polyacrylonitrile were found less foulant than polyethersulfone and poly vinylidenedifluoride when human serum albumin and polyethylene glycol were the fouling agents

The decrease of flux is due to an increase in the resistance of the membrane to permeation over time by the accumulation of materials (such as cake/gel formation,

concentration polarization, and adsorption on the membrane surface), pore blocking (66), and adsorption (67) to pore walls.

Negative consequences of membrane fouling are obvious and include the need for pretreatment, membrane cleaning, limited recoveries and feed water loss, and short lifetimes of membranes. In that sense, membrane fouling is closely related to other problems such as concentrate treatment and membrane stability and lifetime: a total control of fouling would reduce the need for cleaning and would enhance the permeate yield.

Pressure driven membrane process such as NF membrane can be prepared from a large number of different materials [1,2,3]. It can be fabricated from organic or inorganic materials (such as ceramic) and polymers. Inorganic membranes (such as ceramic membranes) are produced from inorganic materials such as aluminum oxides, silicon carbide, and zirconium oxide. Inorganic NF membranes are very resistant to the action of aggressive media (acids, strong solvents). They are very stable chemically, thermally and mechanically. Even though inorganic membranes have a high weight and substantial production costs, they are ecologically friendly and have long working life. The most of commercially membranes are utilized in separation process are made of polymeric. Organic (polymeric) membranes lead the membrane separation industry market because they are very competitive in performance and economics. Many polymers are available. It has to be compatible with chosen membrane fabrication technology. The polymer has to be obtainable and reasonably priced to comply with the low cost criteria of membrane separation process. The most common polymers in membrane synthesis are cellulose acetates, and esters, polysulfone (PS), polyamide, polyimide, polyethylene and polypropylene (PE and PP), polytetrafluoroethylene (PTFE), polyvinylidene fluoride (PVDF), polyvinylchloride (PVC)[1,2].

Escoda et al. [68] investigated influence of salts on the rejection of polyethyleneglycol by an NF organic membrane. Rejection rate measurements were carried out with a single polyethyleneglycol (PEG) solution and mixed PEG/inorganic salt solutions for a nanofiltration polyamide membrane. It was observed that PEG rejection is significantly lower in mixed-solute solutions. C.P. Athanasekou et al. [69] studied grafting of alginates on UF/NF ceramic membranes for wastewater treatment and reported that the grafting process led to the development of alginate layers with adequate stability under acidic regeneration conditions and metal retention enhancement of 25–180%, depending on the silane involved as grafting agent and the solvent of silanisation.

Tsuru et al. [70] prepared inorganic nanofiltration membranes from silica–zirconia composite colloidal sol (molar ratio Si/Zr=9/1) using a sol–gel process and reported that Silica–zirconia membranes were stable in aqueous solution for periods in excess of four months. Molecular weight cut-off (MWCO) was successfully controlled between 200 and 1000 g/mol by regulating the colloidal diameters of sol solutions in the final coating stage.

Membrane separations processes are useful techniques to purify or fractionate valuable biomolecules from wastes or byproducts. P. Jaouen et al. [71] and others reserchers reported recovery of proteins [72], aromas [73] or polysaccharides [74] from liquids effluents. The particular application of the ultrafiltration technique to the treatment of milk for making cheese was covered in a French patent in 1969. The Effluent biomolecules characteristics in the feed water play an important role in membrane fouling in wastewater applications. The composition of biomolecules is quite complex and heterogeneous. For example, it contains any organic molecule that is produced by a living organism, including large polymeric molecules such as polysaccharides, proteins, and nucleic acids as well as small molecules such as primary metabolites, secondary metabolites, and natural products [75]. The polysaccharides have the greatest fouling potential [75]. biomolecules cause fouling problems in NF and must be removed to improve membrane performance.

P. Bourseau et al. [76] reported the impact of a two-step UF/NF process producing four different fractions on two industrial fish protein hydrolysates (FPH) with different hydrolysis degrees. The NF fractionation produces a permeate enriched with respect to the FPH smaller than a molecular weight of about 600–750 g/mol, and a retentate enriched in large peptides (above the same MW). A similar behaviour is found for the UF fractionation. Comparing the impact of the UF fractionation on the two hydrolysates allows concluding that the membrane cut-off is well-suited when comprised between the MWs of the biggest and the most abundant peptides in the FPH.

Reverse Osmosis (RO)

Reverse Osmosis (RO) is the tightest possible liquid membrane separation process; it is generally considered that only water molecules can pass through the dense swollen membrane. The comparison between the four membrane processes is summarized in Fig.(9.1). Table 3.1 illustrates the characteristics of feed, permeate and concentrate for some

applications of RO, NF and UF. Total worldwide use of membranes, based on membrane surface area, is approximately presented in Fig.(10.1)

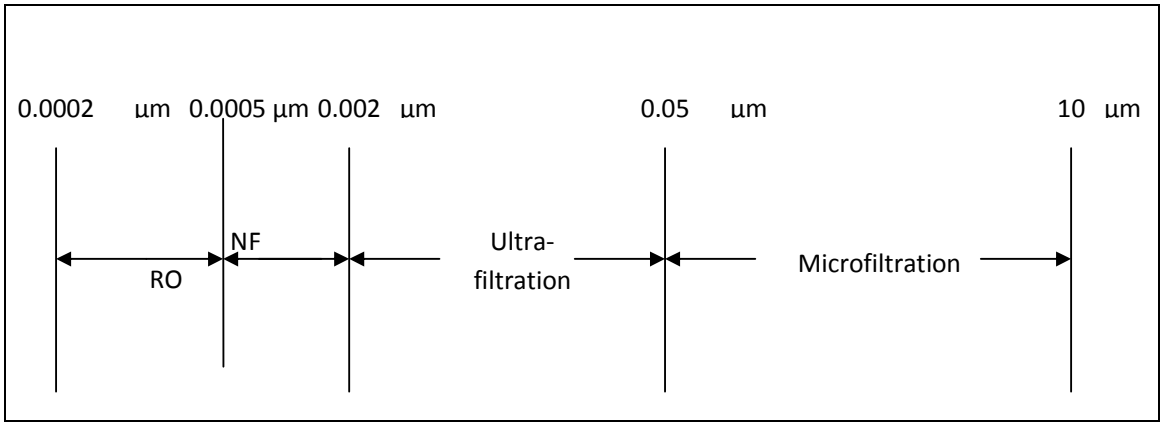

Figure 9.1: Definitions of pressure-driven membrane processes based on the smallest particle (molecule) retained.

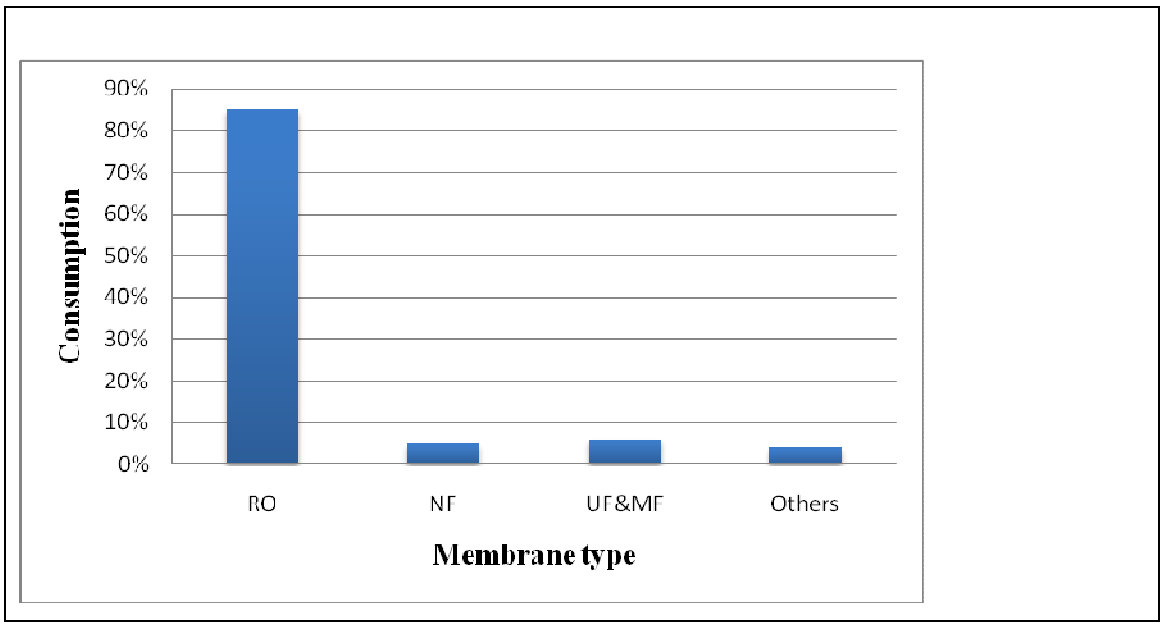

Figure 10.1: Classified use of membrane in the world based on surface-area [54].

Table 3,b .1: illustrates the characteristics of feed, permeate and concentrate for some applications of pressure-driven membrane system [54].

	Feed	**Permeate**	**Concentrate**
RO	Dyeing effluent	Clean water	BOD, salt , chemicals, waste products
	See water	Low salinity water	Salty water
	Whey	Low BOD permeate	Whey concentrate
NF	Antibiotics	Salty waste product	Desalted, concentrated antibiotics
	Dyeing effluent	Clean, salty water	BOD/COD, color
	Polluted water	Softened water	Waste product
	Whey	Salty waste water	Desalted whey concentrate
UF	Antibiotic	Clarified fermentation broth	Waste product
	Bio-gas waste	Clarified liquid for discharge	Microbes to be recycled
	Enzymes	Waste product	High value product
	Milk	Lactose solution	Protein concentrate for cheese production
	Oil emulsion	Oil free water (< 10ppm)	Highly concentrated oil emulsion
	Washing effluent	Clarified water	Dirty water (waste product)

Membrane retention [2]

In general, membranes exhibit retention for any molecules near their pore size. Ideally, the membrane should be capable of retaining completely all solutes or particles above some specified molecular weight or size and of passing completely all species below that size. Molecular weight is only an indirect, albeit convenient, parameter to estimate size. As a general rule, flexible molecules in solution (free-draining chains) tend to be retained to a lesser degree for a given molecular weight than do the more highly structured molecules such as branched polymers.

Molecular Weight Cut-Off *(*MWCO) and Pore Size [2]

What Researchers mean by the molecular weight cut-off (MWCO) of a "diffuse cut-off" membrane should be clearly defined. The convention states that the molecular weight cut-off of the membrane is equal to the molecular weight of molecules which are 90%

retained by the membrane. The molecular weight at which the rejection curve crosses retention of 90% is the "molecular weight cut-off" of the membrane. This means that larger molecules are rejected by the membrane and smaller molecules are succeed to pass.

The retention (R) may be defined as follows:

$$R\%=100(1-(c_p/c_f))$$

Where Cp = concentration of the solute in the permeate

Cf = concentration of the solute in feed

1.3.3 Problem of the extraction of low molecular weight organic compounds from water by membranes

Previous researchers have shown that nanofiltration (NF) membranes are effective technology to reject organic compounds when the solute sizes are larger than the membrane pore sizes or organic compounds have ionizable functional groups causing electrostatic repulsion. However, these previous studies have typically considered relatively large organic molecules (e.g., molecular weight (MW) > 150 g/mol) [77]. Only a few researchers have developed the retention of small uncharged organic compounds by RO and NF membranes. These previous studies have reported that the rejections for uncharged small compounds such as urea are quite low [78,79].

The investigation on the rejection of low molecular weight organic compounds by reverse osmosis (RO) membrane was studied by Ozaki et al. [80]. The results showed that the percentage removal of organic compounds increased linearly with the molecular weight as well as with the molecular width.

Some of the existing studies [81,82] reported that RO and NF succeeded in retention of the higher molecular weight molecules (e.g. humic acids) typically quantified as dissolved organic carbon and biodegradable dissolved organic carbon. However, the lower molecular weight molecules typically quantified as assimilable organic carbon (e.g. acetic acid and amino acids) were retented to varying degrees related to the membrane material and probably the solution environment.

Nevertheless the rejection is not purely a function of molecular weight. Some results of other studies suggested that the shape of the molecule (estimated via the solute radius) is a better parameter to predict the rejection of solutes than the molecular weight [83]. In addition the polarity of the solute can also have a significant effect on its rejection from water solutions.

1.3.4 Interest of nanofiltration

Nanofiltration (NF) technology, a high pressure driven process, has proved to be an alternative process for the drinking water treatment, due to its high water flux, its superior removal of disinfection by-product precursors, its minimal use of chemicals, and its ability to reduce sludge production [83,84]. NF is the most recent membrane separation process in the liquid phase. NF membranes possess a molecular weight cut-off between reverse osmosis membranes (dense structure) and ultrafiltration membranes (porous structure). Their effective pore sizes between 0.5 and 2 nm. An advantage of NF is that it permits operation at low pressure while keeping a relatively high permeate flux compared with that for conventional reverse osmosis.

Recently, nanofiltration (NF) process has become a widely used membrane technology often replacing reverse osmosis (RO), this is because NF need a low energy consumption and has a high flux rate compared to the other membrane technologies, which is usually attributed to larger pore sizes of the material [85], with a molecular weight cut-off (MWCO) range between 200 and 1000 g/mol. On one hand, NF lies between the classical non-porous RO membranes, where separation is mainly a function of solution diffusion coefficient of the dissolved organic and/or inorganic species and the ultrafiltration (UF), which is generally regarded as a pore filtration technology [86]. On the other hand, however, alongside the molecular sive effect, NF membranes have a second separation mechanism, originating in charge effects by the dissociation of surface group such as sulphonated, for instance in the case of polyamide membrane, carboxylate groups can be present on the membrane surface, inducing positive attractions for cations are repulsive ones for anions

Furthermore, nanofiltration membranes have another feature: most of them are electrically charged in aqueous media [87,88]. This is because the ionization of surface functional groups and/or adsorption of charged molecules from the solution onto the membrane surface [89,90]. In addition, the combination of micropores with electrically charged materials means that solute separation is dependent on the micro hydrodynamics and interfacial phenomena occurring at the membrane surface and inside the membrane.

Internationally, nanofiltration membranes, is a promising membrane technique, and made a remarkable progress since the last decade with a large number of applications in the field of process water, water treatment and the production of drinking water [91], where it is used for softening and removal of micropollutants such as pharmaceutically active compounds, pesticides and other relatively small organic solutes. Nanofiltration is used also for more challenging applications, involving fractionation rather than purification. More

specifically, NF can be used to remove (multivalent) ions as well as relatively small organic molecules [92] from liquid streams. However, for a successful implementation of the separation process it is necessary to obtain information about the retention performance of a given membrane.

1.3.5 Separation mechanism with NF membranes

Nanofiltration is a process in which membranes with nano-size pores are used to separate solutes based on size and/or charge [78,93]. Furthermore, several recent studies [94,95] have investigated the transport mechanisms of ionic and organic solutes through NF membranes. These studies have shown that for inorganic and organic compounds the removal depends upon both the membrane properties (i.e., pore size, hydrophobicity, membrane material, membrane charge) and solute characteristics (such as molecule size, charge and polarity), as well as on the membrane-solute interactions.

In nanofiltration, the distribution of neutral organic compounds at the membrane surface is assumed to be realized by a steric exclusion mechanism. Typically, steric exclusion is for nanofiltration but applies also to the others pressure driven membrane processes as ultrafiltration and microfiltration. Due to their size, organic solutes only have access to a fraction of the total surface area of a pore. This leads to a geometrical exclusion of the solute from the membrane. Typically, separation between organic solutes could only take place when the solutes have a difference in size. Two different compounds of the same molecular weight can have different configurations such that their molecular diameter is different. For example, a linear polymer can snake through the membrane pores while a spherical polymer of the same molecular weight, but of greater diameter, is rejected (see Fig. 11.1). Additionally, transport of organic compound takes place by convection due to a pressure difference and diffusion due to a concentration gradient across the membrane.

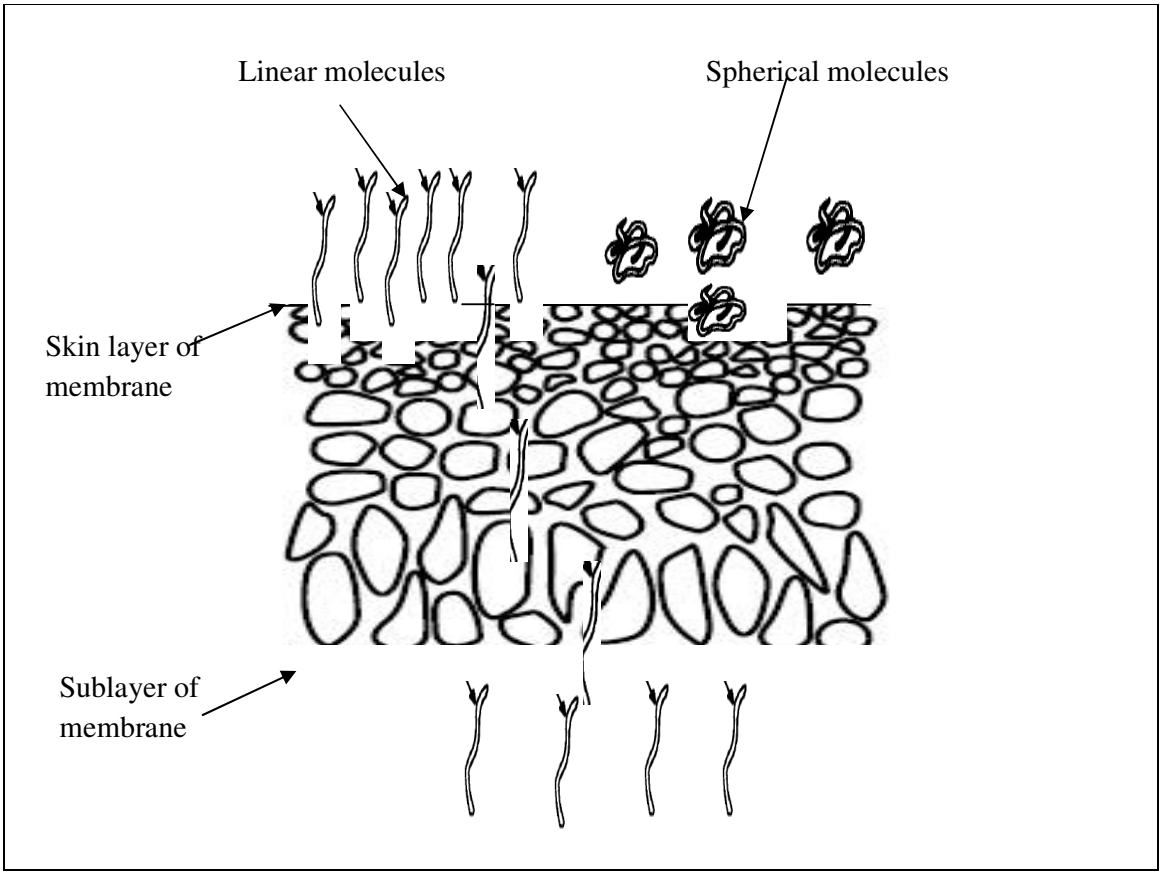

Figure 11.1: Retention of spherical and linear molecules in NF membrane by a steric exclusion mechanism.

Kosutic [96] studied the removal of organics from aqueous solutions by commercial RO and NF membranes, and reported that the rejection of organics is related to the sieving parameters (eg: solute and pore size). Furthermore, B. Van der Bruggen et al. [97] developed the influence of molecular size, polarity and charge on the retention of organic molecules by nanofiltration, and showed that the polarity and the charge of organics could effect on the rejection process, especially when the pore sizes of membranes are large. The removal of uncharged molecules results from size exclusion or may be a result from differences in diffusion rates in a dense structure, which related also on molecular size [98]. Some researchers [2,93,97] reported that the rejection usually remains constant and/or drops slightly with increasing feed concentration .

B. Van der Bruggen [99] developed a model for the retention of organic molecules with nanofiltration membrane as a function of the molecular weight. For uncharged solutes, however, NF membranes are characterized by rejection curve, which results in an insufficient separation between different molecules on the basis of their molecular size. A typical

sigmoidal rejection curve is given in Fig.(12.1). Therefore, the permeate contains molecules with variable size, both below and above the claimed pore size of the membrane. Either the permeate or the retentate is to be considered as a waste fraction.

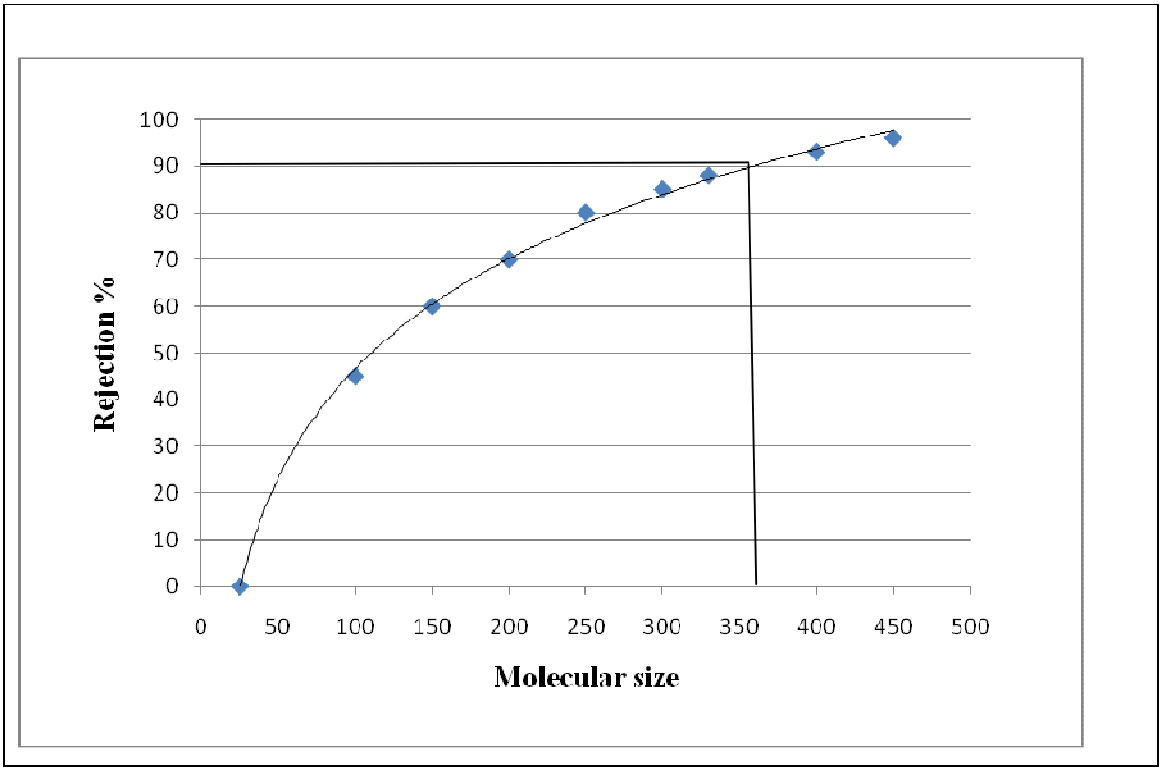

Figure 12.1: Typical sigmoidal rejection curve (rejection as a function of molecular weight) obtained for rejection of uncharged solutes with a nanofiltration membrane [99].

- **For charged solutes two additional distribution mechanisms can be recognised:**

I. **Donnan exclusion** [100,101,102]: Which compared to other membrane processes has an obvious effect on the rejection mechanism in NF. This is may be the effect of the slightly charged nature of the membrane. Compounds with an opposite charge compared to the membrane (counter-ions) are attracted, while molecules with the same charge (co-ions) are repelled. Additionally, at the membrane surface a distribution of co- and counter-ions will take place, thereby causing an additional separation. For charged [103] molecules an electrostatic interaction occurs between the component and the membrane, as most nanofiltration membranes are charged. Thus, the separation performance of NF membranes can be identified as a combination of the sieving (steric hindrance) effect and Donnan (electrostatic) effect [104,105].

II. **Dielectric exclusion** [106]: Because the charge of the membrane and the dipole momentum of water, polarization in the membrane pore takes place by water molecules. This

polarization leads to a decrease of the dielectric constant inside the pore, therefore the charged solute is less favourable to enter.

Additionally, Fane et al. [107,108], reported the applications of nanofiltration to ionic separations, and suggested that the transfer through a charged membrane is governed by three forces:

- dielectric forces,
- coulombic forces: This force is dependent on the sign of the charge of the membrane and on the charge of the ions,
- hydration forces: This force is dependent on the hydration of the membrane and on that of the ionic species.

Furthermore, A. Lhassani et al. [109] developed a selective demineralisation of water by nanofiltration application to the defluorination of brackish water, and suggested that ions are transferred by two mechanisms in NF: (1) convection: the larger ions will be rejected (physical parameters); (2) solubilization- diffusion: a function of the solvation energies and the partition coefficient, the larger the ion, the better it is retained (chemical parameters).

Alami-Younssi et al. [110] studied the rejection of mineral salts in gamma alumina nanofiltration membrane, and showed that the transfer of the charged species through the NF membrane depends not only on the size of the ions but also on their charge and the surface charge of the membrane. In fact, it is necessary to take into account all the forces due to interactions between the membrane and the ionic species during the transfer through the membrane.

F.G. Donnan [111] has already described the effect of membrane charge on the transport of charged solutes. The well-known Donnan exclusion mechanism is often used to give a qualitative explanation for the retention of ions [112,113]. In salt separation, a Donnan effect, stemming from the membrane charge, leads to a difference in rejection according to ion charge. Rejection is low for monovalent ions and high for divalent ions (co-ions).

The Gibbs–Donnan effect [114] is also known as the Donnan effect, Donnan law, Donnan equilibrium, or Gibbs–Donnan equilibrium. The Donnan effect explains the behavior of charged compounds near the membrane. For example, in case of the presence of different charged molecules that are rejected, this produces an uneven electrical charge.

1.3.6 Traditional methods to remove pollutants from water and wastewater

Traditional methods to remove pollutants from water and wastewater are:

1. Absorption	2. Adsorprtion	3. Coagulation
4. Flocculation	5. Sedimentation	6. Sand filtration

7. Ion exchange 8. Electrodeposition 9. Extraction,

10**.** Precipitation 11. Biological degradation.

Most of these methods have disadvantages [112**-**115**]**:

- Disadvantages of operating in a successive steps due to heterogeneous reactions,
- Distribution of raw material between different phases that usually require a long operating period and a large area.

1.3.7 Rejection of organic compounds using nanofiltration (NF) membranes

In the following section, some of previous work for separation of organic compounds in liquid solutions using nanofiltration (NF) were outlined. Rejection of organic micropollutants such as alcohols, pesticides, endocrine disrupting compounds, or pharmaceutical residues is becoming an important concern during water and wastewater treatment applications where nanofiltration (NF) treatment is employed. Recently, Some researchers made a great effort in order to establish the removal efficiency of organic solutes by NF membranes from aqueous solutions and hence the rejection mechanism. Therefore, understanding the key parameters driving the rejection of organic contaminants is very important for assessing treatment efficiencies a priori.

NF membranes differ from the other pressure driven membranes because NF are designed to selectively remove molecules such as multivalent ions or organic pollutants while allowing other solutes to go through [116,117**]**. Furthermore, NF membranes can be operated at lower feed pressures because the molecules in permeate which passed through the membrane do not add a too strong osmotic pressure to the system when their concentration are low [97**]**.

From the knowledge gained during the literature review, it was found that the major rejection mechanism of organic compound by NF is physical sieving of solutes larger than the membrane (MWCO). Other rejection mechanisms such as electrostatic exclusion and hydrophobic–hydrophobic interactions between solute and membrane may considerably influence the rejection of organic compound. Furthermore, solution chemistry and membrane fouling are considered affecting the rejection of organic compound.

The summary of some of previous work studied the factors affecting the rejection of organic solutes during NF/ RO treatment as follows:

I. Molecular weight (MW):

Agenson et al. [118**]** investigated the retention of a wide variety of organic pollutants by NF/ RO membranes, and showed that rejection was dependent on the molecular weight of

solutes but the molecular width was more useful to describe the physical sieving rejection by membranes. Levine et al. [119] studied treatment of trace organic compounds by membrane processes (UF, NF and RO), and demonstrated that low-molecular base neutrals showed the poorest rejection during treatment. Huang et al. [120] developed the rejection of alcohols, amines and aldehydes by RO using crosslinked PAA composite membrane, and reported that the molecule rejection increased with the increase of the molecular weights of alcohols, amines and aldehydes. The order of compound rejection for alcohols and amines with different structures was tert->sec->iso->n-. Some of previous work studied the separations performance by RO membranes for alcohols [121], phenols [122], organic acids [123], and hydrocarbons [124] in aqueous solutions using porous cellulose acetate membranes, and showed that the rejections of aqueous organics solution are relatively low, especially for low molecular weight organics [124,125]. Some researchers, who developed NF full-scale applications, reported a partial rejection of organic solutes with MW below the MWCO of the membranes [126,127].

II. Solute radius (*ri*,s):

Most of the current models describe rejection of organic solutes in the NF process, based on the physical sieving mechanism 'Pores' [97,98,100,128]. Rejection characteristics of organic and inorganic compounds were examined by Richard et al. [129] for six reverse osmosis (RO) membranes and two nanofiltration (NF) membranes. It was shown that the removal of organic compounds is dependent on solute radius and molecular structure. An empirical relation for the dependence of the rejection of organic compounds on the ratio solute radius (*ri*,s) / membrane pore radius (*r*p) was proposed. The rejection for organic compounds is over 75% when *ri*,s/*r*p is greater than 0.8.

III. Phisco-chemical properties :

Kiso et al.[77] examined the rejection properties of 11 non-phenylic pesticides by reverse osmosis (RO) and NF membranes, and reported that the rejection is dependent on hydrophobicity. Moreover, it was shown that all pesticides adsorbed on the membranes and that, the adsorption was controlled by hydrophobicity of the pesticide. B. Van der Bruggen et al.[89,90] indicated that a high dipole moment of a solute might produce a decrease in solute retention while Kiso et al.[78] linked the high hydrophobicity of some pesticide molecules to their increased retention; these effects are related to various types of dipolar interactions

C. Bellona et al. [130], studied factors affecting the rejection of organic solutes during NF/RO treatment, and reported a comprehensive literature review, targeting membrane rejection mechanisms as follow:

I. Key solute parameters which were identified to primarily affect solute rejection include: molecular weight (MW), molecular size (length and width), acid disassociation constant (pK_a), hydrophobicity / hydrophilicity ($\log_{ow}$), and diffusion coefficient (D_p).

II. Key membrane properties affecting rejection that were identified: molecular weight cut-off, pore size, surface charge (measured as zeta potential), hydrophobicity/hydrophilicity (measured as contact angle), and surface morphology (measured as roughness).

III. Feed water composition, such as pH, ionic strength, hardness, and the presence of organic matter, was also identified as having an influence on solute rejection, and also membrane fouling.

1.3.8 Inorganic rejection using nanofiltration (NF) membranes

From table 4.1 it was found out that the multivalent ions (such as SO_4^{2-}) are separated by the NF membrane to a high degree whereas a majority of monovalent ions (such as Na^+) are rejected with a low degree. This phenomenon is explained by the Donnan effect. Monthon et al.[131] studied rejection characteristics of inorganic pollutants by a nanofiltration membrane, and reported that generally the divalent ions such as Ca^{2+} , Mg^{2+} and SO_4^{2-} gave higher rejection than that of the monovalent ions such as Na^+, K^+, Cl^-; however the rejection is also linked to the type of counter ion (monovalent or divalent one), see table 4.1.

Table 4.1: Inorganic rejection using a commercial nanofiltration (NF) membrane

Salt	rejection	Ref.
Na_2SO_4, $MgSO_4$ KCl	95–99% at 5 bar 30–89% at 5 bar	[132]
Na_2SO_4	95% at 10 bar	[133]
$MgCl_2$	70% at 10 bar	[134]
K_2SO_4,Na_2SO_4 Na_2CO_3, K_2CO_3 NaCl, KCl	90-99% at 15 bar 82% at 15 bar 40-55% at 15 bar	[135]

G. Hagmeyer et al.[136] studied the rejection of NaCl and Na_2SO_4 at different concentrations and pressures using NF membranes. Their results showed that the rejection of NaCl and Na_2SO_4 was slightly decreased as the concentration increased. It is worth-while mentioning that a high flux with high rejection was obtained at low salt concentration for all tested membranes, while the flux and rejection were relatively low at high concentration. The same result was reported by [137,138] also.

Table 5.1: Physical properties of the salts ions tested [138,139] .

Ion	Ionic radius (nm)	Hydration radius (nm)	Hydration enthalpy (kJ/mol)
Na^+	0.095	0.365	418
Cl^-	0.181	0.347	338
SO_4^{2-}	0.23	0.38	1138
Mg^{2+}	0.065	0.429	1923
Ca^{2+}	0.1	0.349	1653
Fe^{2+}	0.055	0.435	1981

1.3.9 Rejection of aqueous organic/inorganic by asymmetric polyetherimide membranes

In the following section, some of previous work for rejection of aqueous organic /inorganic compounds using asymmetric polyetherimide membranes has been reviewed in tables (6.1,7.1) .

Table 6.1: Asymmetric PEI ultrafiltration membranes made from monomers for organic solution separation.

Membrane material	Ultrafiltration Process condition	Feed composition	Total flux (kg/m^2 h)	Rejection %	Ref.
monomers: BAPS-m)ODPA, **Solvent** :NMP	pressure 1 kg/cm^2, flow rate 2.5 L/min at 25 ^oC	solutes (1000mg/L) (PEG MW 6000,1000,and 20000) in water	water flux:375-470 (kg/m^2 h)	10-98% Rejection *	[140]

* Rejection Increase with increase MW of PEG and polymer wt %.

Table 7.1: Comparison of nanofiltration performance of the asymmetric PEI membranes prepared from commercial pure polymers for organic liquid solution separation.

Membrane material	NF Process Condition	Feed composition	Total flux	Rejection%	Ref.
PEI (UItem 1000, General Electric) **Solvent**: NMP, DGDE	14 bar, 2.5 l/min flow rate at 25°C, membrane area 18.6 cm^2	1000 ppm solution of PEG 600 in DI water	water flux (53 kg/ m^2 h)	83%	[141]
PEI (UItem 1000, General Electric) **Solvent**: DMF	The PEG600 solution flux was measured at 14 bar, 2.5 L/min of flow rate at 25 ^oC.	1000 ppm PEG 600 in DI water	6-100 kg/ m^2 h	25-75% Rej. Increase with increase polymer wt% While flux decrease	[142]
soluble polyimide (HQDPA-DMMDA)	Pressure 5 to 20 bar at 10-14 ^oC	Thee benzylpenicillin sodium solutions concentration of 7.2, 13.0, and 19.7 g/L.	0.8-9.5 kg/m^2 h Flux increase with increase pressure	62-85% The rejection reached 85% for 19.7 g/L under 2.0 MPa.	[143]
P84 copolyimide **Solvent**: DMF	Pressure 13.8 bar , at room temperature.	Solution Salts: $CaCl_2$,NaCl , Na_2SO_4 0.2-2.0 g/L	50 (kg/m^2 h) for 2.0 g/L NaCl solution	50.9 ± 5.1% salt rejection.The rejection sequence of $CaCl_2$ > NaCl > Na_2SO_4	[144]

* Whers: *N*-methyl-2-pyrrolidone (NMP) and diethylene glycol dimethyl ether (DGDE), DI distilled water

1.4 Part 2: Membrane preparations

The preparation of symmetric (such as dense membrane), asymmetric and composite membranes made from polymeric materials, to be used in the different membrane processes and applications, are reported in this part. In this work we intend to prepare membranes using polyimide, thus the first part is dedicated to this polymer.

1.4.1 Interest of polyimide membranes

Polyimides are well known as polymeic materials and they have been used since the last three decades as specialty polymers in numerous applications [145]. One of the reason is the outstanding physical properties of aromatic polyimides (PI): the polymer backbone induces high thermal stability, high electrical insulating properties and good chemical resistance in addition to mechanical toughness [146]; therefore PI have been widely employed in various technical fields such as coatings, composite matrices, adhesives, fibers, foams moldings, electrical and electronic applications [147] and also in the field of membranes [148,149].

Polyimides have high gas permeabilities. Therefore, the polyimide membranes have been used for gas separation since the last two decades [150,151]. From the statistical analysis, 47% of polyimide membranes are used in gas separation and about 5% in pervaporation technologies [152]. Furthermore, polyimides are used for the analysis of the mechanism of permeation and diffusion. However, tailored polymers are required to give the desirable applications, such as nanofiltration, pervaporation and gas separations in membrane processes [153].

Most of the polyimides polymers exhibit a higher permeability as well as a higher selectivity than many other glassy polymers; thus they are widely studied polymers. In addition, the modification in the chemical structure of polyimides plays a good role in gas solution and transport in these polymers [154]. Some researchers have been studying the effect of fillers . Such fillers are in general introduced in the polymeric matrix so as to form an heterogenous membrane. Such membranes are able to improve the separation properties of polymers for pervaporation [155,156].

1.4.1.1 General introduction on polyimides

The polyimide polymers show a high performances through the combination of excellent properties: high thermal stability, low dielectric constant, high glass transition temperature and high resistance to solvents [157]. They are mechanically and chemically resistant, and they often replace glass and metals such as steel and highly demanding industrial applications such as aerospace.

A polyimide is a polymer with imide function. There are two types of polyimide: linear polyimide and ring polyimide shown in Fig.(13.1).

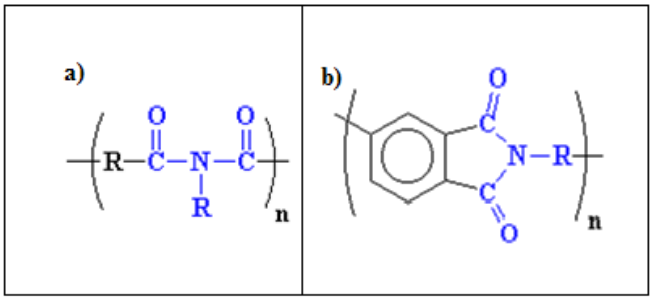

Figure 13.1: Structure of a polyimide a) linear b) heterocyclic aromatic.

Aromatic polyimides are used as linear polyimides, they represent the majority of commercial polyimide such as Ultem and Kapton shown in Fig. (14.1)

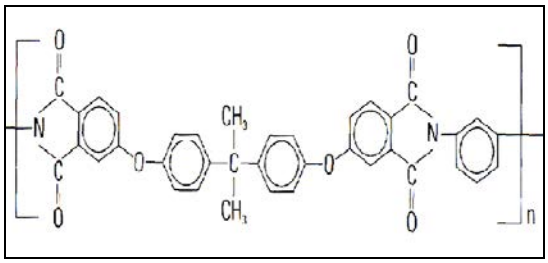

Ultem

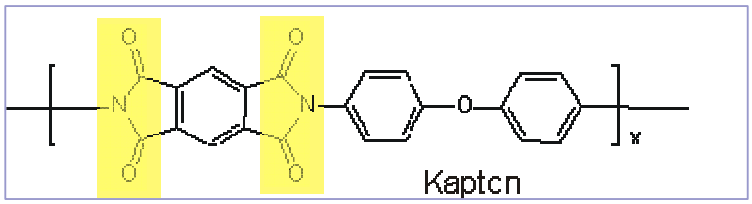

Figure 14.1: Structure of Ultem and Kapton.

- **Principle of polyimide synthesis**

The polyimides polymer are obtained by the addition mixing reaction of a dianhydride and a diamine. As shown in Fig. 15.1, this reaction involves two consecutive steps [158]:

I. The dianhydride and the diamine react at room temperature to give polyamic acid (PAA) .

II. The PAA is converted into polyimide (PI) by thermal treatment under vacuum.

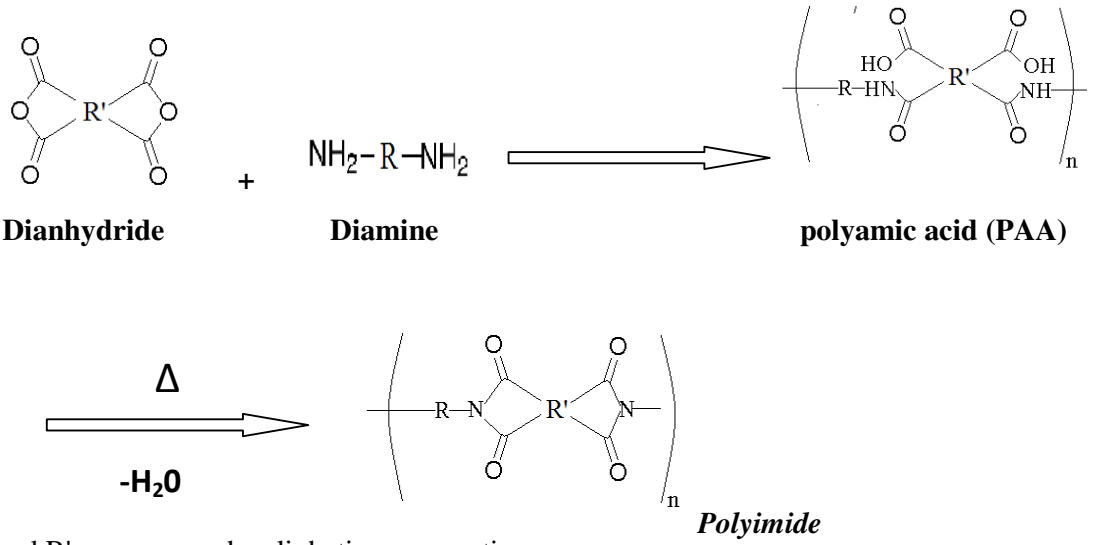

* R and R' groups may be aliphatic or aromatic.

Figure 15.1: General reaction for synthesis of a polyimide

Polyetherimides (PEI) have the general formula presented in Fig. (16.1)

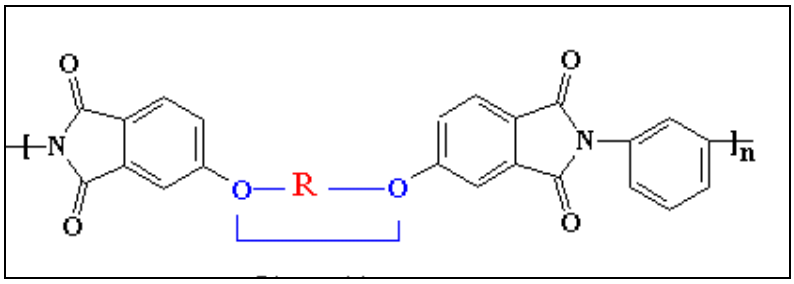

Figure 16.1: Structure polyetherimides (PEI).

1.4.2 Preparation of membranes [1,2]

Typically, the preparation of polymeric membranes, with different physical structures, takes place by two methods [2]:

(1) Physical treatment of a certain polymer membrane (such as: annealing, elongation, etc.),

(2) Preparation of the membranes from a certain polymer by several membrane formations processes (casting process such as wet and dry phase inversion).

There are difference between two methods. On one hand, the physical structure is created by the treatment after preparation of the membranes. On the other hand, in the second case, the structure is created at the same time as membrane formation.

Fortunately, all kinds of different synthetic materials can be used for membrane formation process. In addition, there are a number of different techniques to prepare the

required membrane, some of these methods can be used to prepare polymeric as well as inorganic membranes. The equilibrium thermodynamic properties of the ternary system polymer/solvent/nonsolvent play an important role in the description of membrane preparation process. Thus, depending on the choice of the ternary system, three possible results can occur during membrane formation process there are [159,160]:

(i) Non-porous film (symmetrical dense membrane),

(ii) Porous film (symmetrical porous membrane),

(iii) Asymmetric membrane which has a thin dense top layer on a porous supporting layer.

The asymmetric membrane is the desired structure in this study. An explanation of these results could be dependent on two sets of factors:

(I) The ternary system (polymer/solvent/ nonsolvent) and its equilibrium thermodynamic properties (such as liquid-liquid phase separation and solidification),

(11) The effect on the kinetics of the above-mentioned demixing phenomena and the exchange of solvent and nonsolvent during membrane preparation process .

The preparation process of asymmetric membranes could include two sets of factors. The preparation of symmetric, asymmetric and composite membranes are reported in this section.

1.4.3 Symmetrical membrane [161]

- **Dense symmetrical membranes (nonporous membrane)**

These types of membranes are capable of separating molecules of approximately the same size from each other (such as toluene/heptane). On one hand, dense symmetrical membranes are widely applied in research, development and other laboratory studies for characterizing membrane properties (such as: swelling, mechanical propertes). On the other hand, these types of membranes are however, rarely used commercially; because the membranes permeate flux is very low for practical separation processes. Morever, such membranes are used in some applications as pervaporation, vapour permeation, gas separation and dialysis. The dense membranes are prepared by two step mechanism, solution casting and thermal melt-pressing process as described below.

I. Two step mechanism

The polyimide membranes were obtained by addition mixing reaction of a dianhydride and a diamine in presence of suitable solvent, this reaction involves two consecutive steps there are:

a) The dianhydride and the diamine react at room temperature to give polyamic acid (PAA) .

b) The PAA is casted on a glass plate or teflon to give PAA membrane, after the casting has been drawn; the casted film is dryed at high temperature, thus the solvent will evaporates to leave a thin film. The PAA membrane is converted into polyimide (PI) membrane by thermal treatment under vacuum.

- **Solution casting (dry phase inversion)**

Solution casting uses a casting knife to cast polymer solution across a casting plate. After the casting has taked place, the solvent evaporates to leave a thin film. The best casting solution concentrations are in the range 15-20 wt% polymer in order to prevent the spreading of polymer over the casting plate. Solvents having high boiling points are unsuitable for this method, because their low volatility needs too long evaporation times.

- **Melt pressing (melt forming)**

Some polymers do not dissolve in suitable casting solvents. For example, polyethylene, polypropylene, and nylons, which have to be formed into membranes by melt pressing. Melt pressing process occurs by sandwiching the polymer at high pressure between two heated plates. A pressure of 136-340 bar is used for 0.5 to 5 minutes, while holding the plates almost above the melting point of the polymer.

1.4.4 Preparation of porous membrane

In fact, this class of membrane induces separation mechanism by discriminating between solute size. Typically, porous polymeric films can be prepared by several ways, such as sintering, stretching, track etching and phase inversion processes. Really, the final morphology of the prepared membranes is dependent on the properties of the polymer solution and the process conditions. Furthermore, the majority of membranes are formed by controlled phase separation of polymer solutions into two phases: In the former one with a high polymer concentration (rich polymer phase), and in the latter one with a low polymer concentration (poor polymer phase). The rich polymer phase solidifies immediately after phase separation, and forms the membrane. The membrane performance is dependent on the morphology of the prepared membrane.

1.4.4.1 Preparation of porous membranes by phase inversion techniques

Phase inversion can be defined as " a process whereby a polymer is changed in a controlled manner from a liquid state to a solid state" [1]. Phase inversion of polymer

solutions can be induced in several ways [162]. The four main techniques for the preparation of polymeric membranes by phase inversion are [163,164 ,165]:

i. Immersion precipitation

Most commercially available membranes are formed by immersion precipitation. The phase inversion process induced by immersion precipitation is a well-known technique to get asymmetric polymeric membranes. A polymer solution is casted as a thin film on a plate support (as glass), and is immediately immersed in a coagulant bath. Precipitation can take place because the good solubility between solvent and nonsolvent in the polymer solution .

ii. Thermally induced phase inversion (TIPS)

The TIPS is dependent on the theory that solubility of the polymer in a solvent usually decreases when the temperature is decreased. After the demixing process is occurred, the solvent is removed by extraction, evaporation or freeze drying.

iii. Precipitation from the vapour phase

This process was used as early as 1918 by Zsigmondy. Phase separation of the polymer solution is induced, during this method, by a nonsolvent vapour which penetrates in the polymer solution.

iv. Air-casting of a polymer solution (precipitation by solvent evaporation) [166,167]

The most simple technique to form phase inversion membranes is precipitation by solvent evaporation. This process was already used in the early years of this century. In this technique, the polymer is dissolved in a mixture of solvent (volatile) and nonsolvent (less volatile). During the evaporation of the solvent, the solubility of the polymer decreases then the composition of mixture will shift to a higher nonsolvent and polymer content. This leads eventually to the polymer precipitation and then phase inversion can take place leading to the formation of skinned membrane.

It was clearly that the differences between the four techniques originate from differences in desolvation mechanisms.

1.4.5 Asymmetric membrane preparation and phase inversion process

Most of the membranes in use today are phase inversion membranes (asymmetric structure membranes) obtained by immersion precipitation [1,168]. These membranes are asymmetric since their cross-section reveals an asymmetric structure: dense skin layer (dense permselective layer $<0.1\mu m$) supported by a porous sublayer (more open porous substrate $\geq 15\mu m$). In industrial applications, symmetrical microporous membranes, which induced by

precipitation from the vapour phase, have been almost completely displaced by asymmetric membranes, which have much higher liquid fluxes with a good quality.

The asymmetric membrane structure was not recognized until Loeb and Sourirajan [169] prepared the first asymmetric membranes according to the wet phase inversion process (Loeb- Sourirajan technique) in 1962. The Loeb- Sourirajan technique made a critical breakthrough in membrane process technology. Since, the asymmetric membranes were prepared by Loeb and Sourirajan, the research and developments in asymmetric membrane preparation methods and properties were accelerated by using scanning electron microscopes, which enabled the effects of structural modifications to be easily assessed. More importantly, the demonstration of the advantages of the asymmetric membrane structure open the way to improve the membrane separation processes. In addition, the development of the phase inversion process has preceded many systematic studies on the effects of membrane formation parameters and mechanism.

Figure 17.1 shows a schematic of the phase inversion process induced by immersion precipitation. This process consists of four main steps:

i. **Casting step**: the polymer solution is casted by using a film applicator to form a thin film of a polymer solution on a suitable substrate (i.e: glass support)
ii. **Pre-concentration step**: the casted film is left for a certain evaporation time at room temperature (pre-concentration time).
iii. **Immersion step (phase inversion step)**: the casted film is immersed into an appropriate coagulation bath (i.e: water). During this step, the solvent will pass into the coagulation bath while non-solvent will penetrate the polymer solution. The exchange of diffusion of a solvent and a nonsolvent through the interface in a polymer casting solution and a nonsolvent will yield the phase inversion process for polymer casting solution with different exchange rates which induce membranes with symmetric or asymmetric structures (the interchange of solvent and non-solvent coagulant due to the diffusion form membrane). The exchange rate is induced by the difference between solubility parameters, the diffusion force of nonsolvent and physical factors of the phase inversion process [170]. Furthermore, the properties of the polymer casting solution are presumed to affect the structure of the resulting membrane [171,172**].**
iv. **Drying step:** this step removes traces of water and solvent from the prepared membranes.

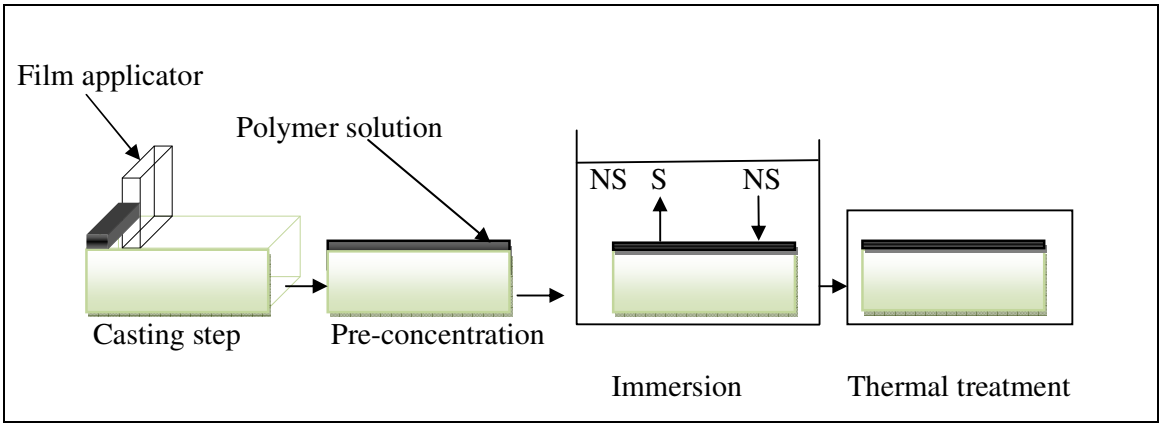

Figure 17.1: Phase inversion process by immersion precipitation, S; solvent, NS; nonsolvent [173].

1.4.6 Thermodynamic description of phase inversion

It known that the state of any system, open, closed or isolated can be described by state functions; entropy, enthalpy and free energy. The thermodynamic state of a system of binary, ternary or more components with limited miscibility can be described in terms of the free energy of mixing. At constant pressure and temperature, three different states can be distinguished [1] with the modification of the composition:

(1) A stable state: the solution remains homogeneous: the free energy of mixing is negative

$\Delta G < 0$ (P, T = const) (2)

(2) An unstable state: the homogeneous solution separates spontaneously into two phases corresponding to a miscibility gap, the free energy of mixing is positive

$\Delta G > 0$ (P, T = const) (1)

(3) An equilibrium state: given by the phase boundary composition, the free energy of mixing is zero

$\Delta G = 0$ (3)

Mechanism of microporous formation by thermal gelation of a binary system [1, 2]

The phase inversion process (phase separation) induced by several techniques in a homogeneous solution to form microporous membranes can be related to three basic procedures [2]:

(1) Thermogelation of a homogeneous solution of a binary system, ternary system or more components;

(2) Evaporation of a volatile solvent from a homogeneous solution;

3) Addition of a nonsolvent or nonsolvent mixture to a homogeneous solution.

All three procedures may result in symmetric microporous structures or in asymmetric structures with a more or less dense skin at one or both surfaces suitable for nanofiltration, reverse osmosis, ultrafiltration or microfiltration. The free energy of polymer homogeneous mixing under certain conditions of temperature and composition is negative (stable state) that is the only thermodynamic presumption for all three basic preparation procedures; thus the system must have a miscibility gap over a defined concentration and temperature range.

Typically, a binary mixture of a polymer and a solvent should be assumed for understanding the mechanism of liquid-liquid demixing. Phase separation induced by thermal gelation, evaporation of solvent and addition of nonsolvent can be illustrated with the aid of the phase diagram of a polymer mixture solution. On one hand, the starting point for preparing phase inversion porous membranes is a thermodynamically stable state for homogeneous solution, for example the point A at a temperature T_1 (Fig. 18.1). On the other hand, the simplest procedure to yield a microporous system is by thermogelation of a binary (two component) mixture. At high temperature, thermogelation of a binary system forms a homogeneous solution for all compositions, but a miscibility gap over a wide range of compositions is shown at a lower temperature. This behavior is illustrated schematically in Fig. 18.1, which shows a phase diagram of a binary mixture of a polymer and a solvent as a function of temperature.

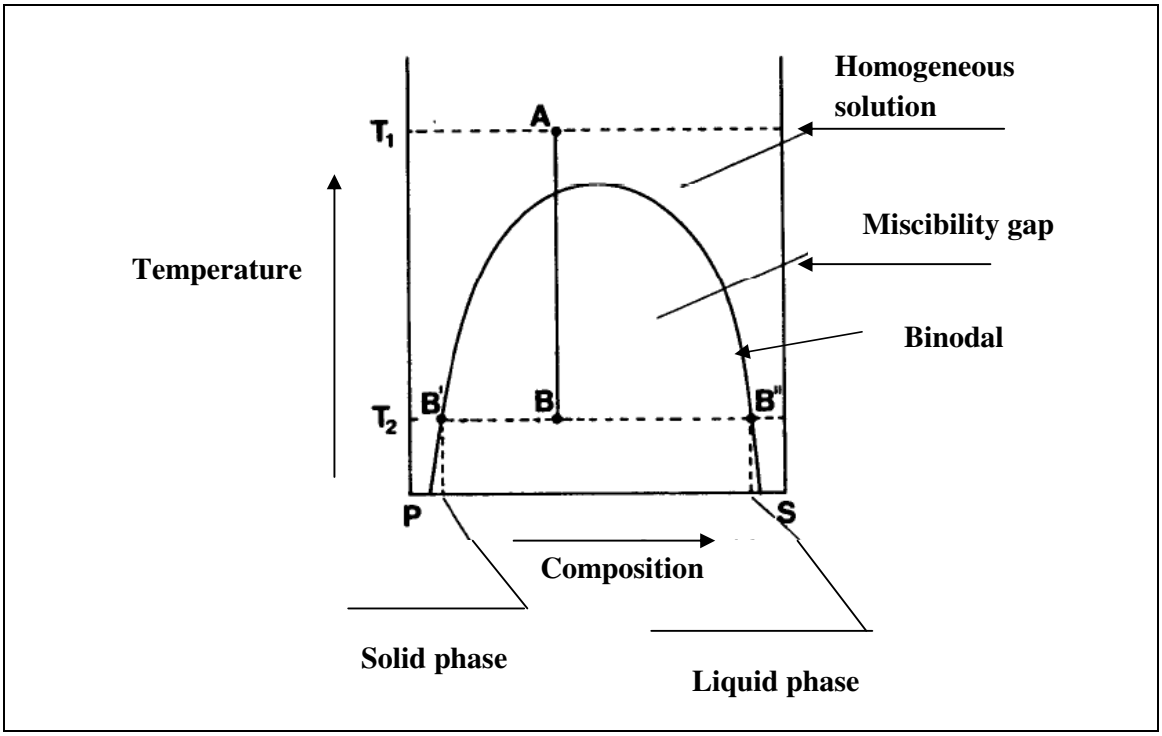

Figure 18.1: Schematic diagram showing the formation of a microporous system by thermal gelation of a binary (two-component) mixture exhibiting a miscibility gap at certain conditions of temperature and composition [1,2].

From figure 18.1, the points P and S indicate the pure components of polymer and solvent respectively while points on the line P-S indicate mixtures of these two components. When the temperature of the system decreases, demixing of the homogeneous solution will take place when the binodal is reached. Furthermore, the homogeneous solution will demix into two phases and this is referred to as liquid- liquid demixing. Thus, if a homogeneous solution mixture of the composition Xp, at a temperature T_1, as represented by the point A (Fig. 18.1), is cooled to the temperature T_2, as represented by point B, and lies inside demixing (miscibility) gap, it is not stable thermodynamically, and will separate into two different phases, the composition of which are represented by the points B' and B". The point B' shows the (polymer- rich, solvent- poor) solid phase and the point B" shows the (solvent- rich, polymer- poor) liquid phase. The lines B'-B and B"-B represent the ratio of the amounts of the two phases in the mixture, that is, the overall porosity of the obtained microporous system.

1.4.7 Phase inversion process and ternary phase diagram

Phase inversion process (phase separation process) is the most important technique used to prepare both asymmetric and symmetric polymeric membranes. The morphology and

membrane performances strongly depend on the membrane preparation process parameters [174]. From a thermodynamic point of view, study on polymer–solvent– nonsolvent system can be well depicted in a ternary phase diagram, as illustrated in Fig. 19.1. The Flory-Huggins theory [175] was found to be a convenient and useful framework for thermodynamic analysis of component mixing in a membrane preparation system.

The systems include mixture of ternary components: a polymer, a solvent and a third component, which may be a non-solvent. This ternary system is completely miscible over a certain composition range but shows a miscibility gap over another composition range, as shown in Fig. 19.1, which shows an isothermal phase diagram of the ternary components. The pure components are represented at the corners of the triangle while boundary lines between any two corners of triangle represent mixtures of two components, and any point inside the triangle diagram represents a mixture of all three components. The main elements of ternary-phase diagram are: binodal and spinodal curves, a critical point, tie lines, and a glassy region shown in Fig. 19.1. For the studied ternary system, the interaction parameters evaluated for the binary mixture allowed a remarkably accurate prediction of the ternary phase diagram.

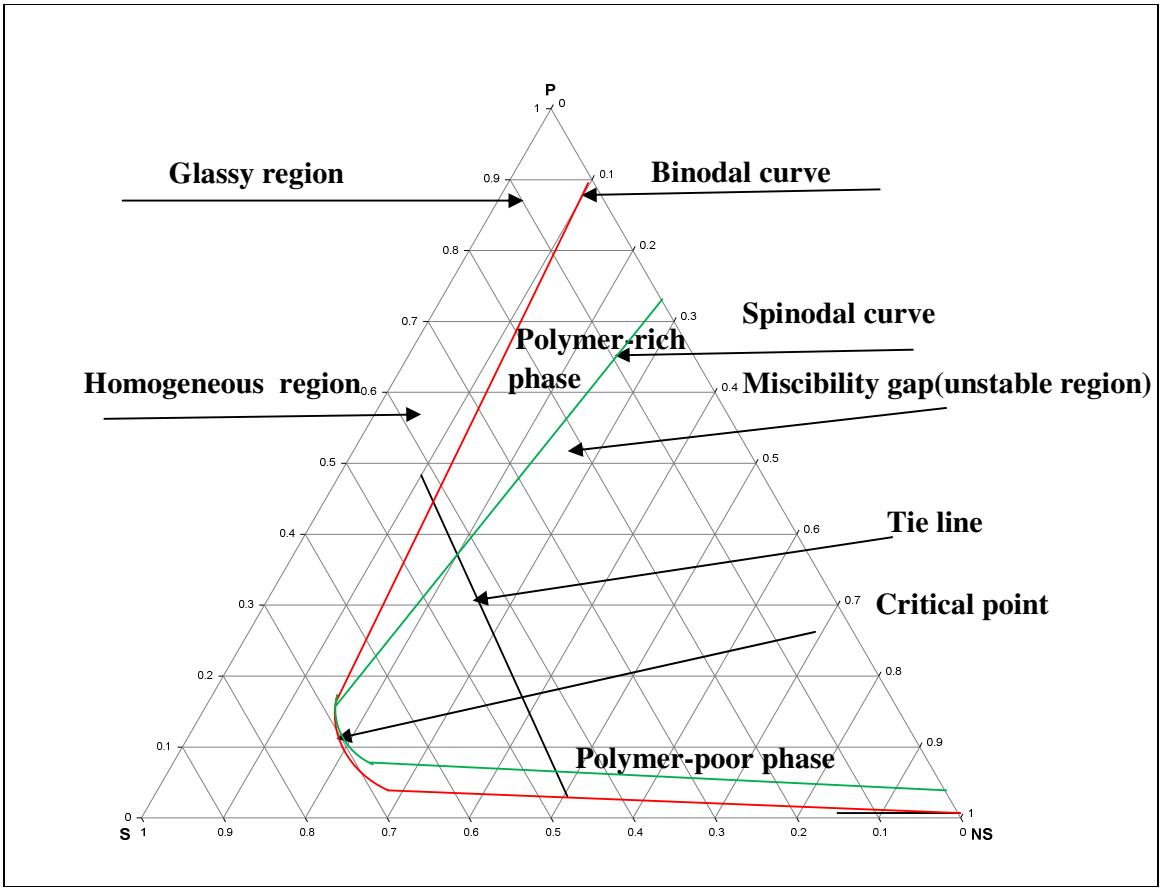

Figure 19.1: Ternary-phase diagram of polymer(P)–solvent(S)–nonsolvent(NS) system.

If a nonsolvent (such as water) is added to a homogeneous solution consisting of binary mixture of polymer and solvent [2], the membrane casting solution composition is represented by the point A as shown in Fig. 20.1. Thus, if the solvent is removed from the polymer solution (this takes place by immersion precipitation), the composition of the casting solution mixture will change to follow the line A-B. At point C, the composition of the yield system will reach the demixing gap and therefore two produced phases will start to form: a polymer- rich phase at the upper boundary of the demixing gap and a polymer-poor phase at the lower boundary of the demixing gap. The polymer concentration in the polymer-rich phase will be high enough to be considered as solid; this occurs at a certain composition of the ternary mixtures, which is represented by point D in Fig. 20.1. At this point, the membrane structure is more or less formed. Further exchange of solvent and nonsolvent will lead to the final composition of the membrane, the porosity of which is determined by point B (pore fraction=(56/90)=59.8%). Point B represents a mixture of the solid polymer-rich phase and the liquid solvent-rich phase as represented by points B1 and B2 respectively.

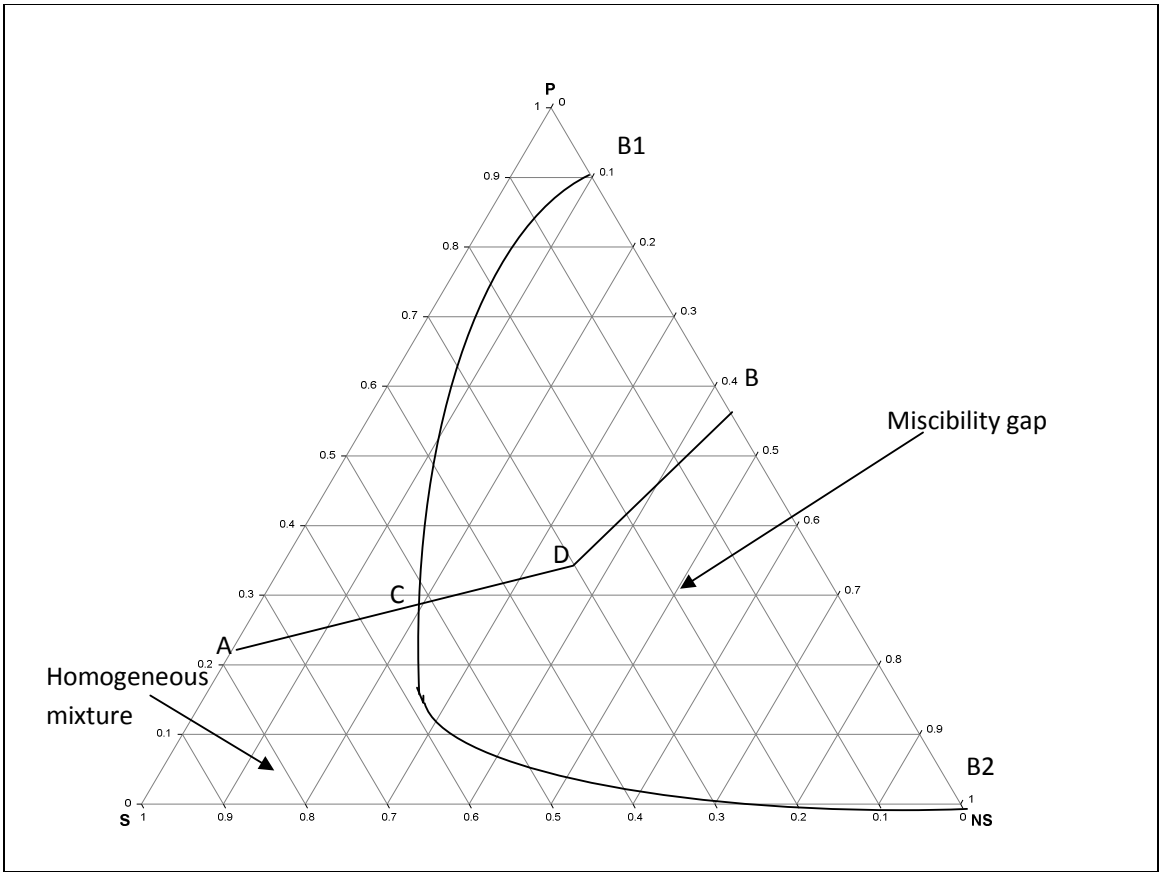

Figure 20.1: Schematic diagram showing the formation of a microporous system by addition of a nonsolvent to a homogeneous polymer solution in a ternary mixture exhibiting a miscibility gap at certain conditions of temperature and composition (P : polymer; S : solvent; NS: nonsolvent)[2].

The main important step for membrane formation from such ternary systems is always to prepare a homogeneous polymer solution (thermodynamically stable). This will often represent a point on the polymer/solvent axis as point A in Fig. 20.1. However, it is also possible to add nonsolvent to such a binary mixiture that all the polymer solution components are still miscible (homogeneous region) before the binodal curve is reached.

1.4.8 Demixing types in a ternary system [176]

In a ternary system consisting of a polymer/solvent/nonsolvent, changes in composition can cause demixing (Fig. 20.1). The demixing types that can occur are:

(a) Liquid-liquid phase separation:

The addition of such an amount of nonsolvent can induce demixing process when the polymer solution becomes thermodynamically unstable (Fig 20.1). When the binodal is

reached, liquid-liquid demixing will take place. Free enthalpy of the polymer solution decreases by separating into two liquid equilibrium phases. Demixing can take place by two ways: (1) nucleation and growth of droplets of the second phase (2) and instantaneous spinodal demixing. The composition area surrounds the spinodal demixing gap where phase separation (inversion) by nucleation and growth occurs.

(b) Crystallization or gelation:

As a matter of fact, many polymers are partially crystalline. Crystallization can take place if the temperature of the solution is lower than the melting point of the polymer. Gelation is a considerable important phenomenon during membrane preparation to form the skin layer (top layer) [1]. When gelation takes place, a dilute or more viscous polymer solution is transformed into a system of infinite viscosity, i.e. a gel. As demixing starts, the free enthalpy of the solution is decreased by polymer molecules to form ordered structures. On one hand, single crystals can be formed at low polymer concentrations. On the other hand, at higher concentrations of polymer, very small crystalline regions could work as physical crosslinks between the polymer molecules and the result is a thermoreversible gel.

1.4.9 **Mechanism of formation skin toplayer and porous sublayer** [176,177]

1.4.9.1 Mechanism of formation asymmetric membrane

In the phase inversion process induced by immersion precipitation, a polymer casting solution, cast on a support (i.e: glass, teflon), is immersed in a coagulation bath containing a nonsolvent (as water). The solvent moves from polymer solution to nonsolvent while the nonsolvent penterates the casted polymer solution.

The mechanism of membrane formation has been reported by some researchers. On one hand, C. Smolders et al. [178] suggested that the porosity of the sublayer (bottom layer) proves to be liquid-liquid phase separation while the formation of pores may be ascribed to nucleation and growth of the dilute polymer phase. On the other hand, Koenhen et al. [179] suggested that the mechanism for the formation of the sponge-like structure can be ascribed to liquid-liquid phase separation with nucleation and growth of the diluted polymer phase. Furthemore, Bokhorst et al. [180] studied formation of asymmetric cellulose acetate membranes, and reported that the toplayer is formed by gelation while liquid-liquid phase separation forms the sublayer of the membrane.

Hence, the skin layer (toplayer) is formed by gelation and the porous sublayer (bottom layer) is the result of liquid-liquid phase separation by nucleation and growth. On one hand, the factor which is determining the type of phase inversion at any point in the cast sheet is the local polymer concentration at the moment of precipitation. On the other hand, in the first

split second after immersion in the coagulation bath there is a fast depletion of solvent from the casted film and a relatively small penetration of nonsolvent. Thus, this means that the concentration of polymer in the film / bath interface increases, which crosses the gel boundary (transition C to A in Fig. 21.1). The thin and dense gel-layer which is induced by this way will work as a resistance to solvent out-diffusion and at positions beneath the skinlayer (toplayer). At lower polymer and higher nonsolvent concentrations, demixing process will take place. Thus, the type of demixing process in that case will be liquid- liquid phase separation (transition C to B in Fig. 21.1). At the end of the process, the demixing gap is entered at the polymer-rich side of the critical point (CP), so the nuclei consist of the polymer-poor phase, and a porous sublayer structure is formed, the pores of which are filled with the dilute solvent/nonsolvent phase.

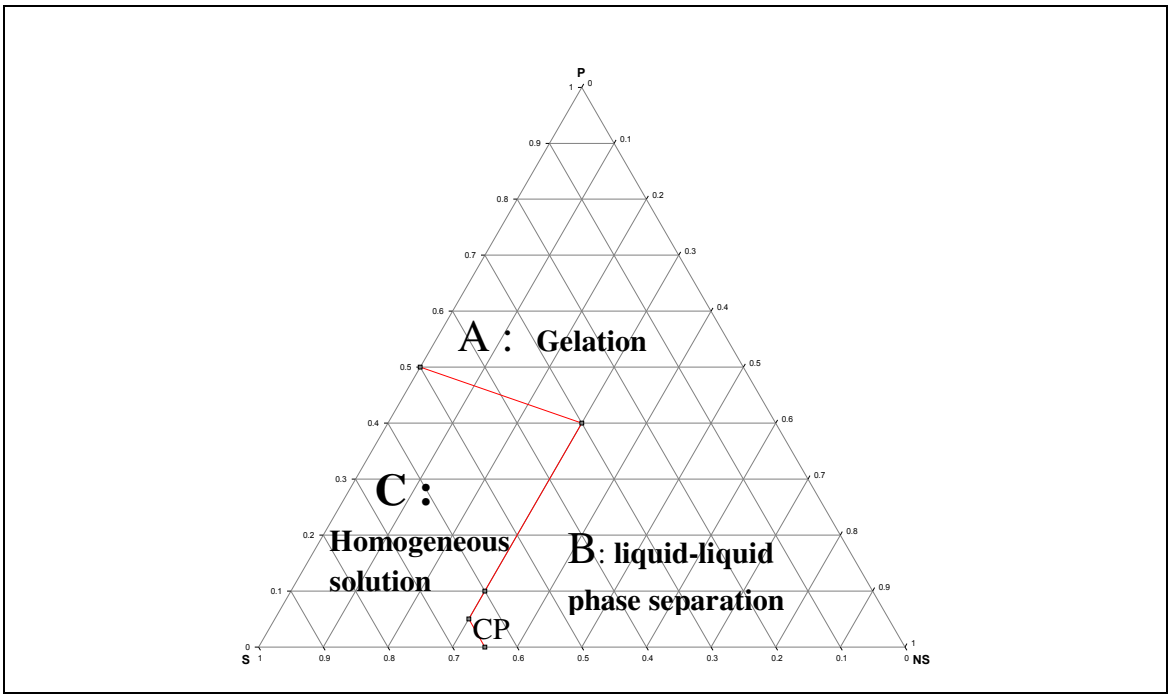

Figure 21.1: Mechanism of formation of asymmetric membrane, ternary phase diagram containing ; P : polymer; S: solvent; NS: nonsolvent; CP: critical point; A: gelation (gel region); B: liquid-liquid phase separation(two phase region); C: homogeneous solution(one phase region).

1.4.9.2 **Mechanism of formation symmetric microporous membrane**

Conversely to the case of precipitation from the vapour phase, the casted polymer solution, in this case, is in contact directly with a nonsolvent vapour phase. In addition, the nonsolvent vapour phase is saturated with the solvent used. On one hand, in this process there is no solvent outflow from polymer casted solution but only a nonsolvent inflow to polymer casted solution. On the other hand, the only possible demixing mechanism is liquid-liquid

phase separation to form symmetric microporous membrane without a dense toplayer. The change of composition in the casted film is illustrated in Fig. 22.1 (transition D to E).

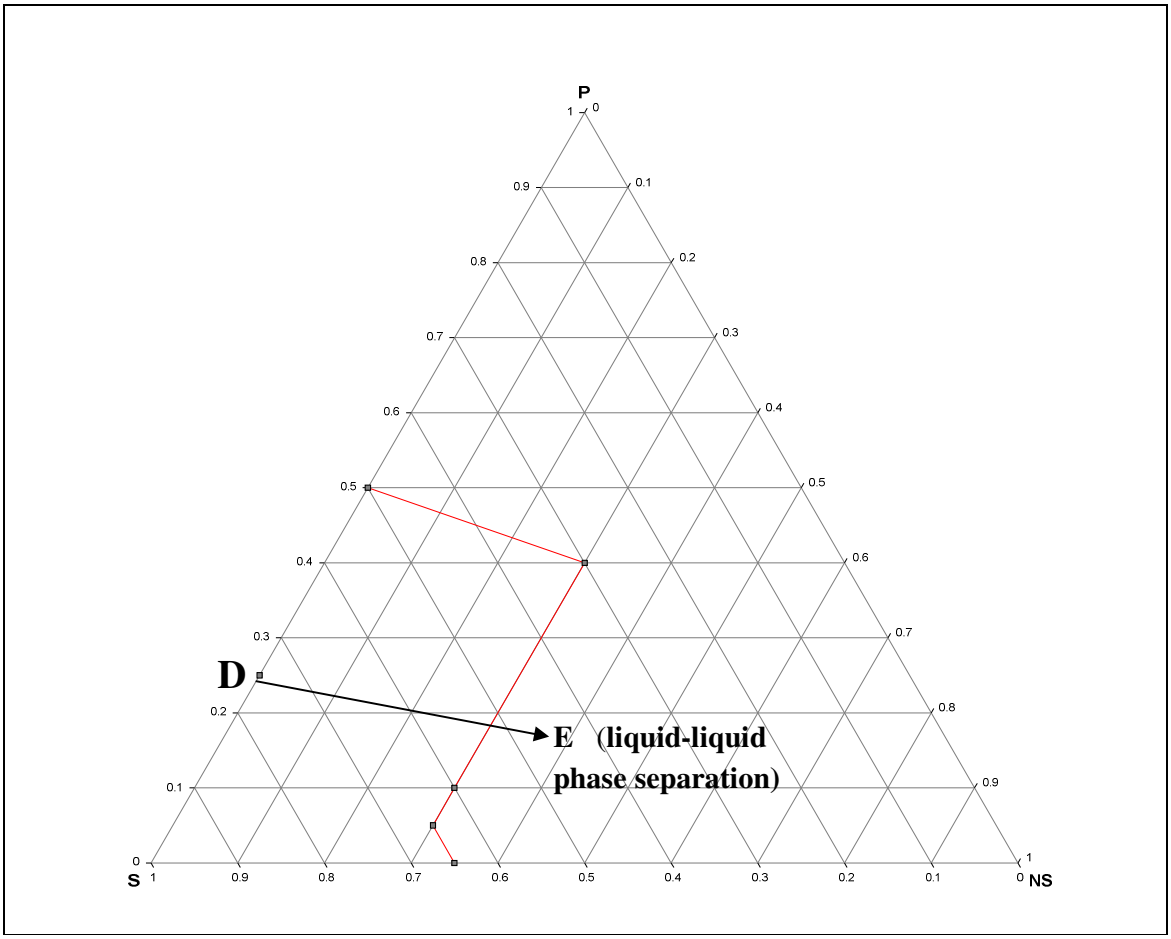

Figure 22.1: Formation symmetric microporous membrane of a polymer film with initial composition D when brought in contact with a nonsolvent vapour phase saturated with solvent.

1.4.10 Study of some parameters which have an influence on membrane morphology

In this section, the influence of some parameters on membrane morphology will be described. It is known that there two different types of membranes can be obtained, porous membranes (i.e: nanofiltration and ultrafiltration) and nonporous membranes (i.e: dense membrane), depending on the type of formation mechanism, i.e instantaneous demixing or delayed onset of demixing.

It is obvious that the kinetics of phase separation during the immersion of a polymer/solvent mixture in a nonsolvent bath plays a major role in the control of membrane morphology [181]. The accelerated rate of phase separation due to the addition of nonsolvent additive may be restricted in rearrangement of polymer aggregates, resulting in the formation

of membrane with small macrovoids. Surface properties of membranes can be controlled depending on the casting conditions, polymer solution, and coagulation bath temperature and compositions [1,2,182].

The following factors will be described in this section:

- The choice of solvent/ nonsolvent (coagulant)systems;
- The polymer concentration;
- The effect of bath temperature;

There are a number of other parameters, in addition to those listed, which will not be considered here.

1.4.10.1 Solvent effect: (1) with a higher affinity with coagulant bath (2) addition of solvent or co-solvent with a lower affinity with coagulant bath.

In order to obtain an optimal membrane structure, an additive or co-solvent is frequently used. The addition of a fourth component to a casting solution or a nonsolvent coagulant bath is an important method used in membrane modification. Many researchers studied the effects of additive materials in a coagulation bath with other factors, which can influence membrane formation.

The choice of solvent/ nonsolvent is one of the main variables in the wet phase inversion process which is influenced the membrane formation. Generally, the membrane morphology can be characterized by scanning electron microscopy (SEM). In case of delayed liquid-liquid demixing, a sponge-like structure can be formed and in case of instantaneous demixing finger-like structure can be formed [1]. Generally, in case of higher affinity between the solvent and coagulant, however, instantaneous demixing process takes place, but for a lower affinity between the solvent and coagulant, the delayed demixing process takes place [2].

By addition of co-solvent to polymer/solvent solution with low affinity with coagulant, the polymer solution system will be shifted from instantaneous demixing to delayed demixing process. This is due to the lower affinity of co-solvent with coagulant than solvent. In case of delayed demixing, a dense skin layer is formed; this inhibits the inflow of nonsolvent (water) into the polymer solution. Further, in the case of delayed demixing, the number and the size of nuclei of polymer-poor phase become smaller. Therefore, macrovoids significantly disappear. By increasing the amount of co-solvent, the number of macrovoids become smaller, and the top layer shows a very packed and dense shape. When the ratio of co-solvent to solvent is increased, almost all the macrovoids disappear and the spongy

structure starts formation. Without the addition of co-solvent, large fingers are formed because of instantaneous demixing and the upper part of the membrane is porous.

Water-miscible solvent (wms) and water-immiscible solvents (wis) can be used in the casting solution in order to prepare asymmetric membranes. Because (wis) is immiscible with water, it is left in the membrane after coagulation and can further modify the membrane structure through its solvency power.

Kim et al. [182], developed formation of integrally skinned asymmetric polyetherimide nanofiltration membranes by phase inversion process, and showed that the polymer solution system is shifted from instantaneous demixing to delayed demixing process. This is due to the lower affinity of 1,4-dioxane (co-solvent) with water (nonsolvent) than DMF (solvent). By increasing the amount of 1,4-dioxane, the number of macrovoids became smaller and the top layer shows a very packed and dense shape. Without the addition of 1,4-dioxane, large fingers were formed because of instantaneous demixing and the upper part of the membrane was porous.

Shieh et al. [183], studied preparation of polyetherimide membranes from Water-Miscible/Immiscible mixture Solvents, and reported that the PEI/NMP/H_2O system exhibits an instantaneous liquid–liquid phase separation property, but the phase separation rate reduces with the addition of methlyene chloride (MC) into the casting solution. The decrease in the phase separation rate may be mainly due to the difference in solubility parameters; water is 47.9 $(MPa)^{1/2}$, while MC is 19.8 $(MPa)^{1/2}$. The elongated macrovoids diminish gradually as the MC content increases, and no macrovoids are formed when the MC content is 30 wt% in the casting solution.

1.4.10.2 **Effect of coagulation bath temperature (CBT) on membrane morphology**.

Coagulation bath temperature is an important parameter in membrane morphology and performance. It was found that with asymmetric membranes, the porosity increases with the increase of the immersion bath temperature [184]. Raising the temperature increases mutual diffusivities between the nonsolvent (as water) and the solvent (as DMF) in the casting solution during de-mixing process. In addition, in the former case, the increase of coagulation bath temperature [185], rises the speed of nucleus growth of polymer-poor phase, that is increases the formation of porous structure in the membrane. Conversely, in the latter case, at the reduction of the temperature, the speed of nucleus growth is limited and the formation of a large number of small nucleuses is increased; so a great number of pores/voids are formed in the bottom layer of the asymmetric membranes. Therefore, formation of macrovoids is prevented and denser membrane structures are obtained.

Kim et al. [186], prepared skinned asymmetric polyetherimide nanofiltration membranes by phase inversion process, and reported that light transmittance of experiment showed an increase with coagulation bath temperature; demixing of the casting solution was gradually shifted from delayed demixing to instantaneous demixing. When the casting solution [PEI/DMF/1, 4-dioxane (16/28/56)] was coagulated at the temperature of 25 ^{o}C, porous spongy-like structure was formed. However, lower coagulation temperature (<10 ^{o}C) makes the membrane structure dense spongy.

1.4.10.3 Effect of polymer concentration on membrane morphology

Generally, increasing polymer concentrations in the casting solution, slows down the demixing process, leads to a much higher polymer concentration at the interface [186,187], and increases the thickness of the top layer and decreases the porosity of the membrane. The macrovoid formation will be diminished, and the pore size will decrease. Conversely, the reduction of the polymer concentration in the casting solution indeed leads to a more open and porous structure with large pores. Such a phenomenon has been reported in cellulose acetate/ dimethyl sulfoxide/water [188] and Nomex/*N*,*N*-dimethylacetamide/water systems [189]. Furthermore, mechanical properties of the membranes prepared with a low polymer concentration are lower than for a membrane prepared with a high polymer concentration.

1.4.11 Preparing new asymmetric block copolyimide membranes: Asymmetric polyetherimide (PEI) copolyimide membranes

In this work we discuss the modification of polyimides to improve the separation selectivity as well as the permeation flux rate. The target is to prepare and develop new polymeric asymmetric block copolyimide membranes which might give rise to high performance membrane systems for applications in liquid-liquid separations.

To tackle the permeability-selectivity problem, we decided to use aromatic polymers like polyimides, which are well-known to be solvent resistant; this approach has been previously reported with oligooxyethylene [190,191] or oligosiloxane blocks [192]. The objectives was to prepare asymmetric membranes thanks to the glassy properties of the rigid block, and to modify the aromatic PI structure by the incorporation of a water-selective block, in order to get asymmetric membranes able to combine selectivity and high permeability. However, it was not possible to predict the exact influence of this second type of block on the preparation of asymmetric membranes or to know if molecular separation could be achieved in nanofiltation with such asymmetric membranes.

Hence two objectives have been targeted: first, the selection of water selective materials, and secondly the preparation of high flux membranes for the recovery of water and retention of organic molecules from polluted water mixtures. Thus, achieving both high flux and high rejection of organic is an important challenge for NF membranes to ensure an efficient and economic treatment in purification of drinking water.

This work explores this synthesis approach, using α,ω-alkoxyether diamines, i.e. Jeffamine® ED-series, as precursor blocks for selective water permeation. Both dense and asymmetric copolyether-imide membranes (PEI) were prepared with different ether-aromatic block contents; the phase inversion procedure was tuned to favour the formation of highly porous sub-structure retaining on its top side a tight film as thin as possible under the conditions used. The separation properties of these membranes were compared for the separation of alcohol-water, organic-organic and aqueous mixture chosen as a feed model.

References Chapter 1

1. M. Mulder, (1996). Basic principles of membrane technology (2 ed.). Kluwer Academic: Springer. ISBN 0-7923-4248-8.
2. M.C. Porter, (1990).Handbook of industrial membrane technology. Noyes publications, park Ridge, New Jersey, U.S.A P 61-70.
3. S. Loeb and S. Sourirajan, Sea water demineralization by means of an osmotic membrane, Adv. Chem. Ser.,38 (1962) 117.
4. A.L Zydney, L.J Zeman, (1996). Microfiltration and ultrafiltration: principles and applications. New York: CRC. ISBN 0-8247-9735-3.
5. http://en.wikipedia.org/wiki/Membrane (selective_barrier).
6. R. W. Baker, Membrane Technology and Applications, 2004 John Wiley & Sons, Ltd ISBN: 0-470-85445-6
7. A. Rezvanpour, R.Roostaazad, M. Hesampour, M. Nyström, C. Ghotbi, Effective factors in the treatment of kerosene–water emulsion by using UF membranes, J.Hazard.Materi.161 (2009) 1216 -1224.
8. J.Zeng, H.Ye, Z.Hu, Application of the hybrid complexation–ultrafiltration process for metal ion removal from aqueous solutions, J.Hazard.Materi, 161 (2009) 1491-1498.
9. E. Blond, N. Richet, Thermo-mechanical modelling of ion-conducting membrane for oxygen separation, J.Europ.Ceram.Soc, 28 (2008) 793-801.

10. R. Sharma, R. Agrawal and S. Chellam, Temperature effects on sieving characteristics of thin-film composite nanofiltration membranes: pore size distributions and transport parameters, J. Membr. Sci. 223 (2003) 69–87.
11. M. Wiesner and S. Chellam, The promise of membrane technology, J. Environ. Sci. Technol. 33 (1999) 360A–366A.
12. K. Scott, R. Hughes, Industrial membrane separation technology, London: Blackie Academic & Professional, Springer; ISBN-13: 978-0751403381, 1996.
13. W.L Luyben, Control of a column/pervaporation process for separating the ethanol/water azeotrope, Ind. Eng. Chem. Res. 48 (2009) 3484-3495.
14. M. Peng, L.M. Vane and S.X. Liu, Recent advances in VOC's removal from water by pervaporation, J. Hazard. Mater. B 98 (2003) 69–90
15. B. Smitha, D. Suhanya, S. Sridhar and M. Ramakrishna, Separation of organic–organic mixtures by pervaporation—a review, J. Membr. Sci. 241 (2004) 1–21.
16. F. Lipnizki, S. Hausmanns, P. Ten, R. Field, G. Laufenberg, Organophilic pervaporation: prospects and performance, Chem. Eng. J. 73 (1999) 113–129
17. M.Kréa , D. Roizard, N. Mustefa, D. Sacco, Synthesis of polysiloxane-imide membranes - Application to the extraction of organics from water mixtures, Desalination 163 (2004) 203 – 206.
18. N. Hilmioglu, S. Tulbentci, Pervaporation of MTBE/methanol mixtures through PVA membranes, Desalination 160 (2004) (3) 263-70.
19. X. Zhang, Q. Liu, Y. Xiong, A. Zhu, Y. Chen, Q. Zhang, Pervaporation dehydration of ethyl acetate/ethanol/water azeotrope using chitosan/poly (vinyl pyrrolidone) blend membranes, J. Membr. Sci. 327 (2009) 274-280
20. S. Sridhar, B. Smitha, A. Shaik, Pervaporation-based separation of methanol/MTBE mixtures - A review, Separation and Purification Reviews 34 (2005) 1-33.
21. W. Guo and T.Shung, Study and characterization of the hysteresis behavior of polyimide membranes in the thermal cycle process of pervaporation separation, J. Membr. Sci. 253 (2005) 13-22.
22. D. Roizard, E. Favre, Chap.9: Trends in design and preparation of polymeric membranes for pervaporation, in Advanced materials for membrane preparation, Bentham e-Book (in print, 2010). Editors: M.G. Buonomenna and G. Golemme.
23. P. Kober, Pervaporation, perstillation and percrystallization, J. American Chem. Soc. 39 (1917) 944-948.

24. R. Binning, R. Lee, J. Jennings, E. Martin, Separation of liquid mixtures by permeation, Preprints 3 (1958)131-141.
25. A. Jonquières, R. Clément and P. Lochon, industrial state-of-the-art of pervaporation and vapour permeation in the western countries, J. Membr. Sci. 206 (2002)87-117.
26. A. Ballweg, W.H. Schneider, Pervaporation Membranes,in Proceeding as of the Fifth International Alcohol Fuels Svmsosium, Auckland, New Zealand, 13-18 May 1982, John McIndoe, Dunedin, New Zealand (1982).
27. H. Brüschke, "State of the Art of Pervaporation," in Proceeding as of third international conference on pervaooration in the chemical Industry, Nancy, France, R. Bakish (Ed.) (1988).
28. I. Blume, J. Wijmans and R. Baker, "The Separation of Dissolved Organics from Water by Pervaporation", J. Membr. Sci. 49 (1990) 253-286
29. M. Chen, G. Markicwicz and K. Venugopal, Development of membrane pervaporation TRIM process for methanol recovery from CH3OH/MTBE/C4 mixtures, AlChE Symp. Ser. 85 (1989) 82-88.
30. A. Jonquières, R. Clément and P. Lochon, Permeability of block copolymers to vapors and liquids, Prog. Polym. Sci. 27 (2002) 1803–1877.
31. T. Yamaguchi, Y. Miyazaki, S. Nakao, T. Tsuru, S. Kimura, Membrane Design for Pervaporation or Vapor Permeation Separation Using a Filling-Type Membrane Concept, Ind. Eng. Chem. Res. 37 (1998) 177-184.
32. M. Yoshikawa, H. Yokoi, K. Sanui, N. Ogata and T. Shimidzu, Separation of water and ethanol by pervaporation through polymer membranes containing N-substituted imide groups, Polym. J. 16 (1984) 653.
33. M. Yoshikawa, N. Ogata, T. Shimidzu, Polymer membrane as a reaction field. III. Effect of membrane polarity on selective separation of a water–ethanol binary mixture through synthetic polymer membranes, J. Membr. Sci. 26 (1986) 107.
34. P. Aptel, J. Neel, Synthetic Membranes: Science, Engineering and Applications; Bungay, P. M. ; Lonsdale, H. K. ; de Pinho, M. N. , Eds.; D. Reidel Publishing Company: Dordrecht, Holland, (1986) 403.
35. T. Shimidzu and M. Yoshikawa, Polymer membranes as a reaction field, I. A characterization of environment of polymer, Polym. J. 15 (1983) 135-138.
36. A. Fouad and F. Xianshe, Use of pervaporation to separate butanol from dilute aqueous solutions: Effects of operating conditions and concentration polarization, J. Membr. Sci. 323 (2008) 428-435.

37. A. Jonquières, R. Clement and P. Lochon, New film-forming poly(urethane-amide-imide) block copolymers: influence of soft block on membrane properties for the purification of a fuel octane enhancer by pervaporation, Eur. Polym. J. 41 (2005) 783–795.
38. S. Kalyani, B. Smitha, S. Sridhar and A. Krishnaiah, Separation of ethanol-water mixtures by pervaporation using sodium alginate/poly(vinyl pyrrolidone) blend membrane crosslinked with phosphoric acid, Ind. Eng. Chem. Res. 45 (2006) 9088–9095.
39. J. Villaluenga, A. Mohammadi, A review on the separation of benzene/cyclohexane mixtures by pervaporation processes, J. Membr. Sci. 169 (2000) 159-174.
40. B. Dutta, S. Sikdar, Separation of azeotropic organic liquid mixtures by pervaporation, AIChE J. 37 (1991) 581-588.
41. X**.** Yexin, C. Cuixian, L. Jidijng**,** Experimental study on physical properties and pervaporation performances of polyimide membranes, Chem. Eng. Sci. 62 (2007) 2466-2473.
42. R. Huang, V. Lin, Separation of mixtures by using polymer membranes. I. Permeation of binary organic liquid mixtures through polyethylene, J. Appl. Polym. Sci. 12 (1968) 2615-2617.
43. I. Cabasso, J. Grodzinski, D. Vofsi, Polymeric alloys of polyphosphonates and acetyl cellulose. I. Sorption and diffusion of benzene and cyclohexane, J. Appl. Polym. Sci. 18 (1974) 2117–2136.
44. H. Karlson, G. Trangardh, Pervaporation of dilute organic– water mixtures. A literature review on modelling studies and applications to aroma compound recovery, J. Membr. Sci. 76 (1993) 121–146.
45. H. Karlson, G. Trangardh, Aroma compound recovery with PV-feed flow effects - An experimental and theoretical study on concentration polarization in PV, J. Membr. Sci. 81 (1993) 163– 171.
46. R. Psaume, P. Aptel, Y. Aurelle, J. Mora, J.L. Bersillon, Pervaporation: importance of concentration polarization in the extraction of trace organics from water, J. Membr. Sci. 36 (1988) 373.
47. D. Roizard, A. Nilly, and P. Lochon, Preparation and study of crosslinked polyurethane films to fractionate toluene-n-heptane mixtures by pervaporation, Sep. Puri. Techn. 22 and 23 (2001) 45-52.
48. D. Roizard, A. Jonquières, C. Léger, I. Noezar, L. Perrin, Q. T. Nguyen, R. Clément, H. Lenda, P. Lochon and J. Néel, Alcohol/ether separation by pervaporation. High performance membrane design, Sep. Sci. Technol. 34 (1999)369 - 390.

49. N. Schneider, A. Allen and L. Dusablon, Water vapor permeability of ultrathin polyurethan films. J. Macromol. Sci. Phys B3 (1969)767–776.
50. R. Roudman and F. DiGiano, Surface energy of experimental and commercial nanofiltration membranes: Effects of wetting and natural organic matter fouling, J. Membr. Sci. 175 (2000) 61–73.
51. Y. Fusaoka , T. Inoue , M. Murakami,M. Kurihara, Drinking water production using cationic and anionic charged nanofiltration membranes, Proceedings of the AWWA Membrane Technology Conference, San Antonio, TX, 2001.
52. A. Mohammad and N. Ali, Understanding the steric and charge contributions in NF membranes using increasing MWCO polyamide membranes, Desalination 147 (2002) 205–212.
53. J. Drewes, M. Reinhard and P. Fox, Comparing microfiltration-reverse osmosis and soil-aquifer treatment for indirect potable reuse, Water Res. 37 (2003) 3612–3621.
54. J. Wagner, ‘‘Membrane Filtration Handbook Practical Tips and Hints ’’, Second Edition, Revision 2, Printed by Osmonics, November 2001.
55. P. Eriksson, Nanofiltration extends the range of membrane filtration, Environ. Prog. 7 (1988) 58–62.
56. C. Ventresque, G. Bablon, The integrated nanofiltration system of the Mery-sur- Oise surface treatment plant (37 mgd), Desalination 113 (1997) 263–266.
57. W.R. Bowen, A.W. Mohammad, A theoretical basis for specifying nanofiltration membranes-dye/salt/water streams, Desalination 117 (1998) 257–264.
58. W.R. Bowen, A.W. Mohammad, Characterization and prediction of nanofiltration membrane performance—a general assessment, Trans. IChemE 76 (1998) 885–893.
59. M. Mänttari, A. Pihlajamäki, E. Kaipainen and M. Nyström, Effect of temperature and membrane pre-treatment by pressure on the filtration properties of nanofiltration membranes, Desalination 145 (2002) 81–86.
60. M. Nilsson, F. Lipnizki, G. Trägardh and K. Östergren, Performance, energy and cost evaluation of a nanofiltration plant operated at elevated temperatures, Sep. Purif. Technol 60 (2008) 36-45.
61. A. Ghermandi, R. Messalem, The advantages of NF desalination of brackish water for sustainable irrigation: The case of the Arava Valley in Israel, Desalin. Water Treat. 10 (2009) 101–107.

62. K.O. Agenson, T. Urase, Change in membrane performance due to organic fouling in nanofiltration (NF)/reverse osmosis (RO) applications, Sep. Purif. Technol. 55 (2007) 147–156.
63. D. Trebouet, J.P Schlumpf, P Jaouen, F Quemeneur, Stabilized landfill leachate treatment by combined physicochemical–nanofiltration processes, Water Res. 35 (2001) 2935-2942
64. B. Van der Bruggen, C. Vandecasteele, T. Van Gestel, W. Doyen and R. Leysen, Pressure driven membrane processes in process and waste water treatment and in drinking water production, Environ. Progr. 22 (2003) 46–56.
65. A.R. Roudman, F. A. DiGiano, Surface energy of experimental and commercial nanofiltration membranes: effects of wetting and natural organic matter fouling, J. Membr. Sci. 175 (2000) 61-73
66. M. Meireles, P. Aimar, V. Sanchez, Albumin denaturation during ultrafiltration: effects of operating conditions and consequences on membrane fouling, Biotechno. Bioeng. 38 (1991)528–534.
67. P. Aimar, S. Baklouti, V. Sanchez, Membrane–solute interactions: influence on pure solvent transfer during ultrafiltration, J. Membr. Sci. 29 (1986) 207–224.
68. A. Escoda, P. Fievet, S. Lakard, A. Szymczyk and S. Déon, Influence of salts on the rejection of polyethyleneglycol by an NF organic membrane: Pore swelling and salting-out effects, J. Membr. Sci. 347 (2010) 174-182
69. C.P. Athanasekou, G.E. Romanos, K. Kordatos, V. Kasselouri-Rigopoulou, N.K. Kakizis and A.A. Sapalidis,Grafting of alginates on UF/NF ceramic membranes for wastewater treatment, J. Hazardous Materials 182 (2010) 611-623
70. T.Tsuru, S. Wada, S. Izumi, M. Asaeda, Silica–zirconia membranes for nanofiltration, J. Membr. Sci. 149 (1998) 127-135
71. P. Jaouen, M. Morancais-Bothorel and F. Quemeneur, Membrane filtration for waste protein recovery, Fish Processing Technology, Blackie, 1992.
72. C. Jarusutthirak, G. Amy and J.P. Croue, Fouling characteristics of wastewater effluent organic matter (EfOM) isolates on NF and UF membranes, Desalination 145 (2002) 247-255.
73. L. Vandanjon, S. Cros, P. Bourseau and P. Jaouen, Recovery by nanofiltration and reverse osmosis of marine flavours from seafood cooking waters, Desalination 144 (2002) 379–385.

74. B. Lignot, V. Lahogue and P. Bourseau, Enzymatic extraction of Chondroitin Sulfate from skate cartilage and concentration-desalting by ultrafiltration, J. Biotechnol. 103 (2003) 281–284.
75. R. Atra, G. Vatai, E. Bekassy-Molnar, A. Balint, investigation of ultra- and nanofiltration for utilization of whey protein and lactose, J. Food Eng. 67(2005)325-332
76. P.Bourseau, L.Vandanjon, P. Jaouen, M. Chaplain-Derouiniot, A. Massé , F. Guérard, A. Chabeaud, I. Johansson, Fractionation of fish protein hydrolysates by ultrafiltration and nanofiltration: impact on peptidic populations, Desalination 244 (2009) 303-320
77. Y. Kiso, Y. Nishimura, T. Kitao, K. Nishimura, Rejection properties of non-phenylic pesticides with nanofiltration membranes, J. Membr.Sci. 171 (2000) 229–237.
78. Y. Kiso, Y. Sugiura, T. Kitao, K. Nishimura, Effects of hydrophobicity and molecular size on rejection of aromatic pesticides with nanofiltration membranes, J. Membr. Sci. 192 (2001) 1–10.
79. Y. Yoon, M. Richard, Removal of organic contaminants by RO and NF membranes, J. Membr.Sci. 261 (2005) 76–86.
80. H. Ozaki, H. Li, Rejection of organic compounds by ultra-low pressure reverse osmosis membrane, Water Res. 36 (2002) 123-130.
81. I. Sibille, L. Mathieu, J. Paquin, D. Gatel, J. Block, Microbial, characteristics of a distribution system fed with nanofiltered drinking water, Water Res. 31 (1997) 2318–2326.
82. K. Agbekodo, B. Legube, P. Cote, Organic in NF permeate, J. Am. Water Works Assn. 88 (1996) 67–74.
83. L.D. Nghiem, A.I. Schäfer, M. Elimelech, Removal of natural hormones by nanofiltration membranes: measurement, modeling, and mechanisms, Environ. Sci. Technol. 38 (2004) 1888–1896.
84. A.I Schäfer, L.D. Nghiem, T.D Waite, Removal of the natural hormone estrone from aqueous solutions using nanofiltration and reverse osmosis, J. Environ. Sci. Technol. 37 (2003) 182–188.
85. L. Raman, M. Cheryan, N. Rajogaopalan, Consider nanofiltration for membrane separations, Chem. Eng. Prog. 3 (1994) 68-69.
86. R. Rautenbach, A. Gröschl, Separation potential of nanofiltration membranes, Desalination 77 (1990) 73-84.

87. A. Szymczyk, M. Sbaï, P. Fievet and A. Vidonne, Transport Properties and Electrokinetic Characterization of an Amphoteric Nanofilter, Langmuir 22 (2006) 3910-3919.
88. T. Tsuru, D. Hironaka, T. Yoshioka and M. Asaeda, Titania membranes for liquid phase separation: effect of surface charge on flux, Sep. Purif. Technol. 25 (2001) 307-314.
89. J. Schaep and C. Vandecasteele, Evaluating the charge of nanofiltration membranes, J. Membr. Sci. 188 (2001) 129-136.
90. C. Labbez, P. Fievet, A. Szymczyk, A. Vidonne, A. Foissy and J. Pagetti, Analysis of the salt retention of a titania membrane using the "DSPM" model: effect of pH, salt concentration and nature, J. Membr. Sci. 208 (2002) 315-329.
91. B.Van der Bruggen and C. Vandecasteele, Removal of pollutants from surface water and groundwater by nanofiltration: overview of possible applications in the drinking water industry, Environ. Pollut. 122 (2003) 435–445.
92. V. Freger, T. Arnot and J. Howell, Separation of concentrated organic/inorganic salt mixtures by nanofiltration, J Membr Sci 178 (2000) 185–193.
93. A.Verliefde, S. Heijman, E. Cornelissen,G. Amy, B. Bruggen,J. Van Dijk, Rejection of trace organic pollutants with high pressure membranes (NF/RO), Environ. Prog. 27 (2008)180-188
94. L. Nghiem, A. Manis, K. Soldenhoff, A.I. Schäfer, Estrogenic hormone removal from wastewater using NF/RO membranes, J. Membr.Sci. 242 (2004) 37–45.
95. P. Lipp, F. Sacher, G. Baldauf, Removal of organic micro-pollutants during drinking water treatment by nanofiltration and reverse osmosis, Desalin. Water Treat. 13 (2010) 226-237
96. K. Kosutic and B. Kunst, Removal of organics from aqueous solutions by commercial RO and NF membranes of characterized porosities, Desalination 142 (2002) 47–56.
97. B.Van der Bruggen, J. Schaep, D. Wilms and C. Vandecasteele, Influence of molecular size, polarity and charge on the retention of organic molecules by nanofiltration, J. Membr. Sci. 156 (1999) 29–41.
98. B.Van der Bruggen and C. Vandecasteele, Removal of pollutants from surface water and groundwater by nanofiltration: overview of possible applications in the drinking water industry, Environ. Poll. 122 (2003) 435–445
99. B.Van der Bruggen and C. Vandecasteele, Modelling of the retention of uncharged molecules with nanofiltration, Water Res. 36 (2002)1360–1368.

100. S. Chellam and J. Taylor, Simplified analysis of contaminant rejection during ground- and surface water nanofiltration under the information collection rule, Water Res. 35 (2001) 2460–2474.

101. J. Schaep, B. Van der Bruggen, C. Vandecasteele and D. Wilms, Influence of ion size and charge in nanofiltration, Separ. Purif. Technol. 14 (1998) 155–162.

102. J. Peeters, Characterization of nanofiltration membranes, PhD Thesis, Twente University, Dordrecht (1997).

103. B. Chaufer, M. Baudry, L. Guihard, G. Daufin, Retention of ions in nanofiltration at various ionic strength, Desalination 104 (1996) 37-46.

104. R. Levenstein, D. Hasson and R. Semiat, Utilization of the Donnan effect for improving electrolyte separation with nanofiltration membranes, J. Membr. Sci. 116 (1996) 77-92

105. C.Wang, P. Ouyang, The possibility of separating saccharides from a NaCl solution by using nanofiltration in diafiltration mode, J. Membr. Sci. 204 (2002) 271-281

106. J. Bontha, P. Pintauro, Water orientation and ion solvation effects during multi-component salt partitioning in a nafion cation exchange membrane, Chem. Eng. Sci. 49 (1994) 3835-3851.

107. A. Fane, A. Awang, M. Bolko, R. Macoun, R. Schofield, Y. Shen and F. Zha, Metal recovery from waste water using membranes, Water Sci. Technol. 25 (1992) 5-18.

108. R. Macoun, Y. Shen, A. Fane and C. Fell, Nanofiltration theory and applications to ionic separations, Proceedings 9th Australian Engineering Conference, Newcastle, Australia, Chemical (1991) 398-405.

109. A. Lhassani, M. Rumeau, D. Benjelloun and M. Pontie, Selective demineralisation of water by nanofiltration application to the defluorination of brackish water, Water Res. 35 (2001) 3260–3264.

110. S. Alami-Younssi, A. Larbot, M. Persin, J. Sarrazin and L. Cot, Rejection of mineral salts in gamma alumina Nanofiltration membrane. Application to Environmental process, J. Membr. Sci. 102 (1995) 123-129.

111. F.G. Donnan, Theory of membrane equilibria and membrane potentials in the presence of non-dialysing electrolytes. A contribution to physical–chemical physiology, Z. Phys. Chem. 17 (1911) 572.

112. J. Gilron, N. Gara and O. Kedem, Experimental analysis of negative salt rejection in nanofiltration membranes, J. Membr. Sci. 185 (2001) 223–236.

113. P. Baticle, C. Kiefer, N. Lakchaf, A. Larbot, O. Leclerc, M. Persin, J. Sarrazin, Salt filtration on gamma aluminananofiltration membranes fired at two different temperatures, J. Memb. Sci. 135 (1997) 1.

114. http://en.wikipedia.org/wiki/Gibbs Donnan effect.

115. N. Saffaj, H. Loukili, A. Alami-Younssi, A. Albizane, M. Bouhria, M. Persin and A. Larbot, Filtration of solution containing heavy metals and dyes by means of ultrafiltration membranes deposited on support made of moroccan clay, Desalination 168 (2004) 301–306.

116. R. Liikanen, I. Miettinen and R. Laukkanen, Selection of NF membranes to improve quality of chemically treated surface water. Water Res. 37 (2003) 864–872.

117. X. Wang, T. Tsuru, S. Nakao and S. Kimura, The electrostatic and steric-hindrance model for the transport of charged solutes through nanofiltration membranes. J. Membr. Sci. 135 (1997) 19–32.

118. K. Agenson, J. Oh, T. Urase, Retention of a wide variety of organic pollutants by different nanofiltration/reverse osmosis membranes: Controlling parameters of process , J.Membr. Sci. 225 (2003) 91-103.

119. B. Levine, K. Madrireddi, V. Lazarova, M. Stenstrom and M. Suffet, Treatment of trace organic compounds by membrane processes: at the lake arrowhead water reuse pilot plant. Water Sci. Technol. 40 (1999) 293–302.

120. J. Huang, Q. Guo, H. Ohya, The characteristics of crosslinked PAA composite membrane for separation of aqueous organic solutions by reverse osmosis, J. Membr. Sci. 144 (1998) 1-11.

121. T. Matsuura, S. Sourirajan, Physicochemical criteria for reverse osmosis separation of monohydric and polyhydric alcohols in aqueous solutions using porous cellulose acetate membranes, J. Appl. Polym. Sci. 17 (1973) 1043.

122. T. Matsuura, S. Sourirajan, Physicochemical criteria for reverse osmosis separation of alcohols, phenols, and monocarboxylic mono-carboxylic acids in aqueous solutions using porous cellulose acetate membranes, J. Appl. Polym. Sci. 15 (1971) 2905.

123. T. Matsuura, S. Sourirajan, Reverse osmosis separation of organic acids in aqueous solutions using porous cellulose acetate membranes, J. Appl. Polym. Sci. 17 (1973) 3661-3683.

124. A. Schäfer, A. Fane and T. Waite, Fouling effects on rejection in the membrane filtration of natural waters, Desalination 131 (2000) 215–224.

125. K. Kosutic, L. Kunst and B. Kunst, Porosity of some commercial reverse osmosis and nanofiltration polyamide thin-film composite membranes, J. Membr. Sci. 168 (2000) 101–108.

126. I. Najm and R. Trussel, NDMA formation in water and wastewater, J. Am. Water Works Assoc. 93 (2001) 92–99.

127. M. Reinhard, N.L. Goodman, P.L. McCarty and D.G. Argo, Removing trace organics by reverse osmosis using cellulose acetate and polyamide membranes, J. Am. Water Works Assoc. 78 (1986) 163–174.

128. B. Van der Bruggen, J. Schaep, W. Maes, D. Wilms and C. Vandecasteele, Nanofiltration as a treatment method for the removal of pesticides from ground waters, Desalination 117 (1998) 139–147.

129. M. Richard, Y. Yoon, Removal of organic contaminants by RO and NF membranes, J. Membr. Sci. 261 (2005) 76–86.

130. C. Bellona, E. Drewes, P. Xu and G. Amy, Factors affecting the rejection of organic solutes during NF/RO treatment— a literature review, Water Research 38 (2004) 2795–2809.

131. T. Monthon, K. Yamamotob, O. Jeong, K. Chood, S. Choi, Rejection characteristics of organic and inorganic pollutants by ultra low-pressure nanofiltration of surface water for drinking water treatment, Desalination 145 (2002) 257-264.

132. H. Al-Zoubia, N. Hilala, N. Darwishb, A. Mohammadc, Rejection and modelling of sulphate and potassium salts by nanofiltration membranes: neural network and Spiegler–Kedem model, Desalination 206 (2007) 42–60.

133. J. Schaep, C. Vandecasteele, W. Mohammad and R. Bowen, Modelling the retention of ionic components for different nanofiltration membranes, Separ. Purif. Technol. 23 (2001) 169–179.

134. M. Afonso, G. Hagmeyer and R. Gimbel, Streaming potential measurements to assess the variation of nanofiltration membranes surface charge with the concentration of salt solutions. Separ. Purif. Technol. 23 (2001) 529–541.

135. A.Orecki, M. Tornaszewska, K. Karakulski, A.W. Morawski, Surface water treatment by the nanofiltration method, Desalination 162 (2004) 47-54.

136. G. Hagmeyer and R. Gimbel, Modelling the salt rejection of nanofiltration membranes for ternary ion mixtures and for single salts at different pH values, Desalination 117 (1998) 247–256.

137. N. Hilal ,H. Al-Zoubi , N. Darwish , A. Mohammad, Nanofiltration of Magnesium Chloride, Sodium Carbonate, and Calcium Sulphate in Salt Solutions, Sep. Sci. Technol. 40 (2005) 3299 – 3321.

138. L. Firdaous, F. Quemeneur, J. Schlumpf, J. Maleriat, Modification of the ionic composition of salt solutions by electrodialysis, Desalination 167 (2004) 397–402

139. S. Madaeni, V. Kazemi, Treatment of saturated brine in chlor-alkali process using membranes, Sep. Purificat. Tech. 61 (2007) 72–78

140. C. Kim, J. Kim, K. Lee, T. Tak, Preparation of soluble polyimides and ultrafiltration membrane performances. J. Appl. Polym. Sci. 75 (1999) 1-9.

141. I. Kim, K. Lee and T.Tan, Preparation and characterization of integrally skinned uncharged polyetherimide asymmetric nanofiltration membrane, J. Membr. Sci. 183 (2001) 235–247.

142. I. Kim, Y. Hyung, K. Lee, Formation of integrally skinned asymmetric polyetherimide nanofiltration membranes by phase inversion process, J. Appl. Polym. Sci. 84 (2002) 1300-1307.

143. S. Baoli, Q. Zhang, H. Zhang, Z. Liu, X. Zhang, Concentration of benzylpenicillin sodium by polyimide nanofiltration membrane J. Appl. Polym. Sci. 104 (2007) 3077-3081.

144. B. Chaoyi, J. Langer and J. Economy, Chemical modification of P84 copolyimide membranes by polyethylenimine for nanofiltration, J. Membr. Sci. 327 (2009) 49-58.

145. T. Takekoshi, Polyimides- Fundamentals and Applications, Ed. Ghosh, M.K. and Mittal, K.L., Marcel Dekker, New York, 1996, Chapter 2.

146. P. Hergenrother, K. Watsona, J. Smith , J. Connella, R. Yokota, Polyimides from 2, 3, 3, 4-biphenyltetracarboxylic dianhydride and aromatic diamines, Polymer 43 (2002) 5077–5093

147. T. Yamaguchi, Y. Miyazaki, S. Nakao, T. Tsuru, S. Kimura, Membrane Design for Pervaporation or Vapor Permeation Separation Using Filling-Type Membrane Concept, Ind. Eng. Chem. Res. 37 (1998) 177-184.

148. J. Jansen , M. Macchione , E. Drioli, High flux asymmetric gas separation membranes of modified poly(ether ether ketone) prepared by the dry phase inversion technique, J. Membr. Sci. 255 (2005) 167–180.

149. F. Tsai, D. Harding, S. Chen and T. Blantan, High-permeability fluorinated polyimide microcapsules by vapor deposition polymerization, Polymer 44 (2003) 995–1001.

150. R. Huang and X. Feng, Pervaporation of water ethanol mixtures by an aromatic polyetherimide membrane, Sep. Sci. Technol. 27 (1992) 1583- 1597.

151. Y. Wang, S. Huang, C. Hu, C. Li and K. Lee, Sorption and transport properties of gases in aromatic polyimide membranes, J. Membr. Sci. 248 (2005) 15–25.

152. H. Ohya, V. Kudryavtsev and S. Semenova, Editors, Polyimide membranes, applications, fabrications, and properties, Gordon and Breach Publishers, Amsterdam (1996).

153. M. Butt, Z. Akhtar, M. Zafar-uz-Zaman and A. Munir, Synthesis and characterization of some novel aromatic polyimides, Euro. Polym. J 41 (2005) 1638–1646.

154. S. Stern, Polymers for gas separation; the next decade, J. Membr. Sci. 94 (1994) 1–65.

155. H. Hennepe, D. Bargeman, M Mulder and C. Smolders, Zeolite-filled silicone rubber membranes. Part 1. Membrane preparation and pervaporation results, J. Membr. Sci. 35 (1987) 39-55.

156. M. Goldman, D. Frankel and G. Levin, zeolite/polymer membrane for the separation of ethanol-water azeotrope, J. Appl. Polym. Sci. 37 (1989) 1791-1800.

157. J. Lizhong, W.Wencai, W. Xiaowein, W. Dezhen, J. Riguang, Effect of water on the preparation, morphology and properties of polyimide/silica nanocomposite films prepared by sol-gel process, Wiley Inter Science (2006).

158. G. Eastmond,J. Paprotny**,** Scope on the synthesis and properties of poly(etherimide)s, Reactive & Functional Polymers 30 (1996) 27-41.

159. F.W. Altena, C. Smolders, Calculation of liquid-liquid phase separation in a ternary system of a polymer in a mixture of a solvent and a nonsolvent, Macromolecules 15 (1982) 1493-1497.

160. M. Frommer, M. A.; Lancet, D, In “Reverse Osmosis Membrane Research”; Lonsdale, H. K.; Podall, H. E., Eds.; Plenum Press: New York (1972) 85.

161. Baker, R.W. ; Cussler, E.L. ; Eykamp, W. ; Koros, W.J. ; Riley, R.L. ; Strathman, R.H., Membrane separation systems: recent developments and future directions, ndc, Membrane Technology and Research, Noyes Publications, Mill Road at Grand Ave., Park Ridge, NJ 07656 (USA) 1991.

162. P. Witte , P. Dijkstra, J. Berg, J. Feijen , Review Phase separation processes in polymer solutions in relation to membrane formation, J. Membr. Sci. 117 (1996) 1-31.

163. H. Strathmann, Production of microporous media by phase inversion processes, ACS Symp. Ser., 269 (1985) 165-195.

164. H. Strathmann and K. Koch, The formation mechanism of phase inversion membranes, Desalination, 21 (1977) 241-255.

165. J. Wijmans and C. Smolders, Preparation of asymmetric membranes by the phase inversion process, in H.K. Londsdale and M.H. Pinho (Eds.), Synthetic Membranes: Science, Engineering and Applications, Reidel, Dordrecht, The Netherlands, 1986, pp. 39-56.

166. L. Zeman and T. Fraser, Formation of air-cast cellulose acetate membranes. Part I. Study of macrovoid formation, J. Membr. Sci. 84 (1993) 93-106.

167. L. Zeman and T. Fraser, Formation of air-cast cellulose acetate membranes. Part II. Kinetics of demixing and microvoid growth, J. Membr. Sci. 87 (1994) 267-279.

168. K. Scott, R. Hughes, Industrial membrane separation technology, London: Blackie Academic & Professional, Springer; ISBN-13: 978-0751403381, 1996.

169. M. Loeb, S. Sourirajan, Sea water demineralization by means of an osmotic membrane, Adv. Chem. Ser. 38 (1962) 117.

170. K. Chun, S. Jang, H. Kim, Y. Kim, H. Han, Y. Joe, Effects of solvent on the pore formation in asymmetric 6FDA–4,40ODA polyimide membrane: terms of thermodynamics, precipitation kinetics, and physical factors. J. Membr. Sci. 169 (2000) 197–214.

171. A. Dyukevick, T. Yatskova, Compaction on ultrafiltration membrane under the effect of working pressure, Khim.Tekhnol.Vody. 13 (1991) 544-547.

172. A. Bulte, E. Naafs, F. Eeten, M. Mulder, C. Smolders, H. Strathmann, Equilibrium thermodynamics of the ternary membrane- forming system nylon, formic acid and water, Polymer 37 (1996) 1647- 1655.

173. A. El-Gendi, S. Ahmed, H. Talaat, Preparation and evaluation of flat membranes for phenols separation, Desalination 206 (2007) 226-237.

174. A. Ismail, L. Yean, Review on the Development of Defect-Free and Ultrathin-Skinned Asymmetric Membranes for Gas Separation through Manipulation of Phase Inversion and Rheological Factors, J. Appl.Polym.Sci. 88 (2003) 442–451.

175. P.J. Flory, Principles of Polymer Chemistry, Cornell University Press, Ithaca, NY, 1969.

176. J. Wijmans, J. Baaij and C. Smolders, The mechanism of formation of microporous or skinned membranes produced by immersion precipitation, J. Membr. Sci. 14 (1983) 263-274.

177. M. Frommer, I. Feiner, O. Kedem and R. Bloch, The mechanism for formation of "skinned" membranes. II. Equilibrium properties and osmotic flows determining membrane structure , Desalination 7 (1970) 393-402.

178. C. Smolders, L. Broens, F. Altena, D. Koenhen, Asymmetric membrane structures as a result of phase separation phenomena, Desalination 32 (1980) 33- 45.

179. D. Koenhen, M.H.V. Mulder and C.A. Smolders, Phase separation phenomena during the formation of asymmetric membranes, J. Appl. Polym. Sci. 21 (1977) 199.

180. H. Bokhorst, F. Altena and C. Smolders, Formation of asymmetric cellulose acetate membranes, Desalination 38 (1981) 349-360.

181. A. Bottino, G. Roda, G. Capannelli, S.Munari, The formation of microporous polyvinylidene difluoride membranes by phase separation, J. Membr. Sci 57(1991) 1-20.

182. I. Kim, H. Yoon, K. Lee, Formation of integrally skinned asymmetric polyetherimide nanofiltration membranes by phase inversion process, J. Appl. Polym. Sci. 84 (2002) 1300-1307.

183. J. Shieh and Tai-Shung Chung, Phase-Inversion Poly(etherimide) Membranes Prepared from Water-Miscible/Immiscible Mixture Solvents, Ind. Eng. Chem. Res. 38 (1999) 2650–2658.

184. C. Smolders, A. Reuvers, R. Boom, I.. Wienk, Microstructures in phase inversion membranes. Part 1. Formation of macrovoids, J. Membr. Sci. 73 (1992) 259–275.

185. M. Amirilargani, M. Sadrzadeh, T. Mohammadi, Synthesis and characterization of polyethersulfone membranes, J. Polym. Res. 17 (2010) 363–377.

186. E.Saljoughi, M. Sadrzadeh, T. Mohammadi, Effect of preparation variables on morphology and pure water permeation flux through asymmetric cellulose acetate membranes, J. Membr.Sci. 326 (2009) 627–634.

187. L.Y. Lait, F.C. Lin, T.T. Wu, D.M. Wang, on the formation of macrovoids in PMMA membranes, J. Membr.Sci. 72 (1999) 31-43.

188. M. Frommer, R. Messalam, Mechanism of Membrane Formation. VI. Convective Flows and Large Void Formation during Membrane Precipitation, Ind. Eng. Chem., Prod. Res. Dev. 12 (1973) 328-333.

189. H. Strathmann, K. Kock, P. Amar, R. Baker, the Formation Mechanism of Asymmetric Membranes, Desalination 16 *(*1975) 179-203.

190. N. Tanihara, N. Umeo, T. Kawabata, K. Tanaka, H. Kita, K. Okamoto, Pervaporation of organic liquid mixtures through poly(ether imide) segmented copolymer membranes, J. Membr. Sci. 104 (1995) 181-192.

191. X. Yu, C. Song, C. Li, S.L. Cooper, Polyether-polyimide thermoplastic elastomers. I. Synthesis and properties, J. Appl. Polym. Sci. 44 (1992) 409-417.

192. M. Kréa, D.Roizard, N. Moulai-Mostefa, D.Sacco, New copolyimide membranes with high siloxane content designed to remove polar organics from water by pervaporation, J. Membr. Sci. 241 (2004) 55-64.

Chapter (2)

Materials and Methods

Table of contents Chapter 2

Chapter (2) *123*

Materials and Methods *123*

2.1 Materials and Methods *123*

2.1.1 Materials *123*

2.1.2 Part 1: Preparation of PEI and Kapton™ membranes *124*

2.2 Part 2: Membrane characterizations *132*

2.2.1 Phase diagram *132*

2.2.2 Scanning electron microscopy (SEM) *134*

2.2.3 Thermo-mechanical property *134*

2.2.4 Thermo-gravimetric analysis (TGA) *134*

2.2.5 FTIR characterizations *135*

2.2.6 Swelling properties *135*

2.3 Part 3: Separation properties *136*

2.3.1 Pervaporation (PV) experiments *136*

2.3.2 Nanofiltration (NF) system experiments *143*

2.3.3 Characteristic flow rates of NF set-up *150*

References chapter 2 ..... *154*

Chapter (2)

Materials and Methods

This chapter describes the adopted experimental program for investigating the parameters affecting the preparation of polyetherimide (PEI) membrane by phase inversion. The membrane characterization and the performance evaluation of the casted membrane are also outlined. This chapter represents the description of the basic laboratory devices, raw materials, chemicals and the methodology adopted for membrane preparation and performance evaluation under the investigated conditions.

2.1 Materials and Methods

2.1.1 Materials

Jeffamine® ED-600 (Jeff), an α-,ω alkoxyether diamine of average Mw=600g/mol, was purchased from Aldrich; others monomers 4,4'-oxydianiline (ODA), 1,2,4,5-benzenetetracarboxylic anhydride (PMDA) were purchased from Acros Organics Inc. and Fluka Chemical Corp. N,N-dimethylformamide (DMF) was obtained from Aldrich, purified and stored over molecular sieves (4 Å). Commercial Kapton precursor poly(amic acid) (PAA) 11 wt% solution in NMP/ aromatic hydrocarbon and 15 wt% solution in NMP were purchased from Aldrich. The characteristics of different raw materials are presented in table 1.2 and figure 1.2.

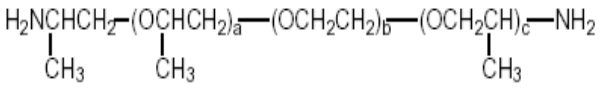

Jeffamine ED-600

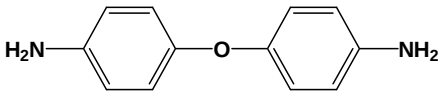

ODA

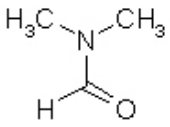

N,N-Diméthylformamide (DMF)

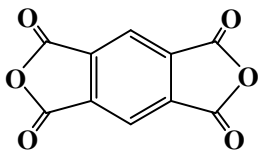

PMDA

Figure 1.2: Chemical structures of the raw materials

Table 1.2: Characteristics of different raw materials

Reagent	***Source***	***Formula***	***Molecular weight (g/mol)***	***Density(g/ml)***	***Boiling point/ Melting point***
4,4' Oxydianiline (ODA)	Acros Organics , Fluka and Aldrich	$C_{12}H_{12}ON_2$	*200.24*	1.166	*190-192°C*
1,2,4,5-Benzenetetracarboxylic anhydride (PMDA)	Acros Organics. and Fluka Chemical Corp	$C_{10}H_2O_6$	*218.12*	1.68	*283-286°C*
N,N-dimethylformamide (DMF)	Aldrich	C_3H_7NO	*73.10*	*0.944*	*153°C*
Jeffamine® ED-600 (Jeff)	Aldrich	C_3H_9NO	600	1.056	m.p 22
Kapton (PAA 11%, PAA 15%)	Aldrich				174

2.1.2 Part 1: Preparation of PEI and Kapton™ membranes

Fortunately, membranes can be prepared from a large number of different materials. Moreover, a large number of preparation techniques exist which enable a membrane to be constructed from a given material. Typically, the kind of technique employed depends mainly on the material used and on the desired membrane morphology which in turn is dependent on the separation problem. To be effective for separation, membrane materials should ideally possess the following properties:

- Mechanical stability,
- Chemical resistance to feed,
- Stable operation,

- Thermal stability,
- High permeability,
- High selectivity.

In this part, the preperation of PEI and Kapton™ membranes are reported by phase inversion to prepare asymmetric membranes following the two steps mechanism; the dense membrane used as a reference is also reported.

2.1.2.1 Preparation of PEI dense and asymmetric membranes

Standard operating conditions:

- Solvents are dried on sieve 4 Å several days. All the synthesis were carried out at ambient temperature, under Argon atmosphere.
- To investigate the different factors affecting the preparation of membrane by casting, the following considerations have been emphasized:
  - The PAA polymer solution should not be stored for long period.
  - Before casting, the polymer solution should be degassed by vacuum.
  - Mixing of polymer solution should be completed when other additives were added.
  - Glass support should be cleaned very carefully.

2.1.2.1.1 Preparation of PEI dense membrane.

The amine ratio 0.4/0.6 allowed the preparation of asymmetric membranes of good mechanical properties to be used further in pervaporation and nanofiltration. For the others PAA having higher than 0.4 Jeffamine® contents, despite the variations of the phase inversion conditions, i.e. polymer dope concentration, concentration time, coagulation bath temperature, liquid film thickness, it was not possible to prepare reproducible asymmetric films usable in pervaporation or nanofiltration experiments, so we prepare dense and asymmetric PEI membranes with amine ratio 0.4/0.6. The preparation of PEI dense membranes by two synthesis steps is described and shown in the figure 2.2 as follow:

i. Preparation of casting PAA solution (Argon, room temperature)

The polyamic acid (PAA: PAA solution Jeff600-PMDA-ODA (0.4/1/0.6), 30 wt% in DMF is prepared in the first step by solubilisation of Jeffamine in DMF (a solution of 15wt.% of solid), then the anhydride (PMDA) is added very slowly in solid form; the reaction time is 5 hours under magnetic stirring (IR control). Finally, the aromatic amine (ODA) is added in solid form to the reaction medium and the reaction is stopped after 36h. The structure of PAA prepared is shown in figure 2.2.

Example for synthesis of PAA solution Jeff600-PMDA-ODA (0.4/1/0.6), 30 wt% in DMF:

- 0.4 mmole of Jeffamine 600 (0.4*600*1/100) = 2.4g) in DMF (4 g)
- +1mmol of PMDA (1*218.12*1/100)= 2.18g) in DMF(6g).
- after 5h + 0.6 mmol ODA (0.6*200.24*1/100)=1.20043g) in DMF (3.26 g).
- Quantities: monomers: 5.78004g; solvent: 13.26 g
- Concentration PAA solution in weight= 5.78/(13.66+5.78)= 30 wt.%

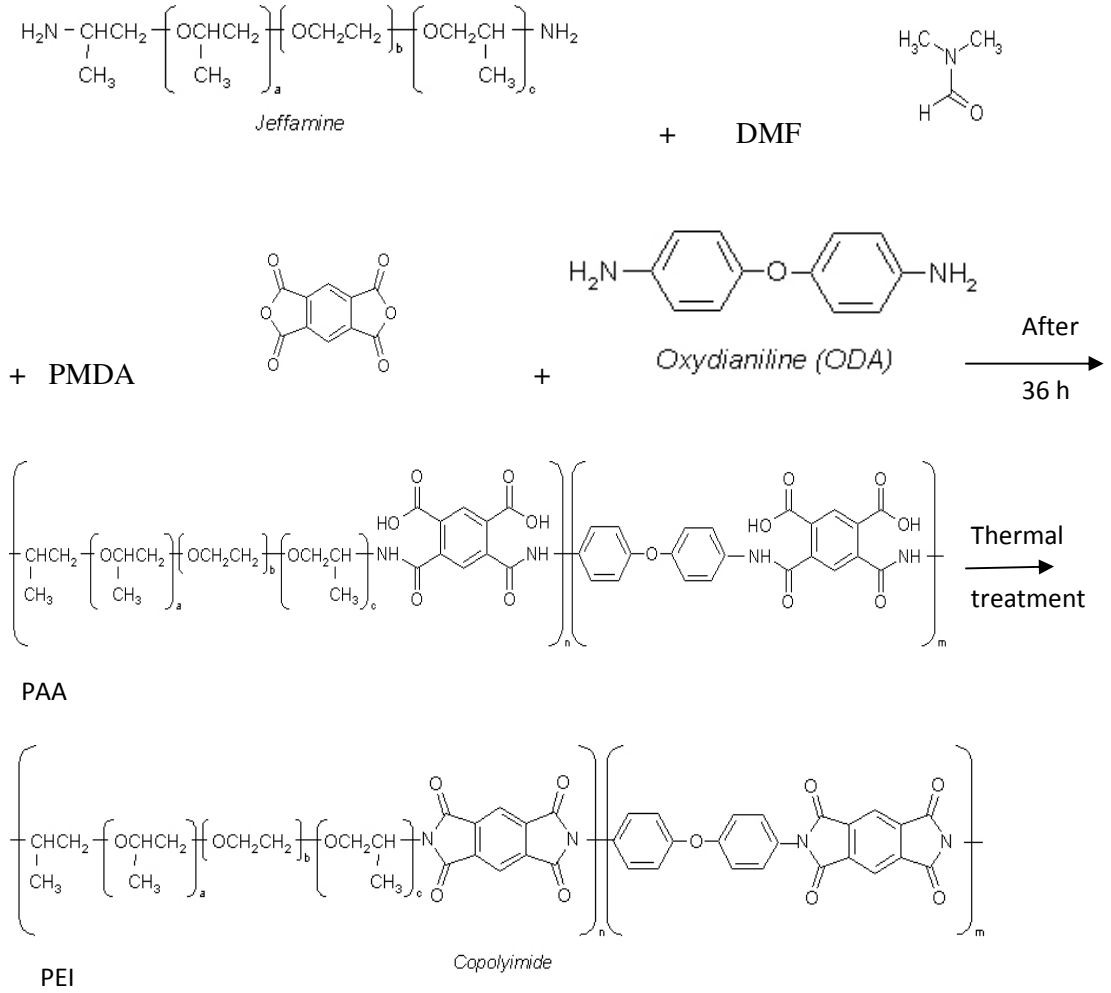

Figure 2.2: PAA and PEI synthesis with two steps mechanism

ii. Casting step

The casting step can be induced by two different methods:

Method 1: Thin liquid films of PAA were cast on glass plates using a film applicator (Fig.3.2). Then these films were placed into a dryer for 12 h at 80 °C to remove most of the solvent. The remaining solvent is then removed using vacuum.

Method 2: The PAA solution is casted on glass plates (carriers) by using film applicator with drawdown thickness 100- 500 µ m to form flat sheets films. These liquid films are preserved at ambient temperature from 1 to 3 days to be sure that the evaporation of the solvent from the casted film is completed.

It was found that the mechanical property of films prepared by method 1 is better than the films prepared by method 2.

iii. Cyclization step

Thermal conversion of the PAA membranes to the corresponding polyimides was performed by heating in a vacuum oven for 3 h, successively at 100 (1h), 150 (1h) and 200 °C (1h). At last dense slightly yellow films with good mechanical properties were obtained; this colour does not changed with time, up to several months meaning no oxidation seems to occur.

. The structure of PEI prepared are shown in figure 2.2.

The obtained PEI is composed of two different blocks:

- An aliphatic block: it is a soft block which gives flexibility to the polymer
- An aromatic block:it is a rigid block which gives good mechanical property to the polymer

2.1.2.1.2 Preparation of asymmetric polyimide membranes

The preparation of asymmetric polyimide membranes by the wet phase inversion procedure is described below and shown in the figure 3.2.

I. Preparation of casting solution [Mixing step]

The polyamic acid (PAA) was prepared by solution condensation polymerization at ambient temperature as described before in the first step of dense membrane preparation. Before casting, the PAA solution must be carefully degassed to avoid the formation of bubbles in the liquid films.

II. Casting Step

The polymer solution is casted on glass plates (carriers) by using film applicator with drawdown thickness 100-500 µm to form flat sheets films having wet thickness of about 100-500 µm at a time ranges from (1– 3) minute as pre-concentration step.

III. Immersion Step

The glass plates are immersed into a coagulating bath (volume= 5liters) containing pure water at controlled temperature (5 to 20 ^{0} C) for a duration varying from (60 to180) min. The coagulation occurs immediately with in water bath; the PAA precipitates as a white-pale yellow film.

IV. Drying Step

The casted flat sheets were dryed in the air (several hours) at ambient temperature.

V. Cyclization step

The cyclization of the casted PAA films to the corresponding polyimide PEI are carried out by heating during 1 H at the respective temperatures of 100, 150, and 200 ^{0} C under vacuum.

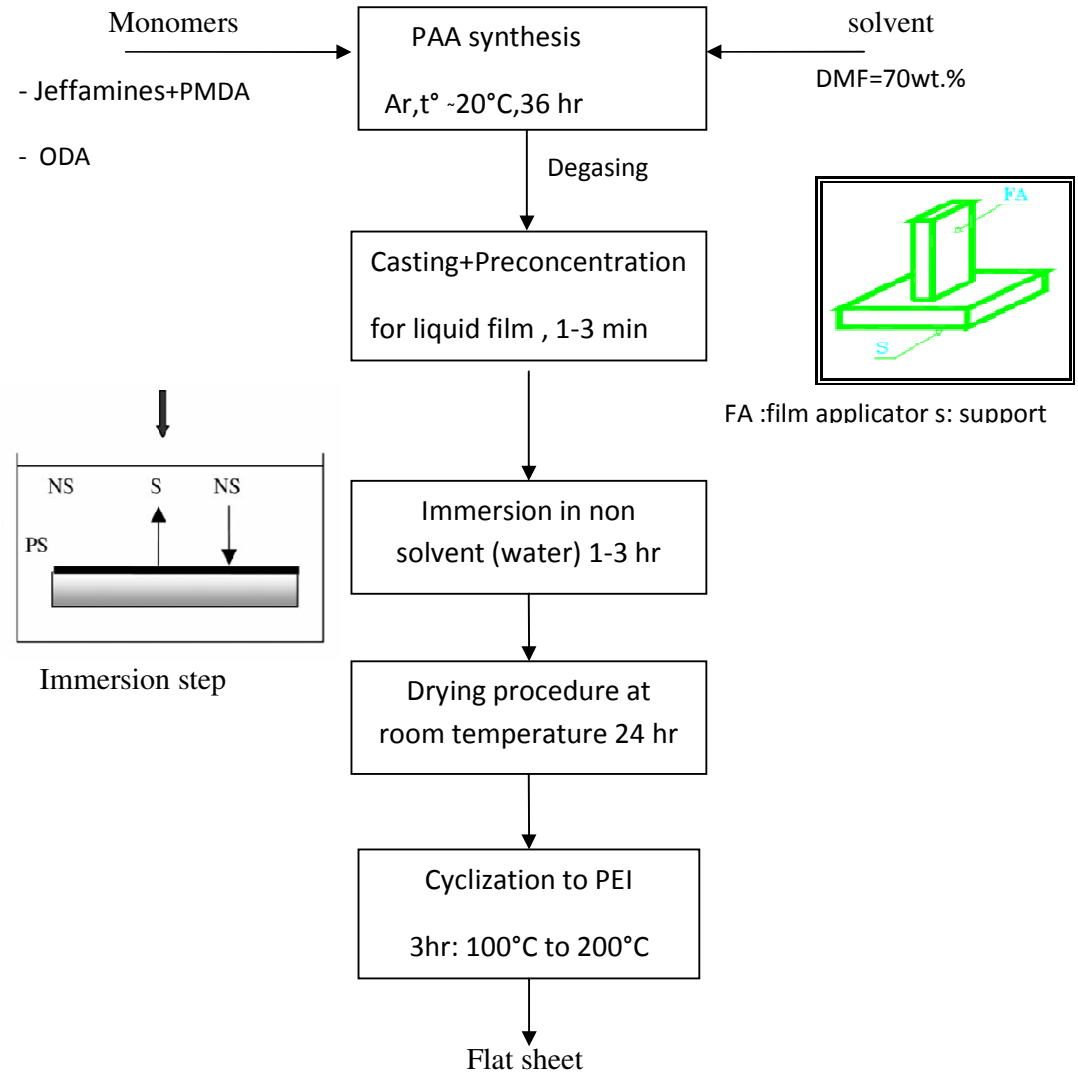

Figure 3.2: Process flow sheet for asymmetric PEI membranes preparation.

The effect of several parameters on the morphology of the PAA and PEI films was studied as follows:

- The initial PAA concentration
- The evaporation delay (pre-concentration step), ranging from 1 to 3 minutes
- Effect of addition of small quantities of water to PAA solution.
- Effect of additives in the coagulant water bath (DMF, ethanol,…)
- Effect of addition of co-solvents to PAA solution such as toluene.
- The type of non solvent of the coagulant bath
- The time of immersion, ranging from 1 to 3h.
- Coagulation bath temperature
- Using different immersion bath in series.

2.1.2.2 Preparation of Kapton™ (PI) asymmetric and dense membranes

2.1.2.2.1 Preparation of Kapton™ dense membrane

Kapton™ (PI) dense polyimide membranes are prepared by two steps as described below; using commercial Kapton precursor poly(amic acid) (PAA) solution of 11 wt% in NMP/ aromatic hydrocarbon.

I. Casting step

Thin liquid films of commercial PAA were casted on glass plates using a film applicator.Then these films were placed into a dryer at least 12 h at 80 °C to remove most of the solvent.

II. Cyclization step

Kapton™ dense membranes were obtained with a thermal treatment up to 300°C in a vacuum oven for 3 h, successively. At last dense slightly yellow films with good mechanical properties were obtained.

2.1.2.2.2 Preparation of asymmetric Kapton™ (PI) membranes.

The so-called wet phase inversion method was used to induce the formation of homogenous asymmetric Kapton™ membranes with water as a non-solvent. The Kapton precursor poly(amic acid) (PAA) solution of 15 wt% in NMP solution was casted onto a glass substrate using a film applicator before immersion in a water bath to produce phase inversion. Then, Kapton™ membranes were obtained with a thermal treatment up to 300°C in a vacuum oven for 3 h.

2.1.2.3 Asymmetric PEI membranes preparation with mechanical support

The aim is to improve the mechanical properties of thin asymmetric PEI membranes for nanofiltration (NF) experiments.

Two types of porous support without dense layer are prepared:

1- PEI symmetric support from (i.e: PAA 20 wt% in DMF +10 wt % water)

2- Kapton symmetric support which is prepared from commercial PAA 11% in NMP/ aromatics

General procedure for preparing PEI asymmetric membranes with support:

1. Casting of PAA at ambient temperature (coating liquid thickness: 300 microns for PEI; 500 microns for Kapton).
2. Drying time in air for 1 min.
3. Then immersion in pure water at 10°C during 1h, to get asymmetric porous PAA films.
3. Drying at ambient temperature in air for the PAA membranes, and supports.
4. Curing under vacuum 1 h at 100 ^{0}C ,150 ^{0}C and 200 ^{0}C for the PEI membranes and PEI support.
5. For Kapton support the curing treatments under vacuum lasted 3 h up to 300 ^{0}C.
6. Coating of the second PAA layer.

2.1.2.4 Preparation of the hybrid silica- PEI membranes

The modification of polymers properties by changing the structure and/or chemical characteristics has been also studied with the synthesis of hybrid membranes constituted of two different matrices (inorganic and organic).

In this part, we intended to study the properties of some hybrid Polyetherimide (PEI). The dense membrane PEI Jeffamine-PMDA-ODA is a reference for all our studies. To improve the properties of the PEI membrane separation, various modifications were made. These modifications concern three different aspects of the membrane:

• **Morphology**: preparation of the asymmetric membranes by phase inversion.

• **The chemical nature**: preparation of hybrid membranes by the incorporation of silica particles in the polymer matrix. In our case these inorganic particles have been introduced either directly using SiO_2 nanoparticles or generated in situ from the TMOS sol-gel process.

• **The chemical architecture**: by changing the proportions of the amines used (Jeffamine,ODA).

2.1.2.4.1 The aim of work in this part.

The effect of using either SiO_2 fillers or inorganic silica precursors, i.e. TMOS by the sol-gel technique on the morphology and transport properties of a polyimide film was studied.

2.1.2.4.2 Material

PAA(Jeff600-PMDA-ODA (0.4/1/0.6) Concentration= 15-30 wt% in DMF, fumed silica was used nanoparticles (AEROSIL 200; 12 nm hydrophilic) Evonik-Degussa Chemicals, Germany and tetramethyl orthosilicate (TMOS; >99%; Sigma-Aldrich Inc.).

2.1.2.4.3 Methods

Two methods were used to get polyimide-silica hybrid membranes with SiO_2 particles. The first one consists to mix the PAA solution and SiO_2 powders, using hydrophilic nanoparticles (12 nm hydrophilic). The second one uses the sol-gel process with addition of tetramethoxysilane (TMOS) to PAA solution stirred for 6 h at 80°C. Then the hybrid dense and asymmetric PAA membranes were imidized to PEI as described before.

The sol–gel process consists of a two-step reaction, hydrolysis/condensation, as shown in figure 4.2.

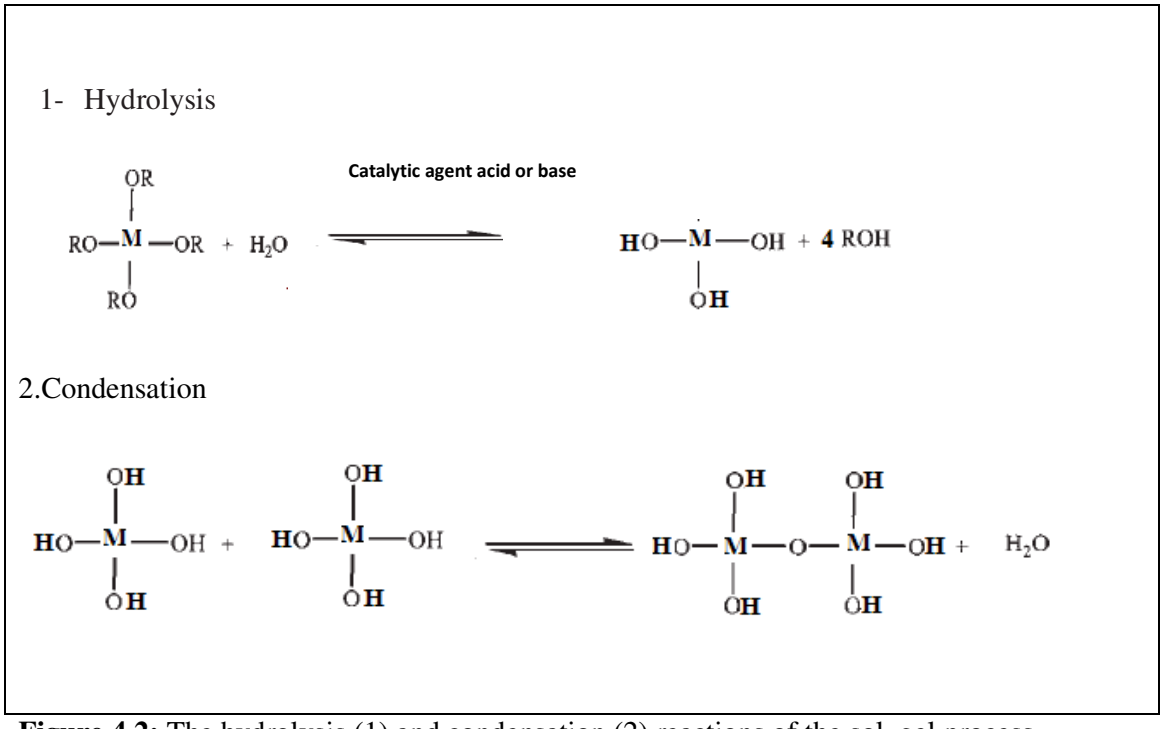

Figure 4.2: The hydrolysis (1) and condensation (2) reactions of the sol–gel process.

2.2 Part 2: Membrane characterizations

2.2.1 Phase diagram

In the ternary phase diagram (polymer (p)/solvent (s)/nonsolvent (ns)) a miscibility gap with metastable regions exists. According to the theory of phase separation three modes of phase separation can take place in such ternary system: nucleation and growth of the polymer lean phase, spinodal phase separation and nucleation and growth of the polymer rich phase. Since polymer is one of the components of the ternary system, solidification of a part of the system can take place.

2.2.1.1 Phase diagram and the determination of the binodal demixing curve by alternating addition of nonsolvent (cloud point, ○) and solvent (clearing point, ●) to the polymer solution [1].

Phase diagrams of the PAA/DMF/water systems could be obtained by drop-wise addition of alternatingly nonsolvent and solvent under continuous stirring, as shown schematically in Fig.5.2. The cloud point was observed visually by sudden occurrence of turbidity (upon water addition) or by sudden clearing of the mixture (upon solvent addition).

To perform the titration technique, distilled water was slowly added into the PAA solution (30 wt.% in DMF) under continus stirring. During titration, the solution temperature was controlled at 10°C with a water bath. The addition of pure water was continued until the clear polymer solution visually turned to a cloudy solution. After observation of the first sign of turbidity, addition of nonsolvent was stopped and the cloudy solution was agitated for an additional 20-60 min to see whether the turbid solution changes to a clear solution or not. If the cloudy solution (milky like) turned to a clear solution, more nonsolvent was added, otherwise the determined point was considered as the onset of real cloud point. Then, the pure solvent (DMF) was added until the cloudy polymer solution visually turned to clear solution.The composition of each point was then determined by the amount of nonsolvent, solvent, and polymer present in the bottle .

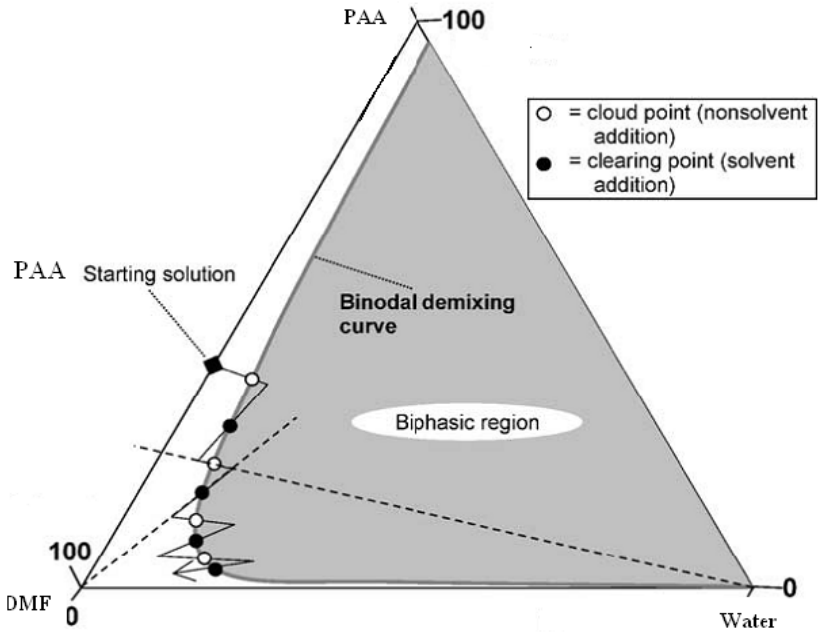

Figure 5.2: Schematic representation of the phase diagram and the determination of the binodal demixing curve.

2.2.1.2 Determination of turbid points values and phase diagrams

In this work we intended to study PAA/DMF/water (non solvent) systems to report the agreement between experimental work to get asymmetric PEI membranes and the ternary phase diagram miscibility gaps for the evaluations of a membrane-forming system**.** The phase diagram of the polymer/solvent/nonsolvent combinations systems was determined by cloud point measurement. Hence**,** the ternary phase diagram (turbid points curve) was obtained by the following method: PAA solutions with different compositions were placed in glass-ware reactor under stirring and the coagulant were slowly added to the PAA solutions until the clear solutions remain milky-like. For this purpose, starting polymer solutions with concentrations of 1, 2, 5, 10, 20, and 30 wt% PAA in DMF were used in the glass-ware reactor. To achieve homogeneous polymer solutions, these mixtures were stirred by a magnetic stirrer. The ternary phase diagram was obtained from the turbid points.

To reach the turbid point, distilled water was added slowly into the polymer solution under stirring. During titration, the solution temperature was controlled at 10°C with water bath and the addition of pure water was continued until the clear polymer solution visually turned to look milky-like. After observation of the first sign of turbidity, addition of nonsolvent was stopped and the solution was stirred for an additional 40 min to see whether the turbid solution changes to a clear solution or not. If the solution turned to a clear solution,

more nonsolvent was added, otherwise the determined point was considered as the onset of real turbid point.The ternary composition of turbid point was then calculated from the amount of nonsolvent, solvent and polymer present in the glass-ware.

2.2.2 Scanning electron microscopy (SEM)

Scanning electron microscopy (SEM) was used to characterize the morphology of the dense and asymmetric membranes. The samples were prepared by freeze cut in liquid nitrogen and metalized with gold using polaron sputter coater with magnetron head before SEM examination (Gold sputtering device: Jeol JFC-11-E, SEM: Jeol JSM-T330A). The registered pictures show the membrane morphology views of cross-sections.

2.2.3 Thermo-mechanical property

Tensile strength of PEI and PI were measured by using an Instron Tensile Tester 5569 (universal tensile testing machine). The mechanical properties of PEI prepared were determined using test specimens (length 23mm, width 8mm, area 50mm^2). The test specimens were prepared as the standard method. These specimens are cut from PEI and PI films with thicknesses of approximately 200 μm. Young modules, tensile stress and elongation at break are reported the average of several measurements (at least 3).

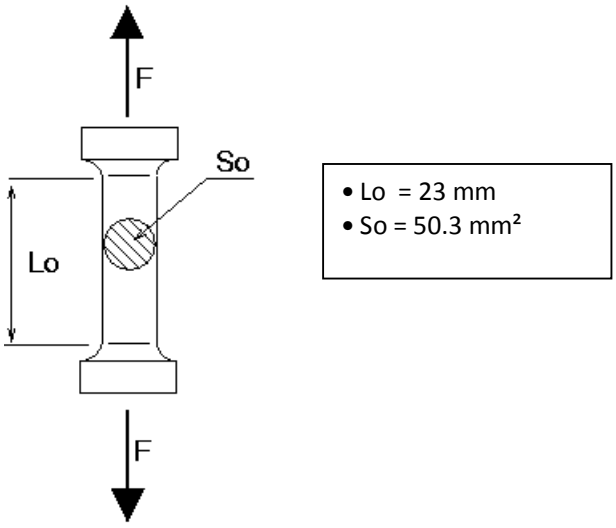

Figure 6.2: Shape and dimensions of PEI and PI specimens used in mechanical testing.

2.2.4 Thermo-gravimetric analysis (TGA)

Thermo-gravimetric analysis (TGA) was conducted with a SETARAM, Setsys TG-12 System at a heating rate of 10 °C/ min. The thermal stability and the loss of 10 wt% of the

PEI and Kapton™ as a function of temperature were evaluated using a magnetic microbalance of high accuracy 2.10^{-6}g. The PEI samples were cut from the prepared membranes and dried under vacuum. The TGA measurements were carried out in nitrogen atmosphere from 30 to 1000^0C at a heating rate of 10^0C / min.

2.2.5 FTIR characterizations

The poly(amic acid), the polyetherimide and Kapton™ synthesis steps were analyzed by FT-IR spectroscopy using a Thermo Nicolet 370 (FT-IR) using ATR method. The main attributions of the wavenumbers (cm^{-1}) are as follows. Poly(amic acid) (PAA). 2400-3200: O-H (COOH) and NH_2; 1660, 1700, 1710, 1735, 1775, 1780 and 1340, 1370, 1380: C=O group vibrations; 1600: CONH amide deformation; Polyetherimide (PEI). 1500: C-N; 1230, 1240, and 1260: C-O-C; 811 and 720: CO imide.

2.2.6 Swelling properties

The membrane swelling degrees were determined under steady-state conditions. Well dried samples were precisely weighed and then immerged into liquids at room temperature until swelling equilibrium was reached. From time to time, the swollen samples were removed from solvent, quickly wiped of excess solvent with tissue paper and immediately weighed in a close flask. The initial sample weight, recorded before immersion, is noted as Wd and the final sample weight noted as Ws.

The swelling degree at equilibrium was calculated according to the formula:

$$\text{Swelling degree } (\%) = 100.\ (Ws - Wd) / Wd \quad [1.2]$$

2.2.7 Membrane porosity measurement

Porosity of asymmetric PEI membranes was measured. Membrane porosity plays an important role in describing its performance. In order to evaluate porosity of the membranes, they were initially impregnated with water then weighed after wiping superficial water with filter papers. After that, the wet membranes were placed in an air-circulating oven at 80°C for 24h to be completely dried and finally, the dry membranes were weighed. The porosity of membranes was calculated using the following equation [**2**]:

$$P\ (\%) = 10000 * [(W_O - W_1)/ V] \quad [2.2]$$

Where P is the membrane porosity; W_O and W_1 are the weights of wet and dry membranes (g), respectively; V= A*t where A is the membrane surface area (cm^2) and t is the membrane

thickness (cm). In order to minimize the experimental errors, the membrane porosity of each sample was measured several times and the results were reported in average.

Other method used to get Porosity for asymmetric membrane based in its density:

P_d (%) = 100*(V- V_d/V) [3.2]

V_d = W_1/ density of PEI= volume of PEI dense membrane has the same weight of asymmetric membrane, density of PEI=1.15 gm/cm^3 (obtained by He pycnometry), volume of pore= V- V_d.

2.3 Part 3: Separation properties

It is obvious that, the requirements for separations in the process industries are many although they can be classed generally into two areas, those where materials are present as a number of phases and those where species are dissolved in a single phase. Fortunately, membranes separation process can be used to achieve both types of separations through their ability to perform one or more of the following functions:

- Prevent permeation of certain species,
- Change the composition of a solution,
- Regulate permeation of certain species,
- Chemically or physically properties that effect of a permeating species.

Transport of selected species through the membrane is achieved by applying a driving force across the membrane. This gives a broad classification of membrane separation in the way or mechanism by which material is transported across a membrane. The driving forces are either pressure, concentration, temperature or electrical potential. In many cases the transport rate (permeation) is proportional to the driving force.

In this part the prepared PEI and Kapton membranes were tested by pervaporation (PV) and nanofiltration (NF) to characterize the separation properties of the dense and asymmetric membranes.

2.3.1 Pervaporation (PV) experiments

PV Experiments with mixtures of organic-organic (toluene/ heptane), and water/ alcohols were carried out to characterize the separation properties of the dense and asymmetric membranes. All the experiments were carried out under steady state conditions with a downstream vacuum of 1mmHg, keeping the temperature constant for feed mixtures. The composition of the permeate trapped in liquid nitrogen was determined by gas chromatography (FID- TCD; columns used, Mark 102G). For each mixture, the permeate enrichment and flux of permeation (J) were measured for several membrane samples (specific

membrane area of 2.1 10^{-3} m^2). A feed tank with a magnetic stirrer of 100 cm^3 capacity was used for the pure liquids or the mixtures at different wt % respectively. The effect of the temperature on the membrane performances was studied in the range 30 to 70 °C. The downstream side pressure of the process was maintained at 1 mbar with a vacuum pump. For each experiment with pure solvent, experiments were carried out for a minimum of 7 days. The weight of permeate was determined using a precise balance ($\pm 10^{-3}$ mg). Each experiment was repeated several times and the results were averaged to minimize the errors. The PV set-up is shown in Fig.7.2.

Te pervaporation performances were evaluated by the separation factor (α) and total flux (*J*). The separation factor is defined by

$$\alpha = (Y_i * X_j)/(X_i * Y_j) \qquad [4.2]$$

Where;

Y_i: represent the weight fractions of the fastest compound in the permeate (toluene, water)

Y_j: represent the weight fractions of the slowest compound in the permeate (heptane, alcohols)

and X_i , X_j represent the weight fractions of the component in the feed. The membrane flux has been calculated according to the following equation after the steady state has been reached:-

$$J = Q/A*T \qquad [5.2]$$

Where;

J: Flux	(kg / m^2 h)
Q: the total mass of permeate collected	kg
A: effective area of membrane	m^2
T: time of sampling	h

The tests for pure solvents and mixtures were carried out in series as follow:

- Pure toluene,
- Pure n-heptane,
- A mixture Toluene/n- Heptane,

The mixture contains 50 wt.% Toluene/n- Heptane. The main characteristics of these solvents are given in Table 2.2.

- Pure water,
- Ethanol,
- Alcohol aqueous solution,

The mixture contains water / ethanol mixtures 20 to 80 wt.%.

- alcohols mixtures: ethanol 95 wt.% and n- butanol 95 wt.%,

Table 2.2:The properties of the non-polar mixture (Toluene/n-Heptane).

Componant	Toluene	n- Heptane
Formula	C_7H_8	C_7H_{16}
Structure	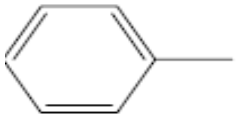	
Molacular weight (g/mol)	92.14	100.21
Density (g/ml)	0.864	0.68
Boiling point (°C)	110.6	98-99
Source	Sigma aldrich	Fisher scientific

Table 3.2: Properties of alcohols.

Alcohol	ethanol	n- butanol
Formula	C_2H_6O	$C_4H_{10}O$
Molacular weight (g/mol)	46.07	74.12
Density (g/ml)	0.7896	0.81
Boiling point (°C)	78.5	116-118
Source	Carls Erba	Fluka

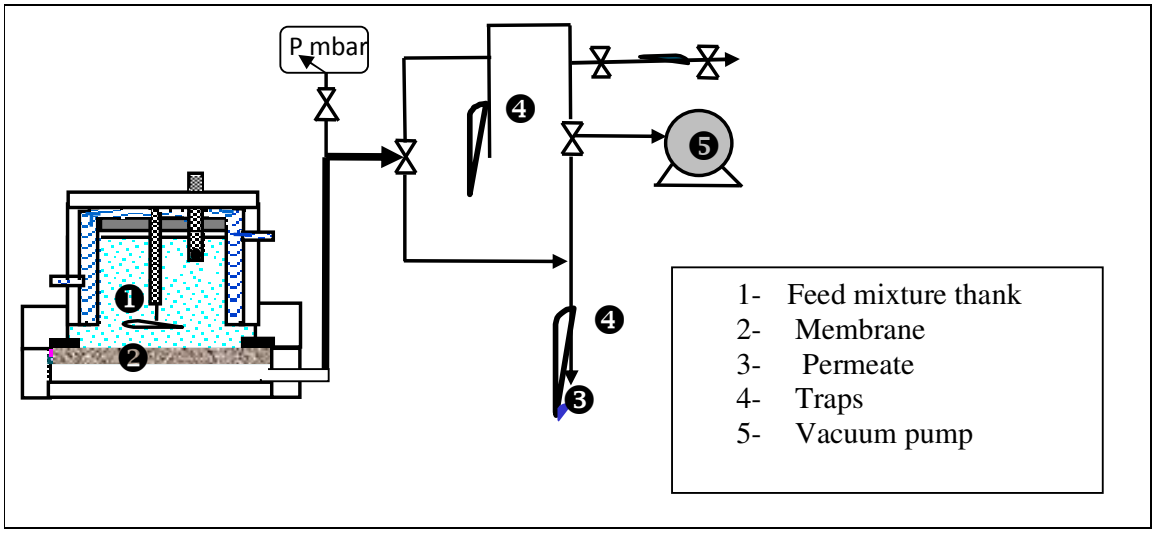

Figure 7.2: Schematic diagram of the pervaporation experimental set-up.

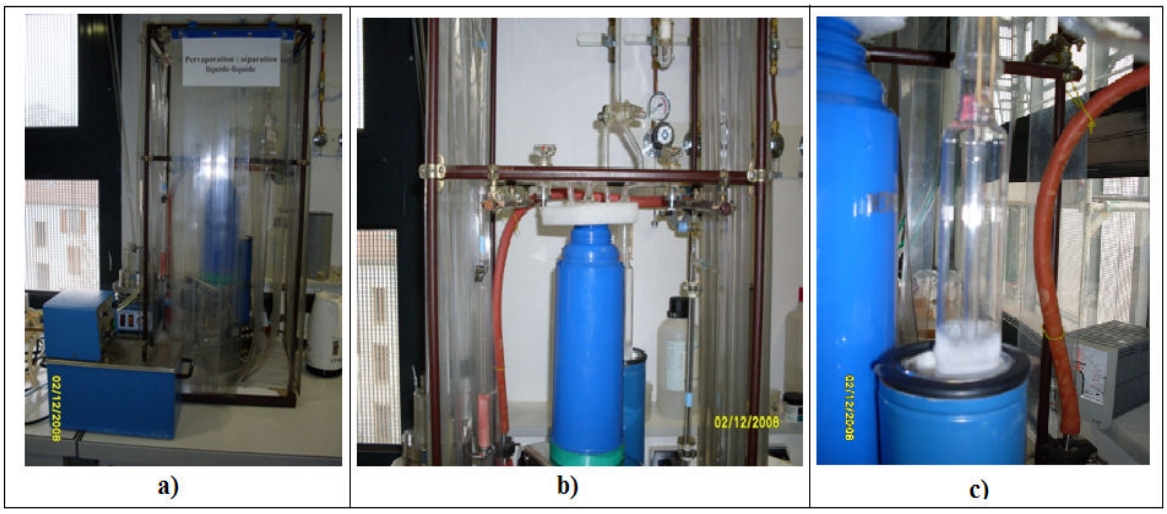

Figure-8.2: a) the pervaporation unit b) trap during pervaporation c) Condensation of the permeate through contact with liquid nitrogen

2.3.1.1 **Analytical Methods**

a- Analysis of permeation by gas chromatography(GC)

The permeate samples from the pervaporation of toluene– heptane and water-alcohol were analyzed by GC; for this reason, we established the calibration curves of toluene–heptane and water-alcohol. The calibration curve (Fig. 9.2) represents the area ratio between toluene and heptane as a function of mass ratio of these two components. Analogous calibration curves (Figures: 10.2, 11.2) were obtained between water and alcohol (ethanol or

n-butanol). The equation of the calibration curve for toluene/heptane has the form (the same for the calibration curves of water and alcohols):

$$\frac{A_T}{A_H} = p \times \frac{m_T}{m_H} \iff \frac{m_H}{m_T} = p \times \frac{1}{\frac{A_T}{A_H}} \qquad [6.2]$$

where:

p = slope of the calibration

m_T = mass of toluene

m_H = mass of heptane

R_A = area toluene/area heptane = $\frac{A_T}{A_H}$

In fact, the selectivity of the membrane can simply be represented by the concentration of toluene in the permeate Cp, which is given by the formula:

$$C_p = \frac{m_T}{m_{T+m_H}} \iff \frac{1}{C_p} = \frac{m_{T+m_H}}{m_T}$$

$$\frac{1}{C_p} = 1 + \frac{p}{R_A} \iff C_p = \frac{1}{1 + \frac{p}{R_A}} \qquad [7.2]$$

With the slope p and the ratio obtained in the GC analysis, we can calculate the selectivity of the studied membranes.

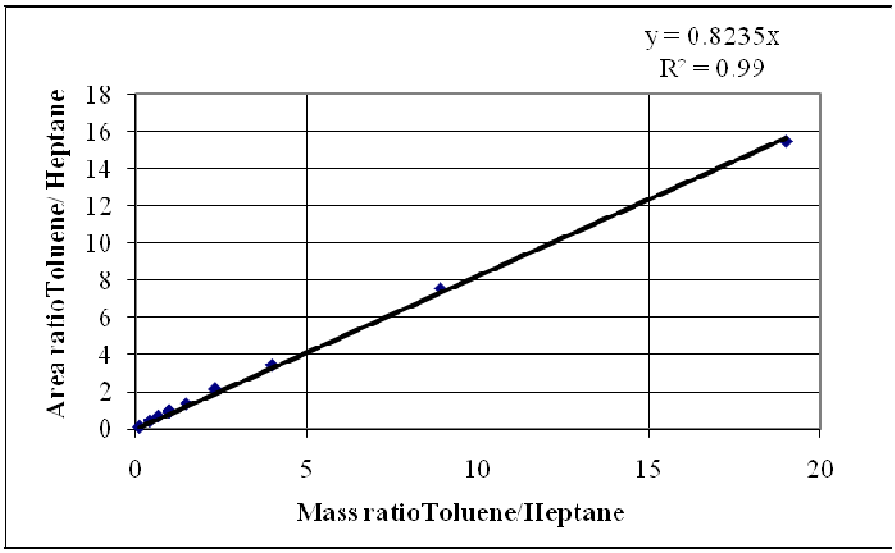

Figure 9.2: Calibration curve of toluene – heptane (gas chromatography-FID, Model no : 7675 Capillary : 25 m * 530 um * 5 um nominal).

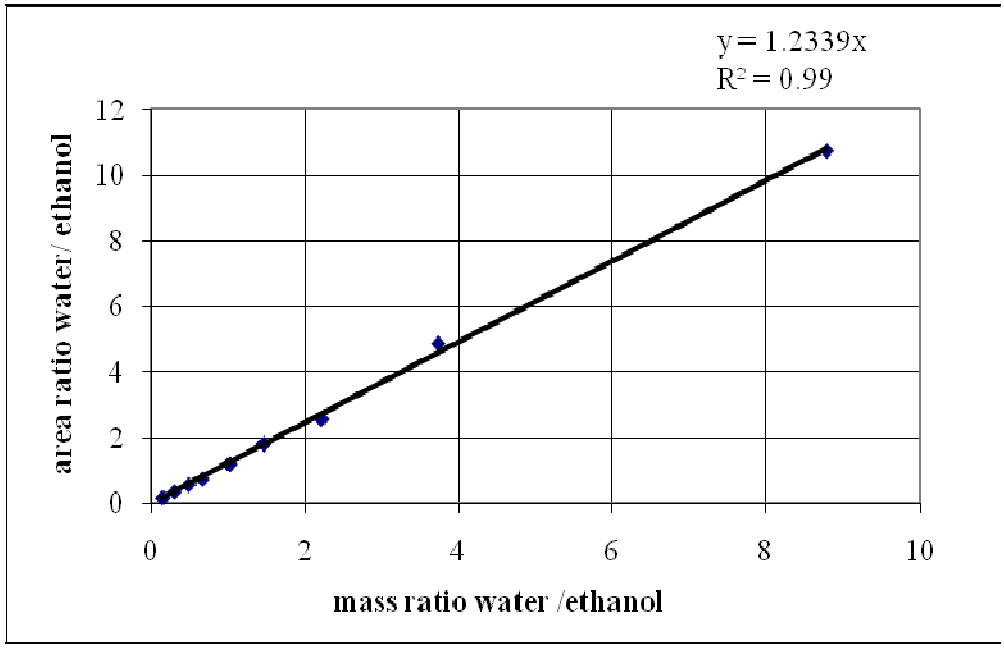

Figure 10.2: Calibration curve of water – ethanol (gas chromatography-TCD, Model no: 8570 Capillary: 30 m * 530um * 2 um nominal).

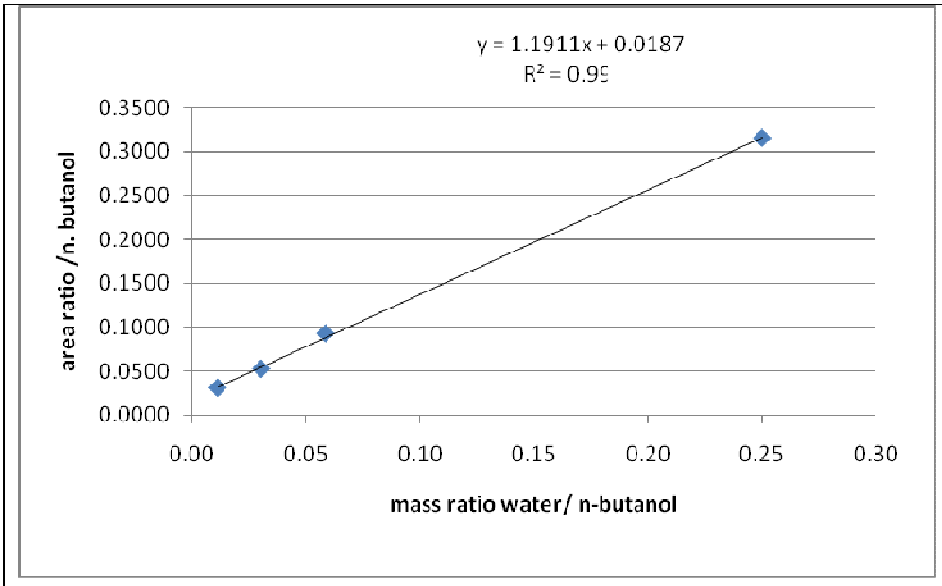

a- At high % of butanol .

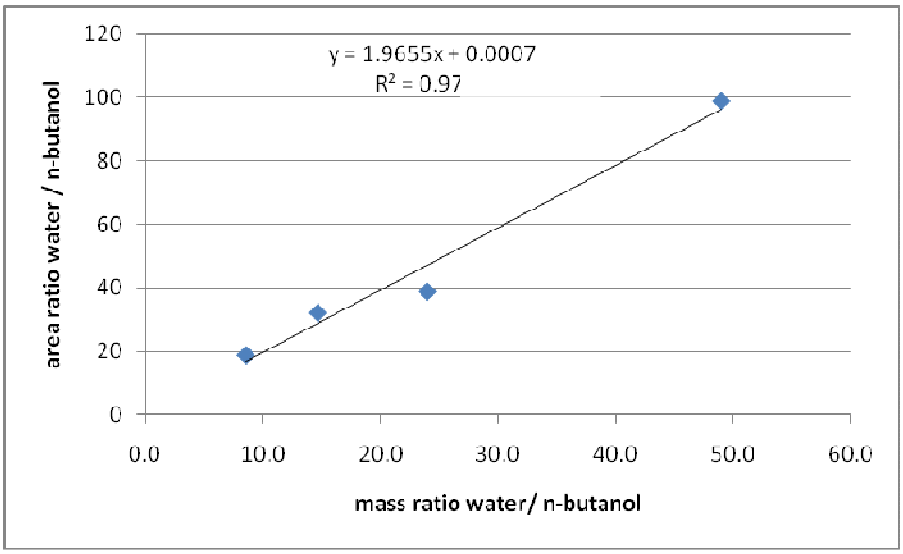

b- At high % of water.

Figure 11.2: Calibration curve of water – butanol (gas chromatography-TCD, Modle no: 8570 Capillary: 30 m * 530um * 2 um nominal)

2.3.2 Nanofiltration (NF) system experiments

2.3.2.1 Implementation of assembling nanofiltration (NF) set-up.

Implementation and creation of a new experimental set-up of NF water system was carried out. The new installation of NF is assembled with pump, reservoir, fluid circulation, cell permeation and device analysis (TOC). In year 2007 the NF cell (The SEPA CF II Membrane Element Cell) was purchased from Sterlitech Corporation USA (Fig. 12.2). Then, we asked the workshop to make the reservoir and fluid circulation conections, then analytical to make another permeation cell with a smaller area. In addition, we ordered an analytical device able to measure low concentrations of organic compound in water (TOC).

The first test in NF assembly without TOC took place on 9 December 2008, hence NF assembly took one year.The first series of tests took place to understand and characterize the NF set-up:

- Regulation of flow rate
- Control of up stream pressure
- Control of membrane sheet(GE Osmonics)

Figure 12.2: The SEPA CF II Membrane Element Cell

2.3.2.2 NF System configuration

The SEPA CF II membrane element cell is bought from Sterlitech Corporation USA. This cell is a lab scale cross flow filtration unit. Figure 13.2 illustrates the typical configuration of a standard SEPA CF II membrane element cell system. This figure shows the three major components of the system:

I. Cell Body
II. Feed Pump
III. Cell Holder

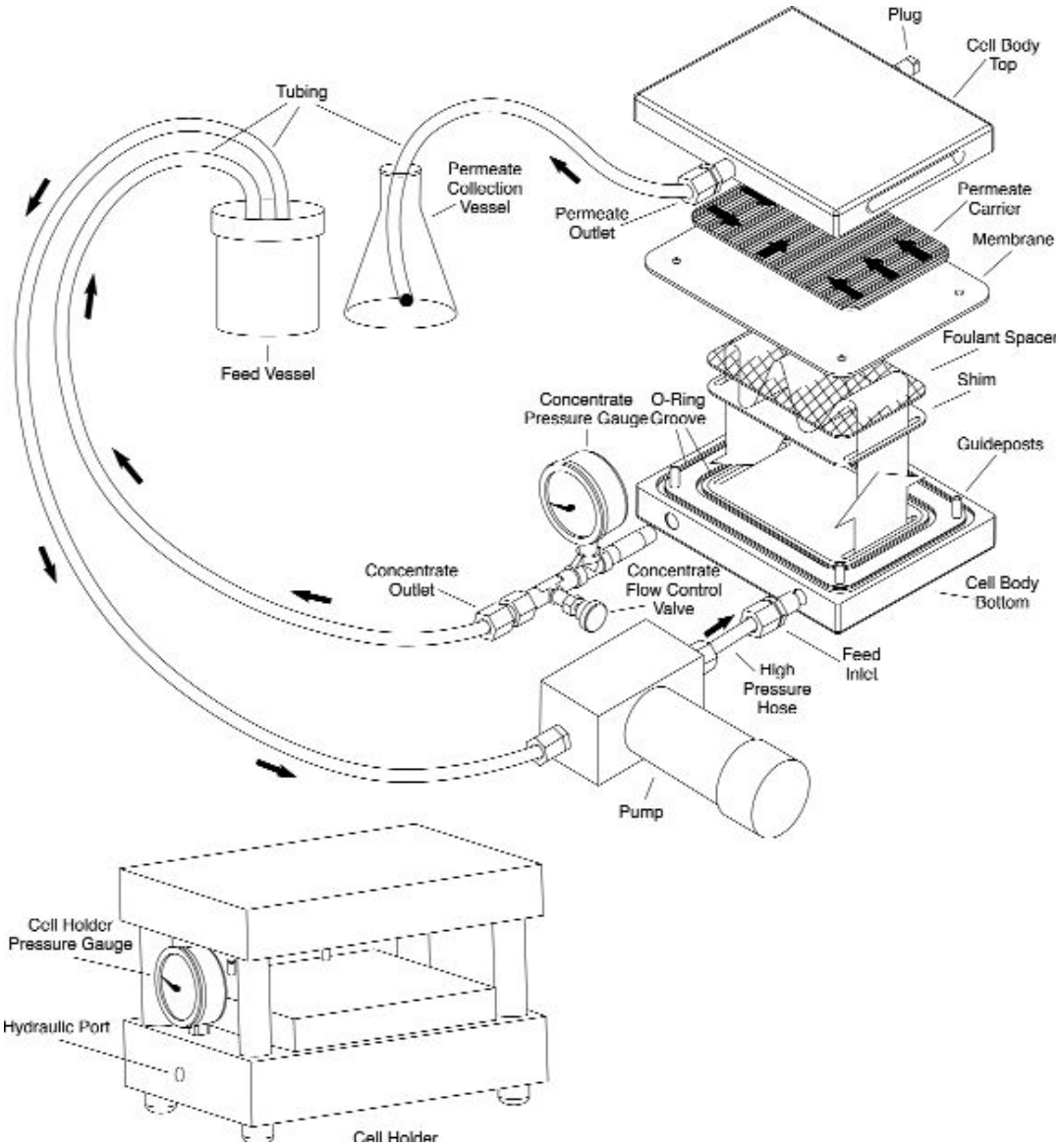

Figure 13.2: SEPA CF II Membrane element cell major components and flow sequence

2.3.2.3 Preparation and start-up of NF system principles of operation

a- Assembly of cell body

A single piece of rectangular membrane is installed in the cell body bottom (Fig.13.2) on top of the feed (foulant), spacer and shim (optional). The permeate carrier is placed in the recess on the cell body top. The cell body top fits over the guideposts of the cell body bottom. The guideposts assure proper orientation of the cell body halves.

b- Assembling of the cell body with cell holder

The assembled cell body is inserted and centered into the cell holder. Hydraulic pressure is applied through a fitting in the bottom of the cell holder. The hydraulic pressure causes the piston to extend upward and compress the cell body against the cell holder top. Double O-rings in the cell body provide a leak-proof seal.

c- Start-up with feed pump

The feed stream is pumped from the user supplied feed vessel to the feed inlet. The feed inlet is located on the cell body bottom. Flow continues through a manifold into the membrane cavity. Once in the cavity, the solution flows tangentially across the membrane surface. A portion of the solution permeates the membrane and flows through the permeate carrier, which is located in the cell body top. The permeate flows to the center of the cell body top, is collected in a manifold, and then flows out through the permeate outlet connection into a user-supplied permeate collection vessel. The concentrate stream, which contains the material rejected by the membrane, continues sweeping over the membrane and collects in the manifold. Then, the concentrate flows through the concentrate flow valve back into the feed vessel.

The feed pressure is less than or equal to the piston pressure on the cell holder/cell body. It was verified by comparing the reading on the piston cell holder pressure gauge (Fig. 13.2) to the reading on the concentrate pressure gauge. The operating parameters for NF cell system are presented in table 4.2.

Table 4.2: Operating parameters for NF cell system

Effective membrane Area	41 cm^2
Maximum pressure	69 bar (1000 psig)
Maximum temperature	177°C (350°F)
pH Range:	Membrane dependent
Maximum flow	1.3L/min (78 $L.h^{-1}$)
Liquid stream thickness	1000 µm

2.3.2.4 Membrane replacement

Steps of membrane replacement in NF system:

1. Turn the feed flow pump off.
2. Turn the knob (counterclockwise) on the pressure relief valve on the hydraulic pump to release the hydraulic pressure in the system.
3. Slide the cell body out of the cell holder.
4. Separate the cell body top from the cell body bottom.
5. Replace the membrane.
6. Replace the permeate carrier and feed spacer, if necessary.
7. Install new membrane in the cell body bottom (Fig. 13.2) on top of the feed (foulant) spacer and shim (optional).
8. Reassemble the cell body top and bottom.
9. Return the cell body to the cell holder.
10. Reactivate the piston mechanism.
11. Turn the feed flow pump on.

2.3.2.5 Characteristics of flow rates

The first tests of NF were performed with pure water for calibration of the system and control the relations of (flow- pressure). The relations between flow at outlet of (pump, permeate) with open of pump valve and flow at concentrate outlet with pressure is tested. The maximum possible pressure is 60 bar, for flow rates of approximately 1.3L/min.

2.3.2.6 Permeation tests for PEI and Kapton^{TM} membranes with NF (experimental part)

Aim of work**:** testing nanofiltration with PEI membranes using pure water as feed to check the structure of dense and asymmetric PEI membranes and to understand the effect of

the operating pressure and hydraulic parameters on flux and permeability. Then, testing of inorganic/water and organic/water mixtures to check molecular separation and to reach optimum characterization of asymmetric membrane with flux and selectivity.

Evaluations of membrane performances as a function of different operating parameters have been investigated. Pure water flux and permeability as a function pressure were studied. Further, the prepared membrane sheets have been tested to check their mechanical strength under different applied pressures.

It was observed that the PEI membranes with dense and spongy like strucures do not exhibit permanent deformation due to the applied pressure while the PEI membranes with finger like structure are irreversibly compacted.

The permeation tests for PEI membranes were carried out at ambient temperature under an operating pressure up to 50 bar and a pump feed with flow rate of 1.3L/min using the NF cell, the feed solution has capacity of 31 L. The effective surface membrane area was 41cm^2. Membranes first were conditioned in the test cell with pure water by gradually increasing the pressure up to 20 bar for at least one day. Each test of the aqueous (organic or inorganic) solution was circulated over the membrane surface under test conditions for at least 24 h prior to collecting the permeate samples. In each experiment, the real flux (J) of pure water and that of the aqueous(organic or inorganic) solution was determined from equation:

$J = Q/ (A*Tt)$ [8.2]

Where;

Q: permeate mass in kg

A: membrane active area in m^2

Tt: time in hour

When the aqueous (organic or inorganic) solution was tested, the rejection (R) was calculated as:

$R(\%) = (1 - C_p/C_f) \times 100\%,$ [9.2]

where ;

C_f : the concentration of the feed solution

C_p: the concentration of the permeate

The concentrations of C_p and C_f were measured with the TOC device. In addition, all membranes were tested with a single-solute solution. The concentration of inorganic solute in the feed solution was 5 and 10 g/L for NaCl and 5 g/L for $CaCl_2$ while aqueous organic solution with feed prepared in range 100-500 ppm depends on the solubility of organic solute

in water. The tests of pure water and aqueous (organic or inorganic) solution were carried out in series as follows:

- Pure water
- aqueous inorganic solution
  NaCl,$CaCl_2$
- aqueous organic solution

Nanofiltration of aqueous organic feed solutions through an asymmetric PEI membranes was investigated. In this work different types of polar and non-polar organic chemicals were used in order to characterize membrane performances.The tested solutions were as follow:

i. aqueous organic of 50, 80 wt% H_2O/ EtOH mixtures

ii. The molecular weight cut-off (MWCO)

for the molecular weight cut-off (MWCO) the solution concentration of aqueous organic range 100-500ppm depends on the solubility of organic on water, the tested solutes are:

a. Hydrophilic compounds: EtOH (46),2-propanol(60), butanol(74), Urea (60), TEG (150), PEG av. 400, PEG av.1000, PEG av.2000, PEG av.6000
b. Hydrophobic compounds: Cyclohexane (84) max solubility: 100ppm, Toluene (92) max solubility: 500ppm, terathane (TTEG) 250, 650, 1400.

The main characteristics of these organics are given in Table 5.3. which summarises their most important properties. The NF system is presented in figure 14.2

Table 5.3: Characteristics of organic

Organic compound	*Source*	*Formula*	*MW (g/mol)*	*Density(g/ml)*	*Boiling point/melting point*
Ethanol	*Carlo Erbo*	C_2H_6O	*46.07*	*0.7896*	*78.5*
2-Propanol	*Fluka*	C_3H_8O	*60.1*	*0.786*	
n-butanol	*Fluka*	$C_4H_{10}O$	*74.12*	*0.81*	*116-118*
TEG	*Aldrich*		*150*		
PEG400	*Eastman kodak*	$(C_2H_4O)n$ H_2O	*400*	*1.128*	*m.p:6*
PEG1000	*Fluka*	$(C_2H_4O)n$ H_2O	*950-1050*		*m.p: 37-40*
PEG2000	*Aldrich*	$(C_2H_4O)n$ H_2O	*2000*		*m.p: 55-58*
	Fluka	$(C_2H_4O)n$ H_2O	*1900-2200*		*m.p: 50-52*
PEG6000	*Merck – schuchardt*	$(C_2H_4O)n$ H_2O	*5000-7000*		
Urea	*Fluka*	CH_4N_2O	*60.06*		*m.p: 130-132*
Cyclohexane	*Prolabo*	C_6H_{12}	*84.16*	*0.778-.0779*	

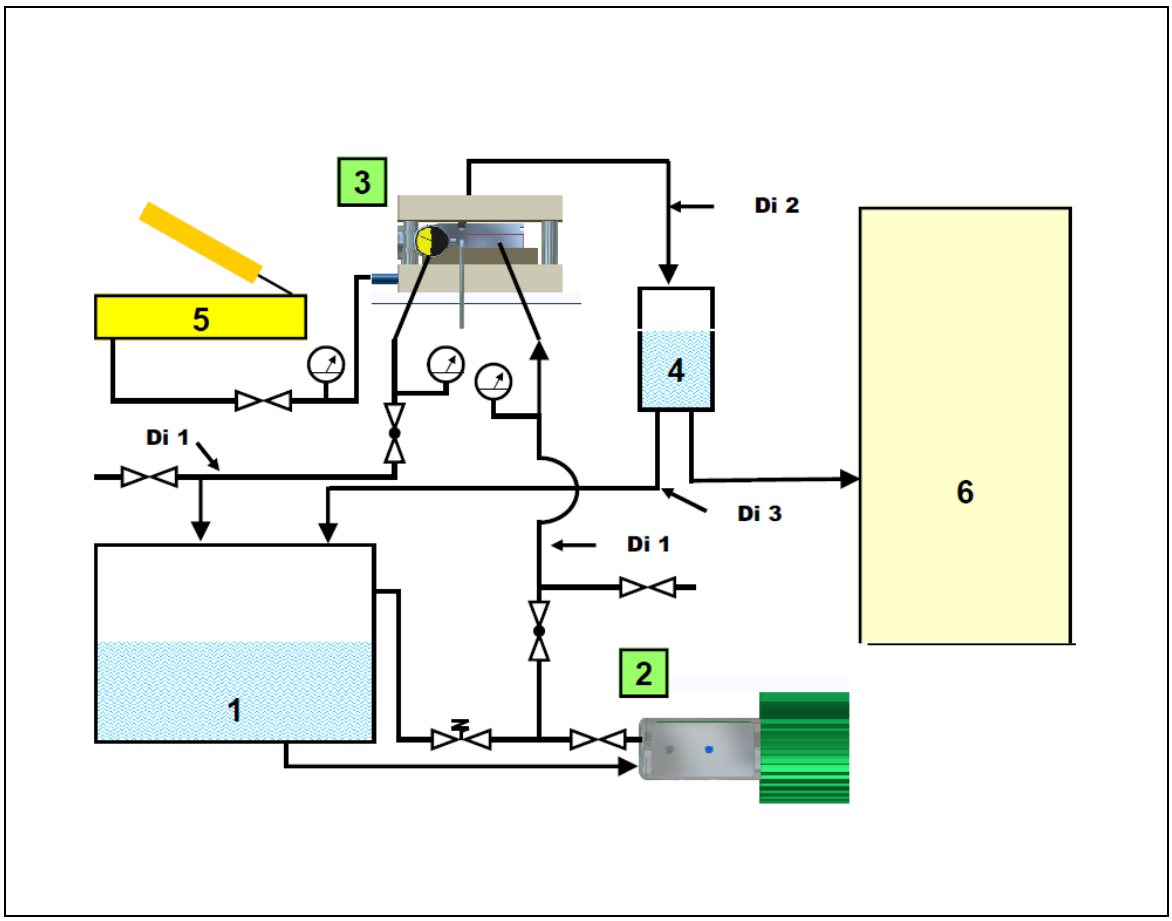

Figure14.2: NF permeation system set-up Where; 1: Feed tank,2: Feed pump,3: Membrane cell,4: Permeate, 5: pump ,6: Total organic carbon analyser, Di1:1/4", Di2:1/2", Di3:1/4"

2.3.3 Characteristic flow rates of NF set-up

The first test of NF (Fig.15.2) was carried out with pure water for calibration of the system and control of the flow- pressure relations without membrane film. The relations between the pressure and the flows at the outlet of the pump and outlet of the permeate are presented in Fig. 16.2. The maximum possible pressure is 60 bar, with flow rates of approximately 1.35L/min at the cell inlet, and of 1.2L/min at the permeate outlet, the retentate outlet valve being closed. Figure (2,b.5) shows the effect of an open retentate outlet valve on flow rate as a function of pressure (the permeate outlet was closed by using impermeable film), The maximum possible flow rates for the retentate outlet are approximately of 1.19L/min and the maximum pressure 40 bar.

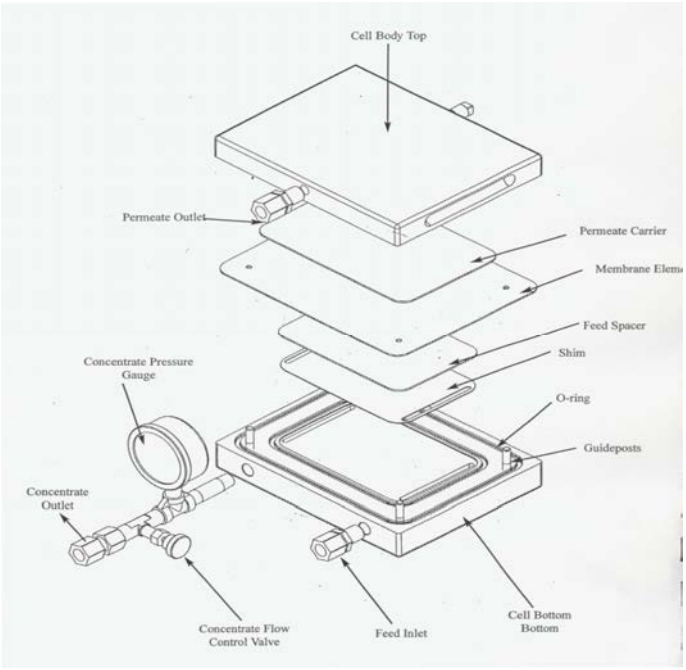

a

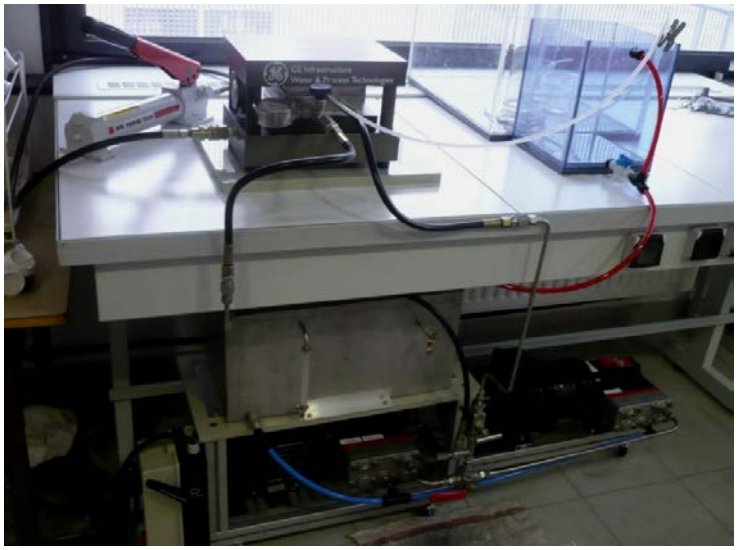

b

Figure 15.2: a, Membrane element cell, b; NF setup.

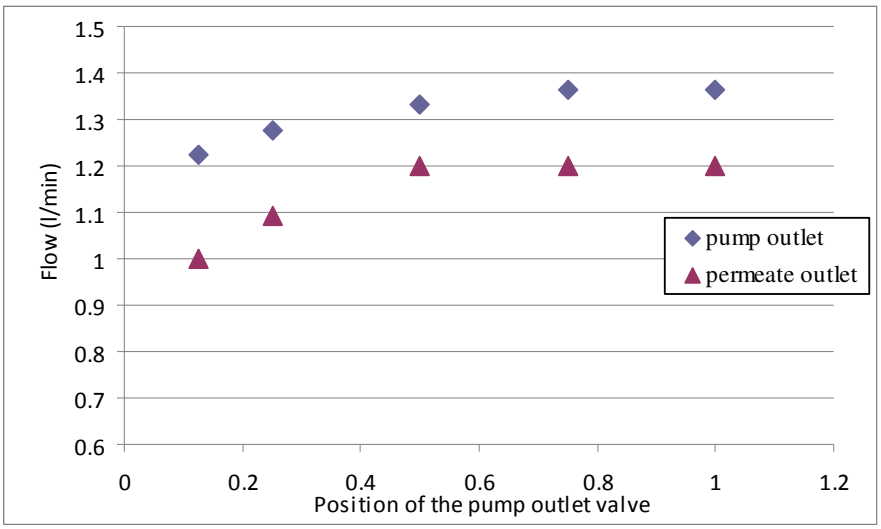

a- Outlet of pump and permeate (retentate outlet valve closed)

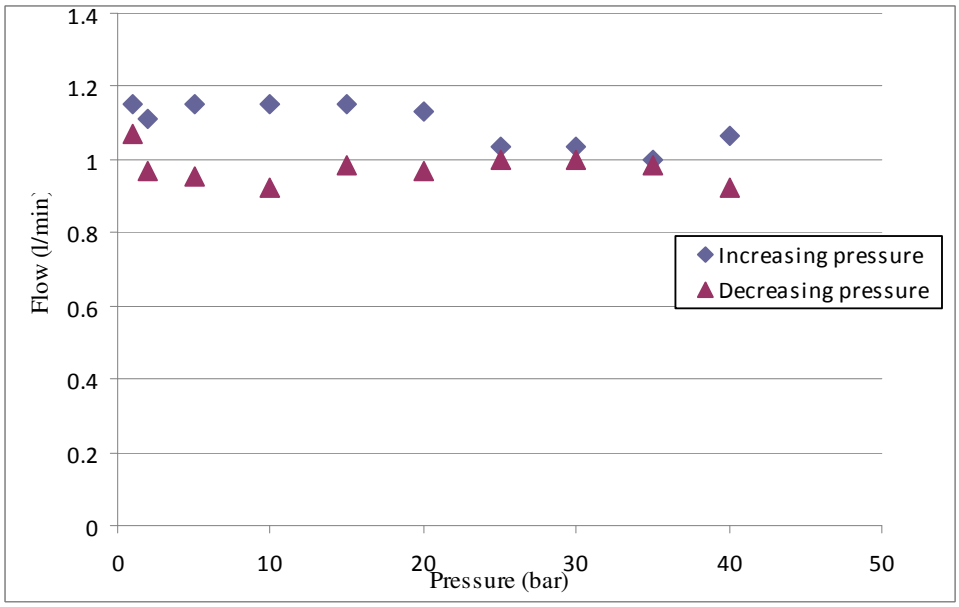

b- Retentate outlet (open of pump valve 0.125, permeate outlet was closed).

Figure 16.2: NF cell tests without membrane with pure water (characteristic of the cell hydrodynamics).

Velocity and Reynolds number

For a pipe the characteristic length is the hydraulic diameter. The Reynolds Number for pipe can be determined from the equation:

$Re = \rho v d_h / \mu$

Re =Reynolds number (non dimensional)

Where;

d_h = hydraulic diameter (m)

v = velocity (m/s)

μ = kinematic viscosity (1 cSt = 10^{-6} m^2/s)

The Reynolds Number can be used to determine if flow is laminar, transient or turbulent. The flow is:

- **laminar** when Re < 2300
- **transient** when 2300 < Re < 4000
- **turbulent** when Re > 4000

I. **Calculating the** Reynolds Number in feed pipe of NF set up

$Re = \rho v d_h / \mu$

d_h (diameter)=0.635 cm A=0.316 cm^2 Q in feed pipe =1300 (cm^3/min)

Velocity in feed pipe= v =Q/A= 0.6845 m sec^{-1}

Kinematic Viscosity (μ) =0.00000081 (m^2/s) at 30°C

Re= 5366 flow is turbulent in feed pipe

II. **Calculating the** Reynolds Number in retentate pipe of NF set up

d_h (diameter)=0.635 cm A=0.316 cm^2 Q in retentate pipe =1000-1300 cm^3/min

v= Q/A= 0.527 m sec^{-1}

Re= 4127 flow is turbulent in retentate pipe

III. **Calculating the** Reynolds number in membrane cell of NF set up

For shapes such as rectangular (where the height and width are comparable) the characteristic dimension for internal flow situations is taken to be the hydraulic diameter, D_H:

$D_H=4A/P$

D_H: Hydraulic diameter

A: Cross-sectional area.

P: The wetted perimeter that are in contact with the flow

A=5.4*0.1=0.54 cm^2

P=2(5.4+0.1) =11cm

D_H=4A/P= 0.196cm

$Q = A*v = 1300\ (cm^3/min) = 21.67\ (cm^3/sec)$ velocity (v) $= 21.67/0.54 = 40$ cm/sec $= 0.4\ m\ sec^{-1}$

$Re = \rho\ v\ d_h / \mu = 967$ **flow is laminar in membrane cell**

2.3.4 Effect of PAA concentration and composition on membrane performance

The effect of polymer and/or additive concentrations on the membrane performance (flux, permeability, separation) is investigated and analysed.This has been carried out by using different precasted membrane samples with PV and NF.

2.3.5 Effect of operating pressure on permeate flux

The effect of operating pressure on the permeate flux is investigated and analysed.This has been carried out by using different precasted membrane samples with NF. All the membranes were tested with operating pressures in the range 0 up to 50 bar.

2.3.6 Effect of operating temperature on membrane performance

The effect of operating temperature on the membrane performance is investigated and analysed.This has been carried out by using different precasted membrane samples with PV with operating temperature ranging from 30 up to 70 °C.

References Chapter 2

1. J. Jansen, M. Macchione and E. Drioli, High flux asymmetric gas separation membranes of modified poly(ether ether ketone) prepared by the dry phase inversion technique, J. Membr. Sci. 255 (2005) 167-180
2. Q. Zheng, P.Wang, Y. Yang, D. Cui, The relationship between porosity and kinetics parameter of membrane formation in PSF ultrafiltration membrane, J. Membr. Sci. 286 (2006) 7–11.

Chapter 3

Results and discussion of Synthesis and Characterization of membranes

Table of Contents Chapter 3

Results and discussion of Synthesis and Characterization of membranes

Table of Contents Chapter 3

Chapter 3 ..... *161*

Results and discussion of synthesis and characterization of membranes *161*

3.1 Membrane preparation *161*

3.2 Phase diagrams *161*

3.2.1 Phase diagram and the determination of the binodal demixing curve by alternating addition of nonsolvent (cloud point) and solvent (clearing point) to the polymer solution. *162*

3.2.2 Turbid points values (binodal demixing curve) and phase diagrams *164*

3.3 Studing of membrane morphology with scanning electron microscope (SEM) *166*

3.3.1 Preparation of PEI dense membrane *166*

3.3.2 Preparation of PEI asymmetric membranes by phase inversion process *167*

3.3.2.8 Effect of addition of co-solvents to PAA solution and effect of additives addition with water in coagulation bath *190*

3.3.3 SEM for Hybrid silica-PEI membranes *193*

3.3.4 Kapton membranes preparation *194*

3.3.4.1 Preparation of Kapton (PI) dense membrane *194*

3.3.4.2 Preparation of Kapton membrane by phase inversion *195*

3.3.5 Asymmetric PEI membranes preparation with strong mechanical support *198*

3.4 Study of the stability of PEI dense membranes in organic solvents and in water ... *200*

3.5 Physical characterizations *207*

3.5.1 Infrared spectra (FT-IR) *207*

3.5.2 Mechanical property *210*

3.5.3 Thermogravimetric analysis (TGA) *211*

Conclusions and Recommendations for Future work *217*

References **219**

Chapter 3

Results and discussion of synthesis and characterization of membranes

3.1 Membrane preparation

Polyimides(PI) are well known as a polymer materials and they have been used since the last three decades as specialty polymers in numerous applications. In addition, there are many different methods to prepare aromatic polyimides, the most popular method being the two steps procedure, i.e. the reaction of an aromatic dianhydride (1 equivalent) with an aromatic diamine (1 equivalent) to form a soluble poly(amic acid), followed by its thermal imidization to polyimide. For example, Kapton™, one of the very typical aromatic polyimide, is prepared from PMDA and ODA, leading to the corresponding poly(amic acid) (PAA); then Kapton™ films can be subsequently obtained by thermal treatment. In this work we introduce alkoxy soft blocks in the basic PI structure to modify both the physico chemical properties of the polyimide structure and the permeation properties, the later one being known to be very small with fully aromatic polyimides. The prepared dense and asymmetric PEI membranes had stoechiometric amounts of an α,-alkoxyether diamines, i.e. Jeffamine® (Jeff) ranging from 0.4 to 0.6, the other amine used being the aromatic oxydianiline (ODA). The physical features of this set of polyetherimides were studied comparatively to Kapton™ characteristics, and the ability of these polymers to give asymmetric structure determined from their related PAA. The purpose was to prepare rubbery asymmetric copolyimides with a self supported thin dense layer on the topside, thanks to the rigid properties of the aromatic part of the PEI structure and to study the effect of some of operating parameters on membrane preparation to optimize and control the morphology.

However, if asymmetric morphologies can be easily formed by phase inversion methods with glassy polymer such as Kapton™, the effect of the soft blocks in polyimide structure on the ability of preparing such membranes was unknown, not predictable and not yet reported to our knowledge.

3.2 Phase diagrams

Phase diagrams can predict, whether or not a solution of a certain polymer in a certain solvent is suitable for membrane formation. Binary phase diagrams showing the phase boundaries as a function of temperature and composition provide information for the phase inversion process, whereas ternary isothermal phase diagrams are useful for the prediction of

the phase transitions that could occur when phase separation is induced according to one of the other methods. It should be kept in mind that such diagrams only predict which phase transition a polymer solution can undergo during a membrane formation process. An equilibrium phase diagram provides a map for the different phase transitions that are favoured thermodynamically. The kinetics of phase separation processes determine whether or not the thermodynamically favoured transition will occur, and also to what extent the transition will take place. Non equilibrium processes may play an important role during membrane formation. In this part we intended to study polymer/solvent/nonsolvent systems to report the agreement between experimental and miscibility gaps with the evaluations of a membrane-forming system**.**

3.2.1 Phase diagram and the determination of the binodal demixing curve by alternating addition of nonsolvent (cloud point) and solvent (clearing point) to the polymer solution [1].

Phase diagrams of the polymer (PAA)/solvent (DMF)/nonsolent(water) systems were obtained by drop-wise addition of alternatingly nonsolvent and solvent under continuous stirring. The cloud point was observed visually by sudden occurrence of turbidity (upon water addition) or by sudden clearing of the mixture (upon solvent addition). The sections of the ternary phase diagrams that could be determined experimentally are displayed in table 1.3 and Fig.1.3 for the systems PAA/DMF/Water. The phase diagrams represent a detailed picture of the components miscibility and they contain useful thermodynamic information about the phase separation process. The composition of each point was determined by the amount of nonsolvent, solvent, and polymer present in the glass-ware which is presented in table 1.3 and shown in fig.1.3. Experimental determination of the phase diagrams was limited to a maximum polymer concentration of 30wt.% in DMF, in order to avoid inefficient stirring as a consequence of the high viscosity of the solutions or the tendency towards gel formation.

Table 1.3: Points of alternating addition of nonsolvent (cloud point) and solvent (clearing point) to the polymer solution at 10 °C.

test	Clear solution			Cloud Polymer ternary solution(turbid points values)		
	PAA %	**DMF %**	**W %**	**PAA %**	**DMF %**	**W %**
1	30	70	0	22	52	26
2	20	55	25	19.9	53.3	26.8
3	18.8	55.9	25.3	18.46	55	26.54
4	18	57	25	17.4	56.2	26.4
5	16.5	58.1	25.4	16.25	57.4	26.35
6	15.7	58.9	25.4	15.5	58	26.5
7	14.9	58.5	25.6	14.7	58.8	26.5
8	14.3	60	25.7	14.2	59.15	26.65
9	13.7	60.5	25.8	13.5	59.9	26.6

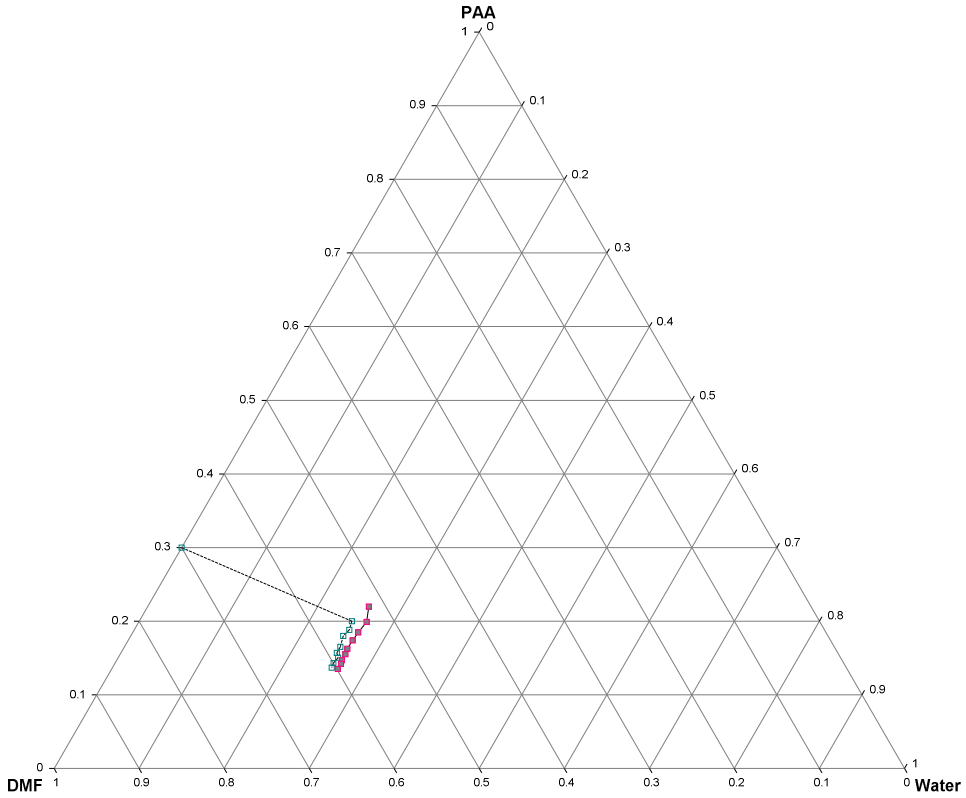

Figure 1.3: Schematic representation of the phase diagram and the determination of the binodal demixing curve by alternating addition of nonsolvent (cloud point■) and solvent (clearing point) to the polymer solution at 10°C.

The overall phase diagram behaviour depends on many factors and a complete description of the thermodynamics would require the knowledge of the Flory–Huggins interaction parameters of the ternary mixture. Qualitative support for the different thermodynamic behaviour of the systems with DMF is given by the physical appearance of the polymer rich phase after phase separation during the cloud point measurements.

For thermodynamic evaluations of a membrane-forming system, the Flory–Huggins theory of polymer solutions[2-3] is typically used to predict the thermodynamic behavior of nonsolvent/solvent/polymer systems, and a ternary phase diagram including binodal and spinodal curves and tie lines is constructed. Binary interaction parameters of nonsolvent/solvent, solvent/polymer, and nonsolvent/polymer are the main input parameters of the Flory–Huggins relation. The magnitude and concentration dependency of these interaction parameters have a large effect on the binodal, spinodal, and critical point positions of a phase diagram [4-5].The effects of these parameters on the phase diagram of a membrane-forming system have been studied by several researchers [6-7] and [8]for various ternary systems. Altena and Smolders [9] were the first who performed a comprehensive thermodynamic study for a wide range of ternary membrane-forming systems. They have studied water/solvent/cellulose acetate and water/solvent/polysulfone systems and their theoretical calculations showed that good agreement can be found between experimental and theoretical miscibility gaps when the nonsolvent/solvent interaction parameter is taken concentration dependent and two other interaction parameters are considered concentration independent. On the other hand, Yilmaz and McHugh [10] have shown that the concentration dependency of the solvent/polymer interaction parameter is more important than that of the nonsolvent/solvent parameter.

3.2.2 Turbid points values (binodal demixing curve) and phase diagrams

In this work we intended to study (PAA/DMF/H_2O) system to report the agreement between experimental work and miscibility gaps with the evaluations of a membrane-forming system**.** The phase diagrams for the system PAA/DMF/H_2O represent a detailed picture of the three components miscibility and they contain useful thermodynamic information about the phase separation (inversion) process. The ternary phase diagram and the determination of the binodal demixing curve of the polymer/solvent/nonsolvent combinations systems was obtained from the turbid (cloud) points measurement which are presented in table 2.3 and Fig.2.3. The PAA used (Jeff600-PMDA-ODA) were made with

stoichiometry: 0.4 mmole of Jeffamine 600; 1mmol of PMDA; 0.6 mmol ODA. The polyamic acid (PAA) with 30 wt. % in the DMF is prepared.

Table 2.3: The composition of turbid point at 10 °C.

Polyamic acid (PAA) Initial binary solution wt.% in DMF	Polymer in ternary solution (PAA wt %)	Solvent in ternary solution (DMF wt %)	Non solvent in ternary solution (water wt %)
100% (PAA membrane)	84%	0	16%
30%	22%	52%	26%
20%	14%	58%	28%
10%	6%	64%	30%
5%	3%	64%	33%
2%	1%	62%	37%
1%	0.1%	61%	38.9%

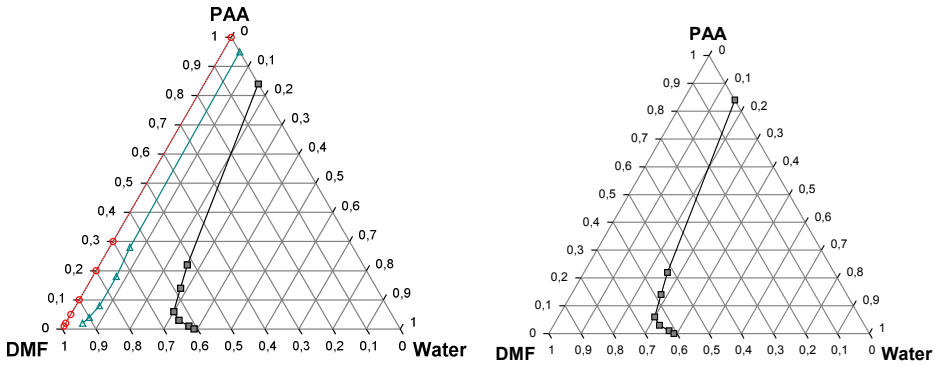

Figure 2.3: Ternary phase diagram and the determination of the binodal demixing curve of PAA-DMF-H_2O system build from turbid points (Starting binary dopes ○; starting ternary dopes ▲ ; final binodal demixing curve ■).

Figure 2.3 shows the experimental cloud points data for PAA/DMF/H_2O system. As this figure shows, the cloud point curve of PAA/DMF/H_2O system is closer to the solvent-nonsolvent axis (DMF-H_2O axis), and so more water (39 wt %) is needed for the precipitation of PAA in this system (because there is a large mixing gap). On the other hand, the lowest binodal points near the DMF/H_2O axis were very dilute, which were close to the critical point. Consequently, the liquid-liquid miscibility gap almost overlapped the DMF/H_2O axis. In addition, the observed results show that the DMF is a good solvent for PAA and therefore a

small demixing gap should be observed for PAA/DMF/H_2O system compared to the other systems reported in literature review as result reported by J. Barzin et.al [6] who studied the theoretical phase diagram calculation for water/solvent (NMP or DMAc)/polyethersulfone systems, he found that water is needed for the precipitation of polyethersulfone in these systems is in range (20 to 25 wt%) (because there is a small mixing gap). The evaluations of a membrane-forming system is available with helping of the SEM pictures recorded on the prepared PEI membranes to show the agreement between the experimental work for the preparation of PEI membranes and miscibility gaps in the ternary phase diagram, this point will be discussed later. In general, trends expected on the basis of the phase diagram were in reasonable agreement with the observed membrane morphology. Hence, we can report the range of addition of non-solvent to polymer solution, the effect of this range on the membrane morphology to predict the behavior of (PAA/DMF/non solvent) systems with helping of these tests. Thus, we can predict that the PEI membranes cannot be prepared when the addition of nonsolvent (water) is greater or equal than turbid points for example 26 wt% addition of water to 30 wt% PAA in DMF.

3.3 Studing of membrane morphology with scanning electron microscope (SEM)

The scanning electron microscope (SEM) is a type of electron microscope that images the sample surface by scanning it with a high-energy beam of electrons in a scan pattern. The electrons interact with the atoms that make up the sample producing signals that contain information about the sample's surface topography, composition and other properties such as electrical conductivity.The prepared membranes are examined by SEM, and the SEM views results are being outlined below.

3.3.1 Preparation of PEI dense membrane

The SEM views of flat membranes of PAA and the corresponding PEI - Jeff600-PMDA-ODA (0.4/1/0.6) prepared by two steps mechanism and solvent evaporation (dry method) revealed that the corresponding structures seem to be pore free either on the top (air side) or on the bottom (glass side) surfaces; thus these samples appeared to be more dense (Fig. 3.3). In addition, the prepared dense PEI membrane is highly transparent with slightly yellow colour. Furthermore, the prepared dense PEI membranes have good mechanical property and are highly stable in large variety of solvents (see result of swelling chapter 3).

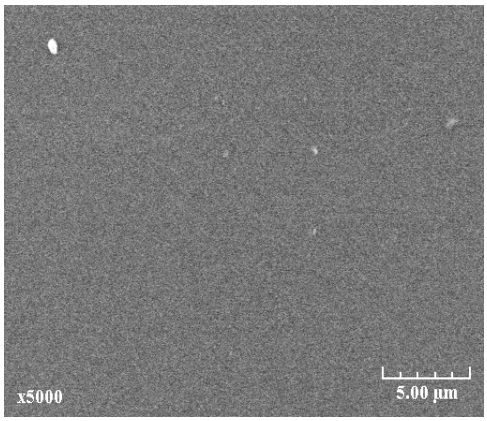

a. PAA dense membrane surface

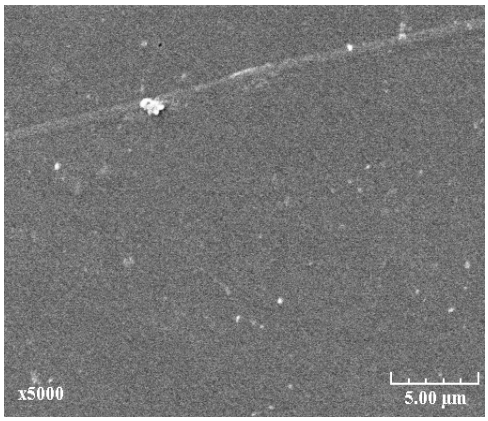

b. PEI dense membrane surface

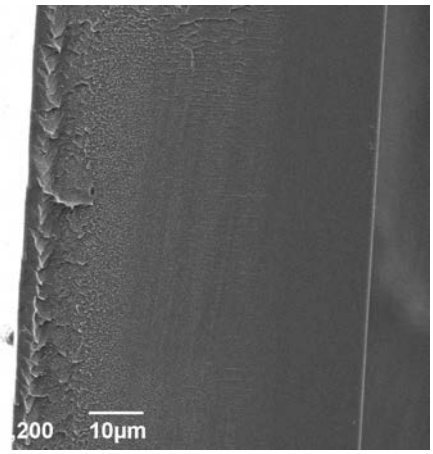

c. cross section for PEI dense membrane (70µm)

Figure 3.3: SEM Photograph of PEI dense membrane.

3.3.2 Preparation of PEI asymmetric membranes by phase inversion process

The preparation of asymmetric membranes was carried out according the wet method using a non solvent bath to induce phase inversion. The effect of some operating parameters on the morphology of PEI membrane were studied, using SEM as tool to optimize the phase inversion conditions in order to prepare PEI membranes having a thin tight top layer self supported on a highly porous sub layer. These parameters results are outlined and shown below.

3.3.2.1 Effect of immersion bath time, ranging from 1 to 3h

The first parameter tested was the residence time (1 to 3h) of the glass plate supporting the polymer solution in the non solvent bath (Table.3.3, tests 1-2). The effect of that parameter is presented in Figures (4.3-9.3) (membranes M_1:M_6). It was found from the SEM view that decreasing the immersion time from 3h to 1h had not a striking effect, except may be the formation of more brittle PAA films probably because the solvent extraction was more complete after a longer immersion time. For the figures, the preparation conditions are expressed as follows (PAA wt%-DMF wt%-Water wt%/preconcentration time/ immersion time/thickness) respectively. It was clear from Figures (4.3-9.3) that porosity is decreased after thermal treatment.

Table 3.3: Operating parameters tested on preparation of PEI membranes.

Membrane	Casting solution			Pre-concentration time (min)	Immersion* Time (h)	Non solvent	test
	DMF	PAA	Water				
M_1	70	30	0	1 min	1 h	Water	1
M_2	"	"	"	"	2 h	"	"
M_3	"	"	"	"	3 h	"	"
M_4	70	30	0	3 min	1 h	Water	2
M_5	"	"	"	"	2 h	"	"
M_6	"	"	"	"	3 h	"	"

*immersion in water bath at 11°C.

3.3.2.2 Evaporation delay (pre-concentration step), ranging from 1 to 3 minutes

The second parameter tested was the evaporation delay (1 to 3min) before inducing phase inversion; it leads to an increase of the polymer concentration at the interface with air (Table.3.3, tests 1-2). The effect of that parameter is presented in Figures (4.3-9.3) (membranes M_1:M_6). It was found from the SEM views that decreasing the time of evaporation from 3min to 1min leads to an increase of the polymer concentration at the interface with air which induced a more porous structure, for example the PEI asymmetric M_1 membrane is more porous than M_4. This effect is due to a less densification of the top surface occurring with the pre-concentration time decrease. It is reported [11,12] that increasing the time of evaporation leads to increase the thickness of dense layer in prepared membranes and to decrease porous structure. It was found from figures (4.3-9.3) that the bottom surface side of all PAA and the coresponding PEI membranes is porous while top surface side is dense.

The thermal treatment from PAA to PEI induces much higher mechanical properties, avoids brittle property, induce densification and may close smaller pores.

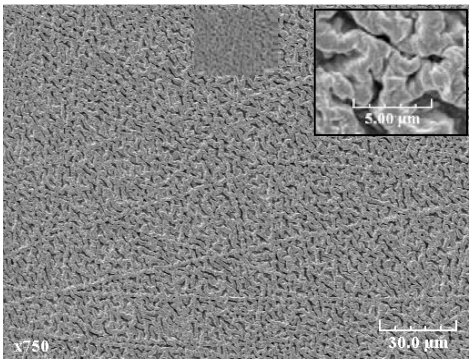

a-Bottom surface of PAA membrane

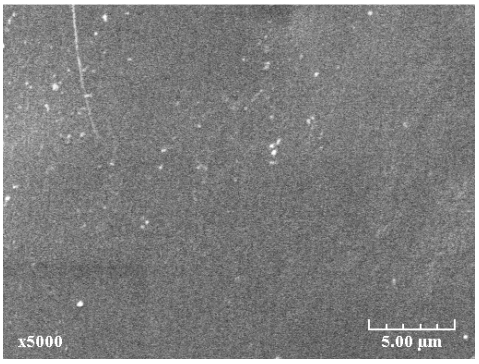

b- Bottom surface of PEI membrane

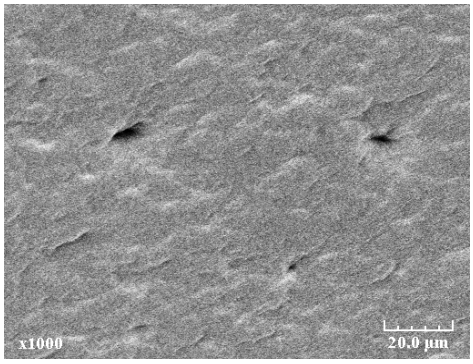

c- Top surface of PAA membrane

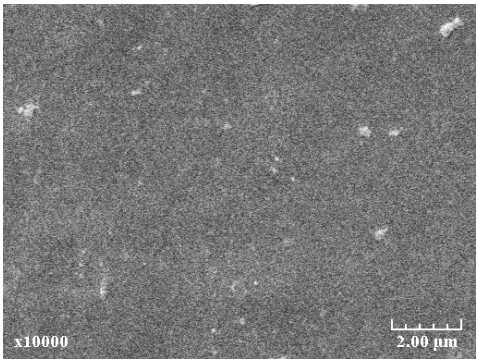

d- top surface of PEI membrane

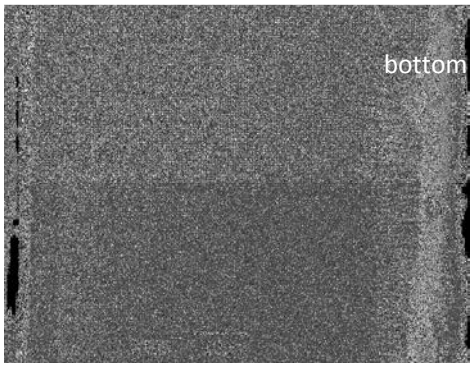

e- Cross sectional view of PAA membrane

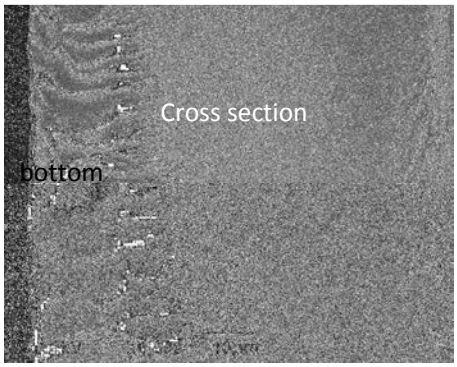

f- Cross sectional view of PEI membrane

Figure 4.3: SEM Photograph surface of M_1 (30%-70%-0/1min/1h/55µm)* where the preparation conditions of each membrane in all figures are (PAA wt%-DMF wt%-Water wt%/preconcentration time/ immersion time/thickness) respectively, film applicator withdraws thickness 300 µm, test1.

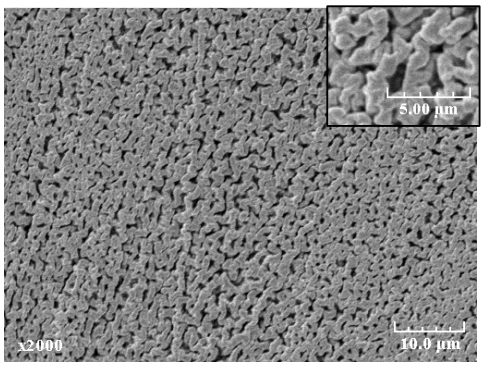

a-bottom surface of PAA membrane

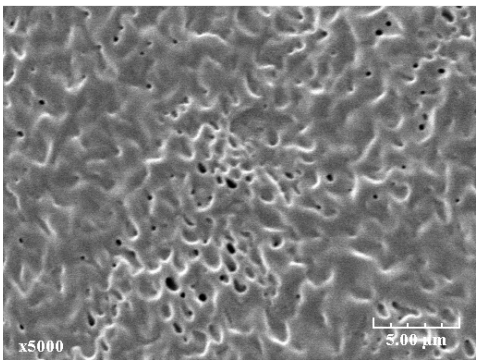

b- bottom surface of PEI membrane

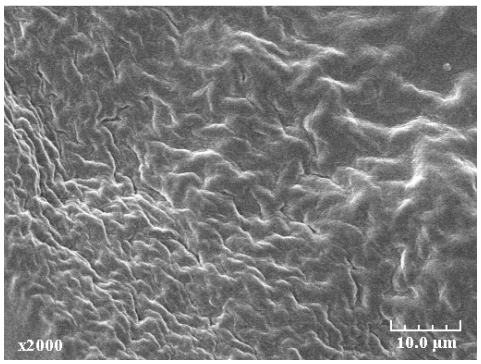

c- top surface of PAA membrane

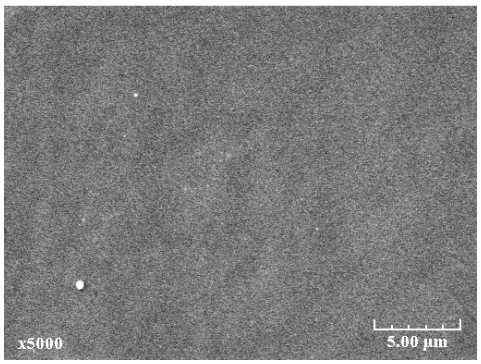

d-top surface of PEI membrane

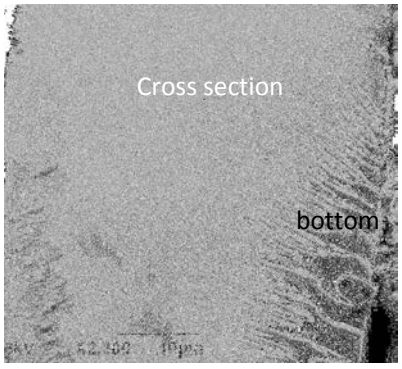

e- Cross section view of PEI membrane

Figure 5.3: SEM Photograph surface of M_2 (30%-70%-0/1min/2h /45µm), film applicator withdraws thickness 300 µm, test1.

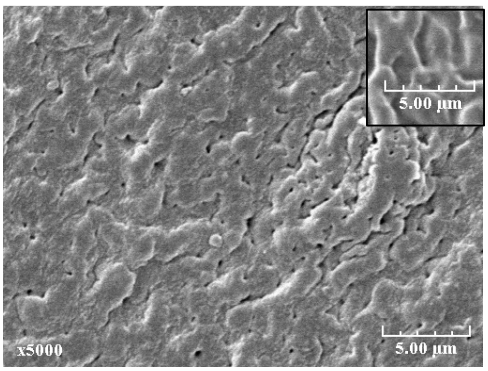

a-bottom surface of PAA membrane

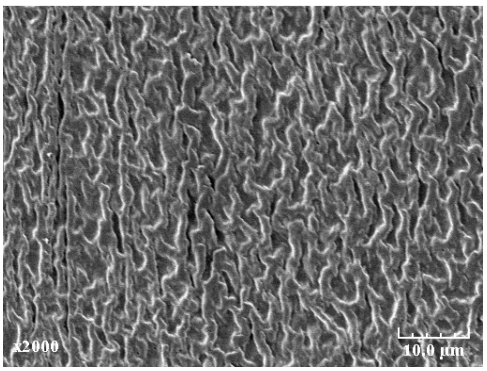

b-bottom surface of PEI membrane

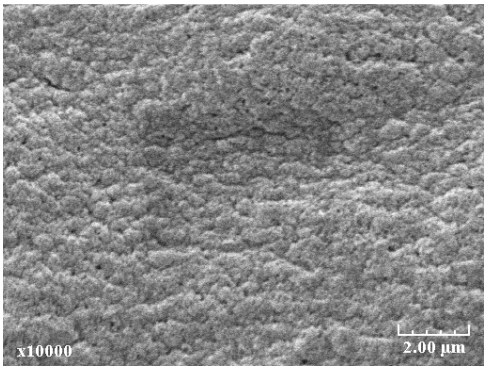

c- top surface of PAA membrane

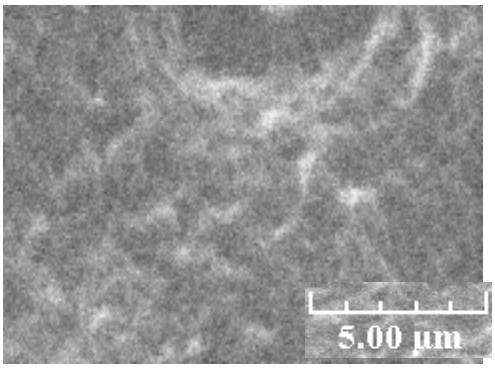

d- top surface of PEI membrane

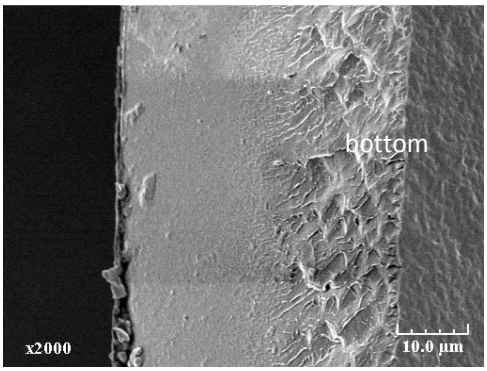

e- Cross sectional view of PEI membrane

Figure 6.3: SEM Photograph surface of M_3 (30%-70%-0/1min/3h/55µm), film applicator withdraws thickness 300 µm, test1.

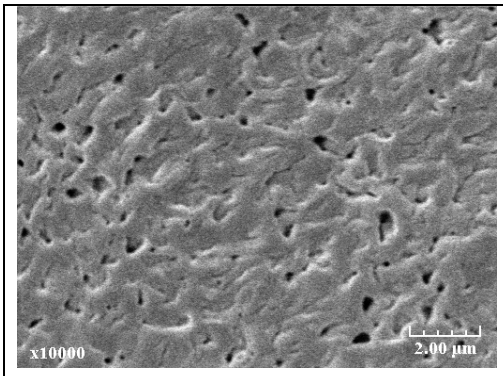

a-bottom surface of PAA membrane

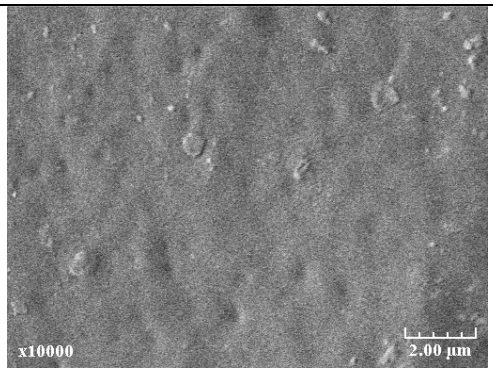

b-bottom surface of PEI membrane

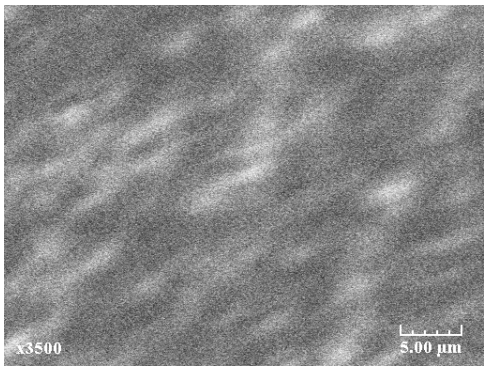

c- top surface of PAA membrane

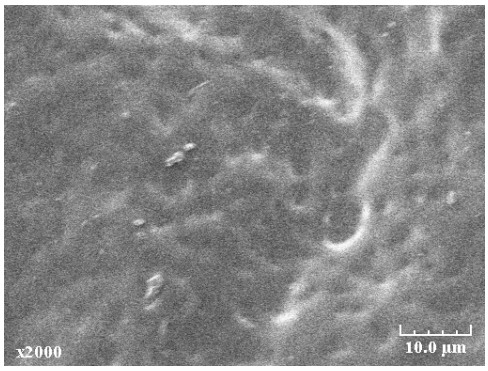

d- top surface of PEI membrane

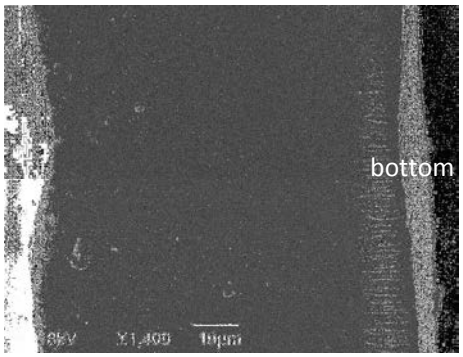

e- Cross section view of PAA membrane

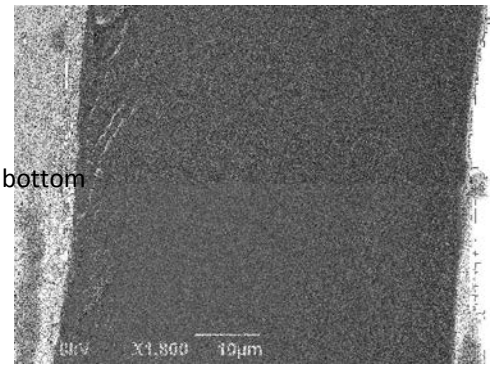

f- Cross section view of PEI membrane(70µm)

Figure 7.3: SEM Photograph surface of M_4 (30%-70%-0/3min/1h/65µm), film applicator withdraw thickness 300 µm, test 2.

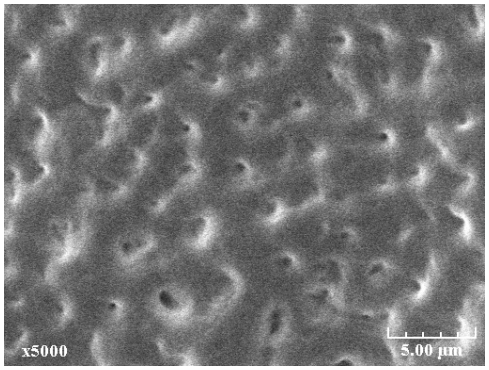

a--bottom surface of PAA membrane

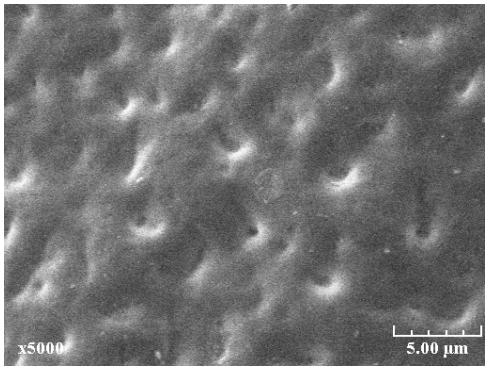

c-bottom surface of PEI membrane

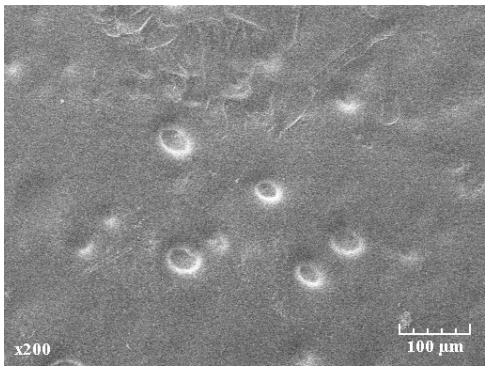

b- top surface of PAA membrane

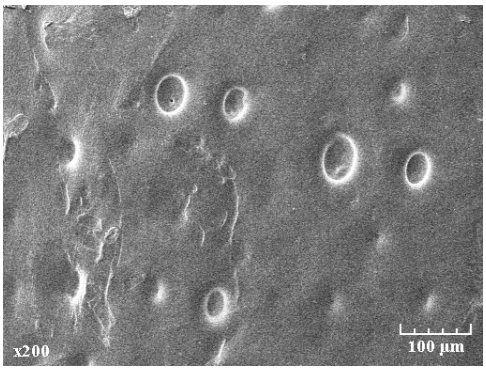

d- top surface of PEI membrane

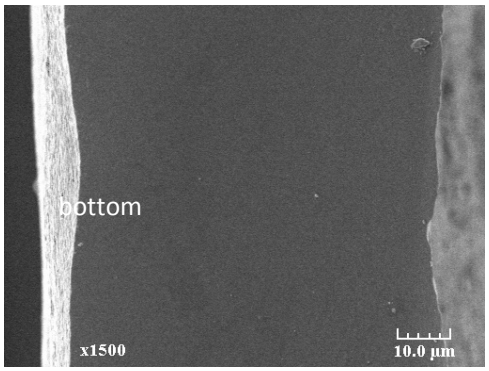

e- Cross section view of PAA membrane

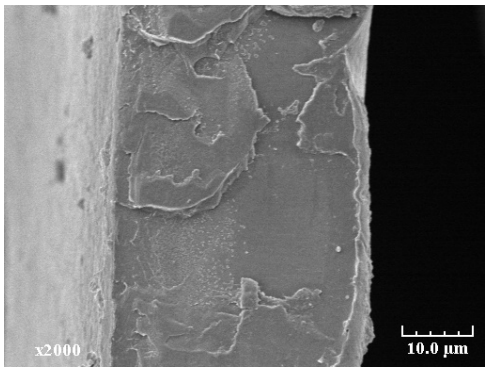

f- Cross section view of PEI membrane

Figure 8.3: SEM photograph surface of M_5 (30%-70%-0/3min/2h/45µm), film applicator withdraw thickness 300 µm, test 2.

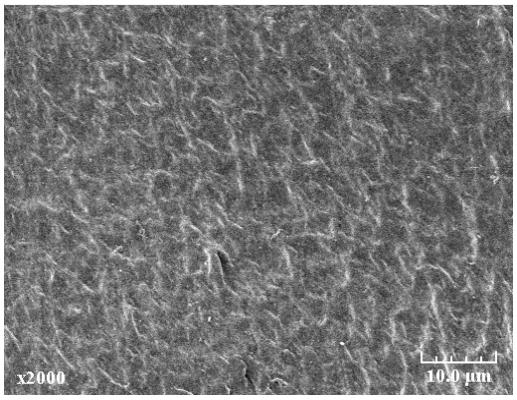

a-bottom surface of PEI membrane

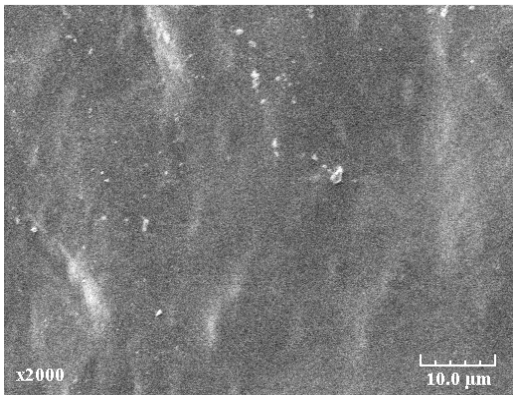

b- top surface of PEI membrane

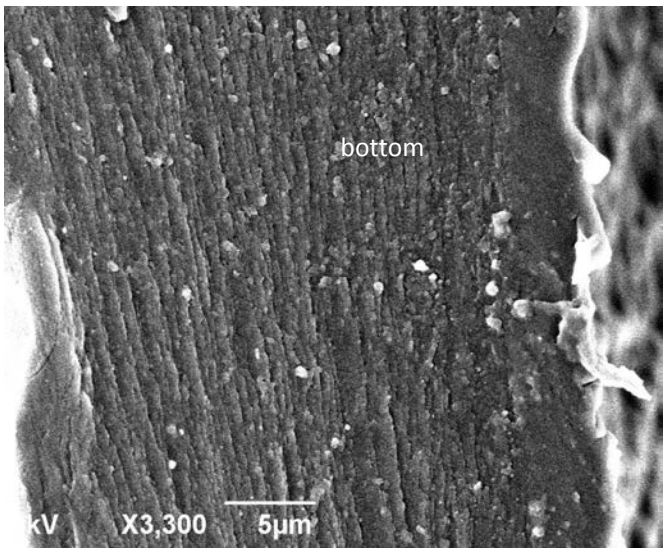

c- Cross sectional view of PEI membrane

Figure 9.3: SEM photograph surface of M_6 (30%-70%-0/3min/3h/40µm), film applicator withdraw thickness 300 µm, test 2.

3.3.2.3 Effect of non solvent (water) addition to polymer solution

The aim of the addition of non solvent to the polymer solution was to change the rate of demixing process and to study its effect on membrane morphology.The effect of non solvent (water) addition to PAA solution on membranes morphology are presented in Figures (10.3 – 14.3, membranes M_7:M_{12}) and the effect of miscibility gap of ternary phase digram on membranes morphology and formation with helping of SEM results are diplayed in Fig.15.3.

Table 4.3: The operating parameters tested for preparation of PEI membranes (membranes M_7:M_{12}).

Membrane	Casting solution wt.%			Pre-concentration time (min)	Immersion* time (h)	Non solvent	test
	DMF	PAA	Water				
M_7	67	28	5	1 min	1 h	Water	3
M_8	60	25	15	"	"	"	"
M_9	56	24	20	"	"	"	"
M_{10}	53	23	24	"	"	"	"
M_{11}	49	20	31	"	"	"	"
M_{12}	42	18	40	"	"	"	"

* starting dope solution before water addition: 30 wt.% PAA; 70 wt.% DMF, immersion in water bath at 11^0C.

It was clear from this 3rd test that the addition of non solvent (water 5-24 wt%, figs.10.3 to 14.3) led to more porous structures. The shape of the pores could also be varied from finger like (water content 15-20 wt %, Figs.11.3-12.3), to highly spongy network which started to appear from water content above 20 wt%; addition of 24 wt % water led to fully spongy cross-section ($M_{10,}$Fig.13.3**).**

Thus, it seemed from SEM characterizations that with the addition of water in the range 5 to 24wt% to the PAA solution, it was possible to get asymmetric membrane having a thin dense top layer connected with long pores. On the other hand the further addition of water (31%) led to a structure formed with very large pores in range of 1000 µm ($M_{11,}$Fig.14.3). At last, above 40wt% of water added in the PAA solution, a two phase system was spontaneous (dimixing gap, Fig.15.3.) formed and no film could be casted(M_{12}**).**

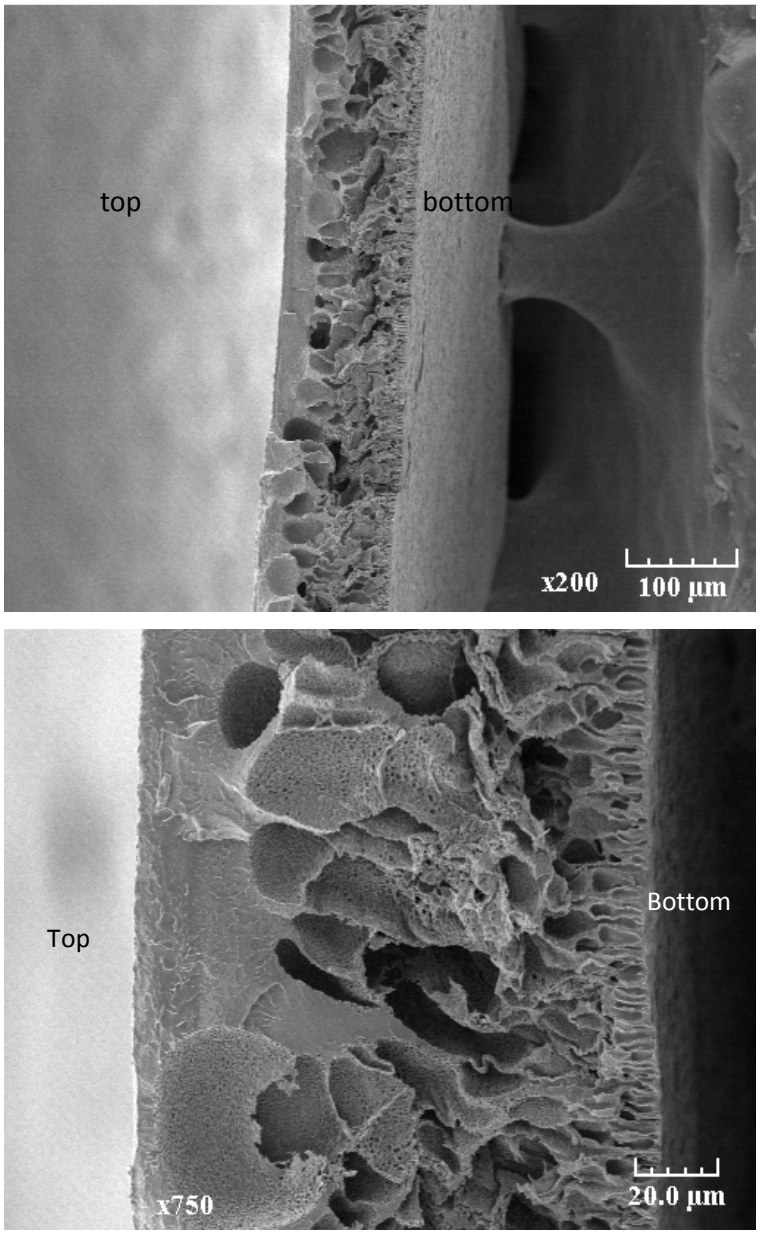

Figure 10.3: Cross section view of asymmetric PEI membrane M_7 (28-67-5/1min/1h/120 µm), film applicator withdraw thickness 500 µm, test 3.

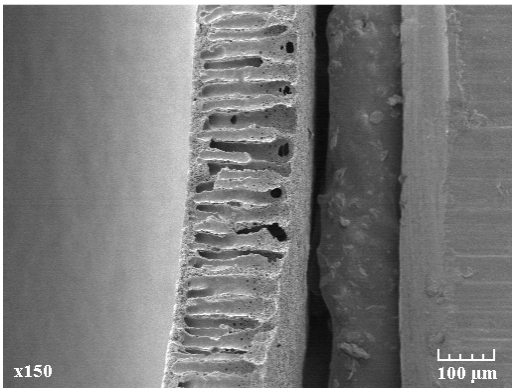

a- Cross section

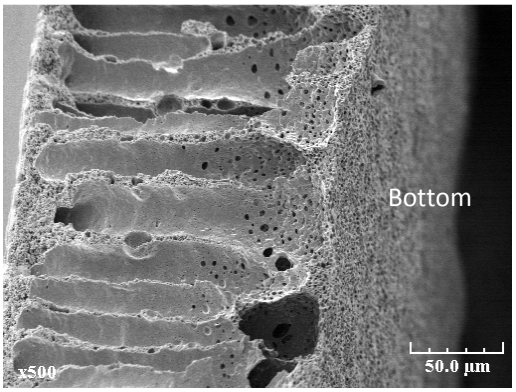

b- Cross section

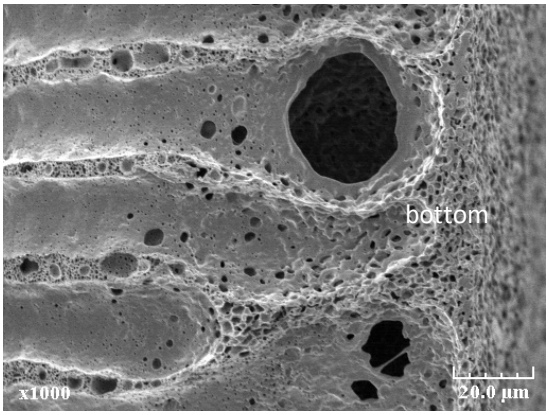

c- Cross section at bottom

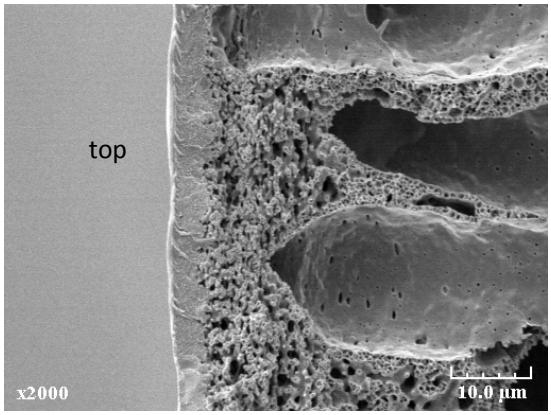

d- Cross section at top

Figure 11.3: Cross section view of asymmetric PEI membrane M_8 (25-60-15 /1min/1h/ 150µm), film applicator withdraw thickness 500 µm, test 3.

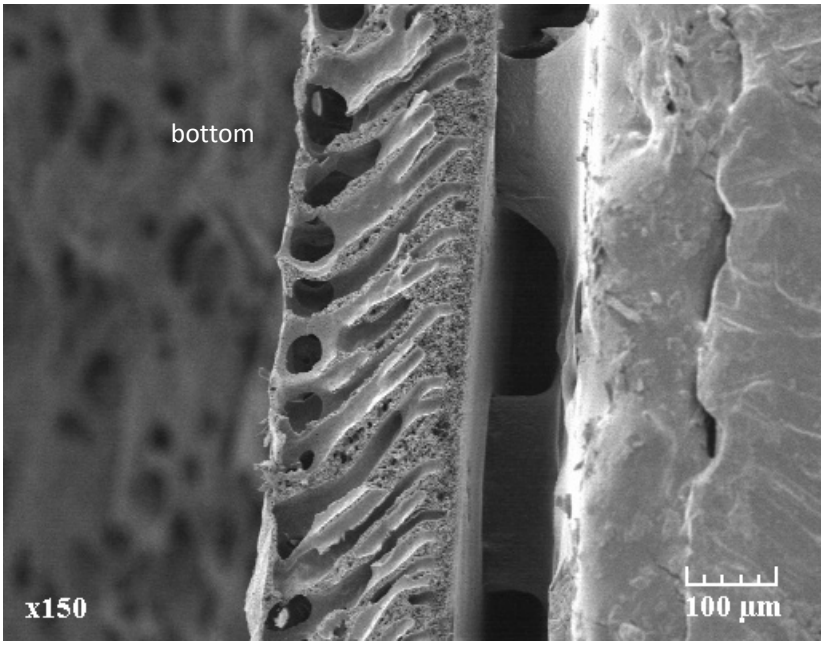

a- Cross sectional view of PAA membrane with thickness 200µm.

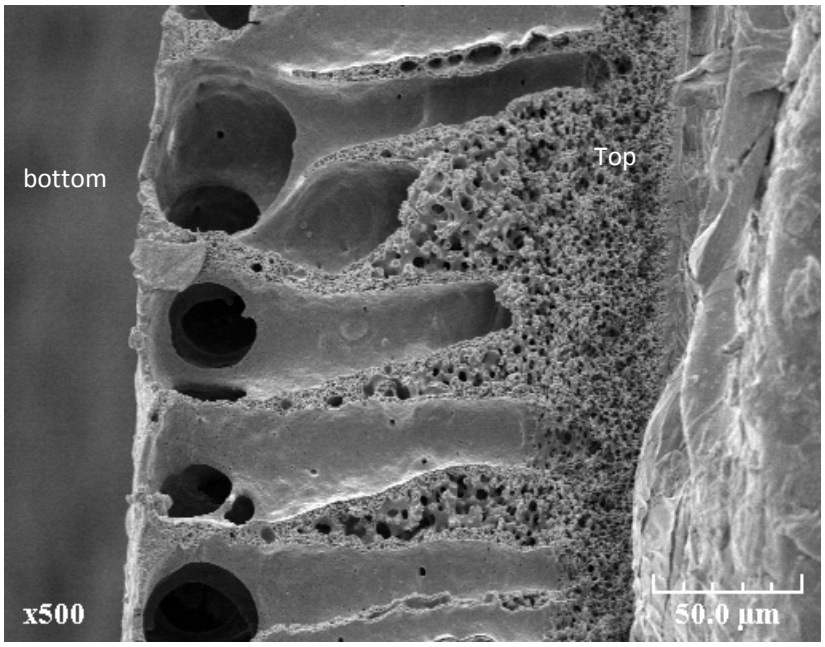

b- Cross sectional view of asymmetric PEI membrane with thickness 170µm

Figure 12.3: Cross section views of M_9 (24-56-20/1min/1h/170µm), film applicator withdraw thickness 500 µm, test 3.

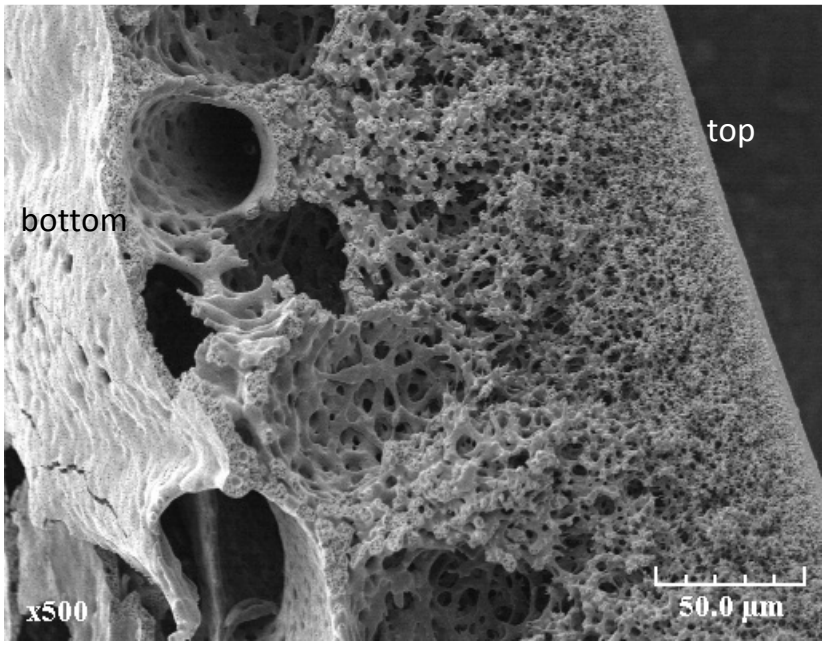

a- Cross sectional view of PAA membrane with thickness 200 µm.

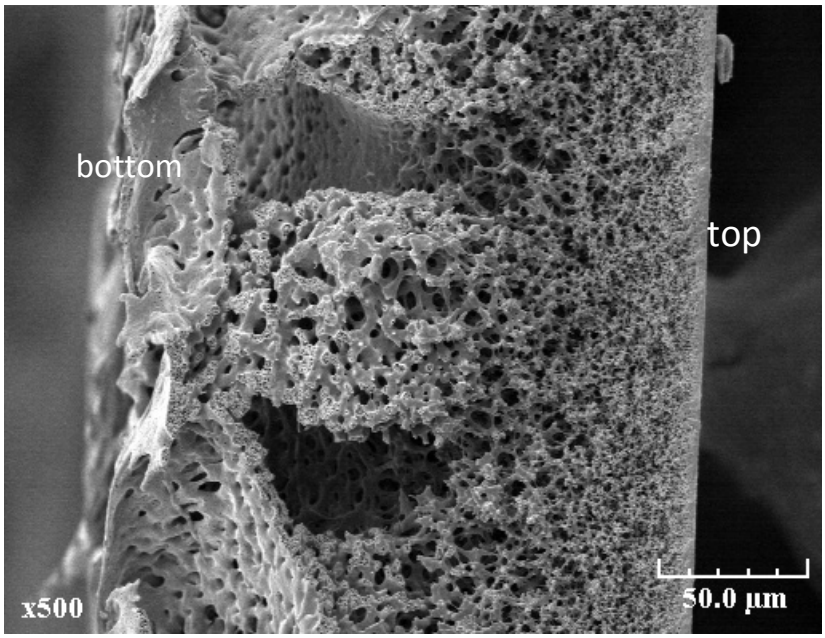

b. Cross sectional view of PEI membrane with thickness 170µm.

Figure 13.3: Cross section view of PEI asymmetric M_{10} (23-53-24/1min/1h/170µm), film applicator withdraw thickness 500 µm, test 3.

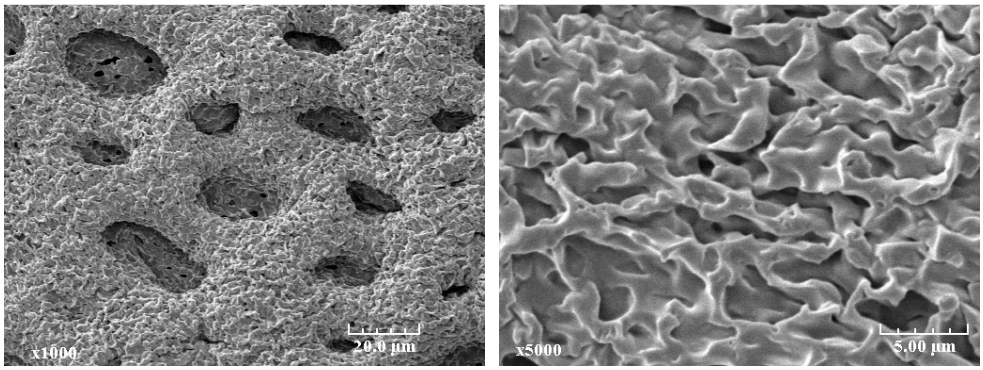

a-PEI bottom side b- PEI top side

Figure 14.3: SEM view of SEM view of M_{11} (PAA-DMF-water: 20-49-31/1min/1h) test 3.

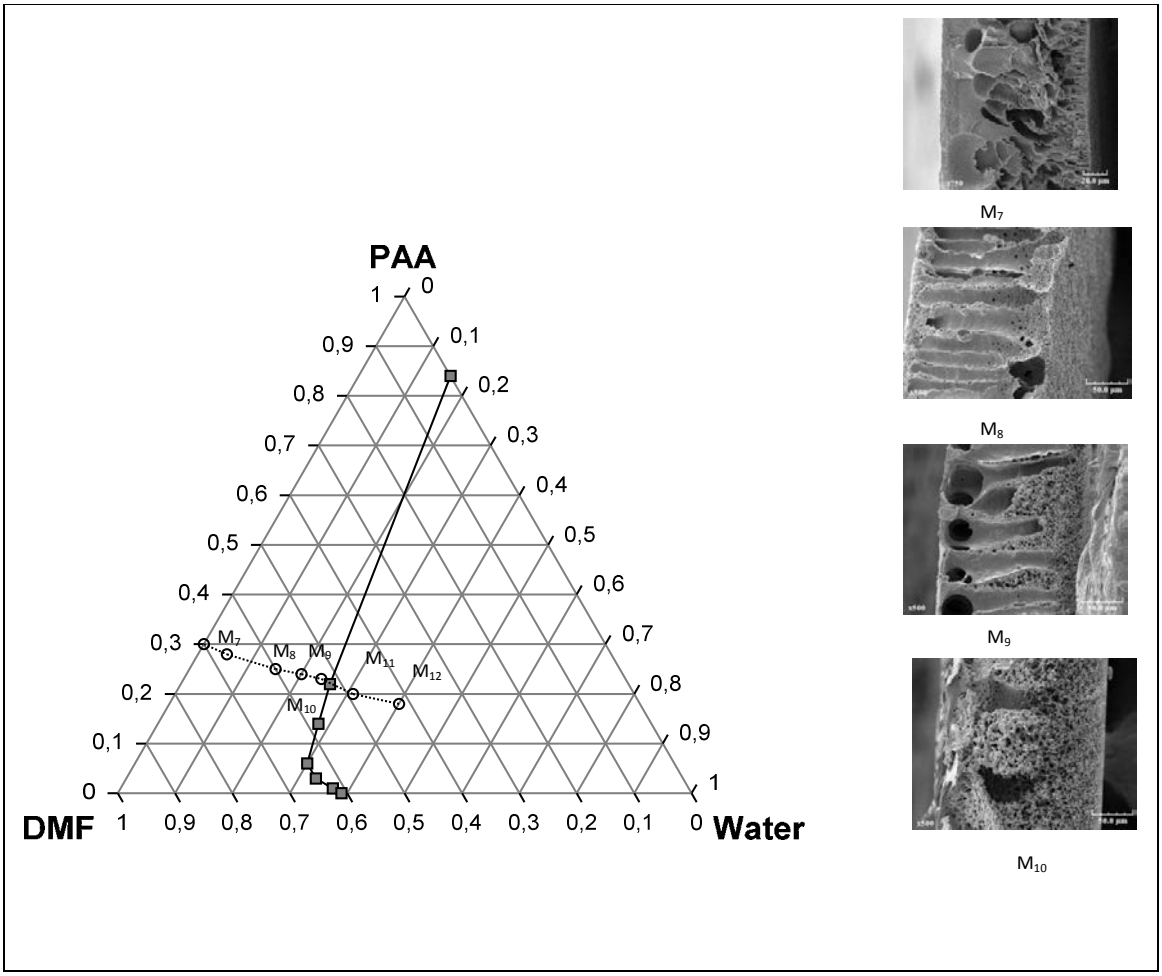

Figure 15.3: Schematic representation of the ternary phase diagram with membrane morphology (ternary solution of PAA membranes M_7-M_{12} --○-- ; binodal demixing curve ■).

The effect of variations of the casting solution composition with water addition for membranes (M_7-M_{12}) is displayed schematically in Fig.15.3, it reports the agreement between

experimental work and miscibility (mixing) gaps with the evaluations of a membrane-forming system**.** From miscibility gap of the ternary phase digram (Fig.15.3) and with helping of SEM results for membranes (M_7-M_{12}), it was found that increasing the water concentration led to change membrane morphology from less porous to highly porous membranes, the addition of water was not possible since the actual concentration (i.e.: 26 wt% water in 30 wt.% PAA in DMF) was already very close to the binodal demixing curve in the ternary phase diagram (i.e.: M_{11} , M_{12})

It is known that membranes with finger-like structure are usually formed when the liquid–liquid phase separation is instantaneous demixing process occurs [11-13]. Furthermore, it has previously been reported that the use of a single nonsolvent as a coagulator results in the formation of finger-like morphologies in systems with a high solvent/nonsolvent affinity and a good solvent for the polymer [14,15], whereas sponge-like structures are formed when a delayed demixing process occurs [16,17]. For delayed demixing, a dense skin layer is formed, which inhibits the inflow of water into the polymer solution. Further, in the case of delayed demixing, the number and the size of nuclei of polymer-poor phase become smaller. Therefore, macrovoids significantly disappeared.

The other parameter known to induce finger like structure in the wet phase inversion method is the affinity between the polymer (in our case PAA), the solvent(DMF) and the non solvent (water) used for the coagulation inversion bath [12,13], in case of higher affinity between solvent and nonsolvent; when the casted film is immersed in the nonsolvent (coagulation bath) the solvent is quickly dissolved in the nonsolvent, and this led to instantaneous demixing process. Conversely sponge-like morphologies are more likely to occur in the opposite case.

Certain membrane structures can be correlated with the rate of precipitation; when very high precipitation rates occur (short gelation times), it leads to asymmetric membranes with a “finger” like structure, while slow precipitation rates (long gelation times) lead to asymmetric membranes with a “sponge” like structure, and very slow precipitation rates very often lead to symmetric membranes with no defined skin at the surface, a structure with a very uniform pore size distribution over the entire cross section of the membrane [13]. If a sponge-type structure is obtained, the pore diameters are inversely proportional to the rate of precipitation. Higher precipitation rates lead to finer pore structures, and lower precipitation rates lead to coarser structures.

The polymer-solvent-precipitant interaction can be approximately correlated in terms of the disparity of the solubility parameter of polymer and solvent.

(1) The smaller the solubility parameter disparity of solvent and polymer, the better the compatibility of solvent and polymer, and the slower the precipitation of the polymer. Thus, the tendency for a change from a sponge to a finger structure membrane increases with decreasing compatibility of solvent and polymer, i.e. higher gelation rates.
(2) The higher this disparity, the less compatible are polymer and precipitant, and the faster will be the precipitation. The tendency to change from a sponge to a finger structure will thus increase with decreasing compatibility of polymer and precipitant.

3.3.2.4 Effect of change polymer solution concentration

The effect of polymer solution concentration is represented in Figure (16.3-17.3, membranes $M_{1,}$ M_{13}:M_{18}) and table 5.3. It was found out that the decreasing concentration of PAA in DMF (from 30 to 15 wt %) led to an increase of the asymmetric structures in the membranes ($M_{1,}$ M_{13}:M_{15}), and in membranes ($M_{8,}$ M_{16}:M_{18}) the asymmetric layer have many pores of higher diameter (from 1µm to 3µm) this is the effect of non solvent addition to polymer solution. The thermal treatment from PAA to PEI improves the mechanical properties, avoids brittle property, induces densification and may close smaller pores.

Table 5.3: The operating parameters tested for preparation of PEI membranes (test 4, test 5)

Membrane	Casting solution			Pre-concentration time (min)	Immersion time (h)	Non solvent	test
	DMF	PAA	Water*				
M_1	70	30	0	1 min	1 h	Water	4
M_{13}	75	25	"	"	"	"	"
M_{14}	80	20	"	"	"	"	"
M_{15}	85	15	"	"	"	"	"
M_8	70	30	15	1 min	1 h	Water	5
M_{16}	75	25	"	"	"	"	"
M_{17}	80	20	"	"	"	"	"
M_{18}	85	15	"	"	"	"	"

*water wt% calculated on the total (PAA+DMF) weight after addition to dope solution, bath temperature 11°C.

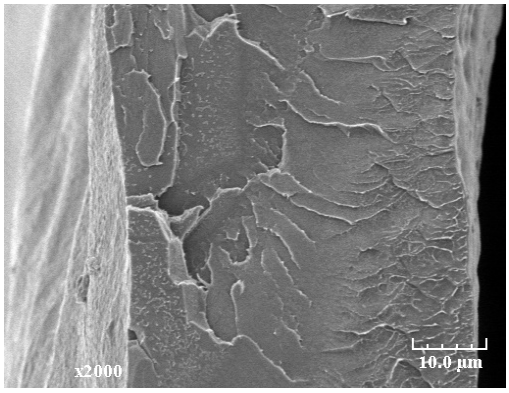

a-M_1 test 4(30%-70%-0 /1min/1h/ 45 µm)

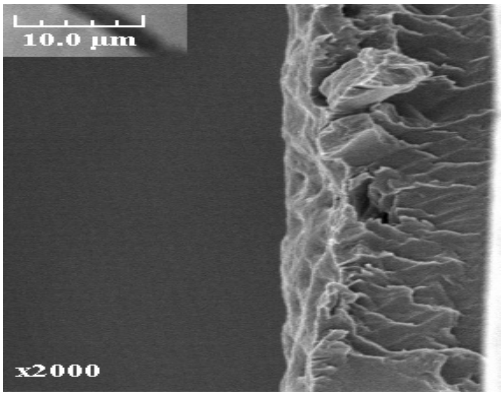

c- M_{14} test 4 (20%-80%-0 /1min/1h/15µm)

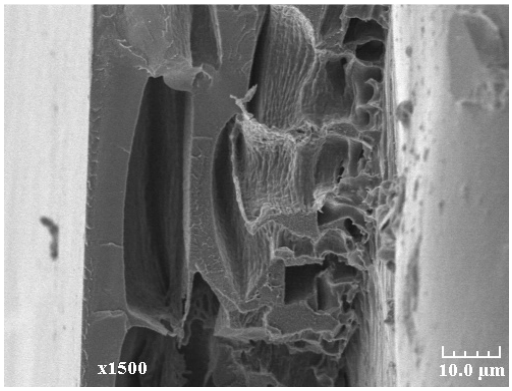

b- M_{13} (25%-75%-0/1min/1h/50µm)

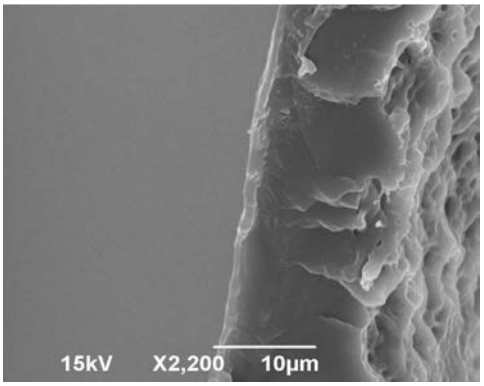

d- M_{15} (15%-85%-0 /1min/1h/15µm)

Figure 16.3: cross section views of PEI asymmetric membranes with change polymer solution composition test 4, film applicator withdraw thickness 300 µm.

Hence, the thickness of the dense layer decreases with decreasing the polymer concentration in casting solution, as reported by [12,13]. In general, the reduction of the polymer concentration in the casting solution indeed leads to a more open and porous structure with large pores (Fig. 17.3). Thus, mechanical properties of the membranes prepared with a low polymer concentration are lower than a high polymer concentration.

It was clear from this 4th set of phase inversion condition that the decrease of polymer concentration led to more porous structures (M_{15})**,** and the shape of the pores is micro-voids with very small dense layer. Thus, Increasing PAA concentration led to slow down the demixing process [12, 13]. This prevents instantaneous demixing growth of nucleuses in the membrane structure. So, a large number of small nucleuses are created and distributed throughout the polymer film and denser membranes are prepared (M_1).

The effect of the nonsolvent (water) addition and of the polymer concentration (test 5) is displayed in Fig.17.3. These systems were further tested by varying the polymer concentration in the casting solution in order to minimize the skin thickness and maximize the liquid permeance. Water as nonsolvent gave the best results for solutions in DMF (from membrane preparation and SEM),when it was added to the casted solution. However, further tests by increasing the water concentration was not possible since the actual concentration (25 %, test 3) was already very close to the binodal demixing curve in the ternary phase diagram. Therefore, instead of increasing the nonsolvent concentration, the polymer concentration was decreased. Upon evaporation of the solvent, both scenarios should lead to a higher nonsolvent/polymer ratio in the demixed system, and thus to a higher final porosity and probably a more open pore structure and a lower skin thickness.

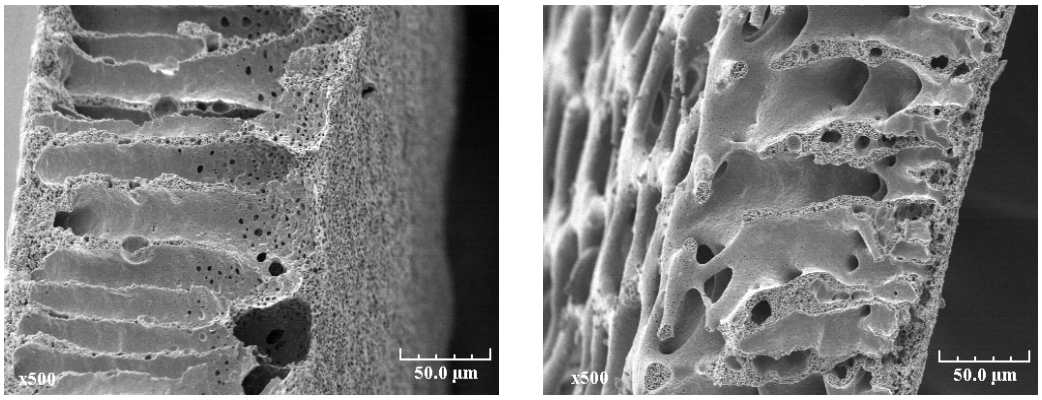

a-M_8 test 5(30%-70%-15%/1min/1h/150µ) b- M_{16} test 5 (25%-75%-15%/1min/1h/100µm)

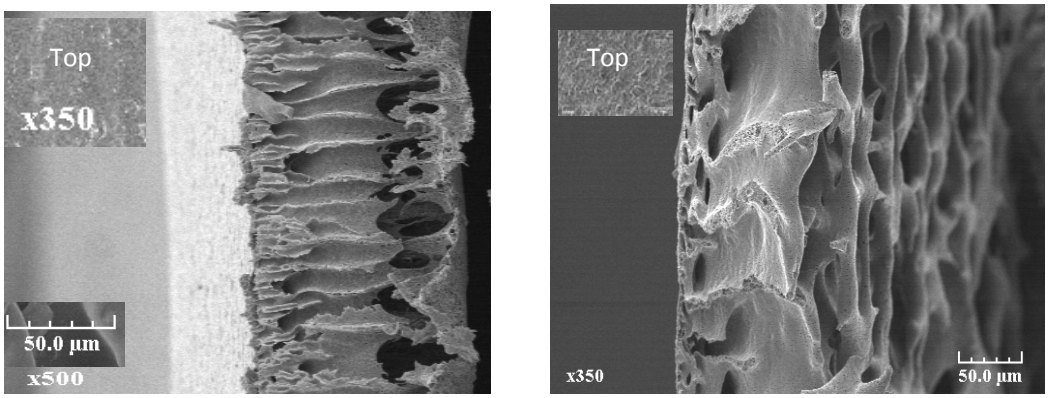

c- M17(20%-80%-15% /1min/1h/75µm) d- M_{18}: (15%-85%-15% /1min/1h/60µm) test 5.

Figure 17.3: Cross section view of PEI membranes versus polymer solution composition film applicator withdraw thickness 500 µm, test 5.

3.3.2.5 Effect of the immersion bath temperature (IBT).

Effects of immersion bath (water) temperature on preparation of asymmetric PEI membrane morphology are shown in Figs.18.3-19.3-20.3(membranes M_{19} to M_{21}). Operating parameters for studying the effect of change of immersion bath temperature is presented in table 6.3. It was found that with asymmetric PEI membranes, the porosity increases with the increase of the immersion bath temperature and the thickness of dense top layer is decreased. Raising the temperature increases mutual diffusivities between the nonsolvent (water) and the solvent (DMF) in the casting solution during de-mixing process. At higher temperature, nucleuses of polymer-poor phase grow rapidly which consequently increases the formation of porous structure in the membrane leading to macrovoids.

Table 6.3: Operating prameters for studying the effect of change of immersion bath temperature.

Membrane	Casting solution			Immersion bath temperature	Membrane features
	DMF	PAA	Water		
M_{19}	70	30	**0**	***5°C***	No pores
				7°C	No pores
				10°C	Asymmetric: pore at bottom surface
M_{20}	75	25	**0**	***7°C***	Pores+dense top layer≈15µm
				10°C	Pores+ dense top layer≈10µm
				16°C	Pores+ thinner top layer ≈2µm
				20°C	Pores
M_{21}	75	25	**1**	***5°C***	Pores+dense top layer≈30µm
				7°C	Pores+ dense top layer≈15µm
				10°C	Pores+ dense top layer≈10µm

Conversely, the reduction of the temperature limits the speed of nucleus growth, giving rise to the formation of a large number of small nucleuses in every part of the cast film; hence a great number of little pores/voids are formed in the sublayer of the PAA membranes. Therefore, formation of macrovoids is prevented and denser PEI structures are obtained after cyclization as shown on Figs.(18.3-19.3-20.3) at the lowest temperature.These results are in agreement with the literature [13,18]. Ehsan Saljoughi et.al [18] found out that increasing coagulation bath temperature (CBT), accelerates diffusional exchange rate of solvent (NMP) and nonsolvent (water) and consequently facilitates formation of macrovoids in the membrane structure.

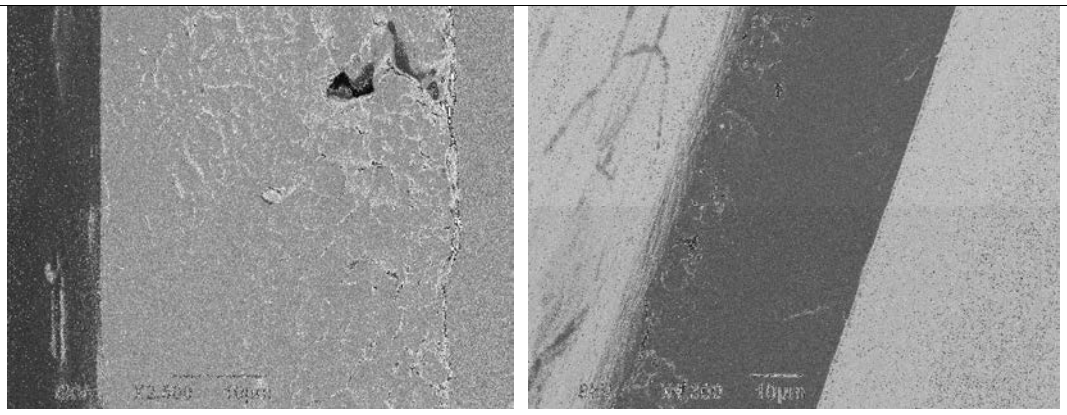

a- PEI membrane at immersion bath 5°C b- PEI membrane at immersion bath 7°C

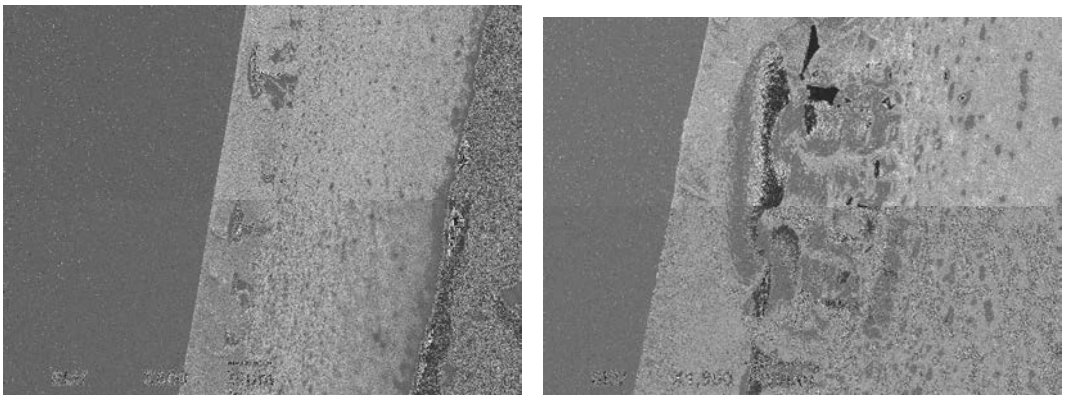

b- PEI membrane at immersion bath 10°C

Figure 18.3: Cross section view of M_{19} (30%-70%-0 /1min/1h/35µm) at immersion bath temperature 5°C, 7°C and 10°C.

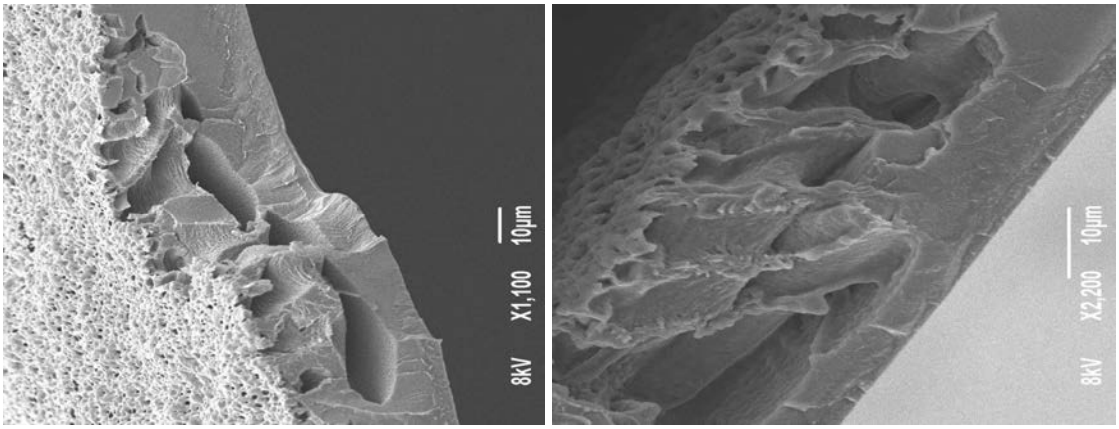

a- PEI membrane at immersion bath 7°C b- PEI membrane at immersion bath 10°C

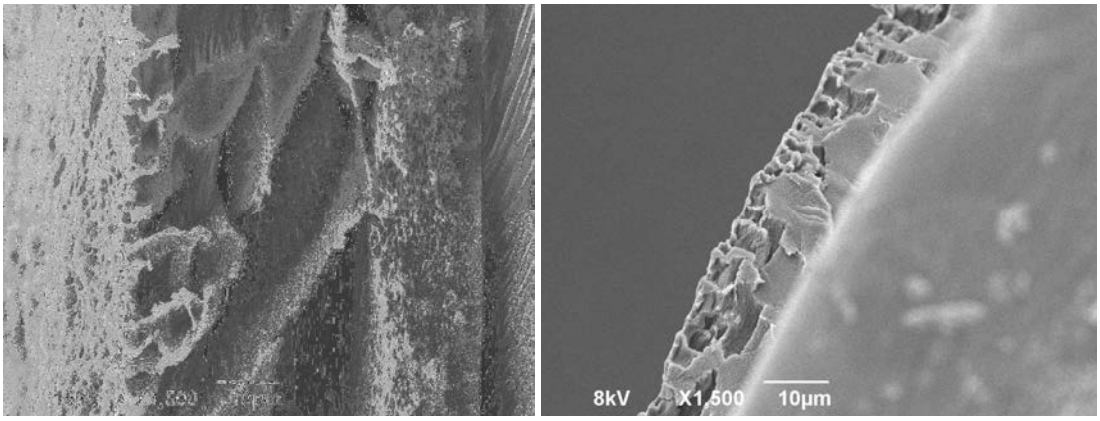

c-PEI membrane at immersion bath 16°C d- PEI membrane at immersion bath 20°C

Figure 19.3: Cross section view of PEI asymmetric M_{20} (25%-75%-0 /1min/1h/20-40µm) at immersion bath temperature 7°C, 10°C, 16°C and 20°C.

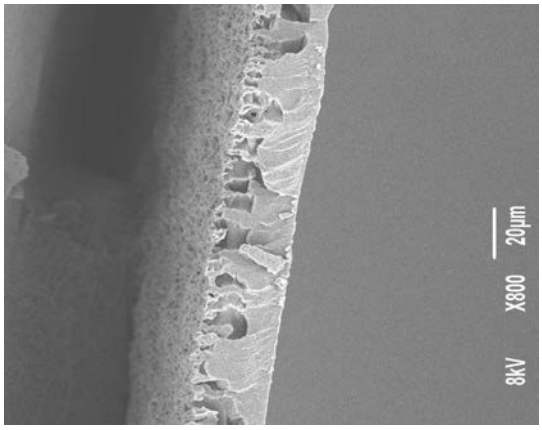

a- PEI membrane at immersion bath ***5°C***

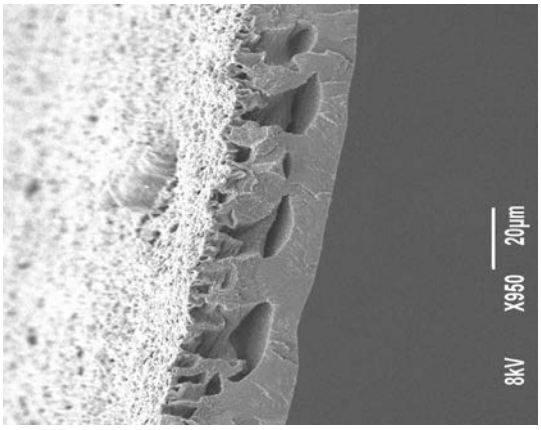

b- PEI membrane at immersion bath ***7°C***

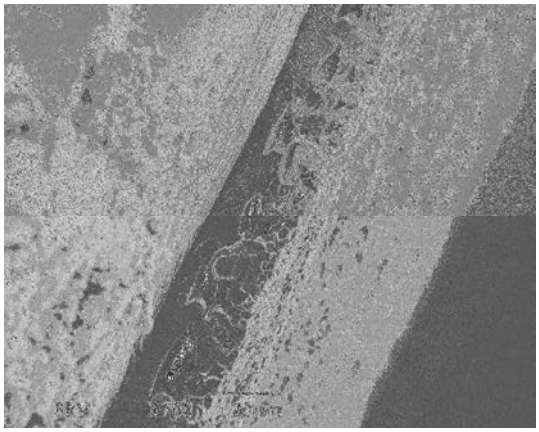

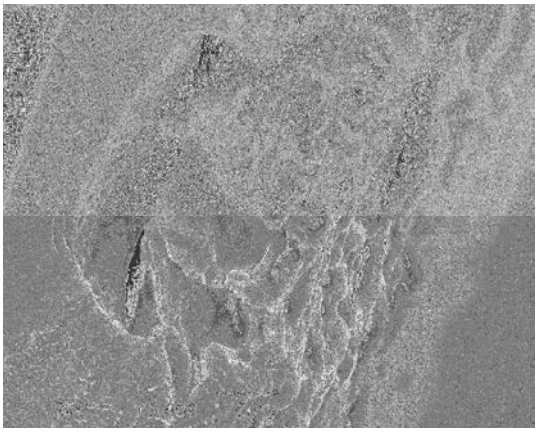

d- PEI membrane at immersion bath ***10°C***

Figure 20.3: Cross section view of M_{21} (25%-75%-1% /1min/1h/30µm) at immersion bath temperature 5°C, 7°C and 10°C**.**

3.3.2.6 Effect of the immersion bath type

Effect of the immersion bath type is presented in table 7.3, membranes M_{22}: $M_{23.}$ In this test we tried to find other non solvents suitable for use as immersion bath. Solubility parameter of non-solvent (NS) follow: H_2O>> CH_3OH >C_2H_5OH.

Table 7.3: The operating parameter tested for preparation of PEI membranes

Membrane	Casting solution			Pre-concentration time in min	Immersion Time in h	Non solvent	test
	DMF	PAA	Water				
M_{22}	70	30	0	1 min	1 h	Methanol	6
M_{23}						Ethanol	

Observation of PAA after immersion in methanol and ethanol

When methanol or ethanol were used as immersion bath, the films were immediately transformed into a sticky paste, leading to the quick formation of numerous holes (up to 1 cm), and to the film destruction with time. Hence, these coagulants liquids were not suitable in this case.

3.3.2.7 Effect of using different immersion bath in series.

The effect of using different immersion bath in series is presented in figure (21.3) (membranes M_{24}-M_{27}), starting with PAA solution, Jeff600-PMDA-ODA (0.4/1/0.6) concentration 30 wt.% in DMF. It was observed that, when methanol or ethanol were used as a second immersion bath, the films were transformed into a sticky paste, leading to the quick formation of numerous holes, and to the film destruction with time, as reported above with a single alcohol immersion bath. The surface morphology exhibits a cloudy porous structure that presents homogenous morphology in bottom surface (Fig.21, a.3).

Thus, it was found that from these tests that only the water immersion tank is suitable as a coagulant (non solvent) in preparation of PEI membranes in our case. When other nonsolvents as methanol and ethanol are used as second bath they induce some swelling and then the formation of pineholes upon drying under vacumm.

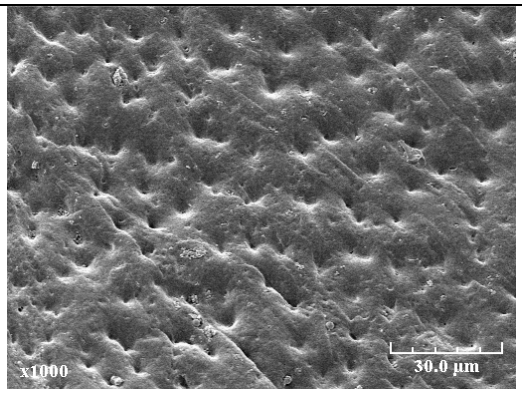

a- bottom surface of PAA membrane

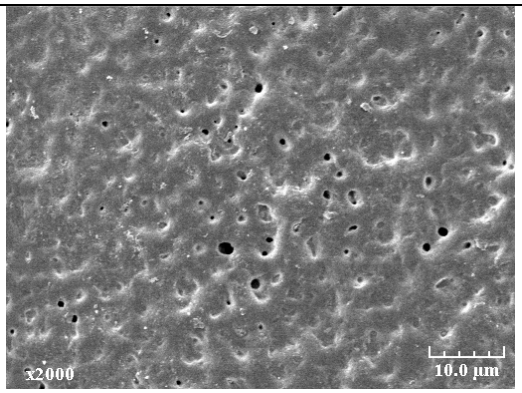

b- bottom surface of PEI membrane

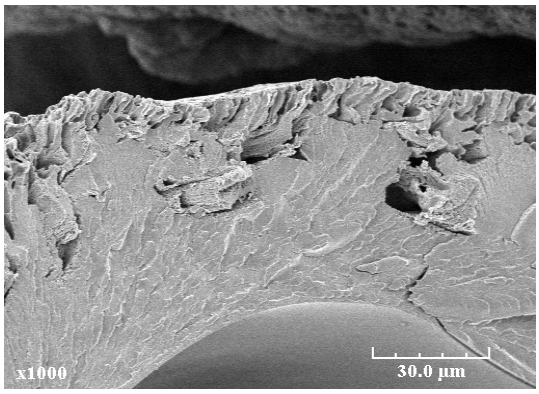

e- Cross sectional view of PAA membrane

Figure 21.3: SEM Photograph surface of M_{24}. Casting at ambient temperature in air for 1 min, then 1st Immersion in water 2h at 11 ^{0} C, then drying at ambient temperature in air 24h, then 2nd Immersion in methanol 1 h, then at ambient temperature in air 24h. Finally curing under vacuum 1 h at 100 ^{0} C, 150 ^{0} C and 200 ^{0} C.

3.3.2.8 Effect of addition of co-solvents to PAA solution and effect of additives addition with water in coagulation bath .

The aim of this work is to study the effect of addition co-solvents (such as toluene) to PAA solution which has a lower affinity with water than with DMF, to delay de-mixing process to get spongy-like structure which is desired versus finger-like because their mechanical properties are higher and also to avoid the formation of large holes. Then, studying the effect of other additives (i.e: DMF, ethanol) with water in the immersion tank for the same purpose. PAA solution used: Jeff600-PMDA-ODA (0.4/1/0.6) with concentration=

15-30 wt% in DMF. All membranes which are prepared are presented in table 8.3 and shown in Fig. (22.3, membranes M_{28}-M_{34}).

Table 8.3: Operating parameter tested for preparation of PEI membranes

Membrane*	Casting solution%			Immersion bath	test
	DMF	PAA	Toluene		
M_{28}	70	25	5	water	1
M_{29}			10		
M_{30}			20		
M_{31}	70	25	-	(95%Water+5%DMF)	2
M_{32}			-	(90%Water+10%DMF)	
M_{33}	70	25	-	(95%Water+5%Ethanol)	
M_{34}			-	(90%Water+10%Ethanol)	

*Drying time in air for 1 min before casting step , immersion bath at 10°C during 1h.

Obervation of PAA after immersion in coagulation bath :

Solubility parameter of non-solvent (NS): H_2O>> CH_3OH >C_2H_5OH. Thus, toluene will delay the time for PAA to reach the glassy state. It was found out that when the PAA casted films are immersed in the coagulant bath immediately a lot of lines are formed on the membrane surface (striated network). This is are observed in all cases of addition of co-solvent (toluene 2.5 to 20%) in PAA or addition of additives in the water bath; the density of these striated network surface increased with increasing the % of co-solvent or additives. Furthermore, all the PEI membranes show a fully dense structure with transperent yellow color. Thus, these type of additives and co-solvents were not suitable in our case.

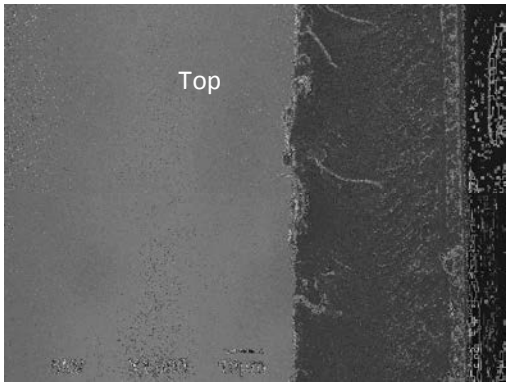

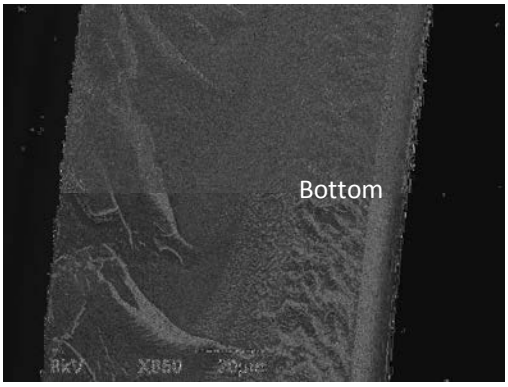

a- M_{28} (25%PAA- 5%Toluene)

b- M_{31}(25%PAA-Im 5%DMF)

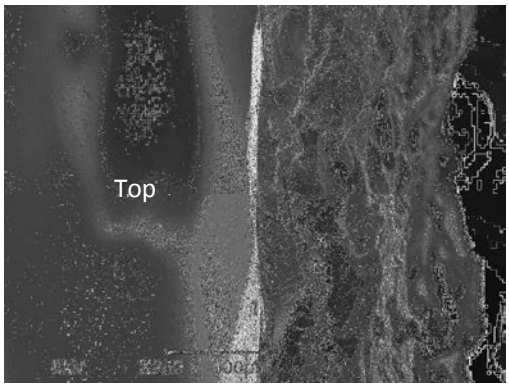

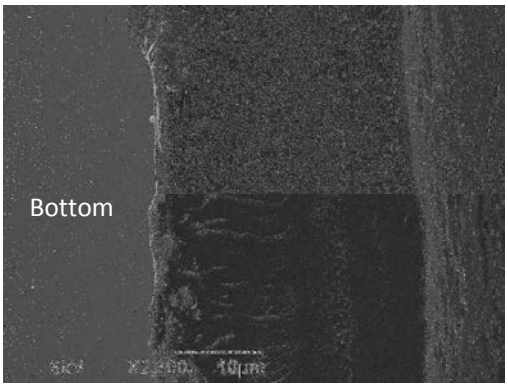

c- M_{32} (25%PAA-Im 10%DMF)

d- M_{33} (25%PAA-Im 5%Ethanol)

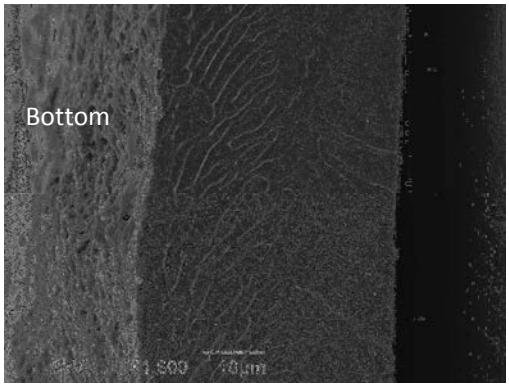

e- M_{34} (25%PAA-Im 10%Ethanol).

Figure 22.3: Cross sections view of PEI membranes, immersion bath at 10°C during 1h.

3.3.3 SEM for Hybrid silica-PEI membranes

The scanning electron microscopy for the hyprid dense PEI membrane is shown in Fig. 23.3 and the asymmetric composite PEI membranes are shown in Figs. (24.3-25.3). From figure (24.3) it is observed that the structures of asymmetric membranes have a large dense layer with a very small asymmetric layer with addition 5% TMOS, with more addition of TMOS the membrane structure is dense.

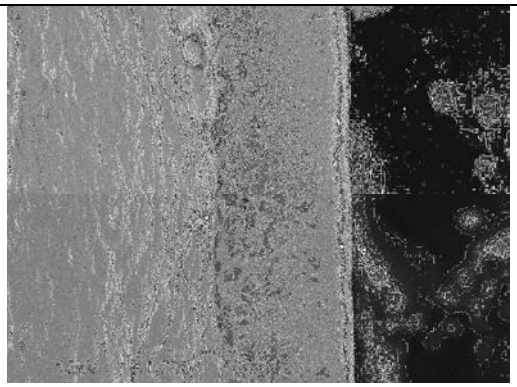

Figure 23.3: Cross section view for hybrid dense PEI membrane M_{dc1} (5%TMOS,95% PAA).

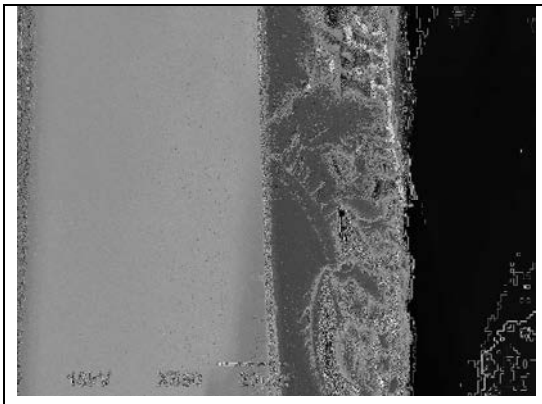

M_{c1} (5%TMOS, 95%PAA)

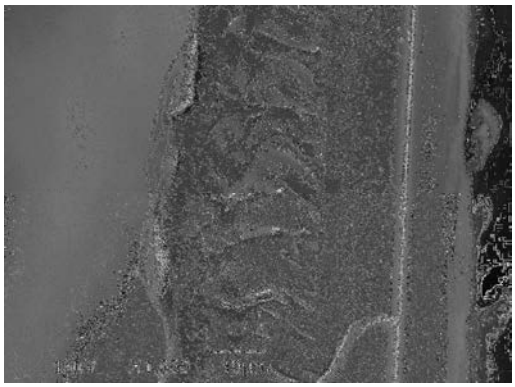

M_{c2}(10 %TMOS, 90%PAA)

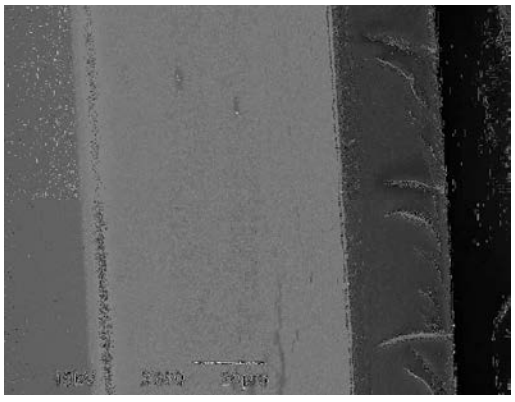

M_{c3} (20 %TMOS, 80%PAA).

Figure 24.3: Cross section views for hybrid asymmetric PEI membrane.

It has been found out that for hybrid membranes, the mechanism of phase inversion did not work properly when using the same experimental protocol as with homogeneous PAA solution. Thus, we can conclude that the sol-gel process alters the conditions of phase inversion and the rate of phase inversion is found to delay demixing with addition of TMOS. It is observed from figure (25.3) that the structure of asymmetric $M_{c4\ (5\%SiO2\ 12\ nm,\ 95\%PAA)}$ membrane has a large asymmetric layer with addition 5% SiO2 (12 nm, hydrophilic). The permeability and selectivity of this type of membrane will be tested to check its structure

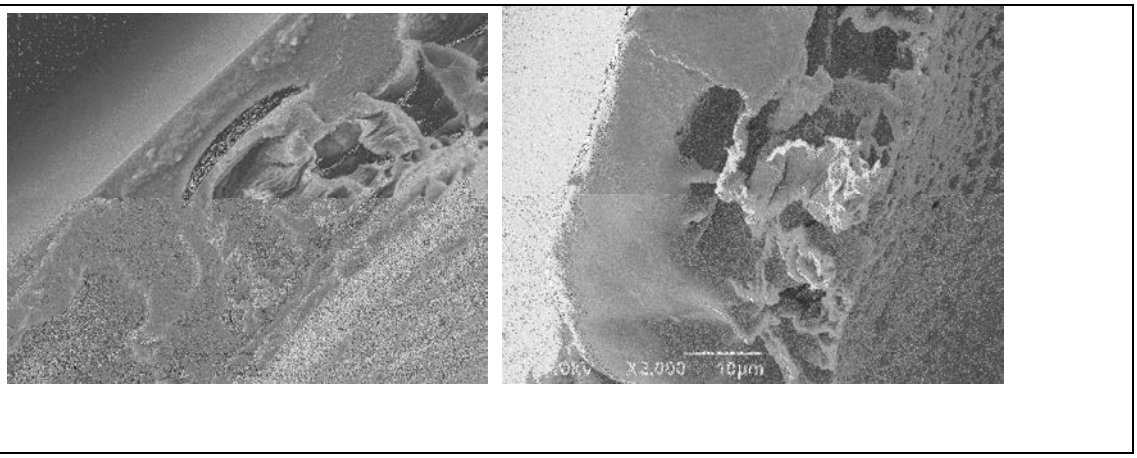

Figure 25.3: cross section views for asymmetric PEI membrane $M_{c4\ (5\%SiO2\ 12\ nm,\ 95\%PAA)}$.

3.3.4 Kapton membranes preparation

3.3.4.1 Preparation of Kapton (PI) dense membrane

The SEM views of flat Kapton membranes prepared by two steps mechanism from PAA solution showed that the corresponding structures seem to be pore free either on the top (air side) or on the bottom (glass side) surfaces. These membranes appeared thus to be dense ones (Fig. 26.3) as expected. In addition, the prepared dense Kapton membrane is highly transparent with slightly yellow color. Furthermore, the prepared dense PI membrane has a good mechanical property.

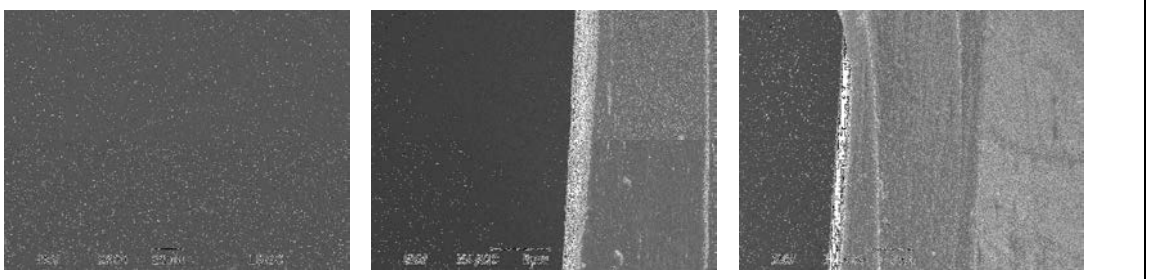

Figure 26.3: Surface view of Kapton (PI) membrane M_{kd1}.

3.3.4.2 Preparation of Kapton membrane by phase inversion

The PI asymmetric membrane and symmetric support layer were made by a phase inversion process. The PAA dope solution (11-15wt%) was casted onto a glass plate. The glass plate was subsequently immersed in a gelation bath consisting of water at 11°C. After a specific period of time, the membrane was removed from the glass plate. It was then rinsed in water at room temperature to remove residual solvent. The membrane was dried at room temperature, then cured. All membranes which are prepared are presented in table 9.3 and shown in figures (27.3-31.3) (membranes M_{k1}:M_{k5}).

Table 9.3: Operating parameters tested for preparation of Kapton membranes

Membrane	Casting solution*		Pre-concentration time in min	Immersion** Time in h	Non solvent
	PAA wt%	NMP wt%			
M_{k1}	11	89	1	1	water
M_{k2}	11	89	60	1	water
M_{k3}	15	85	5	1	water
M_{k4}	15	85	10	1	water
M_{k5}	15	85	15	1	water

*: Kapton is sold as NMP solution.

**: immersion bath at 11°C±2 during 1h, film applicator withdraw thickness 500 µm

From the SEM views it was found out that the prepared Kapton membranes (M_{k1}, Fig.27.3) are almost symmetric with a spongy like structure, the top and bottom surface are highly porous. Thus, that type of membrane can be used as a support for others membranes. In addition, this type of membrane will be tested in NF to check its structure.

When high pre-concentration time were used the SEM views showed that the prepared Kapton membranes (M_{k2}-M_{k5}, Fig. 28.3-31.3) show an asymmetric structure with a finger-like structure with very small dense layer on the top surface while the bottom surface is highly porous. Thus, these types of membranes will be tested in NF to check its structure.

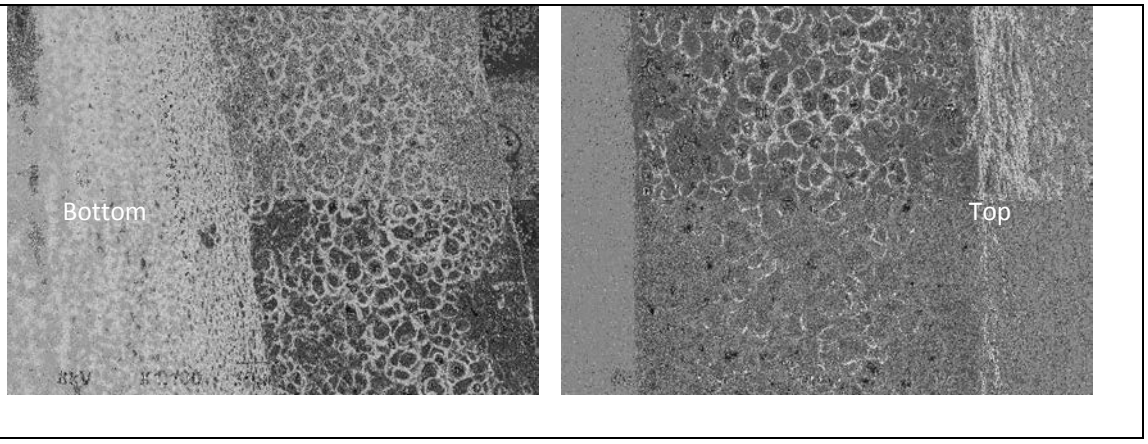

Figure 27.3: Cross section view of Kapton M_{k1} (11PAA%-89NMP%0% /1min/1h/70µm) at immersion bath temperature 11°C, film applicator withdraws thickness 300 µm.

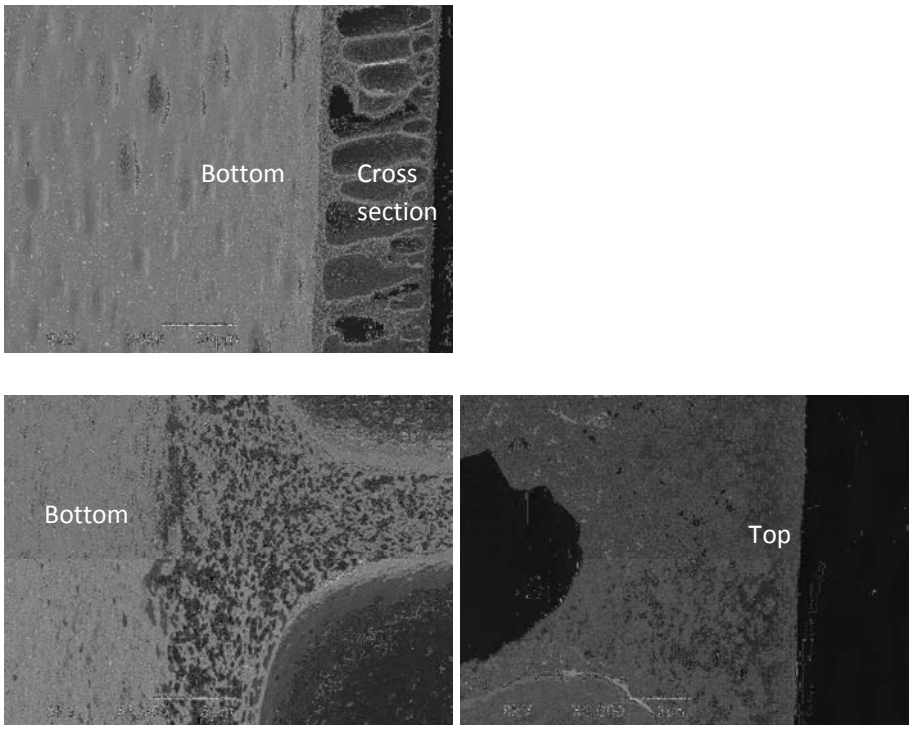

Figure 28.3: Cross section view for M_{k2} (11PAA%-89NMP%/60min/1h/75µm) at immersion bath temperature 11°C, layer dense ≤1µm, film applicator withdraws thickness 300 µm,

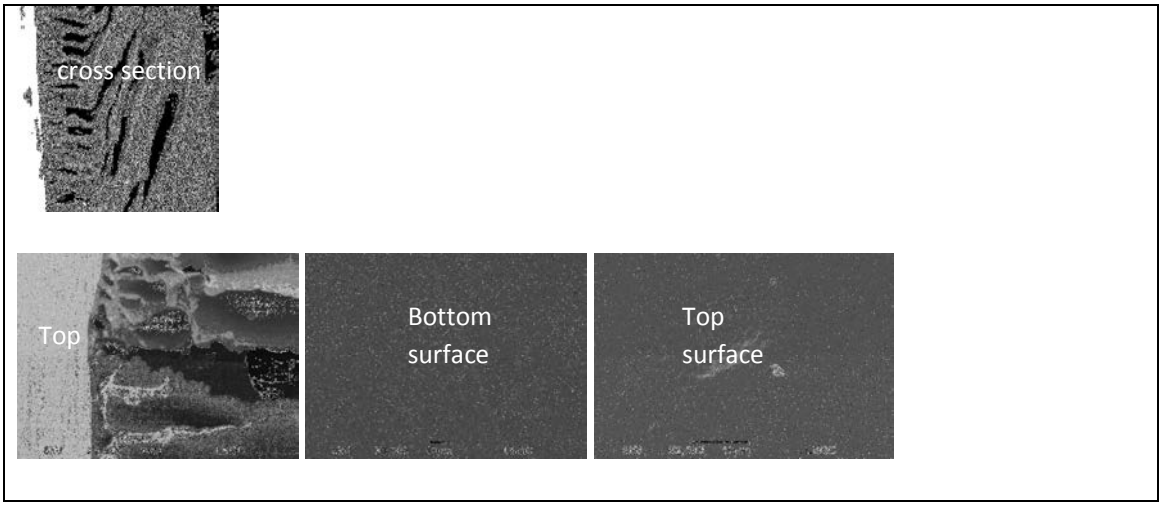

Figure 29.3: SEM view of Kapton M_{k3} (15PAA%-85NMP%/5min/1h/145µm) at immersion bath temperature 11°C, film applicator withdraws thickness 500 µm.

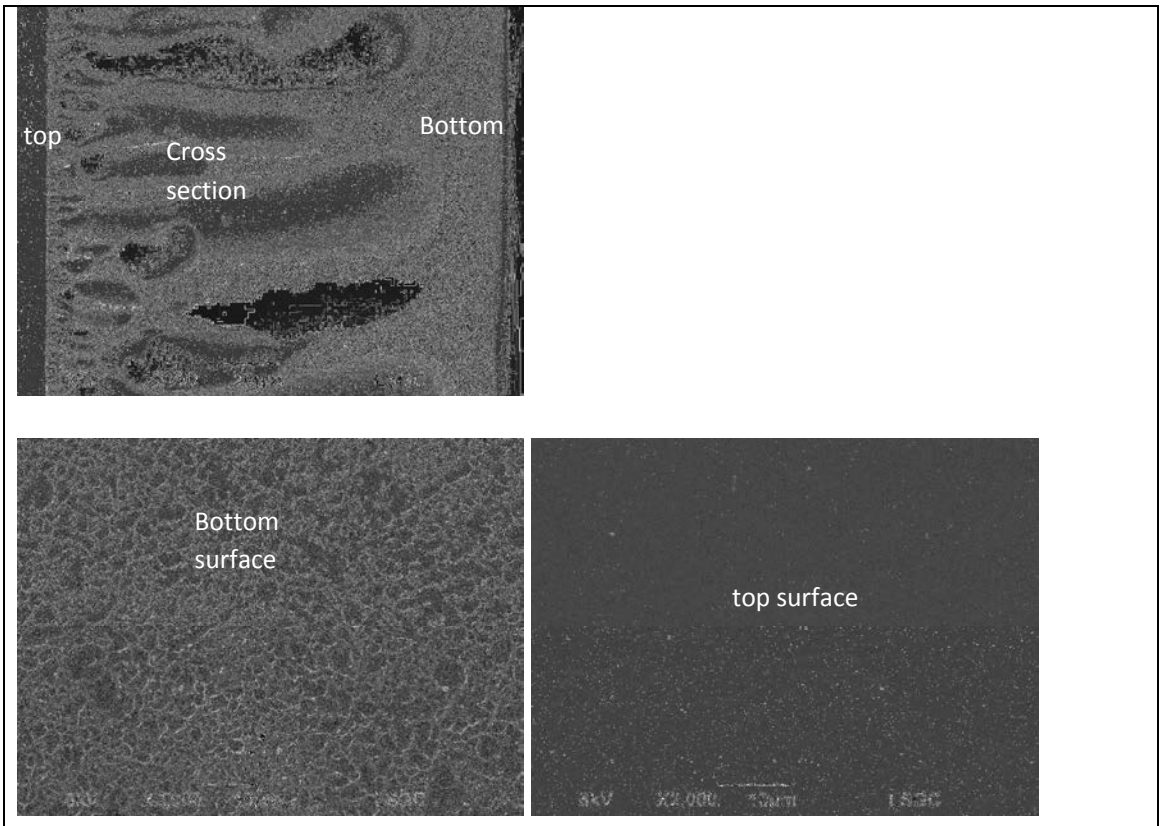

Figure 30.3: SEM view of Kapton M_{k4} (15PAA%-85NMP%/10min/1h/165µm) at immersion bath temperature 11°C±2, film applicator withdraws thickness 500 µm.

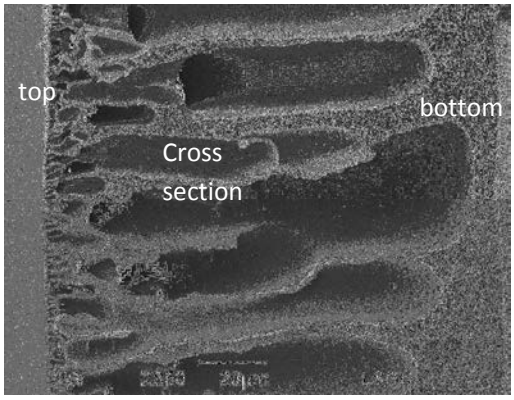

c-Cross section

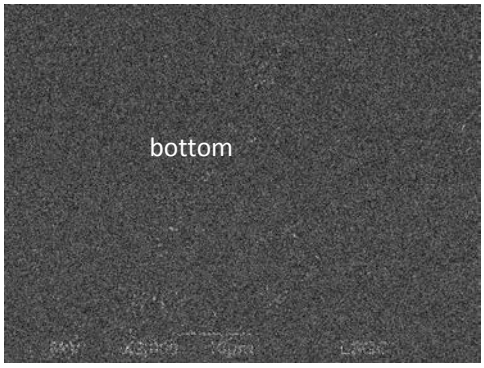

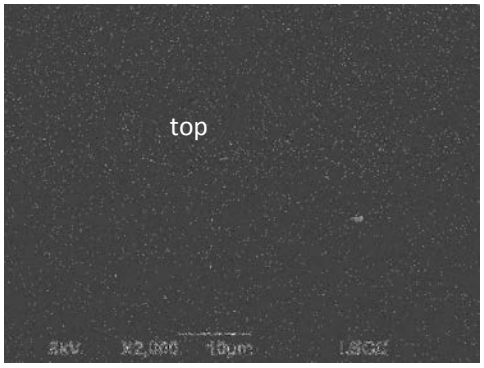

a- Bottom surface b- Top surface

Figure 31.3: SEM view of Kapton M_{k5} (15PAA%-85NMP%/15min/1h/140µm) at immersion bath temperature 11°C±2**,** film applicator withdraws thickness 500 µm.

3.3.5 Asymmetric PEI membranes preparation with strong mechanical support

The aim is to improve the mechanical properties of thin asymmetric PEI membranes for NF experiments. Thus, spongy-like supports are desired versus finger-like because their mechanical properties are better. The prepared membranes are presented in figure (32.3)

From figure (32.3) it was found out that the dense and asymmetric PEI membranes are sucssefully prepared with two types of support (Kapton and PEI). In addition, the prepared (Kapton and PEI) support is almost symmetric.

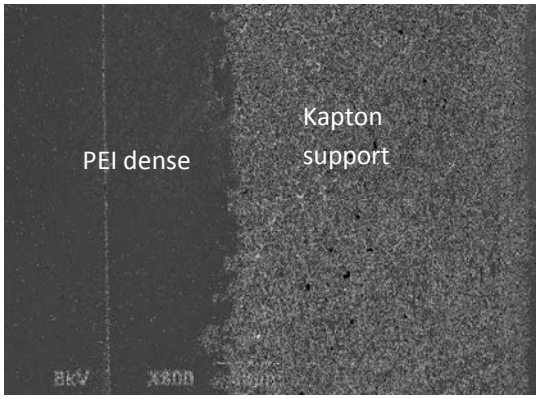

a. PEI dense membrane with Kapton support

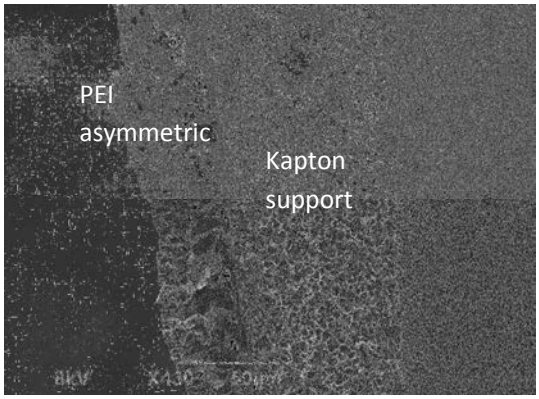

b. PEI asymmetric membrane(25 % PAA in DMF) coated on Kapton support.

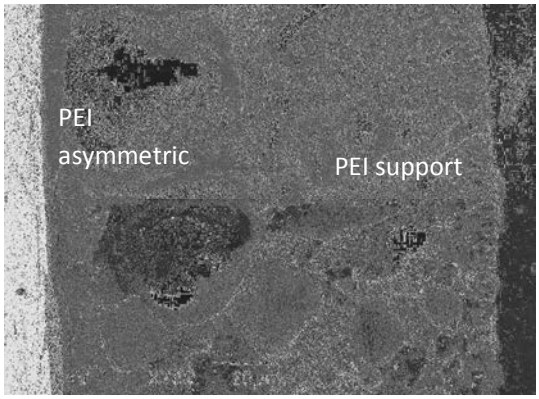

c. PEI asymmetric membrane (25 % PAA in DMF) coated on support PEI (20% PAA in DMF +10% water)

Figure 32.3: Cross sections view of PEI membranes coated on support.

Effect of inversion phase parameters on asymmetric PEI membranes preparation (from figures 5 to 32.3)

- Decreasing time of evaporation from 3min to 1min induces a more porous structure;
- Decreasing immersion time from 3h to 1h has not a stricking effect, may be more brittle films for PAA (may be due to increase of solvent extraction after long immersion time);
- Addition of non solvent (water 5:20wt%) leads to higly porous structures;
- Addition of non solvent (water 5:20wt%) leads to long pores and very thin dense top surface;

- Addition of non solvent (water 15wt%) leads to form finger-like structure ;
- Addition of non solvent (water 24wt%) leads to form spongy-like structure ;
- Decreasing concentration of PAA in DMF (from 30 to 15 wt %) leads to pores of higher diameter (from 1µm to 30µm).

Curing Treatment from PAA to PEI induces much higher mechanical properties, avoids brittle property, induces densification and may be close smaller pores.

The water immersion tank is suitable as a coagulant (non solvent) in preparation of PEI membranes from DMF solution while others nonsolvents such as methanol and ethanol are not suitable. Immersion in MeOH or EtOH leads to gelification (swelling) and membrane destruction.

For the others PAA having higher Jeffamine® contents (≥ 0.5 Jeff), despite the variations of the phase inversion conditions, i.e. polymer dope concentration, concentration time, coagulation bath temperature, liquid film thickness, it was not possible up to now to prepare reproducible asymmetric films usable in permeation experiments.

3.4 Study of the stability of PEI dense membranes in organic solvents and in water

PEI stability was found to be higher in polar solvents like MeOH and EtOH and in alkanes where the lowest swelling degrees (SD) were measured. On the other hand, the PEI dense membranes were significantly swollen in water (uptake up to 30%) and in toluene. The isothermal swelling equilibrium registered with these solvents are presented in Fig. 33.3 and the effect of temperature on swelling in Fig. 34.3. Despite the relatively high recorded SD in water or toluene, it is worth to mention that even after ten months at room temperature in solvent, the PEI membranes remained chemically and mechanically stable.

From Fig. (33.3) the equilibrium state was reached rapidly after about one day. The swelling in water is much larger than the swelling in polar solvents (i.e:methanol, ethanol) and alkanes (i.e: heptane). The toluene swelling is the highest compared to the other solvents while the heptane swelling is the smallest.

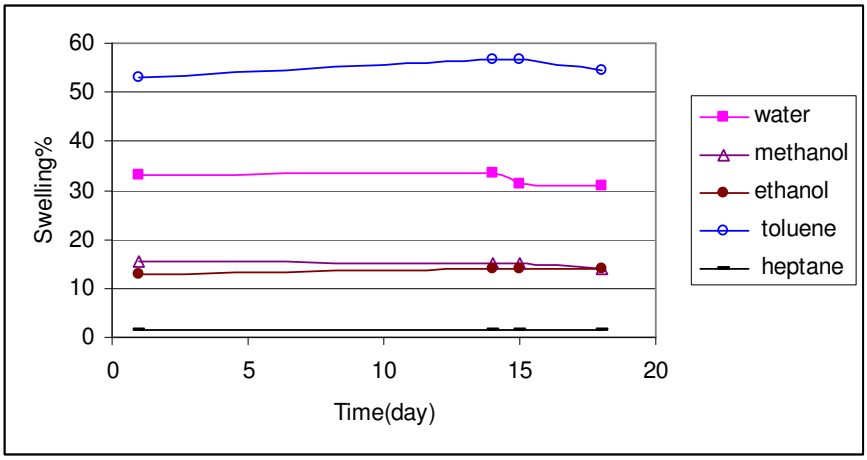

c. PEI dense membrane (0.6 Jeff 600, 1 PMDA,0.4 ODA).

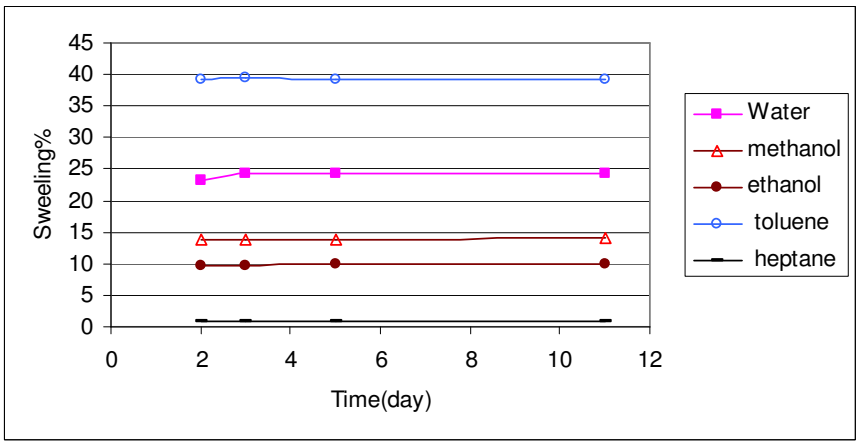

b. PEI dense membrane (0.5 Jeff 600, 1 PMDA,0.5ODA)

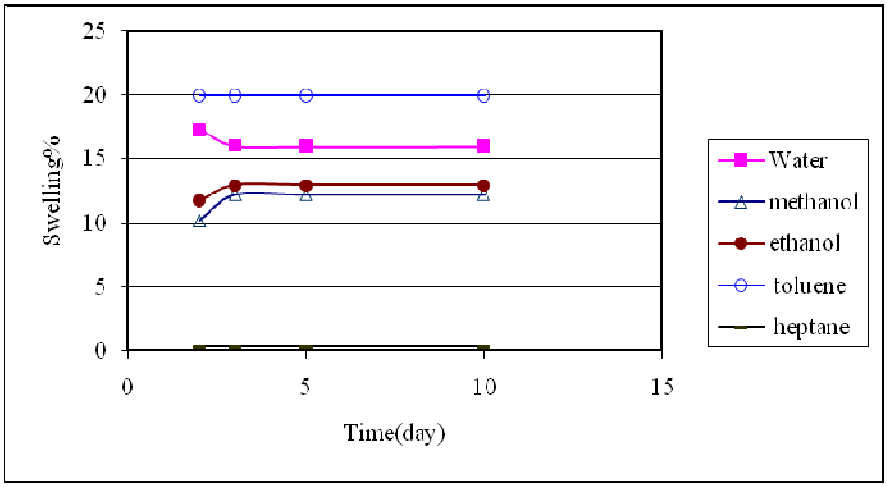

a-PEI dense membrane (0.4 Jeff 600, 1 PMDA,0.6ODA)

Figure 33.3: Isothermal swelling equilibrium of PEI dense membrane at (20^0C).

Fig. (34.3) represented the effect of operating temperature on swelling with PEI Jeff 0.4 and Jeff 0.6. It was observed that the swelling degree decreases only with water when the operating temperature was increased, this means that the swelling of water is exothermic as it is the case with polyethylene-glycol. Conversely, the swelling of the other solvents increased with operating temperature.

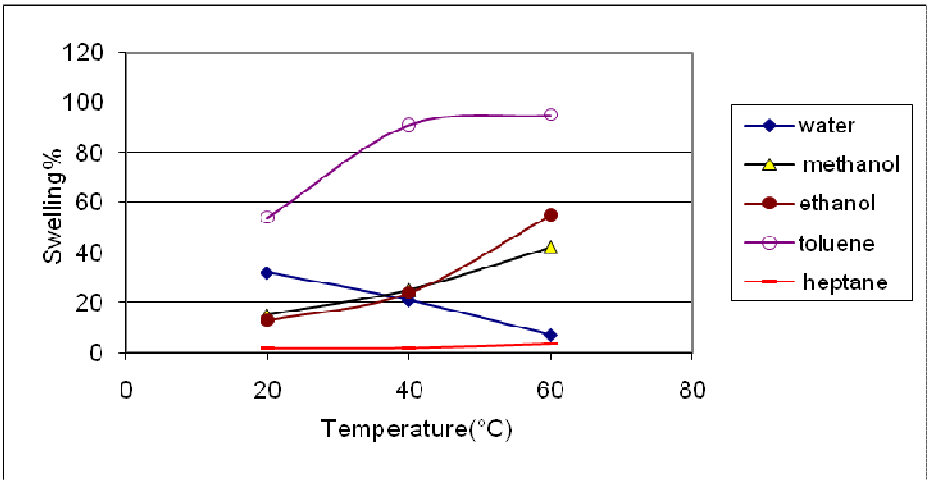

c. PEI dense membranes (0.6 Jeff 600:1 PMDA:0.4 ODA)

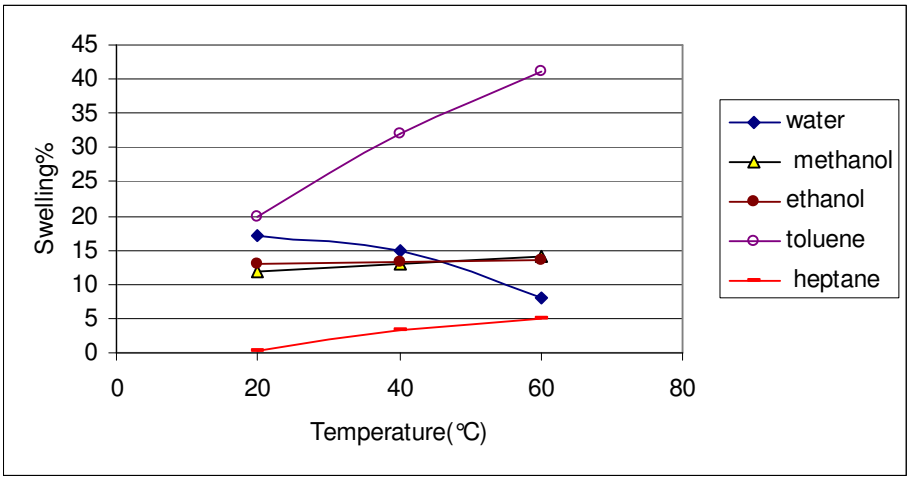

a. PEI dense membranes (0.4 Jeff 600:1 PMDA:0.6 ODA)

Figure 34.3: Effect of temperature on swelling in PEI dense membranes.

Furthermore, the effect of addition of soft blocks (Jeff600) in the swelling of PEI membranes compared with Kapton is presented in table 10.3 and Fig.35.3; it illustrates that the addition of more soft blocks led to increase swelling of PEI membrane. Han et. al. [19] reported that Kapton™ has a low water uptake; about 2-3 wt% at 20°C, and it was expected that the incorporation of alkoxyether groups (Jeff) would enhance the water uptake ability and consequently improve the water permeation properties. In our case, after the addition of the soft block, the swelling of water reached 17-32%, as shown in Fig.35.3.

Table 10.3: Effect of soft block (Jeff600) content on the swelling degree at 20°C.

	Kapton swelling	Swelling PEI (Jeff600:PMDA:ODA) ±3%		
Solvent	0 Jeff(Kapton)	0.4 Jeff	0.5 Jeff	0.6 Jeff
Water	5%	16%	24%	31%
Methanol	6%	12%	14%	14%
Ethanol	3%	13%	13.5%	14%
Toluene	3%	20%	39%	55%
Heptane	0.5%	0.25%	0.9%	1.6%

The swelling degrees of PEI membrane and Kapton™ membranes in different solvents at ambient temperature were calculated as the ratio of the liquid weight uptake per gramm of dry polymer (table 10.3, Fig.35). Whatever the liquid used, it was found that the swelling degree is strongly influenced by the content of Jeff incorporated in the PEI membranes; the more important effect is due to toluene, with a 10 fold increase for PEI 0.4Jeff for instance, whereas heptane has the lowest effect. In the case of water, the effect on PEI swelling degrees is also rather high and the values are 5 to 10 times higher compared to Kapton™.

The increase of the hydrophilic degree of the PEI can be deduced from these measurements as well as a lower packing density compared to Kapton™, where the aromatic blocks act as physical crosslinkers between the polymer chains. As a consequence, it was clear that PEI membranes can be good candidates for applications requiring hydrophilic properties.

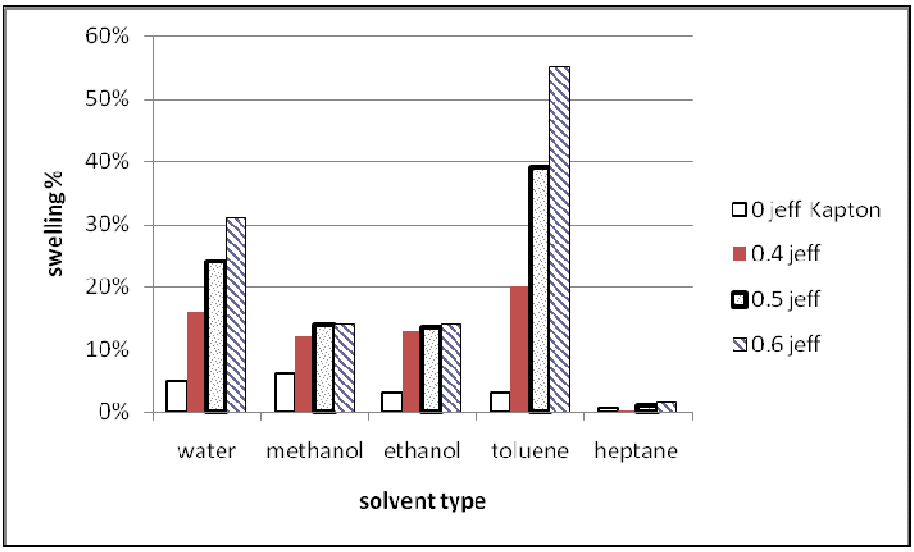

Figure 35.3: Swelling degrees of PEI and Kapton™ dense membranes in different liquids at 20°C.

Relation between solubility parameter of some solvents and swelling percent with dense PEI (0.4 Jeff) is presented in table 11.3 and Fig.36.3. From that figure it was found out that the PEI exhibits two peaks because it contain two blocks. The 1st peak is located at about solubility parameter 20-25 $MPa^{1/2}$ and 25-28 $MPa^{1/2}$ for the 2nd peak; clearly the first step may be related to the presence of the alkoxy soft block, and the 2nd step to the rigid aromatic block (PMDA-ODA).

Table 11.3: Stability of dense PEI (0.4 Jeff) with solvents at room temperature (20^{o}C).

	solvent	Solubility parameter [20] MPa$^{1/2}$	Swelling (wt/wt)%
1	n-Heptane	15.1	0.2
2	Diethyl ether	15.1	0
3	Methyl isobutyl ketone	17.2	4
4	Toluene	18.2	20
5	Ethyl acetate	18.6	5
6	THF[tetrahydrofuran]	18.6	14
7	methyl ethyl ketone	19	10
8	Methyl dichloride	19.8	6
9	acetone	20.3	16
10	Acetic Acid	20.7	53
11	Aniline	21.1	100
12	Triethylene glycol	21.9	17
13	1- butanol	23.3	8
14	Acetonitrile	24.3	5
15	1-propanol	24.3	16
16	dimethylformamide	24.8	52
17	Nitromethane	26.0	91
18	Ethanol	26.0	13
19	Methanol	29.7	12
20	Ethylene glycol	29.9	14
21	Water	47.9	17
22	Chloroform	19	Cracked

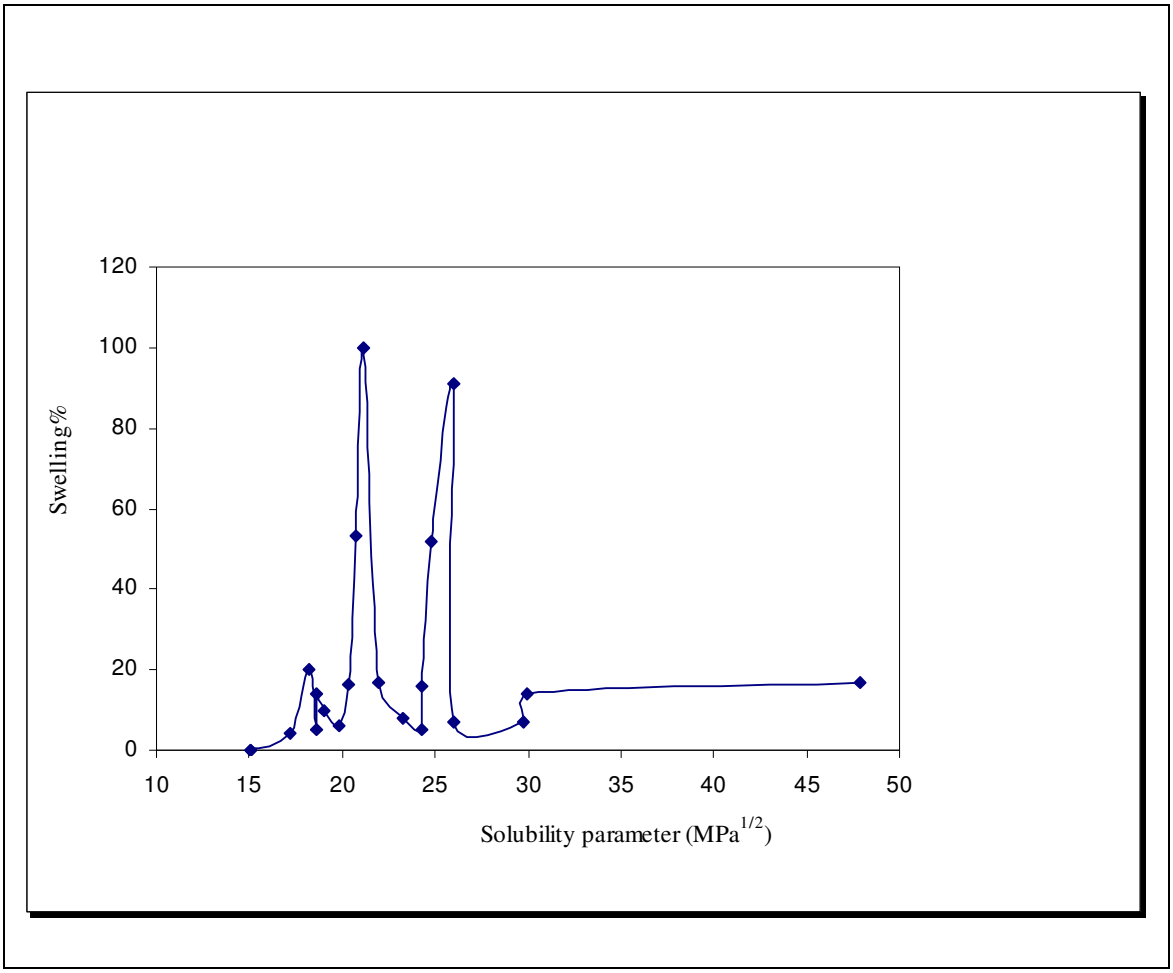

Figure 36.3: Relation between solubility parameter of some solvents and swelling percent of PEI dense membranes.

a) The swelling of water is much larger than the swelling of methanol, ethanol and heptane. It is well known that the diffusion coefficient of water is one of the highest one, it is quite obvious that the membrane will favour the permeation of water compared to the other polar organic molecules.

b) Aniline and nitromethane give the highest swelling degree compared to the other solvents. This affinity for these types of polar compounds can be a disadvantage in nanofiltration (NF) of aqueous solutions containing polar compounds because a slow absorption phenomena of organic compounds can be expected to occur.

3.5 Physical characterizations

3.5.1 Infrared spectra (FT-IR)

To follow the proper course of the PAA, PEI and PI synthetic steps, FTIR was used. The IR spectra obtained for dense and asymmetric PAA (Jeff-PMDA-ODA) are presented on Fig.37.3. The IR spectra obtained for dense and asymmetric PEI and dense PI membranes are presented on Fig.38.3. These spectra exhibit the characteristic peaks expected for the poly(amic acid) (Fig.37.3) and for the polyimide bonds (Fig.38.3). These features indicate that the phase inversion procedure does not inhibit the polymer formation nor the subsequent imide cyclization carried out by thermal treatment, i.e. up to 200°C for PEI membrane and to 300°C for Kapton™ membrane.

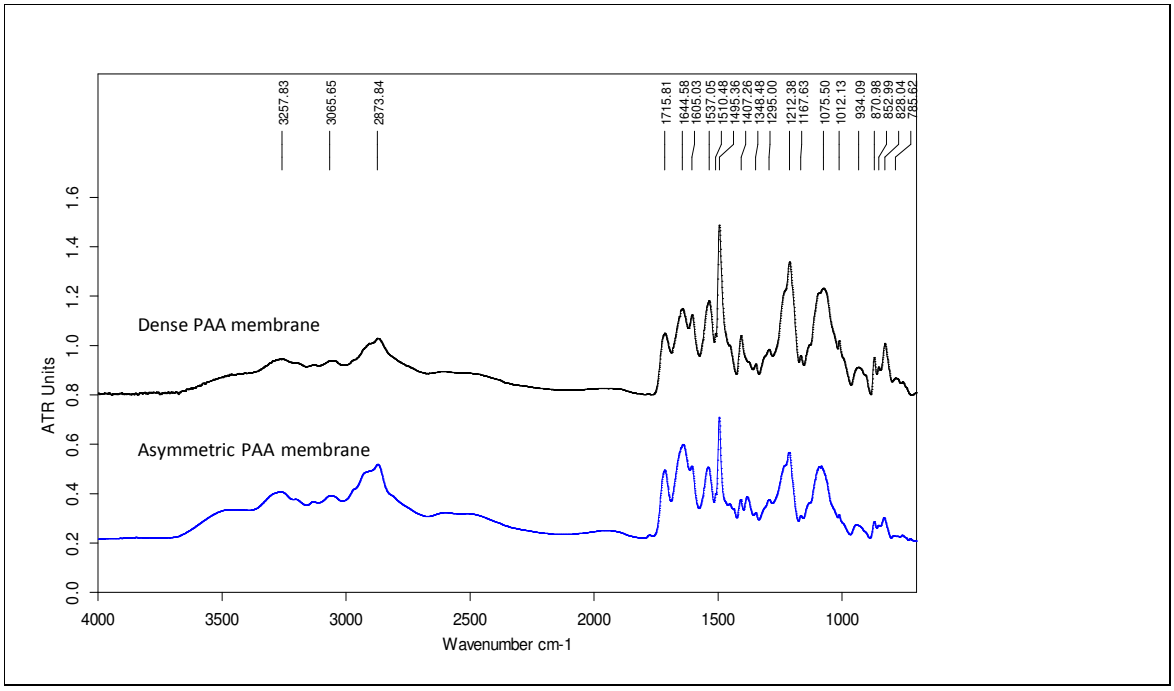

Figure 37.3: Infra-red spectrum for dense and asymmetric PAA membrane 30% PAA in DMF.

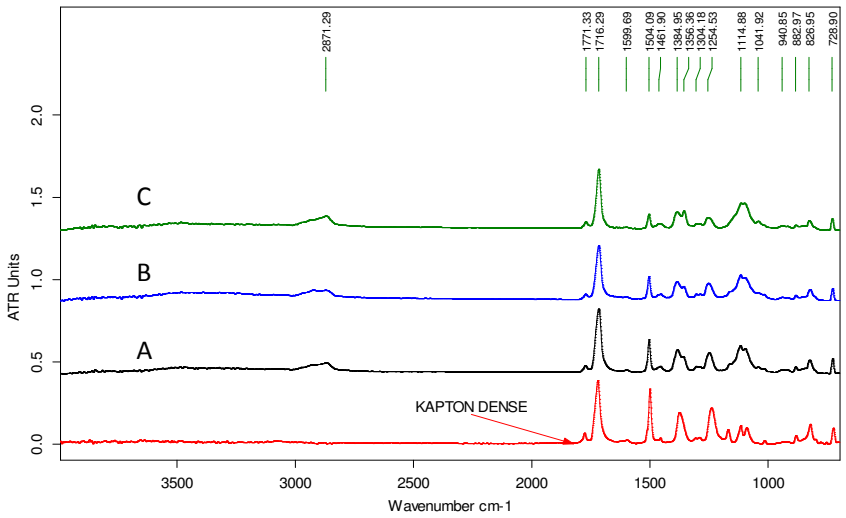

b- Infra-red spectrum for dense Kapton™ and PEI dense membranes (A Jeff 0.4, B Jeff 0.5, C 0.6 Jeff)

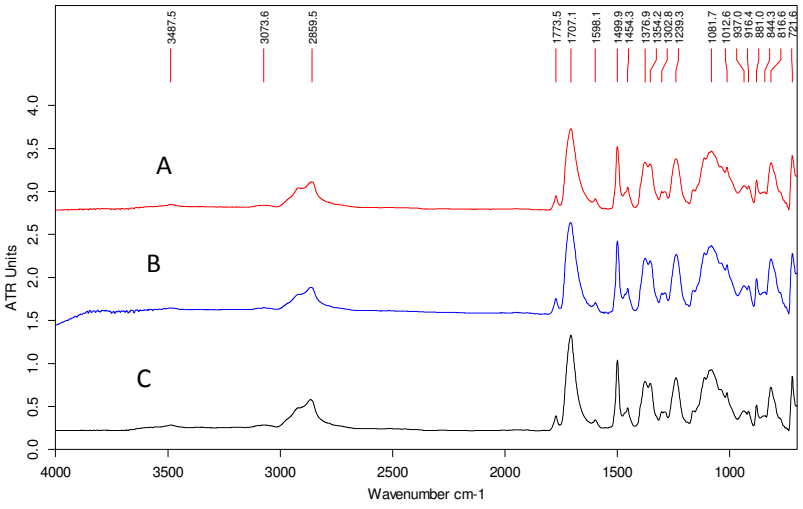

a- Infra-red spectrum for dense PEI (A), asymmetric PEI 25PAA (B) and asymmetric PEI 30 PAA(C), all with Jeff 0.4.

Figure 38 a, b.3: Infra-red spectra for PAA, PEI and Kapton™ membranes.

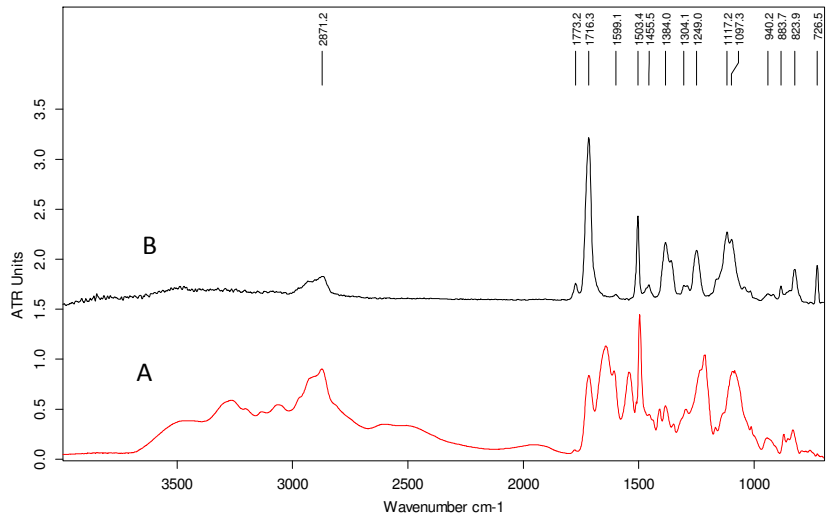

c- Infra-red spectrum for dense PAA (A) and PEI (B) dense membranes with 0.4Jeff.

Figure 38, c.3: Infra-red spectra for PAA, PEI membranes.

These figures showed characteristic spectra of polyimide membranes with peaks corresponding to $\overline{\nu}$ (cm $^{-1}$). The peaks at 3200-3400 were attributed to N-H(CONH), 2400-3200 were attributed to O-H(COOH) where the peaks at 1660 ,1700,1710,1735,1775, 1780 and 1340,1370,1380 cm^{-1} were attributed to the C=O and N-C=O, The peak at 1600 cm^{-1} was attributed to the ---CONH--- coupled deformation of amide, the peak 1500 (CN) was attributed to the mode of aromatic ring, the peaks at 1230,1240 , 1260 cm^{-1} was attributed to the C---O---C stretching vibration between two aromatic rings, and the peaks 811 and 720 was attributed to(CO). In contrast, the characteristic peaks of polyamic acid are absent. These characterizations indicate that the polyamic acid structures seem to be fully imidized to polyimide even when the curing temperature was limited to 200°C for PEI membranes.

Compared to Kapton spectrum, the PEI spectra show aliphatic bonds in the range 2870-3000 cm^{-1}; the intensity of these bonds increase slightly from PEI Jeff 0.4 to PEI Jeff 0.6. Conversely, the strong aromatic bond at 1504 cm^{-1} clearly decreases, as well as also the Ar-O-Ar at 1254 cm^{-1}. The other IR bond due to the alkoyether block is the ether one where the increase is also net at 1114 cm^{-1}. On the other hand, the bond at 728 cm^{-1} handing for the imide formation is steady in all cases.

3.5.2 Mechanical property

In order to improve mechanical properties of (co) polyimides soft block of Jeff 600 was added to PEI membranes. Stress-strain behavior of PEI was observed at ambient temperature on films of thickness of 200 µm.

Previous studies have shown that polyimides prepared with PMDA and ODA monomers (i.e. Kapton™ type) show a high Young modulus and a high tensile strength; conversely such polyimides have low elongations at break values [21,22 ,23 ,24] (Tab.12.3).

To improve the permeability and the water affinity properties of these rigid aromatic polyimides, various contents of Jeff were incorporated in the first synthetic step to give rise to PEI structures. Mechanical behaviour of PEI was recorded at ambient temperature leading to the characteristic parameters gathered in Table 12.3: Young modulus were determined from the initial slope as well as the tensile stress and the elongation at break. To evaluate the impact of the soft block on the mechanical properties of PEI, data related to Kapton™ are also given. The stress-strain curve of PEI with Jeff 600 (0.4) is presented in Fig. 39.3.

Table12.3: Mechanical properties of PEI and Kapton™ (present work and literature data).

Membrane	Young modulus (GPa)	Tensile strength (MPa)	Elongation at break (%)
PI Ref. [21]	3.2	265	60.1
PI Ref. [22]	2.1	104.7	16
PI Ref. [23]	2.3	60.2	35
PI Ref . [24]	0.80/0.62	106/66	18/13
PI [this work]	1.4	66.8	16
PEI 0.4Jeff	0.25	35.9	285
PEI 0.5Jeff	0.1	15.7	287
PEI 0.6Jeff	0.025	6.9	303

It was found that the Young modulus and the tensile strength of the PEI membranes decreased with increasing Jeff content in PEI membranes, while the elongation was increased.

Comparison of the mechanical behavior of Kapton™ shows an increase of Young modulus and a decrease in the elasticity. The evolution of the mechanical properties are really impressive: compared to Kapton™ the elongation at break is about one order of magnitude higher whereas the Young modulus is one or two orders of magnitude lower.

Table 12.3 shows that the PEI membranes have higher elongation than Kapton at break. For example, the Young's modulus for pure Kapton (PI) film is 1.4GPa while for the PEI membrane with 0.4 Jeff 600 it is 0.25GPa. The tensile strength and elongation at break for the pure film are 66 Mpa and 16 %, respectively while for the PEI membrane with 0.4 Jeff 600 it is 35.88 Mpa and 285%. This higher elongation of PEI is due to the fact that a copolyimide (PEI) includes alkyloxy- rubbery blocks (the effect of addition soft block in PEI).

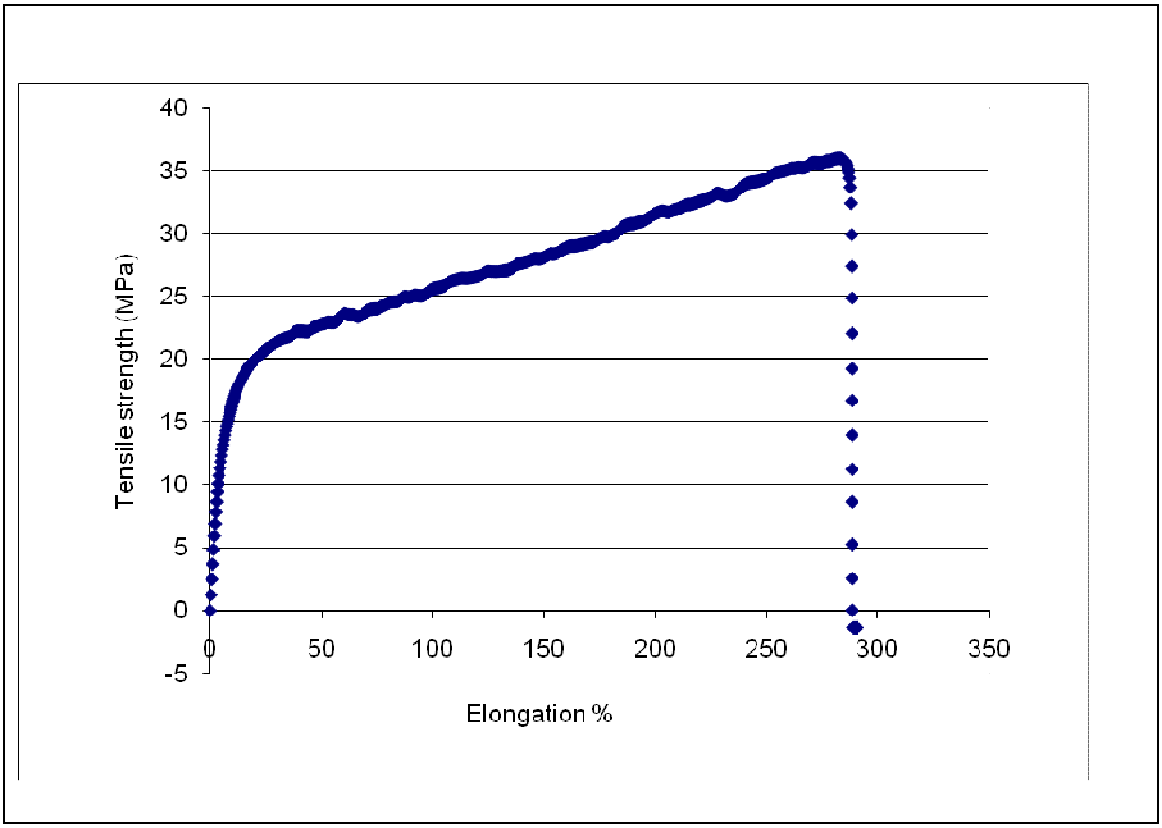

Figure 39.3: Stress-strain curve of PEI with Jeff 600 (0.4).

3.5.3 Thermogravimetric analysis (TGA)

The thermal stability of PEI membranes and PI was determined by thermogravimetric analysis and the results are given in Table 13.3. Compared to Kapton™, PEI exhibits two degradation steps starting at about 250-280°C and 510°C (Fig.40.3); clearly the first step can be related to the presence of the alkoxyimide block: going from PEI 0.4Jeff to PEI 0.6Jeff, the peak intensity increases as shown on Fig.41.3; among PEI, the PEI 0.4 Jeff has the higher

degradation temperature. However, the degradation of the aromatic block of the PEI occurs at the same starting temperature than the aromatic block of Kapton™, i.e. 510°C. At last one can notice that the total weight loss at 800°C is also related to the Jeff content showing that the decomposition of the PEI gives more volatile species than the fully aromatic structure (Fig.42.3).

Furthermore, the temperature corresponding to the degradation of 5% of the mass of the PEI samples are superior to 350° C (table13.3). Note that the initial kinetics of the PEI degradation is different and follows the changes in the rate of Jeff 600. The relationship between temperature T5 % or T10% with the rate of Jeff 600 are shown in fig. 43.3.

Table 13.3: TGA features of PEI membranes

Membrane type	T (°C) at 5% weight loss	T (°C) at 10% weight loss	Final degradation (wt%)
PI (PMDA-ODA)	569	584	42
PEI Jeff/PMDA/ODA (0.4/1/0.6) dense	386	399	68
PEI Jeff/PMDA/ODA (0.5/1/0.5) dense	351	379	73
PEI Jeff/PMDA/ODA (0.6/1/0.4) dense	393	405	77

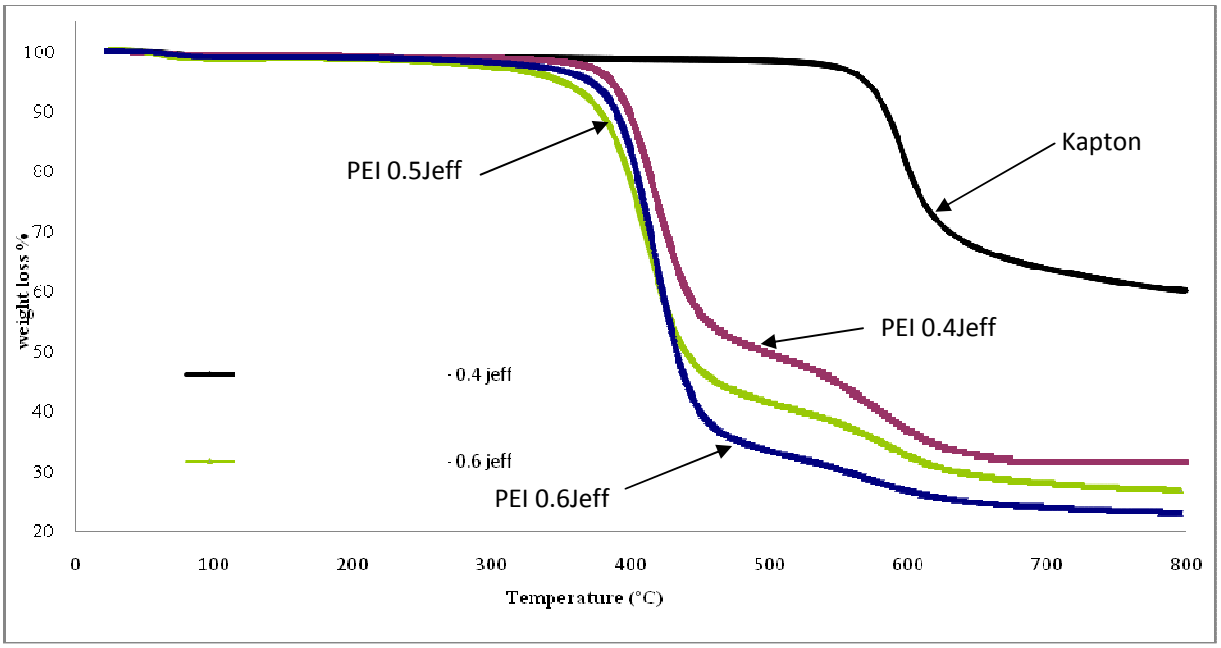

Figure 40.3: TGA showing the membranes weight loss of PEI and Kapton™ (N_2, heating rate: 10°C/min)

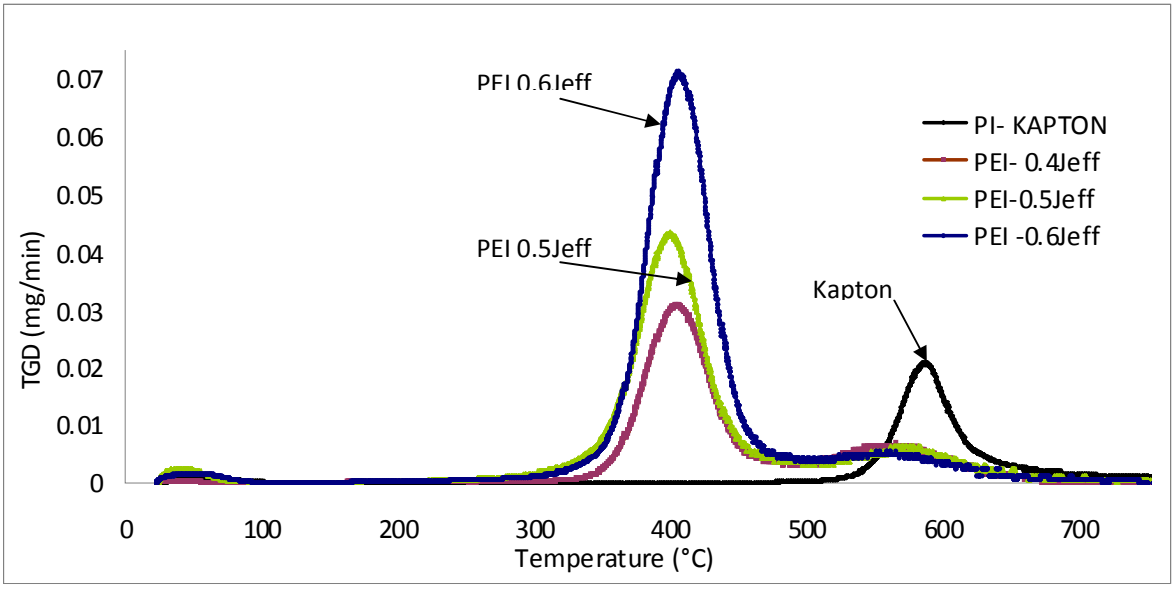

Figure 41.3: Differential curves of the TGA signals of PEI and Kapton™. The influence of the Jeff content is very clear: the more Jeff, the higher rate of polymer degradation.

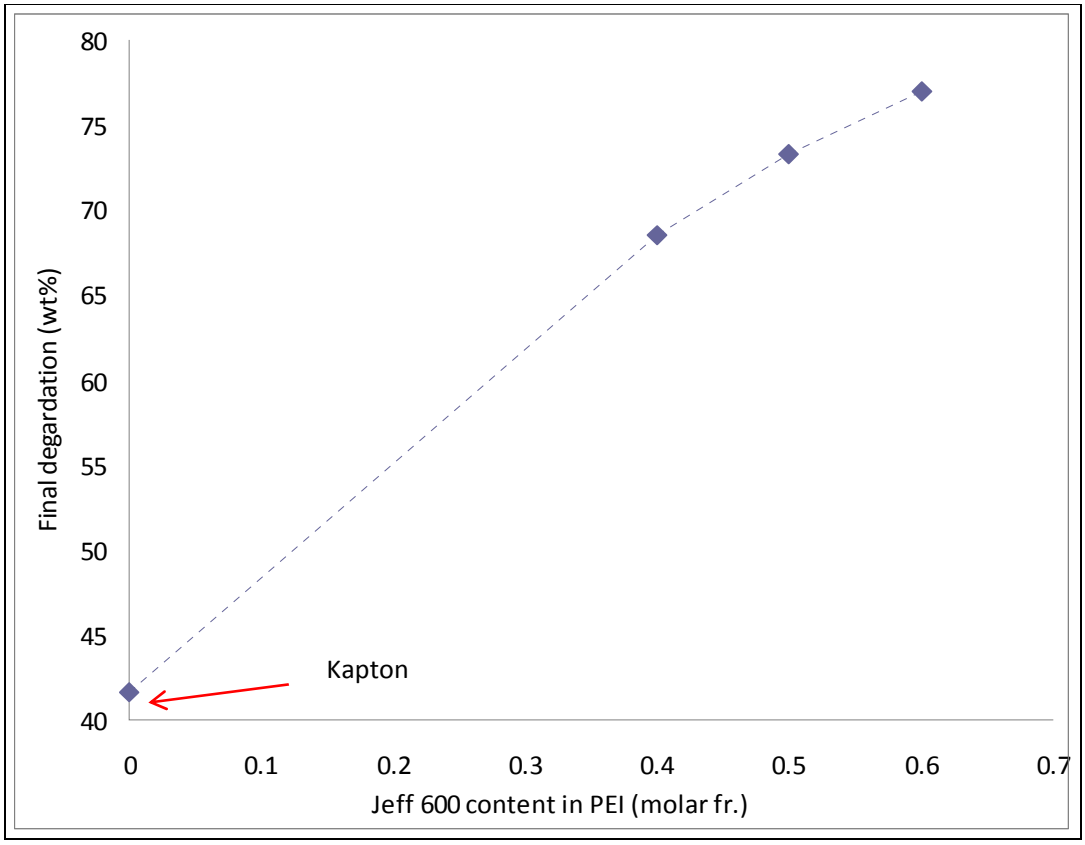

Figure 42.3: Evolution of the total weight loss with the polymer structures after degradation at 800°C.

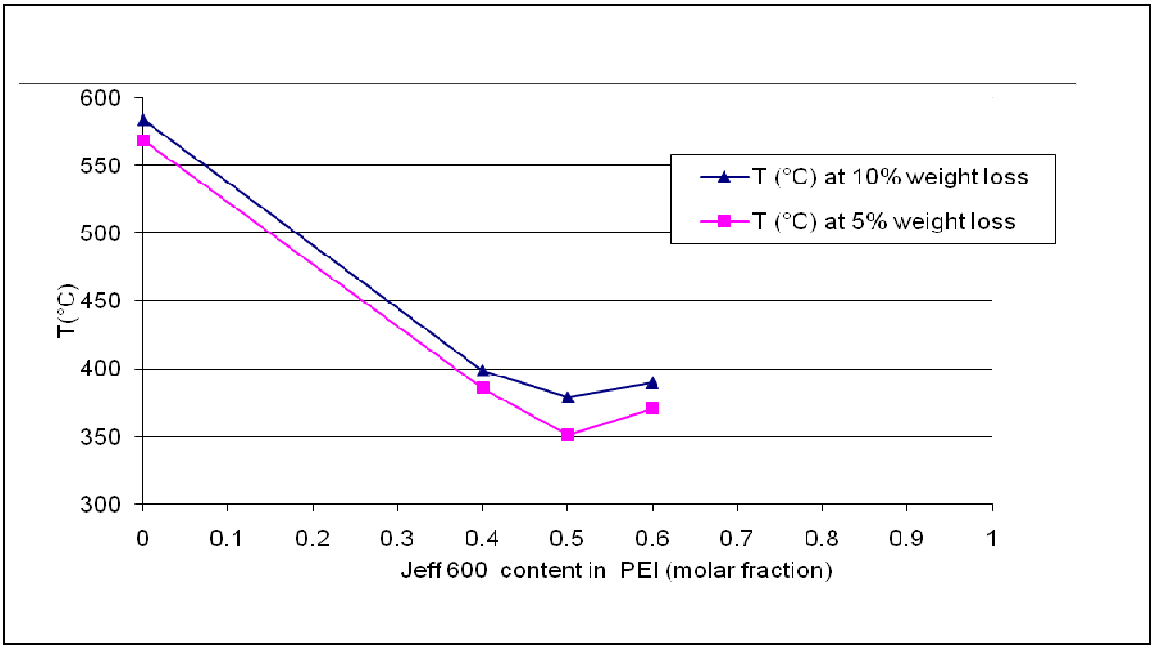

Figure 43.3: Evolution of PEI decomposition temperatures rate of Jeff 600.

Tables (14.3-16.3) below illustrate the effect of operating parameters on the preparation of dense and asymmetric PEI membranes.

Table 14.3: Effect of addition non solvent (water) to polymer solutions (membranes M_7:M_{12}).

Membrane	Casting solution wt %			Pre-concentration	Immers-ion.	Non solvent	test	SEM
	DMF	PAA	Water					
M_1	70	30	0	1 min	1 h	Water		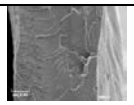
M_7	67	28	5	1 min	1 h	Water	3	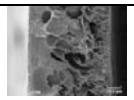
M_8	60	25	15	"	"	"	"	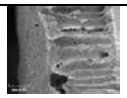
M_9	56	24	20	"	"	"	"	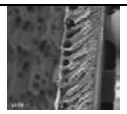
M_{10}	53	23	24	"	"	"	"	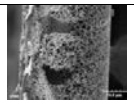
M_{11}	49	20	31	"	"	"	"	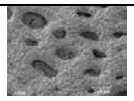
M_{12}	42	18	40	"	"	"	"	Not possible due to initial phase separation

Table 15.3: Effect of the polymer solution concentration

Membrane	Casting solution			Pre-conc. time	Immers -ion	Non solvent	test	SEM
	DMF	PAA	Water*					
M_1	70	30	0	1 min	1 h	Water	4	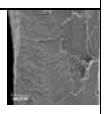
M_{13}	75	25	"	"	"	"	"	
M_{14}	80	20	"	"	"	"	"	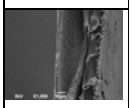
M_{15}	85	15	"	"	"	"	"	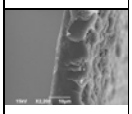
M_8	70	30	15	1 min	1 h	Water	5	
M_{16}	75	25	"	"	"	"	"	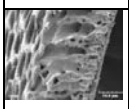
M_{17}	80	20	"	"	"	"	"	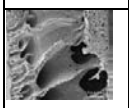
M_{18}	85	15	"	"	"	"	"	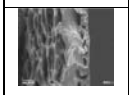

*water wt% calculated on the total (PAA+DMF) weight.

Table 16.3:Effect of change immersion bath temperature

Membrane	Casting solution			Pre-conc. time	Imm.	Non s	test	SEM
	DMF	PAA	Water					
M_{21}	70	30	0	1 min	1 h	water	5°C	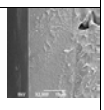
							7°C	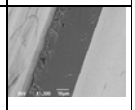
							10°C	

Conclusions and Recommendations for Future work

The final membrane morphology formed during phase inversion (separation) is dependent on the kinetics as well as the thermodynamics of the phase inversion, and the equilibrium ternary phase diagram system is a good tool for understanding and controlling the morphology and the membrane structure. Thus, the cloud points curve (binodal curve) for ternary system of PAA/ DMF/H_2O were determined by a titration method for PAA 30, 20, 10, 5, 2, 1 wt.% in DMF at 10°C. A large amount of water (26-39 wt. % water) was needed to achieve liquid–liquid phase separation in the ternary system. The systems which required a large amounts of nonsolvent to achieve precipitation, to obtain liquid-liquid phase separation, form membranes with nanofiltration and reverse osmosis properties. This observation concerning the thermodynamic properties of the systems.

Phase inversion was found to be a suitable method to prepare asymmetric membranes from rubbery polyetherimides combining soft alkoxyether blocks (from Jeffamine®) and aromatic blocks (from ODA) after condensation with PMDA. Dense PEI membranes were easily obtained with various aliphatic / aromatic diamine ratios; with respect to the ODA-PMDA blocks, these membranes have a structural analogy with the Kapton™ structure. They were used as reference membranes through out this work.

The amine ratio 0.4/0.6 allowed the preparation of asymmetric membranes of good mechanical properties to be used further in pervaporation and nanofiltration. It was shown that the porosity of the membrane sublayers could be tuned according to the initial polymer dope concentration, nonsolvent addition and the temperature of the inversion (immersion) bath.

For the others PAA having higher than 0.4 Jeffamine® contents, despite the variations of the phase inversion conditions, i.e. polymer dope concentration, concentration time, coagulation bath temperature, liquid film thickness, it was not possible to prepare reproducible asymmetric films usable in pervaporation or nanofiltration experiments.

In all cases, the curing treatment from PAA to PEI improved the mechanical properties, avoided brittle properties, and induced some densification of the top surface. On one hand, the decreasing time of evaporation from 3min to 1min induced a more porous structure, while decreasing immersion time from 3h to 1h had not a striking effect. On the other hand, adding non solvent (water 5-15 wt%) to 30% PAA in DMF led to highly porous structure with finger pores and a very thin dense top surface, the shape of the pores could also be varied from finger like (water content 15-20wt%), to highly spongy network which started to appear from

water content above 20 wt%; addition of 24 wt % water led to fully spongy cross-section, whereas decreasing concentration of PAA in DMF (from 30 to 15 wt%) led to an asymmetric structure with pores of high diameter (from 1µm to 30µm). From miscibility gap of ternary phase diagram and based on SEM results, it was found that the addition of more water was not possible since the 26% concentration was already very close to the binodal demixing curve of the ternary phase diagram. Immersion in MeOH or EtOH did not allow the formation of any membrane.

The major variables involved in the membrane preparation procedure, namely, the polymer concentration, the additive content, the immersion bath temperature, immersion bath type and preconcentration time are crucial to tune membrane performances. Continuing work on optimization of membrane casting conditions is needed to improve membrane performances. On one hand, the optimization can be conducted by determining the optimum variables based on design experiments with either permeation flux or separation factor as the response. On the other hand, other apparatus should be used in the casting step such as doctor blade to compare with the other membranes prepared by using a film applicator, to control the thickness of the membrane and to prepare reproducible asymmetric films. In addition, the orginal prepared PAA solution should have the same viscosity for all synthesis. The peeling of asymmetric membrane from glass support after thermal treatment is very difficult, so it is very important to find an easy way to peel off membrane from glass support.

The membrane stability was found to be better in polar solvents where the swelling degree was lower. The PEI membranes were well stable in water and in some organic solvents for more than ten months at room temperature.

The FT-IR characterizations indicate that the poly(amic acid) structures seemed to be fully imidized to polyimide following the curing treatment which was limited to 200°C for PEI membranes; compared to the imidization temperature of Kapton™ i.e. 300°C, this lower value can be related to the presence of the Jeffamine® soft block of much smaller glass transition temperature. Nevertheless, the TGA analysis revealed that the PEI series had still a fairly good thermal stability, with degradation temperatures at 5wt% loss in the range of 350-390°C.

References

1. J. Jansen, M. Macchione and E. Drioli, High flux asymmetric gas separation membranes of modified poly(ether ether ketone) prepared by the dry phase inversion technique, J. Membr. Sci. 255 (2005) 167-180.
2. P.J. Flory, Principles of polymer chemistry, Cornell University Press, Ithaca, NY (1953).
3. H. Tompa, Polymer solutions, Butterworths, London (1956).
4. L. Zeman and G. Tkacik, Thermodynamic analysis of a membrane-forming system water/N-methyl-2-pyrrolidone/polyethersulfone, J. Membr. Sci. 36 (1988) 119–140.
5. J. Kim, H. Lee, K. Baik and S. Kim, Liquid-liquid phase separation in polysulfone/solvent/water systems, J. Appl. Polym. Sci. 65 (1997) 2643–2653.
6. J. Barzin and B. Sadatnia,Theoretical phase diagram calculation and membrane morphology evaluation for water/solvent/polyethersulfone systems, Polymer 48(2007) 1620-1631.
7. J. Wijmans, J. Kant, M. Mulder and C. Smolders, Phase separation phenomena in solutions of polysulfone in mixtures of a solvent and a nonsolvent: relationship with membrane formation, Polymer 26 (1985) 1539–1545.
8. J. Lai, S. Lin, F. Lin and D. Wang, Construction of ternary phase diagrams in nonsolvent/solvent/PMMA systems, J. Polym. Sci. Polym. Phys. 36 (1998) 607–615.
9. F. Altena and C. Smolders, Calculation of liquid-liquid phase separation in a ternary system of a polymer in a mixture of a solvent and a nonsolvent, Macromolecules 15 (1982) 1491–1497.
10. L. Yilmaz and A. McHugh, Analysis of nonsolvent-solvent-polymer phase diagrams and their relevance to membrane formation modeling, J. Appl. Polym. Sci. 31 (1986) 997–1018.
11. M. Mulder(1996), Basic Principles of Membrane Technology, Kluwer Academic Publishers, Dordrecht ISBN 0-7923-4248-8(PB).
12. M. C.Porter, ‘‘Handbook of industrial membrane technology ’’, Noyes publications, park Ridge, New Jersey, U.S.A P 61-70,1990.
13. M. Frommer and R. Messalem, Mechanism of membrane formation, VI, Convective flow and large void formation during membrane precipitation, Ind. Eng. Chem. Prod. Res. Develop. 12 (1973) 328.
14. I. Kim, H. Yoon, K. Lee, Formation of integrally skinned asymmetric polyetherimide nanofiltration membranes by phase inversion process, J. Appl. Polym. Sci. 84 (2002) 1300-1307.

15. J. Shieh and T. Chung, Phase-Inversion Poly(ether imides) Membranes Prepared from Water-Miscible/Immiscible Mixture Solvents, Ind. Eng. Chem. Res. 38 (1999) 2650–2658.
16. C. Smolders, A. Reuvers, R. Boom and I. Wienk, Microstructures in phase-inversion membranes, Part I, Formation of macrovoids. J. Membr. Sci. 73 (1992) 259–275.
17. P. Witte, P. Dijkstra, J. Berg and J. Feijen, Phase separation processes in polymer solutions in relation to membrane formation, J. Membr. Sci. 117 (1996)1-31.
18. E. Saljoughi, M. Sadrzadeh, T. Mohammadi, Effect of preparation variables on morphology and pure water permeation flux through asymmetric cellulose acetate membranes, J. Membr. Sci. 326 (2009) 627-634.
19. H. Han, C. Gryte, M. Ree, Water diffusion and sorption in films of high-performance poly(4,4′-oxydiphenylene pyromellitimide): effects of humidity, imidization history and film thickness, Polymer 36 (1995)) 1663-1672.
20. Barion A FM, solbility parameters, Chem. Rev 1975 , vol 75.
21. P. Ma , W. Nie , Z. Yang , P. Zhang , G. Li , Q. Lei , L. Gao , X. Ji, M. Ding , Preparation and characterization of polyimide/Al_2O_3 hybrid films by sol-gel process, J. Appl. Polym. Sci. 108 (2008) 705-712.
22. Y. Zhai, Q. Yang, R. Zhu, Y. Gu, The study on imidization degree of Poly(amic acid) in solution and ordering degree of its polyimide film, J. Materi.Sci. 43 (2008) 338-344.
23. M. Shaikh , M. Alam, T. Agag, T. Kawauchi, T. Takeichi, organic–inorganic hybrids containing polyimide, organically modified clay and in situ formed polydimethylsiloxane, React. Funct. Polym. 67 (2007) 1218-1224.
24. E. Mazoniene, J. Bendoraitiene, L. Peciulyte, S. Diliunas, A. Zemaitaitis,(Co)polyimides from commonly used monomers, and their nanocomposites, Prog. Solid State Chem. 34 (2006) 201-211.

Chapter 4

Pervaporation results and discussion

Table of contents Chapter 4

Pervaporation results and discussion

Table of contents Chapter 4 Pervaporation results and discussion

Chapter 4 227

Pervaporation results and discussion 227

4.1 Pervaporation performances with pure solvents (Water, Heptane, Toluene) and 50-50 wt% Toluene-Heptane mixtures (organic –organic mixture) 227

4.1.1 Effect of feed concentration and operating temperature on the performances of PEI dense membrane. 229

4.1.2 Effect of membrane (type, thickness) and temperature on membrane performances ……232

4.2 Pure solvents (Water, Ethanol) and 0-100 wt. % aqueous solution of water- ethanol ……..237

4.2.1 Effect of temperature and feed composition on membrane selectivity 240

4.2.2 Effect of temperature and feed composition on membrane flux 246

4.3 Effect of soft block on pervaporation performances of PEI membranes 250

4.3.1 Effect of membrane type and operating temperature on selectivity 251

4.3.2 Effect of operating temperature and membrane morphology on flux 253

4.4 Dehydration of alcohols 254

4.5 Separation properties with the hybrid silica- PEI membranes 260

4.5.1 Effect of operating temperature on flux and selectivity 261

4.5.2 Effect of TMOS content on flux, swelling and selectivity 264

Conclusions and Recommendations for Future work 267

References 269

Chapter 4

Pervaporation results and discussion

Pervaporation is a rate-governed membrane process for the separation of liquid mixtures. Currently, dehydration of alcohols is the best developed application of pervaporation in the chemical processing industries. The pervaporation experiments carried out in our work intended to check which of the phase inversion procedures was able to lead to asymmetric defect-free membranes, i.e. able to achieve molecular mixture separation with selectivity close to the one obtained with dense membranes, together with a much higher flux. The best asymmetric membranes, i.e. exhibiting the best selectivity/flux compromise, would then be selected for further nanofiltration study aiming at the purification of organic water mixtures. Thus, the pervaporation of pure solvents were tested, to check dense and asymmetric structure, in order to estimate dense layer tightness of asymmetric membrane and to understand the effect of operating temperature. Finally, binary mixtures were used to check molecular separation and to reach optimum structure of asymmetric membrane with flux and selectivity.

4.1 Pervaporation performances with pure solvents (Water, Heptane, Toluene) and 50-50 wt% Toluene-Heptane mixtures (organic –organic mixture)

The pervaporation separation performances are governed by the physicochemical nature of the polymer membrane and of the species to be separated, by the membrane morphology and by the process operating conditions. Thus, pure solvents (Water, Heptane, and Toluene) and 50-50 wt% Toluene-Heptane mixtures were used to investigate the dense and asymmetric PEI membranes performances and their temperature dependence in the range 30-70°C. The results are presented in Tables (1.4-3.4) and Figures (1.4- 5.4), for PEI membranes prepared either by the dry or wet method.

First it should be underlined that all the membranes were well stable during the PV experiments even at 70°C and long term PV experiments could be carried out to check the temperature dependence (up to 7 days). As expected, the total flux for pure solvents and mixtures through all the PEI membranes increased with the increase of feed operating temperature following an Arrhenius law (table1, 2.4, Fig.2.4) [1 ,2]. In accordance with the absorption–diffusion model, a higher flux is a consequence of an increased driving force due to the increased vapor pressure of the components in the feed, but also due to an increased mobility of the absorbed species [3,4].

Table 1.4: Pervaporation results of PEI dense and asymmetric membranes with feed 50 wt.% Toluene-Heptane.

Membrane	*t µm	*J (kg/h.m^2) ±10%			*J_T (kg/h.m^2)±10%		
		40°C	55°C	70°C	40°C	55°C	70°C
M_{dense}	40	0.024	0.04	0.054	0.02	0.035	0.048
	60	0.013	0.029	0.037	0.01	0.027	0.033
$M_{1(30PAA)}$	100	0.01	0.02	0.04	0.01	0.013	0.03
	40	0.02	0.05	0.1	0.019	0.045	0.098
$M_{13(25PAA)}$	100	0.45	0.65	0.95	0.33	0.5	0.7
$M_{7(25PAA+5w)}$	150	0.13	0.15	0.20	0.07	0.1	0.11
$M_{8(25PAA+15w)}$	40	0.13	0.33	0.48	0.08	0.2	0.3

*J: total flux, $J_{T:}$ toluene flux, $J_{H:}$ heptane flux, t: thickness, T: toluene, H: heptane, W: water.

Table 2.4: Effect of PEI membranes types on the separation factor (α) and on the permeate enrichment (Cp) with 50 wt% Toluene-Heptane feed(CP ±2-3%).

Membrane type	α 40°C	α 55°C	α 70°C	Cp (40°C)	Cp (55°C)	Cp (70°C)
$M_{dense(60\ um)}$	12	11	10	92%	90%	89%
$M_{dense(40\ um)}$	12	10	9	91%	89%	88%
$M_{1\ (30PAA,\ 40\ um)}$	13	10	9	93%	91%	89%
$M_{1\ (30PAA,100um)}$	11	10	6	90%	90%	85%
$M_{13(25PAA)}$	2.8	2.7	3	74%	73%	75%
$M_{7(25PAA+5w)}$	1.3	1.4	1.4	55%	59%	56%
$M_{8(25PAA+15w)}$	1.8	1.5	1.5	65%	60%	59%

Table 3.4: Pervaporation results of PEI dense and asymmetric membranes with pure solvents and water.

Membrane	*t µm	Feed	*J (kg/h.m^2)		
			J 40°C	J 55°C	J 70°C
M $_{dense}$	60	100 % *w	0.28	0.42	0.55
	60	100 % *T	0.17	0.25	0.34
	60	100 % H	0.003	0.006	0.01
$M_{1(30PAA)}$	40	100% T	0.18	0.33	0.6
$M_{13(25PAA)}$	100	100 % w	0.80	1.3	3.2
$M_{7(25PAA+5w)}$	150	100 % w	0.24	0.47	0.91
	150	100 % T	0.4		

*J: total flux, $J_{T:}$ toluene flux, $J_{h:}$ heptane flux, t: thickness, T: toluene, H: heptane, W: water

4.1.1 Effect of feed concentration and operating temperature on the performances of PEI dense membrane.

The influence of toluene concentration in the feed on the membrane performances for toluene / heptane mixture by pervaporation at different temperatures was studied using PEI dense membranes of 40 to 60 µm thickness.

The effect of temperature on selectivity of PEI dense membrane, i.e. permeate enrichment is shown in Figure 1.4. It was found that the selectivity increased with the increasing of toluene feed content and the two dense membranes give almost the same selectivity. The selectivity has a drop with an increase of operating temperature (table 2.4), due to the effect of toluene swelling and coupling of heptane molecules with toluene molecules which increased with increase of operating temperature. in other words, the dense PEI membranes exhibit a toluene permselectivity over a wide range of feed composition and the selectivity reaches a maximum at a high toluene contents in the feed mixture; this preferential permeation of toluene is mainly due to the alcoxyether soft block [27].

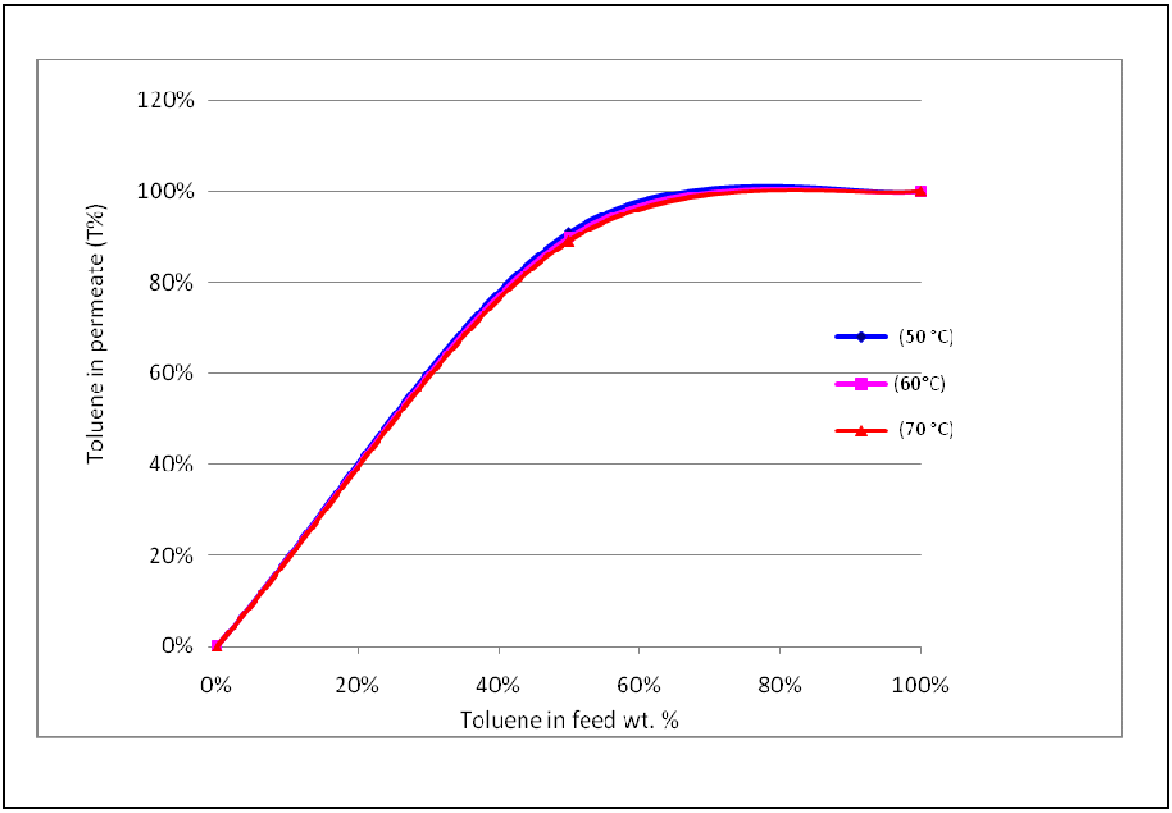

Figure 1.4: Toluene enrichment in PEI dense membrane (60µm).

The effect of feed operating temperature on flux of the dense PEI membranes (40-60µm) is represented in table 1.4. As expected, the total flux increases with the increase of operating temperature.

Figure (2,a.4) illustrates the effect of feed mixture content (toluene/heptane mixture) on the partial normalized flux of toluene for PEI dense membrane. As expected, the partial normalized flux of toluene is increased with the increase of toluene wt.% in feed and also with increase of operating temperature.

However, figure (2,b.4), shows bell shape curve which does not follow heptane activity, but toluene activity; it illustrates the agreement with swelling due to low swelling of PEI dense membrane in heptane and shows the strong plasticizing effect of toluene.

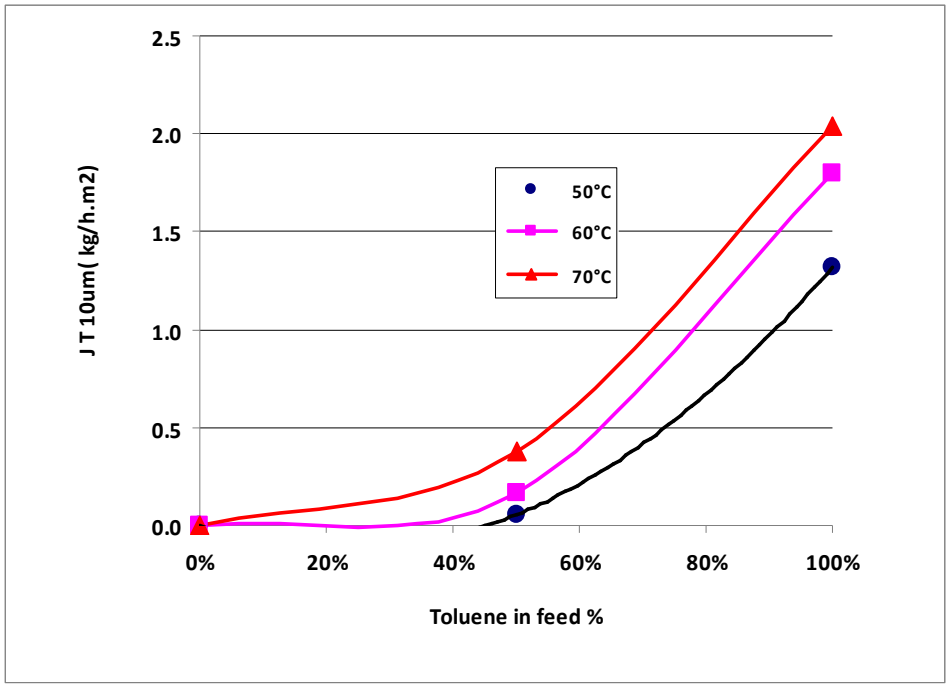

a. Partial normalized flux of toluene (J_T) in PEI dense membrane

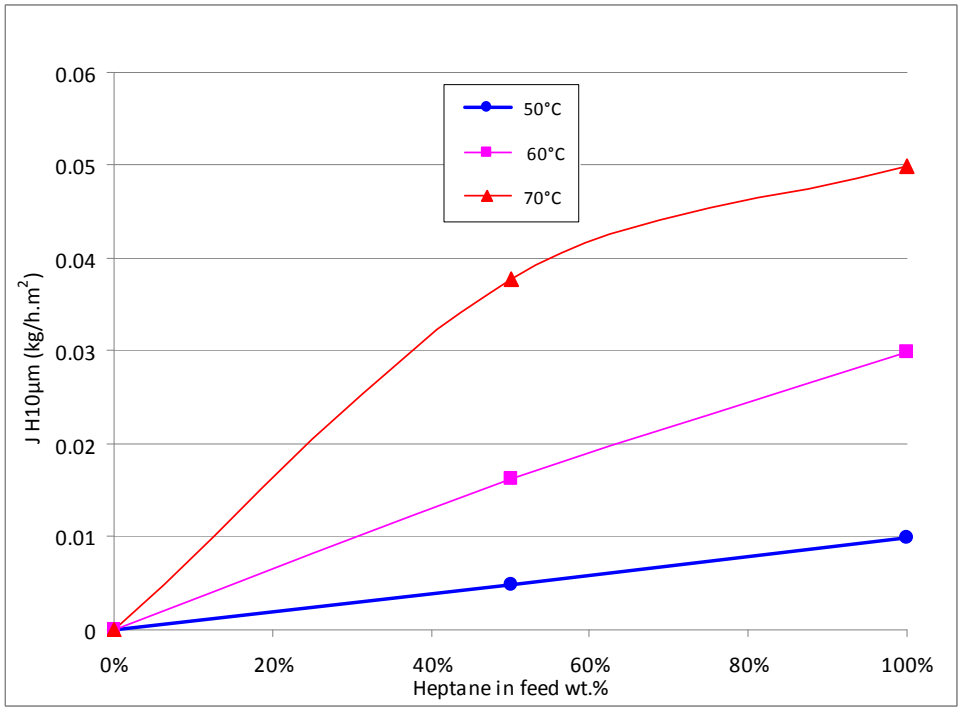

b. Partial normalized flux of heptane in PEI dense membrane

Figure 2.4: Effect of feed wt. % on the partial normalized flux of PEI dense membrane (60µm)

4.1.2 Effect of membrane (type, thickness) and temperature on membrane performances

The membranes are often used to achieve a high flux with a good selectivity, thus the effect of some variables as thickness and membrane type will be evaluated and investigated in this part. The SEM views of the asymmetric PEI membranes tested are presented in Fig. 3.4.

The effect of membrane type and operating temperature on the selectivity, i.e. permeate enrichment and separation factor is shown on Fig. 4.4. The dense membrane (M_{dense}) and asymmetric membrane (M_1) with 30wt% of PAA in DMF have the best selectivity (89-91) but a rather low flux (0.01-0.1 kg/h.m^2). Thus, it means that the asymmetric membrane (M_1) prepared by phase inversion has a very low porosity (P_{wet}=11%) and behaves like a dense membrane structure as M_{dense} while asymmetric membrane (M_{13}) with 25 wt% of PAA in DMF has selectivity (73-75 %) and real flux about ten times higher than of the dense membrane (0.45-0.95 kg/h.m^2). It means that the asymmetric membrane (M_{13}) have structures with a thin top layer and almost defect free. Asymmetric membranes (M_7, M_8) are very porous, so it was difficult to test them in pervaporation due to their high flux. Only two samples were successfully tested (the downstream side pressure of the process was maintained at ≥1 mbar), this effect may explain the membrane performance leading to rather a low selectivity (55-65%) but very high flux (0.13-0.48 kg/h.m^2) compared to dense membranes and a poor selectivity. Their potential in nanofiltration will nevertheless have to be checked carefully in NF because the experimental conditions (pressure, swelling) might lead to more interesting results in NF than in PV.

It is found that the selectivity of asymmetric PEI membranes has a drop with an increase of operating temperature due to the effect of toluene swelling and thus to the coupling of heptane molecules with toluene ones. But interestingly, it can be also noticed that the operating temperature increase led to a steady selectivity with the asymmetric M_{13} membrane. These results show that the dense and asymmetric polyetherimide (PEI) membranes are selective to toluene permeation.

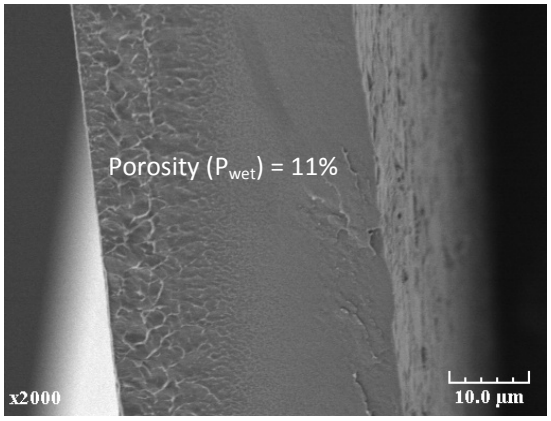

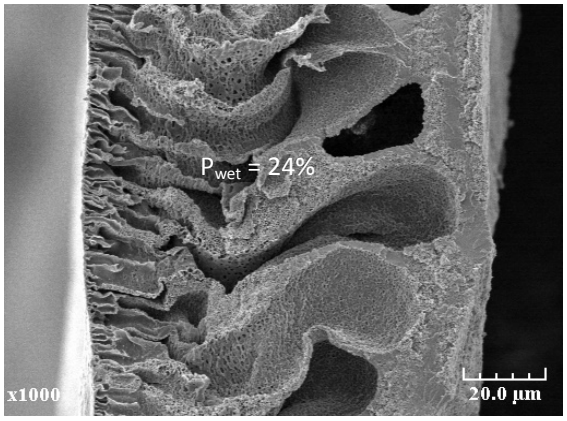

M_1 (30%-70%-0/1min/1h/40µm)

M_{13} (25%-75%-0/1min/1h/100µm)

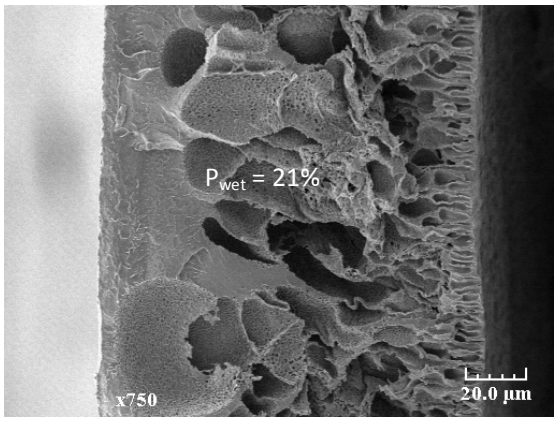

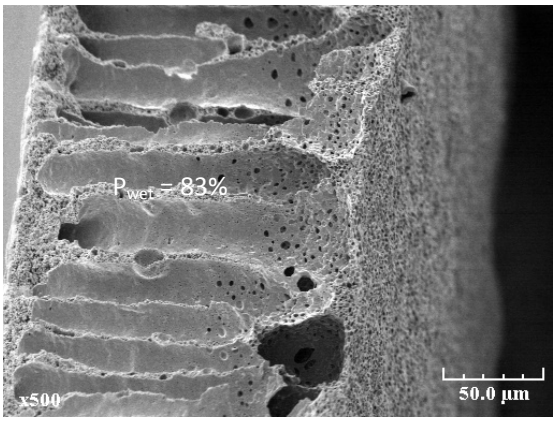

M_7 (28-67-5/1min/1h/150 µm

M_8 (25-60-15 /1min/1h/ 140µm)

Figure 3.4: SEM photographs of the surface of PEI membranes. The conditions of preparation of each membrane are (PAA wt%-DMF wt%-Water wt%/preconcentration time/ immersion time/thickness) respectively.

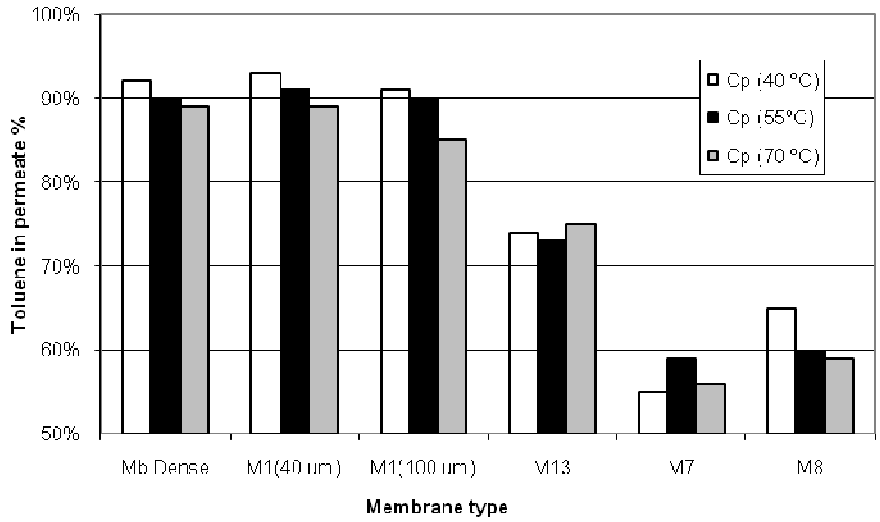

a- Effect of membrane type on the permeate enrichment

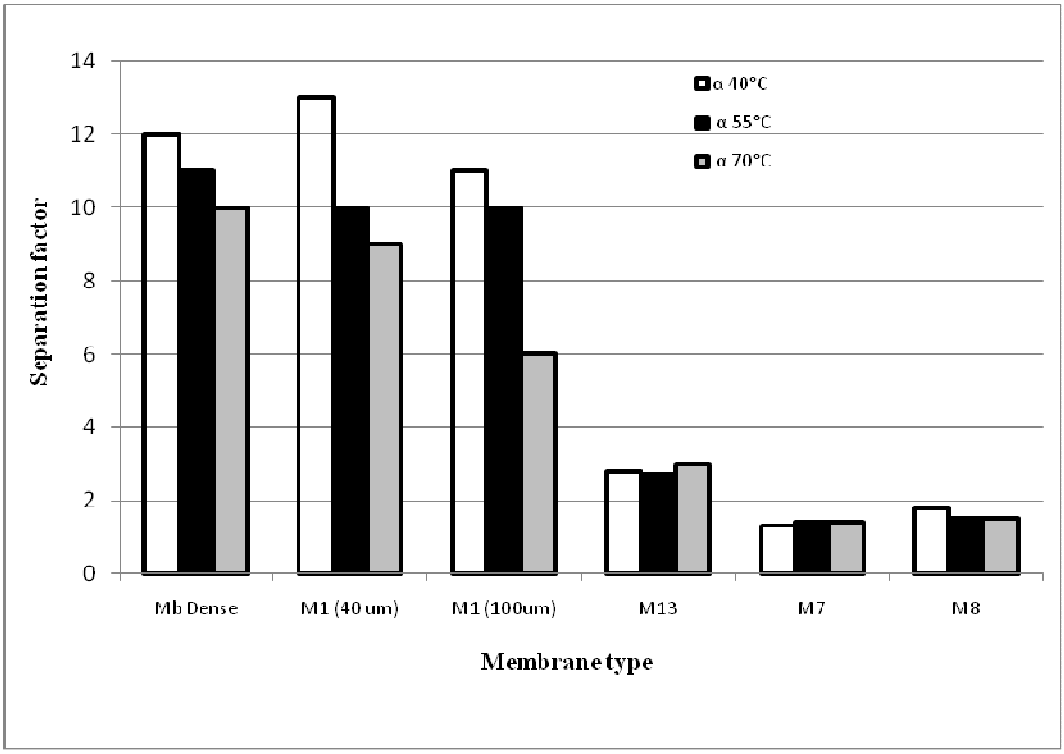

b- Effect of membrane type on separation factor

Figure 4.4: Effect of membrane (type, thickness) and operating temperature on selectivity (feed 50 wt% toluene/heptane).

The effect of dense membrane thickness on the permeate flux was measured at various temperature for the dense PEI membrane with two different thicknesses (40µm, 60µm). The results are plotted in figure 5.4. It was observed that the flux decreased with the increase of dense membrane thickness. in other words, the permeate flux exhibits a very strong dependance on dense membrane thickness.

The effect of asymmetric PEI membrane thickness is shown in figure 5.4. It was found out that the partial real flux of the asymmetric membrane (M_1) decreased with an increase of asymmetric membrane thickness, the partial flux of the asymmetric membrane (M_1,100µm) is lower than the partial flux of the asymmetric membrane (M_1,40µm). Thus, thin asymmetric membranes are logically preferred to achieve high permeation.

It is usually expected that, in an ideal case where the membrane is homogeneous and free of defects, the total permeation flux is inversely proportional to the membrane thickness while the membrane thickness has no impact on the membrane selectivity. This is why in some laboratory studies the reported permeation total fluxes are normalized to a given membrane thickness by assuming a relationship between the permeation normalized or real flux and the membrane thickness.

The effect of membrane type (dense, asymmetric) on flux at the feed 50 wt.% T/H is illustrated in Figure (5.4). It is found that the flux of asymmetric PEI membrane is much higher than the PEI dense membrane. Furthermore, the flux is increased with the increase of feed operating temperature. It explains why in industrial application only asymmetric membranes are used.

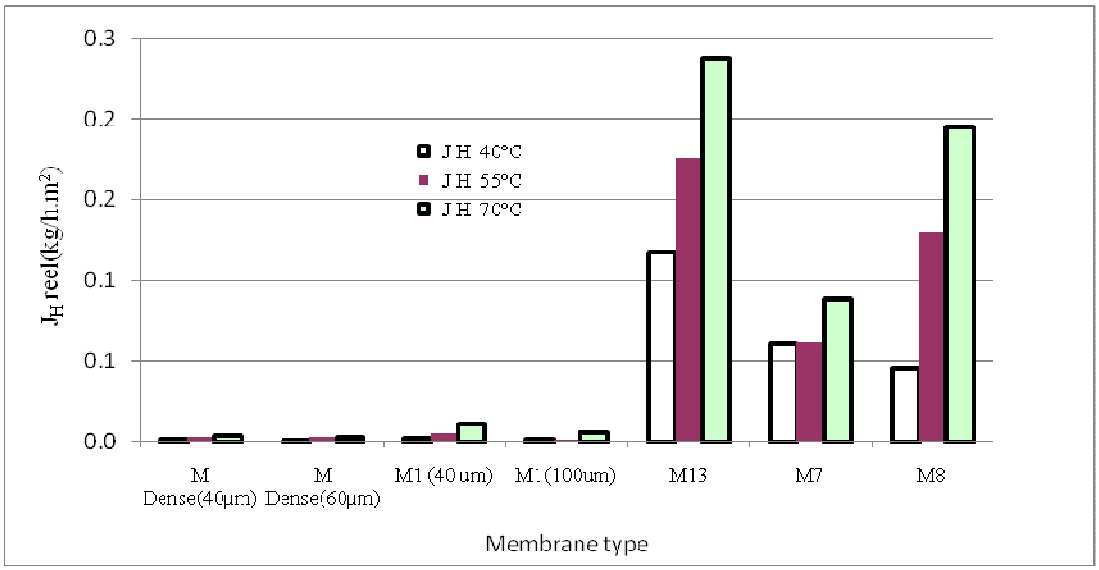

b. Effect of membrane type on Heptane partial flux (feed 50% T/H).

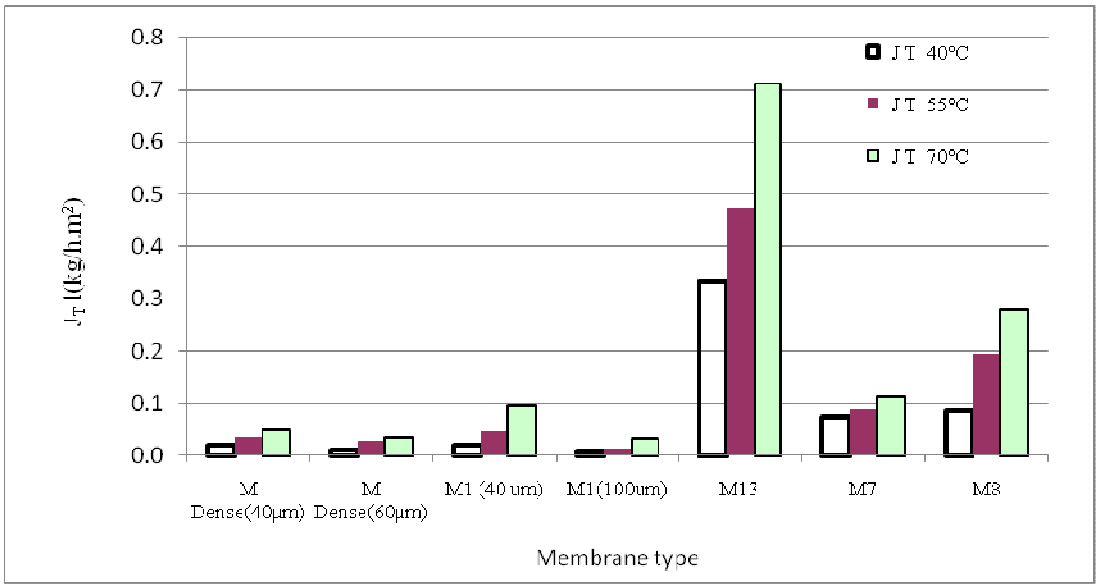

a. Effect of membrane type on Toluene partial flux (feed 50% T/H).

Figure 5.4: Effect of membrane type on partial flux (feed 50% T/H).

4.2 Pure solvents (Water, Ethanol) and 0-100 wt. % aqueous solution of water- ethanol

The main interest of dense membranes used in separation applications is the ability to induce selective permeation of different components (i.e.; solute, organic solvents). Hence, the permeation experiments of pure water, ethanol and aqueous solution of water/ethanol at different temperatures (30, 45, 60^{o}C) were carried out to investigate the dense and asymmetric PEI membranes performances and their temperature dependence in pervaporation. The results are represented in figures (6.4- 12.4) and tables (4.4- 9.4). As expected, the flux for pure solvents and aqueous solution through all the PEI dense and asymmetric membranes increased with the increase of feed operating temperature following an Arrhenius law (tables 4.4-8.4).

Table 4.4: Effect of operating temperature on the total flux of PEI dense and asymmetric membranes.

Feed water/ethanol	Total flux $m_{d1,60\mu m}$* (kg/h m^2)			Total flux $m_{d2,30\mu m}$ *(kg/h m^2)			Total flux $m_{as,60\mu m}$ *(kg/h m^2)		
	30°C	45°C	60°C	30°C	45°C	60°C	30°C	45°C	60°C
ethanol	0.037	0.05	0.1	0.06	0.1	0.18	0.034	0.061	0.1
20 wt % w*	0.08	0.15	0.25	0.18	0.30	0.50	0.19	0.37	0.86
40 wt % w	0.13	0.20	0.40	0.24	0.43	0.83	0.31	0.60	1.21
60 wt % w	0.17	0.25	0.42	0.33	0.53	0.93	0.42	0.61	1.14
80 wt % w	0.18	0.30	0.43	0.37	0.60	0.94	0.43	0.65	1.29
Pure water	0.2	0.31	0.46	0.38	0.64	0.99	0.45	0.84	1.63

*Where: w; water, e; ethanol, PEI dense membrane 30 wt % PAA = $m_{d1,60um}$, PEI dense membrane 25 wt % PAA = $m_{d2,30\mu m}$, PEI asymmetric membrane 25 wt % PAA = $m_{as,60\,\mu m}$

Table 5.4: Effect of temperature on the partial flux of feed with asymmetric PEI membrane 25 wt % PAA ($m_{as,\ 60\ um}$).

Feed water/ethanol	Water partial flux (J_W) (kg/h m^2)			Ethanol partial flux (J_e)(kg/h m^2)		
	30°C	45°C	60°C	30°C	45°C	60°C
20 wt % w	0.13	0.23	0.49	0.051	0.141	0.37
40 wt % w	0.245	0.47	0.87	0.067	0.138	0.339
60 wt % w	0.38	0.53	0.96	0.04	0.08	0.18
80 wt % w	0.45	0.59	1.15	0.02	0.055	0.15

Table 6.4: Effect of operating temperature on the normalized flux for dense PEI membranes.

Feed water/ethanol	Normalized flux m_{d1*} (10µm kg/h m^2)			Normalized flux m_{d2*} (10µm kg/h m^2)		
	30°C	45°C	60°C	30°C	45°C	60°C
Ethanol	0.20	0.30	0.5	0.18	0.3	0.54
20 wt % w*	0.5	1	1.5	0.55	1	1.5
40 wt % w	0.75	1.25	2.5	0.80	1.3	2.5
60 wt % w	1.05	1.5	2.7	0.99	1.5	2.7
80 wt % w	1.1	1.8	2.6	1.15	1.8	2.8
Water	1.2	1.9	2.8	1.2	1.95	3

Table 7.4: Effect of temperature on the partial normalized flux with dense PEI membrane ($m_{d1, 60\mu m}$).

Feed water/ethanol	Water normalized flux m_{d1*}			Ethanol normalized flux m_{d1*}		
	30°C	45°C	60°C	30°C	45°C	60°C
ethanol				0.2	0.3	0.5
20 wt % w*	0.33	0.6	0.9	0.17	0.4	0.61
40 wt % w	0.56	0.9	1.7	0.189	0.38	0.78
60 wt % w	0.97	1.2	2.1	0.23	0.3	0.6
80 wt % w	0.99	1.5	2.4	0.11	0.22	0.4
water	1.2	1.9	2.8			

Table 8.4: Effect of temperature on the partial normalized flux with dense PEI membrane ($m_{d2,30\mu m}$).

Feed water/ethanol	Water normalized flux m_{d2*}			Ethanol normalized flux m_{d2*}		
	30°C	45°C	60°C	30°C	45°C	60°C
ethanol				0.2	0.3	0.5
20 wt % w*	0.33	0.6	0.96	0.143	0.39	0.58
40 wt % w	0.76	0.97	1.7	0.19	0.37	0.77
60 wt % w	0.98	1.2	2.15	0.1824	0.36	0.60
80 wt % w	0.98	1.5	2.41	0.1	0.20	0.40
Pure water	1.2	1.95	3			

Table 9.4: Separation factor of PEI membranes.

Feed water/ethanol	Separation factor m_{d1}			Separation factor m_{d2}			Separation factor m_{as}		
	30°C	45°C	60°C	30°C	45°C	60°C	30°C	45°C	60°C
20 wt % w	10	7	5.8	11	8	6	9	6	5
40 wt % w	5	4.1	3	5	4	3	5.2	5	3.8
60 wt % w	2.6	2.6	2.1	2.8	2.6	2.3	3.3	2.7	2.2
80 wt % w	2.15	1.6	1.45	2.1	1.6	1.4	3.5	2.7	2

4.2.1 Effect of temperature and feed composition on membrane selectivity

The influence of ethanol concentration in the feed on the membrane performances for the separation of ethanol from water by pervaporation at different temperatures was studied using dense and asymmetric PEI membranes. The separation data in Tables (4.4-9.4) are plotted against the corresponding operating conditions (temperature, feed composition) data for the dense and asymmetric membranes, as shown in Figures (6.4:12.4), which explicitly shows that the membrane performance is strongly affected by the membrane morphology and preparation conditions.

The effect of temperature and membrane type on the selectivity, i.e. permeate enrichment is shown on Figs.(6.4:8.4). It is found that the PEI dense and asymmetric is a water selective membrane while the membrane selectivity for water decreases with an increase of feed temperature, but increases with an increase of water concentration in feed at the same temperature. Morever, selectivity is higher at lower temperature because there is less coupling between water and EtOH. The influence of temperature on swelling and the effects of swelling are opposite with water. This can be related to the lower plasticizing effects of the permeants; thus as the polymer free volumes are lower, the water permselectivity is favoured. In other words, the PEI membranes exhibit a water permselectivity over a wide range of feed composition and the selectivity reaches a maximum at high water contents in the feed mixture. The highest selectivity was found at 80 wt.% water in feed at the lowest operating temperature (30°C) while the lowest selectivity was found at 20 wt.% water in feed at the highest operating temperature (60°C) for all dense and asymmetric PEI membranes.

The selectivity of the two PEI dense membranes ($m_{d1(30PAA)}$, $m_{d2(25PAA)}$) and asymmetric PEI $m_{as(25PAA)}$ were almost the same for all temperature (Fig.7.4-8.4, CP ±2-3%). In other words, the H_2O permeate enrichment of the dense and of the asymmetric PEI membranes were almost the same. Clearly, these results means that the PEI asymmetric membrane is really able to achieve molecular separation as well as the PEI dense membrane does, showing that the phase inversion procedure used gave rise to the formation of asymmetric defect-free membrane.

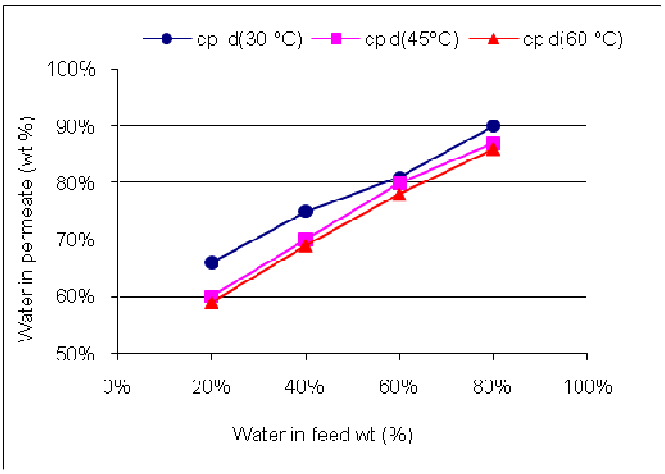

a- dense membrane 30PAA

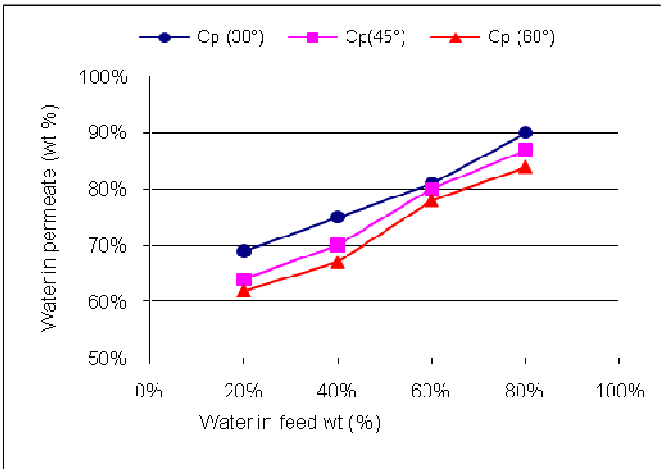

b- dense membrane 25 PAA

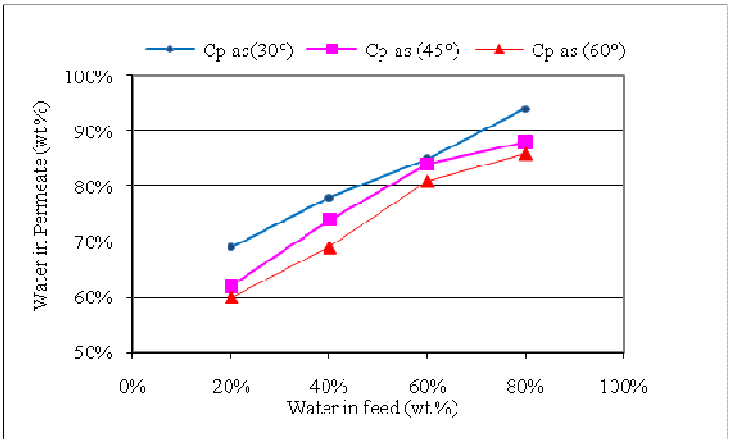

c- asymmetric membrane (25 PAA& 60um)

Figure 6.4: Effect of the feed concentration on separation performance of PEI membranes, CP±2-3%.

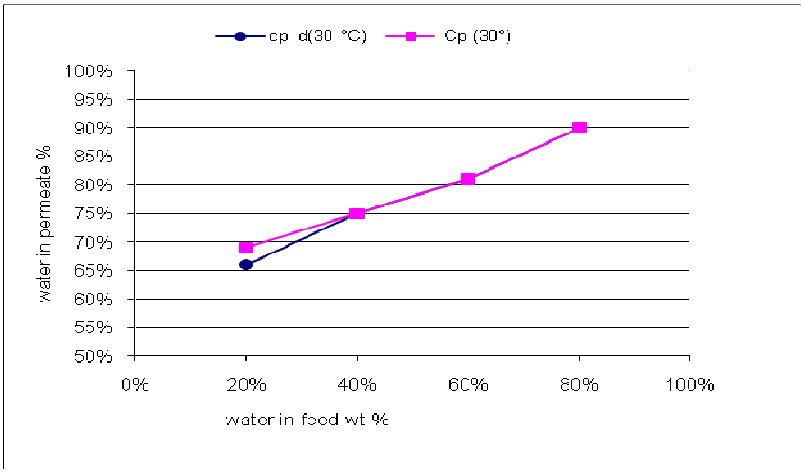

a. Enrichment comparison for the PEI dense membranes (30PAA& 25PAA) at 30^0C.

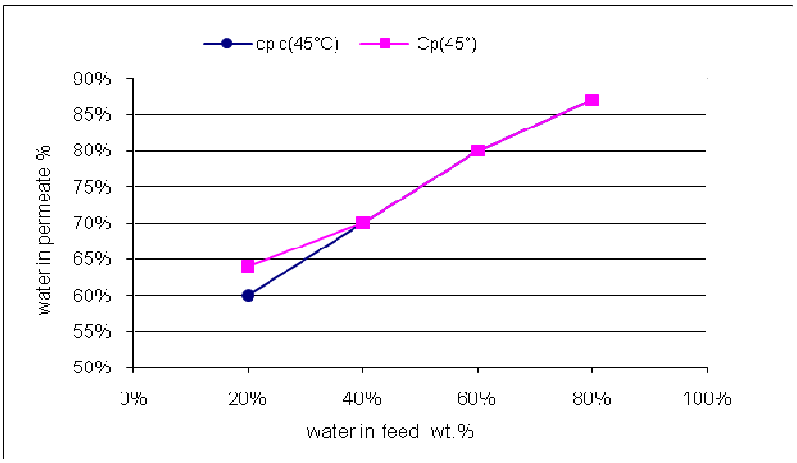

b. Enrichment comparison for the PEI dense membranes (30PAA& 25PAA) at 45^0C.

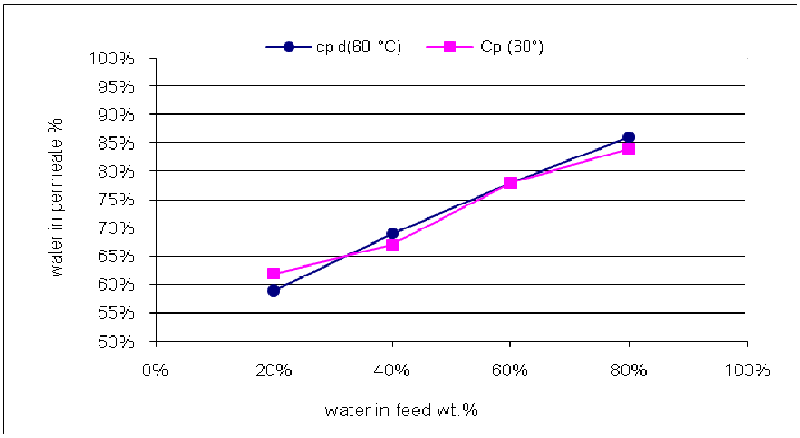

c- Enrichment comparison for the PEI dense membranes (30PAA& 25PAA) at 60^0C.

Figure 7.4 a, b, c: Enrichment comparison for the PEI dense membranes (30PAA& 25PAA) at temperature 30 - 60^0C, where (cp d); (30PAA), CP±2-3%).

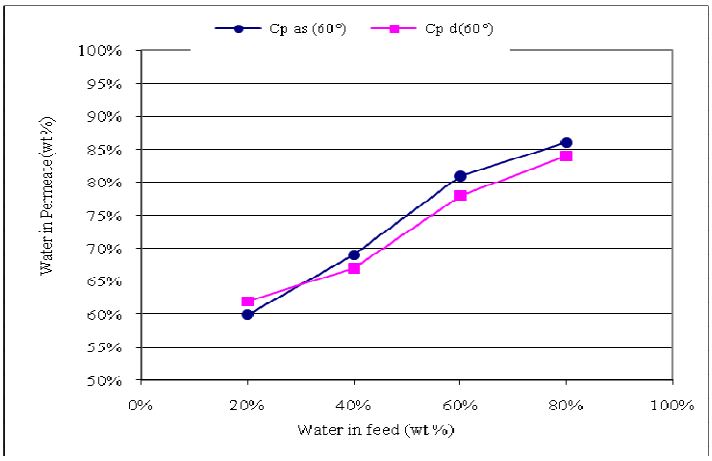

a. Enrichment comparison for the PEI asymmetric and dense membranes at 60^0C.

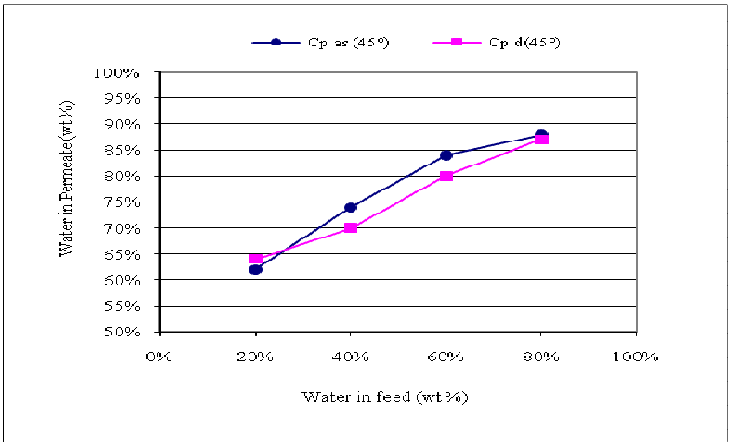

b. Enrichment comparison for the PEI asymmetric and dense membranes at 45^0C.

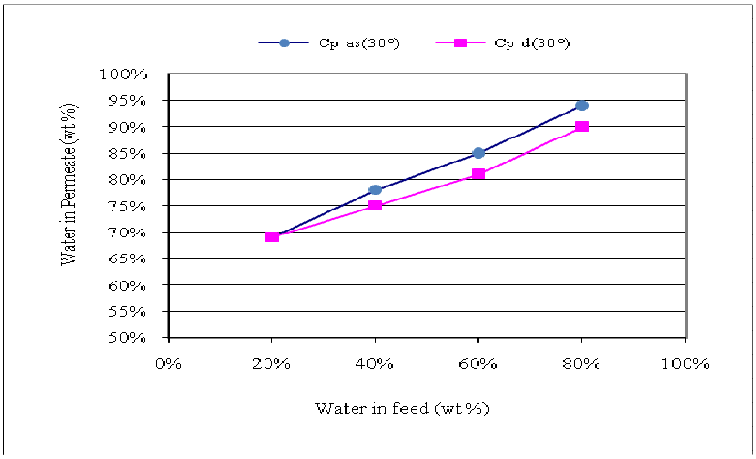

c. Enrichment comparison for the PEI asymmetric and dense membranes at 30^0C.

Figure 8.4, a b c: Enrichment comparison of asymmetric (cp as) / dense membrane (cp d) (25PAA) at temperature 30 - 60 ^{0}C, CP±2-3%.

Furthermore, the effects of operating conditions (temperature, feed composition) on separation factor were shown in (Fig. 9.4). It was observed that the separation factor decreases with increasing feed operating temperature and also with increasing water content in feed. The highest separation factor was found at 20 wt.% water in feed at the lowest operating temperature (30°C) while the lowest separation factor was found at 80 wt.% water in feed at the highest operating temperature (60°C) for all dense and asymmetric PEI membrane (Fig. 9.4, table 9.4).

At low temperature, water molecule only, given its small size can easily move through polymer chains. Ethanol molecular size is about three-fold that of water molecules (the van der Waals volumes of ethanol and water are 96.6 10^{-30} m^3 and 29.9 10^{-30} m^3, respectively). At higher temperature, permeation fluxes of both water and ethanol increase because of expanding free volumes of polymer molecules and plasticizing effects of water molecules in the membrane.

A. Verkerk et al. [5] and J. Elshof et al. [6] reported that the separation factor decreased with increasing water content in feed, this is often attributed to the so-called "drag" effect. In other words, the overall separation factor is governed by contribution of the resistances of both the dense skin-layer and the porous substrate, the separation factor reaches a maximum at low water contents in the feed mixture such as dehydration of alcohols.

Drag (sometimes called air resistance or fluid resistance) refers to forces that oppose the relative motion of an object through a fluid (a liquid or gas). Drag forces act in a direction opposite to the oncoming flow velocity. Unlike other resistive forces such as dry friction, which is nearly independent of velocity, drag forces depend on velocity.

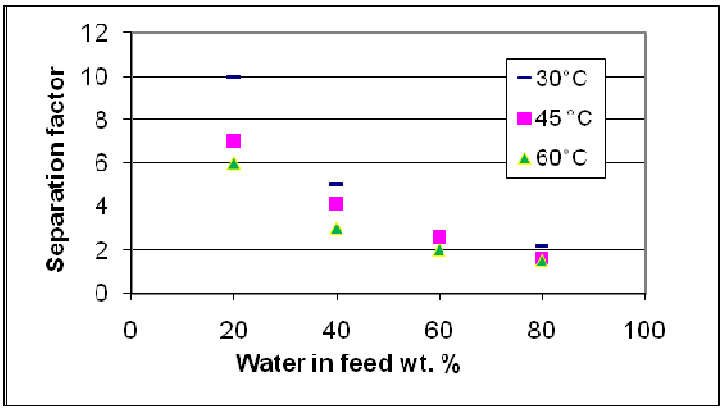

a. Effect of water wt% on separation factor for dense membrane (30%PAA)

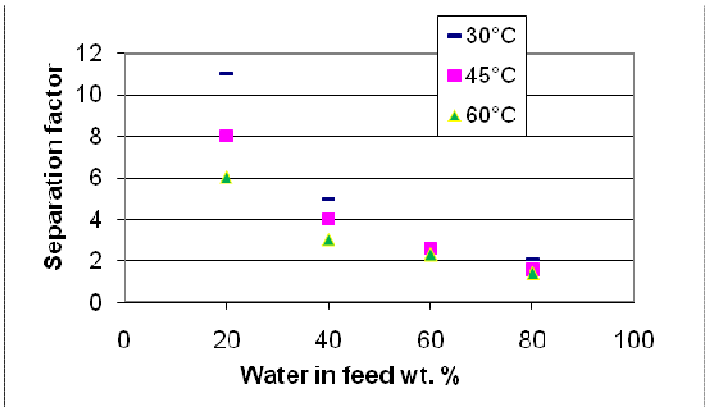

b. Effect of water wt% on separation factor for dense membrane (25%PAA)

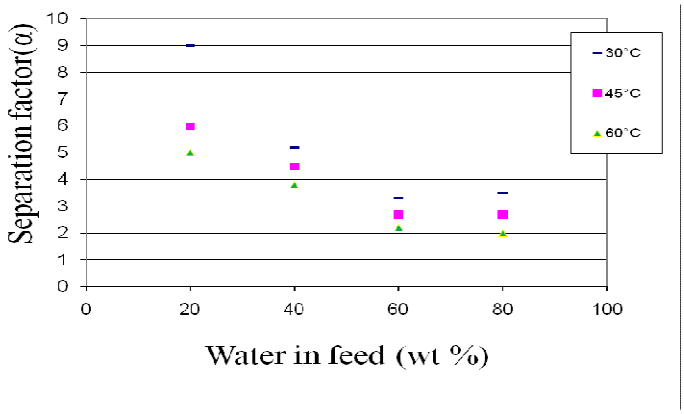

c. Effect of water wt% on separation factor for asymmetric membrane (25%PAA)

Figure 9.4: Effect of operating conditions (temperature, feed composition) and membrane type on separation factor.

4.2.2 **Effect of temperature and feed composition on membrane flux**

The operating parameters (temperature and feed) data are plotted against the corresponding flux data for the dense and asymmetric membranes, as shown in figures (10.4-12.4), which obviously illustrate that the membrane flux is strongly affected by the membrane (type, thickness) and operating conditions.

Figures (10.4-12.4) and tables (4.4-8.4) illustrate the effect of feed mixture content (water/ethanol mixture) and operating temperature on flux. It was observed that the (real, partial, normalized) flux through all the PEI dense and asymmetric membranes increased with increasing water content in feed and also with increasing feed operating temperature following an Arrhenius law.

The real flux of the PEI asymmetric membrane (60µm) is higher than the real flux of the PEI dense membranes (30µm, 60µm); this result is represented in table (4.4). Furthermore, it was found that the parial flux of water is higher than the partial flux of ethanol (Figs. 10.4- 12.4). However, Figures (10,b.4-11,b.4-12,b,.4), show bell shape curves which do not follow ethanol activity, but are linked to water activity. This illustrates the agreement with swelling due to effects of swelling are opposite with water of PEI dense membrane with increasing temperature.

The effect of membrane thickness on PEI dense membrane performance is shown in table (4.4) for the PEI dense membranes (m_{d1}: 30 PAA & 60 µm, m_{d2}: 25 PAA & 30 µm). It was found that the real flux for the dense membrane m_{d2} (25 PAA & 30 µm, 0.1-1 kg/h.m^2) is almost two times higher than the real flux of PEI dense membrane m_{d1} (30PPA, 60µm, 0.07- 0.47 kg/h.m^2), while the normalized flux for the two dense membranes are almost in the same range (0.5-3) kg/h.m^2 at all operating temperature (table 6.4). It is known that the permeation flux is inversely proportional to the membrane thickness while the membrane thickness has no impact on the membrane selectivity. This is why in the dense membrane the reported permeation real fluxes were normalized to a given membrane thickness by assuming a relationship between permeation real flux and the membrane thickness. Thus, thin dense tight membranes are often used to achieve a high water (solute) permeation flux.

The effect of soft block of PEI membrane on flux can be estimated by a comparison of our results with Kapton (PI) membrane. X.Yexin et al. [7] reported that in case of PI (PMDA–ODA) dense membrane (32 µm thickness) with feed of water/ ethanol with mass fraction of water was 10 % the total real flux is 14 to 43 g/h m^2 at an operating temperature of 45 to 75°C while in our case with mass fraction of water was 10%**,** the total real flux for m_{d1},

m_{d2} and m_{as} are 60 to 160, 120 to 350 and 180 to 410 g/h m^2 respectively at operating temperature between 30 and 60°C. Thus, the addition of soft block led to an increase of the flux of PEI dense membrane, at least 10 times higher than the Kapton dense membrane.

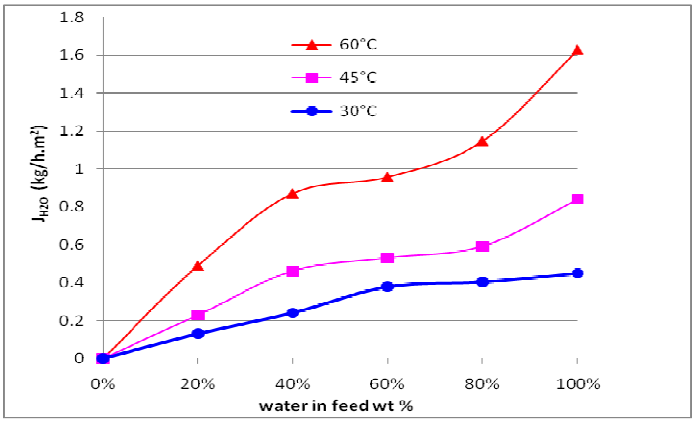

c. Partial real flux of water

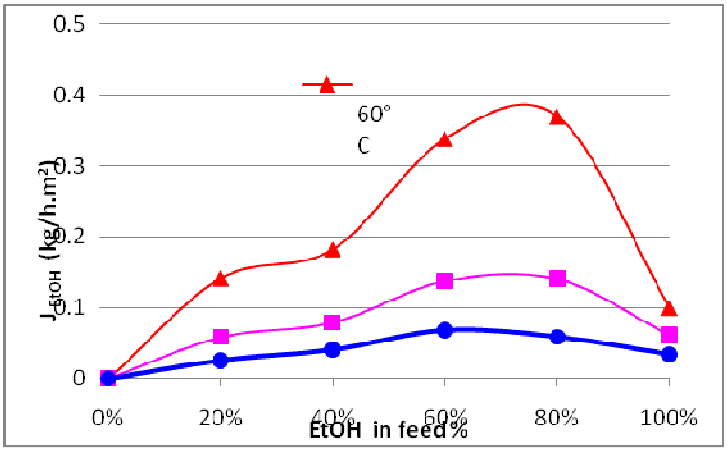

b. Partial real flux of ethanol

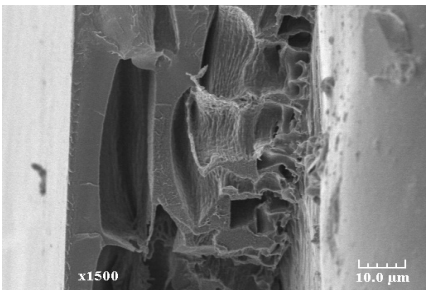

a. Cross section m_{as} (25%-75% 0/1min/1h/60µm) im 11 °C

Figure10.4: Effect of feed concentration on the partial real flux of asymmetric membrane (25 PAA& 60um).

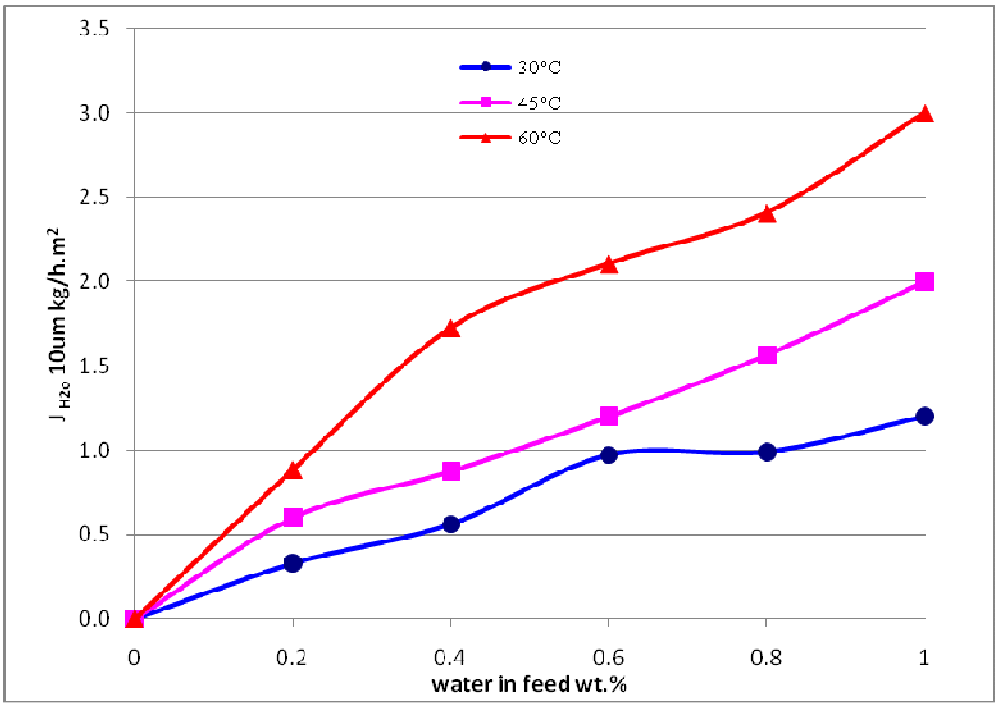

a.Partial normalized flux of water

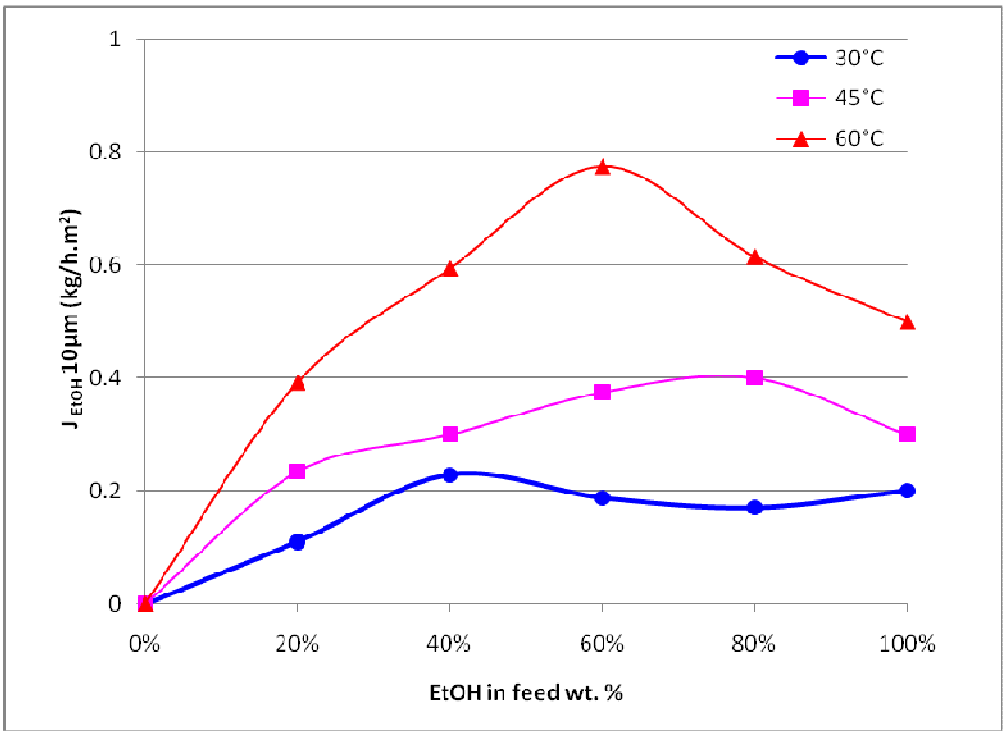

b.Partial normalized flux of ethanol

Figure 11.4: Effect of feed content on partial normalized flux with dense membrane 30 PAA.

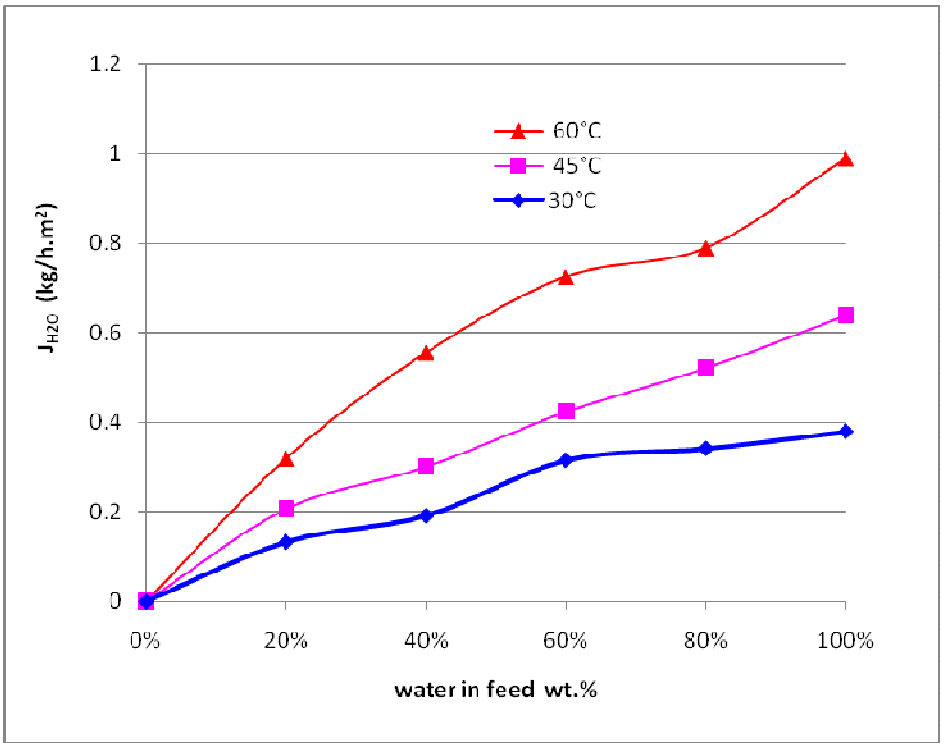

a. Partial water real flux

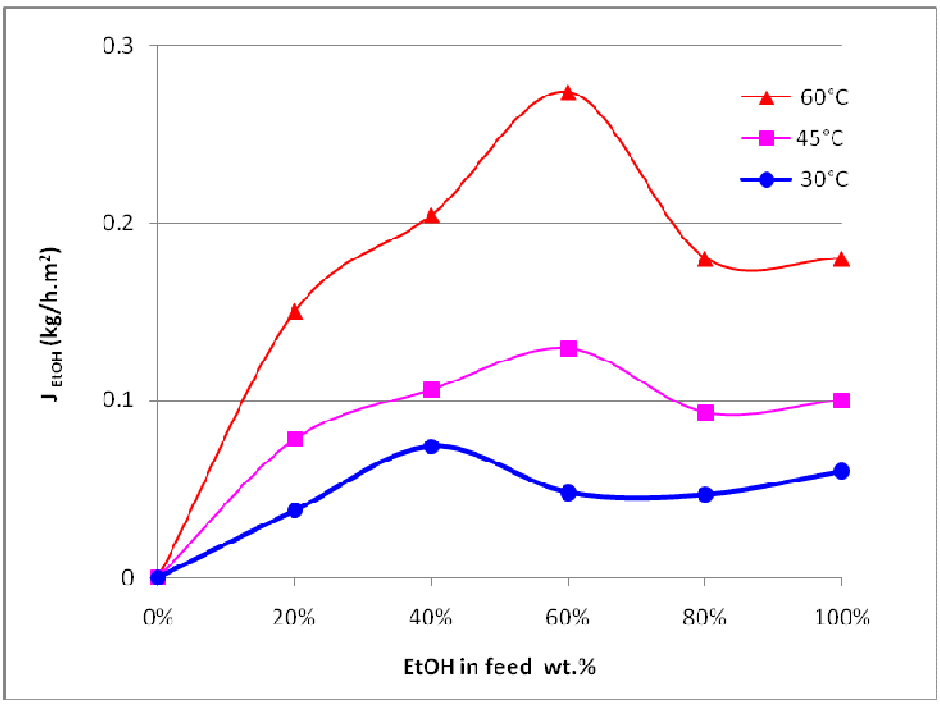

b.Ethanol partial real flux

Figure 12.4: Effect of feed content on partial real fluxes with dense membrane 25 PAA.

4.3 Effect of soft block on pervaporation performances of PEI membranes

The development of high performance asymmetric membranes is a major breakthrough in membrane technology. Thus, this work intends to study the effect of addition of soft blocks on performances of PEI membranes by comparison of performances with a Kapton™ (PI) membrane prepared from commercial PAA. Hence, Water-Ethanol (50-50 wt%) mixtures were used to investigate the dense and asymmetric PEI and PI membranes performances and their pervaporation temperature dependence in the range 30-60°C. Thus, for each membrane, a minimum of three traps with a constant flow was determined before a change in temperature was performed.

The pervaporation (PV) experiments intended to know if it was possible to achieve molecular separation with the asymmetric PEI 0.4Jeff membrane (Fig.13.4) keeping the selectivity close to that obtained with a dense PEI membrane, together with a much higher flux. First it should be underlined that all the PEI 0.4Jeff samples used were well stable during the PV experiments even at 60°C and long term PV experiments could be carried out to check the temperature dependence (up to 7 days).The PV results are presented in Table 10.4 and in Fig. 14.4.

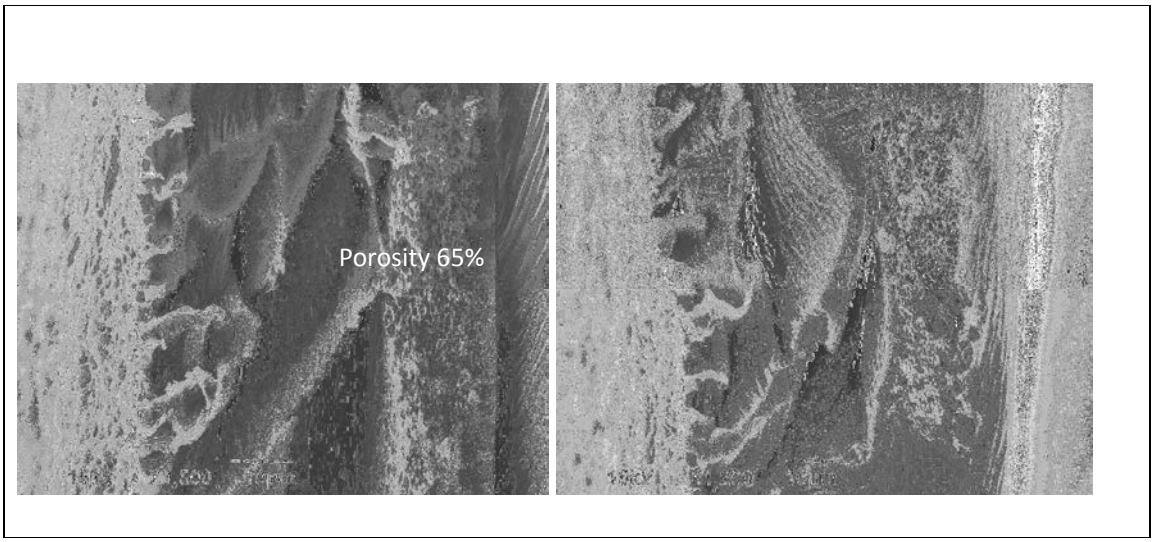

Figure 13.4: Cross section view of PEI asymmetric membrane 25% PAA in DMF at immersion bath temperature 16°C.

Table 10.4: Comparison between dense, asymmetric PEI (0.4 Jeff 600) and dense PI Kapton™ membranes prepared from commercial PAA (feed 50 wt% ethanol/water).

Membrane type	dense PEI (25 % PAA, 0.4 Jeff600)	dense Kapton™ (11 % PAA)	asymmetric PEI (25 % PAA, 0.4 Jeff600)
thickness	30 µm	20µm	50 µm
selectivity%	78-80 at 40 °C 74 at 60 °C	98 at 40 °C 96 at 60 °C	80 at 40 °C 79 at 60 °C
Separation factor (α)	3.5 at 40 °C 3 at 60 °C	38 at 40 °C 24 at 60 °C	4 at 40 °C 3 at 60 °C
Normalized flux (kg/h.m2)	1.48 at 40 ° C 2.82 at 60 °C	0.11 at 40 °C 0.23 at 60 °C	
Real flux (kg/h.m2)	0.55 at 40 °C 0.9 at 60 °C	0.05 at 40 °C 0.115 at 60 °C	4.4 at 40 °C 6.4 at 60 °C

4.3.1 Effect of membrane type and operating temperature on selectivity

The effect of membrane type and of membrane morphology on the selectivity, i.e. permeate enrichment is shown on the Fig.14-a.4. It should be noted that the fully aromatic PI is much more selective for H_2O than the PEI membranes despite the fact that the water affinity of PEI is about three times higher than for the PI Kapton™ . Two factors explain this result: first, the EtOH affinity is also higher for the PEI membranes than for the PI, resulting in lower intrinsic sorption selectivity; second, as far as pervaporation deals with a binary mixture, it is known that a coupling effect can occur giving rise to a higher permeation rate than expected for the compound having the lowest membrane affinity; hence it is the combination of these two phenomena which led to the lower selectivity of PEI compared to PI. But one should note also that the PI flux is extremely low, about 15 times lower than PEI flux, meaning that dense PI membranes could not have any practical use ($J \approx 0.05\text{-}0.1$ kg/h.m^2).

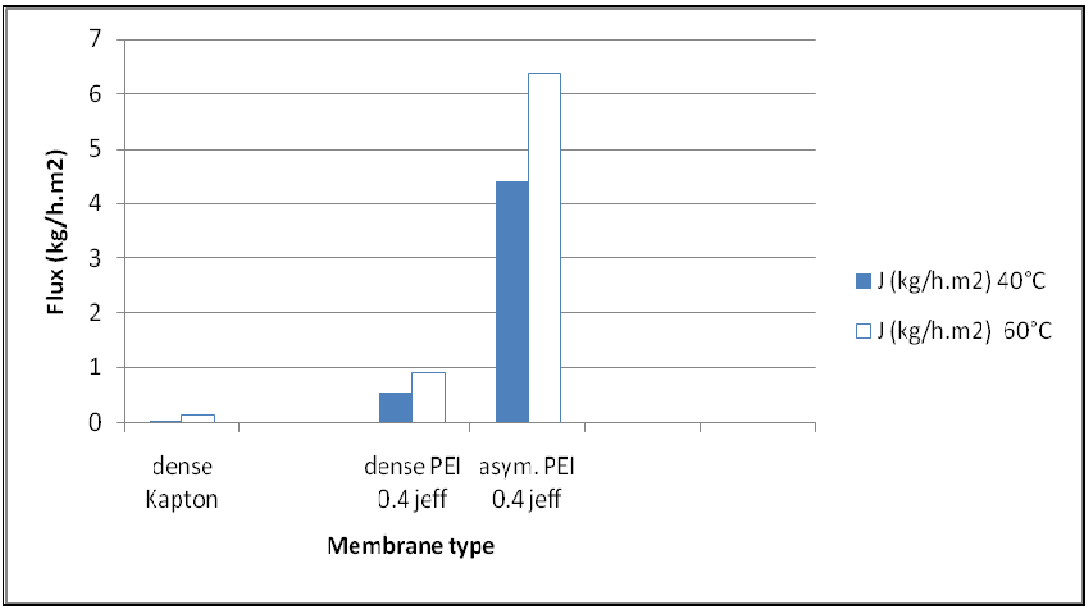

b.Effect of membrane type on the PV flux

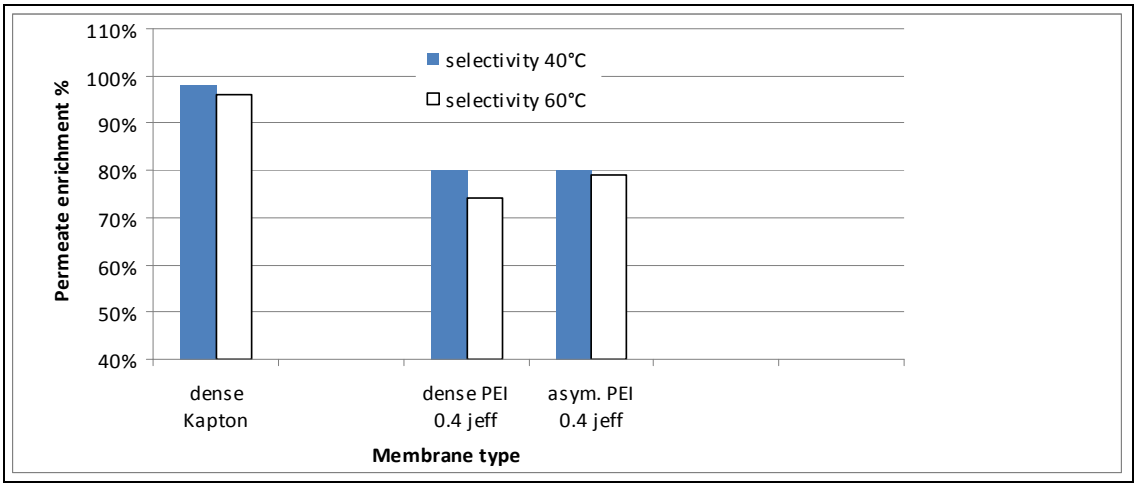

a- Effect of membrane type on the permeate enrichment

Figure 14 a, b.4: PV results obtained with PI or PEI membranes either as dense or asymmetric membranes – Feed mixture: 50 wt% water/ethanol(at 40 and 60°C)

On the other hand, the H_2O permeate enrichment of the dense and of the asymmetric PEI 0.4Jeff membranes were almost the same, i.e. 80wt% at 40°C. These results mean that the asymmetric membrane is really able to achieve molecular separation as well as the dense

membrane does, showing that the phase inversion procedure used gave rise to the formation of a tight layer on the top of the asymmetric membrane.

The effect of the operating temperature on PV selectivity was at first glance rather conventional: the permeate enrichments recorded with PEI and PI membranes were smaller when the temperature was increased. This trend is well-known and has been reported many times in the literature [8]. The higher selectivity at lower temperature is explained by the lower coupling phenomena between H_2O and EtOH, that can be related to the lower plasticizing effects of the permeants; thus as the polymer free volumes are lower, the water permselectivity is favoured.

But interestingly, it can be also noticed that the temperature increase led to a lower decrease of the selectivity recorded with the asymmetric membrane than with the dense one, respectively 79% and 74% at 60°C. Considering the classical solution-diffusion model this finding could not be predicted. So we can only postulate that phase inversion conditions do not lead to the formation of a thin dense layer having exactly the same PEI microphase separation structure than the dense layer prepared by a slow solvent evaporation procedure; but up to now, no analytical proofs of this hypothesis could be obtained.

4.3.2 Effect of operating temperature and membrane morphology on flux

Considering now the PEI flux obtained at 40 or 60°C (Fig.14,b.4), the results obtained were rather expected, showing a much higher flux of the asymmetric membrane up to ≈700% more (i.e. 4.4 to 6.4 kg/h.m^2). But again, one can notice that the range of the temperature effect is different for the dense membranes (PEI or PI, 80% increase or more) and for the asymmetric one, for which the flux increase was relatively lower (only 40%). Hence these experimental results might also indicate that the structure of the dense top layer is not strictly the same for the two types of membranes. This phenomena could be related to the very different conditions prevailing to the formation of the two types of dense layers; for the homogeneous dense membrane, the structure is formed by slow solvent evaporation (DMF) where thermodynamic polymer chain rearrangements are possible to a large extent, i.e. until the Tg is reached, whereas in the other case, the structure of the dense layer is formed on the top of an asymmetric membrane obtained from a very fast polymer gelification due to the phase inversion conditions.

4.4 Dehydration of alcohols

Separation of azeotropic organic solvents , i.e., low molecular weight alcohols and their mixture with water is difficult to be achieved by a conventional process such as distillation. Most aqueous alcohol solutions form azeotropic mixtures. Examples are ethanol (EtOH) and isopropanol (IPA). Aqueous alcohol solutions are concentrated using the distillation process, but purity is restricted by their azeotropes. Further, alcohol dehydration is carried out by means of azeotropic distillation, with the use of either an azeotrope-breaking component (entrainer) or a hybrid system consisting of a multi-stage evaporation and distillation. Such azeotropic distillation consumes large energy and entails cost. As a substitute for those conventional separation processes, prevaporation separation process is an effective method for azeotropic mixtures separation because of its energy saving aspect, low cost and simplicity[9]. Thus, the pervaporation separation process has been applied in the dehydration of aqueous alcohol mixtures.

Polymeric membranes are widely used in solvent dehydration because of their ease of fabrication, reasonable separation performances and low cost [10,11]. The material and structure of the membranes determine its separation performance. A good polymer for the selective permeation of water should have high-sorption centers. Thus, selecting a membrane with one or some of these features incorporated in the polymer chain is often desirable [12,13].

Really, the key to the pervaporation process success is the preparation of suitable membranes. Polyetherimides have been regarded as suitable membrane materials because of their high thermal stability, excellent mechanical strength, and high resistance to organic solvents. However, the disadvantage of dense polyimide membranes when applied to the pervaporation separation process is their low permeation rates. Thus, the dehydration of alcohols will achieved by asymmetric PEI membrane in this part.

The permeation experiments of aqueous alcohols solution of azeotropic ethanol and 95 wt% n-butanol /water at different temperatures (30, 45, 60^{o}C) by PEI asymmetric membrane were carried out. The results are presented in tables (11.4-12.4) and Figs. (15.4-16.4). Pervaporation was carried out to investigate the temperature dependence of pervaporation performances and study the effect of solute molecular weight in separation.

Table 11.4: Pervaporation performances of PEI membranes in aqueous alcohol systems.

Membrane type	**Feed and concentration**	**Operating T (°C)**	**Total flux (Kg/m^2 h)**	**Separation factor**	**Water content**
Asymmetric 25% PAA	95 wt% n-butanol /water	30	0.040	475	98%
		45	0.086	313	97%
		60	0.165	266	96%
	95 wt% EtOH /water	30	0.040	26	57%
		45	0.160	17	46%
		60	0.350	14	42%

Table 12.4: Activation energy for asymmetric PEI membrane.

Feed and concentration	95 wt% EtOH /water	95 wt% n-butanol /water
Et* (J /K mol)	56853	41754

Where; Et: total activation energy

The dehydration of aqueous alcohol solutions of ethanol and n-butanol was studied using asymmetric PEI membrane. Figure (15, b.4) and table 11.4 illustrate that the separation factor and water content in permeate decrease with increasing feed operating temperature as discussed before.

In addition, in the case of PEI membrane with feed of (95wt% n-butanol/water) the separation factor is very high (266-475) while in case of PEI membrane with feed of (95 wt% EtOH/water) the separation factor is low (14-26). This shows that the separation of organic molecules is dependent on the molecular weight of solute. It is known that molecular weight of butanol is higher than ethanol. In other words, the effect of the diameter of butanol (0.69 nm) is higher than the effect of the diameter of ethanol (0.34 nm) while the effective diameter of water is (0.21 nm). So, the probability of butanol rejection is higher than ethanol and that result is consistent with previous studies [Table 13.4].

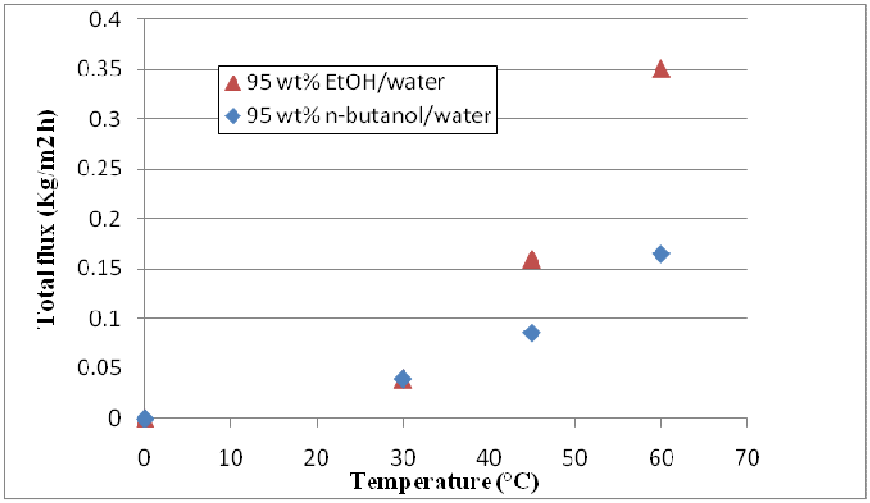

c. Effect of operating temperature on total flux.

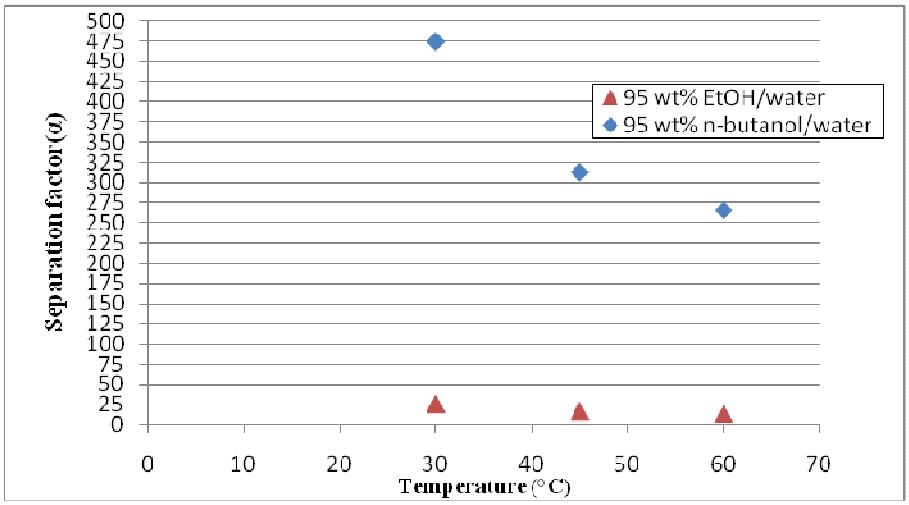

b. Effect of operating temperture on separation factor.

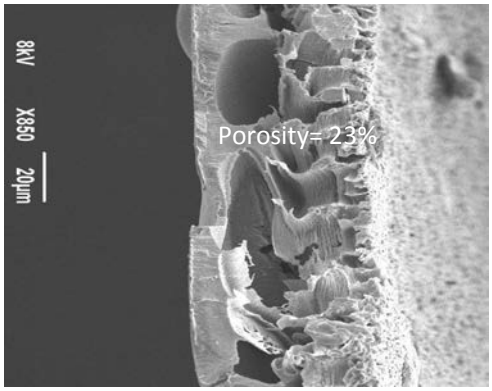

a.Cross section view for M_{13} (25%-75%-0/1min/1h/40µm) im 11°C

Figure 15.4: Asymmetric PEI membrane performances with aqueous alcohol systems.

Figure 15, c.4 showed that the total flux increases with the increase of feed operating temperature. The temperature dependency of the permeation flux is found to follow an Arrhenius low, as shown in Fig. 16.4 (change in logarithm of molar flux(J) flows according to 1 / T for a asymmetric membrane (25%PAA)). Hence, the overall activation energies (*E*t) characterizing the temperature dependencies of the permeation fluxes, can be obtained from the slopes of the straight lines in Fig. 16.4.

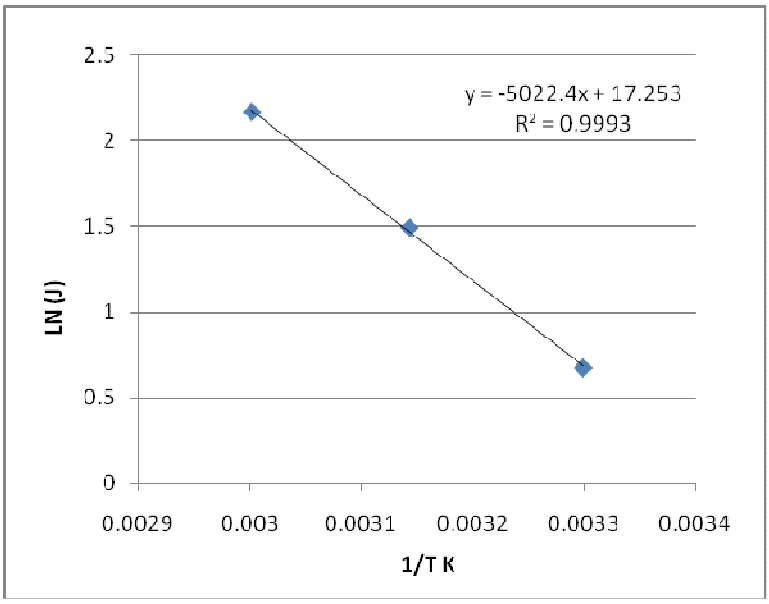

b. Feed aqueous n- butanol

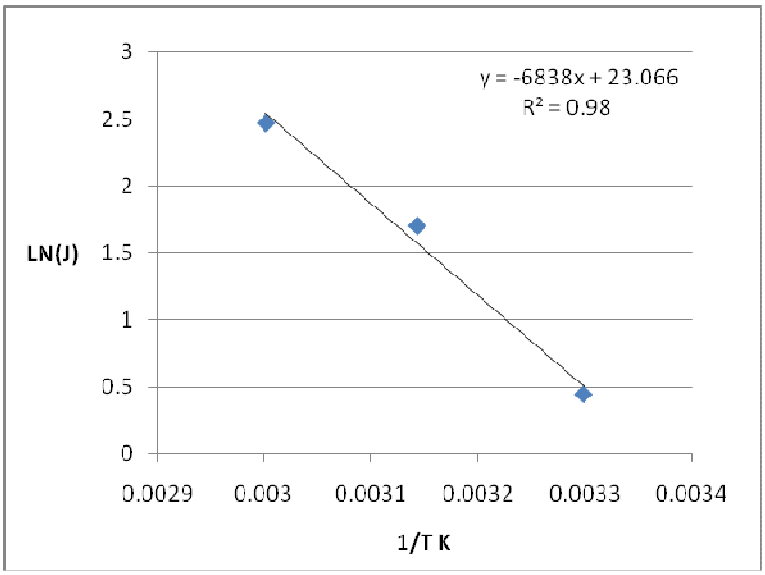

a. Feed aqueous azeotropic ethanol

Figure 16.4: Plot of molar ln(J) / versus 1 / T for the asymmetric membrane (25%PAA).

The table below represents a collection of pervaporation performances of polyimide membranes in aqueous alcohol systems.

Table 13.4: Pervaporation performance of polyimide membranes in aqueous alcohol systems.

Membrane	**Feed and concentration**	**Operation T (°C)**	**Total flux (g/m^2 h)**	**Separation factor**	**Membrane structure**	**Ref.**
(PMDA-ODA)	88.9 wt% EtOH[a]/water	45-75	14-43	347-455	dense	[7]
(PI-2080)	93 wt.% EtOH/water	60	1000	900	asymmetric	[4]
(PMDA - ODA – triethylamine)	93 wt.% EtOH/water	30–60	210	800	composite	[14]
(BTDA/ODA)	93 wt.%) EtOH/water	25	37	1300	composite	[15]
(BPDA-ODA/DABA)	90 wt.% EtOH/water	75	18.49	1800	dense	[16]
(EDA-BMTC)	90 wt.% EtOH/water	40	1700	240	composite	[17]
P84	85 wt.% IPA/water	60	432.3	3866	asymmetric	[18]
		50-250	30-230	3000-1000	dense	
PEI (Ultem 1000)	87.6 wt.% IPA/water	25	36 -507	20-173	asymmetric	[19]
PEI (Ultem 1000)	0.68 0.96 molar fraction IPA/water	25°C		173 384	asymmetric	[20]

Sulzer PERVAP® 2510	85 wt.% IPA/water	60	857	1053	composite	[21]
			64.4	2908	dense	
Matrimid® 5218	85 wt.% *tert*-butanol/ water	25-100	965-2350	41-91	asymmetric	[22]
(BTDA-pPDA)	benzene/cyclohexane (50/50 v/v)	30	450-760	7.3-15.6	asymmetric	[23]
matrimid	95 wt% n-butanol /water	95	1700	57-76	dense	[24]
P84			1400	361		
Torlon			1550	361		
P84	95 wt% EtOH /water	150	3000			
microporous silica membranes	95 wt% n-butanol /water 95 wt% n-propanol /water 90/10 EtOH/H2O	30 60 30 60 80	400 700 420 640 1000	5 100 5 30 800	microporous	[25]
Poly(ether-block-amide) PEBA membrane	(0.03-0.4 wt%) butanol in water	29 40 50 60	100 190 250 370	14-18 21 26 33	Dense	[26]

[a] EtOH: ethanol, IPA: isopropanol

4.5 Separation properties with the hybrid silica- PEI membranes

The modification of membrane polymer by changing the structure and/or chemical characteristics has been extensively investigated. Thus, this work intends to study the effect of using either SiO_2 fillers or organic silica precursors, i.e. TMOS by the sol-gel technique on the morphology and transport properties of a polyimide film. Furthermore, the influence of SiO_2-fillers on the properties of hybrid materials will be determined.

The hybrid silica-PEI membranes were tested in pervaporation with feed 50% toluene and 50% heptane. Each membrane was tested at 3 different temperatures: 40°, 55° and 70°C. For each membrane, we must have a minimum of three traps with a constant flow before change in temperature. The membranes studied are:

• A homogeneous dense membrane, as reference

• A hybrid dense membrane (with silica produced from the TMOS sol-gel process)

• 2 hybrid asymmetric membranes (with hydrophilic silica particles of size equal to 12nm).

•3 asymmetric hybrid membranes (with silica produced from the TMOS sol-gel process)

The enrichment with the hybrid PEI/SiO_2 powders filler for both asymmetric membranes tested in range (55-65%) were quite low. From SEM it was found that the hybrid PEI/SiO_2 is highly porous membrane. This may be explain the low enrichment. Thus, the addition of this filler is not suitable for this type of membrane.

The effect of feed operating temperature and membrane type on flux of PEI composite membranes are presented in (Fig. 17.4, table 14.4). Selectivity and separation factor are presented in (Fig. 18.4, table 15.4). As expected, the total flux increase with increasing temperature according to an Arrhenius law.

Table 14.4: Effect of TMOS content and temperature on flux.

membrane type	Thickness (µm)	J 40°C	J 55°C	J 70°C	J_T 40°C	J_T 55°C	J_T 70°C	J_H 40°C	J_H 55°C	J_H 70°C
M_{dense}	60	0.013	0.03	0.04	0.01	0.027	0.039	0.001	0.003	0.01
$M_{dense5tmos}$	20	0.04	0.08	0.11	0.037	0.07	0.09	0.003	0.01	0.02
M_5tmos	50	0.02	0.04	0.09	0.02	0.035	0.08	0.002	0.004	0.01
M_{10tmos}	50	0.01	0.03	0.07	0.01	0.027	0.06	0.001	0.003	0.01
M_{20tmos}	40	0.01	0.03	0.06	0.01	0.027	0.05	0.001	0.003	0.01

J: total flux, J_T: partial toluene flux, J_H**:** heptane partial flux

Table 15.4: Separation factor (**α)** and permeate enrichment (Cp).

membrane type	α 40°C	α 55°C	α 70°C	Cp (40°C)	Cp (55°C)	Cp (70°C)
M_{dense}	12	11	10	92%	91%	90%
$M_{dense5tmos}$	9	8	6	90%	86%	85%
M5tmos	14	9	9	93%	90%	90%
M_{10tmos}	12	9	9	92%	90%	90%
M_{20tmos}	12	9	9	92%	90%	90%

4.5.1 Effect of operating temperature on flux and selectivity

Figure (17.4) shows that the selectivity decreases with increasing operating temperature due to the effect of toluene swelling and coupling of heptane molecules with toluene molecules which increased with an increase of operating temperature. In other words, the increase in the flux as a function of temperature is accompanied by a decrease of selectivity. This can be explained by the fact that an increase in the flux of toluene causes an increase in the flux of coupled heptane. In addition, it was found out that the selectivity and separation factor of the membranes (M_{5TMOS},M_{10TMOS}, M_{20TMOS}) is higher than $M_{dense5TMOS}$ for each temperature.

Figure (18.4) shows that the real flux increased with the increase of feed operating temperature for all membranes (the morphology of all membrnes are almost dense), in addition the flux of the homogeneous dense membranes is higher than hybrid silica-PEI membranes at each temperature. It was found from SEM views (chapter 3) that silica-membranes prepared by phase inversion have a denser structure than homgenous asymmetric membrane. Hence we will use the normalized flux for the 2 types of silica-membranes which were prepared by (2 steps mechanism ($M_{dense5TMOS}$) and phase inversion (M_{5TMOS}, M_{10TMOS}, M_{20TMOS})). From figure18.4, it was found out that the normalized flux of the membranes (M_{5TMOS},M_{10TMOS}, M_{20TMOS}) is higher than $M_{dense5TMOS}$.

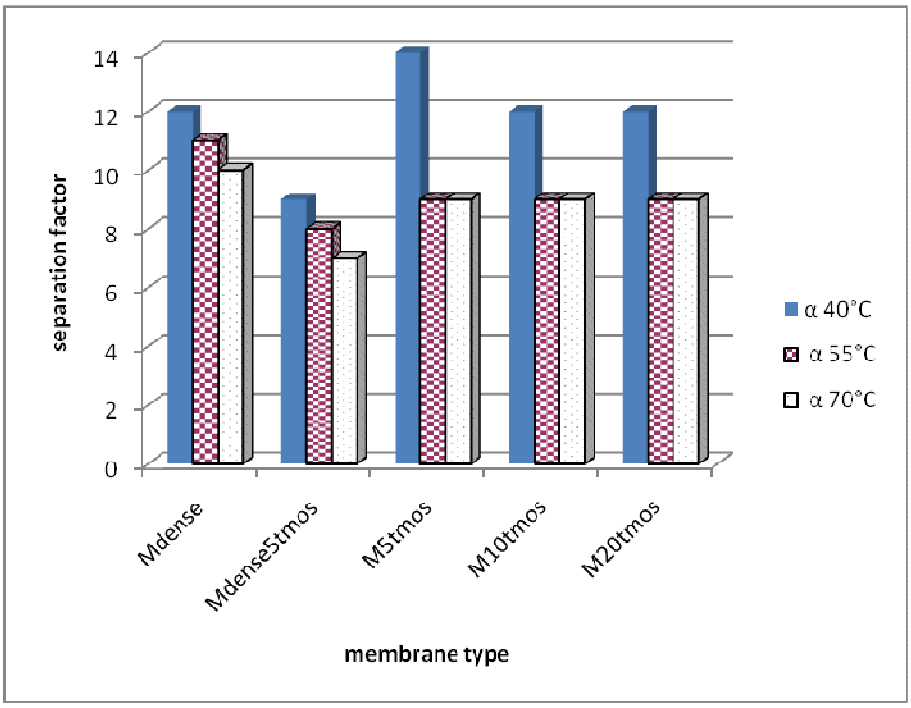

b . Effect of TMOS content and temperature on separation factor

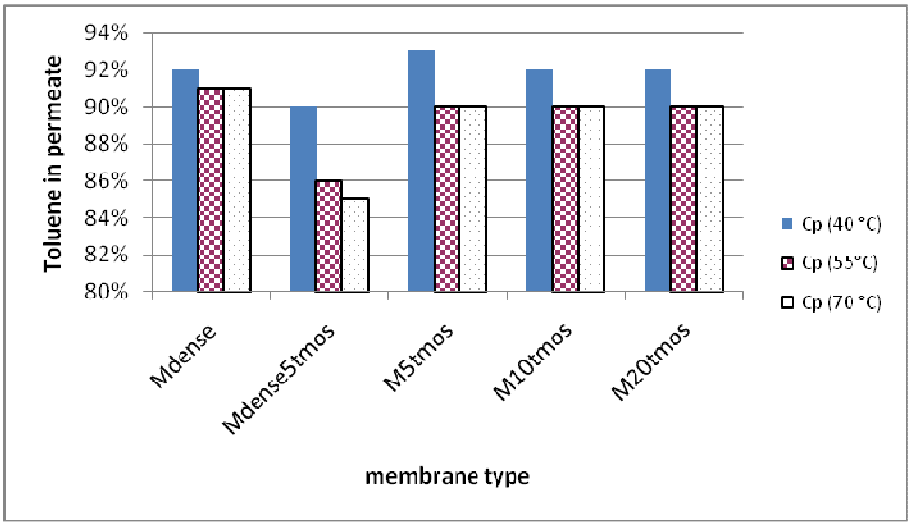

a. Effect of TMOS content and temperature on enrichment.

Figure17.4: Effect of TMOS on membrane performance.

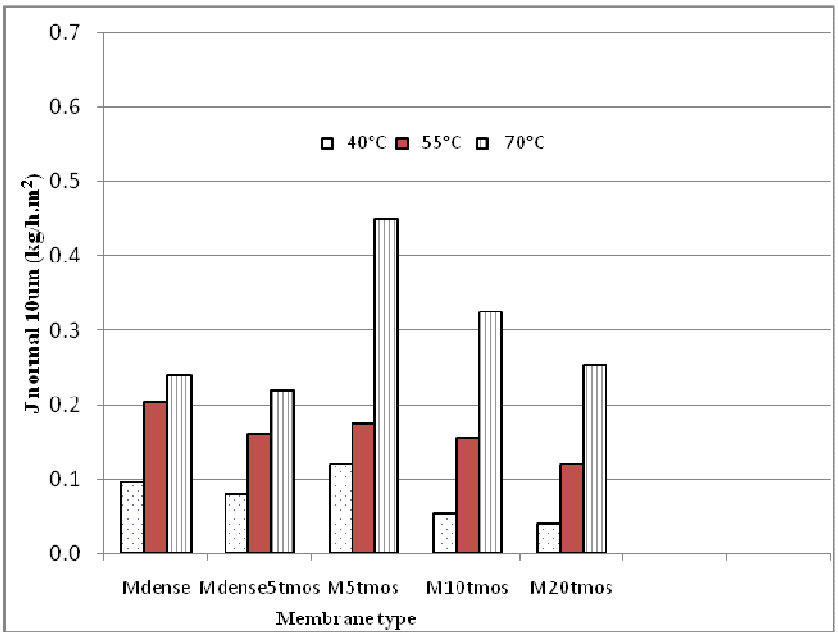

b . Effect of TMOS content on normalized flux.

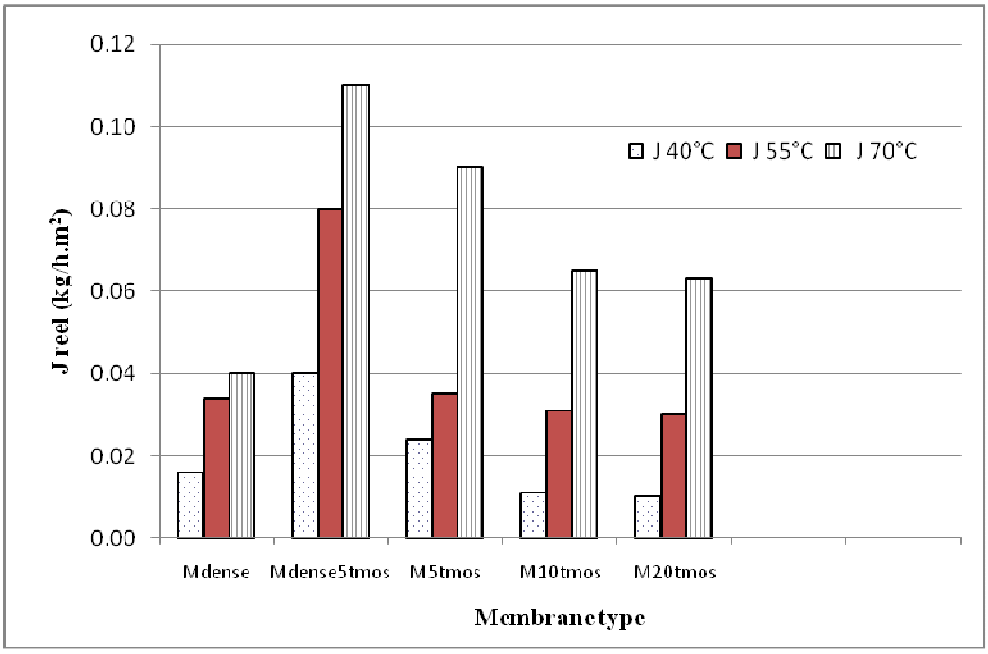

a . Effect of TMOS content on total real flux

Figure 18.4: Effect of operating temperature and membrane type on flux.

The total flux follows an Arrhenius law, as shown by the curve J = f Ln (1 / T) shown on Fig. 19.4 (change in Logarithm of molar flux(J_M) flows according to 1 / T for a hybrid

membrane (20% TMOS)). The resulting curve is a straight line of the form y = a x + b which shows that the flux follows Arrhenius law. In effect $J = J_0 \exp\left(\frac{-Ea}{RT}\right)$ $\leftrightarrow LN(J) - [LN(J]_0) - \frac{Ea}{R} \times \frac{1}{T}$ therefore the slope of this curve is just $-\frac{Ea}{R}$. Hence, the overall activation energies (*E*t) characterizing the temperature dependencies of the permeation fluxes, can be obtained from the slopes of the straight lines in Fig. 19.4.

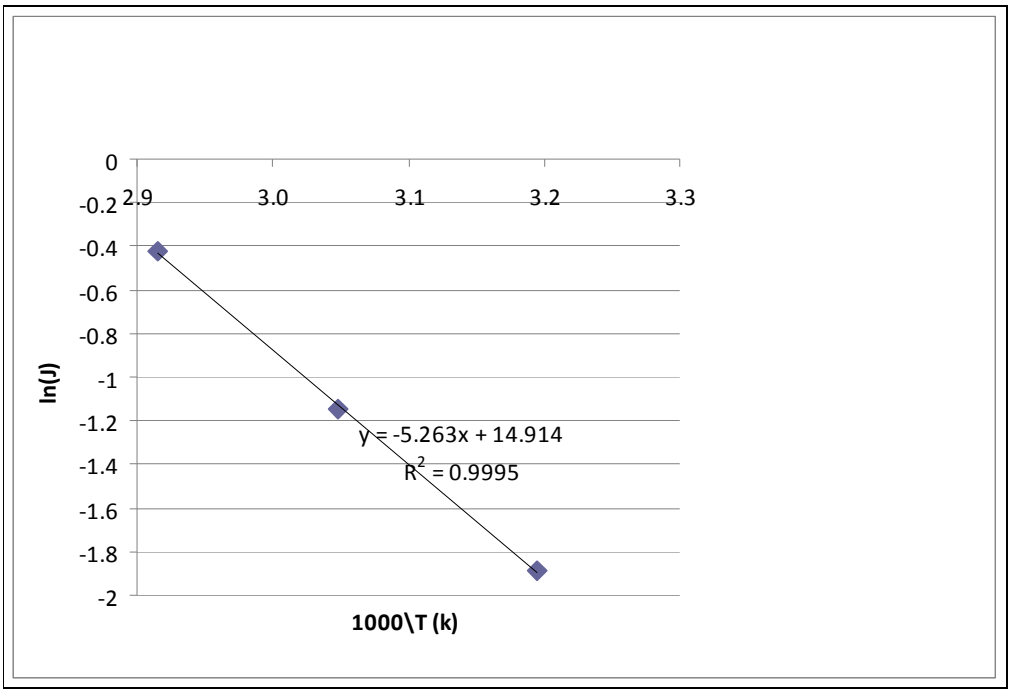

Figure 19.4: Plot of molar ln (j)/ versus 1 / T for a hybrid dense membrane (20% TMOS).

4.5.2 Effect of TMOS content on flux, swelling and selectivity

- **Effect on of TMOS content on flux.**

In literature, it was found out that silica increases the permeability of rigid structures (PMDA+ODA)

In our case two assumptions are possible:

1) Either the silica is mainly fixed on the rigid part of our polymer: then it should lead to an increase in the flux due to an increase in free volume between polymer chains.
2) or the silica is attached to the aliphatic part of the polymer and the silica is surrounded to the flexible aliphatic part which in that case is an impermeable material. Thus, this should reduce the permeability of PEI membranes.

According to Fig. 18.4. it was found that the flux is decreasing with an increase amount of TMOS in all types of PEI membranes for each temperature. Hence, we can conclude that the silica was fixed rather on the flexible aliphatic part of our PEI.

- **Effect of TMOS content in the swelling of the membrane(liquid sorption)** .

The decrease in flux with increasing the amount of TMOS can be due to a decrease in sorption or to a decrease of the diffusion due to tortuosity effect or to both. To study the effect of sorption on TMOS, a swelling test in toluene was made for membranes at different contents of silica.The results presented in Fig.(20.4) show that the amount of swelling decreases with the increase of silica incorporation.Therefore, the decrease of permeate flux with the increasing rate of TMOS is partly due to the reduction of swelling of the membrane.

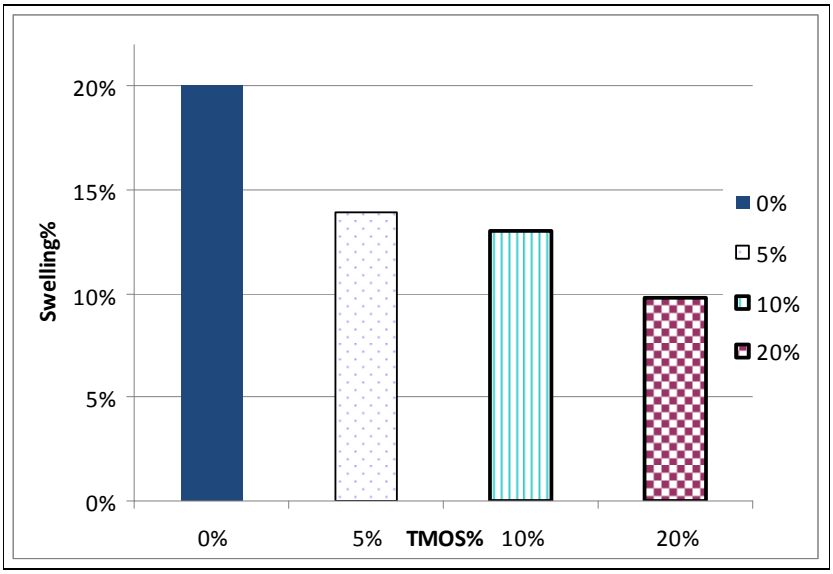

Figure 20.4: Effect of TMOS% on swelling% of silica-PEI membranes.

- **Effect of TMOS content on the selectivity**

According to figure (17.4) it was found out that silica increases slightly the selectivity especially in comparing different hybrid membranes with homogeneous dense membrane (reference) at 40°C. This increase in selectivity is due to the decrease in flux of toluene and consequently a decrease in the flux coupled with heptane. Morever, at 55°, 70°C the selectivity of homogeneous dense membrane (reference) increases slightly in comparison with different hybrid membranes. This increase in selectivity may be due to an increase of the swelling of toluene (swelling%) from 50 % to 90 % at 20°C, 60°C respectively with the

homogeneous dense membrane. Table (16.4) shows review table results of PEI membranes with pervaporation (PV).

Table 16.4 : Review table results of PEI membranes with pervaporation (PV)

Membrane	thickness µm	α 40°C	P α 45°C	SEM
		50%Toluene-Heptane	50 % Water/Ethanol	
Kapton dense	20		38	
M_{dense}	40-60 30	12	4 4	
$M_{1\ (30PAA)}$	40	13		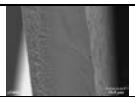
$M_{1\ (30PAA)}$	100	11		
$M_{7\ (25PAA+5w)}$	150	1.3		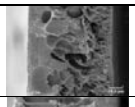
$M_{8\ (25PAA+15w)}$	40	1.8		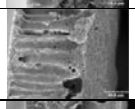
$M_{13(25PAA)}$	100	2.8		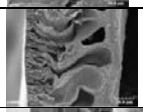
$M_{as(25PAA)}$	60		4	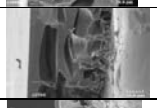
$M_{(25PAA)}$	40		475 with feed 95% n-butanol /water 26 with feed 95% ethanol /water	

Conclusions and Recommendations for Future work

I. Separation properties of PEI membranes with pervaporation

The separation properties of the dense and asymmetric PEI 0.4Jeff were studied by pervaporation with the water/ethanol mixtures, and the recorded permselectivity could be rationalized with the membrane swelling properties which were much higher than for Kapton™ for all the considered solvents. As for the dense membranes, it was first shown that the asymmetric membranes exhibited also molecular separation properties, leading to the selective water permeation from ethanol mixtures. It means that these asymmetric membranes combining rubbery alkoxy and rigid aromatic blocks in the polymer structure had a tight top layer. Compared to the dense membranes, the PEIs show obviously a much higher flux, but also good selectivity.

The most interesting part of this work was the successful preparation of asymmetric membranes by phase inversion from polyether-imide, because these membranes comprise a top dense layer almost free of defects. This was demonstrated by the results obtained in the pervaporation of toluene/heptane mixtures and water/ethanol mixtures (feed=50 wt.%), because the selectivity of the asymmetric membranes tested (Cpermeate: 70-80% for T/H, 80% for W/E) very close to the selectivity of dense films prepared conventionally by evaporation (Cpermeate: 90% for T/H, 80% for W/E). Thus, for most of the asymmetric PEI membranes prepared by optimized preparation methods, it has been possible to verify the expected molecular selectivity. Furthermore, the asymmetric membrane structures had increased dramatically the mass transfer flux.

The pervaporation performances of asymmetric polyetherimide membranes for breaking the ethanol/water azeotrope and the dehydration of n-butanol were investigated. It has been shown that the asymmetric polyetherimide membranes are selective to water permeation and that the membrane performances are strongly influenced by operating temperature and alcohol molecular size.

In the case of water-ethanol mixtures, the goal was double: first, ensuring that asymmetric membranes based PEI prepared by phase inversion can achieve molecular separation as in the previous case of Toluene- Heptane mixtures; secondly, that the selectivity observed corresponds to that of a hydrophilic membrane, since it is the goal for the nanofiltration of aqueous solutions. On both issues, the results have brought positive responses. The asymmetric and dense PEI membranes showed good water selectivity for all concentrations of water-ethanol mixtures used as a feed (eg: Cpermeate: 60-70 % of water

from a feed of 20 wt% water and 80 wt% EtOH at 30 °C). Molecular selectivity is also achieved with a feed of azeotropic composition of ethanol (5wt.% water, 95 wt% EtOH at 30°C) the corresponding permeate enrichment 57% water and also with a feed of butanol (5wt.% water, 95 wt% BuOH at 30°C) the corresponding permeate enrichment 98 % water, which shows the molecular separation and the hydrophilic nature of PEI.

Thanks to pervaporation, it was shown that asymmetric PEI membranes could reach a high level of selectivity with a much higher flux than the one reached with dense membranes. It turns out that these membranes are promising candidates for nanofiltration of organic water mixtures.

II. Separation properties of Hybrid silica-PEI membranes with pervaporation

The pervaporation of Toluene-Heptane mixture was used as a feed to test the performanc of the hybrid silica- PEI membranes. The experiments were conducted on dense and asymmetric hybrid membranes (PEI/SiO_2) with different content of silica (5%, 10% and 20%) and at different temperatures (40 °C, 55 °C and 70 °C).

The SEM images of several membranes prepared by phase inversion have shown that they revealed a fully dense structure and not an asymmetric one as expected. This shows that the incorporation of silica precursors by the sol-gel has changed the results of the phase inversion process. It means that SiO_2 particles formed in situ decrease the solvent exchange moblity, so the polymer solution system seems to be shifted from instantaneous demixing to delayed demixing process.

The all membranes studied are permselective to toluene (Cp=90%, feed 50% T/H). The permeate flux increases with increasing temperature. However, the increase in flux is accompanied by a small decrease in selectivity (not exceeding 2%). This can be explained by the fact that toluene, whose flux increases, induced a higher heptane flux. The permeate flux decreases with increase in the rate of silica. This result is contrary to the results obtained in other studies with fully aromatic PI films (PMDA-ODA), where the silica had remarkably increased flux by increasing the free volume. It was therefore possible to conclude that in our case, silica was fixed on the aliphatic part of the polymer.

Hence, future work in our laboratory intends to find a way to fix the silica on the aromatic part of PEI polymer to obtain the desired effect which is the increase of permeability. Then, the suitable operating conditions of phase inversion with the sol-gel should be determined for preparation of successful asymmetric silica- PEI membranes. The suggestions is to speed up the solvent/nonsolvent exchanges such as: Increase of immersion bath temperature (i.e: 16, 20°C) and changing PAA solution composition.

References

1. W. Guo, T. Chung, T. Matsuura, R. Wang, Y. Liu, Pervaporation study of water and tert-butanol mixtures, J. Appl. Polym. Sci. 91 (2004) 4082-4090.
2. C. Yeom, S. Lee, J. Lee, Pervaporative permeations of homologous series of alcohol aqueous mixtures through a hydrophilic membrane, J. Appl. Polym. Sci. 79 (2001) 703-713.
3. X. Qiao, T. Chunga, K. Pramoda, Fabrication and characterization of BTDA-TDI/MDI (P84) co-polyimide membranes for the pervaporation dehydration of isopropanol, J. Membr. Sci. 264 (2005) 176–189.
4. H. Yanagishita, C. Maejima, D. Kitamoto, T. Nakane, Preparation of asymmetric polyimide membrane for water/ethanol separation in pervaporation by phase inversion process, J. Membr. Sci. 86 (1994) 231-240.
5. A. Verkerk, P. Male, M. Vorstman, J. Keurentjes, Description of dehydration performance of amorphous silica pervaporation membranes, J. Membr. Sci. 193 (2001) 227-238.
6. J. Elshof, C. Abadal, J. Sekulic, S. Chowdhury, D. Blank, Transport mechanisms of water and organic solvents through microporous silica in the pervaporation of binary liquids, Micropor. Mesopor. Mater. 65 (2003) 197-208.
7. X. Yexin, C. Cuixian and L. Jiding**,** Experimental study on physical properties and pervaporation performances of polyimide membranes, Chem. Eng. Sci. 62 (2007) 2466-2473.
8. X. Yexin, C. Chen, J. Li, Sorption and diffusion characteristics of water vapor in dense polyimide membranes**,** J. Chem. and Eng. Data . 52 (2007) 2146-2152.
9. S. Huang, W. Hung, D. Liaw, C. Lo, ,W. Chao,C. Hu,C. Li, J. Lai **,** Interfacially polymerized thin-film composite polyamide membranes: Effects of annealing processes on pervaporative dehydration of aqueous alcohol solutions**,** Sep. Puri. Techn. 72 (2010) 40-47.
10. P. Chapman, T. Oliveira, A. Livingston and K. Li, Membranes for the dehydration of solvents by pervaporation, J. Membr. Sci. 318 (2008) 5–37.
11. W. Qiu, M. Kosuri, F. Zhou and W. Koros, Dehydration of ethanol–water mixtures using asymmetric hollow fiber membranes from commercial polyimides, J. Membr. Sci. 327 (2009) 96–103.
12. S. Semenova, H. Ohya and K. Soontarapa, Hydrophilic membranes for pervaporation: an analytical review, Desalination 110 (1997) 251–286.

13. M. Zhiming, C.Yiming, J. Xingming, K. Guodong, Z. Meiqing and Y. Quan**,** Dehydration of isopropanol–water mixtures using a novel cellulose membrane prepared from cellulose/N-methylmorpholine-N-oxide/H_2O solution**,** Sep. Puri. Techn. 72 (2010) 28-33.
14. H. Yanagishita, D. Kitamoto, K. Haraya, T. Nakane, T. Okada, H. Matsuda, Y. Idemoto and N. Koura, Separation performance of polyimide composite membrane prepared by dip coating process, J. Membr. Sci. 188 (2001) 165-172.
15. H.Yanagisita, D. Kitamoto, K. Haraya, T. Nakane, T. Tsuchiya, N. Koura, Preparation and pervaporation performance of polyimide composite membrane by vapor deposition and polymerization (VDP) , J. Membr. Sci. 136 (1997) 121-126.
16. K. Okamoto, N. Tanihara, H. Watanabe, K. Tanaka, H. Kita, A. Nakamura, Y. Kusuki, K. Nakagawa, Vapor permeation and pervaporation separation of water-ethanol mixtures through polyimide membranes, J. Membr. Sci. 68 (1992) 53-63.
17. K. Jeong, L. Kew and K. Youl, Pervaporation separation of water from ethanol through polyimide composite membranes, J. Membr. Sci. 169 (2000) 81-93.
18. Q. Xiangyi, T. Chung and K. Pramoda, Fabrication and characterization of BTDA-TDI/MDI (P84) co-polyimide membranes for the pervaporation dehydration of isopropanol , J. Membr. Sci. 264 (2005) 176-189.
19. R. Huang, X. Feng, Resistance model approach to asymmetric polyetherimide membranes for pervaporation of isopropanol/water mixtures, J. Membr. Sci. 84 (1993) 15-27.
20. R. Huang, X. Feng, Dehydration of isopropanol by pervaporation using aromatic polyetherimide membranes, Sep. Sci. Technol. 28 (1993) 2035-2048.
21. M. Xiangyi, T. Chung, W. Guo, T. Matsuura and M. Teoh, Dehydration of isopropanol and its comparison with dehydration of butanol isomers from thermodynamic and molecular aspects, J. Membr. Sci. 252 (2005) 37-49.
22. W.Guo and T. Chung, Study and characterization of the hysteresis behavior of polyimide membranes in the thermal cycle process of pervaporation separation, J. Membr. Sci. 253 (2005)13-22.
23. H. Yanagishita, D. Kitamoto, T. Ikegami**,** Preparation of photo-induced graft filling polymerized membranes for pervaporation using polyimide with benzophenone structure, J. Membr. Sci. 203 (2002) 191-199.

24. K. Robert, P. Damian,W. Charles,M. Henk and F. Jaap, High-temperature pervaporation performance of ceramic-supported polyimide membranes in the dehydration of alcohols, J. Membr. Sci. 319 (2008) 126-132.
25. J. Sekuli, J. Elshof, D. Blank, Separation mechanism in dehydration of water/organic binary liquids by pervaporation through microporous silica, J. Membr. Sci. 254 (2005) 267–274.
26. A. Elsayed, F. Xianshe, Use of pervaporation to separate butanol from dilute aqueous solutions Effects of operating conditions and concentration polarization, J. Membr. Sci. 323 (2008) 428–435.
27. D. Roizard, A. Nilly, and P. Lochon, Preparation and study of crosslinked polyurethane films to fractionate toluene-n-heptane mixtures by pervaporation, Sep. Puri. Techn. 22 and 23 (2001) 45-52.

Chapter (5)

Nanofiltration (NF) results and discussion

Table of Contents chapter (5)

Nanofiltration (NF) results and discussion

Table of Contents chapter (5) Nanofiltration (NF) results and discussion

Nanofiltration (NF) results and discussion 279

5.1 Results with PEI-NF.....279

5.1.1 Hydraulic flux of dense membranes.....279

5.1.2 Hydraulic flux of asymmetric membranes.....282

5.2 Separation of aqueous polluted solutions by NF-PEI membranes.....287

5.2.1 Nanofiltration of aqueous inorganic feed solutions with asymmetric PEI membrane 287

5.2.2 Nanofiltration of aqueous organic solutions with asymmetric PEI membrane.....292

Conclusions and Recommendations for Future work.....321

References.....322

General Conclusions and Perspectives.....327

Chapter (5)

Nanofiltration (NF) results and discussion

Nanofiltration (NF) has been increasingly considered as a reliable and affordable technique for the production of high quality water with a high productivity. Thus, the understanding on nanofiltration especially the rejection of uncharged solutes, charged solutes and mixture of solutes is crucial for its application in pure water treatment. Due to this reason, NF membranes are now widely applied in treatment of wastewater.

Nanofiltration (NF) of diluted aqueous organic pollutants appears to be a promising separation tool in chemical industry. In this work, rejection characteristics and permeation of different classes of aqueous organic and inorganic solutions through PEI membranes were measured. As a rule, the pure water flux has been investigated to determine the hydraulic permeability and the membrane properties such as molecular weigh cut-off (MWCO) and solutes rejection have been characterized.

Although separation models and techniques such as pervaporation which is described in the preceding chapter permit characterization of dense-film transport properties of asymmetric membranes, a need exists for improved characterization of the transport behavior of asymmetric membranes under NF conditions.

The following chapter presents information linked to the characterization of the performances of asymmetric PEI membranes. Firstly, the characteristics of the NF set-up system are described; this set-up is assembled with pump, reservoir, fluid circulation, cell permeation and analytical technique (TOC). Secondly, PEI membrane sheets prepared by wet phase inversion are applied to pure water as a feed at different operating pressures to evaluate their performances and flexibility of operation. Finally, rejection characteristics of aqueous solutions (organic, inorganic) by asymmetric PEI membrane sheets are determined.

5.1 Results with PEI-NF

5.1.1 Hydraulic flux of dense membranes

In this part PEI and Kapton^{TM} (PI) dense membranes are tested with feed of pure water, to study the effect of soft block in PEI and to test maximum limiting pressure that the membrane can withstand before being damaged. It was found out that at low pressure and with a pressure up to 15 bar with the 2 types of membranes there is no detectable permeate

flow after one day at each pressure. The permeation starts when the inlet pressure reaches 20 bar (0.7 kg/m^2.h) for dense PEI membrane while for Kapton^{TM} (PI) starts only at 30 bar (0.6 kg/m^2.h). Moreover, the thickness of the dense PEI membrane is 2 times higher than Kapton^{TM} membrane, the water permeation starts with dense PEI membrane at a pressure which is lower than Kapton^{TM} membrane. This is due to the effect of soft block in PEI. The results obtained are presented in Fig. 1.5 and Table 1.5.

Table 1.5: NF test results with dense membranes at 40 bar (active membrane area 41 cm^2).

Membrane type	Thickness (µm)	J (kg/m^2.h)	Jn (10µ kg/m^2.h)	Membrane permeance not normalized (kg/h.m^2.bar)
Dense Kapton(PI)	20	1	2	1/40
Dense PEI	40	1.5	6	1.5/40

From table (1.5) it was obvious that the normalized flux (Jn) of PEI dense membrane is three times greater than Kapton^{TM} (PI), from the sorption test it was found the same relation (swelling of PEI dense membrane is three times greater than Kapton^{TM} membrane), as explained before due to the effect of soft block in PEI membrane. The two types of membranes show a good mechanical resistance (no breakage) against applied pressure up to 40 bar.

Figure 1.5 shows the permeate flux as a function of applied pressure for pure water as a feed. Clearly, the permeate water flux was significantly increased with increasing operating pressure. It is obvious that the real flux (J) of PEI dense membrane is better than the Kapton^{TM} flux. In addition, the membrane permeance is almost stable for the 2 types of membranes.

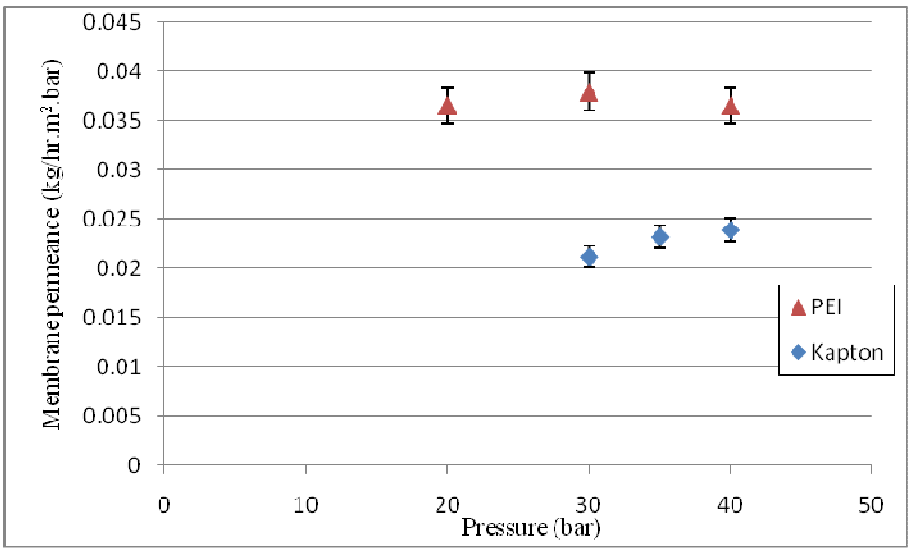

b. Effect of operating pressure on membrane permeance.

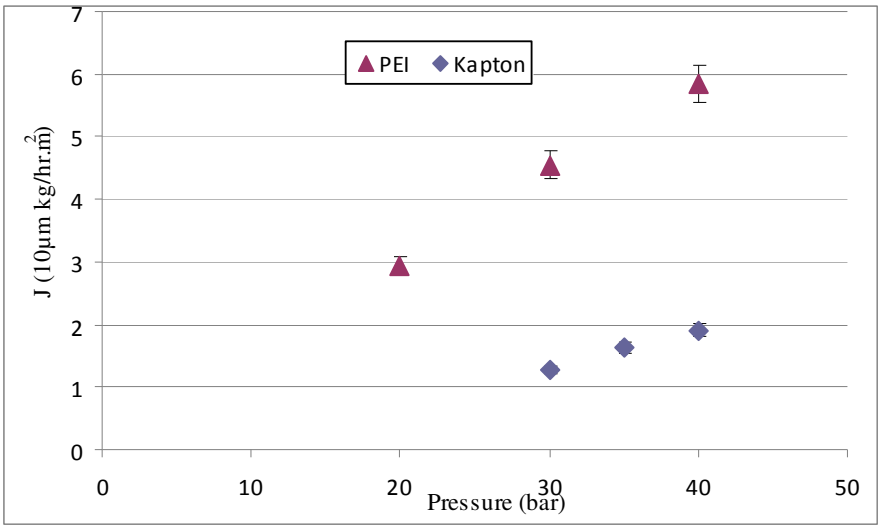

a. Effect of applied pressure on the normalized flux

Figure 1.5: Effect of operating pressure on performance of Kapton™ and PEI dense membranes. Feed: pure water at 30°C±2.

5.1.2 Hydraulic flux of asymmetric membranes

Different PEI membrane sheets prepared by wet phase inversion were tested with pure water as a feed at different operating pressures to evaluate their performances. Furthermore, the membrane samples have been subjected to different operating pressures to define the rupture pressure for each membrane.

The SEM of Kapton^{TM} and PEI membranes prepared by phase inversion is shown in Figs. (2.5:4.5). The results have been summarized in table 2.5 and plotted in Fig. (7.5) which displays the effect of operating pressure on the total flux and membrane permeance of PEI membranes and Kapton^{TM} for active area of membrane =5.4*7.6= 41 cm^2. From SEM it is clear that the supports are highly porous symmetric membranes (MF) while all PEI membranes are highly porous with asymmetric structure and a thin dense layer.

Table 2.5: Nanofiltration results with PEI and Kapton membranes (feed pure water).

Membrane	Total thickness µm	membrane permeance not normalized (kg/h.m^2.bar)	Membrane type
$M_{Kapton(11PAA)}$	100 µm	2600 at 2 bar	porous symmetric MF
$M_{(25PAA)}$	95µm	0.45-0.6(5-20 bar)	Asymmetric NF
$M_{(25PAA+15w)}$	15 µm	10-10.7(5-20 bar)	Asymmetric NF
$M_{(25PAA+20w)}$	140 µm	7.6-8.5 (5-20 bar)	Asymmetric NF
$M_{c(25PAA+ s Kapton)}$	45µm+100µm support	6.7-7(5-20 bar)	Asymmetric NF
$M_{c(25PAA+s15PAA)}$	30µm+50µm support	6.5-7 (5-20 bar)	Asymmetric NF
$M_{c(25PAA+s 20PAA+10w)}$	80µm+80µm support	0.6-1.2(5-20 bar)	Asymmetric NF

Where; s: support type, c: composite membrane, w: water

From table (2.5) it was found that the $M_{Kapton(11PAA)}$ membrane has a high flux at low pressure and the maximum operating pressure is 2 bar (J= 98-4800 kg/h.m^2 at 0 to 2 bar), this is because the Kapton^{TM} membrane is highly porous symmetric membrane (MF) without any dense layer as shown in Fig. (2.5).

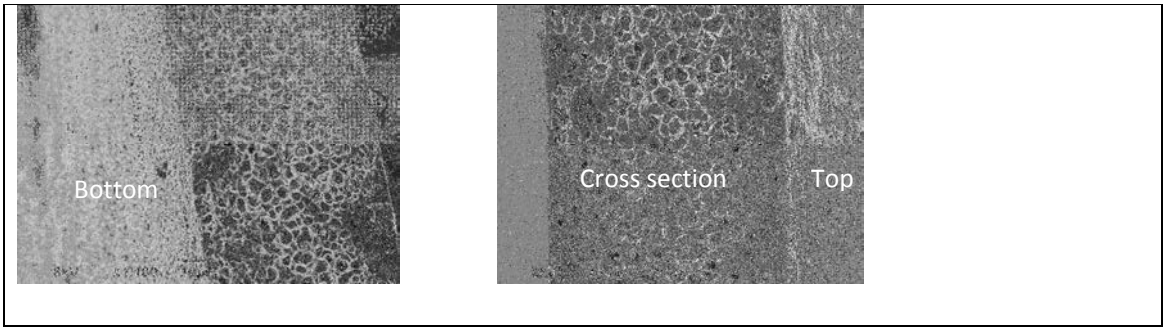

Figure 2.5: Cross section view of porous symmetric Kapton membrane.

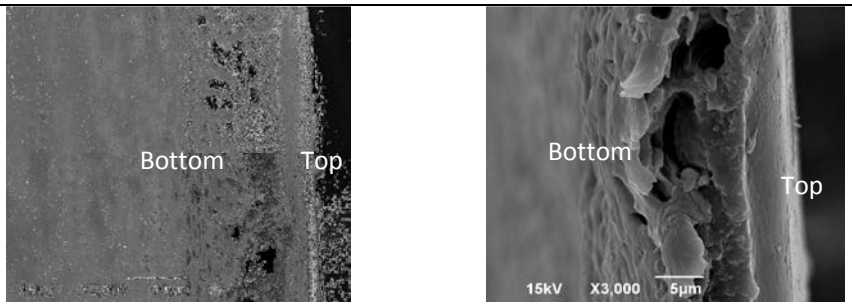

c. Cross section of asymmetric PEI membrane M (25paa+15w).

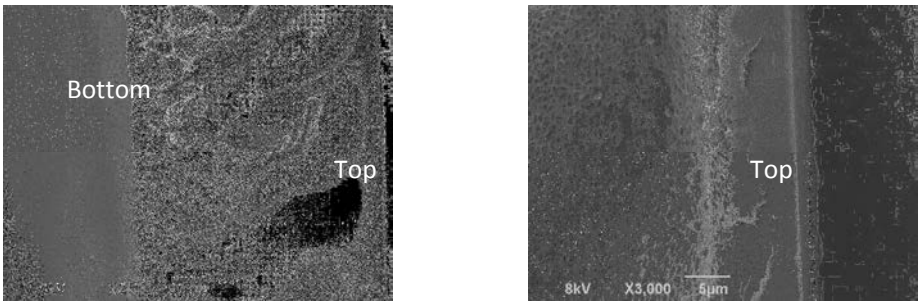

b. Cross section of asymmetric PEI membrane M (25paa+20w) .

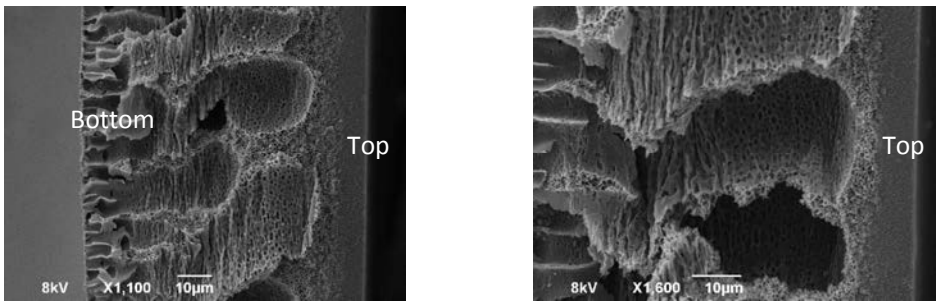

a. Cross section view of asymmetric PEI membrane M (25PAA) .

Figure 3.5: Cross section view of homogenous PEI asymmetric membrane.

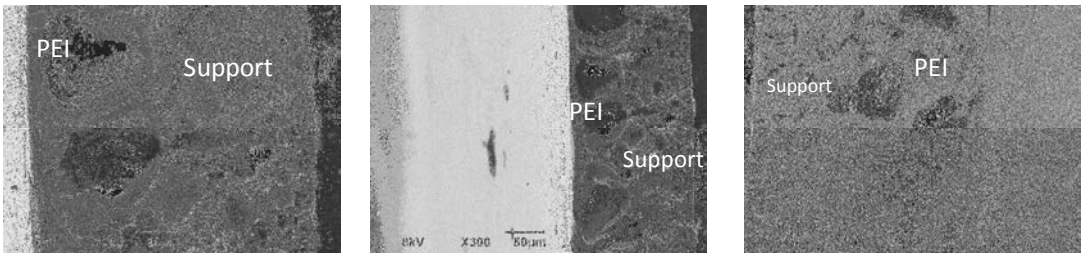

Before testing After testing

c. Cross section view of asymmetric PEI membrane $M_{c\ (25PAA+s\ 20PAA+10w)}$.

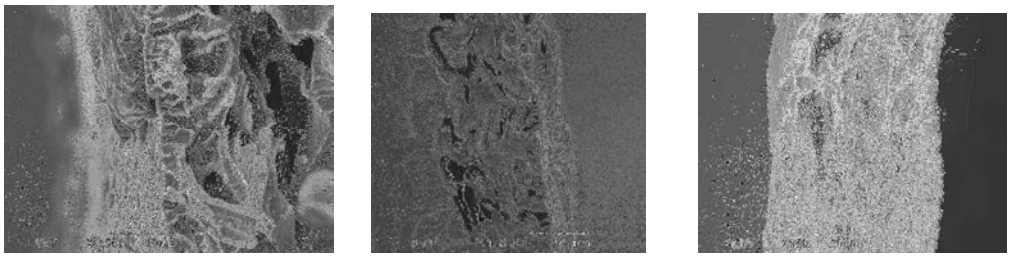

$Mc_{(25PAA+s15PAA)}$ $Mc_{(25PAA+s15PAA)}$ Support $M_{(s15PAA)}$

b. Cross section view of asymmetric PEI membrane $M_{c(25PAA+s15PAA)}$.

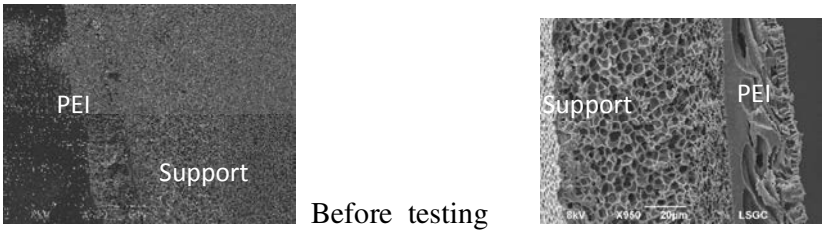

Before testing After testing

a. Cross section view of asymmetric PEI $M_{c\ (25PAA+s\ Kapton)}$ membrane.

Figure 4.5: Cross sections view of composite PEI asymmetric membranes.

Furthermore, it was obvious that from Fig. (5,a .5) the total water flux increased with increasing the applied pressure while the hydraulic permeability (membrane permeance) coefficient is not stable and varied considerably with operating pressure. The presence of

porous sublayer in asymmetric membranes with large macrovoids or finger like structure can induce the compaction of polymeric membranes pores with increasing operating pressure; hence it can explain the observed reduction of flux upon pressure increase, so the reduction of membrane permeance as shown in Fig. (5 b.5) for asymmetric PEI membranes $M_{(25PAA+15w)}$, $M_{(25PAA+20w)}$, $M_{(25PAA+S\ Kapton)}$ and $M_{c(25PAA+s20paa+10w)}$. Asymmetric PEI membranes $M_{(25PAA+s15PAA)}$ and $M_{(25PAA)}$ have almost a constant membrane permeance with change of operating pressure. In addition, significant membrane permeance declines has been observed, the asymmetric PEI $M_{(25PAA+15w)}$ membrane showed a greater membrane permeance decline than the $M_{(25PAA+20w)}$ or the others membranes in sequence:

$M_{(25PAA+15w)}>M_{(25PAA+20w)}>M_{c(25PAA+sKapton)}>M_{c(25PAA+s20PAA+10w)}>M_{c(25PAA+s15PAA}>M_{(25PAA)}$, as shown in Fig.(5b.5).

From Fig.(5.5) it was found out that the flux and membrane permeance decrease with increasing thickness of active dense layer which depends on membrane type which in sequence (average thickness of active dense layer of $M_{(25paa)(7\mu m)} > Mc_{(25paa+s20paa+10w)\ (6\mu m)} > Mc_{(25paa+s15paa)\ (5\mu m)} > M_{c(25paa+Kapton)(4\mu m)} > M_{(25paa+20w)\ (3\mu m)} > M_{(25paa+15w)\ (1\mu m)}$) while the active porous layer has a very small effect on membrane performance compared to the dense layer.

From this result it is clear now that the thickness of the active dense layer plays a key role on asymmetric PEI membrane permeate flux. The transport rate of a liquid through a membrane is inversely proportional to the membrane thickness. High transport rates are desirable in membrane separation processes for economic reasons; therefore, the PEI membrane should be as thin as possible.

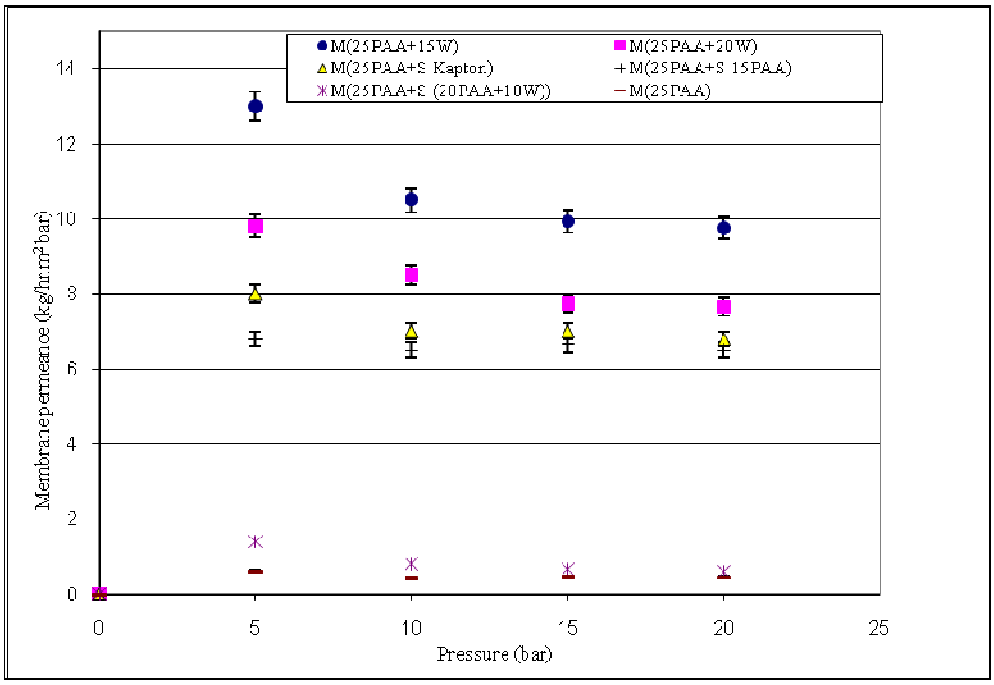

b. Effect of pressure and membrane type on membrane permeance.

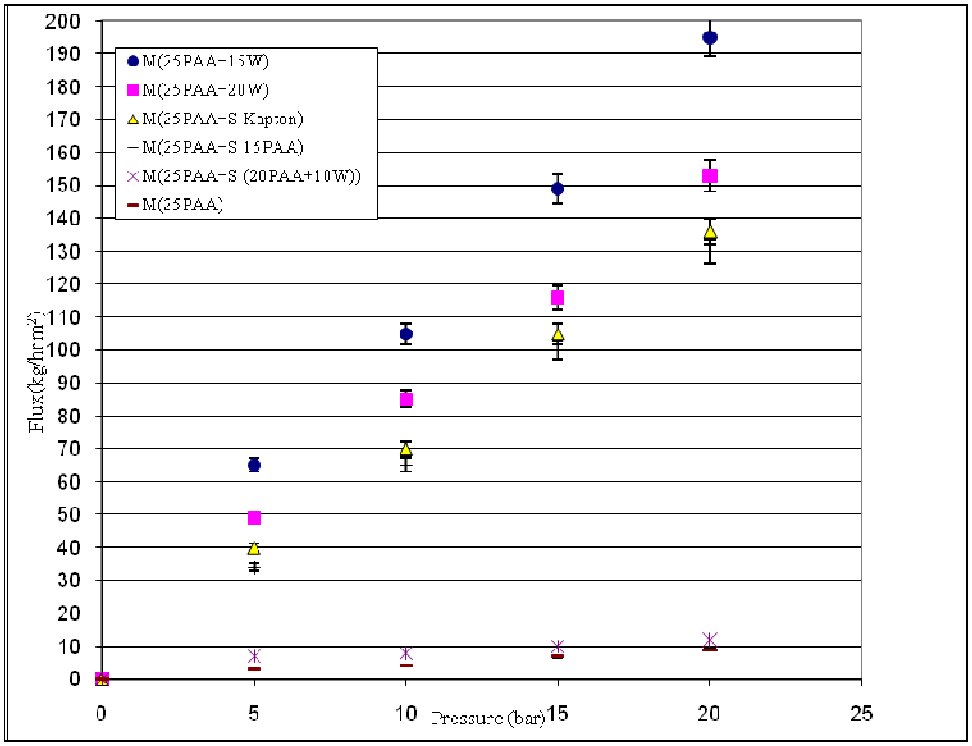

a. Effect of pressure and membrane type on flux

Figure 5.5: Effect of pressure and membrane type on membrane performance (feed pure water).

5.2 Separation of aqueous polluted solutions by NF-PEI membranes

The main objective of this work is the separation of organic from polluted water with high transport rates by NF-PEI membrane, thus the asymmetric membrane will be used for this purpose. When selecting membranes for a separation: the membrane should have good mechanical resistance, high chemical resistance (compatibility), thermal stability, sorption capacity, and good mechanical strength in the solution required to withstand filtration processing conditions. Furthermore, membranes need to be stable in terms of permeability and selectivity under standard operating conditions for extended periods. Membrane stability is vital in solution separations, and is primarily affected by the chemical, mechanical, and thermal properties of the membrane. Rejection experiments of aqueous representative mixtures (organic, inorganic) with asymmetric PEI membrane sheets been carried out at different operating pressures in order to evaluate their performances. The results have been summarized in the following section.

5.2.1 Nanofiltration of aqueous inorganic feed solutions with asymmetric PEI membrane

Separation of aqueous salts feed solutions was investigated using asymmetric PEI $M_{1\,(25PAA+15w)}$ and $M_{2(25PAA+20w)}$ membranes (SEM Fig.6.5). The permeation tests for PEI membranes were carried out at ambient temperature under an operating pressure up to 50 bar and a pump feed with flow rate of 1.3L/min using the NF cell, the feed solution has capacity of 31 L, and with recycling of concentrate and rest of permeat after analysis .The effect of applied pressure and aqueous feed type on membrane performances is presented in Fig. (7.5) and table 4.5. The asymmetric PEI membrane $M1_{(25PAA+15w)}$ is tested for the rejection of aqueous solutions of NaCl at 5, 10 g/L and $M2_{(25PAA+20w)}$ membrane is tested with NaCl at 5 g/L and $CaCl_2$ at 5g/L. As expected, the permeate flux increases with increasing the operating pressure while the membrane permeance is not stable and varied considerably with operating pressure as shown in Fig. (7, b.5) as discussed before. It was found from table 4.5 that the salt rejection was not changed or decreased with increase pressure .

Table 3.5: Physical properties of the salts ions [1-2].

Ion	Ionic radius (nm)	Hydration radius (nm)	Hydration enthalpy (kJ/mol)
Na^+	0.095	0.365	418
Cl^-	0.181	0.347	338
Ca^{2+}	0.1	0.349	1653

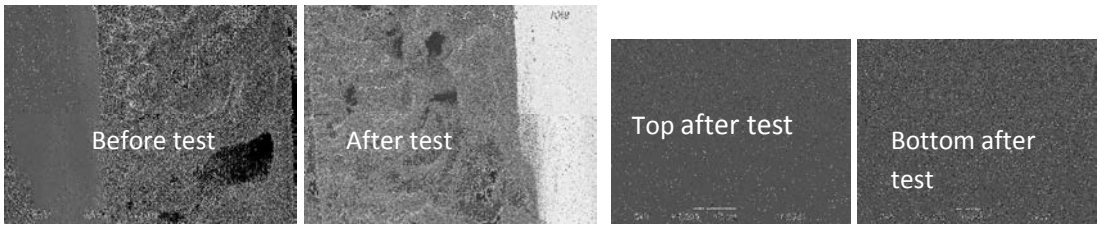

b. Cross section of asymmetric PEI membrane $M_{2(25PAA+20w)}$

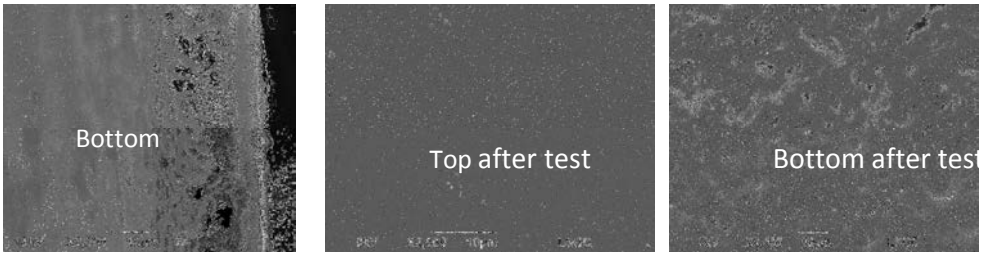

a. Cross section of asymmetric PEI membrane $M_{1(25PAA+15w)}$

Figure 6.5: SEM of asymmetric PEI membranes.

Table 4.5: Results of salt separation with asymmetric PEI membranes, aqueous feed solution at 10 bar, {$M1_{(25PAA+15w)}$, $M2_{(25PAA+20w)}$}.

Salt	Mw (g/mol)	Feed g/L	Rejection %	P_{osm} (bar)	membrane
NaC1	58.5	5 ($85*10^{-3}$ mol.L^{-1})	80 (5-50bar)	2.1	$M1_{(25PAA+15w)}$
		10($171*10^{-3}$ mol.L^{-1})	67 (5-50bar)	4.2	$M1_{(25PAA+15w)}$
		5($85*10^{-3}$ mol.L^{-1})	60 (5-15bar)	2.1	$M2_{(25PAA+20w)}$
$CaCl_2$	147	5 ($34*10^{-3}$ mol.L^{-1})	80 (5-15bar)	0.85	$M2_{(25PAA+20w)}$
NaCl	58.5	0.25-2	50 -70 (13.8 bar)	0.01-0.85	P84 copolyimide
$CaCl_2$	147	0.25-2	80-92 (13.8 bar)	0.04-0.34	asymmetric [3]

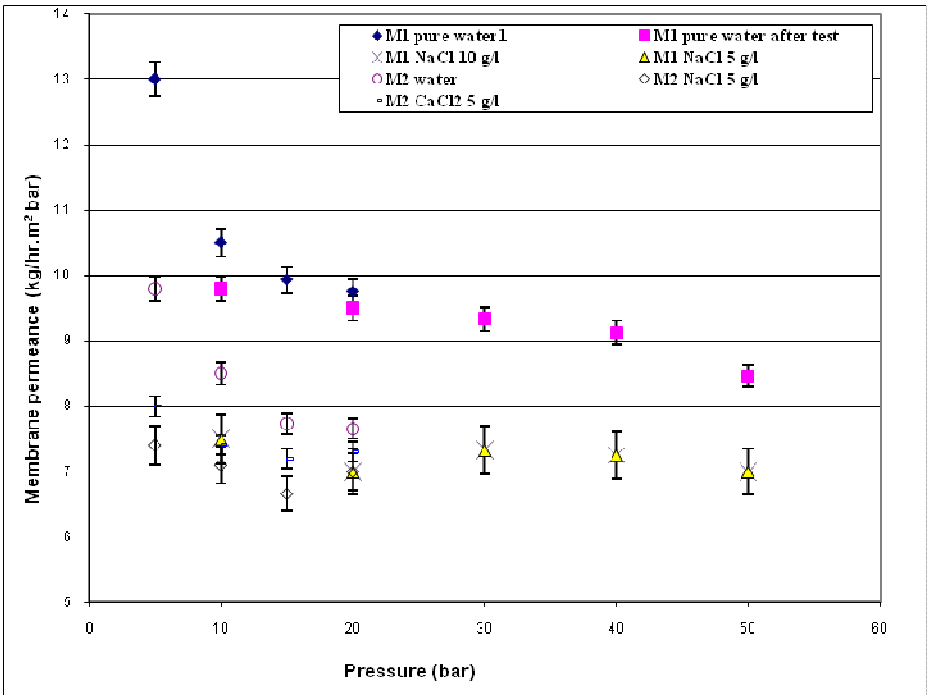

b. Effect of pressure and feed on membrane permeance.

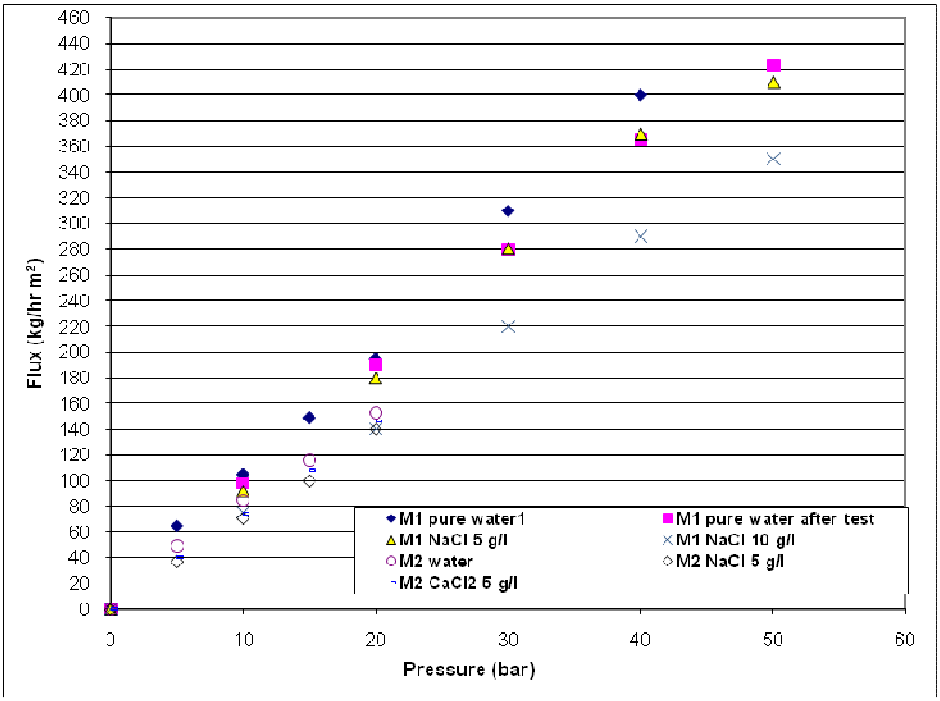

a. Effect of pressure and feed on flux

Figure 7.5: Effect of operating pressure on membrane performances (flux, permeability) {$M1_{(25PAA+15w)}$, $M2_{(25PAA+20w)}$}. The flows between 0-5 bar were not measured.

The salt solution flows between 0-5 bar were not measured. From table 4.5, it was found out that the rejection decreases with the increase of salt (NaCl) in feed concentration by using the PEI asymmetric membrane $M1_{(25PAA+15w)}$. The decrease in salt rejection with increasing salt concentration is consistent with the Donnan exclusion model [4]. The rejection of $CaCl_2$ is higher than NaC1 by using the asymmetric PEI membrane $M2_{(25PAA+20w)}$. The rejection sequence of salts depends on the charge of the ions ($CaCl_2$ > NaCl). It is known that the rejection of NaCl and $CaCl_2$ is governed by both size exclusion and electrostatic exclusion [5-3].

From the original flux and membrane permeance vs. applied pressure data (Fig.7.5), it was found, when comparing these results to the pure water permeabilities, that the salt concentration has an influence on decreasing the permeate flux. The salts solution showed a lower flux than pure water flux, The explanations of these results are:

1- The shrinking of the skin layer resulting from either reduction of water activity, and thus, lower swelling; indeed, the swelling is decreased by 47% due to the addition of dissolved salt (sorption of pure water 15%, sorption of NaCl 500ppm 7.5%),
2- Effect resulting from reduction of the net driving force for water due to the osmotic pressure of the feed.

So the effective transmembrane pressure is reduced which lowers flux. Mark [5] reported that the solvent passes through the membrane at a faster rate than the passage of dissolved salts in solution. Hence, the difference of passage rate results in solvent-salts separation.

Our results is in agreement also with Fraeger et al. [6] who studied nanofiltration (NF) of aqueous inorganic mixtures using the FILMTEC™ NF-200B aromatic polyamide membrane, and reported flux of pure water, 4% NaCl and 9% NaCl are 82, 25, 10 kg/h.m^2 respectively while rejection of 4% NaCl, 9% NaCl are 36%, 25 % respectively.

The osmotic pressure (P_{osm}) of a mixture solution in table 4.5 is calculated by the following equation:

$$P_{osm} = R\,(T+273)\Sigma(mi)$$

Where P_{osm} is osmotic pressure in bar, R is the universal gas constant (0.082 L*atm/mol °K), T is the temperature in °C, and Σ(mi) is the sum of molar concentration (molarity) of all constituents in a solution.

It is known that NF is used to achieve a separation of salts and organic compounds from water. Thus, the asymmetric PEI membrane investigated here is NF type. Hence, the asymmetric PEI membrane will be tested in the next section with aqueous organic solutions.

5.2.2 Nanofiltration of aqueous organic solutions with asymmetric PEI membrane

The nanofiltration of aqueous organic solutions through an asymmetric PEI membrane was investigated. Various types of organic molecules were selected to cover a large range of molecular weight and $\log_{ow}$ for testing with the asymmetric PEI and Kapton^{TM} membranes. The effects of solute molecular weights and hydrophobicity were investigated. Generally, organic rejection, often used to describe the rejection efficiency of NF membranes, was found to be appropriate to indicate the potential rejection of organic pollutants. The permeation tests for PEI membranes were carried out at ambient temperature under an operating pressure up to 30 bar and a pump feed with flow rate of 1.3L/min using the NF cell, the feed solution has capacity of 31 L, and with recycling of concentrate and rest of permeat after analysis.

5.2.2.1 Nanofiltration with aqueous organic of 50 and 80 wt. % H_2O/ EtOH mixtures

Separation of aqueous organic (50-80wt.% of H_2O/ EtOH) feed solutions was investigated using asymmetric PEI $Mc_{(25PAA+ s15PAA)}$ and $M_{(20PAA+25w)}$ membranes. The effects of operating pressure and feed on membrane performance are presented in Figs. (8.5-9.5) and table 5.5. With the two asymmetric PEI membranes (Table 5.5) the ethanol rejection is not high (40-50%); This is because the coupling of water and ethanol molecules. Ethanol is a very small, uncharged molecule (MW 48 g/mol), so it is very difficult to reject by size exclusion and it cannot be rejected by charge exclusion. Indeed, the diameter of ethanol (0.34 nm) and the diameter of water (0.21 nm) are close. Previous studies [7,8] have shown that the rejections for uncharged small molecules such as urea (MW 60 g/mol) are even lower (rejection=16% [9]). The flux of $M_{(20PAA+25w)}$ is very low and it may be the effect of big thickness of spongy like strucure (200µ).

Table 5.5: Effect of operating pressure and feed on membrane performances.

Membrane	Feed H_2O/ EtOH	Flux (kg/m2 h)	Pe(kg/h.m^2 bar)	Rejection %
$Mc_{(25PAA+s15PAA)}$ SEM: Fig 4.5	50 wt.% of H_2O 80 wt.% of H_2O pure water	20-30(10-30bar) 20-50(10-30bar) 65 (10 bar)	1.5-1 1.75-1.6 7	50 40
$M_{(20PAA+25w)}$ SEM: Fig 9.5	50 wt.% of H_2O Pure water	3-7 (10-30 bar) 8 at 10 bar	0.4-0.2 0.85	50

From table 5.5 it was found out that the rejection decreases with an increase in water content in feed. The lower rejection at (lower ethanol, higher water) content in feed is explained by the higher coupling phenomena between H_2O and EtOH, that can be related to the higher plasticizing effects of water; thus as the polymer swelling is higher, the water and ethanol fluxes are higher and the permselectivity are lower.

Figs.(8.5-9.5) showed that the flux of asymmetric PEI membranes increases with pressure and confirms that all membranes obey Darcy's law while flux was decreased with increase ethanol concentration in feed. It was found when comparing these results to the pure water flux that it is clear that the ethanol concentration has an influence on decreasing the initial permeate flux as shown in Figs.(8.5-9.5). This is may be due to low swelling and osmotic pressure (P_{osm}) of ethanol concentration. In addition, the membrane permeance also decreases with increase of ethanol content in feed, and there is almost no change with an increase of pressure.

Fraeger et al. [6] studied nanofiltration (NF) of aqueous organic mixtures using the FILMTEC™ NF-200B aromatic polyamide membrane, and reported flux of pure water, lactic acid 2% are 82, 58 kg/h.m^2 at 10 bar respectively.

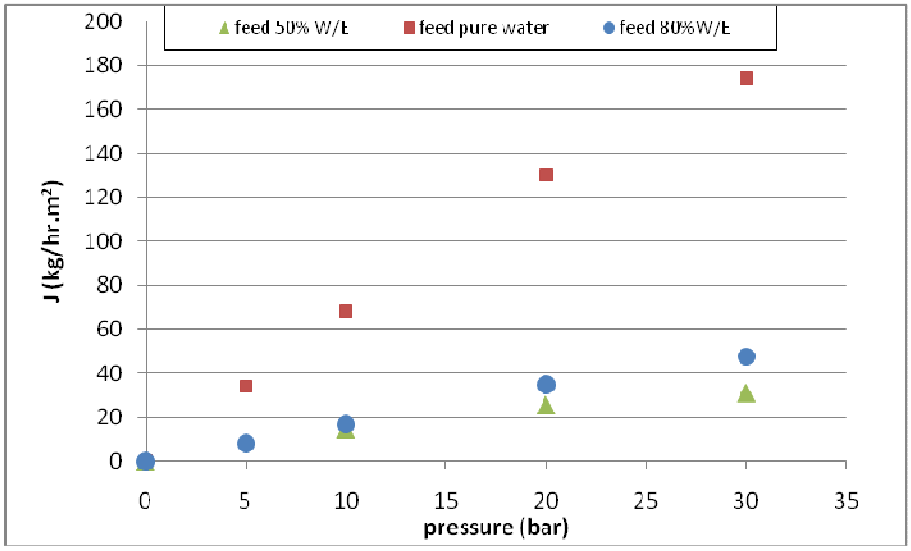

b. Effect of pressure and feed on flux.

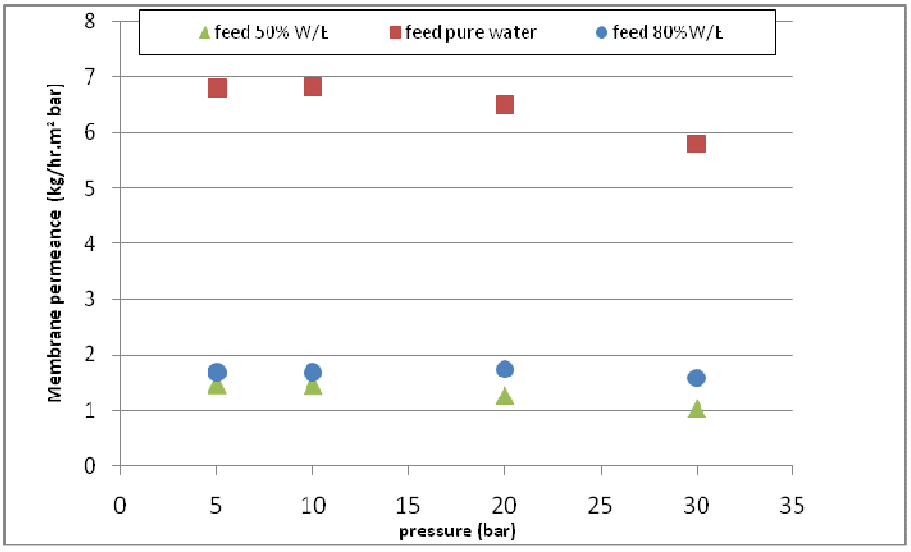

a- Effect of pressure and feed on membrane permeance.

Figure 8.5: Effect of operating pressure and feed on performances of $Mc_{(25PAA+s15PAA)}$.

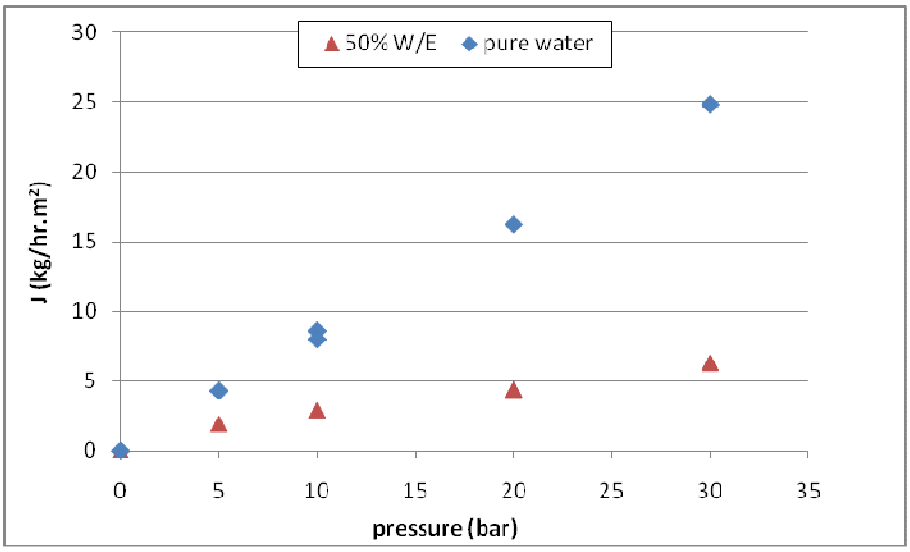

a- Effect of pressure on flux

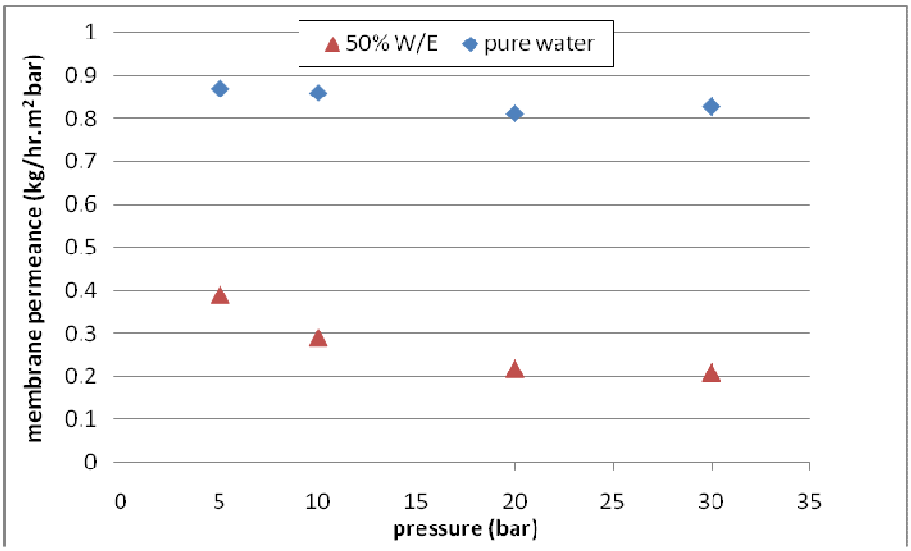

b- Effect of pressure on membrane permeance.

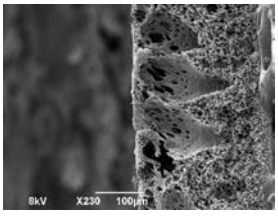

Cross section

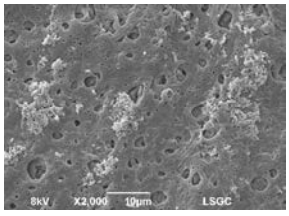

Bottom

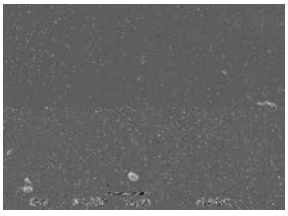

Top

Figure 9.5: Effect of operating pressure and feed on performance of M (20PAA+25w).

Y. Yoon et al. [9] studied the removal of organic contaminants by RO and NF membranes, and reported that inorganic compounds such as NaCl, $(NH_4)_2CO_3$ and organic solutes as urea had flux declines ranging from 9 to 73% of the pure water flux, depending on the membrane and the water composition. X. Zhou et. al.[10] studied the effect of different organic fractions such as hydrophobic acids, weakly hydrophobic acids, charged hydrophilic on membrane flux declines, and showed that in filtration of raw water, flux declines with PES, PVDF and CA membranes are 67%, 59% and 19% of the initial water flux. C. Jarusutthirak et al. [11] studied factors affecting nanofiltration performances in natural organic matter rejection and flux decline with thin-film polysulfone nanofiltration membrane, and reported that an increase in natural organic matter (NOM) concentration decreased permeate flux, increased permeate flux decline and increased NOM rejection, enhancing NOM accumulation on membrane surface. Thus, our experimental results are in agreement with these previous studies.

5.2.2.2 Nanofiltration of aqueous feed containing highly diluted organic compounds (100-500 ppm)

In this work the asymmetric PEI and Kapton™ as reference membranes have been fully characterized using different types of aqueous organic solutions. In order to explain the retention of the organic compounds, the size of the molecule and polarity are the main factors that determine the membrane performances and retention. For each parameter, the relationship with membrane performances and retention of organic molecules was studied in detail. The results obtained are listed in tables (6.5-10.5) and plotted in Figs.(10.5: 21.5).

5.2.2.2.1 Rejection properties of the tested membranes

Organic rejection is a property that is often used by NF membrane manufacturers to characterize membrane rejection properties. Table 6.5 summarizes the rejection results of the tested organic compounds by asymmetric PEI and Kapton™ membranes. The results obtained in this study imply that each membrane polymer material for NF membranes would exhibit different trends in terms of rejection of organic pollutants, which is determined by different factors such as physico-chemical properties of the organic pollutant compounds. Therefore, understanding the factors driving the rejection of organic pollutants is essential in order to get required separation. The effect of operating parameters, membrane type and properties of the organic compounds on rejection properties are reported.

Table 6, a.5: Operating parameters for preparing asymmetric PEI membranes.

Membrane	Casting solution%			Porosity % wet / dry	Thickness μm
	PAA	DMF	Water*		
$M_{(25PAA)}$	25	75	0	56/48	95
$M_{(25PAA+15W)}$	25	75	15	86/63	75
$M_{(20PAA+25W)}$	20	80	25	97/59	60
$M_{(15PAA+25w)}$	15	85	25	97/63	110

*Water wt% calculated on the total (PAA+DMF) weight after addition to dope solution. Immersion in water bath 1 h at 18^0C, pre-concentration time 1 min.

Table 6, b.5: Effect of Mw on average rejection of aqueous organic by PEI membranes (feed 500 ppm of organic/water, pressure 10 bar).

Organic compound	Mw g/mol	Rejection %				
		$M_{(25PAA)}$	$M_{(25PAA+15W)}$	$M_{(20PAA+25W)}$	$M_{(15PAA+25w)}$	$M_{K5(15PAA)*}$
Ethanol	46	11	6	6		
2-propanol	60	13	11	9		
Butanol	74	16	17	15		30
Urea	60	14	9	14-15		
Cyclohexane	84		25-42			
Toluene	92	63	51-56	43	30	
TEG	150	24-30	30	11-33		35
PEG400	400		79			37
PEG1000	1000	65-82.5	82	37	20	
PEG2000	2000		87			41
PEG6000	6000	100	100	45	50	51

*Where: TEG: triethylene glycol, PEG: polyethylene glycol, results with Kapton $M_{K5(15PAA)}$ at 20 bar.

I. Effect of membrane type on rejection

In this section, the retention of a series of organic molecules by asymmetric membranes was studied, in order to correlate the retention with the membrane type and microstructure, the main factors that determine retention. For each membrane, the correlation with organic molecule retention in nanofiltration experiments was calculated. Two types of

asymmetric membranes were tested, the asymmetric PEI $M_{(25PAA)}$, $M_{(25PAA+15w)}$, $M_{(20PAA+25W)}$ and $M_{(15PAA+25w)}$ membranes and asymmetric Kapton $M_{k1(11PAA)}$, $M_{k3(15PAA)}$, $M_{k4(15PAA)}$ and $M_{k5(15PAA)}$ membranes. The retentions results for the organic compounds with a comparable molecular weight are given in table 6,b.5 for the asymmetric PEI and Kapton™ membranes.

Figure 10.5 shows the effect of the membrane type on organic molecule rejection. The PEI asymmetric membranes exhibited a rejection between 6 and 100% while rejection determined with asymmetric Kapton™ was between 30 and 51%. Given that the organic rejection with asymmetric PEI is higher than asymmetric Kapton™ membranes (Table 6,b.5), that effect is because the PEI membranes are hydrophlic membranes with two blocks: the soft block has affinity with water and the rigid block gives good mechanical properties.

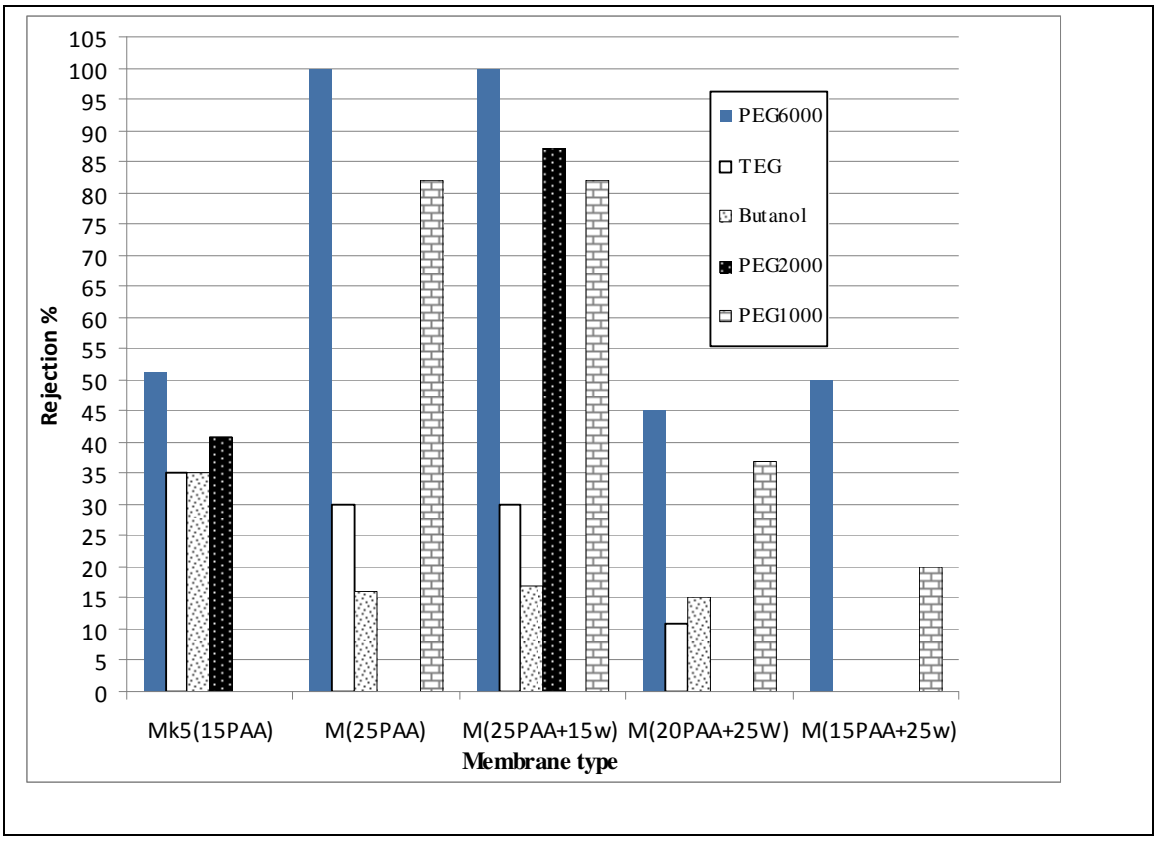

Figure 10.5: Effect of membrane type on organic molecule rejection (10bar, feed 500ppm).

The rejection of aqueous organic compounds determined with asymmetric Kapton™ $M_{k1(11PAA)}$, $M_{k3(15PAA)}$ and $M_{k4(15PAA)}$ membranes exhibited no rejection; this means that these membranes ($M_{k1(11PAA)}$, $M_{k3(15PAA)}$, $M_{k4(15PAA)}$) have no tight dense layer sufficient for organic separation. In other words, from SEM in Fig.(11.5) of these membranes it is observed that the cross section, top and bottom surfaces of these membranes are very porous, thus these membranes are microfilters.

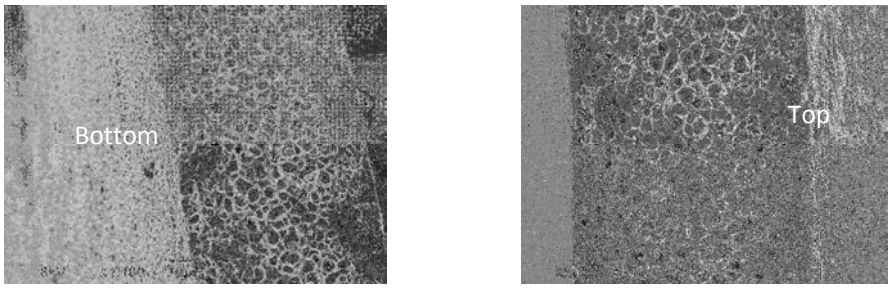

Figure 11,a .5: Cross section view of Kapton M_{k1} (11PAA%-89NMP%/1min/1h/50µm) at immersion bath temperature 11°C**.**

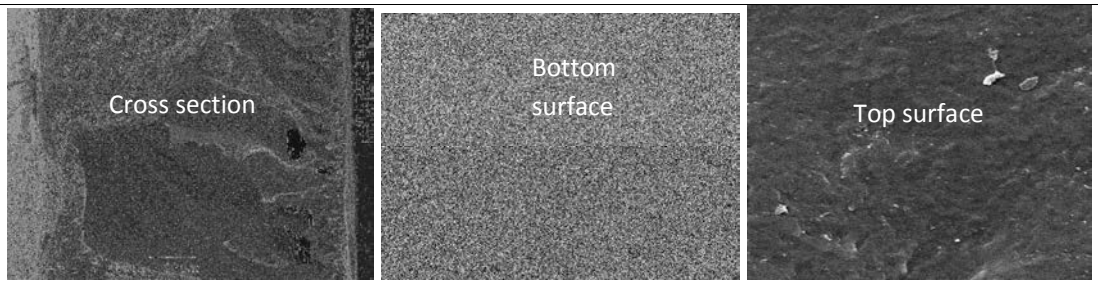

b.SEM view of Kapton M_{k3}(15PAA%-85NMP%/1min/1h/95µm), immersion bath 12°C**.**

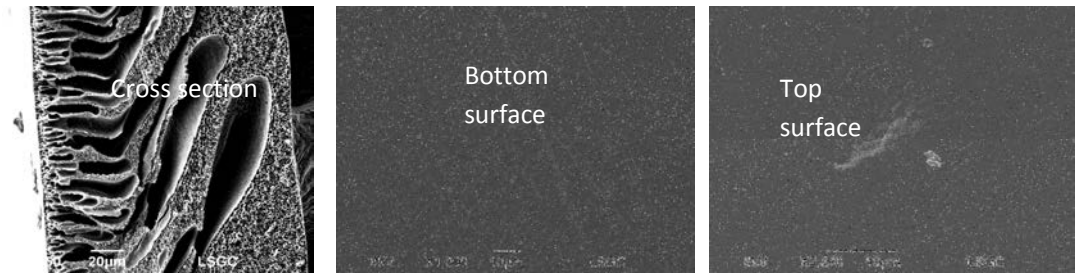

c.SEM view of Kapton M_{k4}(15PAA%-85NMP%/5min/1h/120µm), immersion bath 12°C**.**

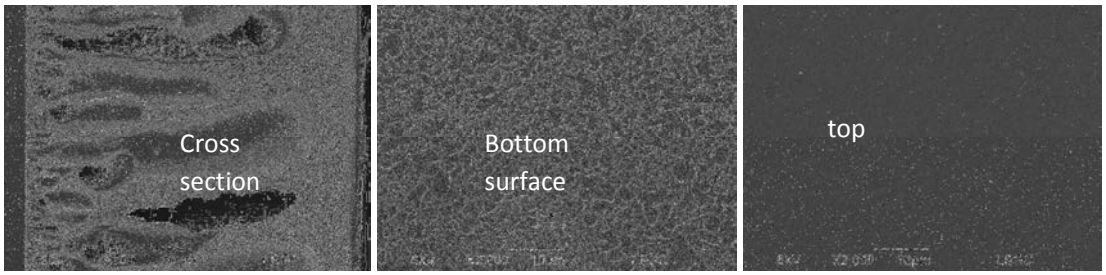

d. SEM view of Kapton M_{k5} (15PAA%-85NMP%/10min/1h/130µm), immersion bath 12°C.

Figure 11, b,c,d.5: SEM view of Kapton™ at immersion bath temperature 12°C**.**

The rejection determined with asymmetric PEI membranes considerably fluctuated and sometimes exhibited very low rejection between 5 and 50% with some asymmetric PEI $M_{(20PAA+25W)}$ and $M_{(15PAA+25w)}$ membranes. However, the organic rejection with the asymmetric PEI $M_{(25PAA)}$ and $M_{(25PAA+15w)}$ membranes have almost the same rejection, between 6 and 100%, which is better than asymmetric PEI ($M_{(20PAA+25W)}$ and $M_{(15PAA+25w)}$) membranes. Thus, the asymmetric PEI $M_{(25PAA)}$ and $M_{(25PAA+15w)}$ membranes have a tight dense layer sufficient for a complete retention of organic molecules as PEG6000. Looking at the rejection data of the organic compounds in table 6,b.5, it becomes clear that the asymmetric PEI $M_{(15PAA+25w)}$ membrane had the lowest retention and hence the largest pore size followed by $M_{(20PAA+25W)}$ membrane. The organic rejection follows the order, $M_{(25PAA+15w)} \approx M_{(25PAA)} > M_{(20PAA+25w)} > M_{(15PAA+25w)}$, as shown in figure (10.5).

Figure 12.5 showed the effect of membrane type on organic molecule rejection for asymmetric PEI $M_{(25PAA+15W)}$ membrane at 10bar, feed 500ppm and asymmetric PEI (UItem 1000) at 4:14 bar, feed 1000ppm [12]. The organic rejection with asymmetric PEI $M_{(25PAA+15W)}$ membrane is higher than with asymmetric PEI (UItem 1000) membrane.

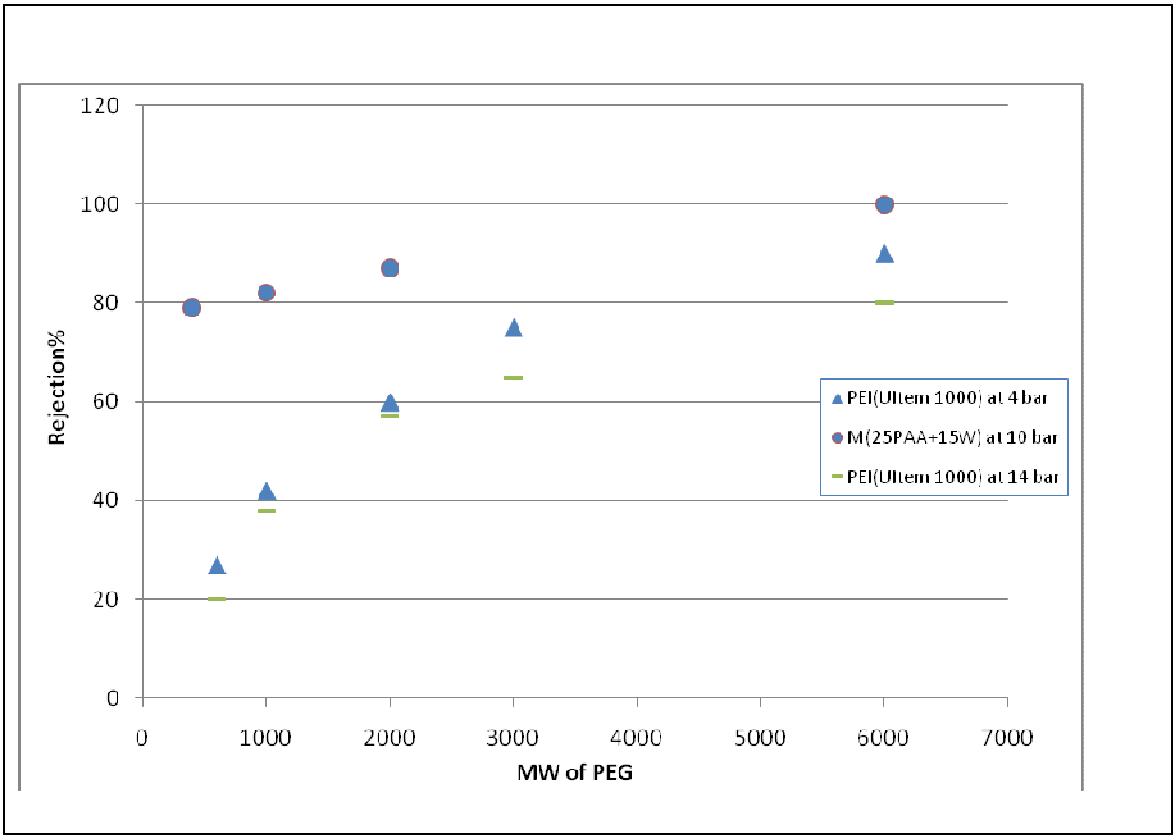

Figure 12 .5: Effect of membrane type on organic molecule rejection for $M_{(25PAA+15W)}$ (10bar, feed 500ppm) and PEI (UItem 1000) (4:14 bar, feed 1000ppm).

II. Effect of organic solute molecular weight on rejection

The PEI asymmetric membranes were characterized for the molecular weight cut-off (MWCO) of solute rejected. Thus, the separation properties of asymmetric PEI and Kapton^{TM} membranes for a series of organic molecules were studied. A summary of all determined characteristics is given in table 6,b.5.

Looking at the rejection data on the organic compounds in table 6.5, it becomes clear that ethanol had the lowest retention of 6-12% corresponding to the smallest molecular weight, followed by 2-propanol, urea and n-butanol. This is because these solutes are uncharged with very small molecular weight, so it is very difficult to reject either by size exclusion and or by charge exclusion.

It also states that the molecular weight of the compound is the most important parameter to describe the retention: a lower molecular weight gives rise to a lower retention. Starting from these rejection data, the MWCO can be calculated by fitting the rejection curve, rejection as a function of the molecular weight which is shown in figure 13.5.

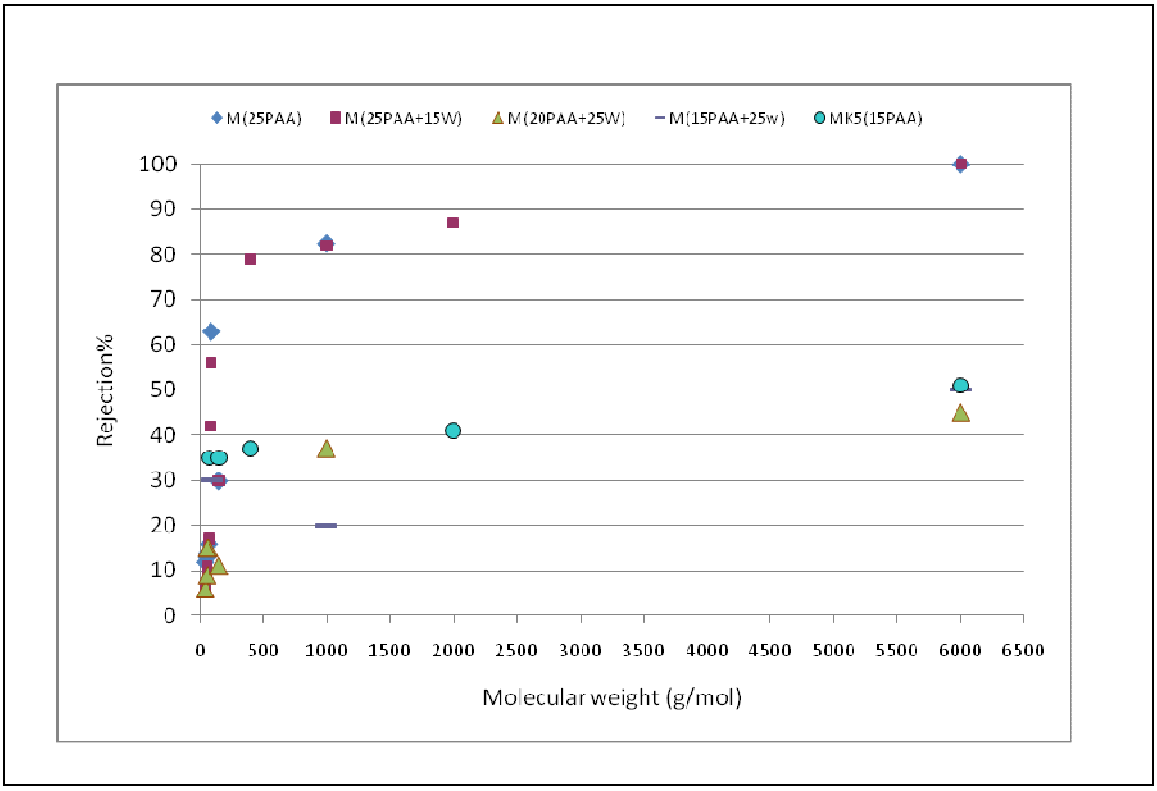

Figure 13.5: Effect of organic solute molecular weight on rejection.

Figure 13.5 shows the relationship between rejections determined in this work and molecular weight of the organic compounds tested. With respect to asymmetric PEI and Kapton membranes, the trend was rather clear. It was obvious that the rejection of organic solute by NF membranes is dependent on the Mw. The higher the molecular weight was, the higher the rejection.

The rejection characteristic of a NF membrane is often quantified by the molecular weight cut-off (MWCO). Usually, the MWCO is defined as the MW of a solute that is rejected at 90 percent [13]. Morever, this definition is not explicit and it can vary between 60 and 90 percent depending upon protocols used by various manufacturers [14]. Variations in solute characteristics, solute concentration, solvent characteristics, as well as flow conditions such as dead-end versus cross-flow filtration, make comparison of results from different manufacturers difficult.

MWCO, however, has no absolute meaning because the rejection depends on membrane type and solute physico-chemical properties. According to the convention that MWCO is the molecular weight of a standard compound (in this work PEG2000 with rejection 87%) that can be rejected by 90%, compounds with molecular weight of >2000 should be rejected more than 87%, at least by the asymmetric PEI $M_{(25PAA+15w)}$ and $M_{(25PAA)}$ membranes. Given that the MWCO of $M_{(25PAA+15w)}$ and $M_{(25PAA)}$ membranes were evaluated to be ≤2000. Furthermore, the retention of PEG6000 was 100% for asymmetric PEI $M_{(25PAA)}$ and $M_{(25PAA+15w)}$ membranes, showing that the molecular weight of PEG6000 is higher than the MWCO of both membranes. However, the retention of PEG6000 was 45-51% for asymmetric PEI $M_{(20PAA+25W)}$ and $M_{(15PAA+25w)}$ membranes and asymmetric Kapton $M_{k5(15PAA)}$ membrane. This indicates that the molecular weight of PEG6000 is lower than the MWCO of the three membranes. Thus, the MWCO of asymmetric PEI $M_{(20PAA+25W)}$ and $M_{(15PAA+25w)}$ membranes and asymmetric Kapton $M_{k5(15PAA)}$ membrane was evaluated to be higher than 6000. Furthermore, the rejection of solutes with low molecular weight as urea and alcohols in all membranes are low based on the MWCO of the membranes.

Thus, based on this study, the MWCO concept is based on the logical observation that molecules generally get larger as their molecular weight increases. Hence, as molecules get larger, sieving effects due to steric hindrance increase and the molecule is rejected by the membrane more often than a smaller molecule. Furthermore, it should be noted that the MWCO may also be related to diffusion, because a bigger molecule will diffuse more slowly than a smaller molecule.

III. Effect of organic solute radius ($r_{i,s}$) on rejection

The size exclusion of organic compounds, expressed as solute radius, can be a useful parameter to understand the specific retention of organic compounds. Figure 14.5 shows the relationship between rejections determined in this study and solute radius (table 7.5) of the organic compounds tested for the asymmetric PEI membranes. It was observed that the higher the radius was, the higher the rejection (Fig.14,b.5). The most easily accessible parameter indicates that the solute radius remains useful for the description of organic solute rejection by asymmetric NF membranes.

Table 7.5: Organic solutes size taken from literature [9-15].

Organic compound	Effective diameter (nm)/radius(nm)
Ethanol	0.34/0.17
2-propanol	0.52/0.26
Butanol	0.69/0.345
Urea	0.36/0.18
Cyclohexane	0.66/0.33
Toluene	0.5/0.25
Water	0.21/0.105
TEG	5.8/2.9
PEG400	6.3/3.15
PEG1000	7.1/3.55
PEG2000	8/4
PEG6000	10/5

Thus, it is important to consider the effect of solute radius on solute rejection. It was obvious that the rejection of organic solute by NF membranes is dependent on the solute radius. The asymmetric PEI $M_{(25PAA)}$ and $M_{(25PAA+15w)}$ membranes with small pore sizes (SEM) had a better rejection than $M_{(20PAA+25W)}$ and $M_{(15PAA+25w)}$ indicating that the solute radius is at least partially responsible for the rejection.

From figure 14, a.5, it appears that the rejection curves are somewhat scattered for solute radius as toluene and cyclohexane, this is because of the polarity; this effect will be discussed later.

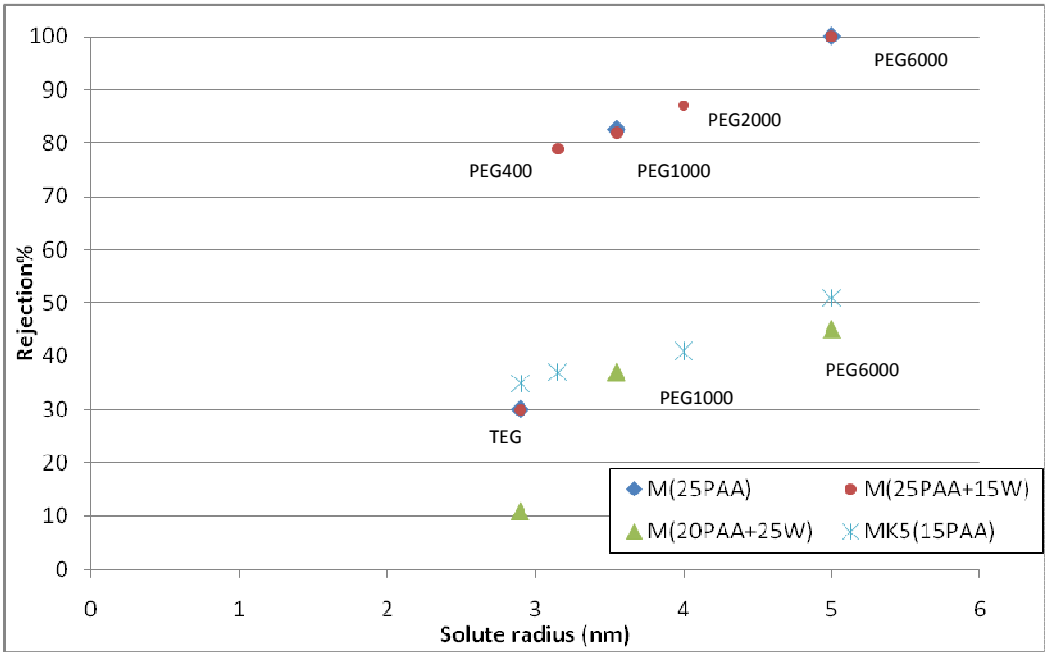

b. Solute rejection as a function of solute radius (with large radius of PEG family).

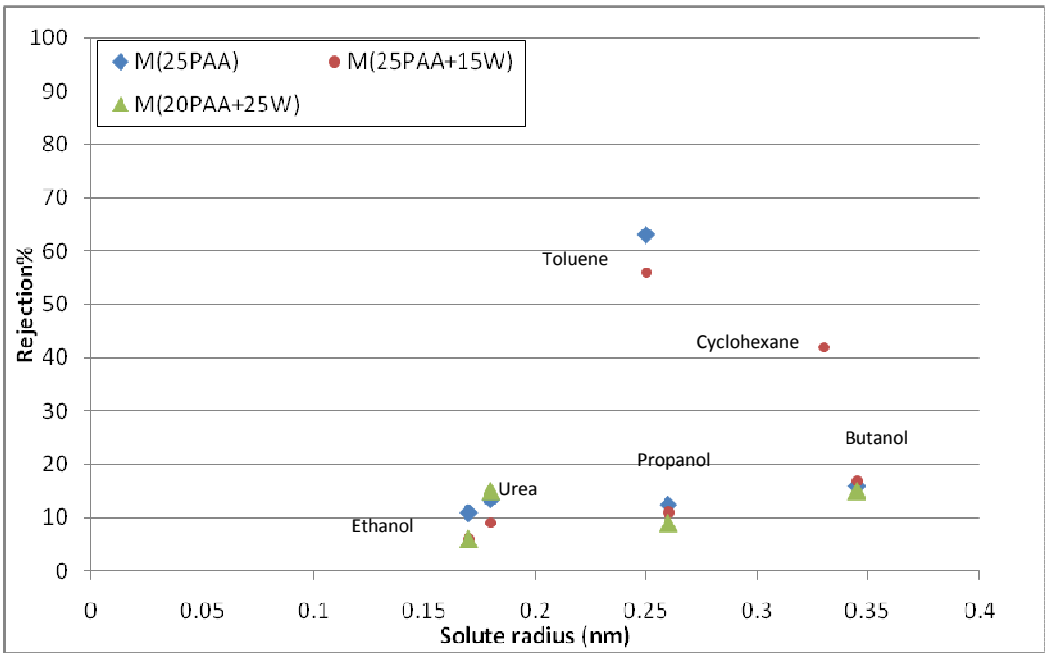

a. Solute rejection as a function of solute radius (with a small radius of alcohol series).

Figure 14.5: Solute rejection as a function of solute radius.

The retention of the alcohols compounds ranged from 12% to 16%, 6% to 17% and 6% to 15% for the asymmetric PEI $M_{(25PAA)}$, $M_{(25PAA+15w)}$ and $M_{(20PAA+25w)}$ membranes (Fig. 14,a.5) respectively. Typically, the retention of ethanol, with the smallest effective radius, is among the lowest retentions (respectively 12% , 6% and 6% for the asymmetric PEI $M_{(25PAA)}$, $M_{(25PAA+15w)}$ and $M_{(20PAA+25w)}$ membranes while the retention of PEG family, with a relatively high effective radius, is high for the asymmetric PEI $M_{(25PAA)}$ and $M_{(25PAA+15w)}$ membranes. This is also illustrated in figure 14.5, where a significant correlation between the rejection and the effective radius is obtained. Therefore, the effective radius is sufficient to describe the retention behaviour of organic compounds (such as alcohols and PEG family) in this work except for hydrophobic solutes such as toluene and cyclohexane in that case the effective raduis is not sufficient. This proves that the rejection is a result of a mere sieving effect at least for hydrophlic solutes.

From figure 14,b.5 it was found that the rejections of PEG6000 was 100%, thus the PEG6000 has a radius above the effective membrane pore radius(r_p), for asymmetric PEI $M_{(25PAA)}$ and $M_{(25PAA+15w)}$ membranes. The retention of PEG400, PEG1000 and PEG2000 was above 75% for asymmetric PEI $M_{(25PAA+15w)}$ membrane and the retention of PEG2000 was above 75% for asymmetric PEI $M_{(25PAA)}$ membrane. Thus, the organic solute radius of these compounds to the effective membrane pore radius ($r_{i,s}$ /r_p) is higher than 0.8. However, the retentions of alcohols are low based on the radius of solute to the membranes. Y. Yoon et al. [8] reported that the rejection for organic compounds is over 75% when $r_{i,s}/r_p$ is greater than 0.8. The transport of organic solutes is controlled mainly by diffusion for the compounds that have a high $r_{i,s}/r_p$ ratio, while convection is dominant for compounds that have a small $r_{i,s}/r_p$ ratio.

IV. Effect of solute hydrophobicity on rejection

The influence of hydrophobicity on retention of organic solutes is investigated by testing a series of organic molecules in aqueous solution with asymmetric PEI and Kapton membranes as follow:

a. Hydrophilic compounds:

- EtOH (46), Urea (60), TEG (150), PEG average 400, PEG ave.1000, PEG av.2000, PEG ave.6000

b. Hydrophobic compounds:

- Cyclohexane (84) max solubility: 100ppm, Toluene (92) max solubility: 500ppm, TTEG 250, 650, 1400 max solubility: 100ppm.

The influence of hydrophobicity on rejection of aqueous organic solution can be represented by the logarithm of the octanol–water partition coefficient (log_{ow}) as presented in table (8.5). For the tested organics, the log_{ow} is plotted as a function of rejection in figure 15.5.

Table 8.5: Selected physico-chemical properties of the organic compounds tested [16].

Solvent	log $_{ow}$	Dipole moment (Debye)μ^{O}	Avg. rejection %
Ethanol	-.032	1.7	9
2-Propanol	0.26	1.66	12
Butanol	0.88	1.66	16
Toluene	2.69	0.4	50
Cyclohexane	4.15	0.3	42

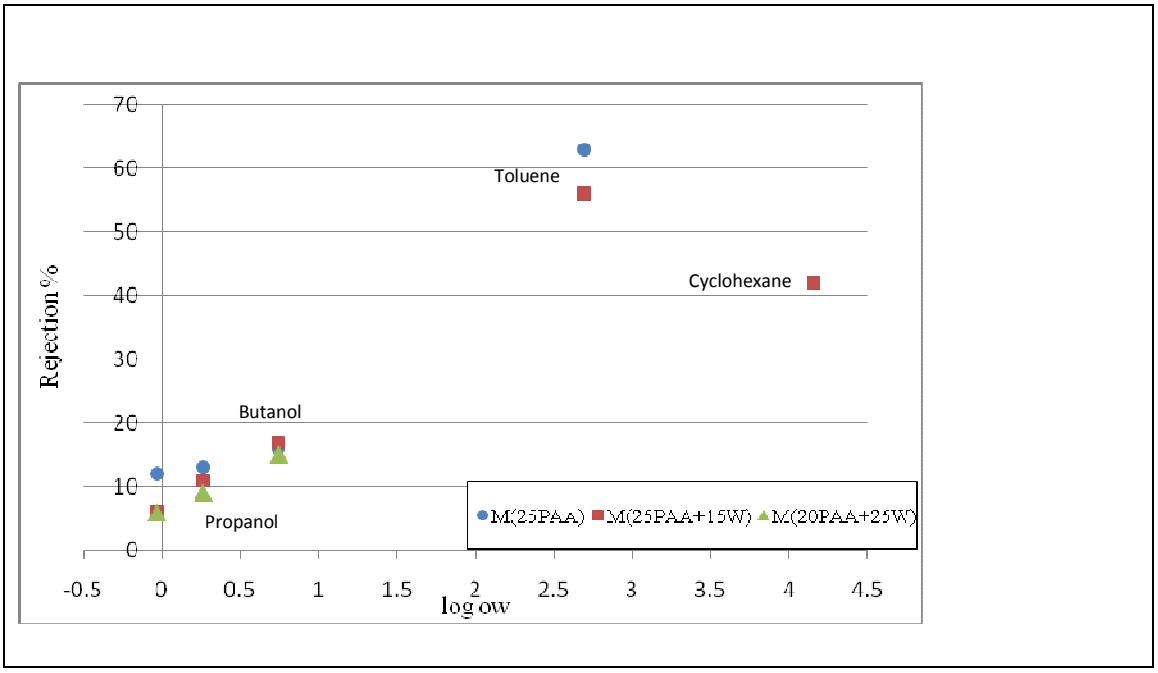

Figure 15.5: Correlation between solute hydrophobicity expressed as log $_{ow}$ and retention of PEI asymmetric membranes for 3 aliphatic alcohols, toluene and cyclohexane.

It is obvious that organic rejection increases with increasing hydrophobicity (log $_{ow}$) as seen in figure 15.5, for the asymmetric PEI $M_{(25PAA)}$, $M_{(25PAA+15w)}$ and $M_{(20PAA+25w)}$ membranes. As appears from figure 15.5, a nearly linear correlation between log $_{ow}$ and organic rejection exists for asymmetric PEI membranes. A compound with a high value of log $_{ow}$ (hydrophobic

compound- postive high value of log $_{ow}$), is rejected relatively easily while a molecule with a high affinity for the water phase (hydrophlic compound- small value of log $_{ow}$) has a small rejection value because these organic compounds permeate relatively easily through the asymmetric PEI membranes.

Y. Kiso et al. [17] reported that an increase of aromatic pesticides rejection with increasing hydrophobicity by nanofiltration membranes. K. Agenson et al. [18] reported that a higher retention will be obtained for a more hydrophobic organic molecule with a larger width and length with nanofiltration membranes. The correlation coefficients for molecular width, length and log $_{ow}$ were all negative indicating that retention of membranes will be lower for a more hydrophilic molecule (as ethanol in our work) with a smaller width and length. Thus, the solutes with larger widths, larger lengths and higher logarithm of octanol–water partition coefficients will have higher retentions for all the membranes used. The rejection by membranes with these three parameters gave the best correlation. This shows that solute molecules with smaller width, length and log $_{ow}$ will easily pass through the membrane. Thus, our experimental results are in agreement with these previous studies.

Moreover, this present study seems to be in contradiction with the results of L.Braeken et al. [19],who reported a decrease of rejection with increasing hydrophobicity by a crosslinked polyamide nanofiltration membrane. However, K.Kimura et al. [20] pointed out that for the relationship between the rejection and $\log_{ow}$ of the tested neutral endocrine disrupting compounds (EDCs) and pharmaceutical active compounds (PhACs), no significant correlation is recognized between the rejection and log $_{ow}$ for the RO membrane (polyamide, cellulose acetate). To better explain rejection by membrane, other parmeters for polarity need to be considered.

Thus, the dipole moment (μ°) of the organic molecules considered is summarized in Table 8.5. In general, hydrophilic compounds are likely to have higher values of dipole moment. It appears that the molecules with the highest dipole moments (hydrophilic compounds) consistently show a lower retention than molecules with a lower dipole moment (hydrophobic compounds such as toluene). For all membranes, the retention of hydrophilic compounds molecules is significantly lower than hydrophobic compounds of approximately the same size.

B. van der Bruggen et al. [13] showed that molecules with dipole moment of >3 debye consistently showed a lower rejection than molecules of approximately the same size but with a lower dipole moment. However, K.Kimura et al. [20] reported that the higher the dipole moment was, the higher the rejection by RO membrane (cellulose acetate) was. Further, the

plotted curve of rejection as a function of dipole moment could not explain the rejection tendency with respect to RO membrane (polyamide).

Thus, this differences in results obtained may be explained by the difference in membrane materials used in all studies and solutes type.

5.2.2.2.2 Membrane performance (flux, membrane permeance)

The permeate flux and membrane permeance of asymmetric PEI and Kapton membranes was reported, to determine the most suitable membranes. Tables 9.5-10.5 summarizes the results of the tested aqueous organic solutions by membranes. Further, the effects of membrane type and operating conditions such as pressure is plotted as a function of membrane permeance in figures (16.5- 21.5). From these figures and tables it was found out that membrane performances depend on membrane type and morphology.

I. E**ffect of membrane type on permeate flux**

The permeate flux of a series of aqueous organic solutions by asymmetric PEI and Kapton membranes was investigated in order to correlate the membrane performance (flux, membrane permeance) with the membrane type. The PEI asymmetric membranes exhibited a flux between 1.3 to 71 (kg/h.m^2) at 10 bar as represented in table 9.5. With asymmetric Kapton $M_{k5\ (15PAA)}$ membrane, it was found out that up to 10 bar there is no permeate flow. The measurable flux occurs only when the inlet pressure reaches 20 bar. Flux determined with asymmetric Kapton $M_{k5\ (15PAA)}$ membrane between varied 0.23 to 0.5 (kg/h.m^2) at 20 bar. In other words, flux of asymmetric PEI membranes is 10 to 140 times higher than asymmetric Kapton $M_{k5\ (15PAA)}$ membrane (Table 9.5). It was surprising that asymmetric PEI apparently exhibited better flux than asymmetric Kapton membrane. As explained before, that effect probably results from the fact that the PEI membranes have two blocks; the soft block has affinity with water and rigid block to give good mechanical properties.

With the other asymmetric Kapton $M_{k1(11PAA),}$ $M_{k3(15PAA)}$ and $M_{k4(15PAA)}$ membranes the permeate flux started at 0 bar giving respectively 98, 438, 4.3 (kg/h.m^2). Thus, again these membranes are microfilters and can easily break.

Table 9.5: Flux of aqueous organic compounds by asymmetric PEI membranes (feed 500 ppm of organic/water, pressure 10 bar for asymmetric PEI membrane and 20 bar for asymmetric Kapton^{TM} membranes).

Organic compound	Flux (kg/h.m^2)				
	$M_{(25PAA)}$	$M_{(25PAA+15W)}$	$M_{(20PAA+25W)}$	$M_{(15PAA+25W)}$	$M_{k5(15PAA)}$
Pure water	3-3.5	12	9.3	71	0.6
Ethanol	1.5	8.5	9.3		
2-propanol	1.7	8	7.1		
Butanol	1.7	7.3	7.1		0.5
Urea	2.7	8	7.3		
Cyclohexane		10			
Toluene	2.5	9.5	7.6		
TEG	2.6	8	9		0.23
PEG400		8			0.49
PEG1000	1.3	8	6	43.5	
PEG2000		8.2			0.29
PEG6000	1.7	9.5	6	45	0.32

Comparing the permeate flux of water and aqueous organic solutions by asymmetric PEI membranes, it is observed that the asymmetric PEI $M_{(15PAA+25w)}$ membrane has the highest permeate flux, but it has the lowest rejection of solutes while the asymmetric PEI $M_{(25PAA)}$ membrane has the lowest flux, with a good level of rejection of solutes. Both the decrease in pore size near the membrane surface and the increase of the top dense layer may be responsible for the decrease in permeation flux observed in the $M_{(25PAA)}$ membrane. The permeate flux and membrane permeance (Fig.16.5) follows the order, $M_{(15PAA+25w)} > M_{(25PAA+15w)} \geq M_{(20PAA+25w)} > M_{(25PAA} > M_{k5(15PAA)}$. From Figure 16.5 and table 9.5, it was obvious that the flux and membrane permeance of different aqueous organics are lower than the flux and membrane permeance of pure water as discussed before.

Table 10 .5: Membrane permeance of aqueous organics by PEI membranes (feed 500 ppm of organic/water, pressure 10 bar for asymmetric membranes and 20bar for asymmetric Kapton).

Organic	Membrane permeance (kg/h.m^2 bar)				
	$M_{(25PAA)}$	$M_{(25PAA+15W)}$	$M_{(20PAA+25W)}$	$M_{(15PAA+25W)}$	$M_{k5(15PAA)}$
Pure water	0.35	1.2	0.93	7.1	0.02
Ethanol	0.15	0.86	0.93		
2-propanol	0.17	0.78	0.71		
Butanol	0.17	0.73	0.71		0.025
Urea	0.27	0.78	0.73		
Cyclohexane			1		
Toluene	0.25	0.95	0.76		
TEG	0.26	0.8	0.9		0.01
PEG400		0.78			0.02
PEG1000	0.13	0.78	0.6	4.35	
PEG2000		0.82			0.015
PEG6000	0.17	0.95	0.6	4.5	0.016

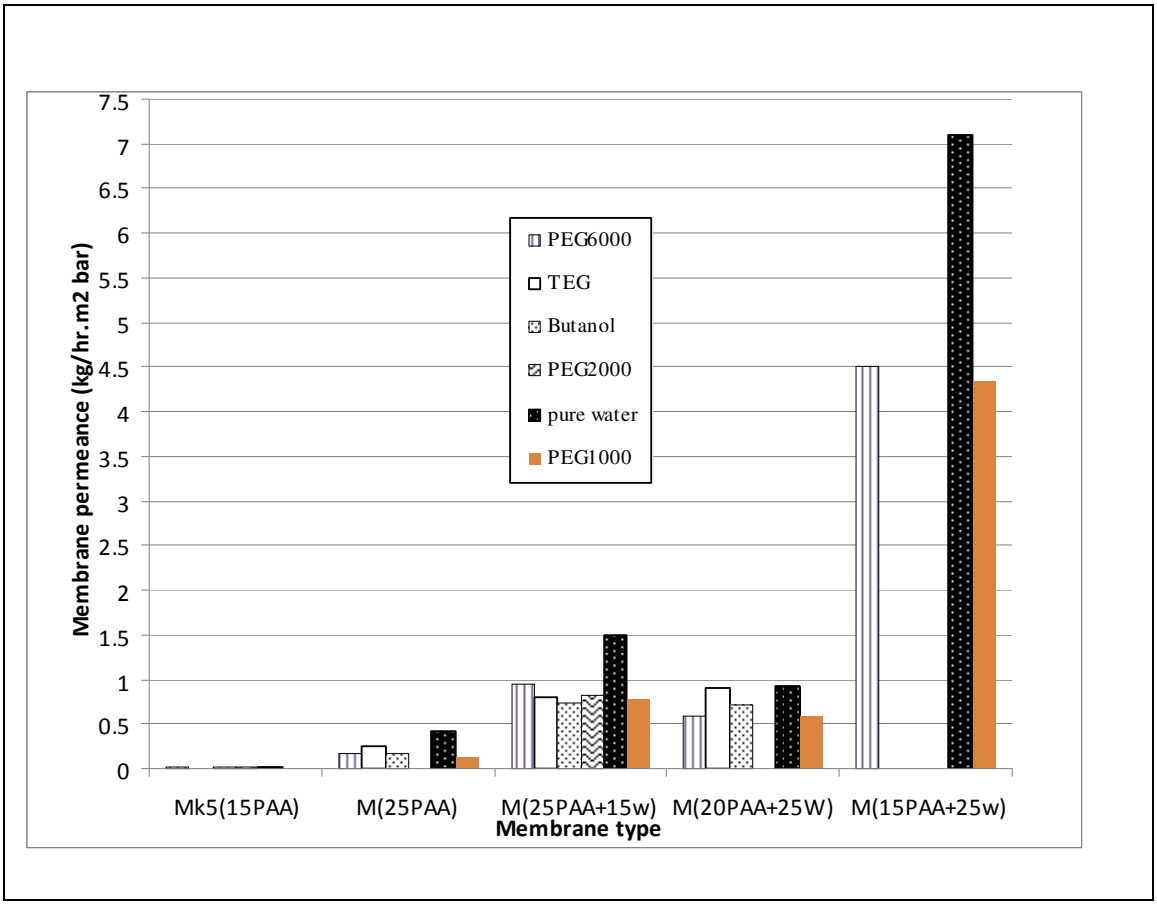

Figure 16.5: Effect of membrane type on membrane performances at 10 bar and feed 500ppm.

II. Effect of operating pressure on permeate flux

Influence of operating pressure on flux and membrane permeance of water and aqueous organic solutions was investigated using asymmetric PEI membranes. The observed flux (J) and membrane permeance are plotted against applied pressure for water and different aqueous organic feed solutions.

Figure (17.5) showed that the flux of asymmetric PEI membranes increased with an increase of applied pressure. This confirms that all membranes follow Darcy's law. Further, the permeate flux and membrane permeance for pure water is better than the aqueous organic solutions. Thus, it is clear that the aqueous organic solution has an influence on decreasing the flux and membrane permeance. This type of result is not surprising and has been observed previously by other studies [6,9,10,11,21,22] as discussed before.

The membrane permeance is not stable and varied considerably with pressure. The presence of large macrovoids or finger like structure (SEM as shown in figs. 18-21.5) can result in compaction or collapse of polymeric membranes with increasing operating pressure and hence it leads to reduction of flux in high pressure application. Hence the membrane permeance will decrease with increasing pressure, as shown in Fig.(17.5) for membranes $M_{(25paa+15w)}$, $M_{((20paa+25w)}$. Membrane $M_{(25paa)}$ has almost a stable membrane permeance with change of operating pressure.

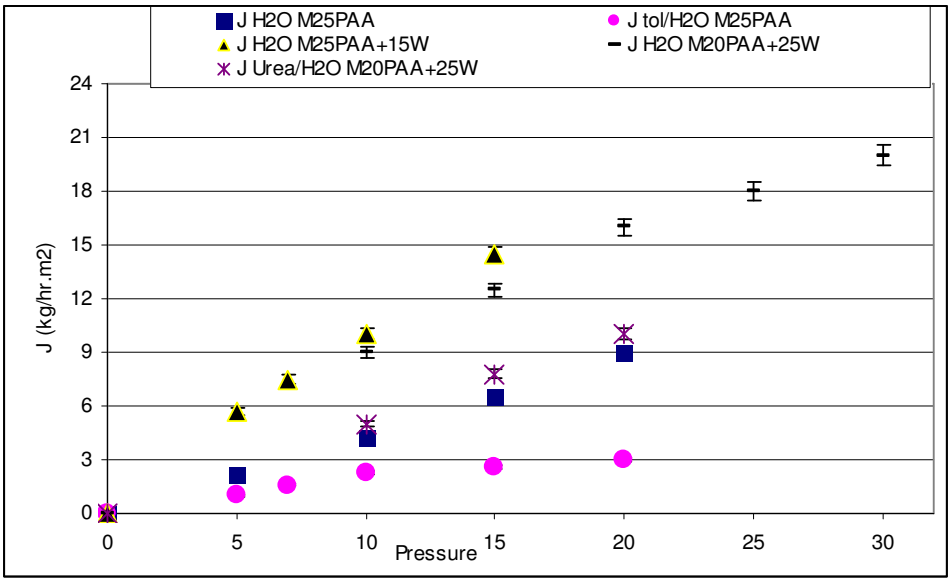

a. Effect of pressure on membrane flux.

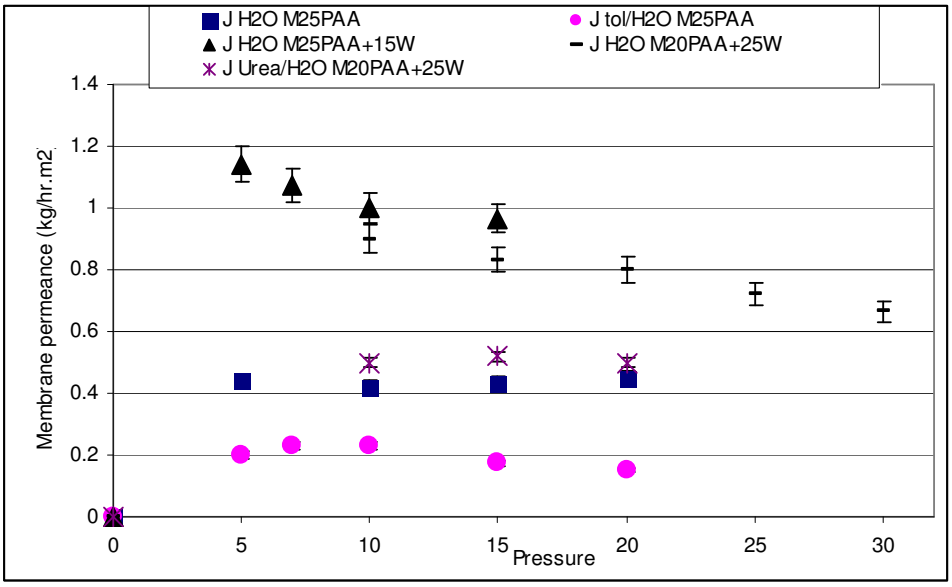

b. Effect of pressure on membrane permeance.

Figure 17.5: Effect of operating pressure on flux and on membrane permeance by asymmetric PEI membranes (aqueous organic feed 500 ppm).

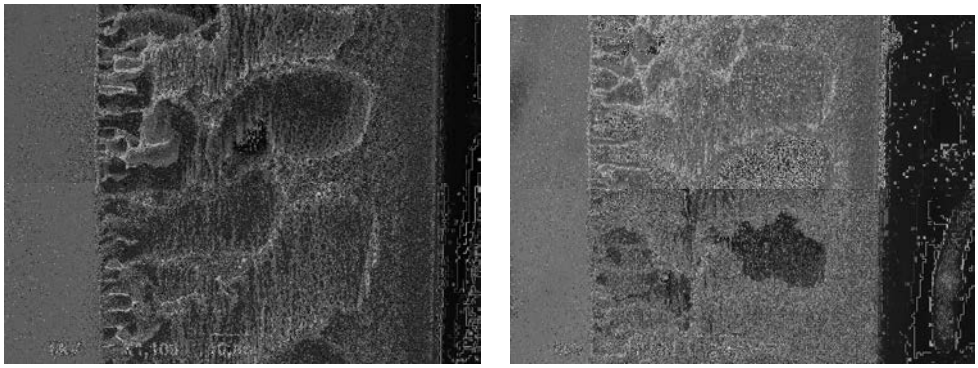

Cross section before test

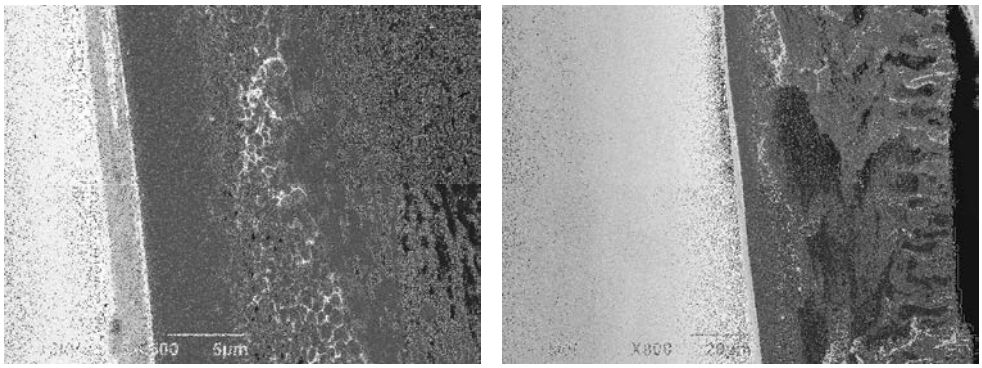

Cross section after test

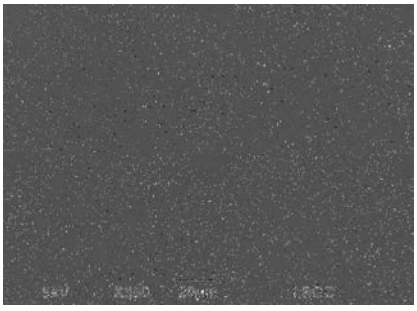

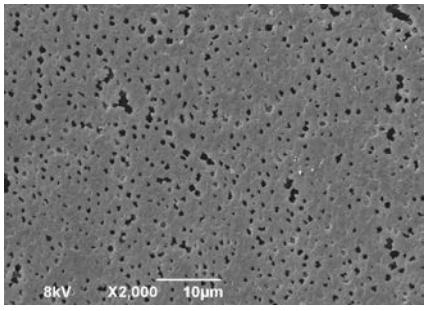

Top Bottom

Figure 18 .5: SEM for asymmetric PEI $M_{(25PAA)}$ membrane.

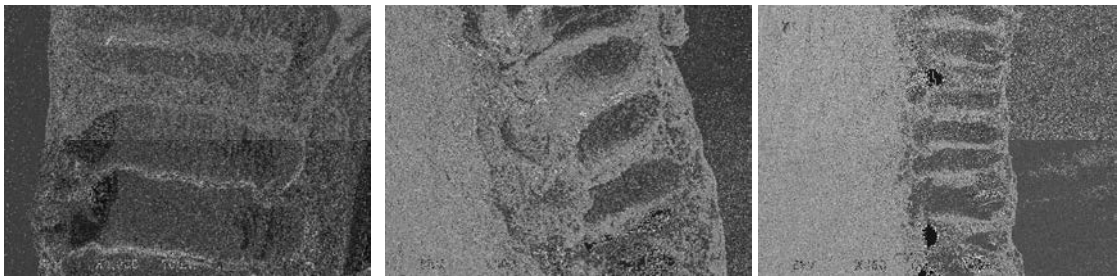

Cross section before testing

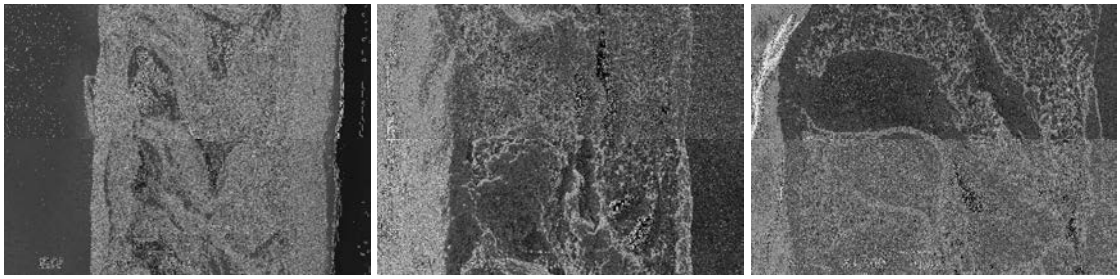

Cross section after testing

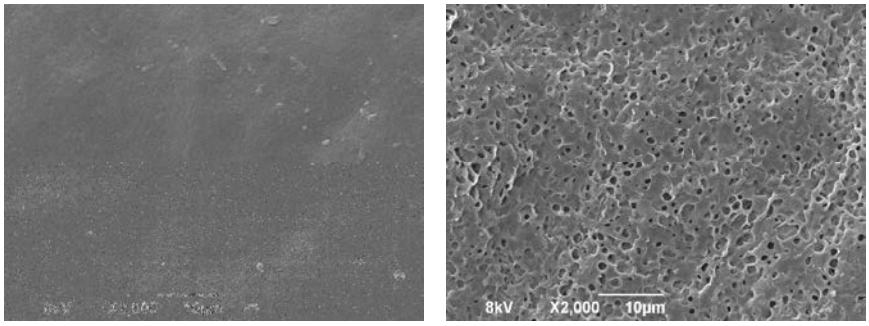

Top surface Bottom surface

Figure 19 .5: SEM for asymmetric PEI $M_{(25PAA+15W)}$ membrane .

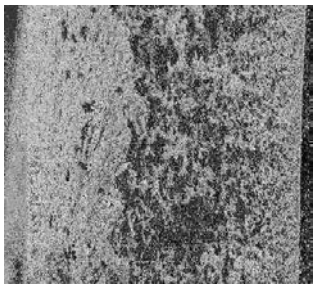

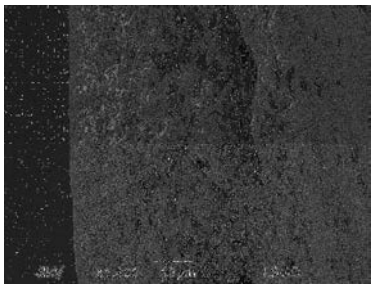

Before testing

After testing

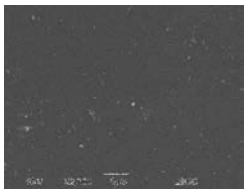

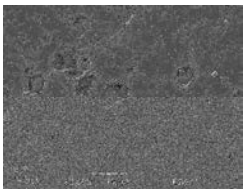

Top view

Bottom view

Figure 20.5: SEM for asymmetric PEI $M_{(20PAA+25W)}$ membrane.

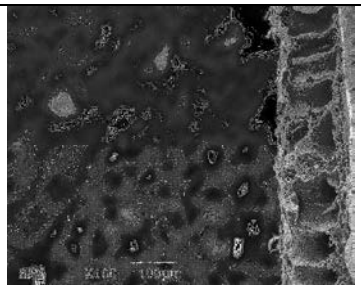

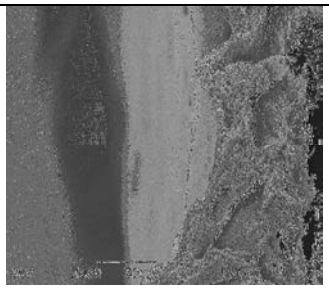

Before testing

After testing

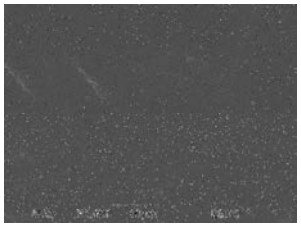

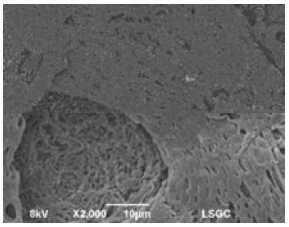

Top

Bottom

Figure 21.5: SEM for asymmetric PEI M $_{(15PAA+25W)}$ membrane.

5.2.2.3 PEI-NF membrane performances with aqueous organic/inorganic solutions

This section considers the nanofiltration (NF) of 500 ppm of aqueous organic/inorganic mixtures using PEI membrane (SEM: Fig. 22.5). Mixtures of salt NaCl and series of organic solutes (500ppm) were used as model solutions to investigate the effects of the dissolved salt on the NF flux and the organic rejection. The results are presented in table 11.5. For all solutions under study, the salt rejection was in range 55-65%, while the organic rejection decreased when dissolved salt was added to an aqueous organic solution. In addition, when dissolved salt was added, the flux also was found to decrease. The maximum in the organic rejection can apparently be explained by the combination of molecular weight.

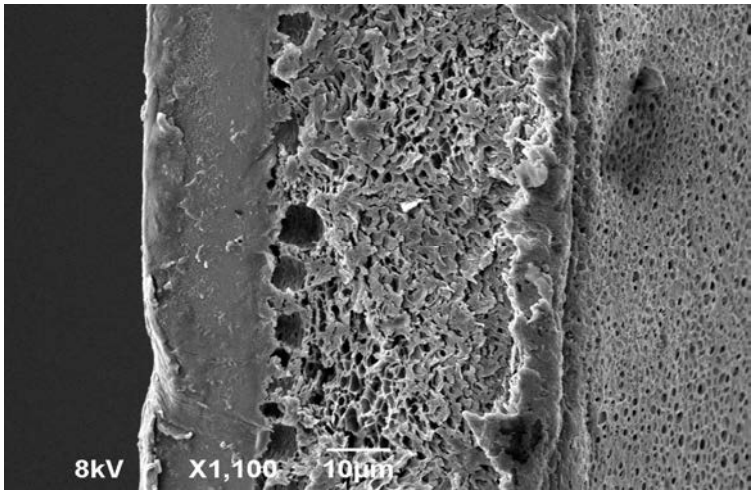

Cross section

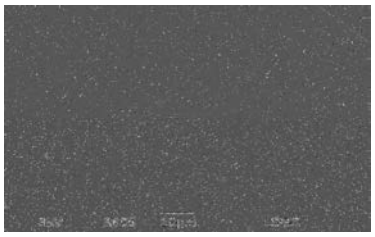

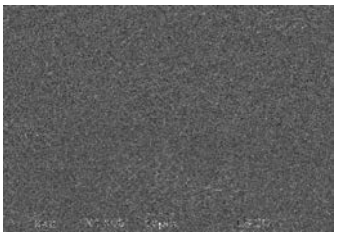

Top Bottom

Figure 22 .5: SEM for Mc (30PAA+ support Kapton 11PAA)·

Table 11.5: Effect of dissolved salt (NaCl) on performances of PEI-NF membrane ($feed_1$= 500 ppm organic, $feed_2$ = 500 ppm organic+500 ppm NaCl, R%= ±3, 10 bar, 20°C ±2).

Feed	M_W (g/mol)	R_1%	R_2%	Rs	J_1(kg/h.m^2)	J_2(kg/h.m^2)	P_{2osm} (bar)
PEG6000	6000	50	31	65	0.95	0.55	0.214
PEG2000	2000	50	34	55	0.8	0.5	0.218
PEG 400	400	31	24	60	0.82	0.61	0.243
Urea	60	14	7	55	0.85	0.82	0.419

Where; R_1= rejection at $feed_1$, $feed_1$= 500 ppm organic, R_2= rejection at $feed_2$, $feed_2$=500 ppm organic+500 ppm NaCl**,** Rs = salt rejection, J_1 = total flux at $feed_1$, J_2= total flux at $feed_2$, P_{2osm}= the osmotic pressure at $feed_2$, the osmotic pressure of salt P_{osm}= 0.211.

Figure 23.5 shows the organic rejection as a function of molecular weight. It is seen that the addition of 500ppm of NaCl to the $feed_1$ containing 500ppm of organic causes a significant reduction of organic rejection for all organic compounds tested and the rejection level is decreased when M_W of organic compound increase.

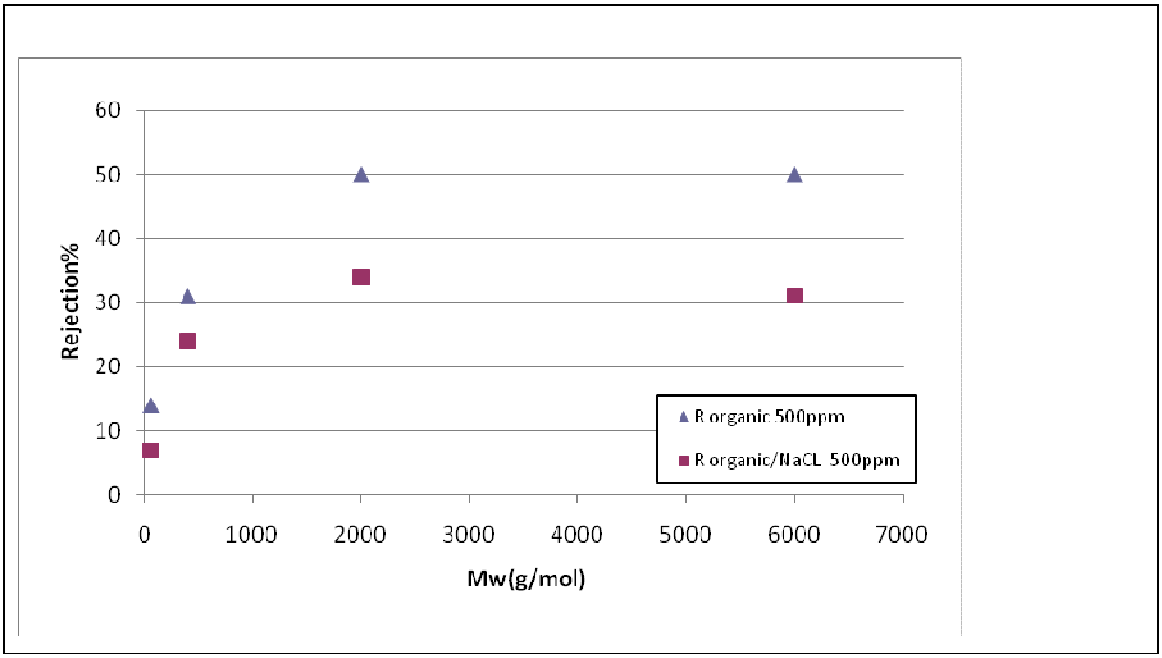

Figure 23.5: Effect of dissolved NaCl (500ppm) on organic rejection as a function of Mw for a series of organic compounds (500ppm) in the feed. The feed temperature was 20°C±2; the pressure was 10 bar, Mc (30PAA+ support Kapton 11PAA).

Table 11.5 and Figure 24.5 shows that fluxes always decrease (25%) with the addition of dissolved salt to an aqueous organic solution.The decrease in flux with the salt

concentration is in agreement with the observations with some of researchers as [5,6,9,10,11,23].

The explanations of these results are:

3- The shrinking of the skin layer resulting from either reduction of water activity, and thus, lower swelling; indeed, the swelling is decreased by 47% due to the addition of dissolved salt (sorption of pure water 15%, sorption of NaCl 500ppm 7.5%),

4- A salting out effect on the organic which leads to increasing of organic activity,

5- Effect resulting from reduction of the net driving force for water due to the osmotic pressure of the feed.

Our results is also in agreement with Freger et al. [6] who studied nanofiltration (NF) of organic/inorganic mixtures using the FILMTEC™ NF-200B aromatic polyamide membrane, and reported flux of pure water, 4% NaCl, 9% NaCl, lactic acid 2% , lactic acid 2% + 4% NaCl and lactic acid 2% + 9% NaCl are 82, 25,10, 58, 23, 8 kg/h.m^2 at 10 bar respectively while rejection of lactic acid 2%, lactic acid 2% + 4% NaCl and lactic acid 2% + 9% NaCl are 60%, 36%, 25 % at 10 bar respectively. Table 12,a,b,c.5 shows summary of results with nanofiltration.

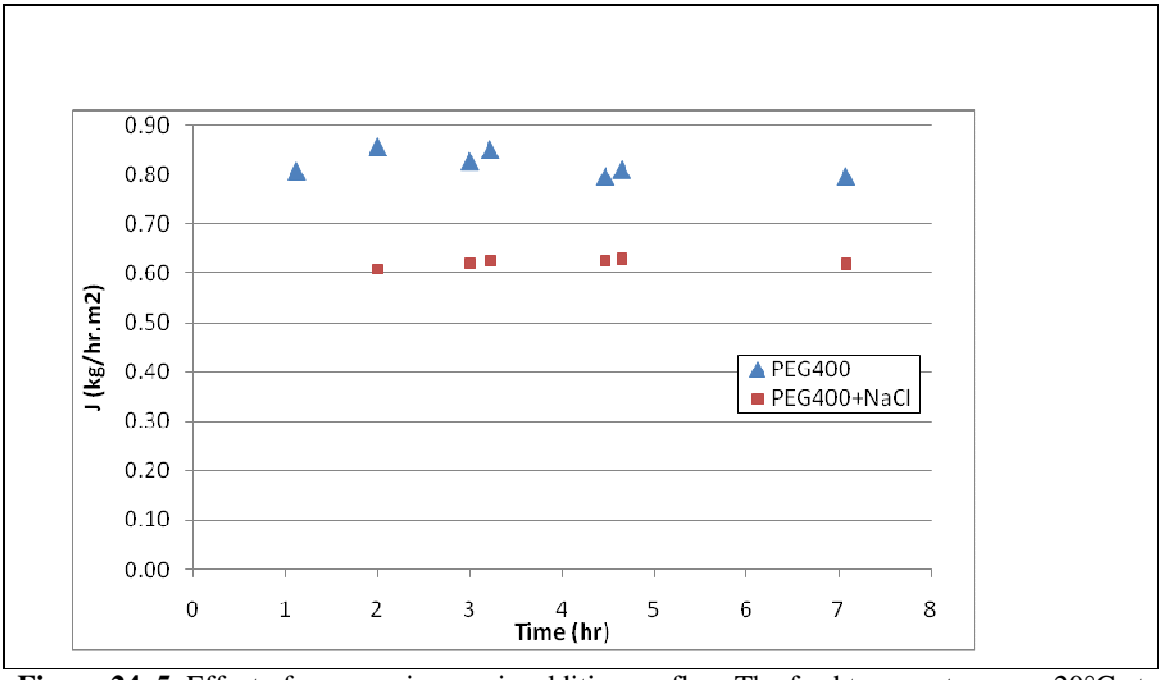

Figure 24 .5: Effect of aqueous inorganic addition on flux. The feed temperature was 20°C at 10 bar.

Table 12,a.5: Nanofiltration results with PEI and Kapton membranes (feed pure water).

Membrane	Total thickness µm	membrane permeance (kg/h.m^2.bar)	SEM
$M_{Kapton(11PAA)}$	100 µm	2600 at 2 bar	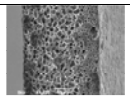
$M_{(25PAA)}$	95µm	0.45-0.6(5-20 bar)	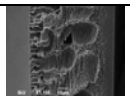
$M_{(25PAA+15w)}$	15 µm	10-10.7(5-20 bar)	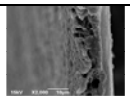
$M_{(25PAA+20w)}$	140 µm	7.6-8.5 (5-20 bar)	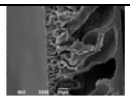
$M_{c(25PAA+ s Kapton)}$	45µm+100µm support	6.7-7(5-20 bar)	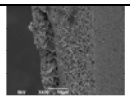
$M_{c(25PAA+s15PAA)}$	30µm+50µm support	6.5-7 (5-20 bar)	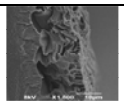
$M_{c(25PAA+s}$ 20PAA+10w)	80µm+80µm support	0.6-1.2(5-20 bar)	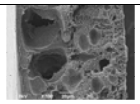

Table 12,b.5: Separation of H_2O/ EtOH mixtures by NF membrane performance.

Membrane	Feed H_2O/ EtOH	Flux (kg/m2 h)	Pe(kg/h.m^2 bar)	Rejection %	SEM
$Mc_{(25PAA+s15PAA)}$	50 wt.% of H_2O 80 wt.% of H_2O pure water	20-30(10-30bar) 20-50(10-30bar) 65 (10 bar)	1.5-1 1.75-1.6 7	50 40	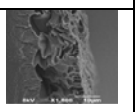
$M_{(20PAA+25w)}$	50 wt.% of H_2O Pure water	3-7 (10-30 bar) 8 at 10 bar	0.4-0.2 0.85	50	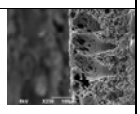

Table 12,c.5: Comparison between nanofiltration and pervaporation

Factor	**PV**	**NF**
Membrane morphology	Dense / Asymmetric	Asymmetric
Driving force	concentration Gradient	Pressure
Transport mechanism	Solution-diffusion	Convection-diffusion
Phase	Liquid-vapor	Liquid–liquid
Pressure	Under vacume	3-35 bar
Ex : asymmetric PEI $M_{(25PAA)}$	Feed =20H_2O/80EtOH J= 0.4 kg/h. m^2 , Cp=70 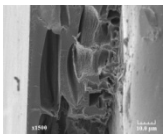	Feed =PEG6000 500ppm, J=1.7kg/h.m^2 , Rejection =100% MWCO 2000 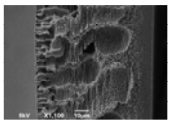
Ex : asymmetric PEI $M_{(25PAA+15w)}$	Feed =50T/50H, J=0.1 kg/h.m^2 , Cp=65% 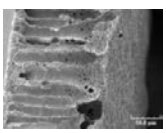	Feed =PEG6000 500ppm , J=9.5kg/h.m^2 , Rejection=100% MWCO 2000 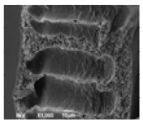

Conclusions and Recommendations for Future work

a) In this work, the rejection characteristics of aqueous organic or inorganic compounds by NF membranes were investigated and discussed. Tested compounds were chosen to cover a large range of molecular weight and $\log_{ow}$ for testing with the asymmetric PEI and Kapton^{TM} membranes. Results obtained in this work can be summarized as follows:

b) The performances of nanofiltration membranes depend on both membrane and feed properties, as it was shown that changing the type of the feed solution implied the selection of another optimal membrane. Comparing the two types of membranes tested (the asymmetric PEI and Kapton^{TM}), the PEI membrane generally exhibited better rejections and much higher fluxes than the asymmetric Kapton^{TM} membrane (PI). These effects are due to hydrophilic nature of the PEI membranes; the soft block has affinity with water and the rigid block gives good mechanical properties. However, even asymmetric PEI did not exhibit complete rejection for the tested compounds. Rejection of organic solutes by asymmetric PEI was in the range of 11:100%, which could be reasonably correlated to solute molecular weight.

c) NF membranes of Kapton have a non measurable flux close to zero when using the same analogous conditions used to test asymmetric PEI-NF membranes, we realize from that result the best interests of the synthesis of PEI and separation efficiency obtained in NF; the insertion of the hydrophilic alcoxyethers chain has permitted to give a strong hydrophilic character to the structure of PEI while ensuring a high rejection for hydrophilic molecules with a molecular weight superior to 150 g / mol.

d) Some of the tested nanofiltration PEI membranes showed high rejection for hydrophilic molecules, like polyethylene glycol, with molecular weight ranging from 400 to 6000 Dalton; according to molecular weight, organic rejection of 79-100% were achieved from 500 ppm aqueous solutions of organic compounds (transmembrane pressure: 10bar, $t° \approx 30$ °C). For example, starting from an aqueous solution containing 500ppm of PEG 2000, the rejection corresponds to 87% ($M_{(25\ PAA\ +15w)}$) or a residual PEG of about 65ppm in water permeat with permeability of about 1L / ($hr.m^2$.bar).

e) The first results obtained with nonpolar molecules are also promising; they indicate organic rejection significantly higher for lower molecular weights compounds. For example, with a hydrophobic molecule such as toluene (Mw = 92g/mole), the rejection is 50% higher than that of triethyleneglycol (Mw = 150g/mole) only of 30% with the same membrane ($M_{(25\ PAA\ +15w)}$).

f) The rejection of the organic molecules by the tight-pore membranes is influenced by both the M_W of the solute and by the physicochemical parameters. With respect to membrane type, rejection was dependent on polarity. Molecules with a high dipole moment (hydrophilic compounds) have lower retentions compared to non-polar molecules (hydrophobic compounds).

g) From the results obtained in this study, it appears that a good correlation exists between rejection and the different parameters (i.e: molecular weight, diameter and polarity). Based on these results, it was hypothesized that the dominant rejection mechanism for NF membranes would be different depending on membrane material and the physico-chemical properties of the target compounds. Better understanding of this aspect could lead to development/modification of PEI membrane for better rejection of organic solutes with low molecular weight (M_W).

h) The rejection of NaCl and $CaCl_2$ is much higher than that for the organic compounds at the same M_W, indicating that the rejection of ionic compounds is governed by electrostatic repulsion.The rejections of divalent ions was higher than those of monovalent ions due to electrostatic effects.

i) In fact, real waste water can be a mixture of several dissolved organic and inorganic compounds. Due to interactions between these compounds, the membrane performances can be improved or get worse. This means that NF experiments with (representative) mixtures of these compounds need to be performed to understand and tune the membrane performances in real applications. Thus, a water mixture containing 500ppm of organic and 500ppm of NaCl in water was tested. It was found that in this case, the organic rejection was lower than organic rejection measured for the binary mixture; probably due to salting out effect which limiting the transmembrane of water flux (lower swelling of the membrane) and also increasing the activity coefficient of organic compound.

References

1. L. Firdaous, F. Quemeneur, J. Schlump, J. Maleriat, Modification of the ionic composition of salt solutions by electrodialysis, Desalination 167 (2004) 397–402.
2. S. Madaeni, V. Kazemi, Treatment of saturated brine in chlor-alkali process using membranes, Sep. Puri. Techn. 61 (2007) 72–78.
3. C. Langer, J. Economy, Chemical modification of P84 copolyimide membranes by polyethylenimine for nanofiltration. J. Membr. Sci. 327 (2009) 49-58.

4. Z. Wang, J. Economy, Novel method to make a continuous micro-mesopore membrane with tailored surface chemistry for use in nanofiltration, J. Membr. Sci. 308 (2008) 191-196.
5. W. Mark(2007), the guidebook to membrane desalination technology, Balaban desalination publications ISBN 0-86689-065-3.
6. V. Freger, T. Arnot, J. Howell, Separation of concentrated organic/inorganic salt mixtures by nanofiltration , J. Membr. Sci. 178 (2000) 185-193.
7. L. Nghiem, A. Schäfer, T. Waite, Adsorptive interactions between membranes and trace contaminants, Desalination 147 (2002) 269–274.
8. L.Nghiem, A. Schäfer, M. Elimelech, Removal of natural hormones by nanofiltration membranes: measurement, modeling, and mechanisms, Environ. Sci. Technol. 38 (2004) 1888–1896.
9. Y. Yoon, R.M. Lueptow, Removal of organic contaminants by RO and NF membranes, J. Membr. Sci 261 (2005) 76-86.
10. X. Zhou, B. Dong, the effect of different organic fraction on membrane flux declines, Environmental Science 30 (2009) 432-438 .
11. C. Jarusutthirak, S. Mattaraj and R. Jiraratananon, Factors affecting nanofiltration performances in natural organic matter rejection and flux decline, Sep. Puri. Techn. 58(2007) 68-75.
12. I. Kim, H. Yoon, K. Lee, Formation of integrally skinned asymmetric polyetherimide nanofiltration membranes by phase inversion process, J. Appl. Poly. Sci. 84 (2002) 1300-1307.
13. B.ven der Bruggen, J. Schaep, D. Wilms and C. Vandecasteele, Influence of molecular size, polarity and charge on the retention of organic molecules by nanofiltration. J. Membr. Sci. 156 (1999) 29–41.
14. C. Cleveland, T. Seacord and A. Zander, Standardized membrane pore size characterization by polyethylene glycol rejection. J. Environ. Eng. 128 5 (2002) 399–407.
15. S. Darvishmanesh,A. Buekenhoudt, J. Degrève, B. Van der Bruggen, Coupled series-parallel resistance model for transport of solvent through inorganic nanofiltration membranes. Sep. Puri. Techn 70 (2009) 46-52.
16. I.M. Smallwood, Handbook of Organic Solvent Properties, Butterworth-Heinemann (1996).

17. Y. Kiso, Y. Sugiura and K. Nishimura, Effects of hydrophobicity and molecular size on rejection of aromatic pesticides with nanofiltration membranes, J. Membr. Sci. 192 (2001) 1–10.
18. K. Agenson, O. Jeong and T. Urase, Retention of a wide variety of organic pollutants by different nanofiltration/reverse osmosis membranes: controlling parameters of process, J. Membr. Sci. 225 (2003) 91–103.
19. L. Braeken, R. Ramaekers, Y. Zhang, G. Maes, B. Bruggen and C. Vandecasteele, Influence of hydrophobicity on retention in nanofiltration of aqueous solutions containing organic compounds, J. Membr. Sci. 252 (2005) 195-202.
20. K. Kimura, S. Toshima, G. Amy and Y. Watanabe, Rejection of neutral endocrine disrupting compounds (EDCs) and pharmaceutical active compounds (PhACs) by RO membranes, J. Membr. Sci. 245 (2004) 71–78.
21. Z. Murthy , S. Gupta, Estimation of mass transfer coefficient using a combined nonlinear membrane transport and film theory, Desalination 109 (1997) 39–49.
22. G. Ludmila, E. Gibbins, S. Satinder, S. Lloyd, P. Roumiana, G. Andrew, Effect of concentration polarization and osmotic pressure on flux in organic solvent nanofiltration , J. Membr. Sci. 236 (2004) 121-136.
23. M. Nystrom, L. Kapia and S. Luque, Fouling and retention of nanofiltration membranes, J. Membr. Sci. 98 (1995) 249–262.

General Conclusions and Perspectives

General Conclusions and Perspectives

The primary objective of this dissertation was to prepare a suitable nanofiltration membrane for retention of relatively small organic molecules from drinking water. As a part of the problems of small organic molecule separations, we have studied from a fundamental point of view, how it was possible to develop new asymmetric elastomeric PEI membrane using phase inversion technology, and to achieve separation of aqueous organic mixtures by pervaporation and nanofiltration.

According to the set of the results obtained, we can draw the following conclusions:

- The feasibility of the synthesis of asymmetric membranes from rubbery polyimide (PEI) have been established clearly, the mechanical properties of these membranes being limited by the rate of the rubbery chain integrated in the imide structure; the morphology of the asymmetrical PEI membrane structure can be controlled by the conditions of phase inversion, and either lead to the formation of pores as a finger like, or to a spongy structure, either again to the formation of a thin dense layer with a very porous support.
- For the PEI membranes comprising a dense skin layer, the molecular selectivity of asymmetric PEI membranes is well proved in pervaporation, whatever the nature of the initial mixture, organic or aqueous, this result indicates that the skin surface is effectively dense, almost exempt of nanometrics pores, and that the separation mechanism corresponds mainly to the solution-diffusion model, as verified in pervaporation.
- In nanofiltration, it appears that the two parameters determining the selectivity of asymmetric PEI membranes are by order of importance polarity and molecular weight of the compound dissolved in water, this is related to the nature of the rubbery phase which hydrophilicity has shown on the one hand, to substantially increase the water flux of the PEI membranes compared to a fully aromatic polyimide and on the other hand, to disfavor the permeation of hydrophobic molecules.These results have the tendency to show that the mechanism of permeation with the prevailing asymmetric PEI membranes do not correspond strictly to that expected by nanofiltration, where predominates the molecular weight compounds in relation with the size of the pores of

the membrane; this seems coherent with the presence of a thin skin layer and essentially devoid of pores in the top surface of the asymmetric PEI membrane.

- The research work presented in this thesis not only illustrates that a rubbery polymer can be a good candidate for liquid-liquid separations such as aqueous organic mixtures, but also provides helpful phase inversion protocols, to improve the membrane performances. The knowledge gained in this thesis can be used to guide future researchers' work in many areas such as modification and development of polymers and aqueous organic treatment by pervaporation and nanofiltration.

Appendix A: List of publications

a- Publications

1. EL-GENDI Ayman, ROIZARD Denis, GRIGNARD Jacques and FAVRE Eric, Investigations of rubbery copolyimides for the preparation of asymmetric pervaporation membranes, Journal Desalin. Water Treat.14 (2010) 67-77

b- Proceedings

1. EL-GENDI Ayman, ROIZARD Denis, FAVRE Eric, Study of asymmetric polyimide films preparation for membrane separation technologies, Proceeding of STEPI 8th June 9-11, 2008

c- Oral presentations

1. ELGENDI Ayman, ROIZARD Denis, FAVRE Eric, Preparation and Evaluation of Asymmetric Polyimide Membranes (PEI) for Separation Organic Compounds from Water, 4 th seminare Franco- Russe 15-17 Octobre 2007, NANCY, France
2. EL-GENDI Ayman, ROIZARD Denis, FAVRE Eric, Preparation of asymmetric polyetherimide membranes for molecular liquid separations, international Conggress on Membranes and Processes (ICOM 2008) July 12-18, 2008, Honolulu, Hawaii, USA.
3. ELGENDI Ayman, ROIZARD Denis, FAVRE Eric, Study of asymmetric polyimide films preparation for membrane separation technologies ,8th European Technical Symposium on Polyimides & High Performance Functional Polymers, Polytech' Montpellier (SETPI 8), Université Montpellier II,S.T.L.; 9-11 june 2008
4. ELGENDI Ayman, ROIZARD Denis, FAVRE Eric,Asymmetric polyimides membranes for pervaporation separations, 5 th seminare Franco- Russe7-10 october 2008.
5. EL-GENDI Ayman, ROIZARD Denis, FAVRE Eric, Etude et préparation de films asymétriques de polyétherimides stables en milieu organique – Application en pervaporation, GFP 2008, Lyon : France (2008)
6. EL-GENDI Ayman, ROIZARD Denis, GRIGNARD Jacques and FAVRE Eric, Investigations of rubbery copolyimides for the preparation of asymmetric pervaporation membranes, Membranes Science and Technology Conference of Vis egrad Countries (PERMEA 2009), Prague Czech Republic, 7-11 June, 2009
7. EL-GENDI Ayman, ROIZARD Denis and FAVRE Eric, Study of asymmetric alkyl polyether-imide nanofiltration membranes, Membranes Science and Technology Conference of Visegrad Countries (PERMEA 2010), Slovakia, 4-8 september

d- Affiches

8. ELGENDI Ayman, ROIZARD Denis, FAVRE Eric, Pervaporation of organic solutions by polyetherimide membranes, 8éme Journée scientifique du GFP Garnd' Est, Mulhouse 17 juin 2008.
9. ELGENDI Ayman, ROIZARD Denis, FAVRE Eric, Pervaporation of organic solutions with polyetherimide membranes, Séminaire de l'Ecole Doctorale RP2E 15 janvier 2009

Appendix B: Résumé Français

Institut National Polytechnique de Lorraine- Ecole doctorale RP2E
Ecole Nationale Supérieure des Industries Chimiques
Laboratoire Réactions et Génie des Procédés

THESE

Présentée pour obtenir le titre de

DOCTEUR DE L'INPL

Spécialité:

GENIE DES PROCEDES ET DES PRODUITS

Présentée par

Ayman Taha ELGENDI

Préparation et Etude de Membranes Asymétriques Polyalcoxyétherimides (PEI) pour la Séparation de Composés Organiques de l'Eau

Soutenue publiquement le 11 Octobre 2010 devant le jury composé de :

Rapporteurs :	**RABILLER-BAUDRY Murielle**	**(Professeur, Université Rennes 1)**
	CABASSUD Corinne	**(Professeur, INSA)**
Examinateurs :	**DERATANI André**	**(Directeur de Recherche, CNRS)**
	LANGEVIN Dominique	**(Chargé de Recherche, CNRS)**
	ROIZARD Denis	**(Directeur de Recherche, CNRS)**
	FAVRE Eric	**(Professeur, INPL)**

Laboratoire Réactions et Génie des Procédés - UPR3349 CNRS – ENSIC

NANCY, France 2010

SOMMAIRE

SOMMAIRE ***337***

Introduction Générale ***343***

1. PARTIE 1: Etude bibliographique ***- 349 -***

2. Partie 2: Matériels et Méthodes ***- 365 -***

2.1 Les matériaux et leurs propriétés ***- 365 -***

2.2 Préparation de membranes denses PEI et membranes asymétriques PEI……- 366 -

2.3 Synthèse de membranes hybrides Organique/Inorganique - 368 -

2.4 Protocoles de préparation de membranes Kapton^{TM} (PI) denses et membranes Kapton^{TM} (PI) asymétriques ***- 370 -***

2.5 Caractérisation des membranes ***- 370 -***

2.6 Propriétés de séparation ***- 373 -***

2.6.1 La pervaporation ***- 373 -***

2.6.2 Mise en place du montage de nanofiltration (NF) - 380 -

3. Partie 3: Résultats et discussions ***- 387 -***

3.1 **Caractérisation des membranes PEI - 387 -**

3.2 Principaux résultats et discussions ***- 403 -***

3.2.1 Etude des propriétés de pervaporation ***- 403 -***

3.2.2 Résultats de Nanofiltration (NF) avec les membranes PEI ***- 419 -***

Conclusion générale ***435***

Nomenclature et Abréviations ***441***

Références bibliographiques ***442***

Introduction Générale

Introduction Générale

Le sujet de cette thèse propose d'utiliser la séparation par membrane pour la purification de mélanges aqueux contenant des molécules polluantes organiques par la perméation préférentielle de l'eau (sélectivité classique) et le rejet des composés organiques. Dans ce cas, le but recherché est le plus souvent la purification de l'eau en aval (production d'eau potable par ultra ou nanofiltration) ou la concentration amont d'espèces organiques (application pour des molécules à hautes valeurs ajoutées). Dans le cas d'une sélectivité inverse ou il y a passage des molécules organiques les plus grosses, le bilan énergétique est beaucoup plus intéressant car c'est l'espèce minoritaire qui permée.

Dans le cas de solutions aqueuses contenant des molécules organiques de petites tailles ou masses moléculaires très petites, les possibilités d'application de la nanofiltration restent encore mal connues. Les objectifs du travail de thèse seront de contribuer à l'amélioration des connaissances dans ce domaine en effectuant des essais de séparation de différents mélanges aqueux contenant des molécules modèles de diverses polarités. Comme cibles potentielles industrielles, on peut citer l'urée, le 2-propanol, le toluène, le pesticides,……

En effet tout en étant une ressource très abondante sur la terre, l'eau disponible est rarement utilisable sans traitement préalable et sa purification est incontournable pour de nombreux usages notamment dans le domaine alimentaire. De plus l'eau est aussi très souvent polluée par les activités humaines industrielles ou agricoles et son utilisation puis son rejet en milieu naturel pose aussi le problème de sa purification. Si les problèmes liés à l'élimination d'espèces organiques, ioniques ou de grosses molécules sont assez bien résolus, le cas de la séparation de petites molécules peu concentrées en milieu aqueux reste problématique.

La thématique correspond au besoin de développement de nouvelles méthodes de purification de mélanges aqueux contaminés par des petites molécules organiques, particulièrement des méthodes de purification par membrane, et à la compréhension des mécanismes mis en jeu pour améliorer l'efficacité de ces méthodes. L'une des solutions possibles est le développement de nouvelles technologies (propres) de dépollution et de régénération pour que les effluents rejetés dans le milieu naturel soient conformes à la réglementation. Depuis quelques années, les procédés membranaires se sont imposés dans ce contexte comme étant des procédés extrêmement efficaces. Ils sont associés non seulement au traitement des effluents mais également à leur recyclage, au développement de la production et aux économies de matières.

Au cours de ce travail, nous nous intéresserons particulièrement à deux techniques membranaires de séparation, que sont la nanofiltration et la pervaporation pour les mélanges liquides. Ce sont des procédés qui mettent en jeu des membranes asymétriques et denses permsélectives à l'un des composants des mélanges à traiter. Pour ces deux procédés, comme pour tout procédé membranaire, la membrane représente l'élément central le plus important, dont les caractéristiques déterminent l'utilité et l'efficacité de tout le procédé. C'est pour cette raison que plusieurs axes de recherches se sont orientés depuis quelques années vers l'élaboration de nouveaux matériaux plus performants et qui permettent d'avoir un compromis entre les deux propriétés fondamentales de la séparation, souvent antagonistes, à savoir la sélectivité et la perméabilité.

Cependant les procédés membranaires ne sont devenus économiquement compétitifs qu'après le développement des membranes polymères hautement perméables. Ces membranes sont moins coûteuses que les membranes inorganiques et leur mise en œuvre est nettement plus facile. Plusieurs types de polymères peuvent être utilisés comme les polysulfones, les polyamides et polyimides ou encore les polyetherimides. Dans notre laboratoire, nous sommes intéressés aux polyalcoxyétherimides, sur lesquels porte le travail de cette thèse.

Les polyetherimides sont des polymères à haute performance grâce à la combinaison d'excellentes propriétés : une stabilité thermique élevée, une résistance mécanique importante ainsi qu'une haute température de transition vitreuse. Des études statistiques rapportent que 47% des membranes polyetherimides sont utilisés en perméation gazeuse contre 5% utilisées en pervaporation [1].

Les polyimides aromatiques sont une classe bien connue de matériaux polymères, qui ont été largement étudiées depuis plus de 20 ans dans le domaine de la séparation par membrane. Comme polymères vitreux, ils possèdent de remarquables propriétés mécaniques et chimiques pour des matériaux organiques, mais en général leurs coefficients de perméabilité sont limités en raison de la rigidité de leur squelette carboné et de leur faible volume disponible; par conséquence leur application en séparation moléculaire est limitée à la séparation de gaz ou aux de procédés de filtration (MF, UF) [2].

Pour contourner ce problème et d'élargir le champ d'application de ces polymères très stables, nous avons étudié les propriétés d'une série de polyimides aromatiques comprenant un bloc éther souple et nous avons préparé des films asymétriques dans le but de parvenir à la réalisation de séparations liquide-liquide en NF. Utilisant diverses conditions expérimentales d'inversion de phase différents types de microstructures correspondant à des membranes de microfiltration ou de nanofiltration asymétriques ayant une surface supérieure dense

pourraient être obtenues et ensuite être testées pour le fractionnement par pervaporation et nanofiltration de modèles de mélanges liquides. Ainsi, l'objectif est le développement de ce type de nouvelles membranes PI asymétriques à blocs pour obtenir des membranes de hautes performances pour des séparations liquide-liquide.

Pour améliorer les performances de ces membranes initialement préparées sous une forme dense et homogène plusieurs modifications ont été apportées, à savoir:

- L'élaboration de copolymères à blocs pour contrôler l'architecture chimique des membranes selon l'application désirée.
- La préparation de membranes asymétriques dans le but de diminuer l'épaisseur de la couche active et augmenter par conséquent les flux des perméats.

Au cours de ce travail, différents types de membranes seront utilisées : des membranes de Kapton^{TM}, comme référence, et des membranes originales de polyetherimide préparées au laboratoire. L'influence de différents paramètres sur l'efficacité de la nanofiltration a été étudiée:

- paramètres moléculaires (masse molaire, forme, polarité),

-effet du type et morphologie de membrane,

-effet de la pression appliquée sur le rejet et le flux transmembranaire.

S'appuyant sur une recherche bibliographique préalable, les principales étapes de la thèse sont:

- la préparation d'une installation du nanofiltration dédiée, comprenant une cellule alimentée par une charge sous pression contrôlée (5-50 bar), une acquisition en ligne permettant de caractériser le flux et la concentration du perméat ;

- la préparation de membranes originales, à peau dense ou de type nanofiltration;

- la caractérisation des membranes (propriétés de surface, porosité, perméabilité à l'eau pure,..)

- l'étude de la séparation de mélanges modèles par nanofiltration et pervaporation (facteur de concentration,..);

- l'analyse des résultats. Une attention particulière sera portée à la compréhension des mécanismes de perméation.

Cette thèse est répartie en 3 parties:

- La première partie est une synthèse bibliographique, dans laquelle nous commençons par la présentation des différentes méthodes de synthèse et de caractérisation des membranes polyetherimides ainsi que le mécanisme de transport dans les films dense qui est celui de la solution-diffusion. Nous introduirons ensuite les deux techniques de séparation

membranaires étudiées à savoir la NF et la pervaporation. Pour chaque technique nous présentons les différentes applications connues, les grandeurs caractéristiques ainsi que les paramètres influençant les performances.

- **La deuxième partie** explique les différentes méthodes et dispositifs expérimentaux utilisés aussi bien pour la synthèse des matériaux que pour leur caractérisation en NF et en pervaporation.
- **La troisième partie** est consacrée a la description des résultats obtenues ainsi qu'à leurs interprétations.

PARTIE 1: Etude bibliographique

1. PARTIE 1: Etude bibliographique

Cette première partie traite de la bibliographie des techniques membranaires, elle donne un rappel détaillé sur les différentes méthodes de séparation, les caractéristiques de la pervaporation et les procédés baro-membranaires sont plus particulièrement détaillées ainsi que les applications, les avantages et les limitations de ces techniques dans le domaine de séparation des mélanges organique (toluène- n heptane), eau – alcools et eau-composés organiques. Les membranes à base de PEI utilisées en technique membranaire sont citées dans cette partie.

1.1 Définition d'une membrane :

Industriellement le terme membrane est utilisé pour désigner un système constitué de trois parties distinctes [3]:

- Un support macroporeux offrant une bonne résistance mécanique,
- Une couche intermédiaire assurant la liaison entre le support et la couche active,
- Une couche finale active de faible épaisseur Cette couche mince de matière permet l'arrêt ou le passage sélectif de substances dissoutes ou non, sous l'action d'une force motrice de transfert.

Dans ce qui suit, et par abus de langage, le terme membrane sera utilisé pour désigner la couche mince active.

Les critères de séparation des particules, des molécules et/ou des ions peuvent être **[4]**:

- La dimension et la forme
- La nature chimique
- L'état physique
- La charge électrique

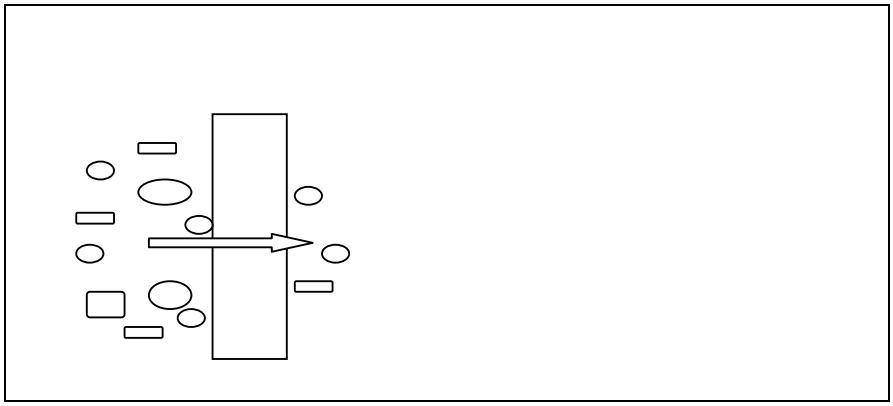

Figure 1.1: Schéma d'exclusion membranaire basée sur l'effet de la taille**.**

1.2 Classification des membranes [5,6 ,7]

1.2.1 Classification selon le mécanisme de séparation

Les mécanismes de séparation dans les membranes sont complexes et encore partiellement compris. Selon leur mécanisme de séparation, les membranes semi perméables peuvent êtres classées en 3 groupes : membranes échangeuses d'ions, membranes poreuses et membranes denses.

- **Membranes échangeuses d'ions:** Ce sont des gels denses ayant une charge positive (échangeuses d'anions) ou négative (échangeuses de cations). Les propriétés de séparation des ces membranes dépendent de la charge et la concentration des ions à leur surface**.** Elles sont utilisées en électrodyalyse pour le dessalement des solutions aqueuses par exemple.
- **Membranes poreuses**: Elles sont constituées d'une matrice solide comportant des trous ou des pores dont le diamètre est compris entre {NF(0.5 nm: 2nm), UF(2nm:5nm), MF (5nm à 10µm)}. En MF et UF, le mécanisme dépend principalement de la taille des pores et du rayon des solutés (convection dans un pore) : une particule est retenue par la membrane si sa taille est supérieure au diamètre des pores.

En NF, le mécanisme est aussi dépendant d'autres paramètres que ceux concernant l'aspect géométrique (i.e. taille soluté / diamètre de pore) : ce sont ceux caractérisant le soluté, la membrane, la charge à traiter dans les conditions de nanofiltration :

- forme moléculaire du soluté (sphérique ou non), charge portée, nature du contre-ion (mono ou divalent, polarité (polarisabilité) du soluté, point isoélectrique pour des protéines, couche d'hydratation pour des ions ;
- propriétés de surface de la membrane : nature hydrophile/hydrophobe, charge résiduelle ;
- pH de la solution aqueuse, force ionique, équilibre de Donnan, vitesse de cisaillement de la charge, pression osmotique pour les solutés concentrés, diffusion en couche limite pour les solutés peu concentrés (polarisation de concentration)

Les membranes poreuses sont préparées principalement par [8]**:**

- Frittage d'une poudre (de céramique, de métal, d'oxydes métalliques),
- Etirement d'un film polymères partiellement cristallisés,
- Irradiation d'un film polymère par des particules à haute énergie suivie d'une réaction de greffage.

- **Membranes denses *:*** Ce sont des membranes non poreuses. La diffusion des espèces a lieu dans les volumes libres situés entre les chaînes moléculaires du réseau de la membrane. Leur sélectivité est étroitement liée à l'affinité chimique du matériau qui les constitue vis-à-vis des espèces qui diffusent. Les membranes denses sont utilisées en perméation gazeuse et

pervaporation. Elles sont généralement obtenues suite à une évaporation lente du solvant : plus l'évaporation du solvant est lente plus l'épaisseur de la couche dense est importante. L'une des techniques les plus utilisées pour la préparation des membranes denses est le « Spin coating » qui consiste à appliquer un film uniforme mince sur un support plat qui est tourné à grande vitesse afin de répandre le fluide de manière homogène. La rotation n'est arrêtée que lorsque l'épaisseur désirée du film est obtenue [9].

1.2.2 Classification selon la morphologie

Selon leur morphologie, les membranes peuvent être classées en deux catégories**:**

- **Membrane symétrique *:*** c'est une membrane ayant la même structure sur toute son épaisseur (structure isotrope)
- **Membrane asymétrique *:*** la structure de la membrane varie d'une couche à une autre (structure anisotrope).

Les membranes asymétriques sont généralement constituées de deux couches : une fine couche dense (0.1µm à 2µm) supportée par une couche poreuse plus épaisse (100µm à 500µm). La couche poreuse sert seulement de support et n'a aucun effet sur les propriétés sélectives de la membrane.

Il existe deux catégories principales de membranes asymétriques:

- **Membranes asymétriques homogènes**

La technique utilisée est l'inversion de phase qui permet de préparer des membranes asymétriques polymériques à partir du même matériau.

La préparation se déroule en 3 étapes consécutives [5**]:**

I. Le polymère est dissout dans un solvant approprié de manière à obtenir une solution avec un pourcentage massique en polymère entre 10% et 30%,

II. Des films d'une épaisseur allant de 100µm à 500µm sont préparés par coulage sur des moules appropriés,

III. Les films sont plongés dans un non solvant du polymère: L'entrée du non solvant dans la solution de polymère provoque une séparation entre une phase riche en polymère. constituant la matrice continue du matériau et une phase discontinue pauvre en polymère à l'origine des pores.

- **Membranes asymétriques composites** :

Ces membranes sont obtenues par la déposition d'une couche polymérique fine et homogène sur une structure poreuse qui sert de support. Plusieurs méthodes sont utilisées pour la synthèse de telles membranes dont la plus ancienne est le moulage d'une solution de

polymère sur une sous couche poreuse. Après évaporation du solvant une couche mince de polymère est obtenue, dont l'épaisseur dépend de la concentration du polymère dans la solution utilisée. L'inconvénient majeur de cette méthode est que le solvant utilisé pour dissoudre le polymère peut parfois attaquer la structure microporeuse. Plus récemment, des méthodes basées sur la polymérisation inter faciale des monomères à la surface de la couche poreuse ont été développées.

1.2.3 Classification selon la nature chimique

I. **Membranes homogènes *:*** Ce sont des membranes constituées d'une seule phase, qui peut être organique ou inorganique.

- **Membranes organiques**: Généralement ce sont des membranes polymérique peu coûteuses (dérivés de la cellulose, polyamides, polyimides, polysulfones, polyethersulfone)
- **Membranes inorganiques**: Ces membranes ont une stabilité chimique, mécanique et thermique supérieure aux membranes polymériques, mais sont par contre plus coûteuses (zircone, oxyde Ti) .

II. **Membranes hybrides:** Ce sont des membranes mixtes faites de polymères et de matériaux inorganiques. L'intérêt de ces membranes réside dans la combinaison des propriétés apportées d'une part, par la matrice polymère (facilité de mise en œuvre, stabilité chimique), et d'autre part, par celles du matériau inorganique (dureté, stabilité thermique) [10]**.**

1.3 Différents types de membranes [7]

1.3.1 La membrane microporeuse (MF, UF)

Elle est constituée d'une matrice solide dont le diamètre des pores est compris entre 0,01 et 10 µm. La plus classique est obtenue par frittage d'une poudre de céramique, de métal ou, d'oxyde métalliques. Elle est fabriquée par étirement normal, à la direction de laminage ou d'extrusion de films polymères partiellement cristallisés. Soit, en soumettant un film mince de polymère à un flux important de particules à haute énergie , puis à une attaque chimique , il est possible d'y former des cavités cylindriques presque parfaitement calibrées, ces membranes sont dites à pores capillaires, leur porosité est fonction de la durée d'irradiation On prépare également des structures microporeuses par attaque chimique sélective de l'un des constituants d'un alliage métallique, ou d'un matériau vitreux (verre borosilicate) obtenu par démixtion. La majeure partie des membranes microporeuses organiques est produite par le procédé d'inversion de phase.

1.3.2 La membrane homogène non poreuse

C'est un film dense. La séparation des substances est alors directement liée à leur vitesse de transfert dans la membrane, c'est à dire leur diffusion et leur concentration dans la matrice membranaire.

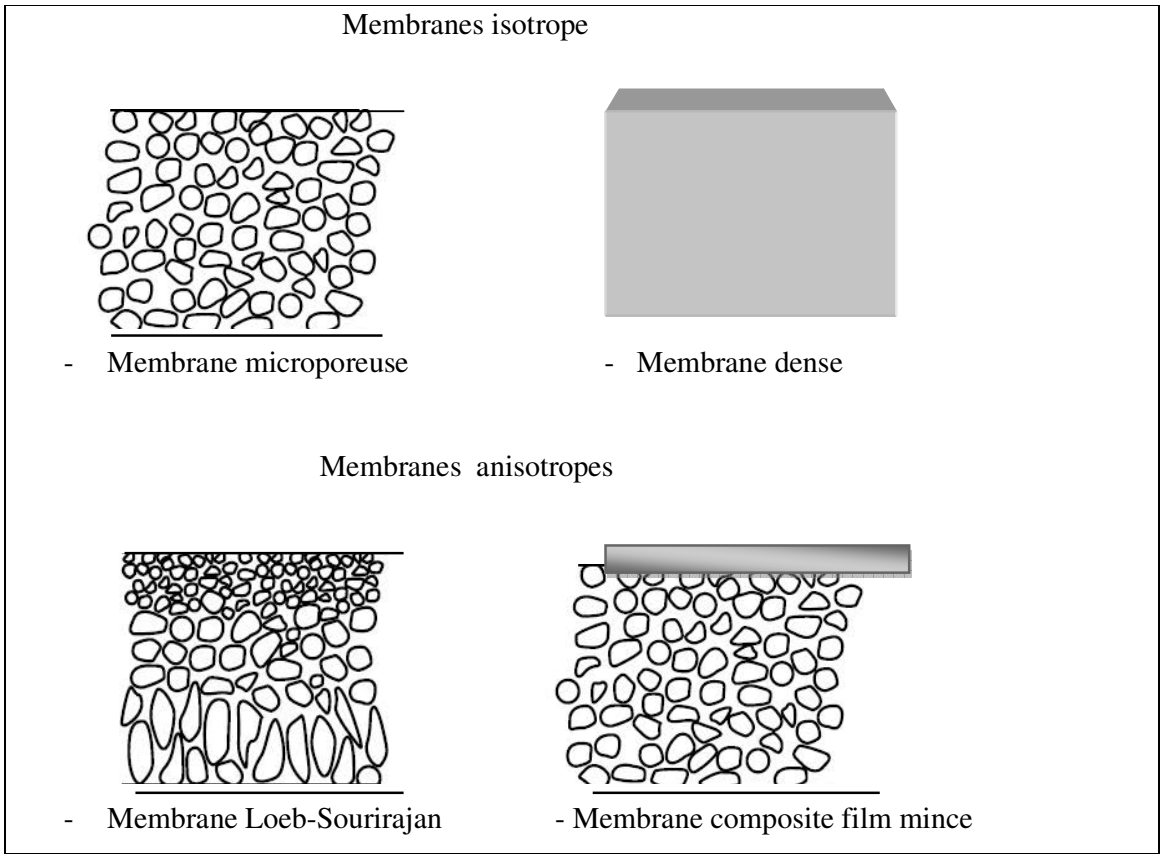

Figure 2.1: Schéma des principaux types de structure membranaire [7]**.**

1.3.3 La membrane échangeuse d'ions

Elle est constituée par un gel gonflé dont les parois des pores sont chargées positivement ou négativement de façon permanente aux pH d'utilisation La séparation est réalisée par l'exclusion de co-ions.

1.3.4 La membrane asymétrique

Les membranes asymétriques sont principalement utilisées pour la séparation d'espèces chimiques. Il faut rappeler à ce propos que les premières membranes qui n'étaient pas asymétriques se colmataient rapidement. Ces membranes sont constituées de deux couches superposées, une mince à 0,1 nm joue le rôle de pellicule semi – perméable et l'autre beaucoup plus poreuse, d'une épaisseur comprise entre 100 et 300 µm joue le rôle de support pour la première. Cette structure est représentée sur la figure 3.1 (a). L'avantage d'une

structure asymétrique réside dans le fait que les particules à séparer ne sont pas retenues à l'intérieur des pores de la membrane**.**

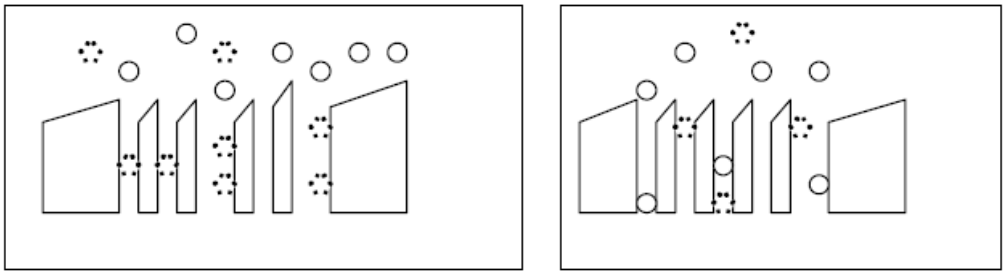

a. membrane asymétrique b. membrane symétrique

Figure 3.1: mode de rétention de particules.

1.4 Les avantages et les limitations des méthodes de séparation membranaire **[**11,12,13**]**

Les procédés de séparations membranaires ont en commun, plusieurs avantages et quelques limitations par rapport aux autres procédés de séparation (une demande énergétique limitée, respect de l'environnement**,….)**

1.4.1 Les avantages

Les méthodes de séparation membranaire permettent de travailler dans les conditions favorables suivantes:

1- procédé propre, grand respect de l'environnement et faible rejet de polluant, pas d'ajout de produits chimiques, ce qui ne signifie donc pas de contamination des perméats et rétentats.

2- Une extraction de produits en continu de milieux entièrement isolés de l'extérieur par le film séparateur et donc l'élimination de toute contamination croisée entre l'amont et l'aval (procédé continu).

3- Un caractère compact et modulaire des installations (intensification) et donc une construction sur mesure par ajout d'éléments standard et une maintenance souple.

4-Une séparation facile à automatiser.

5-Un besoin énergétique limité essentiellement à l'énergie de transport du perméant.

6- Une température modérée favorable à la séparation de composés thermosensibles.

7- La possibilité de concevoir des procédés hybrides, association avec d'autres méthodes de séparation (distillation, lavage de gaz, décantation).

8-Une sélectivité élevée, avec la possibilité de fractionnement des azéotropes.

9- Un coût d'exploitation modéré : énergie électrique comme fonctionnement, pas de produits consommables.

1.4.2 Les limitations

A coté, les nombreux avantages cités, les méthodes membranaires souffrent de certaines limitations:

- des prétraitements nécessaires, parfois très coûteux sont requis
- la durée de vie des membranes limitées à quelques années (4 -10 ans selon les procédés).
- un coût d'investissement relativement élevé et la recherche de matériaux membranaires de grande sélectivité.
- Les résistances chimique et thermique limitées des membranes, surtout les membranes polymère, phénomène de colmatage des pores (essentiellement en MF et UF).

1.5 Les méthodes de séparation membranaire [14]

La membrane est une couche mince qui permet l'arrêt ou le passage de certaines substances de mélanges, entre les deux milieux qu'elle sépare. La partie du mélange retenue par la membrane est appelée rétentat alors que celle qui traverse par la membrane est appelée perméat (Fig.4.1). La séparation se fait sous l'action d'une force motrice de transfert selon un mécanisme de séparation défini par les caractéristiques des membranes: taille de pore, affinités physicochimique, hydrophile. Les performances des membranes sont déterminées par deux paramètres, la perméabilité et la sélectivité.

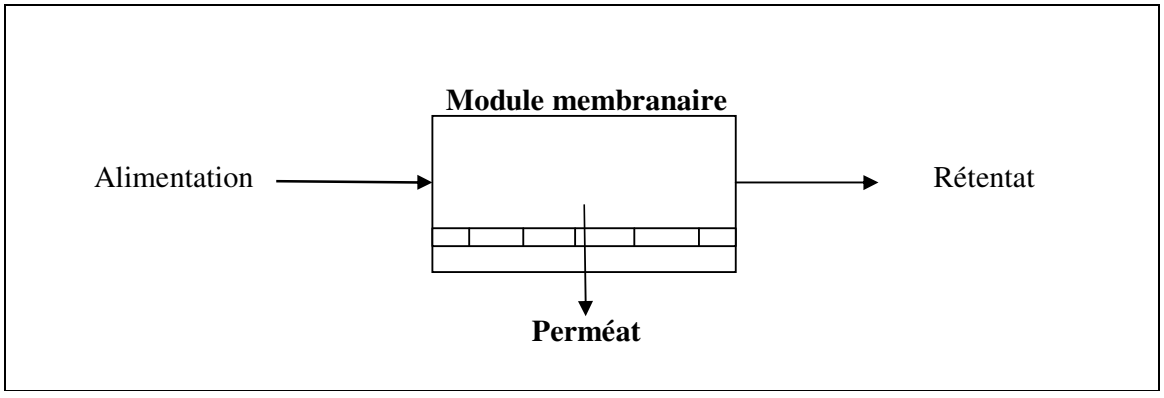

Figure 4.1: Schéma de base d'une séparation membranaire

1.5.1 La Pervaporation (PV)

La pervaporation est généralement utilisée pour fractionner des charges azéotropiques ou des mélanges dont la courbe d'équilibre liquide vapeur tend vers la diagonale du diagramme de Mc Cabe-Thiele. Elle peut dans ce cas se substituer à la distillation ou

l'accompagner dans un procédé hybride distillation-pervaporation. La pervaporation permet en effet de créer un nouvel équilibre de partage au niveau de la face amont de la membrane différent de celui obtenu par l'équilibre liquide-vapeur et peut donc être très sélective là où la distillation ne l'est pas [15-16]. La force motrice de la pervaporation est gradient de concentration . Le mécanisme correspond aux étapes principales de solution- diffusion ; il est expliqué dans la partie résultats.

Les applications de la membrane dépendent en fait de sa nature: si la membrane est hydrophile, elle permettra une déshydratation des solutions organiques alors qu'une membrane hydrophobe permettra plutôt d'extraire des composants organiques. Les applications industrielles de la pervaporation sont nombreuses [17-18]:

- La déshydratation de l'éthanol (plus compétitif que la distillation azéotropique en présence de Benzène)
- La détoxification du sang à l'aide d'échange gazeux artificiel à membrane.

1.5.2 Procédés Baro-membranaires.

Ces procédés sont devenus une alternative aux méthodes classiques de traitement de l'eau. Les procédés membranaires sont souvent utilisés, pour éliminer des constituants tels que les solides dissous, des molécules neutres, molécules chargées, des composés organiques, des eaux usées d'origine industrielles ou municipales [19]. La fréquence et la prévalence des micropolluants organiques tels que les pesticides et autres micropolluants organiques deviennent une vraie problématique dans l'eau potable, eaux usées. Les procédés membranaires sont de plus en plus répandus dans le traitement des eaux polluées et la valorisation des eaux usées pour des applications de réutilisation [20,21 ,22].

Il existe quatre principaux types de procédés de séparation membranaire dont la force motrice est la pression (Fig. 5.1):

I. Microfiltration (MF),
II. Ultrafiltration (UF),
III. Nanofiltration (NF),
IV. L'osmose inverse (RO).

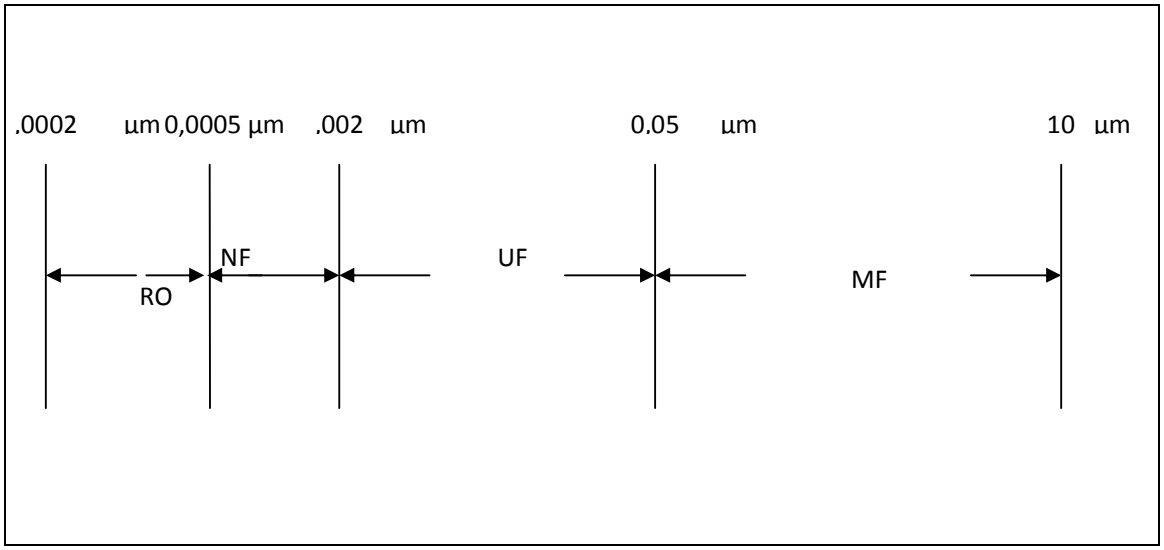

Figure 5.1: Définitions des procédés baro-membranaires sur la base de la taille des particules (molécules) retenues.

1.5.2.1 **Intérêt de nanofiltration** (NF)

La nanofiltration est une méthode barométrique bien connue et largement utilisée pour son efficacité dans le domaine de la production d'eau potable en utilisant une membrane organique hydrophile, il est possible en dépassant la pression osmotique de faire perméer l'eau et de retenir les sels en amont de la membrane.

La nanofiltration (NF), s'est révélée être un processus alternatif pour le traitement de l'eau potable, en raison sa forte perméabilité, de son aptitude à la désinfection, avec une utilisation minimale des produits chimiques, et de ses capacités à réduire la production de boues [23**,**24 **,**25**]**.

Des nombreux travaux ont étudié les mécanismes de rejet de soluté organique et du déclin de flux dans des membranes de NF. La matière organique peut être efficacement retenue par NF, par une combinaison de mécanismes de diffusion, de convection, et de mécanismes de répulsion électrostatiques. Les mécanismes dominants le transport de la matière organique par NF dépendent de nombreux paramètres autres que les strictes conditions de pression transmembranaire et la taille des corps dissous ; on peut ainsi citer les charges portées par les espèces et/ou la membrane, le type de contre-ion (mono ou divalent), la polarité (pour les espèces neutres), la formation de micelles (cas de la caséine), le pH (selon le point isoélectrique des protéines, la température, la vitesse de circulation de la phase liquide. Néanmoins, aucune directive claire n'a été établie pour choisir des membranes de NF pour l'usage dans le traitement d'eau potable.

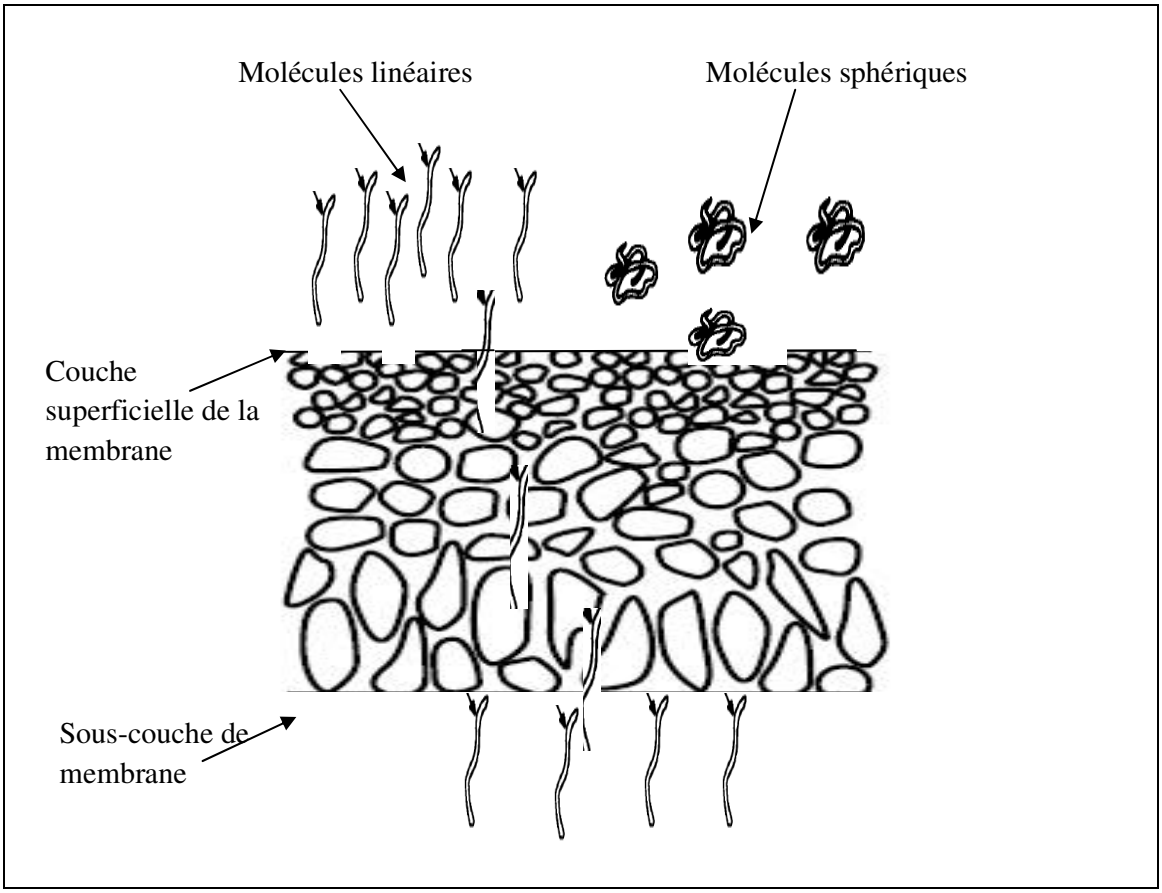

Figure 6.1: Rétention des molécules sphériques et linéaires par une membrane de NF par un mécanisme d'exclusion stérique.

1.6 Méthodes de préparation des PEI

1.6.1 Introduction générale sur les polyimides

Les polyimides sont des polymères de hautes performances grâce à la combinaison d'excellentes propriétés : une stabilité thermique élevée, une faible constante diélectrique, une température de transition vitreuse élevée et une grande résistance aux solvants [26]**.** Ils sont tellement résistants mécaniquement, chimiquement et thermiquement qu'ils remplacent souvent le verre et des métaux comme l'acier dans des applications industrielles très exigeantes comme l'aérospatiale**.** Les polyimides sont des polymères avec une fonction imide [27]. Il existe deux types de polyimide: des polyimides linéaires et des polyimides cycliques (Figure 7.1).

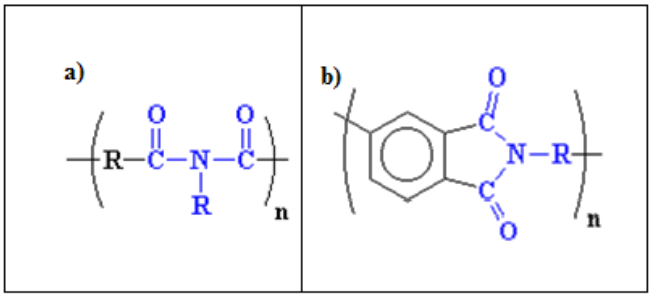

Figure 7.1: Structure d'un polyimide a) linéaire b) aromatique hétérocyclique [26]

Les polyimides aromatiques sont plus utilisés que les polyimides linéaires, ils représentent de ce fait la majorité des polyimides commerciaux (comme l'Ultem de G.E et le Kapton™ de Dupont Fig.8.1).

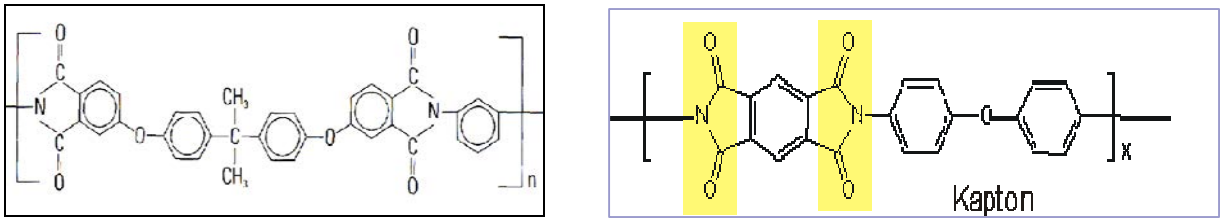

a. Ultem de G.E b. Kapton™

Figure 8.1: Formules de l'Ultem de G.E et du Kapton**.**

Les polyimides doivent leur grande résistance à un transfert de charge important entre les unités adjacentes sur une chaîne de polymère (Figure 9, a.1). Le transfert de charge fonctionne aussi entre les chaînes qui vont s'empiler les unes sur les autres (Figure 9, b.1)

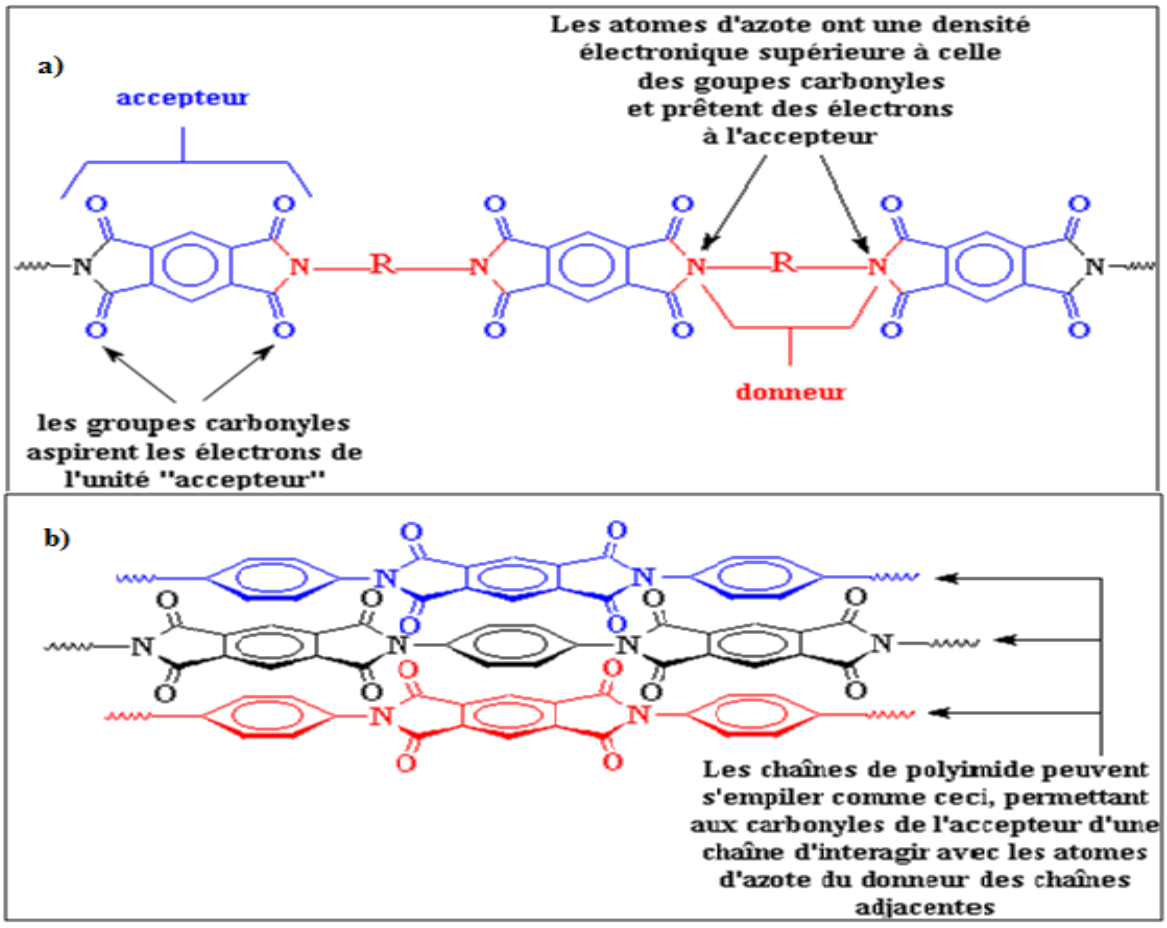

Figure 9.1: Transfert de charge dans un polyimide a) entre les unités adjacentes d'une même chaîne de polymère b) entre des chaînes différentes [8].

Certes ce transfert de charge confère aux PI une grande résistance mécanique, mais il diminue en contre partie leur solubilité ce qui rend difficile leur mise en œuvre, d'où la nécessité de faire des PI plus souples. Ceci peut être réalisé par l'introduction d'une liaison éther. Cette liaison donne au polymère plus de flexibilité sans pour autant diminuer de façon importante sa résistance intrinsèque.

Les polymères obtenus ainsi sont des polyalcoxyétherimides (PEI) et ont la formule générale présentée dans la figure 10.1.

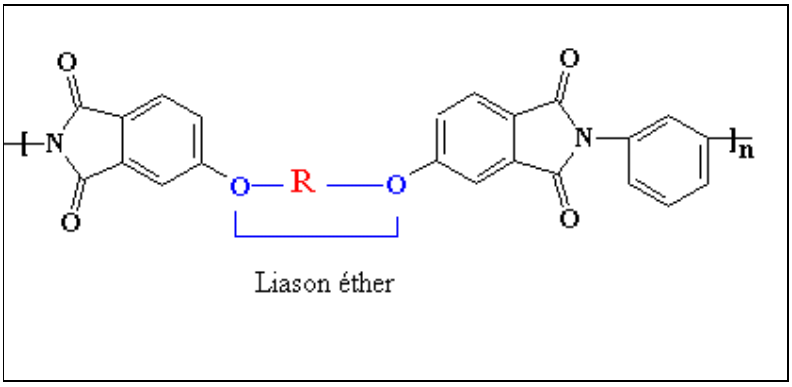

Figure 10.1 : Structure d'un polyalcoxyétherimide [8]

1.6.1.1 Principe de synthèse des polyalcoxyétherimides (PEI)

Les polyimides sont obtenus par la réaction d'un dianhydride et une diamine. Comme le montre à la Figure 11.1, cette réaction se fait en deux étapes consécutives **[26]:**

1. Le dianhydride et la diamine réagissent à température ambiante pour donner l'acide polyamique (APA) qui est un précurseur soluble du polymère,
2. L'APA est transformée en polyimide par cyclodéshydratation.

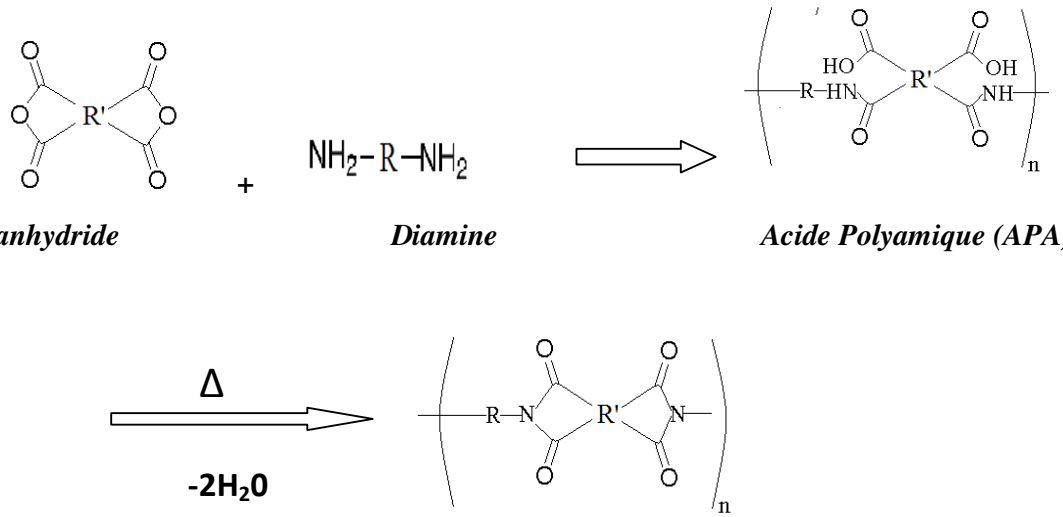

* R et R' peuvent être des groupements aliphatiques ou aromatiques.

Figure 11.1 : Réaction générale de synthèse d'un polyimide

L'introduction de la liaison éther dans ces polymères peut se faire de différentes méthodes:

- Par une réaction de substitution nucléophile (Figure 12.1) : Dans ce cas le polyimide est préparé comme expliqué ci-dessus (Figure 11.1) puis la liaison éther est créée par une réaction

de substitution nucléophile entre le OH phénolique d'un diol et un groupement partant (X) du polyimide **[9].**

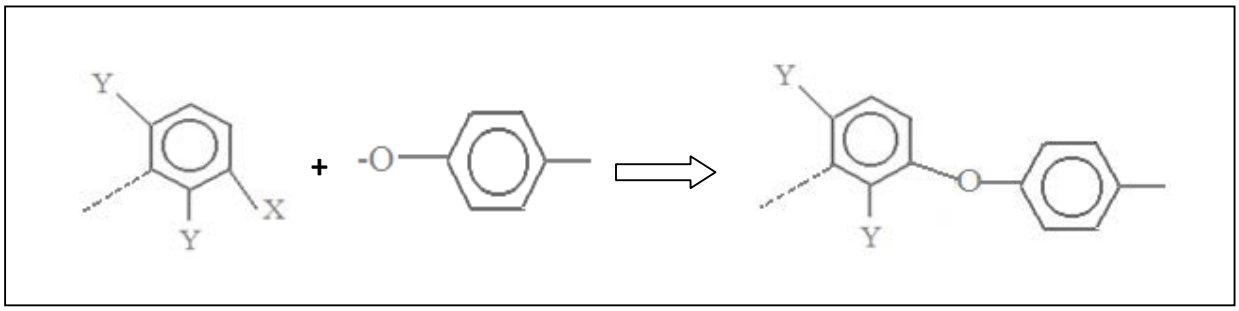

Figure 12.1 : Formation de la liaison éther par substitution nucléophile

Le groupement partant (X) est généralement un halogène ou un groupement nitro (NO_2), qui doit être activé par un groupement Y en ortho ou en para.

L'inconvénient majeur de cette méthode, est que tous les diols aromatiques ne sont pas forcément adéquats à la réaction de substitution, leur choix dépend de la structure de l'anhydride, ce qui limite les structures possibles des PEI synthétisés.

- En utilisant dans la réaction générale de synthèse des polyimides (Figure 11.1) des diamines comportant déjà une liaison éther. Ceci permet d'éviter une étape supplémentaire dans la synthèse et donne plus de choix dans les structures des polyalcoxyétherimides obtenus.

Partie 2: Matériels et Méthodes

2. Partie 2: Matériels et Méthodes

Les membranes de polyétherimide (PEI) requièrent deux étapes de synthèse pour préparer des membranes denses, et une étape d'inversion de phase pour préparer membrane asymétrique suivie de la cyclisation de l'acide amique en imide.

2.1 Les matériaux et leurs propriétés

Le polymère qui sera étudié au cours de ce travail est un copolymère à bloc obtenu par la réaction d'un dianhydride: l'anhydride 1, 2,4, 5-Benzènetétracarboxilique aussi connu sous le nom de dianhydride pyroméllitique (PMDA) avec deux diamines: une diamine aliphatique (la Jeffamine) et une diamine aromatique: la 4,4' Oxydianiline (ODA). Le solvant dans lequel se fait la réaction est le N, N- diméthylformamide (DMF).

- Jeffamine, Hunstman: Jeff600 – Jeff2000 Aldrich

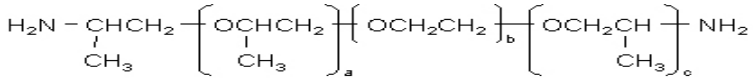

Jeffamine

Figure1, a .2: **Jeffamine**

- **4,4' Oxydianiline (ODA)**

Fournisseur: Aldrich NB : existe sublimé

Formule brute: C12H12ON2

Masse Molaire (g/mol): Mw= 200,24

Point de fusion (°C):190-192°C

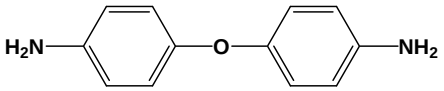

Figure1, b.2: **ODA**

NB: variations avec isomères 2,2' et 2,3' (F° 61 à 71° seulement)

-Anhydride 1, 2, 4,5-Benzenetetracarboxylique (PMDA)

Fournisseur: p160 Aldrich 97% (remainder free acid)

Formule brute: C10H2O6

Masse Molaire (g/mol): Mw= 218,12

Point de fusion (°C): 283-286°C.

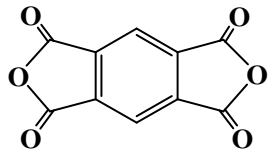

Figure1, c .2: **PMDA**

-**N, N-Diméthylformamide(DMF).**

Un solvant commun pour les synthèses des copolyimides. Il permet la solubilisation des réactifs et des oligomères de l'acide amique.

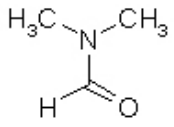

N,N-Diméthylformamide (DMF)

Figure1, d .2: DMF

2.2 Protocoles de préparation de membranes denses PEI et membranes asymétriques PEI

Conditions opératoires types:

- Solvants séchés sur tamis 4A plusieurs jours.
- Toutes les synthèses de Jeff600-PMDA-ODA ont été faites avec la même stoechiométrie: 0,4 mmole de Jeffamine 600; 1mmol de PMDA; 0,6 mmol ODA. On obtient ainsi l'acide polyamique (APA) à 30 masse % dans la DMF.
- Toutes les préparations ont été réalisées à t° ambiante, sous atmosphère Argon.

2.2.1 *Protocole de préparation membrane dense*

Les membranes de référence pour notre étude sont des membranes denses homogènes. La préparation de membranes denses est faite en deux étapes essentielles, la première étape une réaction addition entre une diamine et un anhydre pour former l'acide polyamique, la deuxième étape consiste à transformer l'acide polyamique en polyimide par une cyclodéshydratation thermique, autrement dit par élimination des molécules d'eau. La préparation de membranes dense PEI est décrite dans la Fig. 2.2.

2.2.1.1 Synthèse en deux étapes

i. Etape 1: Préparation de l'acide polyamique (APA)

Après solubilisation des Jeffamine dans du DMF (une solution de 15% de solide), l'anhydride (PMDA) est ajouté doucement sous forme solide; le temps de réaction est de 5 heures. L'amine aromatique (ODA) est ajoutée sous forme solide au milieu réactionnel et la réaction est arrêtée après 36h. Le groupement R représente la partie aliphatique ou aromatique de la diamine qui réagir avec l'anhydre.

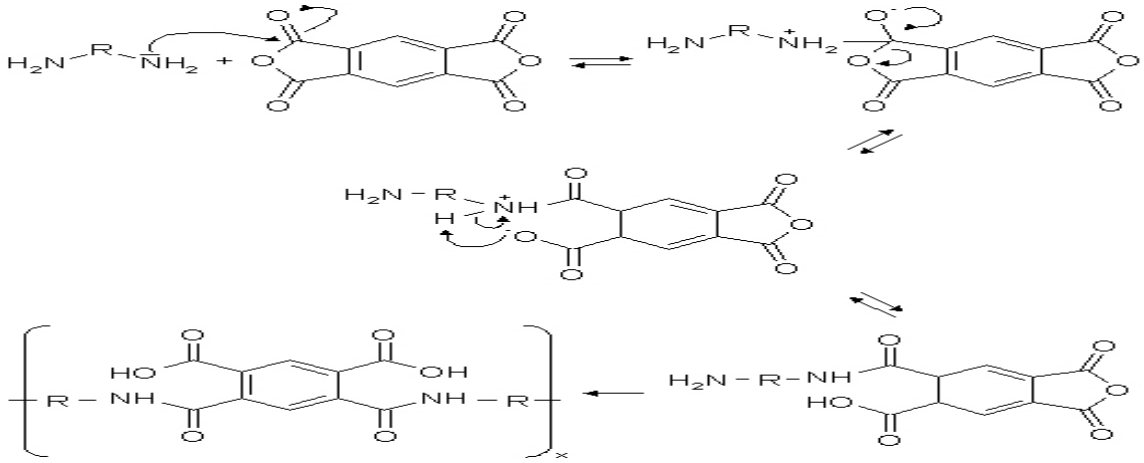

Figure 2, a .2 : préparation de l'acide polyamique.

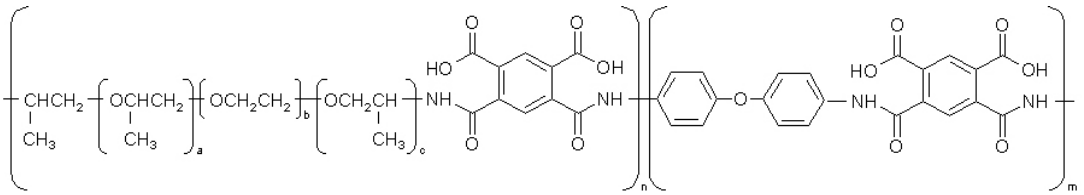

Figure 2, b.2: Formule de l'acide polyamique obtenu.

ii. Deuxième étape: préparation du PEI

Dans la deuxième étape, l'acide polyamique formé est coulé sur des moules en téflon ou en verre. Une période de 12 heures à 80-90°C est nécessaire pour l'évaporation du solvant; puis le film subit un traitement thermique classique de cyclodéshydratation sous vide: 1heure à 100, 1heure à 150, 1heure à 200°C consécutivement, le polymère (PEI) obtenu est un copolymère à bloc comportant deux parties différentes:

Une partie aliphatique: qui confère au polymère une certaine souplesse,

Une partie aromatique: qui constitue la partie rigide du polymère.

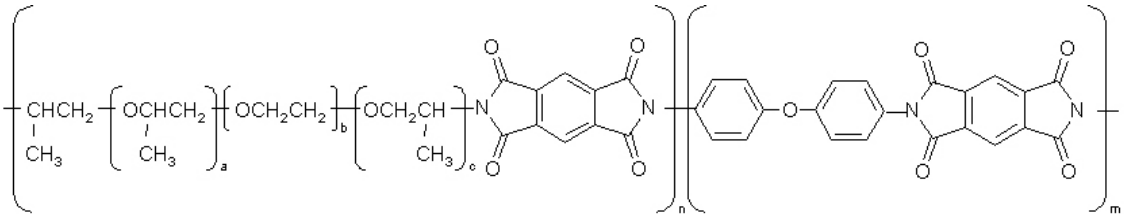

Figure 3.2: Formule du PEI obtenu.

2.2.2 *Protocole de préparation des membranes asymétriques*

Conditions opératoires types: comme pour les membranes denses

La PEI membrane asymétrique est préparé par inversion de phase dans les étapes suivantes.

I. Préparation de solution [étape de mélange]

L'acide polyamique (APA) est prépare comme pour la première étape de la membrane dense par polymérisation en condensation de solution à la température ambiante.

II. Étape de préparation des films

Le dégazage pour l'acide polyamique (APA) sous vide pendant 1 h est importante pour éviter de formation de bulles en membrane. Après dégazage, la solution de copolymère est coulée sur des plaques de verre en utilisant un applicateur de film permettant d'obtenir un film

plan dont l'épaisseur avant séchage est d'environ de 100 à 500 µm selon l'applicateur. Ces films liquides sont conservés à température ambiante de 1 à 3 minutes avant immersion dans un bain de non solvant ce qui permet une pré-concentration.

III. Étape d'immersion

Les plaques de verre sont immergées dans un bain de coagulation contenant l'eau pure à une température comprise entre10 à 20^0C pendant 1 à 3h. Aussitôt le film de polymère immergé devient blanc-jaune et perd sa transparence. Selon le temps de pré-concentration à l'air, le film se décolle plus ou moins facilement de la plaque de verre.

IV. Étape de séchage à l'air

Après d'immersion dans l'eau, les moules sont retirés et laissés sécher 1 ou 2 jours à température ambiante à l'air, on obtient un film qui redevient presque blanc-jaune, plus résistant. Résistance mécanique: les films non secs peuvent être manipulés facilement sans se déchirer.

V. Étape de cyclisation sous vide

La cyclisation des films d'APA en polyimide correspondant est réalisée thermiquement par chauffage sous vide pendant 1 h aux températures respectives de 373, 423 et 473 K. Après cyclisation, nous avons décollé la membrane film du support.

2.3 Synthèse de membranes hybrides Organique/Inorganique

Pour modifier les propriétés des PEI (résistance mécanique, perméabilité,…) différents charges de silice ont été incorporées aux solutions d'acide amique.

L'intérêt de ces matériaux hybrides réside dans la synergie des propriétés à la fois de la matrice polymère (facilité de mise en œuvre, flexibilité,...) et du matériau inorganique (dureté, stabilité thermique...).

2.3.1 *Synthèse de la phase inorganique par le procédé sol-gel*

Le procédé sol-gel est un procédé permettant l'obtention d'un réseau d'oxyde à partir d'alcoolates $M(OR)_n$ (où M est un métal ou le silicium et R un groupement organique alkyle C_nH_{2n+1}) par une suite de réactions d'hydrolyse et de condensation à une température modérée (20 à 150 °C). Comme le montre la Figure 4.2, la réaction se divise en deux étapes principales **[26]**:

1) L'hydrolyse des groupements alcoxy (OR) en groupement hydroxy (OH) lorsque les précurseurs $M(OR)_n$ sont mis en présence d'eau. Cette réaction est catalysée en milieu basique et en milieu acide, sa vitesse est minimale à pH 7.
2) Condensation des groupements hydroxy pour former un pont M-O-M.

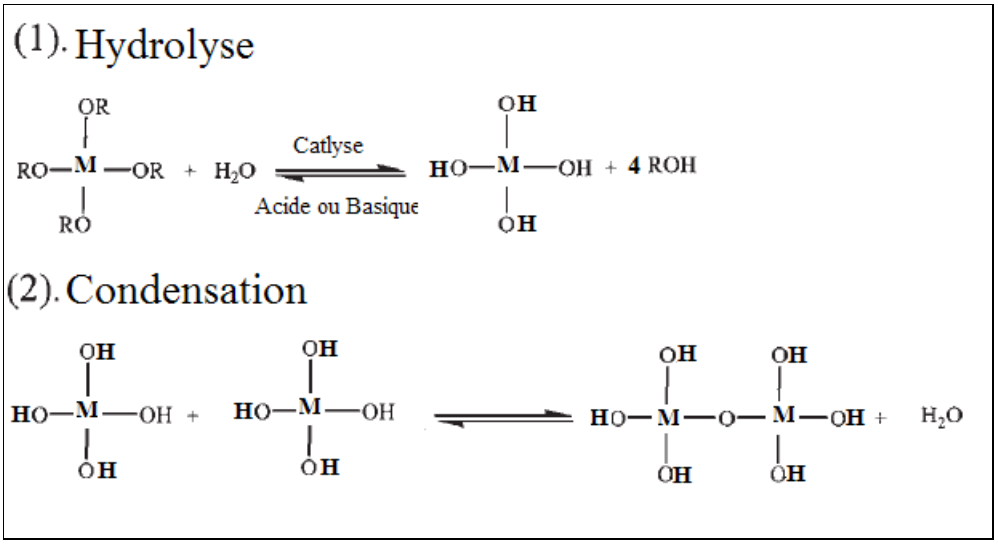

Figure 4.2: Réactions générales du procédé sol-gel [7,26]

- **<u>Avantages et inconvénients du procédé sol-gel</u>**

L'avantage du procédé sol gel est qu'il permet de contrôler non seulement la morphologie mais aussi la taille des particules de silice. Les particules ainsi obtenues sont de formes sphériques et relativement mono-disperses.

2.3.2 *Protocole de préparation de membranes hybrides dense*

La solution d'APA est préparée selon le même protocole décrit précédemment Les charges inorganiques peuvent êtres incorporées dans le matériau polymérique de deux manières différentes :

- Par voie directe: En incorporant des particules solides nanométriques du matériau inorganique dans la solution d'APA.
- Par voie indirecte: par la synthèse in situ de particules inorganiques .Cette synthèse se fait par la méthode Sol-Gel à partir du tétra-méthyle-ortho-silicate (TMOS).

Voie directe

- Les particules nanométriques non poreuses de SiO_2 sont ajoutées à la solution d'APA selon le pourcentage massique souhaité.

  On dispose de un type des particules de silice: silice hydrophile (12nm).
- La solution est mélangée pendant 6 heures à température ambiante.
- La solution d'APA est coulée sur des moules en verre pour former des films minces de polymères.
- Le solvant est évaporé pendant une nuit à 80°C.

- Les films subissent une cyclodéshydratation sous vide à 3 températures successives: 100°C, 150°C puis 200°C (1 heure pour chaque température).

Voie indirecte

Le procédé qui sera utilisé pour la synthèse des particules de silice est le procédé sol- gel sans ajout d'eau.

- Le TMOS est ajouté à la solution d'APA.
- La solution est mélangée pendant 6 heures à 80°C un réacteur inerté par N_2.
- Puis le reste de la procédure est analogue au cas précédent.

2.3.3 *Préparation de membranes hybrides asymétriques*

La synthèse de ce type de membrane se fait par le même protocole que les membranes PEI asymétriques avec une étape supplémentaire d'incorporation de silice ou de TMOS comme expliqué auparavant.

2.4 Protocoles de préparation de membranes Kapton^{TM} (PI) denses et membranes Kapton^{TM} (PI) asymétriques

2.4.1 Préparation de membranes Kapton^{TM} (PI) denses

L'acide polyamique (APA) commercial est coulé sur des moules en téflon ou verre. Une période de12heures à 80-90°C est nécessaire pour l'évaporation du solvant; puis le film subit un traitement thermique classique de cyclodéshydratation sous vide: 3heures à 300°C consécutivement sont nécessaire pour obtenir PEI.

2.4.2 Préparation de membranes Kapton^{TM} (PI) asymétriques

L'acide polyamique (APA) commercial est coulé sur plaques de verre. Les plaques de verre sont immergées dans un bain de coagulation contenant l'eau pure à la température 10^0C pendant 1 h. Après une heure d'immersion dans l'eau, les moules sont retirés et laissés sécher 1 ou 2 jours à température ambiante. Les films subissent les mêmes étapes de cyclodéshydratation que pour les membranes Kapton denses.

2.5 Caractérisation des membranes

2.5.1 Caractérisation des membranes par la Microscopie Electronique à Balayage (MEB)

Les structures de peau de membrane pour les films plats asymétriques et denses de PAA&PEI - Jeff600-PMDA-ODA (0.4/1/0.6) ont été examinées en utilisant la microscopie électronique (MEB). La MEB permet de produire des images de haute résolution de la surface de la membrane. Dans notre cas, on a eu recours à cette méthode pour savoir si la membrane

est dense ou asymétrique et pour évaluer le taux d'asymétrie. Pour la membrane hybride, les images obtenues ne permettent pas d'avoir une idée sur la dispersion des particules nanométriques de silice car elles permettent seulement d'observer les particules dont la taille est supérieure à 1µm.

2.5.2 Spectroscopie infrarouge (FT-IR)

Pour suivre le bon déroulement de la synthèse de la membrane PEI, la spectroscopie infrarouge à transformée de fourier est employée.

2.5.3 *Propriété mécanique*

Les propriétés mécaniques des PEI synthétisés ont été déterminées en utilisant des éprouvettes de dimensions et de forme décrites dans la Figure 5.2. Ces éprouvettes sont découpées à partir de films (PEI et PI) ayant des épaisseurs de 200 µm. Les tests de traction ont été faits avec une machine de type INSTRON 5569, instrument piloté par PC. Les modules de Young, les contraintes rupture et les élongations correspondantes mentionnées dans cette étude sont la valeur moyenne de 3 mesures successives.

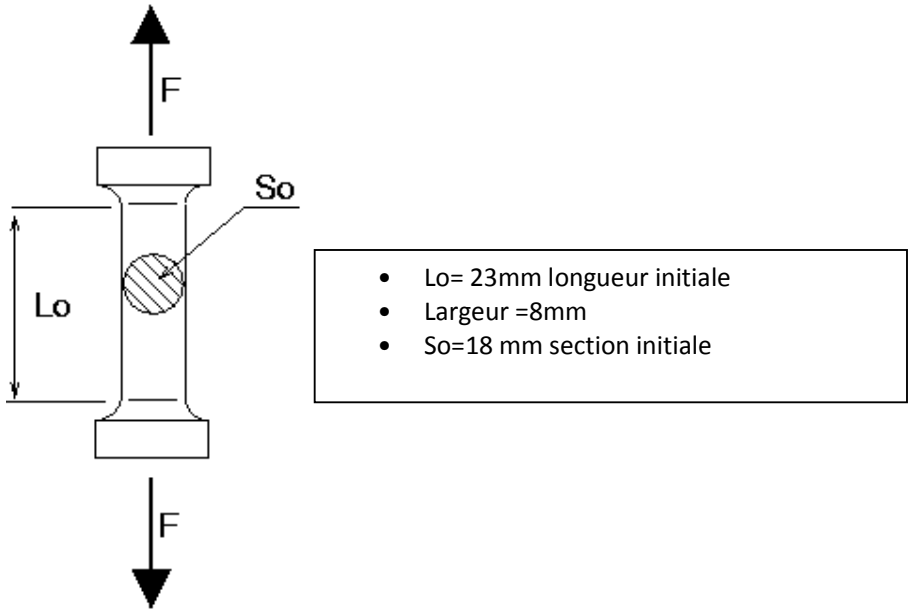

Figure 5.2: Forme et dimensions des éprouvettes de PEI utilisées dans les tests mécaniques.

2.5.4 *Analyse thermo-gravimétrique (ATG)*

Les analyses thermo-gravimétriques (ATG) ont été réalisées avec une microbalance de précision SETARAM, Setsys TG-12 avec un Système de chauffage de 10 C/ min(max 800 °C , précision $2*10^{-6}$g, balayage N_2). La perte de 10% en poids des PEI en fonction de la température ont été mesures en utilisant des échantillons de PEI sous ferme de disques coupés à partir des membranes préparées et séchées sous vide et ayant des épaisseurs de 200µm.

2.5.5 Propriétés du gonflement

Les tests de gonflement consistent à mesurer la variation de masse d'une membrane immergée dans une solution donnée en fonction du temps. Ces tests doivent être effectués avec le maximum de précision possible, car la variation de masse est généralement peu importante, ce qui peut conduire à une l'erreur expérimentale importante (>20%).

Ces tests sont effectués selon protocole suivant:

I. Une membrane parfaitement séchée de masse connue est introduite dans un récipient fermé contenant la solution. La membrane testée ne doit pas avoir une grande surface pour limiter les erreurs expérimentales sur les mesures.

II. Après 24h d'immersion, la membrane est retirée du récipient. Elle est séchée avec du papier, mise dans une boite hermétiquement fermée et pesée. Cette étape doit être effectuée le plus vite possible pour éviter l'évaporation du liquide absorbé. L'essuyage e est effectué pour enlever juste le liquide de surface.

III. Cette opération est répétée tous les jours jusqu'à stabilisation de la masse des échantillons.

IV. Le poids de l'échantillon initial enregistré avant l'immersion est noté (Wd) et le poids de l'échantillon final est noté (Ws). Le degré gonflement à l'équilibre a été calculé selon la formule suivante:

$$\text{Degré de gonflement } (\%) = 100.\ (Ws - Wd) / Wd \qquad (1.2)$$

2.5.6 Détermination des valeurs de coagulation (les points de trouble) pour la construction des diagrammes de phase

Les valeurs de coagulation ont été obtenues par des expériences appropriées. On a supposé que les conditions expérimentales étaient semblables à un pseudo système ternaire polymère-solvant-nonsolvant de comportement Fickien. En d'autres termes, problématique de diffusion couplée, le problème de frontière mobile, et la dépendance de concentration du coefficient de diffusion n'ont pas été considérés.

La valeur de coagulation a été déterminée par la méthode rapide de titrage décrite comme suit: l'eau différente (coagulant) a été titrée dans les solutions de 1 à 30wt.% PAA jusqu'à ce que la solution soit devenue blanc laiteux, correspondant aux points de trouble obtenus. La quantité de coagulant supplémentaire a été enregistrée comme valeurs de coagulation.

2.6 Propriétés de séparation

2.6.1 La pervaporation

La technique de pervaporation est appliquée pour la séparation mélanges organiques, des mélanges azéotropiques et la déshydratation d'alcool, à toutes les gammes de concentration, à condition de choisir la membrane appropriée. Les efforts de recherche effectués concernent la séparation des mélanges azéotropiques, de mélanges de constituants ayant des températures d'ébullition voisines et d'isomères structuraux. En général, c'est l'élimination du composé minoritaire, dans le mélange qui est recherché.

2.6.1.1 Propriétés de séparation par pervaporation des membranes PEI.

L'objectif est d'évaluer et de contrôler la porosité des membranes préparées par inversion de phase à partir de mesures de pervaporation, pour sélectionner des membranes de porosité les plus faibles possibles pour les études de nanofiltration. Des expériences de PV avec des mélanges (toluène-heptane, Eau-alcool) ont été effectuées pour essayer les membranes dense et asymétrique. Toutes les expériences ont été effectuées dans un état d'équilibre continu avec un vide aval de 1mmHg et une température constante d'alimentation pour des mélanges d'alimentation. La composition du perméat condensé par l'azote liquide est déterminée par chromatographie en phase gazeuse (FID- TCD; Mark 102G). Les sélectivités et flux de perméation (j) ont été mesurés pour plusieurs membranes analogues.

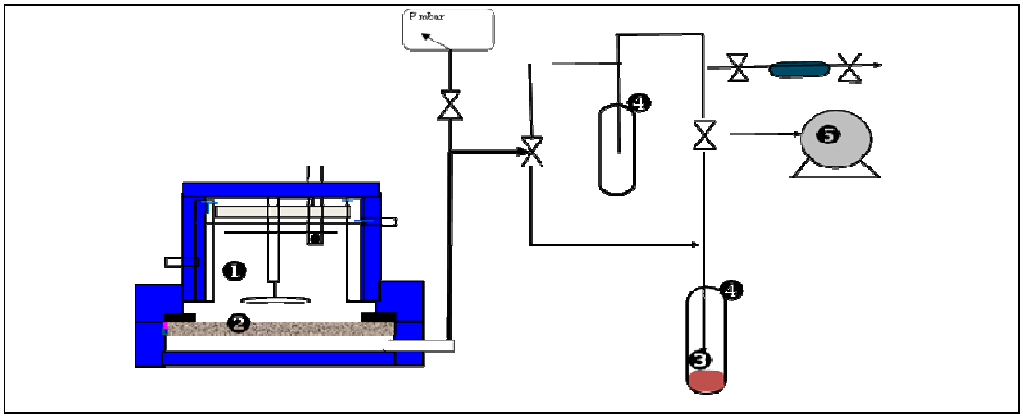

1- alimentation 2-Membrane 3- Perméat 4- Pièges 5- Pompe à vide

Figure 6.2: Schéma de l'appareillage de pervaporation.

Les différentes photos de la figure 7.2 représentent l'unité de pervaporation sur laquelle ont été menées les différentes expériences.

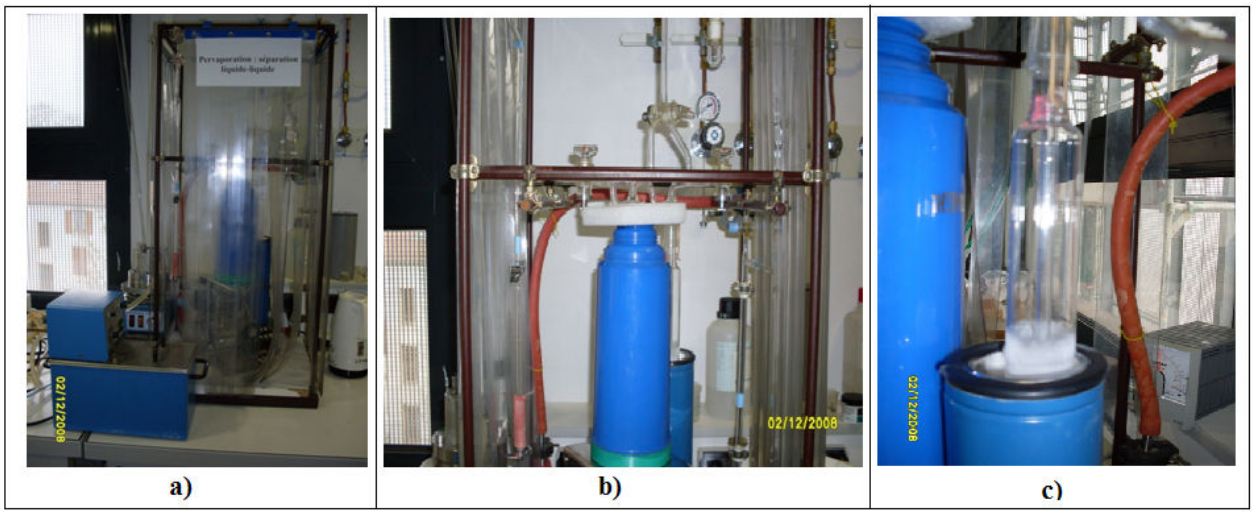

a) b) c)

Figure7.2:- a) Vue globale de l'installation de pervaporation b) Piège en cours de pervaporation c) Condensation du perméat par contact avec de l'azote liquide

I. 1er Cas: Séparation d'un mélange organique Toluène/n- Heptane (non polaire)

Le toluène et le n-heptane sont tous les deux des molécules organiques, apolaires, de tailles et de masses molaires très proches. La première est aromatique et non polarisable alors que la seconde est aliphatique et non polarisable. Les principales caractéristiques de ces solvants sont données dans le tableau 1.2.

Tableau 1.2: Les composants du mélange non polaire

Organique	Toluène	n- Heptane
Formule	C_7H_8	C_7H_{16}
Structure	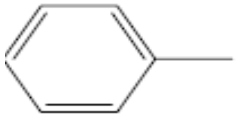	
Masse molaire (g/mol)	92.14	100.21
Densité (g/ml)	0.864	0.68
Pont d'ébullition (°C)	110.6	98-99
Fournisseur	Sigma Aldrich	Fisher Scientific

II. 2em Cas: Séparation d'un mélange aqueux (alcool, eau)

Ce deuxième test correspond à la déshydratation d'alcool (n-butanol, mélange azéotropique de l'éthanol).

Tableau 2.2: Les composants des mélanges alcool- eau

Alcool	éthanol	n- butanol
Formule	C_2H_6O	$C_4H_{10}O$
Masse molaire (g/mol)	46,07	74,12
Densité (g/ml)	0,7896	0,81
Pont d'ébullition (°C)	78,5	116-118
Fournisseur	Carlo Erba	Fluka

2.6.1.2 Grandeurs caractéristiques de la pervaporation [28,29 ,30]

Pour caractériser le comportement d'une membrane utilisée en pervaporation pour le fractionnement d'un mélange binaire A-B, deux grandeurs essentielles sont utilisées : le flux et la sélectivité.

1. **Le flux**

Le flux (J) est généralement exprimé en Kg/h.m^2. Au niveau du laboratoire cette grandeur est souvent rapportée à une épaisseur proche des épaisseurs utilisées industriellement (1µm, 5µm ou 10µm) pour s'affranchir du problème de variation de l'épaisseur d'un film à un autre, et pouvoir comparer les différentes valeurs. On parle alors de flux normés [13].

$J=Q/A*T$ (2.2)

Avec:

J: le flux total (kg / m^2 h)

Q: la masse totale du perméat recueilli kg

A: surface de la membrane m^2

T: le temps du perméat recueilli h

2. La sélectivité

La sélectivité peut être exprimée à l'aide deux facteurs adimensionnels α et β, mais se réfère toujours au composé préférentiellement transféré par la membrane**.**

- **Facteur de séparation α** défini par

$$\alpha= (Y_i*X_j)/(X_i*Y_j) \quad (3.2)$$

Avec ; X_i: Concentration dans la charge du composé préférentiellement transféré, et

X_j le 2^{em} component.

Y_i: Concentration dans le perméat du composé préférentiellement transféré, et Y_j le 2^{em} component.

Ce facteur est plus significatif d'un point de vue physico-chimique, il tend vers l'infini. lorsque la membrane devient parfaitement semi perméable.

- **Facteur d'enrichissement β** défini par $\beta = C_P/C_F = Y_i/X_i$ (4.2)

Avec ; C_P (enrichissement du perméat, la masse en aval) et C_F (concentration d'alimentation, en amont de masse) sont les fractions massiques dans le perméat et dans l'alimentation, respectivement.

2.6.1.3 Paramètres influant le procédé de pervaporation

La figure (8.2) Schématise le fonctionnement d'un module de pervaporation. Il existe plusieurs facteurs qui déterminent l'efficacité de la membrane, qui doivent être gardées en mémoire par touts les chercheurs avant d'essayer de travailler sur pervaporation ils sont:

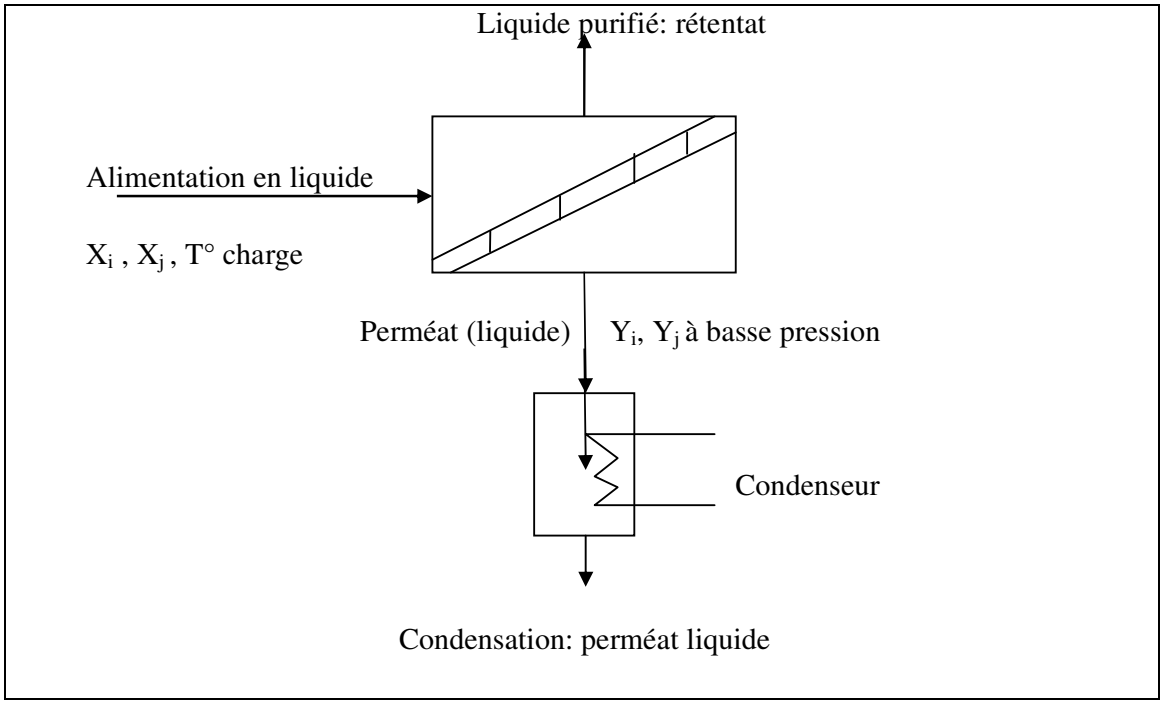

Figure 8.2: Schéma base du procédé de pervaporation [30]

I. **Epaisseur de la membrane** [31]

En général, des membranes fines sont utilisées afin d'obtenir un flux de perméation important. Il est généralement admis que dans un cas idéal la membrane est homogène et exempt de défauts; le taux de perméation est inversement proportionnel à l'épaisseur de la membrane tandis que l'épaisseur de la membrane n'a pas d'incidence sur la sélectivité de la membrane. C'est pourquoi, dans [21,32,33] les flux de perméation rapportés ont été

normalisées à une épaisseur de la membrane de 10µm, selon l'hypothèse d'une relation réciproque entre le flux de perméation et l'épaisseur de la membrane

II. Influence de la composition de la charge d'alimentation [34]

La permsélectivité d'une membrane de pervaporation dépend principalement de l'équilibre de gonflement qui s'établit au niveau de la face amont. Ce gonflement dépend de la composition du mélange étudié, de l'activité chimique de chacun des constituants et des effets de couplage entre eux.

III. Influence de la température [35]

L'influence de la température se manifeste au niveau de la sorption endo ou exothermique et de la diffusion qui est toujours activée par une augmentation de température La variation du flux en fonction de la température peut être décrite selon la loi d'Arrhenius**.**

$$J = J_0 \exp (Ep/RT) \qquad (5.2)$$

Si les énergies d'activation (Ep) pour les deux constituants purs sont équivalentes, la sélectivité est indépendante de la température. Dans le cas contraire, une augmentation de la température engendre une augmentation du flux et modifie la sélectivité.

IV. Influence de la pression [36]

I. Influence de la pression Amont

La pression amont est sans effet notable tant que sa valeur ne dépasse pas quelques Bar. Cependant au-delà de 10bar il peut y avoir deux effets antagonistes. Soit il peut y avoir une diminution du flux due à la compaction de la membrane, soit de façon analogue à l'osmose inverse le transfert sera favorisé au-delà d'une certaine pression dite osmotique **[13].**

II. Influence de la pression Aval

Contrairement à la pression amont, la pression aval a une grande influence sur l'efficacité de la pervaporation. Elle doit être maintenue au dessous de la pression de vapeur saturante du perméat. Dans tous les cas, une augmentation de la pression aval engendre une réduction du flux de perméation. C'est le composé le moins volatil (faible pression de vapeur) qui est le plus affecté et voit sa sélectivité diminuer.

2.6.1.4 Analyse des perméats par chromatographie gazeuse

Les perméats collectés sont analysés par chromatographie gazeuse. On commence tout d'abord par effectuer un étalonnage de la colonne. La courbe d'étalonnage (figure 9.2) représente le rapport d'aire entre le deux composants en fonction du rapport massique de ces deux composants.

L'équation de la droite d'étalonnage est de la forme: $A_T/A_H = p\ (m_T/m_H)$

$\Longleftrightarrow (m_H/m_T) = p\ (A_H/A_T)$

Avec:

p = pente de la droite d'étalonnage

m_T= masse du toluène

m_H= masse de l'heptane

On note RA= aire Toluène/aire Heptane = A_T/A_H

En effet la sélectivité de la membrane peut être représentée simplement par la concentration du toluène dans le perméat Cp qui est donnée par la formule suivante:

$$C_{P=}\frac{m_T}{m_{T+m_H}} \Leftrightarrow \frac{1}{C_p}=\frac{m_{T+m_H}}{m_T}$$

$$\frac{1}{C_p}=1+\frac{p}{R_A} \quad \text{d'où} \quad \Leftrightarrow C_p=\frac{1}{1+\frac{p}{R_A}}$$

Ainsi grâce à la pente p et au rapport R_A obtenu lors des analyses, on peut remonter à la sélectivité des membranes étudiées.

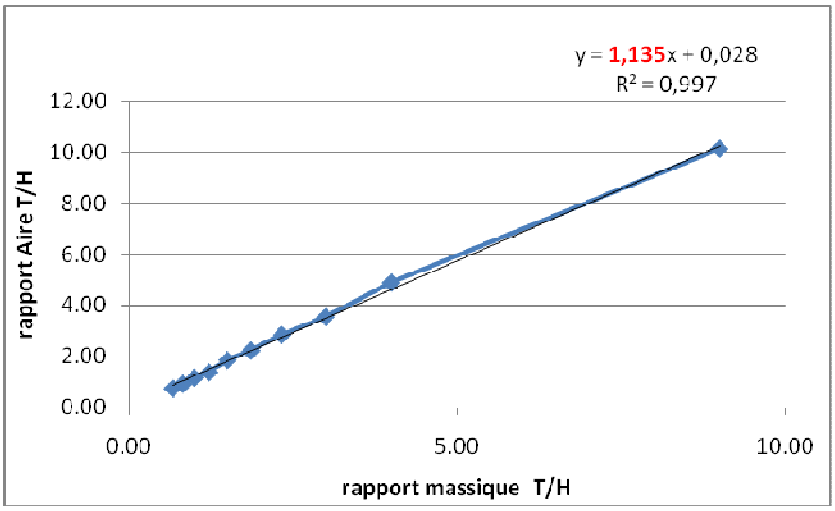

a . Rapport d'aire entre le toluène et l'heptane

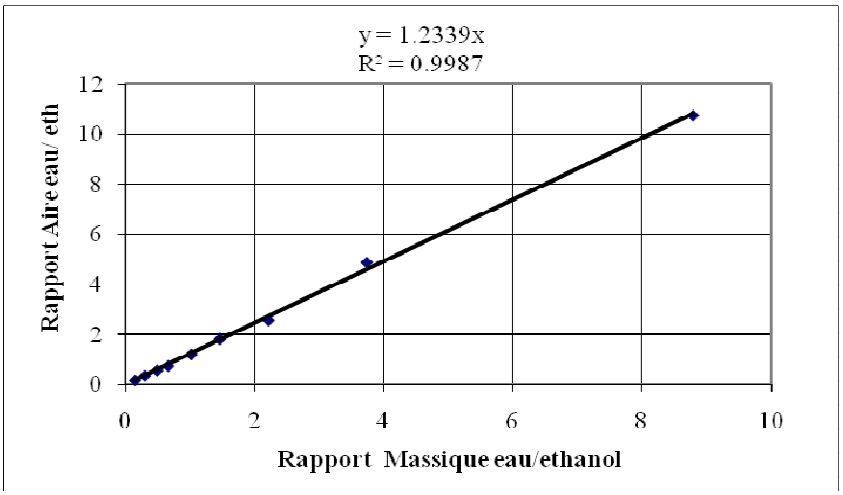

b. Rapport d'aire entre l'éthanol et l'eau

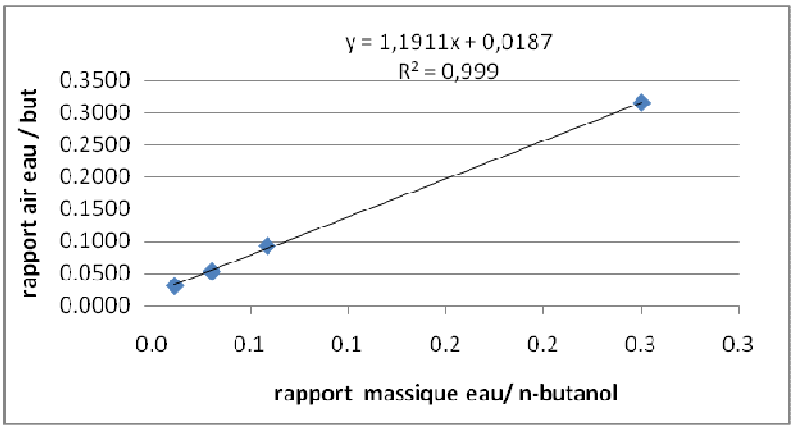

c. Rapport d'aire entre le n-butanol et l'eau

Figure 9.2: Courbes d'étalonnage en chromatographie gazeuse.

2.6.2 *Mise en place du montage de nanofiltration (NF)*

Il s'agissait de réaliser un montage nouveau de NF comprenant pompe, réservoir, circulation des fluides, cellule de perméation et dispositif d'analyse. Les premiers essais de NF avec de l'eau pure ont donc bien pu débuter, après étalonnage du système et contrôle des relations flux–pression. La pression maximum possible est de 60bar, pour des débits d'environ 1,3L/min.

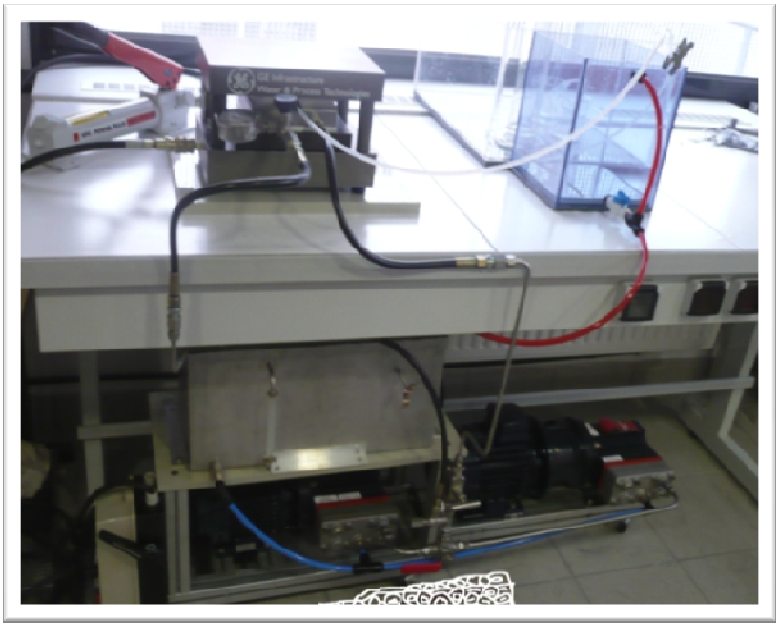

Figure 10: Montage de nanofiltration réalisé.

Tableau 3.2: Paramètres de fonctionnement pour le système cellulaire NF

Surface membranaire	41 cm^2
Pression maximale	69 bar (1000 psig)
Température maximale	177°C (350°F)
Débit maximum	1,3L/min
Epaisseur de la veine liquide	1000 µm

2.6.2.1 Essais de perméation pour les membranes PEI et Kapton^{TM} avec nanofiltration

Des essais nanofiltration avec les membranes PEI utilisant de l'eau pure comme charge ont été effectues pour vérifier la structure des membranes PEI dense et asymétriques et comprendre l'effet de la pression de fonctionnement et les paramètres hydrauliques sur le flux et la perméabilité. Ensuite, des essais avec des mélanges inorganiques/eau et organiques /eau ont été réalisés pour vérifier la séparation moléculaire et optimiser ouatant que possible le préparation de membranes asymétriques avec un flux fort et une bonne sélectivité.

Les essais de perméation des membranes PEI ont été réalisés à température ambiante sous une pression allant de 0 à 50 bar et une pompe d'alimentation avec un débit de 1,3L/min à l'aide de la cellule NF, le réservoir de la solution d'alimentation ayant une capacité de 31 L. La surface de la zone efficace de la membrane était de 41cm^2. Les premières membranes ont été conditionnées dans la cellule d'essai avec de l'eau pure en augmentant graduellement la pression jusqu'à 20 bar pendant au moins un jour. Dans chaque expérience, le flux réel (J) de l'eau pure et celui de la solution aqueuse (organique ou inorganique) ont été déterminés à partir de l'équation suivante:

$$J = \frac{Q}{A \times T_t}$$

avec:

Q: masse en kg de perméat A: surface de membrane active en m^2 Tt: temps en heure

Lorsque la solution aqueuse (organique ou inorganique) a été testée, le rejet (R) a été calculé comme suit:

$R\ (\%) = (1 - C_p / C_f) \times 100\%$,

avec:

C_f: la concentration de la solution d'alimentation Cp: la concentration du perméat

Les concentrations de C_P et des C_f ont été mesurées par dosage du carbone organique total (TOC). Toutes les membranes ont été testées avec une solution contenant un seul soluté. Les principales caractéristiques de ces matières organiques sont données dans le tableau 4.2 qui résume les propriétés les plus importantes. Le système NF est présenté dans la figure 11.2

Tableau 4.2: Caractéristiques des organiques

Composé organique	Source	Formule	MW (g/mol)	Densité (g/ml)	*PE / PF
Ethanol	*Carlo Erbo*	C_2H_6O	*46,07*	*0,789*	*PE:78,5*
2-Propanol	*Fluka*	C_3H_8O	*60.1*	*0,786*	
n-butanol	*Fluka*	$C_4H_{10}O$	*74,12*	*0,81*	*PE:116-118*
TEG	*Aldrich*	$C_2H_6O_2$	*150*		
PEG400	*Eastman kodak*	$(C_2H_4O)n\ H_2O$	*400*	*1,128*	*PF:6*
PEG1000	*Fluka*	$(C_2H_4O)n\ H_2O$	*950-1050*		*PF: 37-40*
PEG2000	*Aldrich*	$(C_2H_4O)n\ H_2O$	*2000*		*PF: 55-58*
	Fluka	$(C_2H_4O)n\ H_2O$	*1900-2200*		*PF: 50-52*
PEG6000	*Merck –*	$(C_2H_4O)n\ H_2O$	*5000-7000*		
Urée	*Fluka*	CH_4N_2O	*60,06*		*PF: 130-132*
Cyclohexane	*Prolabo*	C_6H_{12}	*84,16*	*0,78*	

*Avec ; PE : Point d'ébullition /PF : point de fusion

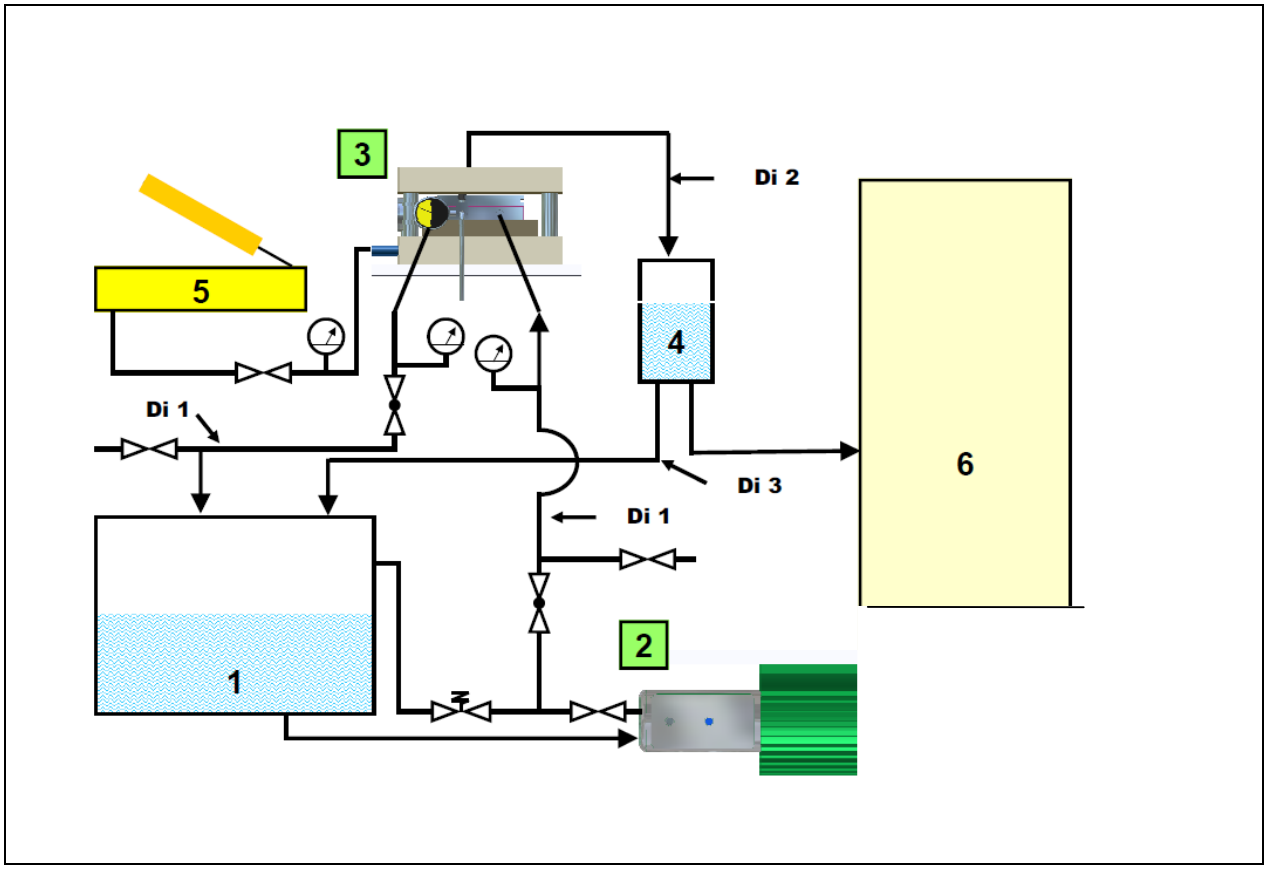

Figure 11.2 : **NF système mis en place** *:*

1: réservoir d'alimentation, 2: Pompe d'alimentation, 3: cellule de NF, 4: Perméat, 5: pompe hydraulique, 6: Analyseur de carbone organique (TOC), Di1:1/4", Di2:1/2", Di3:1/4".

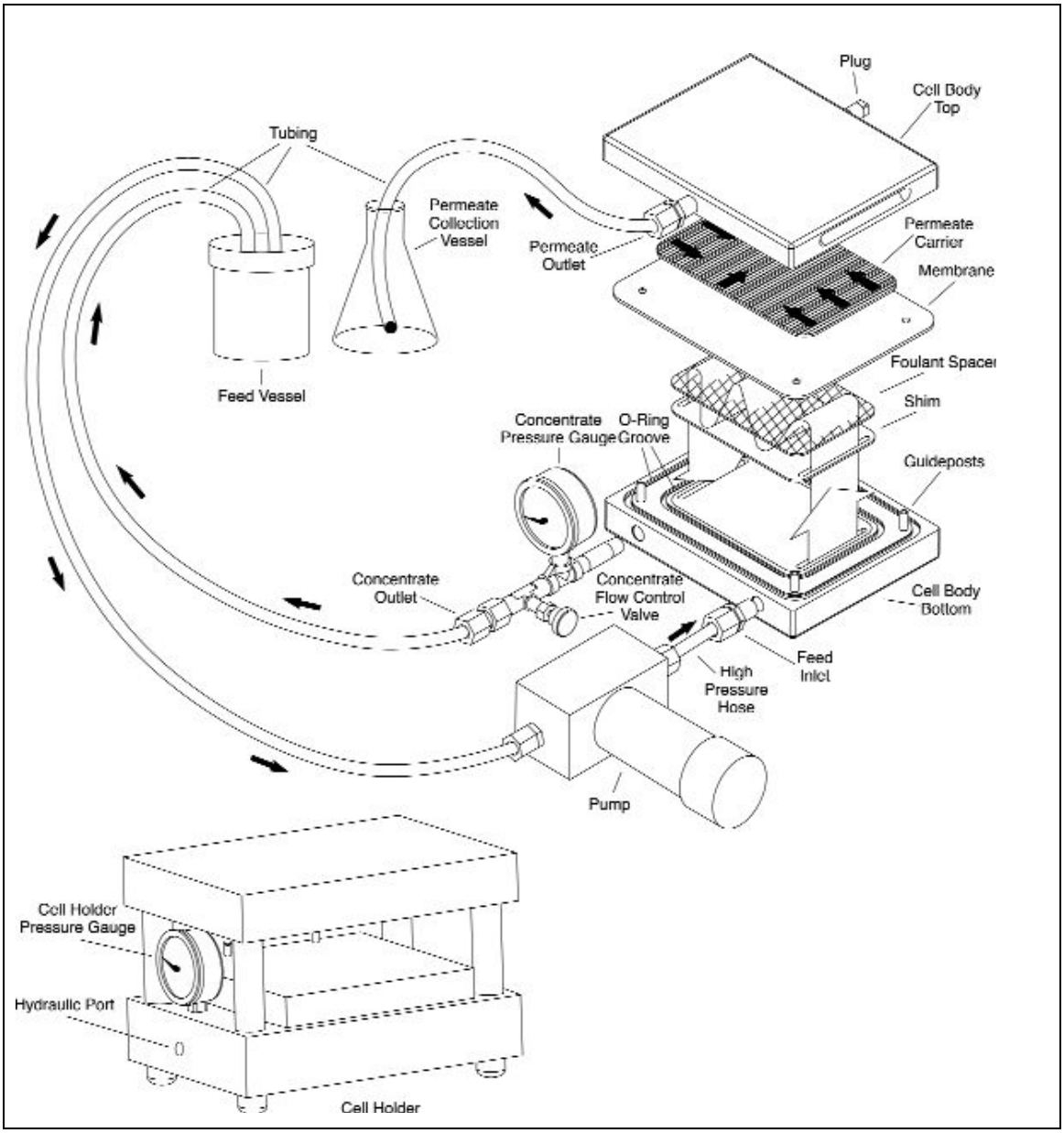

Figure 11.2: SEPA CF II Composants de cellule de NF et circulation des flux.

Partie 3: Résultats et discussions

3. Partie 3: Résultats et discussions

3.1 Caractérisation des membranes PEI

3.1.1 Caractérisation des membranes par MEB

La préparation de deux types de membranes a été prévue pour faire la part de l'influence de la nature du matériau et de sa structure; ainsi, des membranes de type dense, homogène et de type asymétrique comprenant une peau dense extrêmement fine ont été réalisées.

Si l'objectif de séparation moléculaire a bien été atteint facilement avec la membrane dense, il s'agissait de mieux maitriser l'homogénéité de la couche dense superficielle et la structure poreuse inférieure des membranes asymétriques pour des obtenir échantillons reproductibles assez grands pouvant convenir en nanofiltration. En effet par microscopie électronique il a été montré que l'épaisseur pouvait varier de façon significative (de quelques microns à 1 ou 20microns), ce qui était préjudiciable au flux de perméation. De même, la couche inférieure poreuse ne présente pas toujours la même morphologie, pour des conditions supposées identiques de préparation: on observe des structures de type macroporeux ou de type spongieux. Ces dernières étant préférables car mécaniquement plus résistante, on a cherché à optimiser les préparations, notamment en étudiant le diagramme de phase du système ternaire Fig. (3.3).

Les structures des peaux de membrane pour les films plats asymétriques de PAA&PEI - Jeff600-PMDA-ODA (0.4/1/0.6) ont été examinés en utilisant la microscopie électronique (MEB). La morphologie extérieure des membranes est caractérisée par la taille et la structure de réseau de pores. Pour toutes les Figures, les conditions de préparation sont exprimées comme suit (APA masse%/ DMF masse%/ Eau ajoutée masse% / temps pré-concentration / temps d'immersion / épaisseur), respectivement.

Tableau 1.3: Paramètres de préparation des membranes PEI

Membrane	Solution de polymère			Pré-concentration temps en min	Immersion temps en h	Non solvant	test
	DMF	PAA	H_2O				
M_1	70	30	0	1 min	1 h	Eau	1
M_2					2 h		
M_3					3 h		
M_4	70	30	0	3 min	1 h	Eau	2
M_5					2 h		
M_6					3 h		
M_7	70	30	5	1 min	1 h	Eau	3
M_8			15				
M_9			20				
M_{10}			24				
M_{11}			31				
M_{12}			40				
M_1	70	30	0	1 min	1 h	Eau	4
M_{13}	75	25					
M_{14}	80	20					
M_{15}	85	15					
M_8	70	30	15	1 min	1 h	Eau	5
M_{16}	75	25					
M_{17}	80	20					
M_{18}	85	15					
M_{19}	7	30	0	1 min	1 h	Méthanol	6
M_{20}						Ethanol	

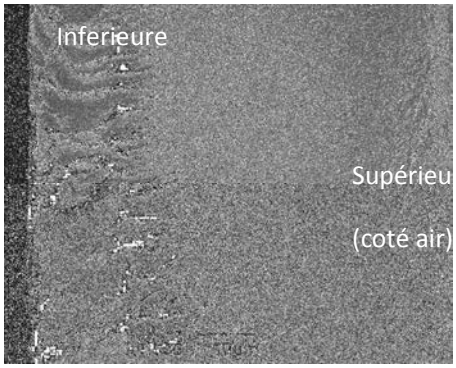

M_1 (30%-70%-0/1min/1h/65µm)

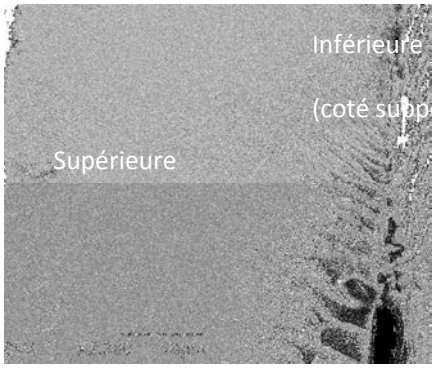

M_2 (30%-70%-0/1min/2h /50µm)

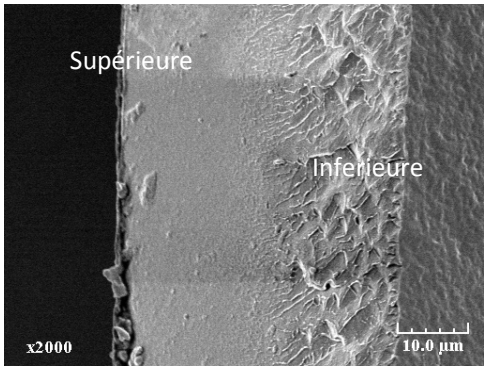

M_3 (30%-70%-0/1min/3h/55µm)

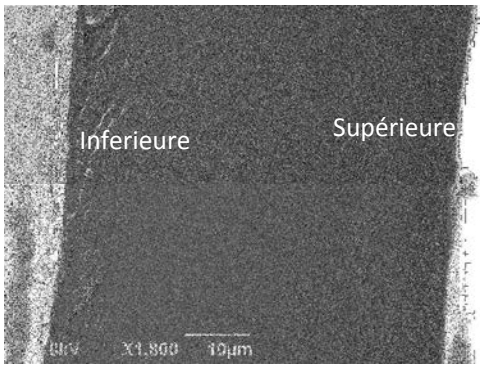

M_4 (30%-70%-0/3min/1h/60µm)

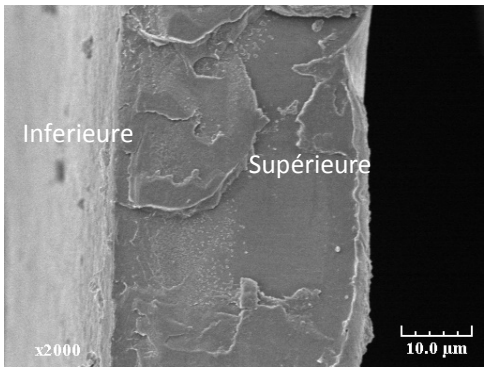

M_5 (30%-70%-0/3min/2h/45µm)

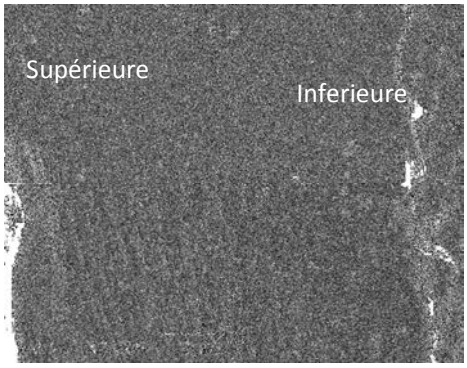

M_6 (30%-70%-0/3min/3h/50µm)

Figure 1.3: Vues en MEB des sections des films de PEI préparent selon protocoles d'inversion de phase pour membranes (M_1- M_6), applicateur de film liquide de 300 µm d'épaisseur.

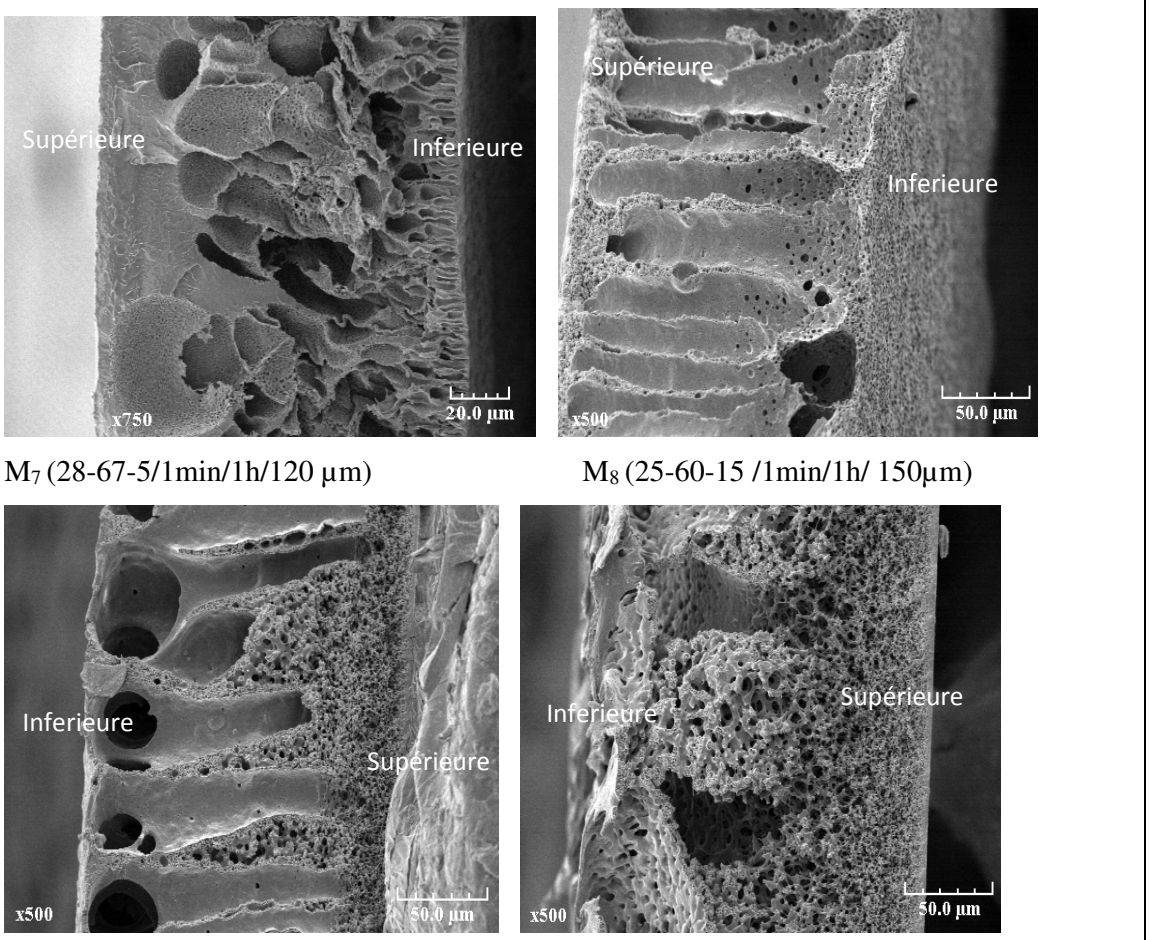

M_7 (28-67-5/1min/1h/120 µm) M_8 (25-60-15 /1min/1h/ 150µm)

M_9 (24-56-20/1min/1h/170µm) M_{10} (23-53-24/1min/1h/170µm)

Figure 2.3: Vues en MEB des sections des films de PEI préparent selon protocoles d'inversion de phase pour membranes (M_7- M_{10}) applicateur de film retirer 500 µm d'épaisseur.

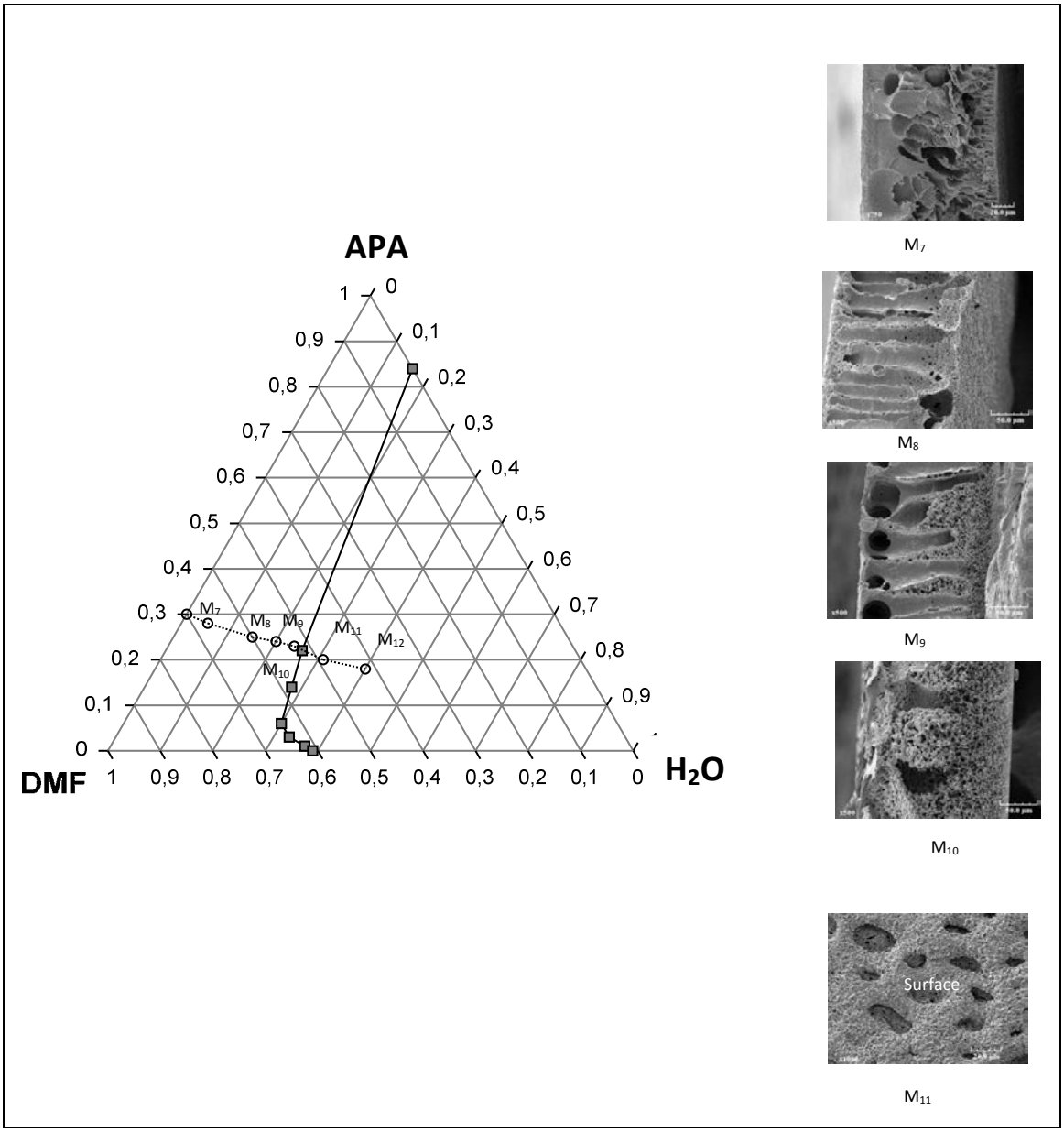

Figure 3 ,a .3: Diagramme de phase ternaire du système APA/DMF/Eau avec la courbe binodale de démixtion et relation avec la morphologie des membranes obtenues par inversion de phase selon la composition initiale de la solution de polymère (solution ternaire de l'APA membranes M_7-M_{12} - ○ -; courbe binodale de démixtion ■).

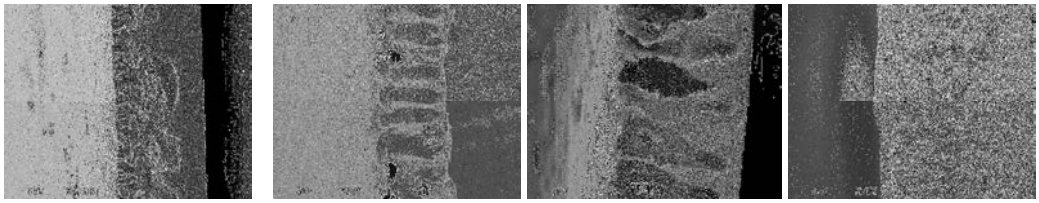

$M_{13(\ 25APA)}$ $M_{8b(\ 25APA,\ 15\ H2O)}$ $M_{9b(\ 25APA,\ 22\ H2O)}$ $M_{10b(\ 25APA,\ 24\ H2O)}$

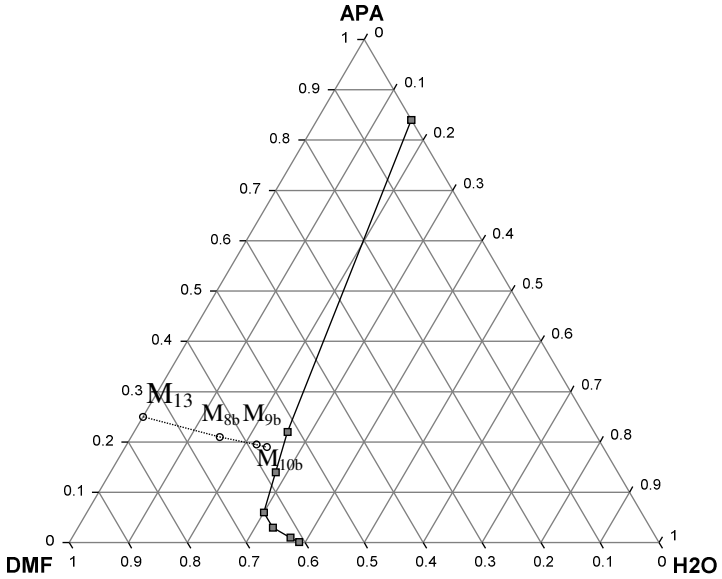

Figure 3 ,b .3: Diagramme de phase ternaire du système APA/DMF/Eau avec la courbe binodale de démixtion et relation avec la morphologie des membranes obtenues par inversion de phase selon la composition initiale de la solution de polymère (solution ternaire de l'APA membranes M_{13}, M_{8b} , $M_{çb}$ et M_{10b} - ○ -; courbe binodale de démixtion ■).

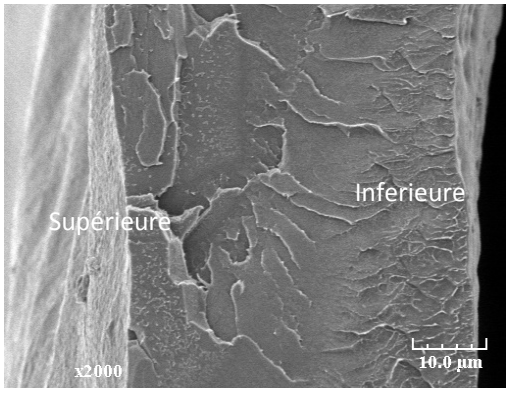

a-M_1 test 4(30%-70%-0 /1min/1h/ 45 µm)

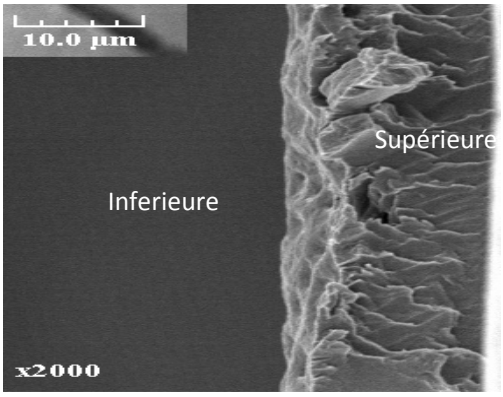

c- M_{14} test 4 (20%-80%-0 /1min/1h/15µm)

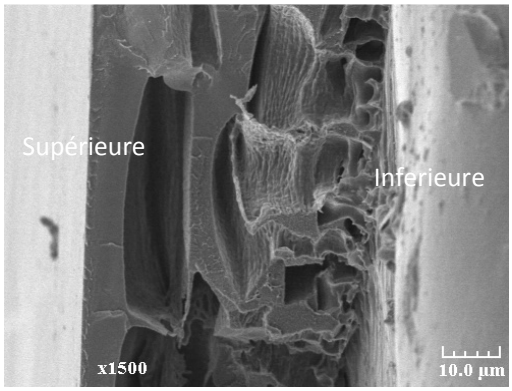

b- M_{13} (25%-75%-0/1min/1h/50µm)

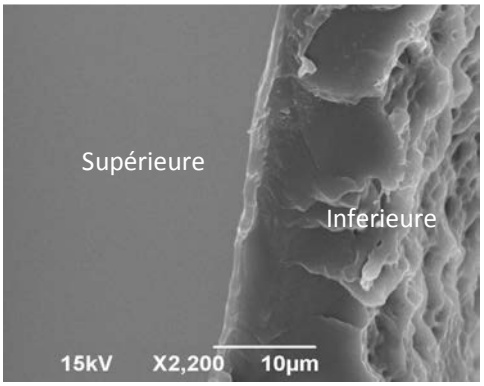

d- M_{15} (15%-85%-0 /1min/1h/15µm)

Figure 4, A.3: Vues en MEB des sections des membranes de polymère PEI changer la composition de solution d'essai 4, applicateur de film liquide 300 µm d'épaisseur.

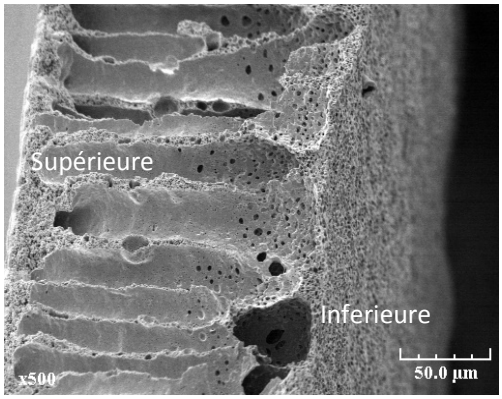

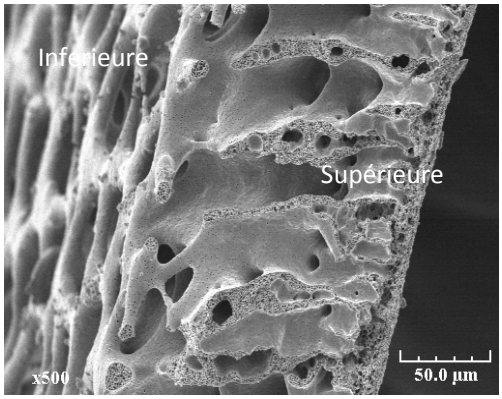

a-M_8 test 5(30%-70%-15%/1min/1h/150µ) b- M_{16} test 5 (25%-75%-15%/1min/1h/100µm)

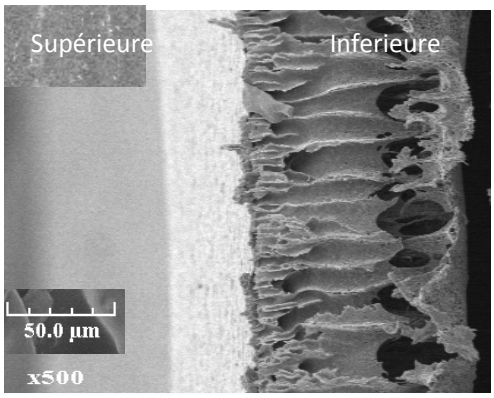

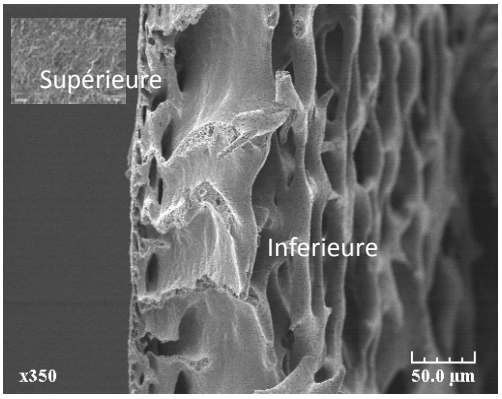

c- M17(20%-80%-15% /1min/1h/75µm) d- M_{18} (15%-85%-15% /1min/1h/60µm)

Figure 4,B.3: Vues en MEB des sections des membranes de polymère PEI en fonction de la composition de solution d'essai 4.

Effet des paramètres d'inversion de phase (Figures1.3- 4.3):

- La période décroissante de l'évaporation de 3min à 1min induit une structure plus poreuse (Figure 1.3).

- Le temps décroissant d'immersion de 3h à 1h n'a pas un effet significatif; il semble peut être rendre les films de APA plus fragile du à 'extraction plus complète du solvant après un long temps d'immersion) (Figure 1.3).

- La porosité augmente fortement lorsque le taux du non solvant passe de 5 à 24 % en masse dans la solution de départ (Figure 2.3).

- l'ajout du non-solvant (l'eau 15 à 24 en masse%) mène à des structures de type macroporeuse ou de type spongieuse et à des pores longs et à une surface supérieure très mince et dense (Figure 2.3).

- la concentration décroissante de PAA dans DMF (de 30 à 15 en masse %) induit la formation de pores d'un diamètre plus élevé (de 1µm à 50µm) (Figure 4.3).

- L'immersion dans MeOH ou EtOH mène à la formation de films gonflés d'APA sans tenue mécanique.

- Le traitement thermique de PAA à PEI confère à des propriétés mécaniques beaucoup plus élevées, évite rend les films de PEI beaucoup usant que les APA induit la densification et réduit peut être aussi la taille des pores.

3.1.2 Infrarouge (FT-IR)

Pour suivre le bon déroulement des étapes de synthèse, la spectroscopie infrarouge à transformée de fournier est employée. Les figures (5.3: 6.3) montrent le spectre infrarouge pour les membranes APA, PEI - Jeff600-PMDA-ODA- et Kapton. Les spectres IR montrent que l'APA est transformée en PEI après le traitement thermique.

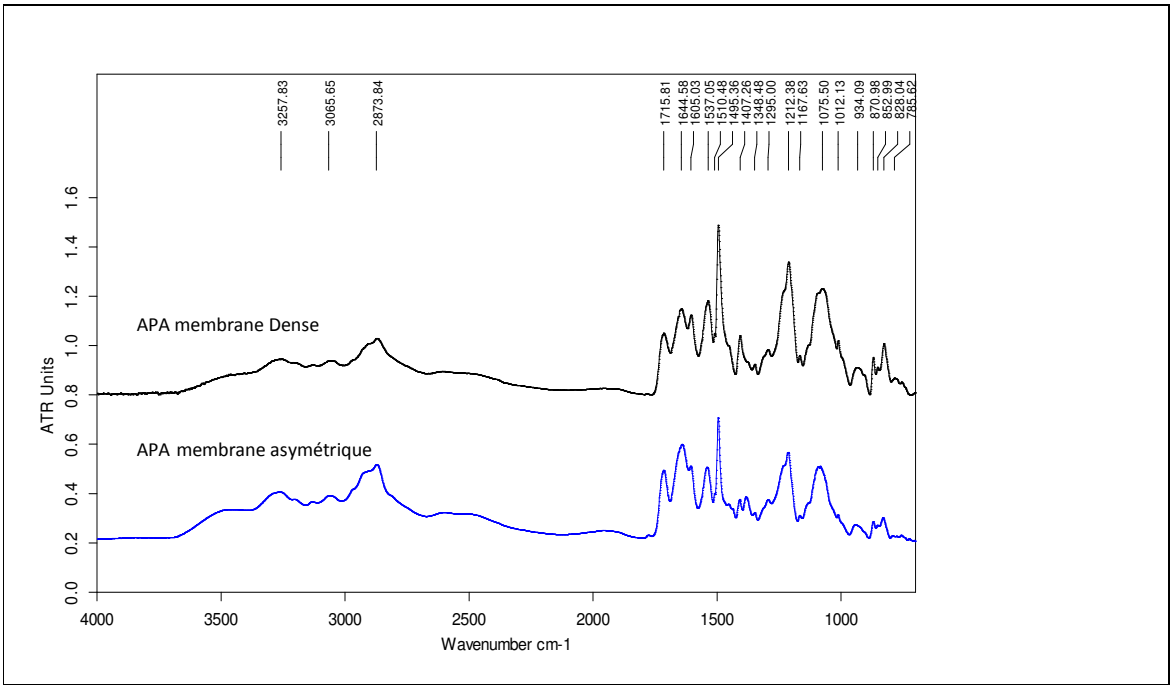

Figure 5.3: Spectres infrarouges d'une membrane APA dense et asymétrique (30% APA dans DMF).

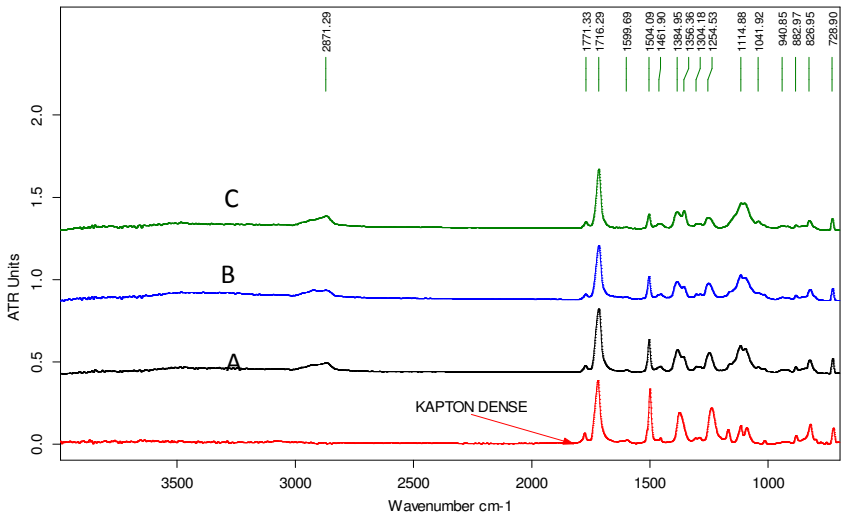

b .Spectres infrarouges des films Kapton™ et PEI denses (A: Jeff 0,4, B: Jeff 0,5, C: 0,6 Jeff)

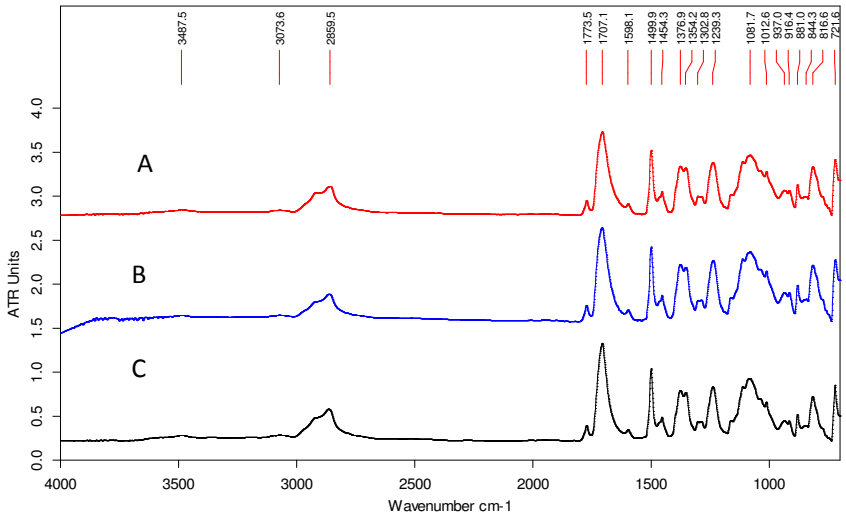

a . Spectres infrarouges des films PEI dense (A), PEI asymétrique (25/APA) (B) et PEI asymétrique (30/APA)(C).

Figure 6 a, b.3: Spectres infrarouges APA, PEI et Kapton™ membranes.

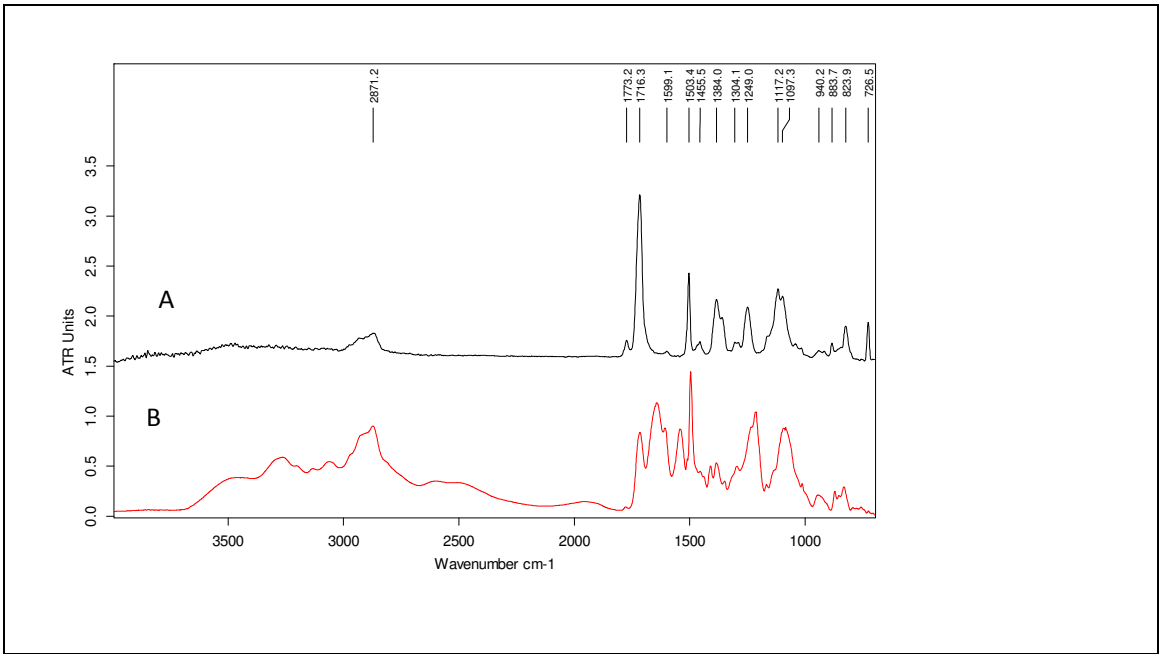

Figure 6, c .3: Spectres infrarouges APA (A) et PEI (B) denses comptions 0,4Jeff-0,6ODA.

3.1.3 Résultats du gonflement des membranes PEI.

Pour étudier l'effet du Jeff600 sur les propriétés physicochimiques, des tests de gonflement aux solvants été effectués pour des membranes à différents taux de Jeff 600.

- Conditions: échantillons PEI séchée 15 heures à 50 °C, puis les échantillons immergés en solvants après 24 heures et 48heures,….. Jusqu'à obtention d'une masse stable, puis essuyage rapide du liquide de surface et pesée dans un flacon fermé.

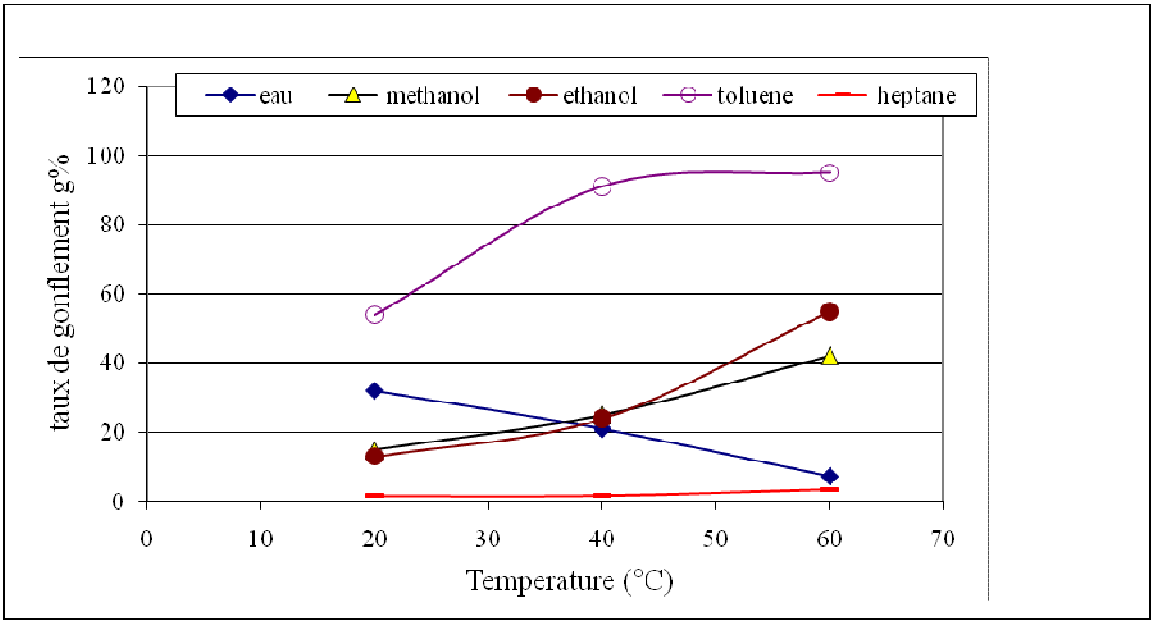

Figure 7.3: Effet de la température sur le gonflement des différents échantillons de PEI (Jeff600 0,4).

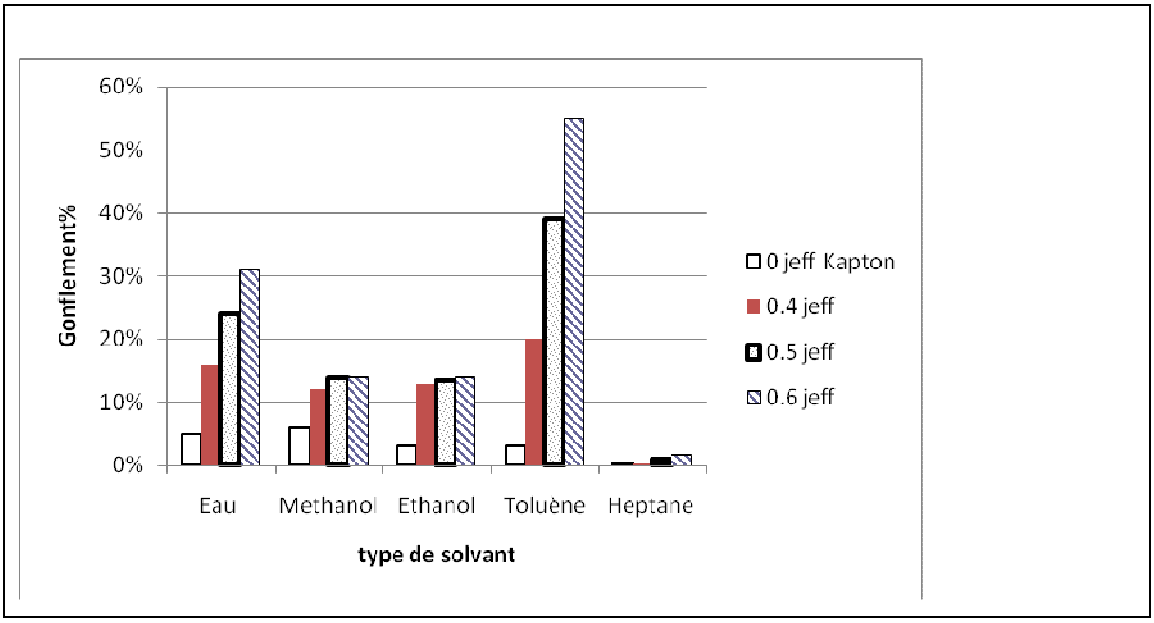

Figure 8.3: Effet du Jeff600 sur le gonflement des différents échantillons de membranes PEI de composition en Jeffamine variable (0,4 à 0,6 Jeff) à (20 °C).

Tableau 2.3: Taux de gonflement de films PEI denses (0,4 Jeff) à température ambiante (20°C).

	Solvant	Paramètre de solubilité [37] $MPa^{1/2}$	Gonflement (masse/masse)%
1	n-Heptane	15,1	0,2
2	Diethyléther	15,1	0
3	Methyl isobutyl Kétone	17,2	4
4	Toluène	18,2	20
5	Ethyl acétate	18,6	5
6	THF[tetrahydrofuran]	18,6	14
7	Methyl ethyl ketone	19	10
8	Chlorure de methylene	19,8	6
9	Acétone	20,3	16
10	Acide acetique	20,7	53
11	Aniline	21,1	100
12	Triethylene glycol	21,9	17
13	1- butanol	23,3	8
14	Acétonitrile	24,3	5
15	1-propanol	24,.3	16
16	diméthylformamide	24,8	52
17	Nitromethane	26	91
18	Ethanol	26	13
19	Methanol	29,7	12
20	Ethylene glycol	29,9	14
21	Eau	47,9	17
22	chloroforme	19	Cassé

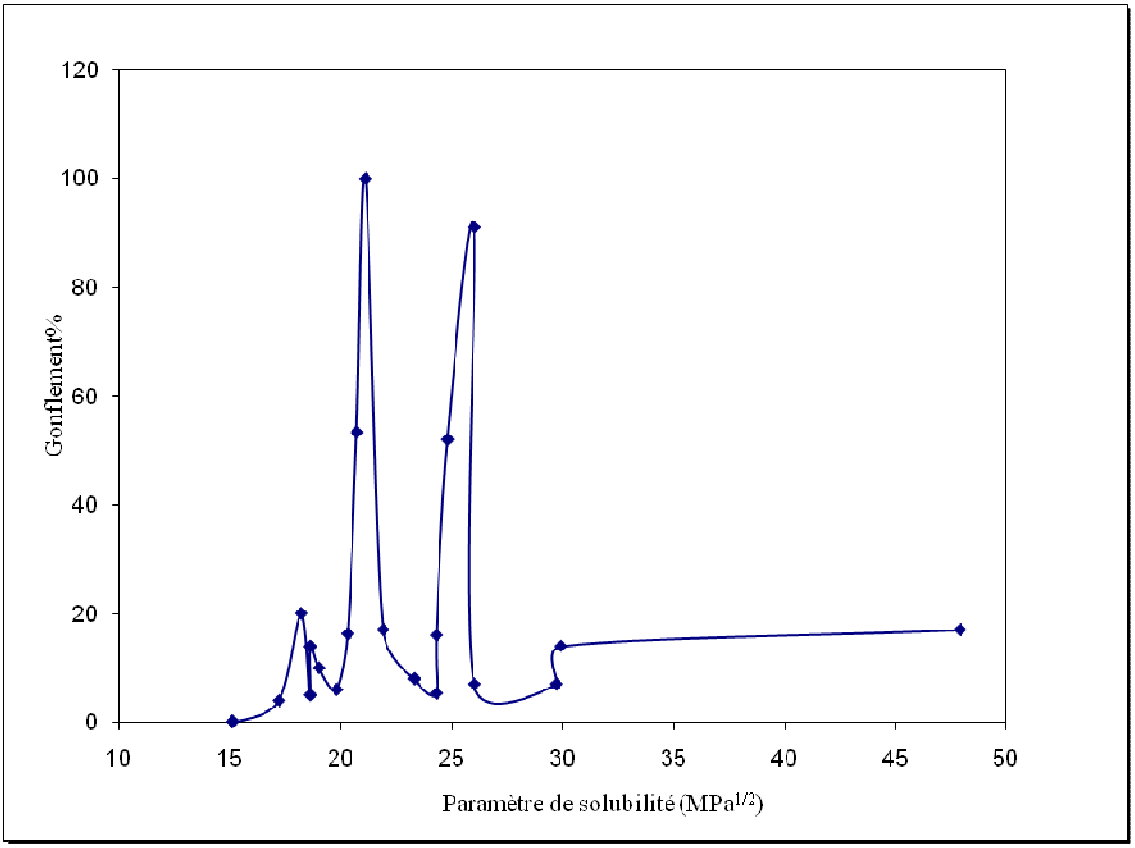

Figure 9.3: Relation entre le gonflement des différents échantillons de PEI membrane et les paramètres de solubilité des solvants.

Prédiction de la sélectivité de perméation (PV)

a) Le gonflement de l'eau est plus grand que le gonflement du méthanol, de l'éthanol ou de l'heptane on peut donc penser qu'en pervaporation. Une membrane dense favorisera la perméation de l'eau par rapport aux autres molécules organiques polaires; l'eau étant la molécule de taille la plus petite, sa perméation sera aussi favorisée du point de vue diffusionnelle.

b) Il faut noter l'influence d'une augmentation de la température (Fig.7.3) qui diminue le gonflement de l'eau alors qu'il l'augmente pour les molécules organiques.

3.1.4 Analyse thermogravimétrique (ATG)

Les analyses thermogravimétriques montrent que la stabilité des PEI enregistrée sous atmosphère d'azote diminue en fonction du taux de Jeff 600 Figs. (10.3-12-3). Cependant, les températures correspondant à la dégradation de 5% de la masse de l'échantillon PEI sont

supérieures à 350 ^{O}C (tableau 3.3). A noter que la cinétique initiale de dégradation des différents PEI est différente et ne suit pas l'évolution des taux de Jeff 600.

Tableau 3.3: Caractéristiques ATG des membranes PEI

Type de Membrane	T (°C) à 5% masse perte	T (°C) à 10% masse perte	Dégradation finale (wt %)
PI (PMDA-ODA)	569	584	42
PEI Jeff/PMDA/ODA (0,4/1/0,6) dense	386	399	68
PEI Jeff/PMDA/ODA (0,5/1/0,5) dense	351	379	73
PEI Jeff/PMDA/ODA (0,6/1/0,4) dense	393	405	77

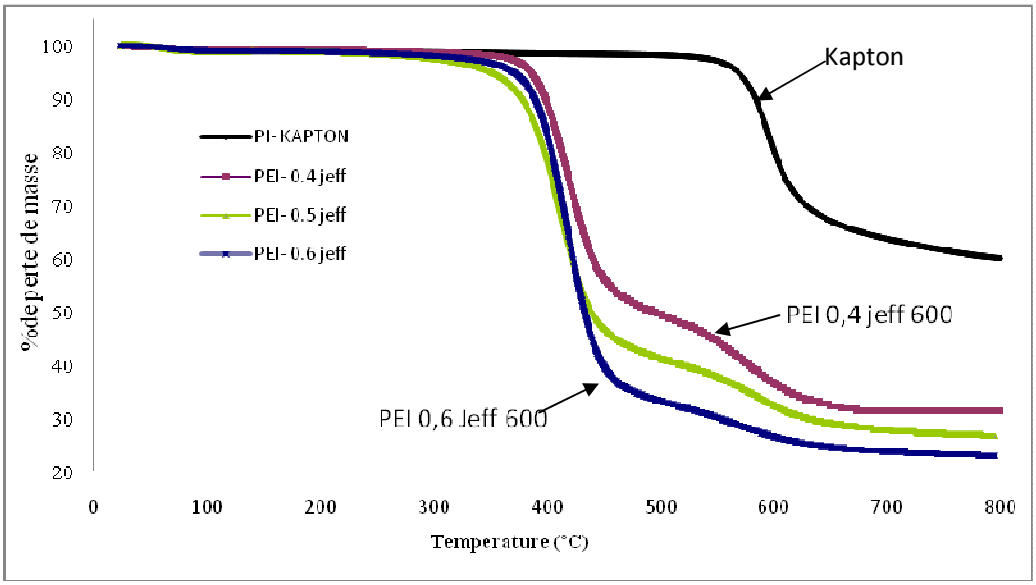

Figure 10.3: ATG montrant la perte de masse des PEI et Kapton ™ membranes (N2, vitesse de chauffage:10 ° C / min).

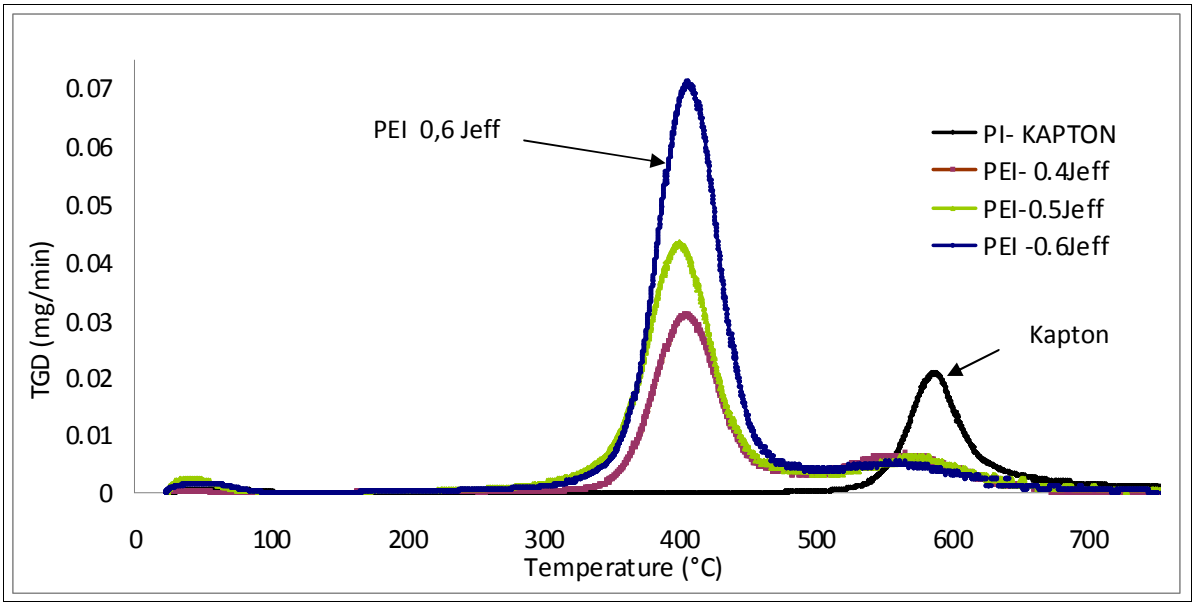

Figure 11.3: Stabilité thermique des PEI, effet du taux de Jeff 600 sur la température de dégradation des PEI.

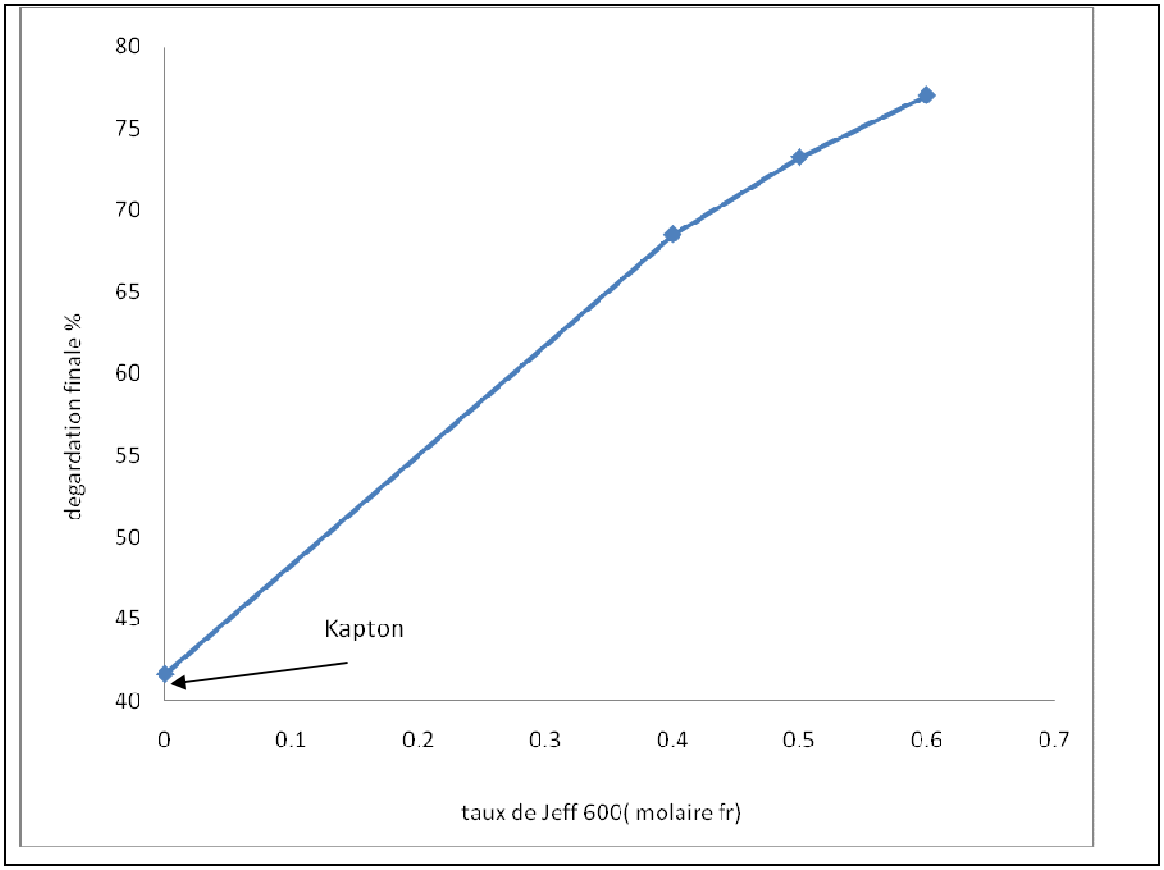

Figure 12.3: Evolution des dégradations finales des PEI en fonction du taux de Jeff 600.

3.1.5 Propriétés mécaniques

Le comportement contrainte-élongation des PEI a été observé à température ambiante sur des films d'épaisseur de 200 µm. Les paramètres suivants sont obtenus à partir des profils contrainte-élongation des échantillons: le module de Young à partir de la pente initiale de la courbe, la contrainte à la rupture et l'élongation à la rupture. Les courbes de tendances des PEI avec différentes compositions en Jeff 600 sont illustrées dans la Fig. (13.3) et les valeurs des paramètres sont résumées dans le tableau 4.3.

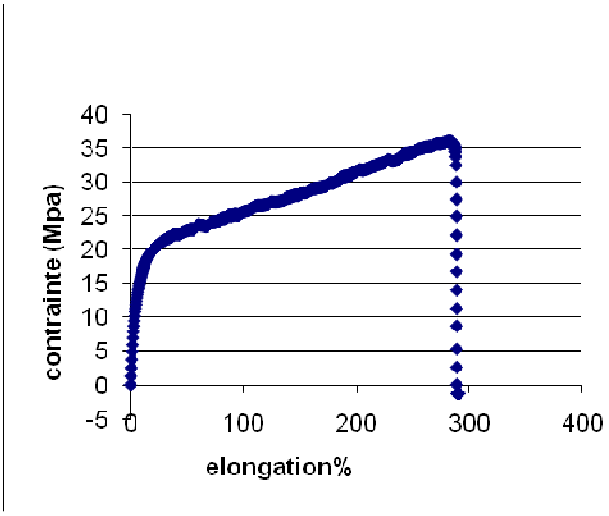

Figure13.3: Relation contrainte allongement des PEI Jeff 0,4.

Tableau 4.3: Propriétés mécaniques des PEI et Kapton™ (notre travail et données de la littérature).

Membrane	Module de Young (GPa)	Contrainte à la rupture (MPa)	Elongation à la rupture (%)
PI Ref. [38]	3,2	265	60,1
PI Ref. [39]	2,1	104,7	16
PI Ref. [40]	2,3	60,2	35
PI Ref. [41]	0,80/0,62	106/66	18/13
PI [this work]	1,4	66,8	16
PEI 0.4Jeff	0,25	35,9	285
PEI 0.5Jeff	0,1	15,7	287
PEI 0.6Jeff	0,025	6,9	303

La comparaison des PEI avec le comportement mécanique du Kapton montre une diminution du module de Young et une augmentation de l'élasticité. L'augmentation du taux

de Jeffamine de 0,4 à 0,6 induit aussi une diminution du module Young importante. Ceci peut être expliqué par une variation de la réticulation physique qu'apporte les jonctions imides et la séparation des phases qui crée des micros domaines rigides limitant l'écoulement des chainons Jeff entre eux.

3.2 Principaux résultats et discussions

Dans travail, nous sommes particulièrement intéressés à l'étude des propriétés de séparation moléculaire de films de type copolyalcoxyétherimide (PEI) à travers deux procédés, à savoir la pervaporation et la nanofiltration. Les membranes de référence pour toutes nos études étaient des membranes denses PEI ou Kapton^{TM} (PI). Afin d'améliorer les propriétés de séparation des membranes PEI, et en mettant à profit les résultats de la littérature, différentes modifications ont été effectuées. Ces modifications concernent trois aspects différents de la membrane:

- La morphologie: en synthétisant des membranes asymétriques par le procédé d'inversion de phase.
- L'architecture chimique: en modifiant les proportions des amines utilisées, à savoir l'amine aliphatique (Jeffamine) et l'amine aromatique (ODA).
- La nature chimique: en synthétisant des membranes hybrides par l'incorporation de particules de silice dans la matrice polymère. Dans notre cas ces particules inorganiques ont été soit introduites directement, soit générées in situ à partir du TMOS à travers le procédé sol-gel (sans addition d'eau).

3.2.1 Etude des propriétés de pervaporation

La pervaporation est une technique de séparation par membrane qui sert à fractionner les constituants d'un mélange liquide par vaporisation partielle à travers une membrane dense permsélective. La force matrice du transfert est la différence des pressions de vapeur du ou des composants perméés entre la face amont et la face aval de la membrane. Ceci est réalisé en maintenant le compartiment aval sous faible pression [42]**.** Le transfert de matière en pervaporation se fait selon un mécanisme de solution-diffusion.

3.2.1.1 Transport des fluides dans les films polymères denses: Mécanisme Solution-Diffusion [6,30,43]

Le transport des fluides dans un film polymère dense dénué de pores est régi par le mécanisme de solution-diffusion. Ce mécanisme se décompose en trois étapes essentielles (Figure 14.3) :

1) ***La sorption*** (ou encore dissolution) du fluide sur la face amont de la membrane (caractérisée par le coefficient de sorption **S).**
2) ***La diffusion*** du fluide à travers la membrane (caractérisée par la diffusivité D)
3) ***La désorption*** des molécules au niveau de la face aval de la membrane.

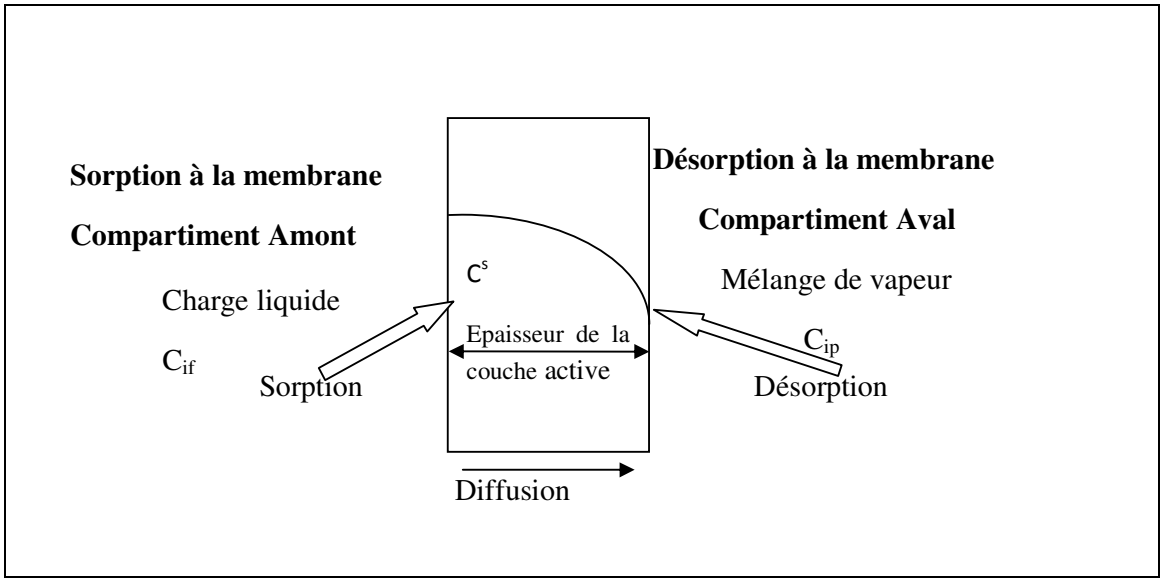

Figure 14.3: Principe du mécanisme de Solution-Diffusion [51].

3.2.1.2 Cas 1: Etude de la séparation de mélanges organique (toluène-heptane)

Le mélange étudié en pervaporation est un mélange organique d'Heptane et de Toluène. Chaque membrane est testée à 3 températures différentes: 40°C, 55°C et 70°C. Pour avoir des résultats reproductibles, on ne procède à des mesures que lorsque le régime stationnaire est atteint, ce qui se traduit par des flux stables. Ainsi pour chaque membrane, on doit avoir au minimum trois pièges avec un flux constant avant de changer de température. Les images MEB de PEI membranes testées sont présentées dans la figure 15.3. Tous les résultats sont présentés dans les tableaux (5.3 à 7.3).

Tableau 5.3: Résultats de pervaporation avec membranes dense et asymétrique PEI (Alimentation 50 % masse Toluène-Heptane).

Membrane	*t µm	*J (kg/h.m^2) ±10%			*J_T (kg/h.m^2)±10%		
		40°C	55°C	70°C	40°C	55°C	70°C
M_{dense}	40	0,024	0,04	0,054	0,02	0,035	0,048
	60	0,013	0,029	0,037	0,01	0,027	0,033
$M_{1(30PAA)}$	100	0,01	0,02	0,04	0,01	0,013	0,03
	40	0,02	0,05	0,1	0,019	0,045	0,098
$M_{13(25PAA)}$	100	0,45	0,65	0,95	0,33	0,5	0,7
$M_{7(25PAA+5w)}$	150	0,13	0,15	0,20	0,07	0,1	0,11
$M_{8(25PAA+15w)}$	40	0,13	0,33	0,48	0,08	0,2	0,3

*J: flux reél total, $J_{T:}$ flux toluène réel, t: épaisseur, T: toluène, H: heptane.

Tableau 6.3: Effet du type membranes PEI sur le facteur de séparation (α) et sur l'enrichissement du perméat (Cp) (Alimentation 50 % masse Toluène-Heptane, C_P ±2-3%).

Type de membrane	α 40°C	α 55°C	α 70°C	Cp (40°C)	Cp (55°C)	Cp (70°C)
$M_{dense(60\ um)}$	12	11	10	92%	90%	89%
$M_{dense(40\ um)}$	12	10	9	91%	89%	88%
$M_{1\ (30PAA,\ 40\ um)}$	13	10	9	93%	91%	89%
$M_{1\ (30PAA,\ 100um)}$	11	10	6	90%	90%	85%
$M_{13(25PAA,\ 100um)}$	2,8	2,7	3	74%	73%	75%
$M_{7(25PAA+5w,\ 150um)}$	1,3	1,4	1,4	55%	59%	56%
$M_{8(25PAA+15w,\ 40um)}$	1,8	1,5	1,5	65%	60%	59%

Tableau 7.3: Résultats de pervaporation avec membranes PEI dense et asymétrique dans des solvants purs et de l'eau.

Membrane	t (µm)	Charge	*J (kg/h.m^2)		
			40°C	55°C	70°C
M dense	60	100 % *w	0.28	0.42	0.55
	60	100 % *T	0.17	0.25	0.34
	60	100 % H	0.003	0.006	0.01
$M_{1(30PAA)}$	40	100% T	0.18	0.33	0.6
$M_{13(25PAA)}$	100	100 % w	0.80	1.3	3.2
$M_{7(25PAA+5w)}$	150	100 % w	0.24	0.47	0.91
	150	100 % T	0.4		

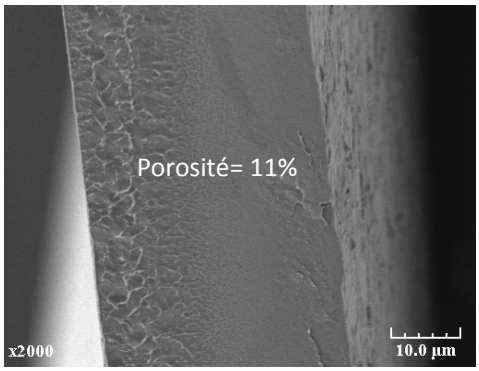

M_1 (30%-70%-0/1min/1h/40µm)

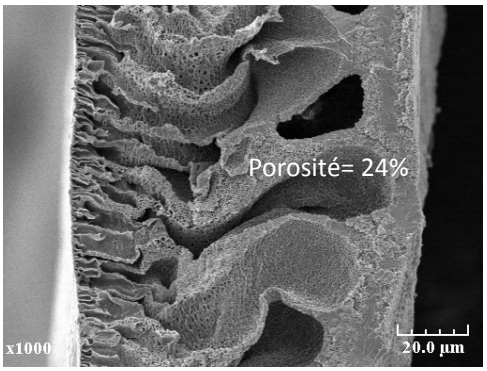

M_{13} (25%-75%-0/1min/1h/100µm)

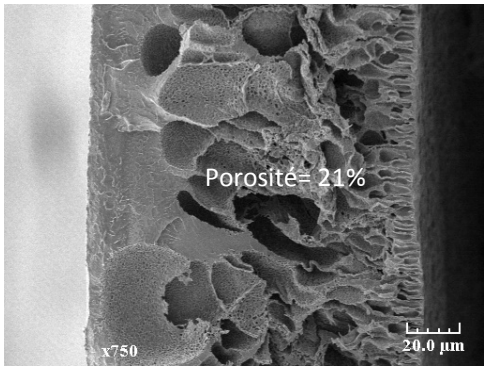

M_7 (28-67-5/1min/1h/150 µm)

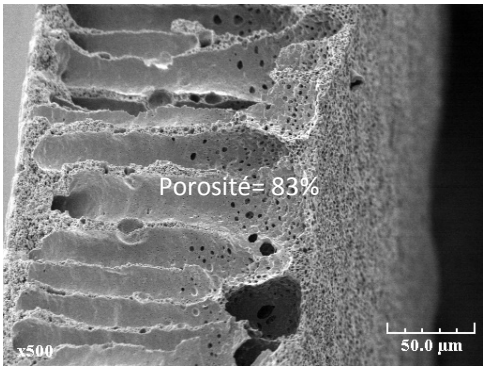

M_8 (25-60-15 /1min/1h/ 140µm)

Figure 15.3: Images de MEB des membranes PEI. Caractéristiques des membranes:(APA % masse -DMF % masse - d'eau % masse/ temps de pré-concentration/ temps d'immersion/ épaisseur).

Le mélange Heptane-Toluène est un mélange dont la courbe d'équilibre liquide vapeur s'approche de la diagonale du diagramme Mc Cabe-Thiele (Fig.16.3). La séparation par simple distillation est ainsi difficile pour tout le domaine de concentration, ce qui n'est pas le cas en pervaporation, qui crée un nouvel équilibre de partage au niveau de la face amont de la membrane.

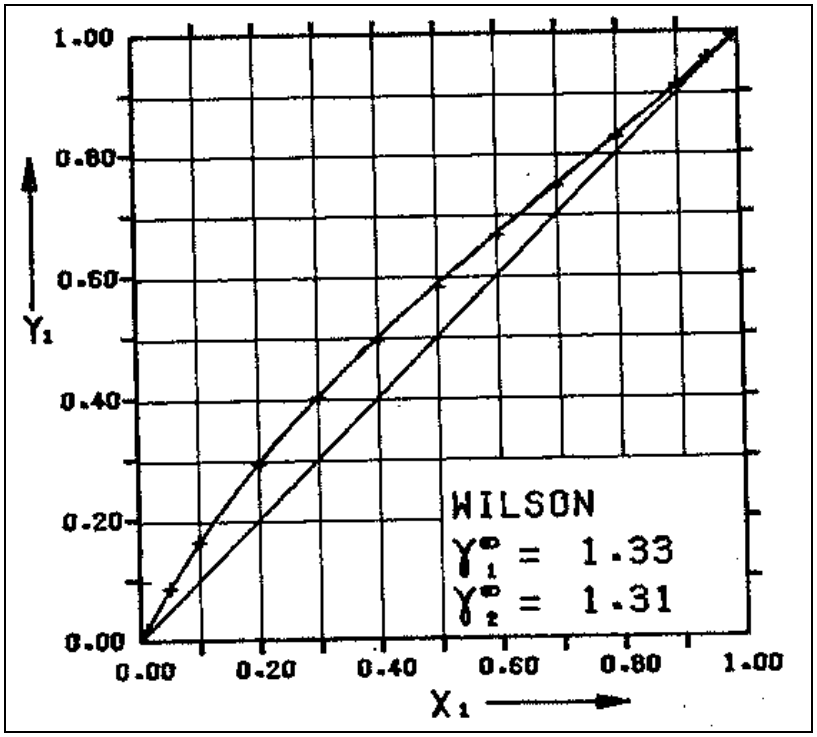

Figure 16.3: Diagramme d'équilibre liquide-vapeur du mélange Heptane-Toluène [44] .

Avec : (1) : Heptane (2) Toluène

X: Fraction molaire dans la phase liquide

Y: Fraction molaire dans la phase vapeur

I. Sélectivité des membranes PEI étudiées

L'analyse des perméats collectés (à partir d'une charge à 50% en masse du mélange Toluène-Heptane) par chromatographie gazeuse montre que les membranes étudiées sont permsélectives au toluène (Fig 17.3). Les chromatogrammes obtenus présentent en fait deux pics: un pic relatif à l'heptane qui apparaît aux alentours de 1,7 seconde et un pic relatif au toluène aux alentours de 2,1 secondes. Ces pics traduisent une grande sélectivité des membranes en faveur du toluène qui est de l'ordre de 90%. Cette grande sélectivité est en

effet l'avantage majeur du procédé de pervaporation par rapport au procédé conventionnel de distillation.

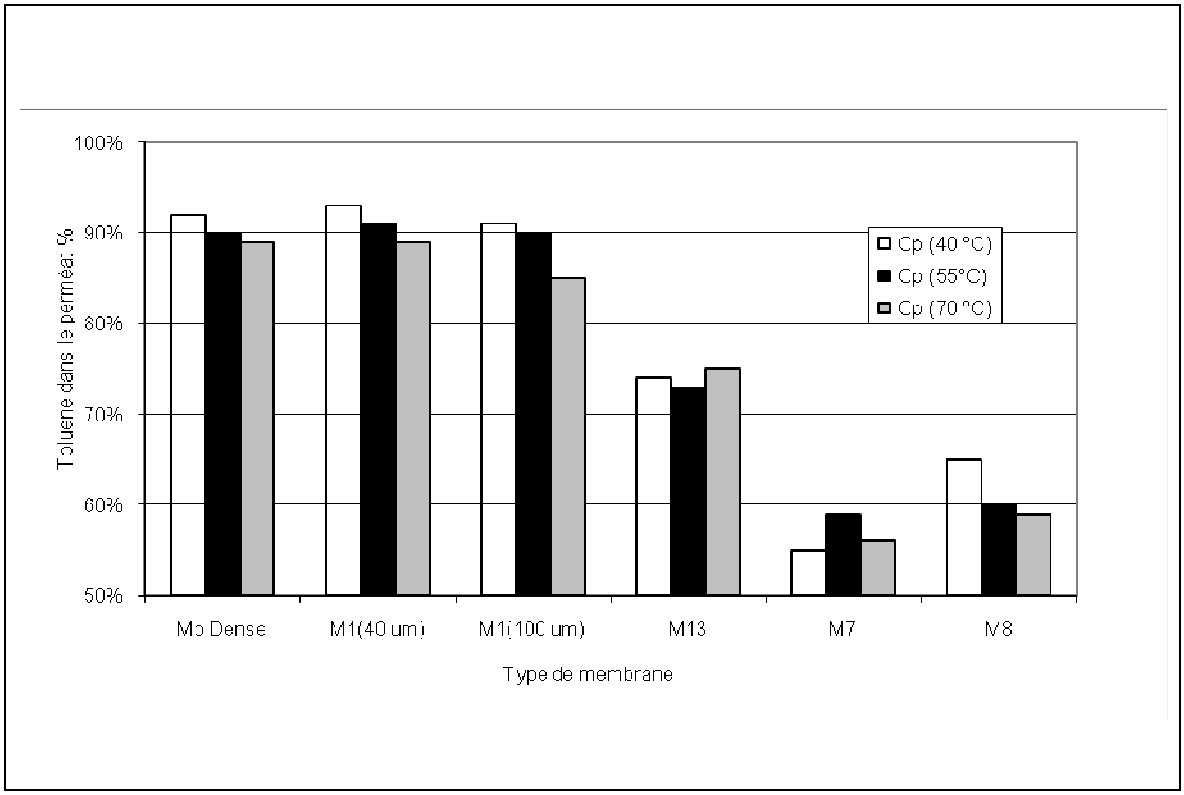

Figure 17.3: Résultats de pervaporation obtenus avec différentes membranes PEI de morphologies asymétriques et dense à partir d'une charge à 50% en masse du mélange Toluène-Heptane. La membrane dense est la référence. On observe une sélectivité analogue ou supérieure avec certains films asymétriques.

Le point le plus intéressant ces essais a été la préparation réussie de membranes asymétriques par inversion de phase à partir de polyéther-imide, car certaines de cas membranes comprennent une couche dense en surface quasiment exempte de défauts. Ceci a été démontré par les résultats de pervaporation obtenu sur le mélange toluène-heptane; en effet la sélectivité des membranes testées (Cperméat : 76-90%) est assez proche de la sélectivité des films denses préparées classiquement par évaporation (Cperméat: 90%) (Fig17.3). De plus, ces membranes asymétriques ont permis d'augmenter de façon très importante les flux de matière transmembranaire (tableau 7.3).

- Effet de la température sur la sélectivité

L'augmentation du flux en fonction de la température s'accompagne d'une diminution de la sélectivité (Fig.17.3). Ceci peut être expliqué par le fait qu'une augmentation du flux du

toluène engendre une augmentation du flux couplé de l'heptane. En d'autre terme, plus le flux du toluène augmente plus il entraîne avec lui de l'heptane.

- Effet de la température sur le flux

Pour les membranes denses, et pour faciliter la comparaison, on peut raisonner en termes de flux normalisés. Dans notre cas, les flux ont été normalisés à une épaisseur de 10µm (Fig.18.3).

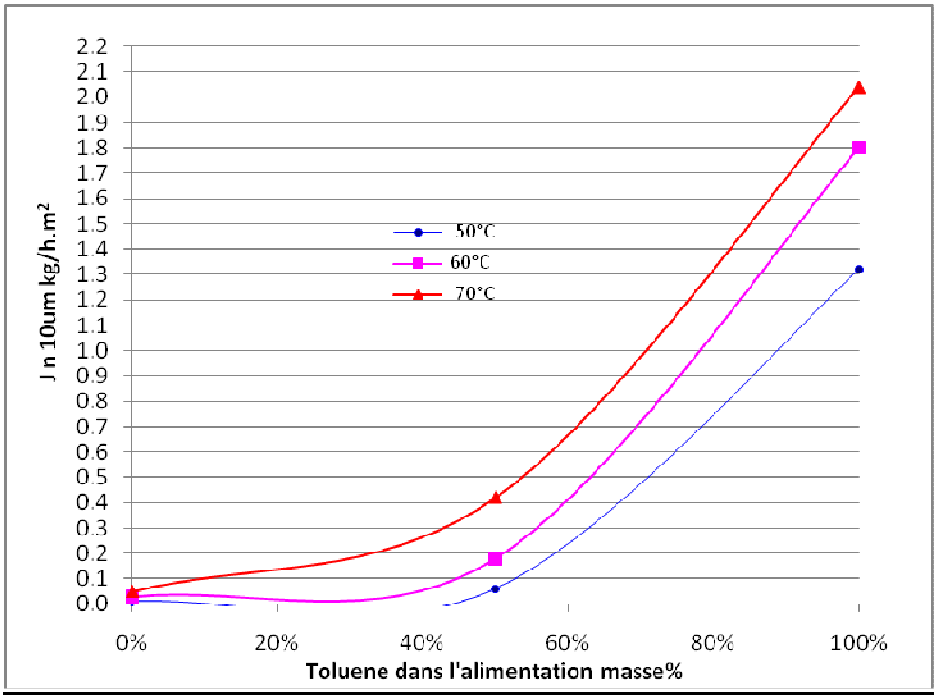

Figure 18.3 Variation du flux normalisé J_n en fonction de la température pour des membranes denses.

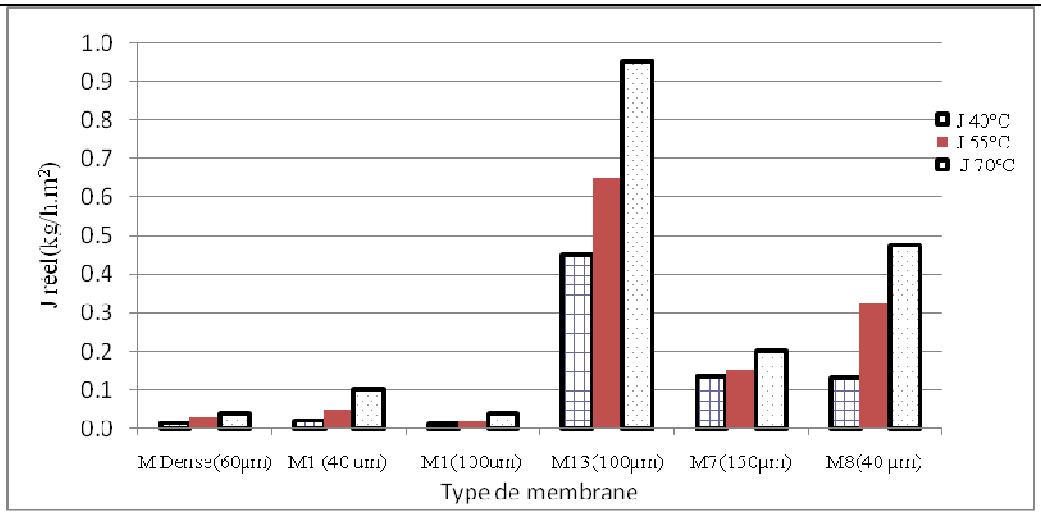

Figure 19.3. Variation du flux réel en fonction de la température pour des membranes denses et asymétriques.

Figure 19.3: Variation du flux en fonction de la température pour des membranes.

D'après la courbe de la Fig. (19.3), en regardant chaque membrane à part, on note que pour toutes les membranes, le flux augmente avec l'augmentation de la température. Il se peut donc que le flux suit une équation type Arrhenius. Pour démontrer cela, on se propose de tracer la courbe Ln J= f (1/T)

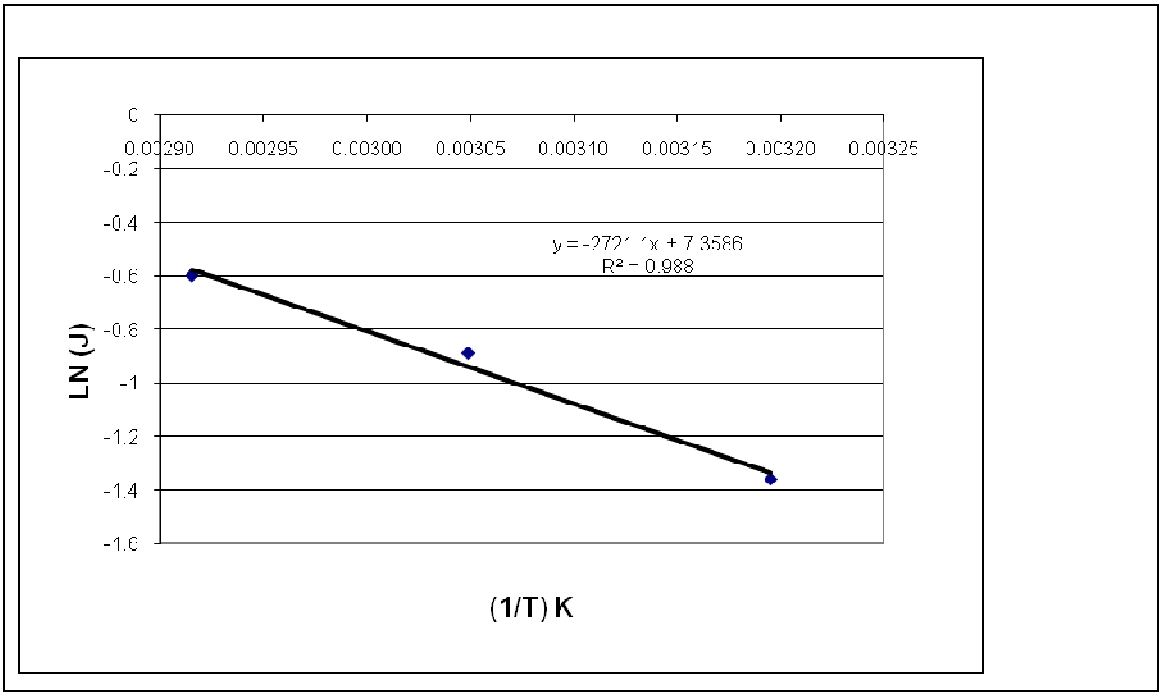

Figure 20.3: Variation du Logarithme du flux molaire JM en fonction de 1/T pour une membrane dense.

La courbe obtenue est une droite linéaire de la forme y = a x+ b ce qui montre que le flux suit bien une loi du type Arrhenius.

En effet $J = J_0 \exp\left(\frac{-Ea}{RT}\right) \Longleftrightarrow \quad LN(J) = (LN(J)_0) - \frac{Ea}{R} \times \frac{1}{T}$ donc la pente de cette courbe est $-\frac{Ea}{R}$.

Les conclusions qui ont pu être tirées de cette partie sont les suivantes:

-Toutes les membranes étudiées sont permsélective au toluène. Les sélectivités en faveur de ce composant sont de l'ordre de 90% pour la membrane dense PEI.

-Le flux du perméat augmente avec l'augmentation de la température, la relation entre les deux paramètres peut être décrite par une loi de type Arrhenius.

Cependant cette augmentation du flux est accompagnée par une faible diminution de la sélectivité (ne dépassant pas les 2%).Ceci peut être expliqué par le fait que le toluène qui voit son flux augmenter, entraine avec lui plus d'heptane.

- Pour les membranes asymétriques, le flux est nettement plus important que pour la membrane dense, cependant la comparaison des différentes membranes n'est pas toujours évidente à cause de la différence du taux d'asymétrie.

3.2.1.3 **2^{em}Cas : Etude de la séparation de mélanges eau- organiques par pervaporation**

Deux mélanges distincts ont été étudiés : eau-éthanol et eau-butanol.

Le mélange étudié en pervaporation est un mélange eau- alcool. Les images MEB de PEI membranes testées sont présentées dans la figure 21.3. Tous les résultats sont présentés dans les tableaux (8.3 à 11.3).

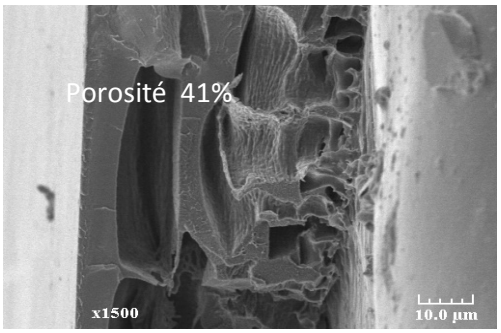

Membrane asymétrique $m_{as\ (25\%\text{-}75\%\text{-}0/1min/1h/60\mu m)}$ Immersion 11°C, testé avec eau /éthanol

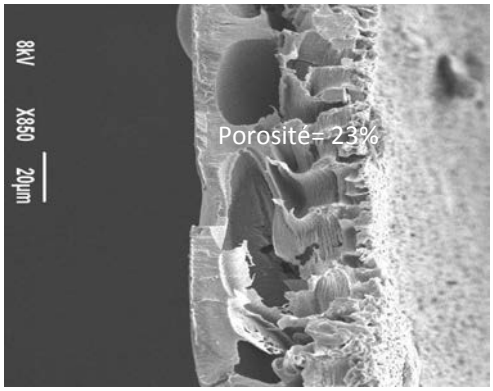

$M_{as2\ (25\%\text{-}75\%\text{-}0/1min/1h/40\mu m)}$ immersion 11°C, testé pour la déshydrations d'alcool

Figure 21.3: Images MEB des membranes asymétriques PEI. Caractéristiques des membranes : (APA masse% -DMF masse% - d'eau masse% / temps de pré-concentration / temps d'immersion / épaisseur).

Tableau 8.3: Effet de la température de fonctionnement sur le flux total réel des membranes PEI denses et asymétriques.

Alimentation Eau/éthanol	Flux réel $m_{d1,60\mu m*}$ (kg/h m^2)			Flux réel $m_{d2,30\mu m*}$ (kg/h m^2)			Flux réel $m_{as,60\mu m*}$ (kg/h m^2)		
	30° C	45°C	60° C	30° C	45° C	60° C	30°C	45° C	60° C
ethanol	0,037	0,05	0,1	0,06	0,1	0,18	0,034	0,061	0,1
20 % w*	0,08	0,15	0,25	0,18	0,30	0,50	0,19	0,37	0,86
40 % w	0,13	0,20	0,40	0,24	0,43	0,83	0,31	0,60	1,21
60 % w	0,17	0,25	0,42	0,33	0,53	0,93	0,42	0,61	1,14
80 % w	0,18	0,30	0,43	0,37	0,60	0,94	0,43	0,65	1,29
Eau	0,2	0,31	0,46	0,38	0,64	0,99	0,45	0,84	1,63

*Avec : W; eau, e; éthanol, PEI membrane dense 30 APA = $m_{d1,60um}$, PEI membrane dense 25 APA = $m_{d2,30\mu m}$, PEI membrane asymétrique 25 APA = $m_{as,60\,\mu m}$, NB: Alimentation Eau/éthanol en % masse

Tableau 9.3: Effet de la température de fonctionnement sur le flux normalisez des membranes denses PEI. NB: Alimentation Eau/éthanol en % masse

Alimentation eau/éthanol	Flux normalisé m_{d1*} (10µm kg/h m2)			Flux normalisé m_{d2*}(10µm kg/h m2)		
	30°C	45°C	60°C	30°C	45°C	60°C
ethanol	0,20	0,30	0,5	0,18	0,3	0,54
20 % w*	0,5	1	1,5	0,55	1	1,5
40 % w	0,75	1,25	2,5	0,80	1,3	2,5
60 % w	1,05	1,5	2,7	0,99	1,5	2,7
80 % w	1,1	1,8	2,6	1,15	1,8	2,8
Eau	1,2	1,9	2,8	1,2	2	3

Tableau 10.3: Effet de la température sur le flux réel et l'alimentation avec la PEI membrane asymétrique 25% APA ($m_{as, 60\ um}$).

Alimentation Eau/éthanol	Eau flux partiel réel (J_W) (kg/h m2)			Ethanol flux partiel réel (J_e)(kg/h m2)		
	30°C	45°C	60°C	30°C	45°C	60°C
*20 % w	0 ,13	0,23	0,49	0,05	0,14	0,37
40 % w	0,25	0,47	0,87	0,07	0,14	0.34
60 % w	0,38	0,53	0,96	0,04	0,08	0,18
80 % w	0,45	0,59	1,15	0,02	0,06	0,15

*NB: Alimentation Eau/éthanol en % masse

Tableau 11.3: Déshydration les systèmes d'alcools aqueux (azéotrope éthanol, et 5% eau, 95% n-butanol).

Type de Membrane	Alimentation	Operation T (°C)	Flux réel (Kg/m^2 h)	Facteur de Separation	Eau perméat % masse
PEI membrane Asymétrique 25% PAA	95 % masse n-butanol / H_2O	30	0.040	475	98%
		45	0.086	313	97%
		60	0.165	266	96%
	95 % masse EtOH / H_2O	30	0.040	26	57%
		45	0.160	17	46%
		60	0.350	14	42%
(PMDA-ODA) dense [45]	88.9 % masse EtOH/ H_2O	45-75	14-43	0,347-0,455	
(PI-2080) Asymétrique [46]	93 % masse EtOH/H_2O	60	1000	0,9	

I. Sélectivité des membranes PEI étudiées

Dans le cas Eau/éthanol, l'objectif était double: d'abord, s'assurer que les membranes asymétriques à base de PEI préparées permettent bien de réaliser des séparations moléculaires comme dans le cas précédent des mélanges Toluène – Heptane; en second lieu, que la

sélectivité observée correspond bien à celle d'une membrane hydrophile, puisque c'est l'objectif pour la nanofiltration de solutions aqueuses.

Sur ces deux questions, les résultats obtenus ont apporté des réponses positives et satisfaisantes. Certaines membranes ont montré une bonne sélectivité (ex. 70% d'eau dans le perméat à partir d'une charge de 20% à 30°C), et pour la plupart des membranes asymétriques testées selon des modes de préparation distincts, il a bien été possible de vérifier la sélectivité moléculaire escomptée. Ainsi partant d'une charge de composition azéotropique (5% eau, 95% EtOH à 30°C), l'enrichissement du perméat correspond varie de 42 à plus de 57% d'eau, ce qui montre bien la séparation moléculaire et le caractère hydrophile des PEI.

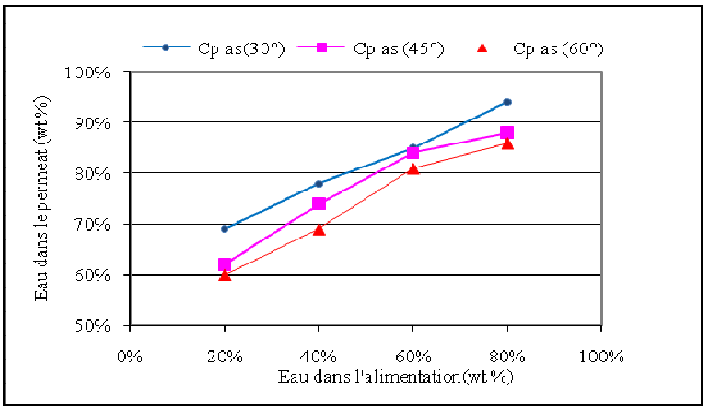

a. asymétrique (25 APA& 60µm).

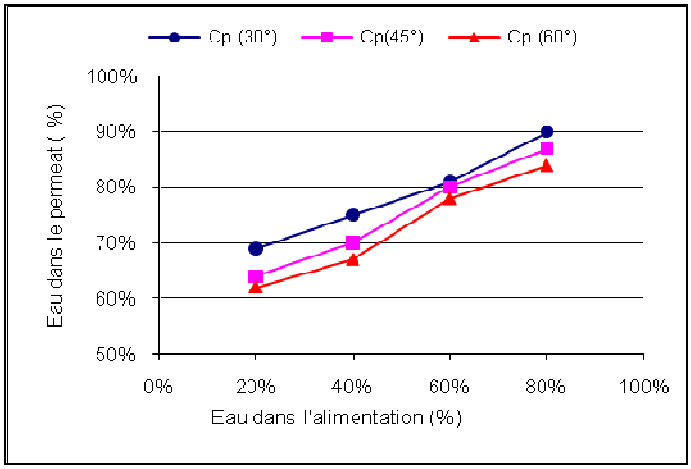

b. Dense (25 APA& 30µm).

Figure 22.3: Effet de la concentration de l'alimentation et température sur la séparation de membrane asymétrique $_{(25\ APA\ ,\ 60um)}$ et membrane dense $_{(25\ APA,30\mu m)}$ (mélange eau/éthanol, C_p±2-3%).

Dans le cas du mélange eau-butanol, il s'agissait de comparer avec les résultats Eau éthanol à la composition azéotropique. Pour une teneur initiale de 5% eau et 95% n-butanol, l'enrichissement du perméat a été de 96 à 98% en eau Fig.23.3, ce qui démontre encore mieux la séparation moléculaire et le caractère hydrophile des PEI.

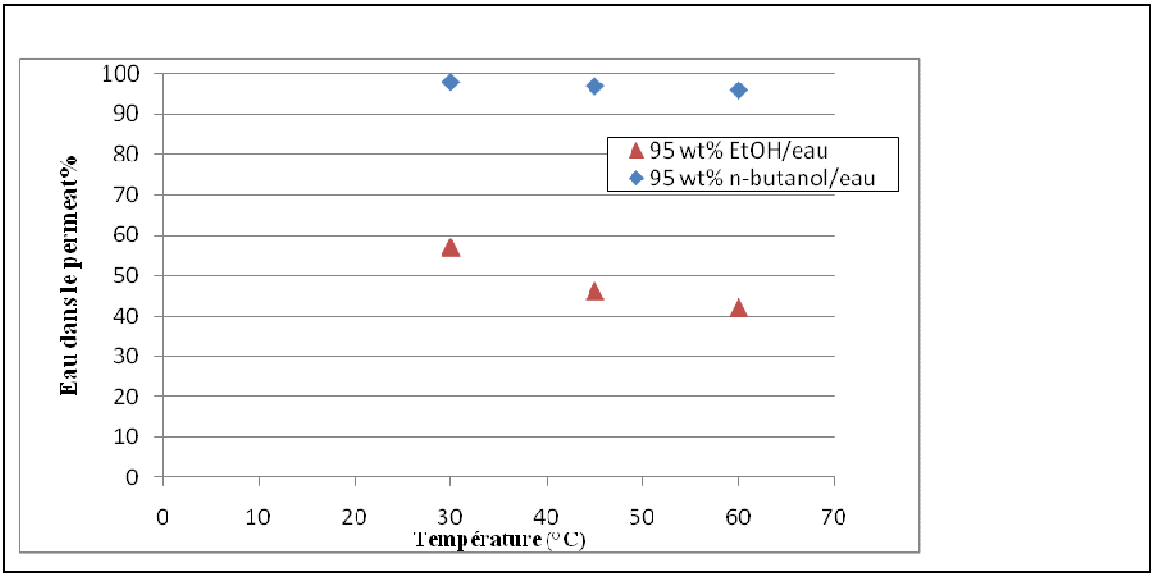

Figure 23.3: Variation de la sélectivité en fonction de la température pour des membranes asymétriques M_{as2} (25%-75%-0/1min/1h/40µm) mélanges H_2O/EtOH et H_2O/nBuOH. NB: il y a démixtion du système H_2O/nBuOH pour 7% masse eau.

- **Effet de la température sur la sélectivité**

L'augmentation du flux en fonction de la température s'accompagne d'une diminution de la sélectivité (Figs.22.3, 23.3). Ceci peut être expliqué par le fait qu'une augmentation du flux de l'Eau engendre une augmentation du flux couplé de l'alcool. En d'autre terme, plus le flux de l'Eau augmente plus il entraîne avec lui de l'alcool.

- **Effet de la température sur le flux**

D'après la courbe de la Fig.24.3, on note que pour toutes les membranes, le flux augmente avec l'augmentation de la température. Il se peut donc que le flux suit une équation type Arrhenius. Pour démontrer cela, on se propose de tracer la courbe Ln J= f (1/T).

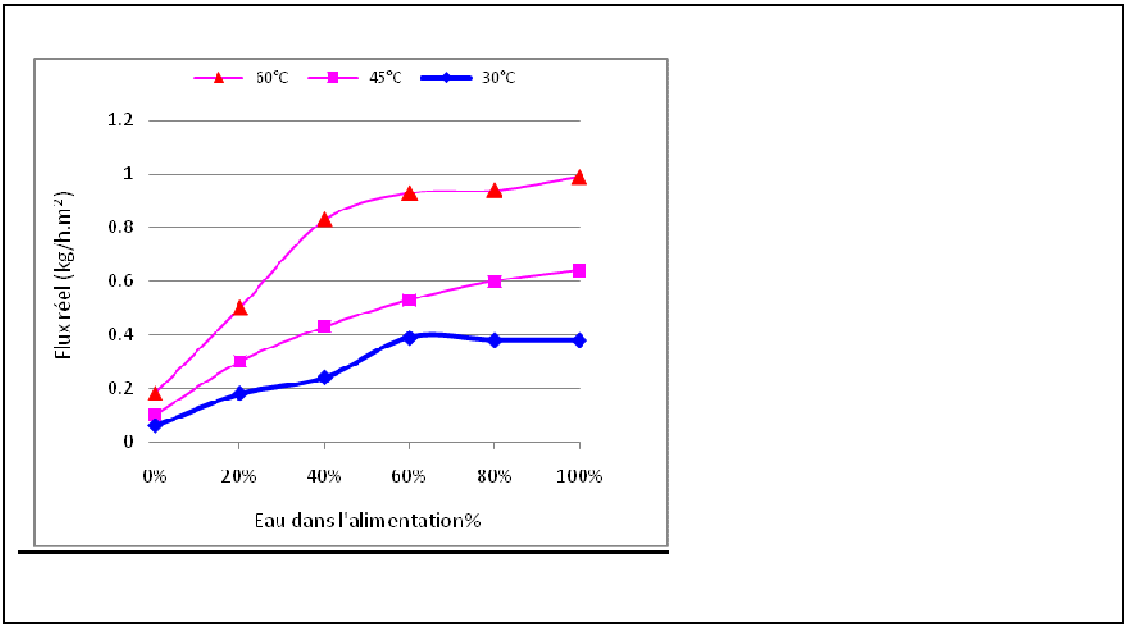

Figure 24,a.3: Variation du flux réel en fonction de la température pour de la membrane dense $M_{d2(25PAA\ ,30\mu m)}$ (25PAA) mélanges H_2O/EtOH.

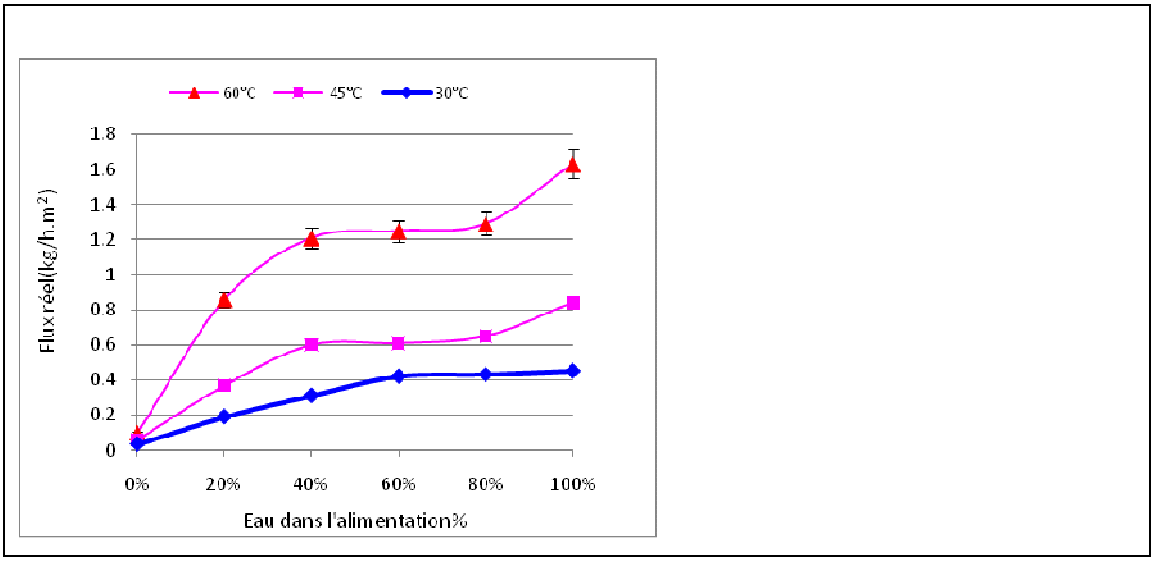

Figure 24,b.3: Variation du flux réel en fonction de la température pour de la membrane asymétrique $M_{as1(25PAA\ ,60\mu m)}$ mélanges H_2O/EtOH.

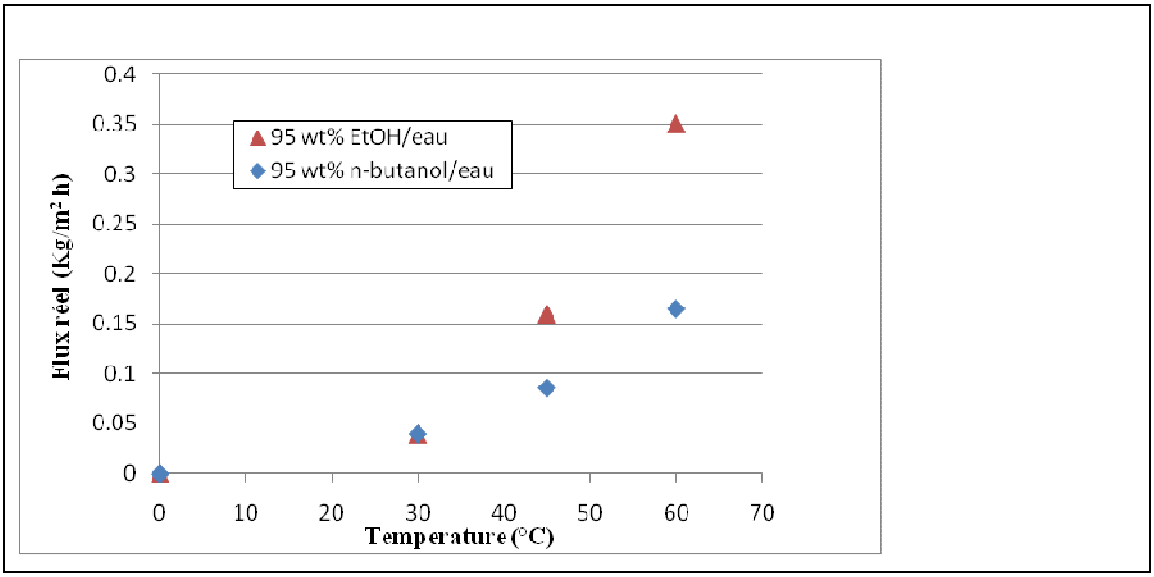

Figure 24,c.3: Variation du flux réel en fonction de la température pour une membrane asymétrique M_{as2}.

La courbe obtenue est une droite linéaire de la forme y = a x+ b ce qui montre que le flux suit bien une loi du type Arrhenius (Fig. 25.3). En effet $J = J_0 \exp\left(\frac{-Ea}{RT}\right)$ $\Leftrightarrow LN(J) = [LN(J)_0) - \frac{Ea}{R} \times \frac{1}{T}$ donc la pente de cette courbe est $-\frac{Ea}{R}$.

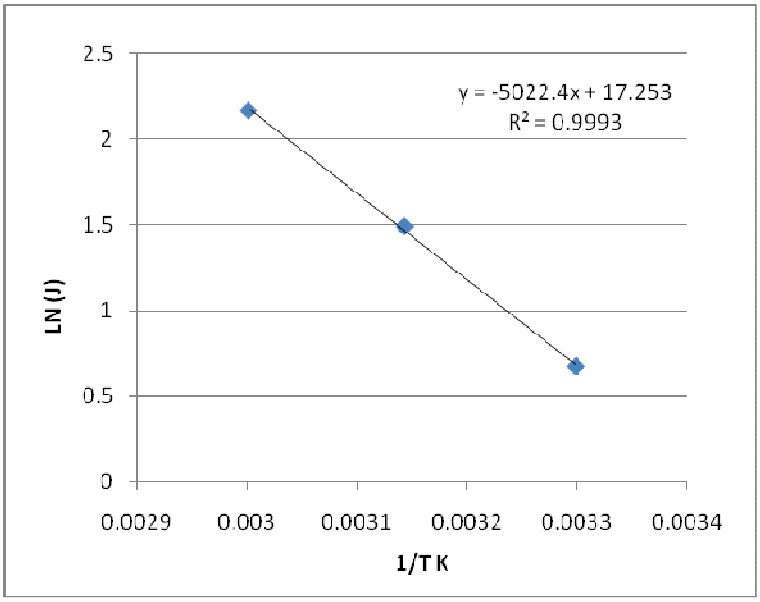

Figure 25.3: Variation du Logarithme du flux molaire J_M en fonction de 1/T pour de membrane asymétrique M_{as2} mélanges H_2O/EtOH.

3.2.2 Résultats de Nanofiltration (NF) avec les membranes PEI

Parmi les méthodes possibles de remédiation, adsorption, absorption, ozonolyse, traitement biologique, etc…, nous nous intéressons à une méthode nouvelle correspondant à la nanofiltration à l'aide de membranes originales synthétisées au laboratoire. Ces membranes, de type polyimide, sont préparées par méthode d'inversion de phase pour obtenir des structures asymétriques très perméables à l'eau, mais pouvant permettre la rétention en amont des molécules organiques.

I. Problème de l'extraction de masse moléculaire faible des composés organiques de l'eau par des membranes

Des études de la littérature ont prouvé que les méthodes d'osmose inverse (OI) et de NF sont des technologies efficaces pour enlever les sels et les composés organiques dessous de fortes masse molaires ou quand les composés organiques dessous ont des groupes fonctionnels ionisables entraînant la répulsion électrostatique. Cependant, ces études ne considèrent que des molécules des relativement grandes [47] (par exemple, masse moléculaire (MW) > 150 g/mol) et/des composés relativement hydrophobes (par exemple, logarithme de coefficient l'octanol-eau > 2.0). Peu d'études ont étudié le rejet de petits composés organiques non-charges par des membranes de OI et de NF. Ces études ont prouvé que les rejets pour de petites molécules non-charges sont très faible comme pour l'urée [48-49], il peut également être très difficile d'enlever d' autres petites, hydrophiles, telles que le méthanol et formaldéhyde en utilisant des membranes d'OI ou de NF.

Plusieurs études récentes ont étudié les mécanismes de transport des corps dissous ioniques et organiques par les membranes de RO ou de NF [50-51]. Ces études ont montré que cela pour les composés organiques le degré de séparation dépend de la taille/de forme et de la polarité/de l'hydrophobicité des corps dissous, alors que pour les composés ioniques le degré de séparation est régi par l'exclusion de taille et l'exclusion électrostatique.

Généralement, de s composés de fortes masse moléculaire ont un meilleur rejet que les composés de faible masse moléculaire. Cependant, le rejet n'est pas purement une fonction de masse moléculaire. Le rejet d'urée (au-dessous de 22%) est sensiblement inférieur à tous autres composés excepté le formaldéhyde et le méthanol (rejet au-dessous de 15%). Ces résultats suggèrent que le rayon de corps dissous soit un meilleur paramètre pour prévoir le rejet des corps dissous que le masse moléculaire [52].

II. Etude de la séparation de solutions aqueuses organiques par des membranes PEI

L'objectif est d'étudié la possibilité de rétention de composés organiques très dilués (100 à 500ppm) dans l'eau par une technique de séparation membranaire, la nanofiltration. En effet, les activités anthropiques conduisent au relargage dans les milieux naturels de molécules organiques (COV, hormones,..) qui provoquent une pollution des eaux de surface d'autant plus difficile à traiter que leur concentration est faible.

Les mélanges étudiés en nanofiltration (NF) sont des solutions organiques aqueuses. Les composés organiques testés ont été choisis pour couvrir une large gamme de masse moléculaire et avoir des propriétés d'hydrophobie (logarithme de coefficient l'octanol-eau (log_{ow})) différentes. Pour avoir des résultats reproductibles, on procède à des mesures en régime stationnaire. Pour chaque membrane, on doit avoir au minimum trois essais avec un flux constant avant de changer de solutions aqueuses organiques. Le Tableau 12.3 montre les paramètres de préparation des membranes asymétriques PEI. Le Tableau 13.3 montre les résultats de rejet moyen des solutions aqueuses organiques par des membranes.

Tableau 12.3: Paramètres de préparation des membranes asymétriques PEI.

Membrane	solution de polymère masse%			Porosité %	Épais µm
	APA	DMF	Eau*		
$M_{(25PAA)}$	25	75	0	56	95
$M_{(25PAA+15W)}$	25	75	15	86	75
$M_{(20PAA+25W)}$	20	80	25	97	60
$M_{(15PAA+25w)}$	15	85	25	97	110

* %eau calculé sur le total (APA + DMF) de masse après l'addition à la solution de polymère. Immersion dans l'eau 1 h à 18±2 °C, temps de pré-concentration de 1 min.

Tableau 13.3: Effet de la Mw sur le rejet moyen de solutions aqueuses organiques par des membranes PEI (Alimentation 500 ppm de matière organique / eau, Pression de 10 bar pour les membranes PEI et 20 bar pour la membrane Kapton PI).

Organique	Mw	Rejet %				
		$M_{(25PAA)}$	$M_{(25PAA+15W)}$	$M_{(20PAA+25W)}$	$M_{(15PAA+25w)}$	$M_{K5(15PAA)*}$
Ethanol	46	11	6	6		
2-propanol	60	13	11	9		
Butanol	74	16	17	15		30
Urée	60	14	9	14-15		
Cyclohexane	84		25-42			
Toluéne	92	63	51-56	43	30	
TEG	150	24-30	30	11-33		35
PEG400	400		79			37
PEG1000	1000	65-82,5	82	37	20	
PEG2000	2000		87			41
PEG6000	6000	100	100	45	50	51

Avec: TEG; triéthylène glycol, PEG; polyéthylène glycol. NB : Résultats pour le Kapton membrane $M_{K5\ (15PAA\ )}$ obtenus à 20 bar.

II.1 Effet du type de membrane et du soluté propriétés sur le rejet organique

La figure 26.3 montre l'effet du type de membrane sur le rejet des molécules organiques:

Les membranes asymétriques PEI présentent un rejet compris entre 6 et 100% alors que le rejet déterminé avec les membranes asymétriques Kapton^{TM} se situe entre 30 et 51%. Ainsi le rejet organique obtenu avec les membranes asymétriques PEI est plus élevé qu'avec les membranes Kapton asymétriques.

Le rejet organique suit l'ordre : $M_{(25PAA +15 W)} \approx M_{(25PAA)} > M_{(20PAA +25 W)} > M_{(15PAA +25 W)}$, comme illustré dans la figure 26.5.

Le rejet organique avec les membranes asymétriques PEI est plus important que les membranes Ultem 1000 asymétriques figure 27,b.3 [53**].**

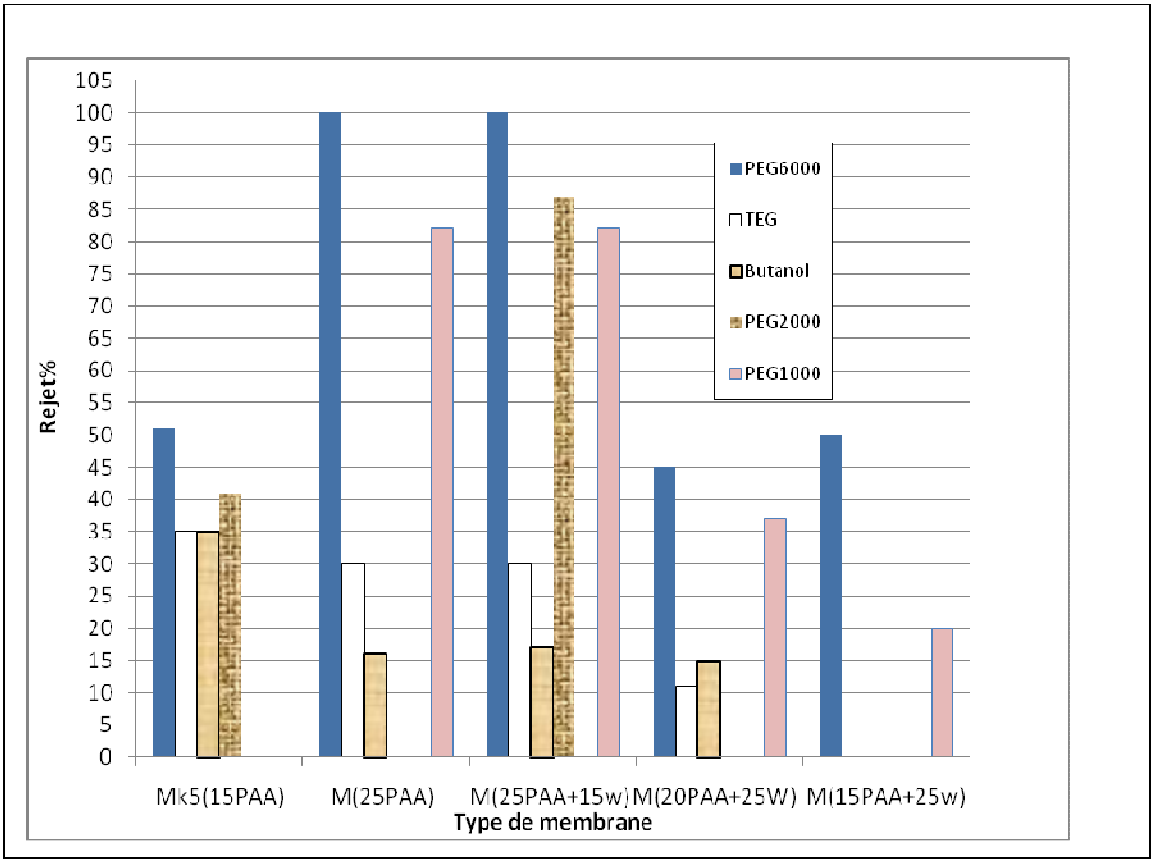

Figure 26.3*:* Effet du type de membrane sur le rejet (alimentation 500 ppm de matière organique / eau, la pression de 10 bar). NB : Résultats pour le Kapton membrane $M_{K5\ (15PAA\ )}$ obtenus à 20 bar.

Figure 27,a.3 montre l'effet de la masse moléculaire sur le rejet des molécules organiques. Généralement, de plus hauts composés de masse moléculaire ont un meilleur rejet que les composés de faible masse moléculaire. Pour les composés organiques relativement petits le rejet du butanol est plus de 17% pour les membranes de PEI. Le rejet d'urée (au-dessous de 14%) est sensiblement inférieur à tous autres composés excepté l'éthanol (rejet au-dessous de 11%). Ces résultats suggèrent que la masse moléculaire est un bon paramètre pour prévoir le rejet.

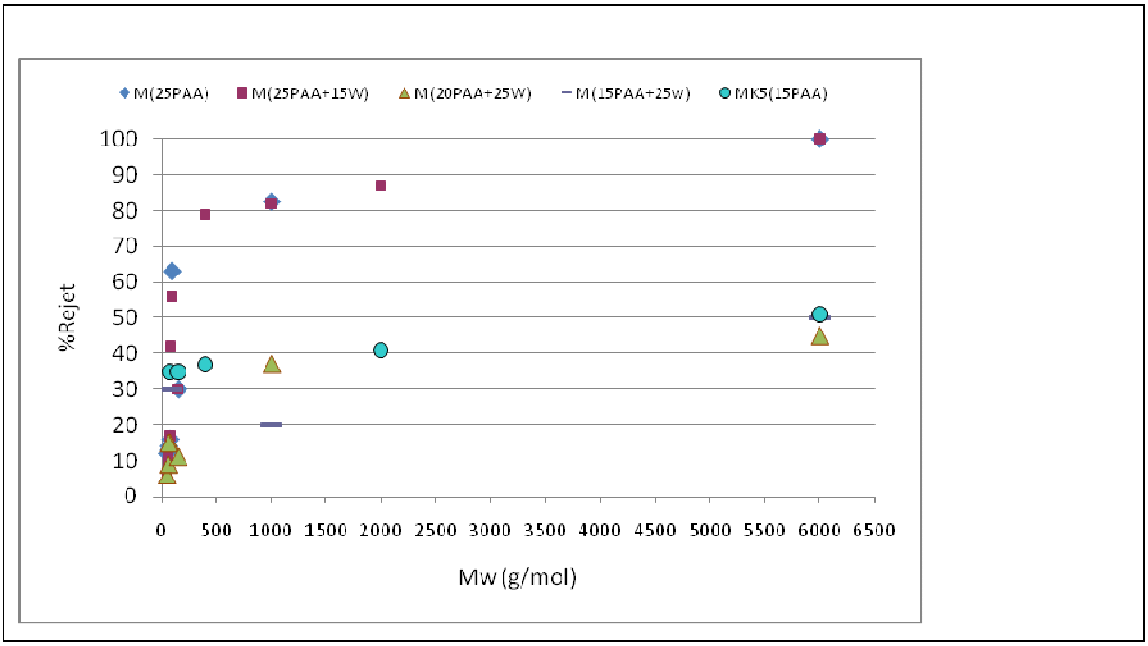

Figure 27,a.3: Effet de la Mw sur le rejet moyen de solutions aqueuses organiques par des membranes PEI (charge 500 ppm de matière organique / eau, pression de 10 bar). NB : Résultats pour le Kapton membrane $M_{K5\ (15PAA\ )}$ obtenus à 20 bar.

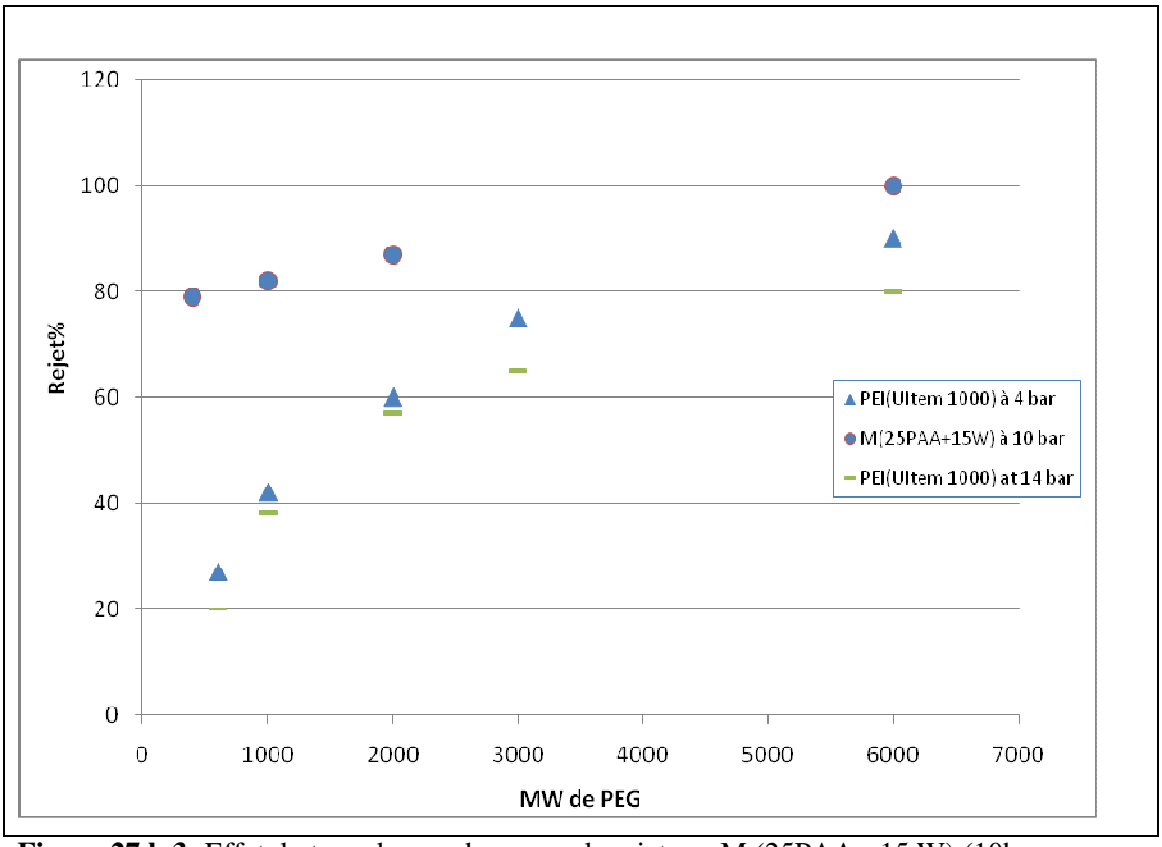

Figure 27,b.3: Effet du type de membrane sur le rejet par M (25PAA+ 15 W) (10bar, aliments 500 ppm) et de PEI (UItem 1000) (4:14 bar, charges 1000ppm).

Figure 28.3 montre l'effet du rayon de soluté sur le rejet des molécules organiques. Généralement, les composés ayant le rayon soluté le plus grand ont un meilleur rejet que les composés de faible rayon.

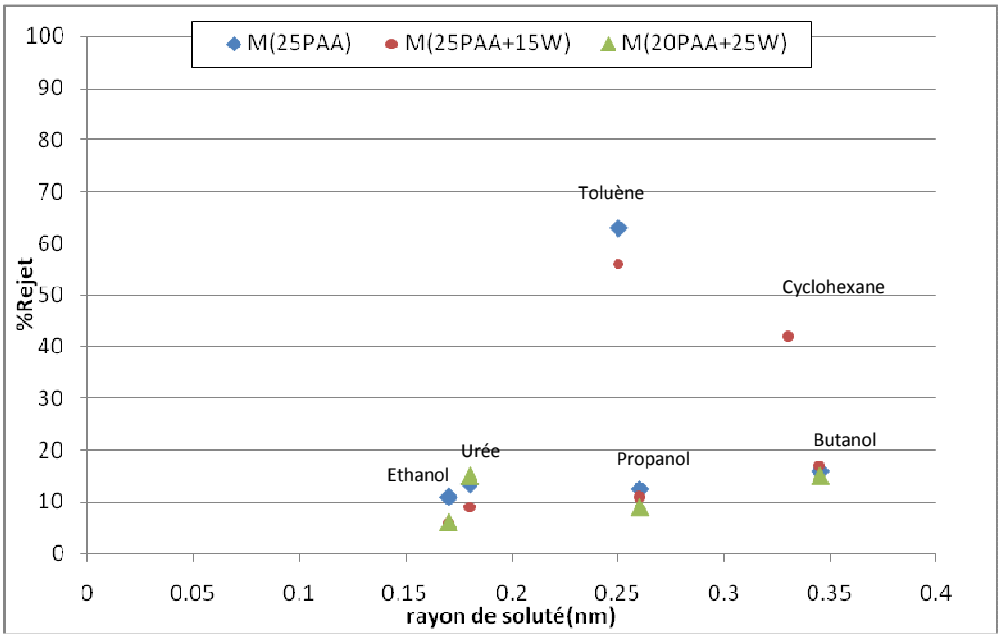

b. Rejet de solutés en fonction du rayon de soluté (cas de solutés de petites masses molaires).

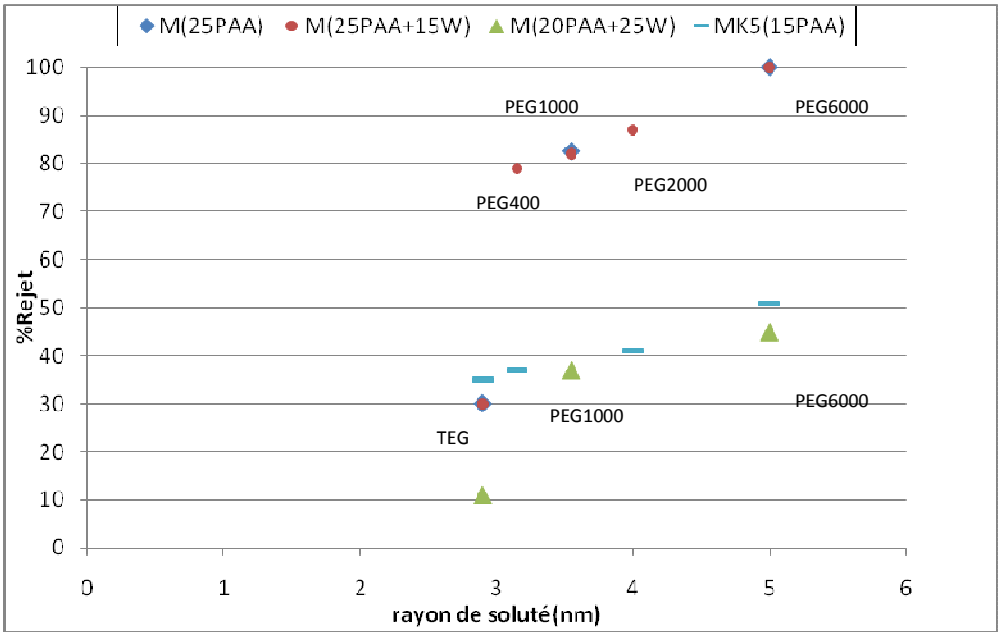

a. Rejet des solutés en fonction d'un rayon de soluté (cas de la famille des PEG).

Figure 28.3: Effet des rayons de solutés sur le rejet moyen de solutions aqueuses organiques par des membranes PEI (charge 500 ppm de matière organique / eau, pression de 10 bar). NB : Résultats pour le Kapton membrane $M_{K5\ (15PAA)}$ obtenus à 20 bar.

L'influence de l'hydrophobicité sur le rejet des solutions organiques aqueuse peut être représenté par le logarithme de la partition octanol-eau (log_{ow}) tel que présenté en figure 29.3. On observe que les composés de forte hydrophobicité ont un meilleur rejet que les composés de faible hydrophobicité pour toutes les membranes testée. Cependant comme le montre la figure 29.3, les membranes asymétriques ayant le meilleur rejet sont dans l'ordre M $_{(25PAA)}$, M $_{(25PAA\ 15\ W)}$ et M $_{(20PAA\ 25\ w)}$.

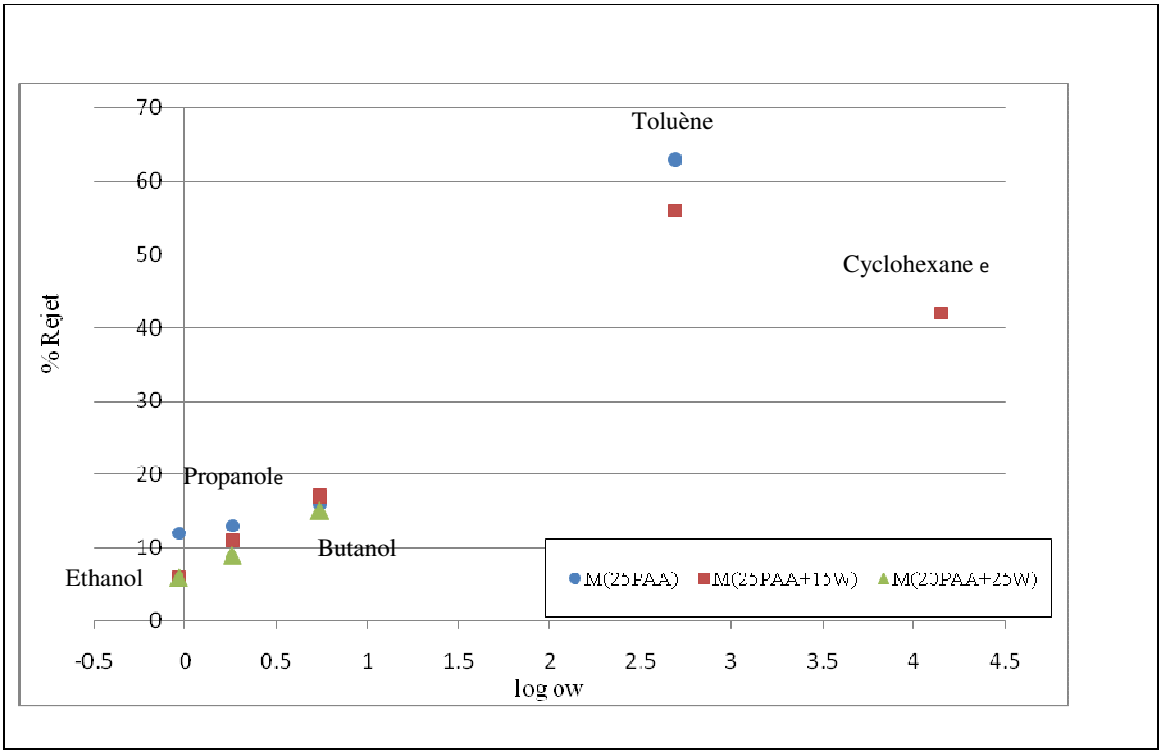

Figure 29.3: Relation entre l'hydrophobicité du soluté exprimée en log_{ow} et la rétention des membranes asymétriques PEI pour 3 alcools aliphatiques, le toluène et le cyclohexane.

II.2 Effet du type de membrane sur le flux réel

Le flux de perméat, d'une série de solutions aqueuses organiques obtenu avec des membranes asymétriques PEI et Kapton, a été étudié dans le but de caractériser la performance de la membrane (flux, perméabilité) avec le type de membrane. Pour chaque membrane, la relation entre le perméat de nanofiltration et les expériences a été calculée. Les tableaux 14.3 et 15.3 montrent les résultats de la nanofiltration (flux réel, Perméabilité) pour des solutions aqueuses et organiques par des membranes.

Tableau 14.3: Flux réels de nanofiltration (NF) obtenus avec les membranes asymétriques PEI (Alimentation 500 ppm de matière organique/ eau, Pression de 10 bar pour les membranes asymétriques PEI et 20bar pour les membranes Kapton^{TM} asymétrique, 30°C±2).

Organique	Flux réel (kg/h.m^2)				
	$M_{(25PAA,95\mu m)}$	$M_{(20PAA+25W, 60\mu m)}$	$M_{(25PAA+15W, 75\mu m)}$	$M_{(15PAA+25W, 110\mu m)}$	$M_{k5(15PAA, 140\mu m)}$
Eau	3-3,5	9 ?3	10-15	71	
Ethanol	1,5	9,3	8,6		
2-propanol	1,7	7,1	7,8		
Butanol	1,7	7,1	7,3		0,5
Ureé	2,7	7,3	7,8		
Cyclohexane			10		
Toluène	2,5	7,6	9,5		
TEG	2,6	9	8		0,23
PEG400			7.8		0.49
PEG1000	1,3	6	7,8	43,5	
PEG2000			8,2		0,29
PEG6000	1,7	6	9,5	45	0,32

Tableau 15.3: Perméabilités obtenus avec les membranes PEI (Alimentation 500 ppm de organique / eau, Pression de 10 bar pour les membranes PEI asymétriques et 20bar pour Kapton asymétrique).

Organique	Permeabilité (kg/h.m^2 bar)				
	$M_{(25PAA)}$	$M_{(20PAA+25W)}$	$M_{(25PAA+15W)}$	$M_{(15PAA+25W)}$	$M_{k5(15PAA)}$
Eau	0,35	0,93	1-1,5	7,1	
Ethanol	0,15	0,93	0,86		
2-propanol	0,17	0,71	0,78		
Butanol	0,17	0,71	0,73		0,025
Ureé	0,27	0,73	0,78		
Cyclohexane		1			
Toluène	0,25	0,76	0,95		
TEG	0,26	0,9	0,8		0,01
PEG400			0,78		0,02
PEG1000	0,13	0,6	0,78	4,35	
PEG2000			0,82		0,015
PEG6000	0,17	0,6	0,95	4,5	0,016

La figure 30.3 montre l'effet du type de membrane sur le flux. Les membranes asymétriques PEI présentent des flux nettement plus élevés que ceux obtenus avec membranes Kapton (15PAA). En effet, les flux varient entre 4,2 et 71kg/h.m^2 à 10 bar pour les membranes asymétriques PEI et entre 0,2 et 0,5 kg/h.m2 à 20 bar pour Kapton (15PAA). Ce résultat et peut être attribué à la structure à deux blocs des membranes PEI. Ainsi, le bloc souple présent une affinité avec l'eau et le bloc rigide permet de bonnes propriétés mécaniques. Le flux suit l'ordre: M (15PAA +25 W)> M (25PAA+15w)> M (20PAA +25 W)> M (25PAA)> M_{Kapton} comme illustré dans la figure (30.5).

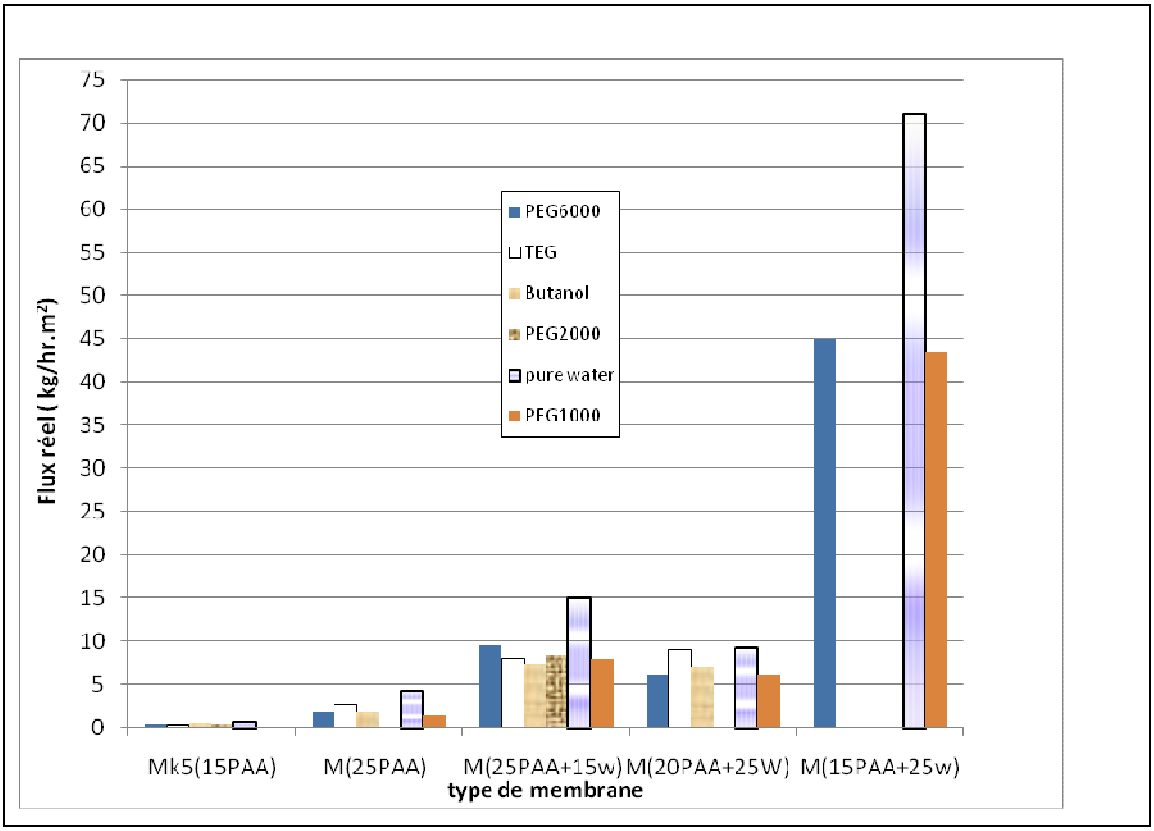

Figure 30.3: Effet du type de membrane sur le flux réel. NB : Alimentation 500 ppm de matière organique / eau, 30°C±2, Pression de 10 bar pour les membranes asymétriques PEI et 20bar pour la membrane Kapton^{TM} asymétrique).

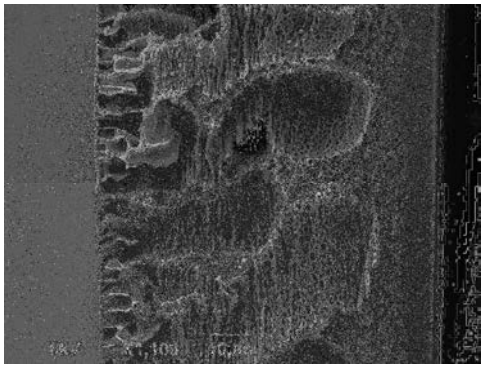

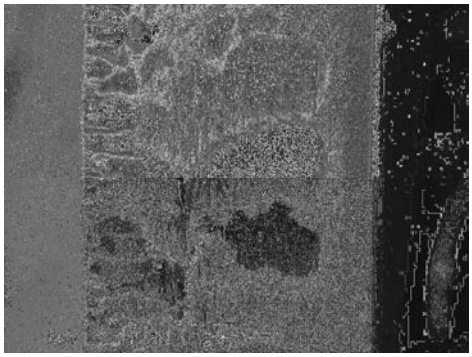

Avant les essais

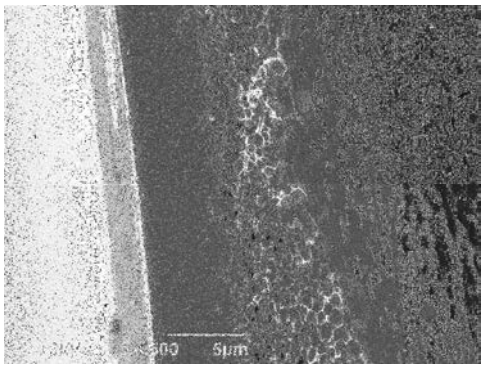

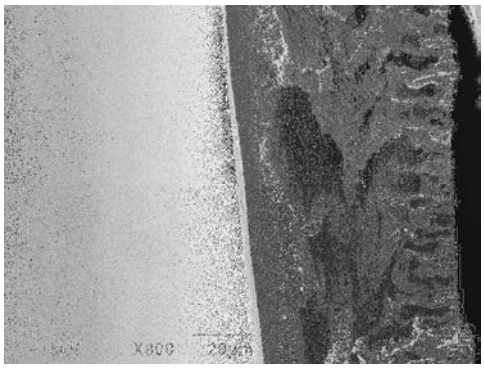

après les essais

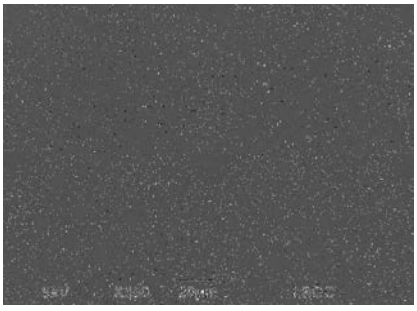

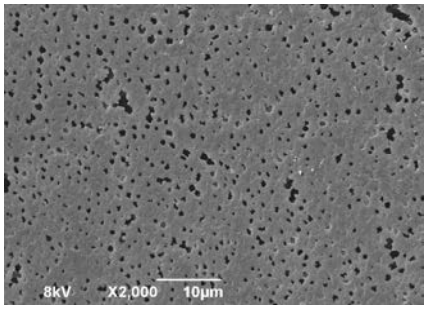

Section supérieure Section inférieure

Figure 31.3: Vues en MEB des sections des films de PEI préparent selon protocoles d'inversion de phase pour membranes M $_{(25PAA,\ 95\mu m)}$, applicateur de film liquide de 500 µm d'épaisseur.

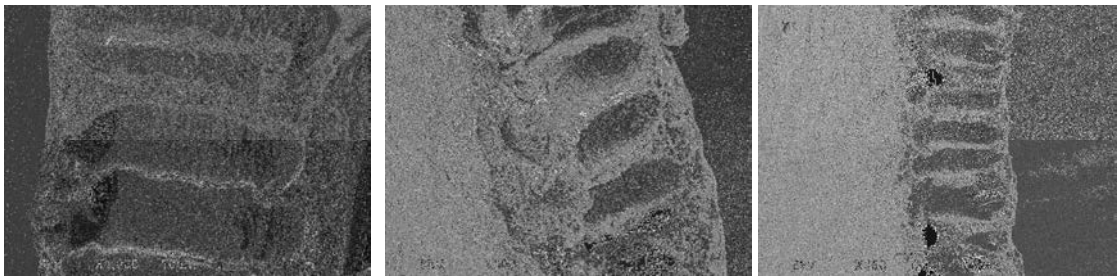

Avant les essais

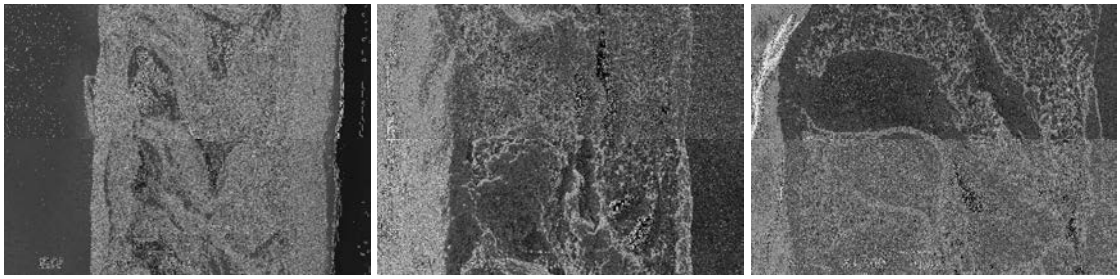

Après les essais

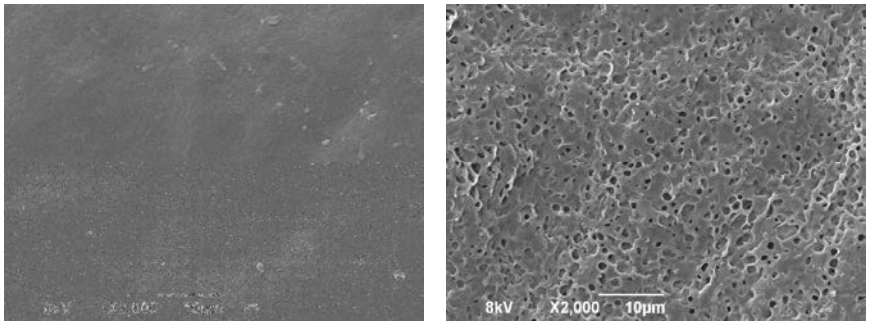

Surface supérieure surface inférieure

Figure 32 .3: Vues en MEB des sections des films de PEI préparent selon protocoles d'inversion de phase pour membranes M $_{(25PAA+15W,75\mu m)}$, applicateur de film liquide de 300 µm d'épaisseur.

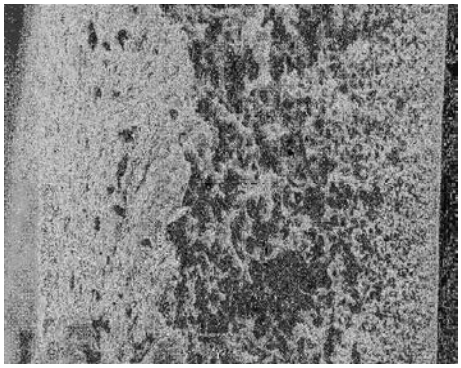

Avant les essais

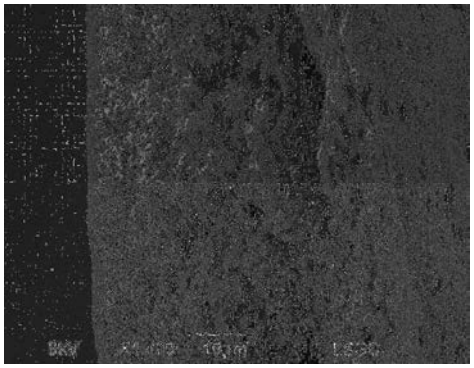

Après les essais

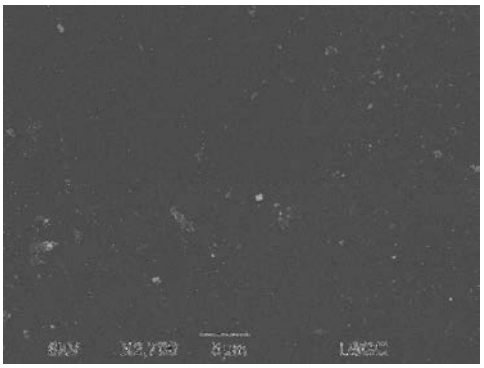

Surface supérieure

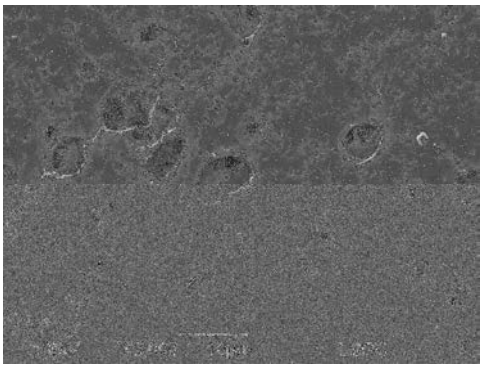

surface inférieure

Figure 33.3: Vues en MEB des sections des films de PEI préparent selon protocoles d'inversion de phase pour membranes M $_{(20PAA+25W,60\mu m)}$, applicateur de film liquide de 300 µm d'épaisseur.

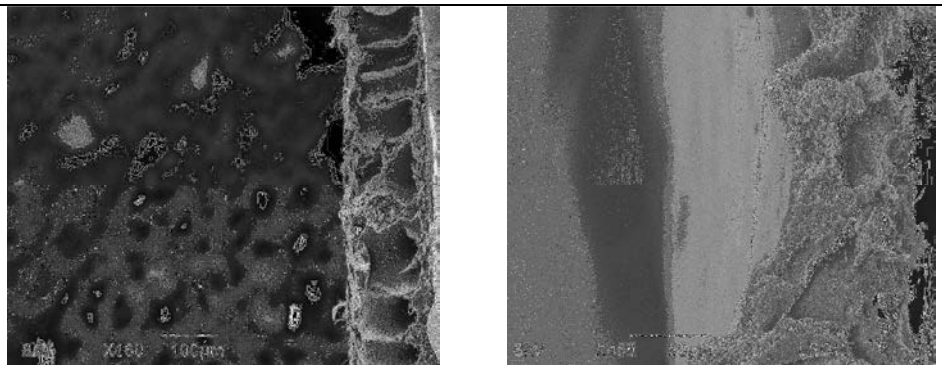

Avant les essais Après les essais

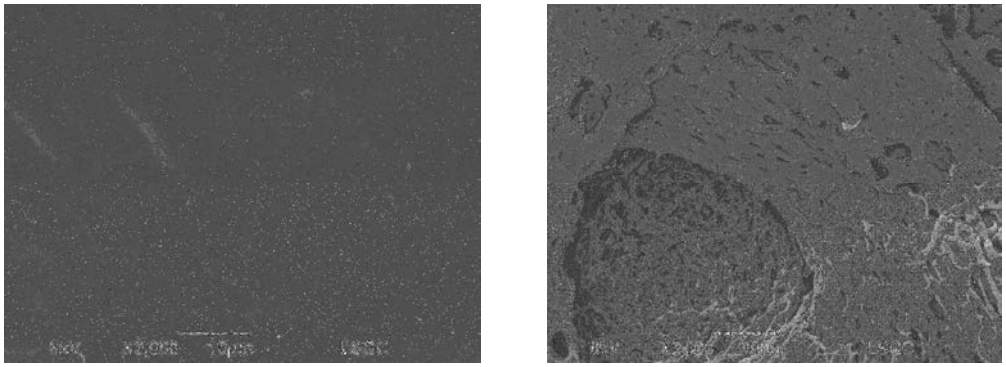

Surface supérieure surface inférieure

Figure 34.3: Vues en MEB des sections des films de PEI préparent selon protocoles d'inversion de phase pour membranes M $_{(15PAA+25w,\ 110\mu m)}$, applicateur de film liquide de 500 µm d'épaisseur.

Conclusion générale

Conclusion générale

La thématique de ce travail s'inscrit dans le contexte actuel de lutte contre la pollution des ressources d'eau potable souvent contaminées par des composés chimiques issus de activité humaine (sociétale ou industrielle) et rejetés avec de faibles concentrations dans l'environnement (molécules pharmaceutiques, pesticides,…). L'objectif était d'étudier la possibilité de rétention de composés organiques, de structures chimiques et de masse molaire variées, très dilués (500 à 100ppm) dans l'eau par une technique de séparation membranaire, la nanofiltration (NF). Etant des procédés propres, les procédés membranaires correspondent pour les industriels à une alternative intéressante pour l'élimination de polluants peu concentrés dans des rejets ; en particulier le traitement d'effluents liquides par NF semble être une solution d'avenir économique qui devrait permettre de respecter les normes de rejet imposées qui sont de plus en plus contraignantes.

Dans le cadre des problématiques de séparations petites molécules organiques, nous avons étudié, d'un point de vue plus fondamental qu'appliqué, la possibilité de développer de nouveaux matériaux pouvant permettre la préparation de membranes asymétriques hydrophiles pour réaliser la purification de mélanges aqueux, en utilisant des technologies membranaires telles que la pervaporation et la nanofiltration.

La préparation de membranes polymères asymétriques est souvent réalisée par la méthode d'inversion de phase, dans laquelle une solution de polymère homogène subie une séparation de phases par l'échange de solvant et de non solvant lors de l'immersion dans un bain de coagulation composé (en général) majoritairement d'eau. La séparation des phases, i.e. une phase riche en polymère en équilibre avec une phase riche en eau, contribue à former la structure asymétrique de la membrane par gélification puis solidification de la phase riche en polymère.

L'inversion de phase est une méthode connue de longue date pour préparer des membranes asymétriques à partir de polysulfones, polyamides ou de polyimides aromatiques (PI). Ce travail a permis de montrer pour la première fois à notre connaissance, qu'il était également d'utiliser des polyalcoxyétherimides élastomères (PEI) combinant des blocs alkoxyéther (obtenus avec des Jeffamines®) et des blocs aromatiques (issus de l'ODA) par condensation avec le PMDA. A partir des acides polyamiques (APA) correspondants, des membranes denses de PEI ont été facilement obtenues avec différentes proportions d'amines aliphatique et aromatique ; ces membranes présentent une forte analogie structurale avec celle du Kapton™ en ce qui concerne les blocs aromatiques composés d'ODA et de PMDA.

Le rapport 0,4/0,6 d'amines aliphatique/aromatique a permis la préparation de membranes asymétriques ayant de bonnes propriétés mécaniques et pouvant être facilement utilisées en pervaporation comme en nanofiltration. Pour les autres APA préparés avec des taux de Jeffamine® supérieurs à 0,4 il n'a en revanche pas été possible de préparer de façon reproductible des films PEI asymétriques par inversion de phase dans des conditions analogues qui soient utilisables en pervaporation ou en nanofiltration ; la variation des conditions d'inversion de phase, telles que la concentration initiale en polymère, le temps de pré-concentration avant immersion, la température du bain de coagulation ou l'épaisseur du film liquide déposé sur la plaque de verre, n'a pas permis non plus la préparation de PEI asymétriques de propriétés mécaniques satisfaisantes .

Le point le plus intéressant de ces travaux a été la préparation réussie par inversion de phase de membranes PEI asymétriques présentant une couche fine quasiment exemptes de pores sur sa partie supérieure ; en effet pour certaines conditions d'inversion de phases, la formation de cette couche dense en surface a permis d'obtenir des membranes asymétriques ayant des propriétés de sélectivité identiques ou analogues à celles de membranes denses, mais avec des flux transmembranaires beaucoup plus grands. Ceci a été démontré particulièrement bien par les résultats de pervaporation obtenus avec les mélanges Toluène/Heptane et eau/alcools montrant des sélectivités fortes (Cperméat: 80% avec T/H ou Eau/Ethanol), proches de la sélectivité des films denses préparées classiquement par pervaporation (Cperméat: 90% avec T/H, Cperméat: 80% avec Eau/Ethanol). Ainsi, pour la plupart des membranes asymétriques préparées selon des modes de préparation optimisées, il a bien été possible de vérifier la sélectivité moléculaire escomptée.

Testées ensuite en nanofiltration, certaines de ces membranes ont aussi montré des taux de rejet élevés pour des molécules très hydrophiles, de type polyéthylène glycol, ayant des masses molaires allant de 400 à 6000 Dalton ; selon les masses molaires, les taux de rejet atteints allaient de 79 à 100% à partir de solutions aqueuses à 500ppm de composés organiques (Pression transmembranaire : 10Bar, t°≈30°). Par exemple, partant d'une solution aqueuse contenant 500ppm de PEG 2000, le rejet correspond à 87% ($M_{(25PAA+15W)}$), soit à une teneur résiduelle en PEG d'environ 65ppm dans l'eau perméée, avec une perméabilité de l'ordre de 1L/(h.m^2.bar).

Si l'on remarque que dans des conditions analogues de NF des membranes asymétriques de Kapton ont un flux non mesurable proche de zéro, on réalise mieux l'intérêt de la synthèse de PEI et des performances de séparation obtenues en NF ; l'insertion des chainons hydrophiles alcoxyéthers a bien permis de conférer un fort caractère hydrophile à la structure des PEI tout

en assurant un taux de rejet élevé pour des molécules hydrophiles de masse supérieure à 150 g/mole.

Enfin, les premiers résultats obtenus avec des molécules peu polaires sont aussi prometteurs ; ils indiquent des taux de rejet sensiblement supérieurs pour des composés de masse molaire inférieure. Ainsi, pour une molécule hydrophobe comme le toluène (M=92g/mole), le taux de rejet est supérieur à 50% ($M_{(25PAA+15W)}$) alors que celui du triéthylèneglycol (M=150g/mole) n'est que de 30%.

Dans la réalité, les eaux usées réel sont des mélanges complexes, souvent constituées de plusieurs des composés organiques et inorganiques. En raison des interactions entre ces composés, les performances de la membrane peuvent être améliorées ou non. Pour cette raison, une série d'expériences de NF a été effectuée avec un mélange modèle aqueux contenant 500 ppm de composé organique et 500 ppm de NaCl. Il a été constaté que dans ce cas, le taux de rejet du constituant organique était inférieur à celui mesuré pour le mélange binaire, probablement en raison d'un effet de sel à la fois limitant le flux d'eau transmembranaire (plus faible gonflement de la membrane) et augmentant le coefficient activité du composé organique.

D'après l'ensemble des résultats obtenus, on peut tirer les trois conclusions suivantes :

- La faisabilité de la synthèse de membranes asymétriques à partir de polyimides élastomères (PEI) a été clairement établie, les propriétés mécaniques de ces membranes étant toutefois limitées par le taux de chainons élastomères intégrés dans la structure imide ; la morphologie de la structure asymétrique des PEI peut être contrôlée par les conditions d'inversion de phase, et conduire soit à la formation de pores en doigts de gant, soit à une structure spongiforme, soit encore à la formation d'une peau fine et dense autosupportée par une couche très poreuse.
- Pour les membranes comprenant une peau dense, la sélectivité moléculaire des membranes PEI asymétriques est bien conservée en pervaporation, quelque soit la nature du mélange initial, organique ou aqueux ; ce résultat indique que la peau de surface est effectivement dense, quasi exempte de pores nanométriques, et que le mécanisme de transport correspond au modèle de solution-diffusion.
- En nanofiltration, il apparait que les deux paramètres déterminant la sélectivité des membranes asymétriques PEI sont par ordre d'importance la polarité et la masse molaire des composés dissous dans l'eau ; ceci est en relation avec la nature de la phase élastomère dont l'hydrophilie avérée permet d'une part, d'augmenter considérablement le flux d'eau par rapport à un polyimide totalement aromatique et

d’autre part, de défavoriser la perméation de molécules hydrophobes. Ces résultats tendent à montrer que le mécanisme de perméation qui prévaut avec ces membranes PEI asymétriques ne correspond pas strictement à celui attendu en nanofiltration, où prédomine la masse molaire des composés en relation avec la taille des pores de la membrane, ce qui semble cohérent avec la présence d’une peau fine et essentiellement dénuée de pores en surface de la membrane asymétrique PEI.

Nomenclature et Abréviations

Nomenclature et Abréviations

APA : Acide polyamique

D : coefficient de diffusion ($m^2.s^{-1}$)

DMF : Diméthylformamide

t : épaisseur de la membrane (cm)

E_D : L'énergie d'activation apparente du processus de diffusion (J/mol)

E_P : L'énergie d'activation apparente du processus de perméation (J/mol)

f : fraction du volume libre dans le polymère

J : flux réel du perméat à travers la membrane ($Kg/h/m^2$)

Jn : flux normalisé du perméat à travers la membrane ($Kg/h/m^2$) pour l'épaisseur de10µm

MEB : Microscopie Electronique à Balayage

MET : Microscopie Electronique à Transmission

ODA : 4,4' Oxydianiline

Pe : Perméabilité de la membrane (barrer avec 1 barrer = 10^{-10} cm^3. cm/cm^2. cmHg.s)

PEI : Polyalcoxyétherimide

PI : Polyimide

S : coefficient de solubilité ($mol.m^{-3}.Pa^{-1}$)

TEOS : Tétraéthylorthosilicate

TMOS : Tétraméthylorthosilicate

α : Facteur de séparation

β : Facteur d'enrichissement

Références bibliographiques

1. X.Shude, Y.M.Robert, F.Xianshe, Synthetic 6FDA-ODA copolyimide membranes for gas separation and pervaporation: Functional groups and separation properties, Polymer 48(2007)5355-5368.

2. R. W. Baker, W. J. Koros (1994), Polymeric gas separation membranes: London, CRC Press.

3. http://www.technologies-propres.com/pdf/livret_fiches_papier.pdf

4. P.Adrian, Étude comparée du colmatage en nanofiltration et en ultrafiltration d'eau de surface, Faculté Des Sciences Et De Génie, Université Laval, 2004.

5. M. C.Porter (1990), Handbook of industrial membrane technology, Noyes publications, Park Ridge, New Jersey, U.S.A P 61-70.

6. M. Mulder (1996). Basic principles of membrane technology (2 ed.). Kluwer Academic: Springer. ISBN 0-7923-4248-8.

7. R. W. Baker (2004) ,Membrane Technology and Applications, John Wiley & Sons, Ltd ISBN: 0-470-85445-6

8. H. Strathmann, Membrane separation process, J. Membr. Sci., 9(1981)121-189.

9. http://www.wikipedia.fr

10. J. Lizhong, W.Wencai, W.Xiaowein, W.Dezhen, J.Riguang, Effect of water on the preparation, morphology and properties of polyimide/silica nanocomposite films prepared by sol-gel process, Wiley Inter. Sci. (2006).

11. R.R. Sharma, R. Agrawal and S. Chellam, Temperature effects on sieving characteristics of thin-film composite nanofiltration membranes: pore size distributions and transport parameters, J. Memb. Sci. 223 (2003) 69–87.

12.M.R. Wiesner, S. Chellam, The promise of membrane technology, J. Environ. Sci. Technol. 33 (1999) 360A–366A.

13. H.Strathmann, L.Giorno, E.Drioli, An introduction to membrane science and technology, consiglio nazionale delle ricerche roma 2006.

14. K. Scott, R. Hughes (1996), Industrial membrane separation technology, London: Blackie Academic & Professional**,** Springer; ISBN-13**:** 978-0751403381.

15. H. Yanagishita, D. Kitamoto, T. Ikegami, H. Negishi, A. Endo, K. Haraya, T. Nakane, N. Hanai, J. Arai, H. Matsuda, Y. Idemoto and N. Koura, Preparation of photo-induced graft filling polymerized membranes for pervaporation using polyimide with benzophenone structure, J. Memb. Sci. 203 (2002) 191-199.

16. X. Feng and R.Y.M. Huang, Liquid separation by membrane pervaporation: a review, Ind. Eng. Chem. Res. 36 (1997)1048–1066.

17. M. Peng, L.M. Vane and S.X. Liu, Recent advances in VOC's removal from water by pervaporation, J. Hazard. Mater. B 98 (2003) 69–90.

18. B. Smitha, D. Suhanya, S. Sridhar and M. Ramakrishna, Separation of organic–organic mixtures by pervaporation - A review, J. Membr. Sci. 241 (2004)1–21.

19. R. Rantenbach, Membrane Processes, WNT,Warsaw, 1996.

20.Y. Fusaoka, T. Inoue, M. Murakami, M. Kurihara, Drinking water production using cationic and anionic charged nanofiltration membranes. Proceedings of the AWWA Membrane Technology Conference, San Antonio, TX, 2001.

21. A. Mohammad, N. Ali, Understanding the steric and charge contributions in NF membranes using increasing MWCO polyamide membranes. Desalination 147 (2002)205–212.

22. J. Drewes, M. Reinhard and P. Fox, Comparing microfiltration-reverse osmosis and soil-aquifer treatment for indirect potable reuse. Water Res. 37 (2003) 3612–3621.

23. A.I. Schäfer, L.D. Nghiem, T.D. Waite, Removal of the natural hormoneestrone from aqueous solutions using nanofiltration and reverse osmosis, Environ. Sci. Technol. 37 (2003) 182–188.

24. L.D. Nghiem, A.I. Schäfer, M. Elimelech, Removal of natural hormones by nanofiltration membranes: measurement, modeling, and mechanisms, Environ. Sci. Technol. 38 (2004) 1888–1896.

25. N.M. Al-Bastaki, Performance of advanced methods for treatment of wastewater: UV/TiO_2, RO and UF, Chem. Eng. Process. 43 (2004)935–940.

26. L. Jiang, W.Wang, X.Wei, D.Wu, R.Jin, Effect of water on the preparation, morphology and properties of polyimide/silica nanocomposite films prepared by sol-gel process, J. Appl. Polym. Sci. 104 (3)1579-1586.

27. Y.C. Wang, S.H. Huang, C.C. Hu, C.L. Li and K.R. Lee, Sorption and transport properties of gases in aromatic polyimide membranes, J. Membr. Sci 248 (2005)15–25.

28. D. Roizard, A. Nilly, and P. Lochon, Preparation and study of crosslinked polyurethane films to fractionate toluene-n-heptane mixtures by pervaporation, Sep. Puri. Techn. 23 (2001) 45-52.

29. D.Roizard, Jonquières, C. Léger, I. Noezar, L. Perrin, Q. T. Nguyen, R. Clément, H. Lenda, P. Lochon and J. Néel ,Alcohol/ether separation by pervaporation. High performance membrane design, Sep. Sci. Technol. 34(1999) 369 - 390.

30. D.Roizard, E.Favre, Chap.9 : Trends in design and preparation of polymeric membranes for pervaporation, in Advanced materials for membrane preparation, Bentham e-Book (2010). Editors: M.G. Buonomenna and G. Golemme (2010 in print)

31. A. Elsayed and F. Xianshe, Use of pervaporation to separate butanol from dilute aqueous solutions: Effects of operating conditions and concentration polarization, J. Memb. Sci. 323 (2008) 428-435.

32. A. Jonquières, R. Clement and P. Lochon, New film-forming poly(urethane-amide-imide) block copolymers: influence of soft block on membrane properties for the purification of a fuel octane enhancer by pervaporation, Eur. Polym. J. 41 (2005)783–795.

33. S. Kalyani, B. Smitha, S. Sridhar and A. Krishnaiah, Separation of ethanol-water mixtures by pervaporation using sodium alginate/poly(vinyl pyrrolidone) blend membrane crosslinked with phosphoric acid, Ind. Eng. Chem. Res. 45 (2006)9088–9095.

34. J.P.G. Villaluenga, A.T. Mohammadi, A review on the separation of benzene/cyclohexane mixtures by pervaporation processes, J. Membr. Sci. 169 (2000) 159-174.

35. X.Yexin, C. Cuixian, L. Jidijng**,** Experimental study on physical properties and pervaporation performances of polyimide membranes, Chem. Eng. Sci. 62 (2007)2466-2473.

36 B.K. Dutta, S.K. Sikdar, Separation of azeotropic organic liquid mixtures by pervaporation, AIChE J. 37 (1991) 581.

37. A. F.M. Barton, Solubility parameters, Chem. Rev., 1975; 75 (6):731-53.

38. P.C. Ma , W. Nie , Z. Yang , P. Zhang , G. Li , Q. Lei , L. Gao , X. Ji, M. Ding , Preparation and characterization of polyimide/Al_2O_3 hybrid films by sol-gel process**,** J. Appl. Polym. Sci. 108 (2008) 705-712.

39. Y. Zhai, Q. Yang, R. Zhu, Y. Gu, The study on imidization degree of Poly(amic acid) in solution and ordering degree of its polyimide film, J. Materi.Sci. 43 (2008) 338-344.

40. Shaikh Md. Mominul Alam, T. Agag, T. Kawauchi, T. Takeichi**,** organic–inorganic hybrids containing polyimide, organically modified clay and in situ formed polydimethylsiloxane, React. Funct. Polym. 67 (2007)1218-1224.

41. E. Mazoniene, J. Bendoraitiene, L. Peciulyte, S. Diliunas, A. Zemaitaitis, (Co)polyimides from commonly used monomers, and their nanocomposites, Progress in Solid State Chem*istry* 34 (2006) 201-211.

42. http://www.cfm-mb.fr

43. V.T.Stannett, R.T.Chern, Separation of gases: Membrane structure and gas separation, The 5th BOC Priestley Conference, Special Publication No.80, Birmingham, 1989.

44. J. Gemehling, U. Onken, W**.** Arlt**,** Vapor-Liquid equilibrium data collection, Chemistry Data Collection, Vol.I, Part 6b.

45. X. Yexin, C. Cuixian and L. Jiding**,** Experimental study on physical properties and pervaporation performances of polyimide membranes, Chem. Eng. Sci. 62 (2007) 2466-2473

46. H. Yanagishita, C. Maejima, D. Kitamoto, T. Nakane, Preparation of asymmetric polyimide membrane for water/ethanol separation in pervaporation by phase inversion process, J. Membr. Sci. 86 (1994) 231-240

47. Y. Kiso, Y. Nishimura, T. Kitao, K. Nishimura, Rejection properties of non-phenylic pesticides with nanofiltration membranes, J. Membr.Sci. 171 (2000) 229–237.

48. Y. Kiso, Y. Sugiura, T. Kitao, K. Nishimura, Effects of hydrophobicity and molecular size on rejection of aromatic pesticides with nanofiltration membranes, J. Membr. Sci. 192 (2001) 1–10.

49. Y. Yeomin, M. Richard, Removal of organic contaminants by RO and NF membranes, J. Membr. Sci. 261 (2005) 76–86.

50. I. Sibille, L. Mathieu, J. Paquin, D. Gatel, J. Block, Microbial, characteristics of a distribution system fed with nanofiltered drinking water, Water Res. 31 (1997) 2318–2326.

51. K. Agbekodo, B. Legube, P. Cote, Organic in NF permeate. Am. Water Works Assoc. 88 (1996) 67–74.

52. L.D. Nghiem, A.I. Schäfer, M. Elimelech, Removal of natural hormones by nanofiltration membranes: measurement, modeling, and mechanisms, Environ. Sci. Technol. 38 (2004) 1888–1896.

53. In-Chul Kim, Hyung-Gu Yoon, Kew-Ho Lee, Formation of integrally skinned asymmetric polyetherimide nanofiltration membranes by phase inversion process, J. Appl. Polym. Sci. 84(2002)1300-1307.

INSTITUT NATIONAL
POLYTECHNIQUE
DE LORRAINE

AUTORISATION DE SOUTENANCE DE THESE
DU DOCTORAT DE L'INSTITUT NATIONAL
POLYTECHNIQUE DE LORRAINE

o0o

VU LES RAPPORTS ETABLIS PAR :
Madame Murielle RABILLER-BAUDRY, Professeur, Université de Rennes 1, Rennes

Madame Corinne CABASSUD, Professeur, INSA, Toulouse

Le Président de l'Institut National Polytechnique de Lorraine, autorise :

Monsieur ELGENDI Ayman Taha

NANCY BRABOIS
2, AVENUE DE LA
FORET-DE-HAYE
BOITE POSTALE 3
F - 54501
VANDŒUVRE CEDEX

à soutenir devant un jury de l'INSTITUT NATIONAL POLYTECHNIQUE DE LORRAINE, une thèse intitulée :

"Préparation et étude de Membranes Asymétriques Polyimides (PEI) pour la séparation de composés organiques de l'eau"

en vue de l'obtention du titre de :

DOCTEUR DE L'INSTITUT NATIONAL POLYTECHNIQUE DE LORRAINE

Spécialité : **« Génie des Procédés et des Produits »**

Fait à Vandoeuvre, le 28 septembre 2010
Le Président de l'I.N.P.L.,
F. LAURENT

INSTITUT NATIONAL POLYTECHNIQUE DE LORRAINE - NANCY

TEL. 33/03.83.59.59.59
FAX. 33/03.83.59.59.55

Préparation et étude de Membranes Asymétriques Polyalcoxyétherimides (PEI) pour la Séparation de Composés Organiques de l'eau

Résumé

Le mémoire rapporte les travaux effectués pour l'élaboration de membranes asymétriques de type co-polyalcoxyéther-imide (PEI) afin d'obtenir des membranes polymères à haut flux, sélectives pour la séparation de molécules organiques à partir de mélanges aqueux par procédés membranaires. La séparation des mélanges liquides (i.e. toluène - heptane, eau - éthanol, soluté organique dilué en solution aqueuse) a été étudiée par pervaporation (PV) et par nanofiltration (NF) à l'aide de membranes PEI originales asymétriques comportant une peau dense autosupportée. Ces membranes ont été préparées dans des conditions expérimentales contrôlées à partir de solutions DMF-H_2O de l'acide polyamique correspondant (APA) en relation avec le diagramme de phase ternaire ; après l'inversion de phase dans un bain d'eau, les membranes d'APA ont été cyclisées en imides par traitement thermique. Les propriétés physiques des membranes (IR, TGA) ont été caractérisées, et les morphologies correspondantes, enregistrées par SEM, ont été utilisées pour optimiser la préparation des membranes asymétriques pour améliorer les propriétés de séparation en ajustant l'épaisseur de la couche dense. Les performances obtenues en pervaporation et en nanofiltration ont été examinées à la lumière de l'influence de trois séries de paramètres, à savoir les paramètres d'élaboration des membranes (composition du collodion, température du bain d'inversion de phase), les conditions expérimentales de perméation (température, pression) et des propriétés moléculaires du soluté (masse molaire, rayon, polarité). Les résultats de pervaporation ont montré que des membranes asymétriques PEI à peau dense pouvaient bien être obtenues, donnant lieu à une sélectivité moléculaire en accord avec le modèle de solution-diffusion. Les résultats obtenus en NF pour des solutés organiques dilués dans l'eau (≈ 500 ppm) ont montré que le degré de rejet des solutés étaient fortement liés aux conditions d'élaboration des membranes PEI et des propriétés des solutés. Les valeurs de seuil de coupure moléculaire des membranes (MWCO) ont été déterminées avec une série de polyéthylène glycol (400 <MW (g/mole) < 6000) pour une pression appliquée allant jusqu'à 10 bar. Il a été montré que le seuil de coupure des membranes était compris entre 400 et 1000g/mol à 30°C. Il a également été constaté pour certaines membranes PEI que de grandes valeurs de flux de perméation associées à de bonnes sélectivités pouvaient être obtenues, conduisant à des performances intéressantes par rapport aux données de la littérature. Ainsi le développement de ces nouvelles membranes asymétriques copolyimides comprenant un bloc élastomère devrait permettre d'obtenir des membranes de hautes performances pour des applications dans les séparations liquide-liquide, en particulier pour les séparations de nanofiltration en milieu aqueux.

Mots-clés : membranes asymétriques de co-polyalcoxyléther-imide ; pervaporation ; nanofiltration; solutions aqueuses diluées de solutés organiques.

Preparation and Evaluation of Asymmetric Polyetherimide Membranes (PEI) for the Separation of Organic Compounds from Water

Abstract

The work aimed to prepare co-polyalkoxyether-imide (PEI) asymmetric membranes in order to get high flux water selective polymeric membranes suitable for the separation of organic molecules from aqueous mixtures by membrane processes. The separation of liquid mixtures (i.e. toluene – heptane, water – ethanol and low concentrated organic solute in aqueous solutions) was studied by pervaporation (PV) and by nanofiltration (NF) using homemade integrally skinned asymmetric PEI membranes. These membranes were prepared under controlled experimental conditions from DMF-H_2O solutions of the corresponding polyamic acid (PAA) with respect to the ternary phase diagram; after the wet phase inversion in a water bath, the PAA membranes were imidized by thermal treatment. The membrane physical properties (IR, TGA) were characterized and the related morphologies, recorded by SEM, were used to optimize the asymmetric membrane preparation to improve the separation properties by tuning the thickness of the dense top layer. The performances of the pervaporation and nanofiltration separations were examined in the light of the influence of three sets of parameters, i.e. membrane elaboration parameters (dope composition, inversion bath temperature), experimental permeation conditions (temperature, applied pressure) and solute molecular properties (molecular weight, radius, polarity). The PV results showed that tight asymmetric PEI membranes could well be obtained, giving rise to a molecular selectivity in agreement with the solution-diffusion model. The NF results obtained with diluted organics in water (≈500ppm) have shown that the degree of rejection of the organic solutes was strongly linked to the PEI elaboration conditions and to the solute properties. The molecular cutoff values (MWCO) of the membranes were determined with a series of polyethyleneglycol (400 < Mw (g/mole) <6000) for an applied NF pressure up to 10 Bar; it was shown that the PEI membrane MWCO could be ranged between 400 and 1000g/mol at 30°C. It was also found with some PEI membranes that high permeation fluxes together with good separation selectivity could be obtained leading to interesting performances compared to literature data. Thus, it is expected that the development of these new asymmetric block copolyimide rubbery membranes might give rise to high performance membrane systems for applications in liquid-liquid separations, in particular in nanofiltration separations.

Keywords: co-polyalkoxyether-imide asymmetric membranes; pervaporation; nanofiltration; diluted organic aqueous solutions